ISSN 0021-9673

VOL. 594 NOS. 1 + 2 MARCH 6, 1992

COMPLETE IN ONE ISSUE

# JOURNAL OF CHROMATOGRAPHY

## INCLUDING ELECTROPHORESIS AND OTHER SEPARATION METHODS



ELSEVIER

# JOURNAL OF CHROMATOGRAPHY

INCLUDING ELECTROPHORESIS AND OTHER SEPARATION METHODS

**Scope.** The *Journal of Chromatography* publishes papers on all aspects of chromatography, electrophoresis and related methods. Contributions consist mainly of research papers dealing with chromatographic theory, instrumental development and their applications. The section *Biomedical Applications*, which is under separate editorship, deals with the following aspects: developments in and applications of chromatographic and electrophoretic techniques related to clinical diagnosis or alterations during medical treatment; screening and profiling of body fluids or tissues with special reference to metabolic disorders; results from basic medical research with direct consequences in clinical practice; drug level monitoring and pharmacokinetic studies; clinical toxicology; analytical studies in occupational medicine.

**Submission of Papers.** Manuscripts (in English; *four* copies are required) should be submitted to: Editorial Office of *Journal of Chromatography*, P.O. Box 681, 1000 AR Amsterdam, Netherlands, Telefax (+31-20) 5862 304, or to: The Editor of *Journal of Chromatography, Biomedical Applications*, P.O. Box 681, 1000 AR Amsterdam, Netherlands. Review articles are invited or proposed by letter to the Editors. An outline of the proposed review should first be forwarded to the Editors for preliminary discussion prior to preparation. Submission of an article is understood to imply that the article is original and unpublished and is not being considered for publication elsewhere. For copyright regulations, see below.

**Publication.** The *Journal of Chromatography* (incl. *Biomedical Applications*) has 39 volumes in 1992. The subscription prices for 1992 are:

*J. Chromatogr.* (incl. *Cum. Indexes, Vols. 551–600*) + *Biomed. Appl.* (Vols. 573–611):
Dfl. 7722.00 plus Dfl. 1209.00 (p.p.h.) (total *ca.* US$ 4880.25)

*J. Chromatogr.* (incl. *Cum. Indexes, Vols. 551–600*) only (Vols. 585–611):
Dfl. 6210.00 plus Dfl. 837.00 (p.p.h.) (total *ca.* US$ 3850.75)

*Biomed. Appl.* only (Vols. 573–584):
Dfl. 2760.00 plus Dfl. 372.00 (p.p.h.) (total *ca.* US$ 1711.50).

**Subscription Orders.** The Dutch guilder price is definitive. The US$ price is subject to exchange-rate fluctuations and is given as a guide. Subscriptions are accepted on a prepaid basis only, unless different terms have been previously agreed upon. Subscriptions orders can be entered only by calender year (Jan.–Dec.) and should be sent to Elsevier Science Publishers, Journal Department, P.O. Box 211, 1000 AE Amsterdam, Netherlands, Tel. (+31-20) 5803 642, Telefax (+31-20) 5803 598, or to your usual subscription agent. Postage and handling charges include surface delivery except to the following countries where air delivery via SAL (Surface Air Lift) mail is ensured: Argentina, Australia, Brazil, Canada, China, Hong Kong, India, Israel, Japan*, Malaysia, Mexico, New Zealand, Pakistan, Singapore, South Africa, South Korea, Taiwan, Thailand, USA. *For Japan air delivery (SAL) requires 25% additional charge of the normal postage and handling charge. For all other countries airmail rates are available upon request. Claims for missing issues must be made within three months of our publication (mailing) date, otherwise such claims cannot be honoured free of charge. Back volumes of the *Journal of Chromatography* (Vols. 1–572) are available at Dfl. 217.00 (plus postage). Customers in the USA and Canada wishing information on this and other Elsevier journals, please contact Journal Information Center, Elsevier Science Publishing Co. Inc., 655 Avenue of the Americas, New York, NY 10010, USA, Tel. (+1-212) 633 3750, Telefax (+1-212) 633 3990.

**Abstracts/Contents Lists** published in Analytical Abstracts, Biochemical Abstracts, Biological Abstracts, Chemical Abstracts, Chemical Titles, Chromatography Abstracts, Clinical Chemistry Lookout, Current Contents/Life Sciences, Current Contents/Physical, Chemical & Earth Sciences, Deep-Sea Research/Part B: Oceanographic Literature Review, Excerpta Medica, Index Medicus, Mass Spectrometry Bulletin, PASCAL-CNRS, Pharmaceutical Abstracts, Referativnyi Zhurnal, Research Alert, Science Citation Index and Trends in Biotechnology.

**See inside back cover** for Publication Schedule, Information for Authors and information on Advertisements.



0021-9673/92/$05.00



This issue is printed on acid-free paper.

Printed in the Netherlands

VOL. 594, NOS. 1 + 2 JOURNAL OF CHROMATOGRAPHY MARCH 6, 1992

# CONTENTS

*(Abstracts/Contents Lists published in Analytical Abstracts, Biochemical Abstracts, Biological Abstracts, Chemical Abstracts, Chemical Titles, Chromatography Abstracts, Current Contents/Life Sciences, Current Contents/Physical, Chemical & Earth Sciences, Deep-Sea Research/Part B: Oceanographic Literature Review, Excerpta Medica, Index Medicus, Mass Spectrometry Bulletin, PASCAL-CRNS, Referativnyi Zhurnal, Research Alert and Science Citation Index)*

## REGULAR PAPERS

*General*

Improved equations for the calculation of chromatographic figures of merit for ideal and skewed chromatographic peaks
by M. S. Jeansonne and J. P. Foley (Baton Rouge, LA, USA) (Received July 24th, 1991) . . . . . 1

*Column Liquid Chromatography*

Modelling of displacement chromatography using non-ideal isotherms
by P. K. de Bokx, P. C. Baarslag and H. P. Urbach (Eindhoven, Netherlands) (Received November 5th, 1991) . . . 9

High-performance liquid chromatographic study of the correlation between the physico-chemical parameters of furan and benzene aldehydes and the rate of their metabolism by yeast.
by V. D. Nemirovskii, N. I. Monakhova and V. G. Kostenko (St. Petersburg, Russia) (Received October 29th, 1991) . 23

Determination of solute–polymer interaction constants via chromatography with polymer capillaries
by D. R. Jenke (Round Lake, IL, USA) (Received October 31st, 1991) . . . . . 29

Retention behaviour of $\beta$-cyclodextrin complexes of anthracene and pyrene using reversed-phase liquid chromatography. The effects of *tert.*-butanol and cyclopentanol
by V. C. Anigbogu, A. Muñoz de la Peña, T. T. Ndou and I. M. Warner (Atlanta, GA, USA) (Received November 8th, 1991) . . . . . 37

Selection of robust combinations of extraction liquid composition and internal standard. Monte Carlo simulation of improvement of assay methods with liquid–liquid extraction prior to high-performance liquid chromatography
by J. Wieling (Zuidlaren and Groningen, Netherlands), P. M. J. Coenegracht (Groningen, Netherlands), C. K. Mensink and J. H. G. Jonkman (Zuidlaren, Netherlands) and D. A. Doornbos (Groningen, Netherlands) (Received October 31st, 1991) . . . . . 45

Computer simulation as a tool for the rapid optimization of the high-performance liquid chromatographic separation of a tryptic digest of human growth hormone
by R. C. Chloupek and W. S. Hancock (San Francisco, CA, USA) and L. R. Synder (Walnut Creek, CA, USA) (Received November 14th, 1991) . . . . . 65

Mixed-mode hydrophilic and ionic interaction chromatography rivals reversed-phase liquid chromatography for the separation of peptides
by B.-Y. Zhu, C. T. Mant and R. S. Hodges (Edmonton, Canada) (Received October 22nd, 1991) . . . . . 75

Suppression of the effect of metal impurities in alkylsilylated silica packing materials
by K. Kimata, N. Tanaka and T. Araki (Kyoto, Japan) (Received December 9th, 1991) . . . . . 87

Ligand–receptor interactions in affinity cell partitioning. Studies with transferrin covalently linked to monomethoxypoly(ethylene glycol) and rat reticulocytes
by C. Delgado, P. Sancho, J. Mendieta and J. Luque (Madrid, Spain) (Received October 29th, 1991) . . . . . 97

Liquid chromatographic separation of all-carbon molecules $C_{60}$ and $C_{70}$ with multi-legged phenyl group bonded silica phases
by K. Jinno, K. Yamamoto, T. Ueda, H. Nagashima and K. Itoh (Toyohashi, Japan) and J. C. Fetzer and W. R. Biggs (Richmond, CA, USA) (Received October 23rd, 1991) . . . . . 105

Liquid chromatographic isolation and structural elucidation of methoxymethylene dimethyl dodecatrienes catalytically synthesized from methanol and three moles of isoprene
by C. Tröltzsch and R. Berger (Greifswald, Germany) and M. Michalik (Rostock, Germany) (Received October 21st, 1991) . . . . . 111

*(Continued overleaf)*

*Contents (continued)*

Identification of the constituent flavanoid units in sainfoin proanthocyanidins by reversed-phase high-performance liquid chromatography
by M. R. Koupai-Abyazani, J. McCallum and B. A. Bohm (Vancouver, Canada) (Received October 30th, 1991) . . . 117

Chromatographic separation of polyols by ligand exchange. Effects of the ion-exchange resin cross-linking and size
by H. Caruel, P. Phemius, L. Rigal and A. Gaset (Toulouse, France) (Received November 7th, 1991) . . . . . 125

Determination of the norlignan glucosides of Hypoxidaceae by high-performance liquid chromatography
by P. Betto, R. Gabriele and C. Galeffi (Rome, Italy) (Received October 31st, 1991) . . . . . 131

High-performance liquid chromatography of okadaic acid and free fatty acids in mussels
by F. Zonta (Trento, Italy), B. Stancher, P. Bogoni and P. Masotti (Trieste, Italy) (Received October 30th, 1991) . . 137

Isolation of aristolochic acids $HA_sI$ and $HA_sII$ by preparative liquid chromatography
by B. Makuch, K. Gazda and W. Cisowski (Gdańsk, Poland) (Received November 8th, 1991) . . . . . 145

Determination of taxol by high-performance liquid chromatography–thermospray mass spectrometry
by S. O. K. Auriola, A.-M. Lepistö, T. Naaranlahti and S. P. Lapinjoki (Kuopio, Finland) (Received October 30th, 1991) 153

Reversed-phase liquid chromatographic behaviour of alkylamines with amperometric detection and its application to trace analysis
by M. Maruyama and T. Nagayoshi (Tokyo, Japan) (Received October 11th, 1991) . . . . . 159

Chromatography of 99 amino acids and other ninhydrin-reactive compounds in the Pickering lithium gradient system
by J. A. Grunau and J. M. Swiader (Urbana, IL, USA) (Received September 10th, 1991) . . . . . 165

Determination of glutamine, glutamic acid and pyroglutamic acids using high-performance liquid chromatography on dynamically modified silica
by B. Polanuer, A. Sholin, N. Demina and N. Rumiantseva (Moscow, Russia) (Received November 7th, 1991) . . . 173

High-performance gel permeation chromatographic analysis of immunoglobulin M produced by hybridoma cell culture
by N. Chauret (Quebec, Canada), J. Côté, J. Archambault and G. André (Montreal, Canada) (Received October 31st, 1991) . . . . . 179

Determination of ascorbic and dehydroascorbic acid in potatoes (*Solanum tuberosum*) and strawberries using ion-exclusion chromatography
by W. D. Graham and D. Annette (Belfast, UK) (Received October 4th, 1991) . . . . . 187

Solvent degradation of cloxacillin *in vitro*. Tentative identification of degradation products using thermospray liquid chromatography–mass spectrometry
by K. L. Tyczkowska (Raleigh, NC, USA), R. D. Voyksner (Research Triangle Park, NC, USA) and A. L. Aronson (Raleigh, NC, USA) (Received October 21st, 1991) . . . . . 195

Determination of dirithromycin purity and related substances by high-performance liquid chromatography
by B. A. Olsen, J. D. Stafford and D. E. Reed (Lafayette, IN, USA) (Received November 4th, 1991) . . . . . 203

Development of stability indicating assay methods for the determination of hydroxamic acids in topical formulations
by J. E. DiNunzio and R. R. Gadde (Buffalo, NY, USA) (Received October 22nd, 1991) . . . . . 209

Determination of the mean ionic charge of the components of three $^{99m}Tc$ bone scanning agents by gel chromatography with two eluents of different electrolyte composition
by W. J. Gelsema, C. L. de Ligny, Y. M. Huigen and J. Schuring (Utrecht, Netherlands) (Received October 23rd, 1991) 217

Determination of major ions in snow and ice cores by ion chromatography
by C. F. Buck, P. A. Mayewski, M. J. Spencer, S. Whitlow, M. S. Twickler and D. Barrett (Durham, NH, USA) (Received October 29th, 1991) . . . . . 225

*Gas Chromatography*

Hydrogen bonding. XXI. Solvation parameters for alkylaromatic hydrocarbons from gas–liquid chromatographic data
by M. H. Abraham and G. S. Whiting (London, UK) (Received September 4th, 1991) . . . . . 229

Preparation and capillary column gas chromatographic characterization of aza-crown ether polysiloxane stationary phases
by C. Wu, J. Cheng, W. Gao, Z. Zeng, X. Lu and S. Gong (Wuhan, China) (Received October 18th, 1991) . . . . . 243

Simultaneous determination of sorbic acid, dehydroacetic acid and benzoic acid by gas chromatography–mass spectrometry
by M. Kakemoto (Tokyo, Japan) (Received October 30th, 1991) . . . . . 253

Analysis of zapatera olives by gas and high-performance liquid chromatography
by A. Montaño, A. de Castro, L. Rejano and A.-H. Sánchez (Seville, Spain) (Received October 29th, 1991) . . . . . 259

Gas chromatographic elution patterns of chlorinated dioxins *versus* column polarity
by J. R. Donnelly and G. W. Sovocool (Las Vegas, NV, USA) (Received September 20th, 1991) . . . . . 269

Determination of $Pb^{2+}$ in water by isotope dilution gas chromatography–mass spectrometry of tetraethyllead formed by reaction with sodium tetraethylborate
by B. J. Feldman, H. Mogadeddi and J. D. Osterloh (San Francisco, CA, USA) (Received September 30th, 1991) . . 275

*Supercritical Fluid Chromatography*

Synthesis of (1*R-trans*)-N,N′-1,2-cyclohexylenebisbenzamideoligodimethylsiloxane copolymers for use as chiral stationary phases for capillary supercritical fluid chromatography
by D. F. Johnson, J. S. Bradshaw, M. Éguchi, B. E. Rossiter and M. L. Lee (Provo, UT, USA) and P. Petersson and K. E. Markides (Uppsala, Sweden) (Received November 18th, 1991) . . . . . 283

Correlation between column surface area and retention of polar solutes in packed-column supercritical fluid chromatography
by T. A. Berger and J. F. Deye (Avondale, PA, USA) (Received October 30th, 1991) . . . . . 291

Effects of collection solvent parameters and extraction cell geometry on supercritical fluid extraction efficiencies
by J. J. Langenfeld, M. D. Burford, S. B. Hawthorne and D. J. Miller (Grand Forks, ND, USA) (Received October 18th, 1991) . . . . . 297

Supercritical carbon dioxide extraction of resin and fatty acids from sediments at pulp mill sites
by H.-B. Lee and T. E. Peart (Burlington, Canada) (Received November 5th, 1991) . . . . . 309

*Electrophoresis*

Charge-reversed, polymer-coated capillary column for the analysis of a recombinant chimeric glycoprotein
by K. Tsuji and R. J. Little (Kalamazoo, MI, USA) (Received November 12th, 1991) . . . . . 317

Capillary modification and evaluation using streaming potential and frontal chromatography for protein analysis in capillary electrophoresis
by T. Wang and R. A. Hartwick (Binghamton, NY, USA) (Received November 1st, 1991) . . . . . 325

Separation of plant growth regulators by capillary electrophoresis
by S. K. Yeo, H. K. Lee and S. F. Y. Li (Kent Ridge, Singapore) (Received October 18th, 1991) . . . . . 335

Finite difference modelling of continuous-flow electrophoresis
by T. M. Grateful and E. N. Lightfoot, Jr. (Madison, WI, USA) (Received November 12th, 1991) . . . . . 341

Continuous-flow electrophoresis: a separation criterion applied to the separation of model proteins
by H. Roux-de Balmann and V. Sanchez (Toulouse, France) (Received October 8th, 1991) . . . . . 351

Continuous separation and purification of proteins by recycling isotachophoresis
by J. Caslavska and W. Thormann (Berne, Switzerland) (Received August 27th, 1991) . . . . . 361

Study of isotachophoretic separation behaviour of metal cations by means of particle-induced X-ray emission. III. Analysis of a crude rare earth chloride from monazite
by J. Hu, T. Hirokawa, F. Nishiyama, Y. Kiso, K. Ito and E. Shoto (Higashi-Hiroshima, Japan) (Received October 31st, 1991) . . . . . 371

*Planar Chromatography*

Quantitative separation of $Cr^{3+}$ from $Mo^{6+}$, $W^{6+}$, $Hg_2^{2+}$, $Cu^{2+}$ and $Pb^{2+}$. Chromatographic behaviour of 51 cations on papers impregnated with Sn(IV)-based inorganic ion exchangers in complex-forming acid systems
by S. D. Sharma and S. Misra (Moradabad, India) (Received November 6th, 1991) . . . . . 379

*(Continued overleaf)*

*Contents (continued)*

SHORT COMMUNICATIONS

*Column Liquid Chromatography*

Primary and secondary amine derivatization with luminarins 1 and 2: separation by liquid chromatography with peroxyoxalate chemiluminescence detection
by M. Tod (Bobigny, France), J.-Y. Legendre (Paris, France), J. Chalom (Les Ulis, France) and H. Kouwatli, M. Poulou, R. Farinotti and G. Mahuzier (Châtenay-Malabry, France) (Received November 21st, 1991) . . . . . 386

Fast protein monitoring in fermentation both using non-porous micropellicular reversed-phase columns
by E. Watson and F. Yao (Thousand Oaks, CA, USA) (Received November 18th, 1991) . . . . . 392

*Gas Chromatography*

Gas chromatography of chloride and bromide as phenylboronic acid/mercuric nitrate derivatives with microwave induced plasma atomic emission detection
by A. Sarafraz-Yazdi, M. Y. Khuhawar and P. C. Uden (Amherst, MA, USA) (Received December 10th, 1991) . . . 395

*Electrophoresis*

Fast and sensitive staining technique for catalase in polyacrylamide gel
by H. Pichorner, S. Loew, S. A. A. Korori, G. Jessner and R. Ebermann (Vienna, Austria) (Received November 5th, 1991) . . . . . 400

BOOK REVIEW

Advances in steroid analysis '90 (edited by S. Görög; guest editor E. Heftmann), reviewed by T. Nambara (Sendai, Japan) . 403

*Author Index* . . . . . 404

*Erratum* . . . . . 407

*Announcement of Special Issue on Principles and Applications of Solid Phase Extraction* . . . . . 408

In articles with more than one author, the name of the author to whom correspondence should be addressed is indicated in the article heading by a 6-pointed asterisk (*).

JOURNAL OF CHROMATOGRAPHY

VOL. 594 (1992)

# JOURNAL of CHROMATOGRAPHY

## INCLUDING ELECTROPHORESIS AND OTHER SEPARATION METHODS




ELSEVIER

AMSTERDAM — LONDON — NEW YORK — TOKYO

0021-9673/92/$05.00



Printed in the Netherlands

*Journal of Chromatography*, 594 (1992) 1–8
Elsevier Science Publishers B.V., Amsterdam

CHROM. 23 889

# Improved equations for the calculation of chromatographic figures of merit for ideal and skewed chromatographic peaks

Mark S. Jeansonne[☆] and Joe P. Foley*,[☆☆]

*Department of Chemistry, Louisiana State University, Baton Rouge, LA 70803-1804 (USA)*

(Received July 24th, 1991)

ABSTRACT

Improved empirical equations based on the graphically measurable parameters peak height ($h_p$), width ($W$) and asymmetry ($b/a$) at 10, 25, 50, 71, 73, 75, 77 and 79% of the peak height have been derived. These equations were developed using the exponentially modified Gaussian function as an asymmetric peak model. Equations are reported for the following chromatographic figures of merit: $\tau$, $\sigma_G$, area, variance, third and fourth statistical moments, excess, and skew. The accuracy and precision of the equations are discussed, along with their applicability.to fronted and overlapped peaks.

## INTRODUCTION

In a recent publication we presented an equation-based approach for the accurate measurement of chromatographic peak statistical moments, excess, and skew [1]. These empirical equations, based on the exponentially modified Gaussian (EMG) function, utilize the peak width, asymmetry, and in some cases, the peak height. The EMG function, resulting from the convolution of Gaussian and exponential decay functions, can model any tailed peak more accurately than a Gaussian function. Due to various intra and extracolumn band broadening process, real chromatographic peaks are seldom symmetrical, so that use of a tailed peak model should be more accurate. The EMG function has been justified both theoretically [2–4] and experimentally [5,6] and has been thoroughly reviewed [7,8]. Because a convenient procedure for verification of the EMG character of chromatographic peaks exists [5], these equations can be confidently applied once EMG peak shape has been established.

A variety of approaches have been used to make this model more practical for routine use [5,9–16]. One particularly popular approach has been to relate the graphical parameters $a$ and $b$, (see Fig. 1), measured at a particular fraction of the peak height, to the fundamental EMG parameters, $\tau$ and $\sigma_G$. Relationships between $a$ and $b$ and the EMG parameters have been reported in the form of both graphical curves and empirical equations. Both techniques circumvent tedious, computer intensive curve fitting. Equations reported by Foley and Dorsey [11] in 1983 have perhaps shown the greatest routine applicability, based on the number of citations. In that work, equations were derived for the calculation of many important chromatographic peak parameters (*i.e.*, $\tau$, $\sigma_G$, statistical moments and efficiency) that were collectively termed chromatographic figures of merit (CFOMs). Equations based on the measurement of $b$ and $a$ at 10, 30 and 50% of the peak height fraction were reported, although

☆ Present address: Chevron Chemical Co., 1862 Kingwood Drive, Kingwood, TX 77339, USA.
☆☆ Present address: Department of Chemistry, Villanova University, Villanova, PA 19085-1699, USA.

0021-9673/92/$05.00 

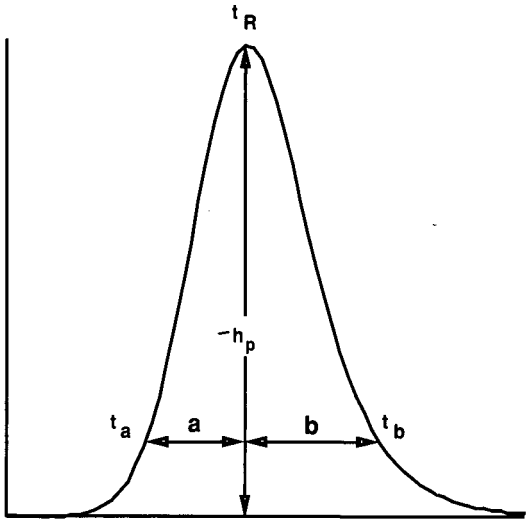


Fig. 1. Graphical parameters necessary for calculation of various chromatographic figures of merit (CFOMs). $h_p$ = Peak height; $W = a + b$ = peak width; $(b/a)$ = peak asymmetry.

only the equations at 10% were recommended for calculation of the CFOMs. The equations at 30 and 50% were intended solely for peak modeling.

Although the CFOM equations reported by Foley and Dorsey earlier are very accurate and precise, they were intended to be used with manually measured $b$ and $a$ values where the accuracy of these measurements was the limiting factor in the accuracy of the equations. Due to the greater accuracy of graphical parameter measurement via modern electronic integrators and data systems, the accuracy of CFOM measurement may be unnecessarily limited by the equations themselves. Two additional limitations are (i) the somewhat narrow asymmetry $(b/a)$ range of the equations; and (ii) the absence of equations based on peak measurements higher than 50% of the peak height.

With regard to (ii), the ability to use $b$ and $a$ from higher peak height fractions is desirable when peaks are overlapped because distortion from the adjacent peak is less. We have shown that accurate measurement of CFOMs utilizing $b$ and $a$ measurements at 75% of the peak height is possible for both overlapping and resolved peaks using improved equations that we did not specify [1]. In this paper we report those improved equations (from the standpoint of the previous limitations) for the measurement of peak area, variance ($M_2$), third ($M_3$) and fourth ($M_4$) statistical moments, excess, and skew.

## EXPERIMENTAL

An Apple Macintosh Plus microcomputer programmed in Microsoft Basic was used for EMG peak generation. The EMG function was evaluated as described before [5], and universal data were obtained via a search algorithm [7]. All polynomial curve fitting was done using commercially available software.

### *EMG peak generation*

Eqn. 1 shows the form of the EMG function used.

$$h_{EMG}(t) = \frac{A}{\tau}\exp\left[\frac{1}{2}\left(\frac{\sigma_G}{\tau}\right)^2 - \left(\frac{t - t_G}{\tau}\right)\right] \cdot \int_{-\infty}^{z} \frac{\exp\left(\frac{-y^2}{2}\right)}{\sqrt{2\pi}}\,dy \quad (1)$$

$A$ is the peak amplitude, $\tau$ is the exponential modifier, $\sigma_G$ is the standard deviation of the unmodified Gaussian, $t_G$ is the retention time of the unmodified Gaussian and $z = (t - t_G)/\sigma_G - \sigma_G/\tau$. The ratio $\tau/\sigma_G$ is used to describe the overall shape of an EMG peak; at $\tau/\sigma_G$ close to zero, the peak approaches Gaussian shape, while higher $\tau/\sigma_G$ values give greater tailing. Values of $A = 1$, $t_G = 100$ and $\sigma_G = 5$ were used for evaluation of the function. The times for $t_R$ (EMG peak apex), $t_a$, and $t_b$ were measured to within 0.001 at $r$ (peak height fraction) = 0.10, 0.25, 0.5, 0.71, 0.73, 0.75, 0.77, and 0.79 (see Fig. 1), from $\tau/\sigma_G = 0$ to 4.5 in 0.05 increments. The peak height ($h_p$) at each $\tau/\sigma_G$ was determined concurrently with $t_R$ using the same search algorithm. Once $t_R$, $t_a$ and $t_b$ were measured, the parameters $a$, $b$, $W (= a + b)$, and asymmetry $(b/a)$ were then calculated. Finally, the values of asymmetry $(b/a)$, $W/\sigma_G$, $(t_R - t_G)/\sigma_G$ and $h_p$, termed universal data, were used in the following derivations.

### *Method of derivation*

A three stage approach was employed for CFOM calculation: (i) derivation of width and asymmetry based equations for $\sigma_G$ and $M_2$; (ii) calculation of $\tau$ via eqn. 2; and (iii) computation via eqns. 3–6 below of the remaining moments, excess, and skew [11].

$$\tau = \sqrt{M_2 - \sigma_G^2} \quad (2)$$

$$M_3 = 2\tau^3 \tag{3}$$

$$M_4 = 3\sigma^4 + 6\sigma^2\tau^2 + 9\tau^4 \tag{4}$$

$$\text{Skew} = \frac{M_3}{M_2^{3/2}} \tag{5}$$

$$\text{Excess} = \frac{M_4}{M_2^2} - 3 \tag{6}$$

We found that the above approach, utilizing equations for $\sigma_G$ and $M_2$ and then eqns. 2–6 above, to be somewhat more accurate than an alternative approach based on equations for $\sigma_G$ and $\tau/\sigma_G$, the calculation $\tau$ from their product, and calculation of the remaining CFOMs via eqns. 3–6. Because of the poorer accuracy of the latter approach, it is not discussed further. Equations based on the first, more accurate approach were derived at several peak heights, with those for $0.71 \leqslant r \leqslant 0.79$ developed for purposes of averaging to reduce uncertainty and bias.

*Derivation of equations for $\sigma_G$*

At each relative peak height ($r$), the quantity $W_r/\sigma_G$ was plotted as a function of asymmetry ($b/a$), giving results similar to Fig. 2 for $r = 0.25$. As shown, the plot is curved at the lower b/a values and linear at the higher values. Therefore, a quadratic least-squares fit was used at lower asymmetries and a linear least-squares fit was used for higher asymmetries, resulting in two (nonoverlapping) equations at each $r$. $\sigma_G$ could then be related to width and asymmetry as shown in eqn. 7.

$$\sigma_G = \frac{W_r}{\mathrm{f}(b/a)} \tag{7}$$

where $\mathrm{f}(b/a)$ is the resulting fitted equation of the form $\mathrm{f}(b/a) = C_0 + C_1(b/a) + C_2(b/a)^2$ [The coefficient $C_2$ is 0 for $\mathrm{f}(b/a)$ resulting from the linear fit.] Table I lists the coefficients obtained at each $r$ for both linear and quadratic fits and their valid asymmetry ranges. The cut point between curved and linear fits was determined so that the relative error in $\sigma_G$ over the entire $b/a$ range was minimized.

*Derivation of equations for $M_2$*

Analogous to the derivations of $\sigma_G$ equations, the quantity $M_2/W_r^2$ was plotted *vs.* asymmetry ($b/a$) at each $r$. However, as shown in Fig. 3 for $r = 0.25$, curvature was evident over the entire $b/a$ range.

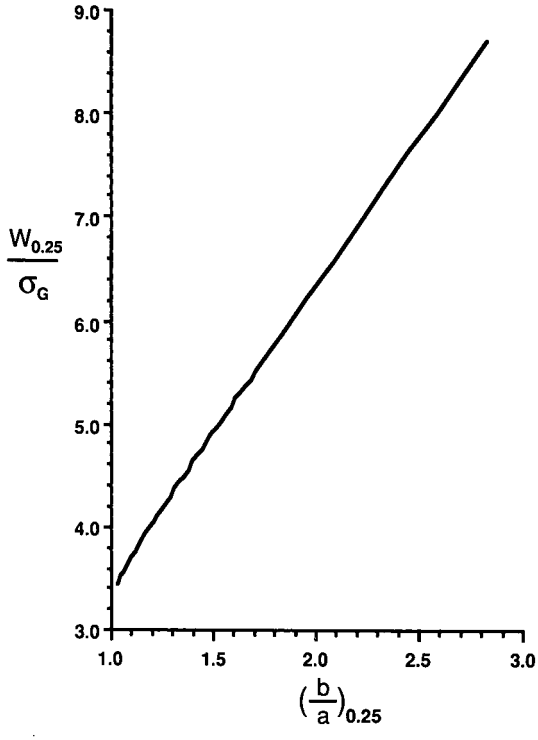


Fig. 2. Determination of $\mathrm{f}(b/a)$ for $\sigma_G$ at $r = 0.25$. Note slight curvature at lower asymmetries. Quadratic fit from $(b/a)_{0.25} = 1.02$ to 1.26, linear fit from $(b/a)_{0.25} = 1.26$ to 2.85.

Moreover, because an accurate quadratic fit over the entire $b/a$ range was not possible, two separate least-squares quadratic fits were used, again choosing the cut point to minimize the relative error over the entire asymmetry range. Eqn. 8 shows the resulting relationship between $M_2$, $W_r^2$ and $\mathrm{f}(b/a)$.

$$M_2 = W_r^2 \cdot \mathrm{f}(b/a) \tag{8}$$

Values of the coefficients of $\mathrm{f}(b/a)$ for calculation of $M_2$ are also given in Table I. At $r$ values of 0.71 to 0.79, the plots were similar to those obtained for the $\sigma_G$ derivations, thereby allowing linear and quadratic fits for the two sections of curves, as before.

*Calculation of remaining CFOMs except peak area*

Using calculated values of $\sigma_G$ and $M_2$ (equations of Table I), values for $\tau$, $M_3$, $M_4$, skew, and excess were calculated at $r = 0.10$, 0.25, 0.5, 0.71, 0.73, 0.75, 0.77, and 0.79 via eqns. 2–6, from $\tau/\sigma_G = 0$ to 4.5 in increments of 0.05. The accuracy and precision of these values is reported in Table II.

TABLE I

COEFFICIENTS, ACCURACY, AND PRECISION OF EQUATIONS FOR CALCULATING $\sigma_G$ AND $M_2$ OF GAUSSIAN AND EMG PEAKS

| Parameter[a] | Peak height fraction, $r$ | Asymmetry range, $\tau/\sigma$ | Asymmetry range, $(b/a)_r$ | Coefficients[b] | | | Maximum error[c] (%) | Relative uncertainty[d] (%) |
|---|---|---|---|---|---|---|---|---|
| | | | | $C_2$ | $C_1$ | $C_0$ | | |
| $\sigma_G$ | 0.10 | 0.30–1.20 | 1.03–1.46 | −1.2951 | 6.6162 | −0.9516 | −0.2, +0.6 | ±0.52 |
| | | 1.20–4.30 | 1.46–3.67 | 0 | 3.3139 | 1.1147 | | |
| | 0.135 | 0.30–0.65 | 1.02–1.14 | −4.1347 | 12.7655 | −4.5742 | −0.2, +0.3 | ±0.53 |
| | | 0.65–4.30 | 1.14–3.42 | 0 | 3.1665 | 1.0051 | | |
| | 0.25 | 0.30–1.10 | 1.02–1.26 | −2.4352 | 8.8715 | −3.0485 | ±0.2 | ±0.52 |
| | | 1.10–4.30 | 1.26–2.85 | 0 | 2.8504 | 0.6888 | | |
| | 0.50 | 0.30–1.30 | 1.01–1.21 | −4.2670 | 12.5178 | −5.8561 | −0.4, +0.8 | ±0.8 |
| | | 1.30–4.30 | 1.21–2.09 | 0 | 2.4685 | 0.0981 | | |
| | 0.71 | 0.30–1.85 | 1.01–1.23 | −2.7901 | 9.0992 | −4.6165 | −0.5, +0.2 | ±1.0 |
| | | 1.85–4.30 | 1.23–1.64 | 0 | 2.2527 | −0.3983 | | |
| | 0.73 | 1.30–1.85 | 1.01–1.22 | −2.9116 | 9.3374 | −4.8028 | −0.5, +0.2 | ±1.0 |
| | | 1.85–4.30 | 1.22–1.60 | 0 | 2.2449 | −0.4666 | | |
| | 0.75 | 0.30–1.25 | 1.01–1.12 | −7.4174 | 18.8306 | −9.8710 | ±0.7 | ±1.2 |
| | | 1.30–4.30 | 1.12–1.56 | 0 | 2.3245 | −0.6604 | | |
| | 0.77 | 0.30–1.85 | 1.01–1.19 | −3.3185 | 10.1672 | −5.3703 | −0.5, +0.2 | ±1.1 |
| | | 1.85–4.30 | 1.19–1.52 | 0 | 2.2326 | −0.6111 | | |
| | 0.79 | 0.30–1.90 | 1.01–1.19 | −3.3724 | 10.2546 | −5.4779 | −0.5, +0.2 | ±1.2 |
| | | 1.90–4.30 | 1.19–1.49 | 0 | 2.2268 | −0.6859 | | |
| $M_2$ | 0.10 | 0.30–1.15 | 1.03–1.46 | 0.1270 | −0.06458 | 0.4766 | −0.2, +0.6 | ±0.6 |
| | | 1.15–4.30 | 1.46–3.67 | −0.0299 | 0.3569 | 0.1909 | | |
| | 0.135 | 0.30–2.85 | 1.03–2.50 | −0.0378 | 0.4993 | 0.1470 | −1.4, +0.5 | ±0.6 |
| | | 2.85–4.30 | 2.50–3.42 | 0 | 0.2493 | 0.5394 | | |
| | 0.25 | 0.30–0.70 | 1.02–1.13 | 2.3418 | −4.1376 | 2.6930 | −0.2, +0.3 | ±0.8 |
| | | 0.70–4.30 | 1.13–2.85 | −0.1842 | 1.6032 | −0.5715 | | |
| | 0.50 | 0.30–1.30 | 1.01–1.21 | 7.9161 | −12.8196 | 6.6750 | −0.6, +0.4 | ±1.5 |
| | | 1.30–4.30 | 1.21–2.09 | −1.3369 | 9.3616 | −6.6407 | | |
| | 0.71 | 0.30–1.30 | 1.01–1.14 | 52.777 | −96.293 | 47.101 | −0.6, +0.8 | ±2.4 |
| | | 1.30–4.30 | 1.14–1.64 | 0 | 25.039 | −22.696 | | |
| | 0.73 | 0.30–1.35 | 1.01–1.14 | 63.545 | −116.389 | 56.743 | −1.0, +0.5 | ±2.6 |
| | | 1.35–4.30 | 1.14–1.60 | 0 | 29.935 | −27.601 | | |
| | 0.75 | 0.30–1.40 | 1.01–1.13 | 84.448 | −157.205 | 77.0333 | −1.3, +0.7 | ±2.8 |
| | | 1.40–4.30 | 1.13–1.56 | 0 | 35.9111 | −33.5484 | | |
| | 0.77 | 0.30–1.70 | 1.01–1.17 | 79.771 | −142.903 | 67.779 | −1.3, +0.7 | ±2.7 |
| | | 1.70–4.30 | 1.17–1.52 | 0 | 44.119 | −41.993 | | |
| | 0.79 | 0.30–1.70 | 1.01–1.16 | 103.956 | −188.641 | 89.840 | −1.3, +0.7 | ±2.9 |
| | | 1.70–4.30 | 1.16–1.49 | 0 | 54.353 | −52.398 | | |

[a] General form of the equations for each parameter: $\sigma_G = W_r/f(b/a)$; and $M_2 = W_r^2 \cdot f(b/a)$, where $W_r$ = width of peak at the peak height fraction given by the subscript, $b/a$ = an asymmetry factor measured at the same peak height fraction as the width, and $f(b/a) = C_0 + C_1(b/a) + C_2(b/a)^2$.

[b] Tabulated values multiplied × 10 for $M_2$.

[c] Maximum relative error of the equations over the stated asymmetry range.

[d] Percent relative standard deviation (%R.S.D.) predicted from error propagation, assuming R.S.D. values of 0.25% and 0.5% for $W_r$ and $b/a$. Note that the precision of $W$ and $b/a$ can be better than what we have assumed for many data acquisition systems. In instances where a range is reported, the larger number refers to the least asymmetric peak (smallest $b/a$ value) and the smaller number refers to the most asymmetric peak (largest $b/a$ value). The uncertainty decreases *exponentially* from the larger value to the lower value as $b/a$ increases.

TABLE II

ERROR AND UNCERTAINTY OF CFOMs CALCULATED FROM $\sigma_G$ AND $M_2$ USING EQNS. 2-6 (TEXT)[a]

| Parameter | Peak height fraction, $r$ | Asymmetry range, $\tau/\sigma$ | Asymmetry range, $(b/a)_r$ | Maximum error (%) | Relative uncertainty (%) |
|---|---|---|---|---|---|
| $\tau$ (eqn. 2, text) | 0.10 | 0.5–4.3 | 1.09–3.67 | −0.4, +0.2 | 2.4–0.3 |
| | 0.135 | 0.5–4.3 | 1.08–3.42 | −0.3, +0.7 | 2.6–0.3 |
| | 0.25 | 0.5–4.3 | 1.07–2.85 | ±0.4 | 3.0–0.3 |
| | 0.50 | 0.5–4.3 | 1.04–2.09 | −0.4, +0.6 | 4.2–0.4 |
| | 0.71 | 0.5–4.3 | 1.03–1.64 | −0,4, +0.6 | 5.8–0.6 |
| | 0.73 | 0.5–4.3 | 1.03–1.60 | −0.7, +0.4 | 6.1–0.7 |
| | 0.75 | 0.5–4.3 | 1.03–1.56 | ±0.8 | 6.5–0.7 |
| | 0.77 | 0.5–4.3 | 1.02–1.52 | −0.5, +1.0 | 7.0–0.8 |
| | 0.79 | 0.5–4.3 | 1.02–1.49 | −0.8, +1.0 | 7.3–0.8 |
| $\tau/\sigma$ | 0.10 | 0.5–4.3 | 1.09–3.67 | −0.8, +0.3 | 2.5–0.6 |
| | 0.135 | 0.5–4.3 | 1.08–3.42 | −0.3, +0.8 | 2.7–0.6 |
| | 0.25 | 0.5–4.3 | 1.07–2.85 | ±0.5 | 3.0–0.6 |
| | 0.50 | 0.5–4.3 | 1.04–2.09 | −1.0, +0.6 | 4.3–0.7 |
| | 0.71 | 0.5–4.3 | 1.03–1.64 | −0.6, +0.9 | 5.9–0.9 |
| | 0.73 | 0.5–4.3 | 1.03–1.60 | −0.6, +0.9 | 6.2–0.9 |
| | 0.75 | 0.5–4.3 | 1.03–1.56 | −0.9, +1.4 | 6.6–1.0 |
| | 0.77 | 0.5–4.3 | 1.02–1.52 | −0.6, +0.9 | 7.1–1.0 |
| | 0.79 | 0.5–4.3 | 1.02–1.49 | ±0.8 | 7.4–1.1 |
| $M_3$ (eqn. 3, text) | 0.10 | 0.5–4.3 | 1.09–3.67 | −1.0, +0.5 | 7.3–0.9 |
| | 0.135 | 0.5–4.3 | 1.08–3.42 | −0.9, +2.2 | 7.8–0.9 |
| | 0.25 | 0.5–4.3 | 1.07–2.85 | −1.2, +1.1 | 8.8–0.9 |
| | 0.50 | 0.5–4.3 | 1.04–2.09 | −1.2, +1.9 | 12.6–1.2 |
| | 0.71 | 0.5–4.3 | 1.03–1.64 | −1.1, +1.7 | 17.5–2.0 |
| | 0.73 | 0.5–4.3 | 1.03–1.60 | −2.0, +1.4 | 18.3–2.0 |
| | 0.75 | 0.5–4.3 | 1.03–1.56 | −2.4, +2.5 | 19.6–2.1 |
| | 0.77 | 0.5–4.3 | 1.02–1.52 | −1.5, +2.9 | 20.9–2.3 |
| | 0.79 | 0.5–4.3 | 1.02–1.49 | −2.5, +2.9 | 22.0–2.4 |
| $M_4$ (eqn. 4, text) | 0.10 | 0.5–4.3 | 1.09–3.67 | −0.6, +0.9 | 3.1–1.2 |
| | 0.135 | 0.5–4.3 | 1.08–3.42 | −0.5, +1.2 | 3.1–1.2 |
| | 0.25 | 0.5–4.3 | 1.07–2.85 | −0.5, +0.9 | 3.5–1.2 |
| | 0.50 | 0.5–4.3 | 1.04–2.09 | ±0.9 | 4.9–1.6 |
| | 0.71 | 0.5–4.3 | 1.03–1.64 | −1.2, +1.6 | 6.7–2.6 |
| | 0.73 | 0.5–4.3 | 1.03–1.60 | −2.3, +1.4 | 7.0–2.7 |
| | 0.75 | 0.5–4.3 | 1.03–1.56 | −2.8, +2.3 | 7.6–2.8 |
| | 0.77 | 0.5–4.3 | 1.02–1.52 | −1.7, +1.6 | 8.0–3.0 |
| | 0.79 | 0.5–4.3 | 1.02–1.49 | −2.9, +1.7 | 8.4–3.2 |
| Skew (eqn. 5, text) | 0.10 | 0.5–4.3 | 1.09–3.67 | −1.0, +0.6 | 7.3–1.2 |
| | 0.135 | 0.5–4.3 | 1.08–3.42 | −0.7, +1.5 | 7.9–1.3 |
| | 0.25 | 0.5–4.3 | 1.07–2.85 | −1.2, +0.9 | 8.9–1.3 |
| | 0.50 | 0.5–4.3 | 1.04–2.09 | −1.2, +1.3 | 12.7–1.6 |
| | 0.71 | 0.5–4.3 | 1.03–1.64 | −1.0, +1.1 | 17.7–2.7 |
| | 0.73 | 0.5–4.3 | 1.03–1.60 | −1.1, +0.7 | 18.5–2.8 |
| | 0.75 | 0.5–4.3 | 1.03–1.56 | −2.3, +1.8 | 19.8–3.0 |
| | 0.77 | 0.5–4.3 | 1.02–1.52 | −0.4, +2.1 | 21.2–3.1 |
| | 0.79 | 0.5–4.3 | 1.02–1.49 | −0.9, +1.8 | 22.2–3.3 |
| Excess (eqn. 6, text) | 0.10 | 0.5–4.3 | 1.09–3.67 | −1.3, +0.8 | 42.1–2.5 |
| | 0.135 | 0.5–4.3 | 1.08–3.42 | −0.9, +2.0 | 45.4–2.6 |
| | 0.25 | 0.5–4.3 | 1.07–2.85 | −1.6, +1.2 | 51.1–2.7 |
| | 0.50 | 0.5–4.3 | 1.04–2.09 | −1.6, +1.8 | 73.0–3.4 |
| | 0.71 | 0.5–4.3 | 1.03–1.64 | ±1.4 | 102–5.5 |

(*Continued on p. 6*)

TABLE II (*continued*)

| Parameter | Peak height fraction, $r$ | Asymmetry range, $\tau/\sigma$ | Asymmetry range, $(b/a)_r$ | Maximum error (%) | Relative uncertainty (%) |
|---|---|---|---|---|---|
| Excess (eqn. 6, text) | 0.73 | 0.5–4.3 | 1.03–1.60 | −1.4, +0.9 | 106–5.8 |
| | 0.75 | 0.5–4.3 | 1.03–1.56 | −3.0, +2.5 | 105–6.1 |
| | 0.77 | 0.5–4.3 | 1.02–1.52 | −0.6, +2.8 | 122–6.4 |
| | 0.79 | 0.5–4.3 | 1.02–1.49 | −1.2, +2.5 | 128–6.8 |

[a] Refer to Table I for an explanation of terms.

*Derivation of area equations*

Area equations based on width, asymmetry, and peak height measurements at $r = 0.10$, 0.25, 0.50, and 0.75 have been previously reported [5] along with the method of their derivation. Additional area equations at $r = 0.71$, 0.73, 0.77, and 0.79, were derived in this report for purposes of comparison. The area equations for these $r$ values are reported in Table III along with the area equations at $r = 0.10$, 0.25, 0.50, and 0.75 previously reported [5].

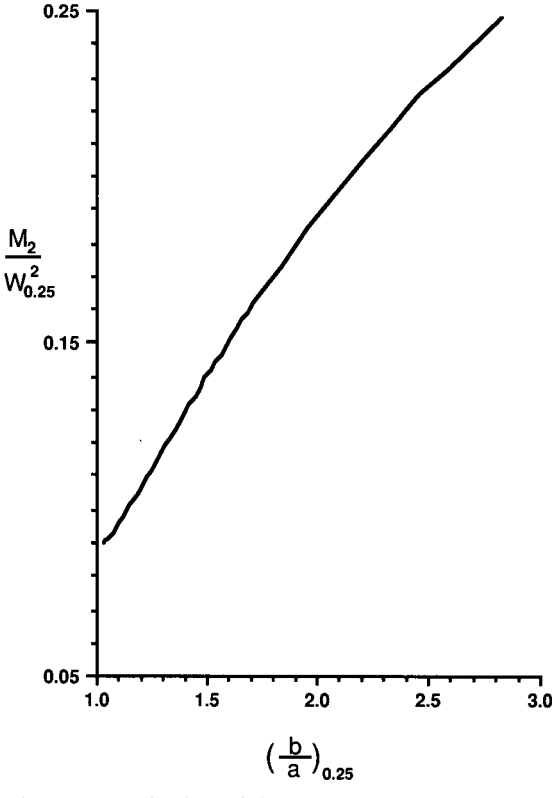


Fig. 3. Determination of f($b/a$) for $M_2$ at $r = 0.25$. Note moderate curvature over entire asymmetry range. First quadratic fit from $(b/a)_{0.25} = 1.02$ to 1.13, second quadratic fit from $(b/a)_{0.25} = 1.13$ to 2.85.

## RESULTS AND DISCUSSION

*Accuracy of CFOM equations*

Tables I and II show the maximum errors over the $\tau/\sigma_G$ range 0.3 to 4.3 for the equations derived for the various CFOMs considered in this study. In general, the equations for $\sigma_G$ are accurate to within 1% while those for $M_2$ are accurate to within 2%. Table IV compares the results of the maximum errors reported for the Foley–Dorsey [11] equations to those reported in Tables I and II. Because Anderson and Walters [13] also derived equations for $M_1$, $M_2$, $\sigma_G$, and $\tau$, the relative errors for their equations are reported in Table IV for purposes of comparison. Only CFOMs at $r = 0.10$ are compared, because the Foley–Dorsey equations at other $r$ values are useful only for peak modeling and should not be used for CFOM calculation. For all CFOMs considered, the accuracy of the present set of equations is better than those derived by the previous methods. Although the Anderson–Walters equations provide a greater valid asymmetry range, most experimental peaks will have asymmetries within the valid range of the present equations. Because our equations give better accuracy than the other methods while providing for the calculation of the higher moments (whereas the Anderson–Walters equations do not), they should be the method of choice in most instances. Also, our equations for higher $r$ (not available previously) allow the calculation of CFOMs when the lower peak height fractions are not accessible due to peak overlap [1,17].

*Precision of CFOM equations*

Also reported in Tables I and II are the relative

TABLE III

PEAK AREA EQUATIONS FOR EMG AND GAUSSIAN PEAKS[a]

| $r$ | Equation | R.E.[b] (%) | R.S.D.[c] (%) |
|---|---|---|---|
| 0.1 | $A = 0.586\, h_p\, W_{0.1}\, (b/a)^{-0.133}$ | ±0.50 | 0.36 |
| 0.135 | $A = 0.631\, h_p\, W_{0135}\, (b/a)^{-0.105}$ | −0.3, +0.6 | 0.36 |
| 0.25 | $A = 0.753\, h_p\, W_{0.25}$ | −1.0, +0.6 | 0.35 |
| 0.50 | $A = 1.07\, h_p\, W_{0.5}\, (b/a)^{+0.235}$ | −1.2, +1.0 | 0.37 |
| 0.71 | $A = 1.514\, h_p\, W_{0.71}\, (b/a)^{+0.591}$ | −1.1, +0.6 | 0.46 |
| 0.73 | $A = 1.58\, h_p\, W_{0.73}\, (b/a)^{+0.651}$ | −0.7, +1.1 | 0.48 |
| 0.75 | $A = 1.64\, h_p\, W_{0.75}\, (b/a)^{+0.717}$ | −1.1, +0.6 | 0.50 |
| 0.77 | $A = 1.73\, h_p\, W_{0.77}\, (b/a)^{+0.763}$ | −0.9, +0.6 | 0.52 |
| 0.79 | $A = 1.82\, h_p\, W_{0.79}\, (b/a)^{+0.835}$ | −1.0, +0.4 | 0.55 |

[a] $A$ = Area of peak, $h_p$ = peak height, $W$ = width of peak at designated peak height fraction, and $b/a$ is the asymmetry factor measured at the same peak height fraction as the width. See Fig. 1.

[b] Largest relative error in area over the interval $0 \leqslant \tau/\sigma \leqslant 4.3$, expressed as a percentage.

[c] Relative uncertainty (percent relative standard deviation) of the area measurement predicted from error propagation, assuming R.S.D. values of 0.25, 0.25 and 0.5% for $h_p$, $W$ and $b/a$. Note that for many data systems the precision of $h_p$, $W$, and $b/a$ can be better than what we have assumed.

uncertainties of the CFOMs based on error propagation, assuming relative standard deviations (R.S.D.) of 0.25 and 0.5% for width ($W$) and asymmetry ($b/a$). Note that the actual precision of the $W$ and $b/a$ measurements are likely to be better with most electronic integration systems, and thus our reported uncertainties are probably overstated. As seen in Table I, the R.S.D. values for $\sigma_G$ and $M_2$ are in general less than than 2%, and less than 1% at some $r$ values. From Table II it is evident that the values of the higher moments, excess, and skew are slightly more imprecise. In instances where a range of uncertainty is reported, the larger number refers to the least asymmetric peak, while the smaller number refers to most asymmetric peak. In general, the uncertainty decreases *exponentially* from the larger to the lower value as the asymmetry increases.

TABLE IV

COMPARISON OF MAXIMUM ERRORS FOR A VARIETY OF CFOM EQUATIONS[a]

| Parameter | This report | | Foley and Dorsey [11] | | Anderson and Walters [13] | |
|---|---|---|---|---|---|---|
| | Valid $b/a$ range | Maximum error | Valid $b/a$ range | Maximum error | Valid $b/a$ range | Maximum error |
| $\sigma_G$ | 1.03–3.67 | −0.2, +0.6 | 1.09–2.76 | −1.0, +0.5 | 1.0–5.21 | −1.3, +1.6 |
| $\tau$ | 1.09–3.67 | −0.4, +0.2 | 1.09–2.76 | −1.0, +3.5 | 1.0–5.21 | −4.0, +0.4 |
| $\tau/\sigma_G$ | 1.09–3.67 | −0.8, +0.3 | 1.09–2.76 | −1.0, +4.5 | [b] | [b] |
| $M_1$ | [b] | [b] | 1.00–2.76 | ±1.0 | 1.0–5.21 | −0.2, +0.1 |
| $M_2$ | 1.03–3.67 | −0.2, +0.6 | 1.00–2.76 | −1.5, +0.5 | 1.0–5.21 | −0.7, +1.0 |
| $M_3$ | 1.09–3.67 | −1.0, +0.5 | 1.09–2.76 | −2.5, +10.5 | [b] | [b] |
| $M_4$ | 1.09–3.67 | −0.6, +0.9 | 1.09–2.76 | −3.0, +1.5 | [b] | [b] |
| Skew | 1.09–3.67 | −1.0, +0.6 | 1.09–2.76 | −1.0, +10 | [b] | [b] |
| Excess | 1.09–3.67 | −1.3, +0.8 | 1.09–2.76 | −1.5, +14 | [b] | [b] |

[a] Equations based on measurement at $r = 0.10$.

[b] Equations not derived for this parameter.

*Accuracy and precision of area equations*

The maximum errors and uncertainties for the area equations derived here, along with those reported previously, are shown in Table III. The errors at all $r$ are well within 1.5%, and are not more than 1.0% in most cases. Assuming a relative uncertainty in $h_p$ of 0.25%, and the same R.S.D. values for $W$ and $b/a$ as before, the resulting uncertainty in area for all of the equations is less than 0.6%.

*Application of equations to fronted and/or overlapped peaks*

We have already demonstrated the advantages of EMG-based equations for both fully resolved [5,11] and overlapping [1,17] *tailed* peaks. However, these equations, including the ones in this report, can also be used with resolved or overlapping *fronted* peaks, provided that: (i) the fronted peak(s) in question resemble(s) the mirror image of an EMG peak; (ii) the definitions of $a$ and $b$ are reversed before using the EMG equations; and (iii) for an overlapped pair of peaks, the equations are applied to the *second* peak instead of the first (as with *tailed* peaks). Note that with regard to (i), the same peak modeling criteria used for tailed peaks [5] can be employed, so long as (ii) is followed. With respect to (iii), the area of the first peak may be obtained by subtracting the calculated area of the second peak (via EMG-based equations) from the total peak area measured electronically.

## CONCLUSIONS

It is hoped that the more accurate equations presented here will facilitate greater use of the EMG peak model within electronic integrators and data systems. Because widths and asymmetries are now commonly measured by many chromatographic data systems, incorporation of these equations into existing software should be easy, thus providing better accuracy for the desired CFOMs. Also, as we demonstrated previously [1], EMG-based equations based on graphical measurements in the upper part of a peak provide for the direct measurement of CFOMs on the less distorted peak in an overlapped pair, even when the valley exceeds 50% of its height.

## ACKNOWLEDGEMENT

The authors gratefully acknowledge the partial support of this work by the Computer-Aided Chemistry Division of the Perkin-Elmer Corporation.

## REFERENCES

1 M. S. Jeansonne and J. P. Foley, *J. Chromatogr.*, 461 (1989) 149–163.
2 E. Grushka, *Anal. Chem.*, 44 (1972) 1733–1738.
3 J. C. Giddings, in J. C. Giddings and R. A. Keller (Editors), *Dynamics of Chromatography*, Vol. 1, Marcel Dekker, New York, 1965, pp. 85–87.
4 J. C. Sternberg, in J. C. Giddings and R. A. Keller (Editors), *Advances in Chromatography*, Vol. 2, Marcel Dekker, New York, 1966, pp. 205–270.
5 J. P. Foley, *Anal. Chem.*, 59 (1987) 1984–1987.
6 P. J. Naish and S. Hartwell, *Chromatographia*, 26 (1988) 285–296.
7 J. P. Foley and J. G. Dorsey, *J. Chromatogr. Sci.*, 22 (1984) 40–46.
8 M. S. Jeansonne and J. P. Foley, *J. Chromatogr. Sci.*, 29 (1991) 258–266.
9 W. W. Yau, *Anal. Chem.*, 49 (1977) 395–398.
10 W. E. Barber and P. W. Carr, *Anal. Chem.*, 53 (1981) 1939–1942.
11 J. P. Foley and J. G. Dorsey, *Anal. Chem.*, 55 (1983) 730–737.
12 K. H. Jung, S. J. Yun and S. H. Kang, *Anal. Chem.*, 56 (1984) 457–462.
13 D. J. Anderson and R. R. Walters, *J. Chromatogr. Sci.*, 22 (1984) 353–359.
14 P. R. Haddad and S. Sekulic, *J. Chromatogr.*, 459 (1988) 79–90.
15 N. S. Wu and M. Hu, *Chromatographia*, 28 (1989) 415–416.
16 N. S. Wu, C. P. Cai and Y. Yang, *Chromatographia*, 30 (1990) 220–222.
17 J. P. Foley, *J. Chromatogr.*, 384 (1987) 301–313.

*Journal of Chromatography*, 594 (1992) 9–22
Elsevier Science Publishers B.V., Amsterdam

CHROM. 23 864

# Modelling of displacement chromatography using non-ideal isotherms

P. K. de Bokx*, P. C. Baarslag and H. P. Urbach

*Philips Research Laboratories, P.O. Box 80 000, 5600 JA Eindhoven (Netherlands)*

(First received July 2nd, 1991; revised manuscript received November 5th, 1991)

ABSTRACT

The chromatographic transport problem in the displacement separation of multi-component mixtures leads to a set of coupled, non-linear partial differential equations. Neglecting axial dispersion, the set of equations can be solved using a transformation of variables ($h$ or $\omega$ transformation) for the case that the multi-component distribution function is considered to be ideal (Langmuirean). If intermolecular interactions (non-idealities) are taken into account in the description of the multi-component distribution equilibrium, such a transformation of variables is no longer possible. The displacement separation of binary mixtures was analysed by applying shock-wave theory to the problem of non-ideal distribution isotherms. A description of the separation as a function of time and distance was obtained (development graph). Experimental results pertaining to the separation of Na–K mixtures using Li as the carrier and Rb as the displacer are presented. Quantitative agreement with predicted development graphs was obtained if non-idealities were taken into account, whereas the use of multi-component Langmuir isotherms yielded agreement with experimental results over only a limited composition range.

## INTRODUCTION

The merits of the displacement mode of chromatography were already recognized by the pioneers of separation science [1,2]. The ability to concentrate sample components in the course of a separation is a particularly important asset of the technique. Owing to both theoretical and technical problems, the advantages of the displacement mode were overshadowed by the success of linear elution chromatography. It was not until the early 1980s that displacement chromatography was revived from its quiescent state, when Horváth and co-workers [3–5] demonstrated that by using modern high-performance liquid chromatographic (HPLC) equipment, the advantages of the displacement mode could be successfully exploited.

In displacement chromatography, the column is first equilibrated with an eluent weaker than any of the feed components (the carrier); the feed mixture is then introduced followed by an eluent stronger than any of the constituents of the feed (the displacer). During the separation, the feed components compete for the sites on the stationary phase; on completion of the separation they are arranged in adjacent pure zones that travel at equal velocities (isotachic state). As the separation is based on mutual interferences among feed components, displacement chromatography is a non-linear technique. This causes the proper selection of the operating parameters required for attaining the isotachic state (*e.g.*, flow-rate, column length, temperature, concentration and nature of carrier and displacer) to be a complex problem.

A large number of different approaches have been proposed to model non-linear separations. Depending on their specific area of interest, different workers have proposed different solutions to the two major problems in non-linear separations: (1) how to incorporate the effect of finite rates (axial dispersion) and (2) how to model the multi-component distribution between stationary and mobile phase.

Early interest in non-linear chromatography de-

0021-9673/92/$05.00 

rived from regenerative operations in fixed beds. Here, mainly the first problem is tackled. Thomas [6] introduced a lumped rate constant to account for slow kinetics. An important extension to the original Thomas approach allowing for other rate-controlling steps (*e.g.*, intra- and extra-particle diffusion) was published by Hiester and Vermeulen [7]. Also, workers studying overloaded elution chromatography used mass-balance equations containing dispersion terms to predict elution profiles. Haarhof and Van de Linde [8] treated non-linearity as a perturbation to the linear solution. Guiochon and co-workers [9,10] used the numerical error introduced by their finite difference scheme to estimate axial dispersion. An exact solution has been derived for a single component following Langmuir-type kinetics, assuming that axial diffusion can be neglected [11]. Owing to the mathematical complexity, the above methods are in many instances limited to a single solute. Thus, multi-component effects, important for practical cases, are not treated by these methods. An interesting exception is the work of Phillips *et al.* [12]. Here, the displacement separation of multi-component mixtures was calculated using a model that incorporates finite mass transfer rates as well as axial diffusion. A numerical technique was employed to approximate the resulting system of coupled non-linear differential equations.

Alternatively, one can assume the column efficiency to be infinite. Hence, equilibrium is assumed and all axial dispersion is neglected. This approximation is generally called ideal chromatography. Although not infinite, the efficiency of present-day HPLC columns is high enough to allow a good comparison between predicted and experimental results [13,14]. Analytical solutions to the multi-component ideal case were obtained by Helfferich and Klein [15] and Rhee and co-workers [16,17] using a very elegant transformation of variables: *h*- [15] or $\omega$-transformation [16]. Golshan-Shirazi and Guiochon [18] presented a solution to the separation of binary mixtures in the overloaded elution mode using shock theory.

The use of the ideal chromatography assumption greatly facilitates the study of non-linear multi-component problems. It is sufficiently accurate to concentrate on the second major problem: how to model the multi-component distribution between mobile and stationary phases. In the literature, the multi-component Langmuir isotherm is used almost exclusively to describe this distribution. The great preference for this particular isotherm can be easily traced to its simple functional form (constant separation factors) and to the fact that solutions for non-linear separations of *N*-component mixtures can be obtained in the Langmuir case by the *h*- or $\omega$-transformation. If separation factors are a function of composition, this is in general not possible. The physical basis for the use of the Langmuir isotherm, however, is weak. The different saturation coverages used for different components have been shown to be inconsistent with basic thermodynamics [19] and the assumed ideality (neglect of interparticle interactions) deserves further investigation. In a number of instances, discrepancies between experimental and predicted results in the modelling of non-linear separations have been attributed to the shortcomings of the Langmuir equation [13,20].

The aim of this work was to compare two models that describe the distribution equilibrium between stationary and mobile phases: the multi-component Langmuir isotherm on the one hand and a multi-component isotherm that accounts for two-body interactions in the stationary phase on the other. As we have recently shown, an isotherm that accounts for two-body interactions in the stationary phase can be derived from first principles for systems that belong to the same compensation class [21–23], a compensation class being defined as a group of similar compounds characterized by a common compensation temperature ($T_c = \Delta H/\Delta S$, where the enthalpy and entropy changes refer to a phase equilibrium). The non-linear system we consider is the displacement separation of binary mixtures. The modelling consists of solving the hyperbolic system of conservation laws of the ideal chromatographic approximation using shock theory. The solutions are presented in the form of development graphs, *i.e.*, plots of time *vs.* distance showing the history of the separation.

More specifically, the system we use to compare the different multi-component isotherms is the displacement separation of K–Na mixtures on an ion-exchange column, using Li as the carrier and Rb as the displacer. We shall show that by using a multi-component isotherm that incorporates non-idealities, a good prediction of the displacement separation is obtained for all compositions of the

K–Na feed. The use of ideal (Langmuir) isotherms in the modelling is shown to yield an adequate description of the separation over only a limited range of composition of the binary feed.

## THEORY

### *General description of the problem for non-ideal isotherms*

Let us consider a system consisting of $m$ components. The molar concentrations of the $i$th component in the mobile and stationary phase are denoted by $c_i$ and $n_i$, respectively. Let $z$ be the distance along the column measured from the inlet and let $t$ denote time with $t = 0$ corresponding to the entry of the sample into the column. The variables $z$ and $t$ are made dimensionless by the length $L$ of the column and by $L/U$, where $U$ is the constant interstitial velocity of the eluent. Neglecting axial dispersion, the conservation law for the $i$th compone nt is

$$\frac{\partial c_i}{\partial z} + \frac{\partial c_i}{\partial t} + \nu \cdot \frac{\partial n_i}{\partial t} = 0 \tag{1}$$

where

$$\nu = (1 - \varepsilon)/\varepsilon \tag{2}$$

$\varepsilon$ being the void fraction. To relate stationary phase concentrations to mobile phase concentrations, we introduce the separation factors $\alpha_{ij}$. To allow for intermolecular interactions in the stationary phase, these separation factors are no longer considered to be constants (the usual assumption), but are a function of all the stationary phase concentrations $n_1, n_2, \ldots, n_m$. It is, of course, here that non-ideality enters into the problem. The separation factors are thus defined by

$$\frac{n_i}{c_i} = \alpha_{ij}(n_1, \ldots, n_m)\frac{n_j}{c_j} \qquad i, j = 1, \ldots, m \tag{3}$$

Consistency demands that

$$\alpha_{ij} = 1/\alpha_{ji} \qquad \text{for all } i, j \tag{4}$$

and

$$\alpha_{ij}\alpha_{jl} = \alpha_{il} \qquad \text{for all } i, j, l \tag{5}$$

We have a total of $m$ conservation laws (1) relating the $2m$ concentrations in the stationary and mobile phases: $c_i$ and $n_i$. One would like to eliminate $m$ of the unknowns by using eqns. 3, 4 and 5, and in view of the general dependence of $\alpha_{ij}$ on the $n_j$, it is natural to try to express the $c_i$ in terms of the $n_j$. However, as we choose to describe the distribution equilibrium using the separation factors that are ratios, there are not enough independent eqns. 3, 4 and 5 to do so. This implies that the set of eqns. 1–5 by itself is not sufficient to determine the development of a separation from its initial conditions. Additional knowledge of the distribution equilibrium needs to be specified for a deterministic description.

To clarify this point, let $\mathbf{C}(z, t) \equiv \sum_{i=1}^{m} c_i(z, t)$ and $\mathbf{N}(z, t) \equiv \sum_{i=1}^{m} n_i(z, t)$ be the total concentrations in the mobile and stationary phases, respectively. From eqn. 3, one obtains

$$\mathbf{C} = \sum_{j=1}^{m} c_j = \sum_{j=1}^{m} \alpha_{ij}(n_1, \ldots, n_m)\frac{n_j}{n_i} \cdot c_i \tag{6}$$

and hence

$$c_i = \mathbf{C} \cdot \frac{n_i}{\sum_{j=1}^{m} \alpha_{ij}(n_1, \ldots, n_m)n_j} \qquad i = 1, \ldots, m \tag{7}$$

Thus, a knowledge of the total mobile phase concentration is required in order to express the $c_i$ in the $n_j$. By adding eqns. 1, it follows that $\mathbf{C}$ satisfies

$$\left(\frac{\partial}{\partial z} + \frac{\partial}{\partial t}\right)\mathbf{C} + \nu \cdot \frac{\partial \mathbf{N}}{\partial t} = 0 \tag{8}$$

By substituting eqn. 7 in eqn. 1, we obtain

$$\left(\frac{\partial}{\partial z} + \frac{\partial}{\partial t}\right)\left\{\mathbf{C} \cdot \frac{n_i}{\sum_{j=1}^{m} \alpha_{ij}(n_1, \ldots, n_m)n_j}\right\} + \nu \cdot \frac{\partial n_i}{\partial t} = 0 \qquad i = 1, \ldots, m \tag{9}$$

Thus, the system of eqns. 8 and 9 can be solved if the total concentration in the stationary phase $\mathbf{N}$ is known as a function of $(z, t)$ or, more generally, if $\mathbf{N}$ is given in terms of all the stationary phase concentrations $\mathbf{N}(n_1, \ldots, n_m)$, because the system of equations then consists of $m + 1$ equations for the $m + 1$ unknowns: $n_1, \ldots, n_m$ and $\mathbf{C}$.

*Non-ideal distribution isotherms with constant total stationary phase concentrations*

In this section we derive a specialized form of eqn. 8 for the case that $\mathbf{N}(z, t)$ is constant. This situation applies to our experimental system: the ion-exchange separation of homovalent ions. Here, electroneutrality requires that the exchanger is always occupied by the same number of ions. Substituting $\mathbf{N}(z, t) \equiv \mathbf{N}$ constant into eqn. 8 shows that $\mathbf{C}$ is constant along curves: $t - z =$ constant. Hence:

$$\mathbf{C}(t, z) = \tilde{\mathbf{C}}(\tau), \qquad \tau = t - z \tag{10}$$

for some function $\tilde{\mathbf{C}}$. Since the linear velocity is unity with respect to the frame $(z, t)$, eqn. 10 implies that a sudden change in the total mobile phase concentration moves with the linear velocity of the eluent. Hence, the total mobile-phase concentration can be determined from the conditions at the inlet $z = 0$. By substitution of this function in eqn. 9, a coupled non-linear system of $m$ equations for the $m$ stationary phase concentrations $n_i$ results.

It will be advantageous to use dimensionless concentrations $x_i$, $y_i$ defined by

$$x_i \equiv c_i/\mathbf{C}, \qquad y_i \equiv n_i/\mathbf{N} \tag{11}$$

Further, it will be helpful to use the independent variables $(\tau, \zeta)$ that are related to $(t, z)$ by

$$\begin{aligned} \tau &= t - z \\ \zeta &= z \end{aligned} \tag{12}$$

Then, for fixed $\zeta$, $\partial/\partial\tau = \partial/\partial t$ and for fixed $\tau$, $\partial/\partial\zeta = \partial/\partial t + \partial/\partial z$. Hence, we obtain from eqn. 9

$$\frac{\partial}{\partial\tau} \cdot y_i + \frac{\tilde{\mathbf{C}}(\tau)}{\nu\mathbf{N}} \cdot \frac{\partial}{\partial\zeta}\left\{\frac{y_i}{\sum_{j=1}^{m} \alpha_{ij}(y_1, \ldots, y_m) y_j}\right\} = 0 \qquad i = 1, \ldots, m \tag{13}$$

where we used the identity

$$\frac{\partial}{\partial\zeta}\tilde{\mathbf{C}}(\tau) = \left(\frac{\partial}{\partial t} + \frac{\partial}{\partial z}\right)\tilde{\mathbf{C}} = 0$$

which follows from eqn. 8 if $\mathbf{N}$ is constant. Also, the separation factors are now considered as functions of the dimensionless stationary phase concentrations $y_i$. By the definition of the $y_i$, we have

$$\sum_{i=1}^{m} y_i = 1 \tag{14}$$

and hence one of the $y_i$ can be eliminated immediately. We shall eliminate $y_m$. Using eqns. 4 and 5, we find for every $i = 1, \ldots, m - 1$

$$\frac{y_i}{\sum_{j=1}^{m} \alpha_{ij} y_j} = \frac{y_i}{\alpha_{im} + \sum_{j=1}^{m-1} (\alpha_{ij} - \alpha_{im}) y_j} = \frac{\alpha_{mi} y_i}{1 + \sum_{j=1}^{m-1} (\alpha_{mj} - 1) y_j} \tag{15}$$

The $\alpha_{mj}$ are now considered as a function of $\vec{y}$, where $\vec{y}$ is the column vector of all independent stationary phase concentrations in the system. Substituting eqn. 15 into eqn. 13, we finally obtain the following coupled system of $m - 1$ non-linear partial differential equations for the $m - 1$ unknowns $y_1, \ldots, y_{m-1}$

$$\frac{\partial}{\partial\tau} \cdot y_i + \frac{\tilde{\mathbf{C}}(\tau)}{\nu\mathbf{N}} \cdot \frac{\partial}{\partial\zeta}\left\{\frac{\alpha_{mi}(\vec{y}) y_i}{1 + \sum_{j=1}^{m-1} [\alpha_{mj}(\vec{y}) - 1] y_j}\right\} = 0 \qquad i = 1, \ldots, m - 1 \tag{16}$$

The concentrations at the inlet of the column $\zeta = 0$ are known at every time $t$. Hence

$$\vec{y}(\tau, \zeta = 0) \tag{17}$$

is given.

Some remarks seem appropriate. First, one can, in principle, derive a system of coupled non-linear partial differential equations which is completely analogous to eqn. 16, but which instead of $y_i$ and $\alpha_{ij}$ involves $x_i$ and $\alpha_{ij}$. However, if the separation factors are not constants, they will in general be specified as functions of the stationary-phase concentrations $y_i$, rather than in terms of the mobile phase concentrations $x_i$. Therefore, the system of eqns. 16 for $y_i$ and $\alpha_{ij}$ is in general more useful than the analogous system for $x_i$ and $\alpha_{ij}$. In the case of Langmuir isotherms, the separation factors are constants and both systems are equally useful, although most workers use the system involving the mobile phase concentrations.

Second, we note that if $\tilde{\mathbf{C}}(\tau)$ is constant, *i.e.*, if the total mobile phase concentration at the inlet is constant, the system has the form

$$\frac{\partial y_i}{\partial\tau} + \frac{\partial}{\partial\zeta} F_i(\vec{y}) = 0 \qquad i = 1, \ldots, m - 1 \tag{18}$$

where the $F_i$ are given by

$$F_i(\vec{y}) = \frac{\bar{\mathbf{C}}}{\nu \mathbf{N}} \frac{\alpha_{mi}(\vec{y}) y_i}{1 + \sum_{j=1}^{m-1} [\alpha_{mj}(\vec{y}) - 1] y_j} \tag{19}$$

Eqn. 18 is called a hyperbolic system if the $(m-1) \times (m-1)$ matrix $\mathbf{A}(y) = (\mathbf{A}_{ij}(\vec{y}))$ given by $\mathbf{A}_{ij}(\vec{y}) = \partial F_i / \partial y_j(\vec{y})$, has $m-1$ real eigenvalues $\lambda_1(\vec{y}), \ldots, \lambda_{m-1}(\vec{y})$ for every state $\vec{y}$. Whether eqn. 18 actually is a hyperbolic system depends on the separation factors $\alpha_{ij}(\vec{y})$, but in the case of constant separation factors (Langmuir) and for the non-ideal distribution isotherm studied in this paper, this is generally so. If the total mobile phase concentration at the inlet is a function of time, the functions $F_i$ depend explicitly on $\tau$ through the factor $\mathbf{C}(\tau)$. Then, the system of eqns. 18 is not hyperbolic. In the experiments considered in this paper the total concentration $\mathbf{C}(\tau)$ is, although not constant, piecewise constant, and the theory of hyperbolic systems can still be used.

*Solution method for binary mixtures*

We consider a binary mixture of K and Na with Li as the carrier and Rb as the displacer. The total stationary phase concentration is constant and the number of components is $m = 4$. The numbering of the components will be in sequence of decreasing affinity for the stationary phase. Thus, $y_1, y_2, y_3, y_4$ correspond to Rb, K, Na and Li, respectively. The numbering convention implies that

$$\alpha_{ij} < 1 \text{ for } i > j \tag{20}$$

We consider the conservation laws 13 for two different isotherms, namely the ideal Langmuir isotherms for which the $\alpha_{ij}$ are independent of the concentrations and the non-ideal isotherms derived in refs. 21–23 that depend on all $y_i$ according to

$$\alpha_{ij}(y_1, y_2, y_3, y_4) = \exp\left[\frac{-(1 - T/T_c)}{RT} \sum_{k=1}^{4} (f_{ik} - f_{jk}) y_k\right] \tag{21}$$

In eqn. 21, $T$ is the absolute temperature and $R$ is the gas constant. $T_c$ is the so-called compensation temperature of the class of compounds under consideration and the $f_{ij}$ are dimensionless parameters describing the two-body interaction between components $i$ and $j$ in the stationary phase. It is important to note that the $f_{ij}$ are structural parameters and do not depend on the composition of the mixture or on the temperature. This is in contrast to the Langmuir case, where it is assumed that multi-component isotherms can be constructed using data obtained from measurements of single-component isotherms; an assumption that has been shown to be untenable [19,24]. It is shown in the cited references that the above distribution isotherm resembles the Fowler–Guggenheim approach [25] to multi-component adsorption, except that in our case the interaction energies are temperature dependent.

For $t < 0$ the column contains only the carrier ($y_4 = 1$). Then, for $0 < t < t_e$, the mixture enters the column and for $t > t_e$ there is only the displacer ($y_1 = 1$). Hence, we have the following boundary condition at the inlet, $x = \zeta = 0$, for the state vector $\vec{y} = (y_1, y_2, y_3, y_4)^T$:

$$\begin{aligned} &\vec{y}(\tau, 0) = (0, 0, 0, 1)^T \equiv \vec{y}^I \text{ (initial state)} \\ &\vec{y}(\tau, 0) = (0, y_2^F, y_3^F, 0)^T \equiv \vec{y}^F \text{ (feed state)} \\ &\vec{y}(\tau, 0) = (1, 0, 0, 0)^T \equiv \vec{y}^E \text{ (end state)} \end{aligned} \tag{22}$$

where the superscript $T$ (transpose) is used to indicate that column vectors are implied.

Let the total mobile phase concentration corresponding to the initial, feed and end state be given by $\mathbf{C}^I$,$\mathbf{C}^F$ and $\mathbf{C}^E$, respectively. It follows from eqn. 10 that there are three regions in the $(z, t)$ plane in which the total mobile-phase concentration is equal to one of these values (see Fig. 1):

$$\begin{aligned} &\mathbf{C}(t, z) = \mathbf{C}^I \text{ for } t < z \\ &\mathbf{C}(t, z) = \mathbf{C}^F \text{ for } z < t < z + t_e \\ &\mathbf{C}(t, z) = \mathbf{C}^E \text{ for } t > z + t_e \end{aligned} \tag{23}$$

The conservation laws 13 thus differ in these three regions of the $(z, t)$ plane. We note that although the governing eqn. 13 has $\tau$ as an independent variable, we shall use time $t$ in the final results and in the plot by using the transformation of eqn. 12.

It is physically obvious, and it can also be verified explicitly, that concentration velocities are smaller than the linear velocity of the eluent, which is equal to 1 with respect to the dimensionless $z$ and $t$ that we use. Hence, below the line $t = z$ only the carrier is present.

The boundary condition 22 consists of three

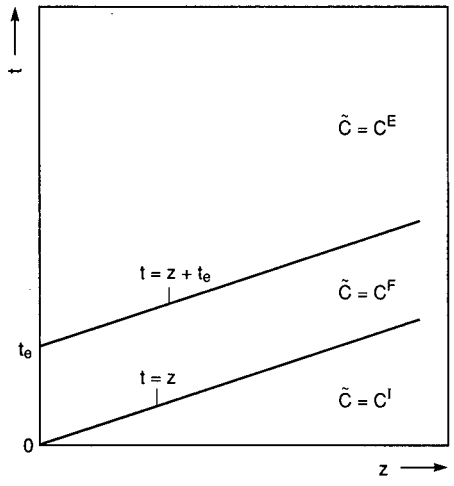


Fig. 1. Schematic diagram of the solution of eqn. 8 in the $(t, z)$ plane showing zones of different total concentration.

constant states separated by discontinuities at $t = 0$ and $t = t_e$. A system of conservation laws with as boundary (or initial) condition two constant states separated by a discontinuity is known as a Riemann problem. Hence, for not too large values of $z$, the solution of our problem can be obtained by separately solving two Riemann problems corresponding to the aforementioned discontinuities. For larger values of $z$ the solutions of the two Riemann problems will, of course, interact.

Let us first consider the Riemann problem corresponding to the discontinuity at $t = 0$ (it might be helpful to refer to Fig. 2 at this point). Since for $t < z$ the state is known to consist of pure Li, only the region $z < t < z + t_e$ is of interest. Hence, we take $\mathbf{C} = \mathbf{C}^F$ in eqn. 13. The displacer obviously plays no role in the distribution process at $\tau = 0$, so that we may put $y_1 \equiv 0$ eqn. 13. Further, using eqn. 14, one of the remaining components, for which we choose $y_4$, can be eliminated. Using eqn. 16, the following set of two conservation laws, involving only $y_2$ and $y_3$, remains:

$$\frac{\partial y_i}{\partial \tau} + \frac{\partial}{\partial \zeta} F_i(\vec{y}) = 0 \qquad i = 2, 3 \tag{24}$$

where $\vec{y} = (y_2, y_3)^T$ and

$$F_i(\vec{y}) = \frac{\mathbf{C}^F}{\nu \mathbf{N}} \cdot \frac{\alpha_{4i}(\vec{y}) y_i}{1 + [\alpha_{42}(\vec{y}) - 1]y_2 + [\alpha_{43}(\vec{y}) - 1]y_3} \qquad i = 2, 3 \tag{25}$$

From the general mathematical theory of hyperbolic systems [26–28], it is known that the solution of a Riemann problem for a system of two components consists of three constant states, $\vec{y}^{\nu}$, $\nu = 1, 2, 3$, with $\vec{y}^1$ the left, $\vec{y}^2$ the intermediate and $\vec{y}^3$ the right state, separated by two shocks and/or simple waves. For the Riemann problem at $\tau = 0$, we have $\vec{y}^1 = (y_2^F, y_3^F)$. Simple waves are continuous transitions which depend on $(\tau, \zeta)$ only through the ratio $\tau/\zeta$. It turns out that for both the ideal Langmuir isotherm and the non-ideal isotherm, all transitions between constant states are shocks. If $s^1 < s^2$ denote the shock speeds, then mass conservation leads to the following jump relationships across the shocks:

$$s^{\nu}(y_i^{\nu} - y_i^{\nu+1}) = F_i(\vec{y}^{\nu}) - F_i(\vec{y}^{\nu+1}) \qquad i = 2, 3 \tag{26}$$

These are four equations for the four unknowns $s^1$, $s^2$, $y_2^2$ and $y_3^2$. Numbers in superscripts are again used to indicate states. Thus, $s^1$ refers to the shock between left and intermediate states, $y_3^2$ is the stationary phase concentration of the third component in the intermediate state, etc. For $\nu = 2$, we add eqns. 26 for $i = 2, 3$. After substitution of eqn. 25 and of $\vec{y}^3 = (0, 0)$ and by using $y_2^F + y_3^F = 1$, one deduces that

$$s^2 = \mathbf{C}^F / \nu \mathbf{N} \tag{27}$$

This value of the speed of the fastest shock is thus independent of the isotherm used. By substituting eqn. 27 into eqn. 26, $s^1$ and $y_2^2$, $y_3^2$ can be calculated. As can be expected, the intermediate state always consists of pure Na, so that $\vec{y}^2 = (0, 1)$. The speed $s^1$ depends on the functional dependence of the $\alpha_{ij}$ on the concentrations $\vec{y}$ and hence is different for different isotherms.

Fig. 2 shows a schematic development graph in the $(z, t)$ plane. The shocks $t = z$ and $t = z + t_e$ between regions of different total mobile phase concentration move at the velocity of the mobile phase (= 1 in our coordinates) and are seen to overtake the shocks with speed $s^1$ [at point $Q = (z_Q, t_Q)$] and with speed $s^2$ [at point $R = (z_R, t_R)$]. As a result, the shock speeds change suddenly to values $\tilde{s}^1$ and $\tilde{s}^2$ which follow from the jump relations 26, but now with $C^F$ replaced by $C^E$. In particular the fastest shock now has speed

$$\tilde{s}^2 = \mathbf{C}^E / \nu \mathbf{N} \tag{28}$$

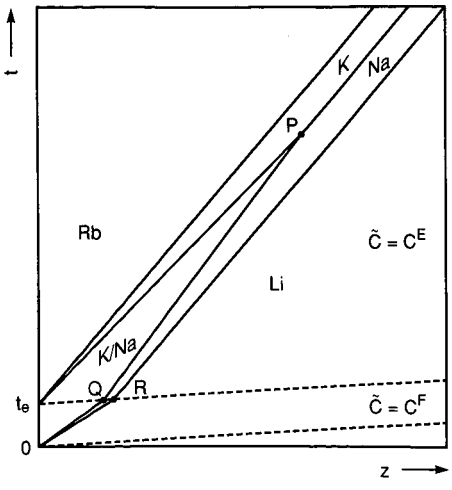


Fig. 2. Development graph of the ion-exchange separation of a binary mixture showing the three characteristic points P, Q and R.

Next consider the Riemann problem at $\tau = t_e$. There, Li is absent so that $y_4 \equiv 0$. By eliminating $y_3$ using $y_3 = 1 - y_1 - y_2$, one obtains a coupled system of two conservation laws involving only $y_1$ and $y_2$. Again, it can be shown that only shocks occur at the transitions between the constant states $\vec{y}^{\nu}$, $\nu = 1, 2, 3$. One now has $\vec{y}^{1} = (1, 0)^T$ and $\vec{y}^{3} = (0, y_2^F)^T$ while the intermediate state $\vec{y}^{2}$ and the shock speeds $s^1$ and $s^2$ follow from the jump equations

$$s^{\nu}(\vec{y}^{\nu} - \vec{y}^{\nu+1}) = F_i(\vec{y}^{\nu}) - F_i(\vec{y}^{\nu+1}) \qquad i = 1,2, \quad \nu = 1,2 \qquad (29)$$

with

$$F_i(\vec{y}) = \frac{\mathbf{C}^E}{\nu\mathbf{N}} \cdot \frac{\alpha_{3i}(\vec{y})y_i}{1 + [\alpha_{31}(\vec{y}) - 1]y_1 + [\alpha_{32}(\vec{y}) - 1]y_2} \qquad i = 1,2 \qquad (30)$$

In particular, if $y_1^2 + y_2^2 = 1$, then eqn. 29 with $\nu = 1$ implies that

$$s^1 = \mathbf{C}^E/\nu\mathbf{N} \qquad (31)$$

If $y_1^2 + y_2^2 < 1$, then by choosing $\nu = 1$ and adding over $i = 1, 2$ the same result is obtained. Further, it is easy to verify that the intermediate state always consists of pure K so that $\vec{y}^{2} = (0, 1)$. Contrary to $s^1$, the speed $s^2$ of the fastest shock depends on the isotherm used.

As can be seen from Fig. 2, the fastest shock corresponding to the Riemann problem at $\tau = t_e$ moves faster than the slowest shock emanating from $\tau = 0$. Hence, the latter is overtaken by the former. At the point of intersection [point P $= (z_P, t_P)$ in Fig. 2], we have yet another Riemann problem. In this problem the left state consists of pure K, whereas the right state consists of pure Na. Hence, only $y_2$ and $y_3$ are relevant. After eliminating $y_3$ using $y_2 + y_3 = 1$, we obtain a single conservation law involving only $y_2$. Hence, there is only one shock emanating from point P, separating the pure K and Na states. The shock speed, $s^1$, follows from

$$s^1(y_2^1 - y_2^2) = F_2(\vec{y}^{1}) - F_2(\vec{y}^{2}) \qquad (32)$$

where

$$F_2(\vec{y}) = \frac{\mathbf{C}^E}{\nu\mathbf{N}} \cdot \frac{\alpha_{32}(\vec{y})y_2}{1 + [\alpha_{32}(\vec{y}) - 1]y_2} \qquad (33)$$

By substituting $y_2^1 = 1$, $y_2^2 = 0$, one finds that

$$s^1 = \mathbf{C}^E/\nu\mathbf{N} \qquad (34)$$

Hence, we conclude (*cf.*, Fig. 2) that for $z > z_P$ four pure states are found that are separated by shocks with equal speeds given by eqn. 34 and independent of the isotherms. Point P is thus the point of complete separation and for $z > z_P$ the isotachic state is attained. Although the isotachic state and the speeds of the shocks separating the pure states for $z > z_P$ are independent of the isotherm used, the position of point P does depend on the isotherms since P is the intersection of the fastest shock emanating from $\tau = t_e$ and the slowest shock emanating from $\tau = 0$. These shocks have speeds that do depend on the isotherm.

Some remarks concerning the computation method outlined above seem appropriate. In general, one does not know beforehand whether a transition between two constant states is a shock or a simple wave. Physically, that is determined by the different magnitudes of the stationary phase concentrations as fixed by the multi-component isotherm. Mathematically, the relative magnitudes of the eigenvalues of the Jacobian matrices $\mathbf{A}(\vec{y}^{\nu})$ and $\mathbf{A}(\vec{y}^{\nu+1})$ determine whether a given transition is a shock or a simple wave. As remarked above, all transitions for both the ideal and the non-ideal isotherms were found to be shocks.

It is well known that in the Langmuir case, *i.e.*, the case that separation factors are constant, computations are facilitated by using the so-called $h$- or $\omega$-transformation [15, 16]. The new dependent variables, $\omega_i$, have the useful property that for a given Riemann problem involving an arbitrary number of components each of them changes across only one of the shocks or simple waves. Dependent variables with this property always exist for a Riemann problem involving only two dependent variables, and therefore we could have made use of them. However, for such small systems the jump relations 26 are just as simple. But for Riemann problems involving more than two dependent variables, the existence of the $\omega_i$s is very special and in fact one can show that for the non-ideal isotherms given by eqn. 21 they do not exist [29].

## EXPERIMENTAL

### *Materials*

All alkali metal salts used were nitrates of Suprapur or comparable quality (Merck, Darmstadt, Germany). The salts were dried overnight at 80°C and cooled to ambient temperature in a desiccator before weighing. High-purity deionized water (> 18 MΩ) was used to make up the solutions. Quartz glassware was used throughout.

All experiments were performed using a polystyrene–divinylbenzene-based strong cation exchanger (IC PAK C, Millipore–Waters, Milford, MA, USA), which was purchased prepacked in a 50 mm × 4.6 mm I.D. column. The total ion-exchange capacity of the column and the column void fraction were determined to be 7.22 μequiv. and 0.42, respectively, using techniques described previously [22].

### *Apparatus*

A modified PU4100 liquid chromatograph (Philips Analytical Chromatography, Cambridge, UK) was used for separations by displacement chromatography. A schematic diagram of the displacement system is shown in Fig. 3. The valves indicated represent a Model 5011P solvent selection switch (A), two Model 7030 three-port valves (B and C) and a Model 7125 six-port injection valve (D), all obtained from Rheodyne (Cotati, CA, USA). A needle valve (E) from Scientific Systems (State College, PA, USA) was installed in the waste line. The pressure differential across the needle valve was adjusted to match the prevailing column pressure drop to allow for switching without influencing the flow-rate delivered by the pump. All tubing used was Tefzel (Omnifit, Cambridge, UK). A feed loop of 2.58 ml was installed within the thermostated compartment of the PU4100 column oven accessory. The column effluent was led to an LDC Conductomonitor Mark III (LDC/Milton Roy, Riviera Beach, FL, USA). The conductivity signal was differentiated with respect to time using a differentiator built in-house and fed to a Philips PU6030 data capture unit. A Philips PU6000 integration system together with a P3202 computer were used for data processing.

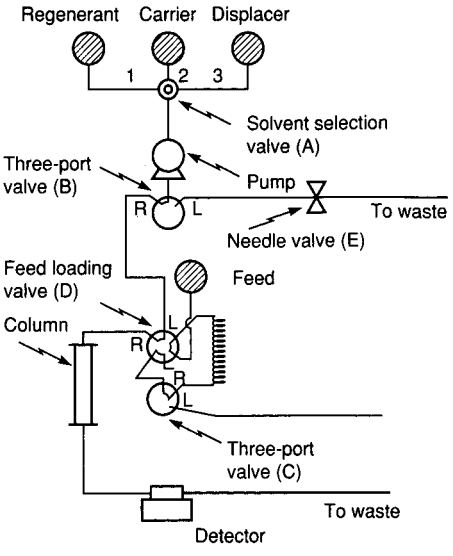


Fig. 3. Diagram of the experimental set-up used for displacement separations. Operational procedures are described in the text.

Optionally, fractions could be collected using a Model 201 fraction collector (Gilson, Villiers le Bel, France). Collected fractions were analysed using a PU4100 chromatograph equipped with a PU4700 autoinjector.

### *Procedure*

The set-up described in the previous section allows a five-position cyclic operation of the displacement system. In the following, the respective positions of the valves A, B, C and D are indicated in

parentheses (refer to Fig. 3). In the load position (2, R, R, R) the carrier solution is loaded on to the column. In the flush position (3, R, L, L) the carrier is flushed from the system and replaced by the displacer up to valve C. The total concentrations of carrier, feed and displacer typically range from 0.5 to 2.5 m$M$. In the feed position (3, L, R, R) the feed loop is filled using a large syringe with the feed solution by flushing with at least five feed-loop volumes. It should be noted that displacer solution is led to waste via the needle valve in the feed position. The run position (3, R, R, L) refers to the actual displacement separation. Flow-rates between 0.5 and 1.5 ml/min were used. After each displacement run, the column was regenerated (1, R, R, R) by flushing with a 0.1 $M$ $LiNO_3$ solution for at least 30 min. The dead volume in the tubing was determined by replacing the column with a zero-dead-volume coupling.

*Numerical calculations*

A computer program was written to compute development graphs. The program decides whether a boundary is diffuse or self-sharpening. If only shocks are encountered, as in this study, all boundary trajectories can be calculated from jump relationships such as eqn. 26. Development graphs are then constructed for a number of preselected concentration ratios of the binary feed. The lengths of pure and mixed zones at the column exit are produced in a dimensional format to facilitate comparison with experimental results.

The input required by the program consists of operating parameters (column void fraction, column capacity, flow-rate, feed-loop volume, total concentrations in carrier, feed and displacer) and isotherm information. The multi-component isotherm used in this paper (eqn. 21) requires the specification of structural parameters, the compensation temperature of the class and the experimental temperature. The experimental temperature was specified as appropriate. The structural parameters for the class of alkali metal ions and the pertinent compensation temperature are listed in Table I.

TABLE I

VALUES FOR THE STRUCTURAL PARAMETERS $f_{ij}$ OF THE COMPENSATION CLASS OF THE ALKALI METAL IONS ($T_c$ = 480 K)

| | Rb | K | Na | Li |
|---|---|---|---|---|
| Rb | 0.0 | | | |
| K | 1.18 | 1.70 | | |
| Na | 2.75 | 3.49 | 6.33 | |
| Li | 3.36 | 4.91 | 9.95 | 12.11 |

## RESULTS AND DISCUSSION

In this section we compare experimental results with those computed using the techniques outlined in the Theory section. As these techniques are general and not restricted to ideal (Langmuir) isotherms, it is our aim to examine critically predictions obtained using different descriptions of the multi-component distribution equilibrium. In the experiments we confine ourselves to the displacement separation of binary mixtures of sodium and potassium. In all experiments Li was used as the carrier and Rb as the displacer.

The results of calculations are presented in the form of development graphs (see Fig. 4), *i.e.*, plots of dimensionless time ($Ut/Z$) *vs.* dimensionless position ($z/Z$). All the information required to compute a chromatogram at any time or place is contained in such a graph. Different characteristic points [*e.g.*, the point of complete separation (P)] can be read directly from the graph. Compositions pertaining to different positions in the graph can be calculated from the known location of shocks and simple waves. As can be seen from Fig. 4, and already noted in the Theory section, only shocks occur in our examples. All displacer concentrations will lead to the desired result of an isotachic train, so that separation always takes place. The displacer concentration can be used as the instrument to control the concentrations at which the pure feed components are eluted. In Fig. 4a, the concentration of the displacer is lower than that of the feed, in Fig. 4b the concentration of the displacer is equal to and in Fig. 4c higher than that of the feed. According to eqn. 23, three regions of different total concentration can be

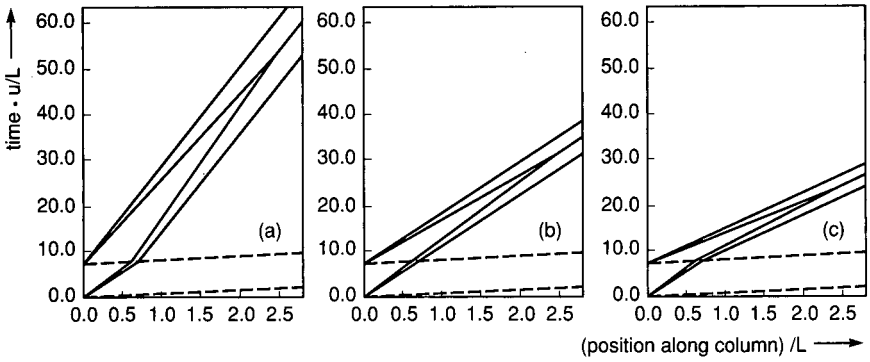


Fig. 4. Development graphs of the displacement separation of a binary mixture consisting of 1.0 m$M$ $KNO_3$ and 1.0 m$M$ $NaNO_3$. The carrier is $LiNO_3$ (2.0 m$M$) and the displacer is $RbNO_3$ at concentrations of (a) 1.0, (b) 2.0 and (c) 3.0 m$M$. The column has a void volume of 0.349 ml and an ion-exchange capacity of 7.22 $\mu$equiv. The feed volume is 2.58 ml and the temperature 295 K. $L$ is the column length and $u$ is the linear velocity of the eluent.

distinguished. As all chromatographic velocities are smaller than $U$, the concentration of the displacer determines the concentrations in the separated zones. Pure zones become narrower and hence more concentrated at higher displacer concentrations, showing the capability of displacement chromatography to enrich sample components during separation.

In Fig. 5 the experimental results are illustrated, the first derivative of the conductivity signal being plotted against time. Compared with Fig. 4, displacement chromatograms refer to a position corresponding to the column outlet ($z = 1$). Our data correspond to the situation of incomplete separation, that is, the feed loaded is so large that the column length is insufficient for the attainment of

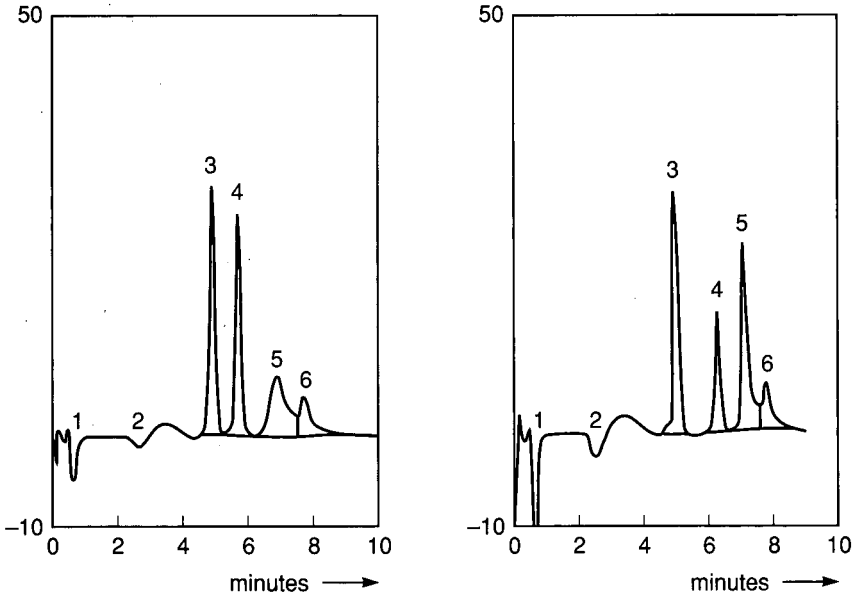


Fig. 5. Displacement chromatograms for two different K–Na mixtures on a Waters IC PAK C column (differentiated conductivity traces). The carrier was $LiNO_3$ (2.0 m$M$) and the displacer was $RbNO_3$ (2.0 m$M$). The feed was 2.58 ml of a solution containing 1.0 m$M$ K–1.0 m$M$ Na (right-hand side) and 0.6 m$M$ K–1.4 m$M$ Na (left-hand side). The flow-rate and the temperature were 1.0 ml/min and 295 K, respectively. The column had a void volume of 0.349 ml and an ion-exchange capacity of 7.22 $\mu$equiv.

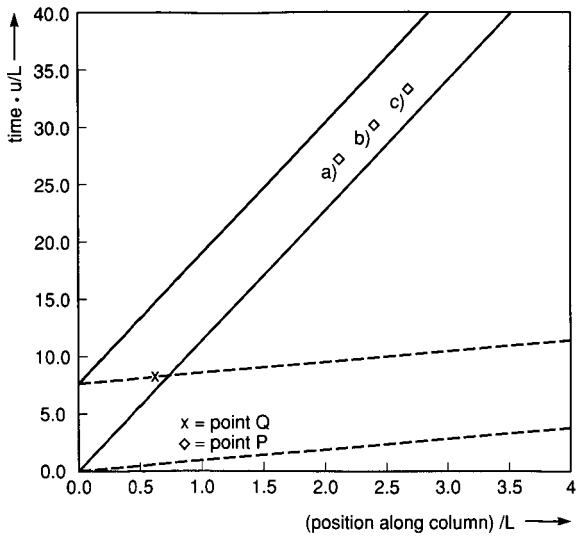


Fig. 6. Development graphs illustrating the shift of the point of complete separation with temperature [(a) 295 K; (b) 308 K; (c) 317 K] of a 1.0 m*M* K–1.0 m*M* Na mixture. The displacer is 2.0 m*M* $RbNO_3$. Other conditions as in Fig. 4.

the isotachic state. In terms of Fig. 4, the column outlet is to the left of the point of complete separation (P). On the left-hand side of Fig. 5, a displacement chromatogram of a 1.0 m*M* K–1.0 m*M* Na mixture is shown, and on the right-hand side, a chromatogram of a 0.6 m*M* K–1.4 m*M* Na mixture. The peaks numbered 3, 4 and 5 refer to the shocks from the carrier state to the pure Na state (3), the pure Na state to the mixed feed state (4) and from the mixed feed state to the pure K state. Peak 6 refers to the shock from pure K to the displacer Rb (5). Peaks 1 and 2 correspond to small changes in the total concentration that are experimentally inevitable. According to eqn. 10, they travel at the velocity of the eluent $U$ and hence emerge at $t_0$ and $t_0 + t_e$. The distances between the peaks, called zone lengths and measured in millilitres of effluent, correspond to the amounts in the different states. In the following, these experimental zone lengths will be compared with predictions using different multi-component distribution functions. It should be realized that when complete separation is attained, *i.e.*, to the right of point P in Fig. 4, zone lengths are no longer a critical test of the distribution function used to model the separation.

Let us first investigate the influence of temperature. In Fig. 6, the development graphs for the separation of an Na–K mixture are given for three different temperatures. It is seen that separation becomes more difficult as temperature is increased, *i.e.*, the point of separation moves to longer column lengths. Numerical results are presented in Table II. A good comparison between the experimental results and those calculated using the multi-component isotherm of eqn. 21 is observed. The result is understandable. As the alkali metal ions belong to the same compensation class, they have, by definition, a common compensation temperature (in this case 480 K). At this temperature the stationary phase composition is equal to the mobile phase composition for all mobile phase compositions, so that all selectivity is lost. Hence, on going from low temperatures towards the compensation temperature, selectivity factors become progressively smaller, making the column length and time required for a complete separation longer.

TABLE II

COMPARISON OF CALCULATED ZONE LENGTHS (USING THE ISOTHERM OF EQN. 21 WITH EXPERIMENTALLY DETERMINED VALUES

| $T$ (K) | Na zone length (ml) | Mixed zone length (ml) | K zone length (ml) |
|---|---|---|---|
| 295 (exp.) | 0.64 | 1.25 | 0.65 |
| 295 (calc.) | 0.64 | 1.30 | 0.64 |
| 308 (exp.) | 0.60 | 1.40 | 0.57 |
| 308 (calc.) | 0.57 | 1.44 | 0.57 |
| 317 (exp.) | 0.56 | 1.46 | 0.54 |
| 317 (calc.) | 0.53 | 1.52 | 0.53 |

We now compare the performance of the multi-component Langmuir isotherm with the isotherm of eqn. 21. Langmuir data used for the K–Na exchange were obtained by fitting frontal chromatography measurements published previously [23] to the Langmuir equation. The values used for $N$ and $\alpha$ were 7.22 $\mu$mol and 0.66, respectively. In Fig. 7, the development graphs for the cases of the Langmuir isotherm and the isotherm of eqn. 21 are depicted on the left- and right-hand side, respectively. The open squares refer to the points of complete separation (P). In each plot, there are eleven such points referring to eleven equidistant K/Na ratios in the

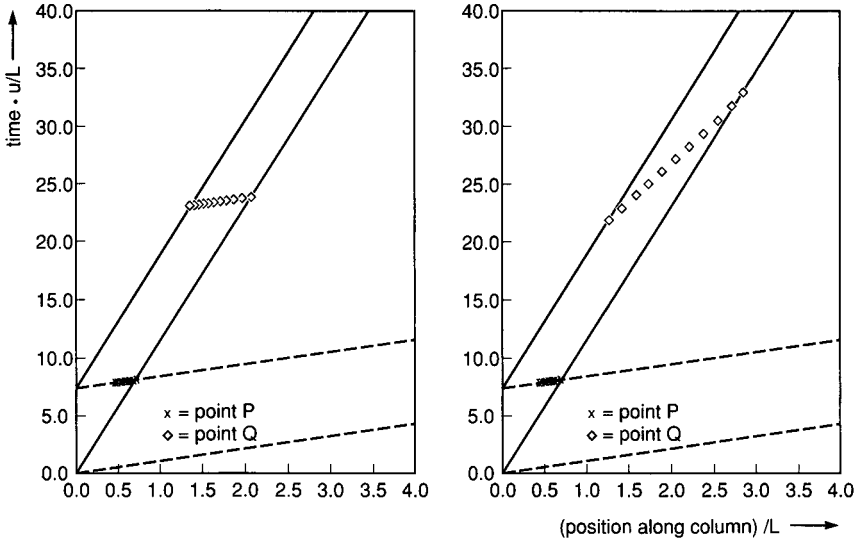


Fig. 7. Development graphs for eleven different K–Na mixtures computed using a multi-component Langmuir isotherm (left-hand side) and the isotherm of eqn. 21 (right-hand side). The points of complete separation correspond to eleven equidistant K/Na ratios in the feed ranging from 0.0 to 1.0. The total feed concentration is 2.0 m$M$, as is the concentration of $RbNO_3$ displacer. Other conditions as in Fig. 4.

feed ranging from 0.0 to 1.0. The difference between the two is apparent. In the Langmuir case, the point of complete separation is only a weak function of the feed composition, whereas a much stronger dependence on the K/Na ratio is observed for the multi-component isotherm in which interactions in the stationary phase are taken into account. Column lengths required for complete separation *ca.* 50% higher are predicted in the latter instance for high potassium contents in the feed. In Fig. 8 the experimental results are compared with the predictions of both models. The lengths of the different zones (in millilitres) are plotted as a function of the composition of the binary feed. The left-hand side

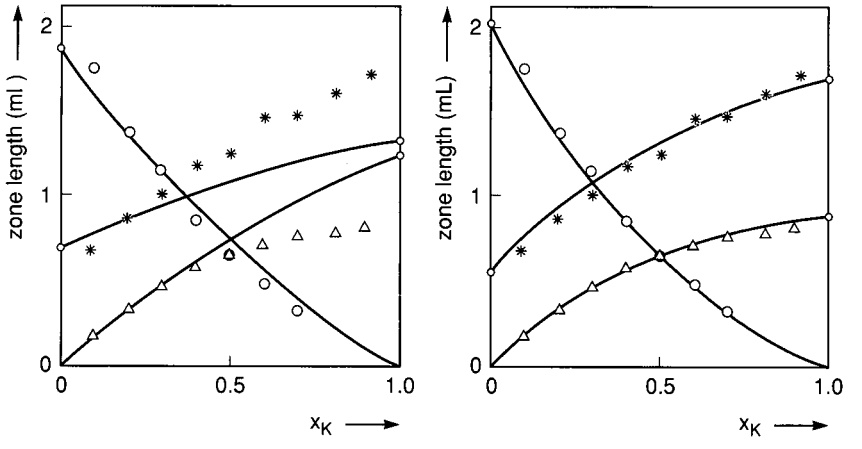


Fig. 8. Lengths of zones in the displacement separation of K–Na mixtures as a function of the potassium content of the feed. Curves in the left-hand figure are computed using a multi-component Langmuir isotherm and in the right-hand figure using the isotherm of eqn. 21. The symbols represent experimental data. Three different zone lengths can be distinguished: (○) the pure Na zone, (✳) the mixed zone and (△) the pure K zone. Total concentrations in carrier, feed and displacer were all 2.0 m$M$. Other conditions as in Fig. 5.

shows the lengths calculated using the Langmuir model, the right-hand side those calculated using the isotherm of eqn. 21. Small open circles on both the Na and K axes represent the limiting lengths of the mixed zone at very small and very high potassium contents, respectively. We feel that the results are convincing: the multi-component distribution isotherm of eqn. 21 shows good agreement with the experimental data over the complete composition range, whereas the Langmuir isotherm predicts experimental results correctly over only a limited composition range. The particular range of fit for the Langmuir isotherm strongly depends on the way Langmuir parameters are extracted from the experimental data, *e.g.*, $\alpha$-values obtained from a fit to the complete isotherm are significantly different from those derived from linear elution chromatographic data. A good prediction over the complete feed composition range is not possible, which reflects the insufficiency of the multi-component Langmuir equation to represent the competitive sorption behaviour.

From Figs. 7 and 8, it is seen that the errors made by using too simple an expression for the distribution isotherm are substantial. Research aimed at obtaining improved descriptions of competitive sorption is sparse, however [30]. As remarked in the Introduction, understanding the sorption process is the key to understanding chromatographic separations. We firmly believe that better descriptions of the distribution equilibrium, such as the isotherm of eqn. 21, are a prerequisite for the quantitative modelling of non-linear separations. Attempts to fine-tune the continuity equations by adding dispersive terms seem dubious as long as inadequate descriptions of the distribution equilibrium are used.

## CONCLUSIONS

The traditional way of solving the coupled set of mass-balance equations that apply to the transport problem in displacement chromatography (*i.e.*, using the $h$- or $\omega$-transformation) cannot be used if the multi-component isotherm describing the distribution between mobile and stationary phases is non-ideal.

For the separation of binary mixtures, the mass-balance equations can be solved for non-ideal isotherms using shock-wave theory, provided that the continuity equations are recast in terms of stationary phase concentrations and that the total concentration in the stationary phase is known at every time and place.

Experimental results for the ion-exchange separation (total concentration in the stationary phase constant) of binary mixtures are only properly described across the complete composition range if non-idealities are taken into account. In extreme cases, ideal sorption behaviour predicts the column length required for complete separation to be *ca.* 50% too short.

For the quantitative modelling of displacement chromatography, multi-component distribution isotherms better than the ideal approximation are a prerequisite.

## REFERENCES


1 M. S. Tswett, cited by L. S. Ettre, in Cs. Horváth (Editor), *High Performance Liquid Chromatography: Advances and Perspectives*, Vol. 1, Academic Press, New York, 1980, p. 25.
2 A. Tiselius, *Ark. Kemi Mineral. Geol.*, 16A (1943) 1.
3 H. Kalasz and Cs. Horváth, *J. Chromatogr.*, 215 (1981) 295.
4 Cs. Horváth, A. Nahum and J. Frenz, *J. Chromatogr.*, 218 (1981) 365.
5 H. Kalasz and Cs. Horváth, *J. Chromatogr.*, 239 (1982) 423.
6 H. C. Thomas, *J. Am. Chem. Soc.*, 66 (1944) 1664.
7 N. K. Hiester and T. Vermeulen, *Chem. Eng. Prog.*, 48 (1952) 505.
8 P. C. Haarhof and H. J. van der Linde, *Anal. Chem.*, 38 (1966) 573.
9 P. Rouchon, M. Schonauer, P. Valentin and G. Guiochon, *Sep. Sci. Technol..*, 22 (1988) 32.
10 G. Guiochon and S. Ghodbane, *J. Phys. Chem.*, 92 (1988) 3682.
11 J. L. Wade, A. F. Bergolde and P. W. Carr, *Anal. Chem.*, 59 (1987) 1286.
12 M. W. Phillips, G. Subramanian and S. M. Cramer, *J. Chromatogr.*, 454 (1988) 1.
13 J. Frenz and Cs. Horváth, *AIChE J.*, 31 (1985) 400.
14 S. Golshan-Shirazi and G. Guiochon, *Anal. Chem.*, 61 (1989) 462.
15 F. Helfferich and G. Klein, *Multicomponent Chromatography, a Theory of Interference*, Marcel Dekker, New York, 1970.
16 H.-K. Rhee, R. Aris and N. R. Amundson, *Philos. Trans. R. Soc. London, Ser. A*, 267 (1970) 419.
17 H.-K. Rhee and N. R. Amundson, *AIChE J.*, 28 (1982) 423.
18 S. Golshan-Shirazi and G. Guiochon, *J. Phys. Chem.*, 93 (1989) 4143.
19 C. Kemball, E. K. Rideal and E. A. Guggenheim, *Trans. Faraday Soc.*, 44 (1948) 948.
20 A. M. Katti and G. Guiochon, *J. Chromatogr.*, 499 (1990) 21.
21 H. M. J. Boots and P. K. de Bokx, *J. Phys. Chem.*, 93 (1989) 8240.

22 P. K. de Bokx and H. M. J. Boots, *J. Phys. Chem.*, 93 (1989) 8243.
23 P. K. de Bokx and H. M. J. Boots, *J. Phys. Chem.*, 94 (1990) 6489.
24 M. D. LeVan and T. Vermeulen, *J. Phys. Chem.*, 85 (1981) 3247.
25 F. Fowler and E. A. Guggenheim, *Statistical Thermodynamics*, Cambridge University Press, Cambridge, 2nd ed., 1960.
26 P. D. Lax, in E. H. Zarantonello (Editor), *Contributions to Nonlinear Functional Analysis*, University of Wisconsin, Madison, WI, 1971, p. 603.
27 P. D. Lax, *Hyperbolic Systems of Conservation Laws and the Mathematical Theory of Shock Waves*, SIAM Regional Conference Series on Applied Mathematics, SIAM, Philadelphia, PA, 1973.
28 J. Smoller, *Shock Waves and Reaction-Diffusion Equations*, Springer, New York, 1983.
29 H. P. Urbach, *Proc. R. Soc. London, Ser. A*, in press.
30 F. D. Antia and Cs. Horváth, *J. Chromatogr.*, 484 (1989) 1.

*Journal of Chromatography*, 594 (1992) 23–27
Elsevier Science Publishers B.V., Amsterdam

CHROM. 23 855

# High-performance liquid chromatographic study of the correlation between the physico-chemical parameters of furan and benzene aldehydes and the rate of their metabolism by yeast

V. D. Nemirovskii*, N. I. Monakhova and V. G. Kostenko

*Institute of Hydrolysis Industry, Kalinina 13, St. Petersburg (Russia)*

(First received April 2nd, 1991; revised manuscript received October 29th, 1991)

ABSTRACT

A kinetic study of the metabolism of furan and benzene aldehydes *in vivo* by *Candida scottii* by high-performance liquid chromatography showed that the biotransformation proceeded via the stages aldehyde → alcohol → carboxylic acid. It was shown by regression analysis that a good correlation exists between the rate constant and chromatographic retention, Hammett's $\sigma$ constant and molar volume for both the furan and benzene derivatives.

## INTRODUCTION

The correlation between structure and biological activity is an important problem in biochemistry, biotechnology and pharmacochemistry. Hansch's approach made it possible to correlate the activity with hydrophobic, electronic, steric and other properties of molecules [1,2]. Recently we used reversed-phase high-performance liquid chromatography (RP-HPLC) to investigate the behaviour of some inhibitors of yeast growth in the presence of *Candida* cells [3–5]. An example of the kinetic curves for the metabolism of furfural is presented below (Fig. 1 [4]). Analysis of the kinetic data showed that the transformation of aldehydes can be described by a general scheme for both furan and benzene derivatives: RCHO → $RCH_2OH$ → RCOOH, where R is substituted furyl or aryl. It is probable that the oxidation of the primary alcohol to the acid proceeds through an intermediate form but we were not able to detect it by kinetic or analytical methods.

Only a few researchers have considered the correlation between metabolism rate and structure [6]. In this work, we investigated the kinetics of aldehyde metabolism by *Candida scottii* cells and attempted to establish its dependence on the structure and physico-chemical properties.

## EXPERIMENTAL

### *Kinetic measurements*

The biomass of *C. scottii* strain [7] was previously grown in buffered medium containing glucose. The fermentation runs were performed in the absence of carbohydrate nutrition in aerobic batch conditions at 30°C. The cell concentration was 20 and 10 g/l for the benzene and furan aldehydes, respectively. In each run 1 mmol/l of the aldehyde was added. Aliquots of 2 ml were filtered, diluted tenfold and analysed by the RP-HPLC method described below. First-order rate constants, $k$, were calculated as average from 6–8 measurements.

### *Chromatography*

The HPLC system consisted of an LKB (Brom-

TABLE I

METABOLISM RATE CONSTANT, RETENTION INDICES, HAMMETT $\sigma$ CONSTANTS AND VAN DER WAALS VOLUMES OF FURAN AND BENZENE DERIVATIVES

| No.[a] | Substance | $k$ (min$^{-1}$) | $k'$ | $\sigma^b$ | $V_w{}^c$ |
|---|---|---|---|---|---|
| 1 | Furylacrylic acid | 0.00136 | 1.50 | −0.22 | 79.9 |
| 2 | 5-Hydroxymethylfurfural | 0.00642 | 1.02 | 0 | 55.6 |
| 3 | Furfuryl alcohol | 0.00832 | 1.00 | 0 | 53.2 |
| 4 | 5-Methylfurfural | 0.0236 | 3.15 | −0.17 | 56.2 |
| 5 | Furfural | 0.0372 | 1.60 | 0 | 45.1 |
| 6 | Furylacrolein | 0.0728 | 6.8 | −0.10 | 61.2 |
| 7 | 5-Nitrofurfural | 0.22 | 1.50 | 0.78 | 59.3 |
| 8 | 5-Nitrofuryl acrolein | 0.517 | 5.5 | 0.68 | 75.5 |
| 9 | Syringaldehyde | 0.00104 | 7.08 | −0.21 | 90.2 |
| 10 | 2,4-Dihydroxybenzaldehyde | 0.00575 | 3.63 | 0.85 | 66.3 |
| 11 | Vanillin | 0.0127 | 4.68 | −0.29 | 75.8 |
| 12 | Veratraldehyde | 0.0157 | 13.49 | −0.19 | 84.7 |
| 13 | 4-Hydroxybenzaldehyde | 0.0266 | 3.31 | −0.37 | 61.5 |
| 14 | 3-Hydroxy-*p*-anisaldehyde | 0.0552 | 5.25 | −0.17 | 75.8 |
| 15 | Protocatechuic aldehyde | 0.126 | 3.02 | −0.27 | 66.3 |
| 16 | 3-Hydroxybenzaldehyde | 0.138 | 3.47 | 0.10 | 61.5 |

[a] Numbers correspond to curve numbers in Figs. 2 and 3.
[b] Taking as zero unsubstituted furfural or benzaldehyde [8].
[c] Taken from ref. 9.

ma, Sweden) Model 2150 pump, a Varian (Vienna, Austria) Model 2080 column oven, a Kratos (Ramsey, NJ, USA) Model 783 UV detector, a Spherisorb $C_6$ (10 $\mu$m) column (25 cm × 4.6 mm I.D.) and a Shimadzu (Kyoto, Japan) Chromatopac C-R3A data system. Previously found absorption maxima for each aldehyde were used as detection wavelengths. The mobile phase was acetonitrile–water (6:94, v/v). The elution rate was 1.5 ml/min and the column oven was thermostated at 60°C.

For kinetic measurements the same conditions were used but for the analysis of aldehydes having long retention times (as furylacrolein, veratraldehyde and syringaldehyde) the acetonitrile concentration in the eluent was 8.5% (v/v).

TABLE II

REGRESSION ANALYSIS OF EXPERIMENTAL DATA FOR FURAN ALDEHYDES (MODELS 1–4) AND BENZALDEHYDES (MODELS 5–8) ACCORDING TO GENERAL EQUATION LOG $k = b_0 + b_1$ LOG $k' + b_2 \sum\sigma + b_3 V_w$

| Model No. | Parameters taken into account | Regression coefficients ($b$), 95% confidence intervals ($S$) and $F$ factors | | |
|---|---|---|---|---|
| | | $b_0$ | | |
| | | $b_0$ | $S_0$ | $F_0$ |
| 1 | Hydrophobicity | −2.05 | 0.86 | 2.25 |
| 2 | Hydrophobicity and molar volume | −0.95 | 5.16 | 0.1 |
| 3 | Hydrophobicity and electronic effect | −2.16 | 0.42 | 4.11 |
| 4 | Hydrophobicity, electronic effect and molar volume | −0.59 | 0.08 | 102 |
| 5 | Hydrophobicity | −0.71 | 1.46 | 0.94 |
| 6 | Hydrophobicity and electronic effect | −0.62 | 1.64 | 0.57 |
| 7 | Electronic effect and molar volume | 1.97 | 3.53 | 1.24 |
| 8 | Hydrophobicity, electronic effect and molar volume | 2.88 | 0.68 | 4.68 |

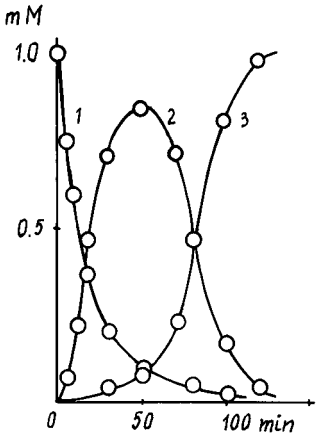


Fig. 1. Kinetics of furfural metabolism by *Candida scottii*. Curves: 1 = Furfural; 2 = furfuryl alcohol; 3 = furan-2-carboxylic acid.

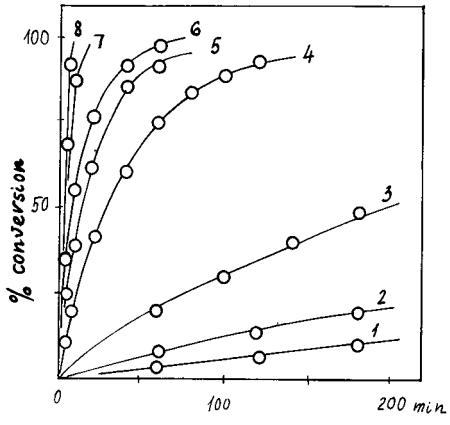


Fig. 2. Dependence of conversion of furan aldehydes on time. For curve numbers, see Table I.

## RESULTS

Kinetic curves for the metabolic transformation of furfural by *C. scottii* are given in Fig. 1. The appearance of these curves is typical of consecutive reactions and shows that metabolism proceeds through two stages: furfural → furfuryl alcohol → furan-2-carboxylic acid. This conclusion was confirmed by experiments in which furfuryl alcohol and furan-2-carboxylic acid were preparatively isolated from fermentation media and their chemical structures were proved [4,5]. The same was established for each furan and benzene derivative.

Kinetic curves describing the first stage of metabolism of furan derivatives are presented in Fig. 2 as conversion–time dependences and in Fig. 3 as logarithm of concentration–time dependences. Data for furfuryl alcohol and furylacrylic acid are given for comparison. It is seen (Fig. 3) that at a constant cell concentration the metabolism is described by a first-order reaction. This is also true for the benzaldehyde derivatives.

We investigated the correlation of the kinetic data with hydrophobic, electronic and steric characteristics of substrate molecules. The chemical and structural parameters were the chromatographic retention index, $k'$, which is proportional to hydrophobicity [8], the sum of the substituent Hammett constants, $\sum\sigma$, calculated as described by Barlin and Perrin [9], and the Van der Waals volume, $V_w$ [10]. These data, which are summarized in Table I, were treated by regression analysis as described by

| Regression coefficients ($b$), 95% confidence intervals ($S$) and $F$ factors | | | | | | | | | $F$ factor (overall) | | Correlation coefficient |
|---|---|---|---|---|---|---|---|---|---|---|---|
| $b_1$ | | | $b_2$ | | | $b_3$ | | | Theory | Calc. | |
| $b_1$ | $S_1$ | $F_1$ | $b_2$ | $S_2$ | $F_2$ | $b_3$ | $S_3$ | $F_3$ | | | |
| 1.58 | 0.72 | 3.36 | – | – | – | – | – | – | 5.99 | 3.37 | 0.60 |
| 1.82 | 1.88 | 4.18 | – | – | – | −0.019 | 0.052 | 0.88 | 5.79 | 1.83 | 0.65 |
| 1.37 | 0.35 | 9.72 | 1.58 | 0.012 | 20.1 | – | – | – | 5.79 | 16.8 | 0.93 |
| 1.65 | 0.16 | 462 | 1.69 | 0.13 | 699 | −0.028 | 0.04 | 173 | 6.59 | 110 | 0.99 |
| −1.43 | 1.42 | 0.66 | – | – | – | – | – | – | 5.99 | 1.43 | 0.44 |
| −1.62 | 1.24 | 1.69 | −0.51 | 0.65 | 0.55 | – | – | – | 5.79 | 0.92 | 0.52 |
| – | – | – | −0.70 | 1.09 | 1.81 | −0.051 | 0.041 | 6.98 | 5.79 | 4.45 | 0.76 |
| 1.56 | 0.87 | 3.12 | −0.72 | 0.48 | 2.26 | −0.078 | 0.018 | 19.4 | 6.59 | 4.49 | 0.80 |

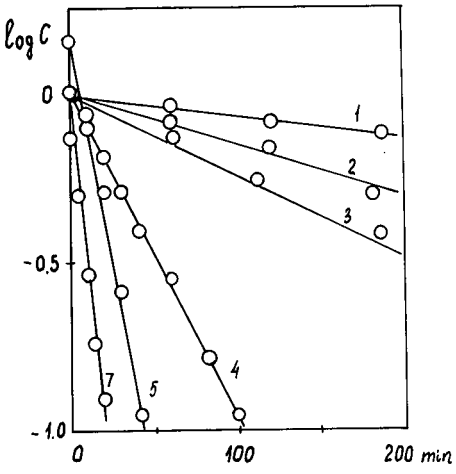


Fig. 3. Conversion of furan aldehydes plotted as logarithm of concentration *versus* time. For curve numbers, see Table I.

Afifi and Azen [11]. Four combinations of independent variables (log $k'$, $\sum\sigma$ and $V_w$) for both furan (models 1–4) and aromatic aldehydes (models 5–8) were considered. For each model the regression coefficients, 95% confidence intervals of the regression coefficients, $F$ factors and correlation coefficients were calculated, and are presented in Table II. Moreover, for each two subsets the squared correlation matrix was calculated (Table III), showing the extent of collinearity of the independent variables.

## DISCUSSION

The results in Tables II and III show that the correlation is high in the furan series but not so high in the benzene series. However, in many instances reported for biological systems poorer correlations were considered to be acceptable [6]. It has been noted in many papers that the correlation is high when the structure of substances is similar within the series. Another factor is, of course, the identity of the set of ferments responsible for the transformation. If we assume that our case is analogous to those reported elsewhere [12], then the alcohol aldehyde dehydrogenase (ADH) is responsible for aldehyde reduction and our results may be explained in terms of the ADH model obtained by Hansch and Bjorkroth [12] from X-ray data treated by a computer graphic method. According to this model, the ferment active site consists of a hydrophobic cavity, one end of which has a polar group, so that complexing of the substrate depends on both hydrophobic and electronic properties of corresponding parts of the molecule.

Our results for benzaldehydes appear to be in agreement with this scheme. Introduction of hydrophobic groups increases the rate of metabolism and we have a positive coefficient for log $k'$ ($b_1$ in model 8). Introduction of electron-attracting groups decreases the electron density on the carbonyl oxygen atom, thus decreasing the rate of metabolism and the coefficient for $\sum\sigma$ ($b_2$) is negative. The influence of hydrophobic properties of the substituents on the rate of metabolism is the same in the series of furan derivatives. The coefficient $b_1$ is also positive in model 4. However, the influence of electronic properties is different here, as the coefficient for the $\sigma$ term in positive. One may assume that another mechanism exists in this instance.

TABLE III

CORRELATION MATRIX

| Model 4 | | | Model 8 | | |
|---|---|---|---|---|---|
| 1.000 | 0.134 | 0.347 | 1.000 | −0.208 | 0.849 |
| 0.134 | 1.000 | 0.176 | −0.208 | 1.000 | −0.271 |
| 0.347 | 0.176 | 1.000 | 0.849 | −0.271 | 1.000 |

## ACKNOWLEDGEMENT

We thank Dr. N. M. Lifshitz for useful discussisons of the statistical analysis results.

## REFERENCES

1 C. Hansch and A. Lee, *Substituent Constants for Correlation Analysis in Chemistry and Biology*, Wiley, New York, 1979.
2 A. J. Hoefnagel and B. M. Wepster, *Collect. Czech. Chem. Commun.*, 55 (1990) 119.
3 V. D. Nemirovskii, M. S. Frid, V. G. Kostenko, A. I. Sizov and I. M. Golubkov, in *5th International Symposium on Furan Chemistry, Abstracts*, Latvian Academy of Sciences, Riga, 1988, Abstract 104.
4 V. D. Nemirovskii, L. A. Gusarova, Y. D. Rahmilivich, A. I. Sizov and V. G. Kostenko, *Biotekhnologiya*, 5 (1989) 285.
5 V. D. Nemirovskii, M. S. Frid, V. G. Kostenko and A. I. Sizov, *Gidrolizn. Lesokhim. Prom.*, 3 (1990) 14.
6 S. P. Gupta, *Chem. Rev.*, 87 (1987) 1183.

7 T. N. Semushina, N. I. Monakhova, V. V. Lukjanova, G. I. Leontieva and D. D. Saveliev, *Byull. Izobret.*, 35 (1977) 212.
8 R. Kaliszan, *Quantitative Structure–Chromatographic Retention Relationship*, Wiley, New York, 1987, p. 303.
9 G. B. Barlin and D. D. Perrin, *Q. Rev. Chem. Soc.*, 20 (1966) 75.
10 A. Bondy, *J. Phys. Chem.*, 68 (1964) 441.
11 A. A. Afifi and S. P. Azen, *Statistical Analysis. A Computer Oriented Approach*, Academic Press, New York, 1979, p. 488.
12 C. Hansch and J. P. Bjorkroth, *J. Org. Chem.*, 51 (1986) 5461.

*Journal of Chromatography*, 594 (1992) 29–36
Elsevier Science Publishers B.V., Amsterdam

CHROM. 23 853

# Determination of solute–polymer interaction constants via chromatography with polymer capillaries

Dennis R. Jenke

*Baxter Healthcare Corporation, William B. Graham Science Center, Round Lake, IL 60073 (USA)*

(First received September 3rd, 1991; revised manuscript received October 31st, 1991)

ABSTRACT

The interaction between model solutes and various polymeric materials was studied chromatographically by measuring dynamic solute absorption. Specifically, the solutes were injected into tubing "columns" manufactured by making thin pieces of tubing out of the polymers of interest. Polymers investigated in this manner included a di(2-ethylhexyl)phthalate-plasticized poly(vinyl chloride), a vinyl acetate–vinyl chloride copolymer and a blend of polypropylene and a styrene–butadiene block copolymer. Linear relationships could be established between the dynamic binding constant of the solute, determined chromatographically, and its equilibrium interaction constant, determined by conventional shake-flask means. Similarly, the dynamic binding constant could be directly related to the solvent–solvent partition coefficients of the solute. The proposed methodology provides a rapid means of assessing the magnitude of polymer–solute interactions.

## INTRODUCTION

Developing polymeric containers for the food and pharmaceutical industries requires the establishment of container–product compatibility. Compatibility revolves around two issues: binding, wherein the container sorbs a component of the product, and leaching, wherein a container component becomes mobilized into the product. Both issues involve partitioning of the solute, regardless of its initial source, between the container and product phases.

Container–solution partition coefficients are usually determined by shake-flask methods wherein the container and solution are equilibrated under controlled conditions and the equilibrium concentration of the solute in the two phases is determined. Such an approach is time intensive (it may take several weeks to reach equilibrium) and must be rigorously controlled to establish (a) that solute loss observed from either phase is truly due to partitioning and not some other loss mechanism such as degradation and (b) that physical difficulties associated with the measurement [1–3] are minimized.

Alternatively, several more or less indirect chromatographic methods exist for assessing material–solute interactions. Inverse gas chromatography and high-performance liquid chromatography (HPLC), in which the polymer of interest essentially becomes the chromatographic support, has been used to study polymer–solute interactions [4–9]. The use of HPLC (reversed-phase) retention characteristics to determine the solvent–solvent partition coefficient of a solute is well documented [10–13]. As solvent–solvent partition coefficients can be directly correlated with polymer–water partition coefficients [14–16], such HPLC methods are directly applicable to the determination of polymer–solution interaction characteristics.

The ability of the chromatographic approaches to predict the polymer–solution interaction rests on how well the chromatographic system mimics the container–solution couple. For methods using a bonded polymeric stationary phase, it is probable that the polymer bonded to the stationary phase bears little resemblance to the material in its container form. This is especially true for the newer classes of container materials which represent mul-

0021-9673/92/$05.00 

ti-layered structures. For the HPLC retention time methods, it is also unlikely that a conventional stationary phase could be found which would mimic the solution interaction of a significant number of the potential container materials, especially given the multi-modal container–solution interactions mechanism that occur.

In this research, container–solute interactions were measured directly by using thin tubes of the container material of interest as the stationary phase in a liquid chromatographic system. Changes in peak size are indicative of the magnitude of the material–solute interaction.

## EXPERIMENTAL

### *Materials*

Polymers studied included a di(2-ethylhexyl) phthalate (DEHP)-plasticized poly(vinyl chloride) (PVC) (Viaflex plastic, Baxter Healthcare, Deerfield, IL, USA), vinyl acetate–vinyl chloride copolymer (VA–VC) (Tygon tubing, Norton, Wayne, NJ, USA) and a blend of polypropylene and a styrene–butadiene block copolymer (PP). The VA–VC tubing had a I.D. of 2 mm and an O.D. of *ca.* 2.5 mm. PVC and PP tubing was extruded in-house; the PVC tubing had an I.D. of 1 mm and an O.D. of 1.5 mm and the PP tubing had an I.D. of 1.5 mm and an O.D. of *ca.* 3 mm. For both tubing types prepared in-house, the sizes prepared were dictated by practical processing constraints.

Test solutes were analytical-reagent grade (98% purity or better) and are listed, together with their solvent–solvent partition coefficients, in Table I. These solutes were chosen as they are analytically expedient, they encompass a fairly wide range in terms of their intrinsic lipophilicity, they exhibit a varying ability to interact with polymers via hydrogen bonding and their polymer diffusion coefficients are relatively large. Other reagents used to prepare mobile phases and other solutions were of analytical-reagent or HPLC grade as appropriate. Water was obtained from a Barnstead NANOpure II water purification system.

TABLE I

MODEL SOLUTES USED

| Model solute | Abbreviation | Log $P_{o-w}$ | Log $P_{h-w}$ |
|---|---|---|---|
| Dimethyl phthalate | DMP | 2.16 | 0.82 |
| Diethyl phthalate | DEP | 3.22 | 1.75 |
| Dipropyl phthalate | DPP | 4.05 | 2.67 |
| 4-Methylbenzoic acid | MBH | 2.27 | −0.4 |
| 4-Ethylbenzoic acid | EBH | 2.97 | 0.4 |
| 4-Butylbenzoic acid | BBH | 3.96 | 1.80 |
| Aniline | AN | 0.9 | −0.1 |
| 4-Methylbenzyl alcohol | MBOH | 1.6 | 0.3 |
| Carbazole | CAR | 3.59 | 2.18 |
| Ethyl 4-aminobenzoate | ETBZ | 2.24 | −0.07 |
| Butyl 4-aminobenzoate | BUBZ | 3.37 | 1.14 |
| Ethyl 4-hydroxybenzoate[a] | ETPB | 2.57 | −1.05 |
| Butyl 4-butylbenzoate[b] | BUPB | 3.59 | 0.5 |
| *n*-Ethylhexylamine | NEHA | 2.00 | −1.80 |

[a] Ethyl paraben.
[b] Butyl paraben.

### *Determination of equilibrium interaction constants*

The equilibrium interaction constant ($E_b$) for a polymer–solute couple was determined by the shake-flask method. Specifically, a known amount of the polymeric material (cut into small pieces to hasten the attainment of equilibrium) was contacted with a known amount of solution which originally contained a known amount of one or more of the test solutes. Replicate polymer test articles and non-polymer-containing control samples was stored at 35°C for 2 weeks with constant gentle agitation. After this time, the solution phase concentration of the solute was determined by HPLC and $E_b$ was calculated.

### *Preparation of tubing columns*

The tubing was made into chromatographic "columns" as follows. For the VA–VC copolymer, the following "columns" were made: coiled, in which a 70-cm length of tubing was just loosely coiled; knotted, in which a 65-cm length of tubing was manually knotted (tightly but without flow stoppage); and knotted with beads, where a 70-cm length of tubing was filled with *ca.* 1 mm diameter glass beads and knotted. For PVC, a knotted "column" was made from a 70-cm length of this tubing. A knotted "column" of PP was made from a 90-cm piece of this material; however, owing to its rigidity, the knots were not a tight as those obtained for the other materials. The various polymer "columns" were fitted with conventional HPLC end fittings. An inert reference "column" was made by coupling two 0.5-ml stainless-steel sample loops together.

*Generation of the dynamic binding chromatograms*

The chromatographic system consisted of conventional HPLC components with the tubing serving as the analytical "column". Typical operating conditions included a mobile phase of 0.05% trifluoroacetic acid at a flow-rate of 0.3 ml/min, UV analyte detection at 215 nm and a sample size of 20 μl. The acidic mobile phase was necessary to ensure that the acidic model solutes were completely protonated. Although the system temperature was usually ambient, some experiments were performed at elevated temperature by placing the tubing in a conventional column oven and preheating the mobile phase in a water-bath.

Dynamic binding experiments were performed as follows. A given "column" was placed in the chromatographic system and equilibrated with the mobile phase. Duplicate injections of the test solutes (at concentrations of *ca.* 5 and 50 ppm) were made and the resulting chromatograms recorded. Sufficient time was allowed between injections so that the baseline was re-established. After elution of all the solutes, another "column" was put into the system and the experiment was repeated. Peak areas of the resulting chromatographic responses were determined by integrating computerized peak traces.

*Definition and calculation of $E_b$ and $D_b$*

The equilibrium interaction constant, $E_b$, is the ratio of the equilibrium solute concentration in the polymer and solution:

$$E_b = (m_p/W_p)/(m_s/V_s) \quad (1)$$

where $m$ is the mass of solute in either phase at equilibrium, $W$ is the polymer weight (in grams), $V$ is the solution volume (in liters) and s and p refer to the solution and polymer phases, respectively. The dynamic binding constant, $D_b$, is defined in a similar manner:

$$D_b = (m_c/W_c)/(m_s/V_s) \quad (2)$$

where $m_c$ is the mass of solute bound by the column, $W_c$ is the column weight, $m_s$ is the mass of solute eluted from the column and $V_s$ is the column void volume.

The quantities $m_c$ and $m_s$ cannot be measured directly but rather require detector calibration. The detector is calibrated by injecting the samples (containing a known concentration, $C_i$, of the solute) into the inert (*i.e.*, no solute absorption) column and noting the peak response ($R_m$) of the eluted solute. The same amount of solute is injected into the polymer columns, producing a detector response $R_c$. If the injection volume is $V_i$, then $m_c$ and $m_s$ from eqn. 2 can be calculated as follows:

$$m_c = (C_i V_i)(1\text{-}R_c/R_m) \quad (3)$$

$$m_s = (C_i V_i)(R_c R_m) \quad (4)$$

## RESULTS AND DISCUSSION

*Equilibrium interaction models*

Equilibrium interaction models (shake-flask experiments) relate $E_b$ to the solvent–water partition coefficient of a solute. For many polymers, a bivariant model is applicable and takes the form

$$\log E_b = a(\log P_{o\text{–}w}) + b(\log P_{h\text{–}w}) + c \quad (5)$$

where o–w refers to octanol–water and h–w refers to hexane–water. The binding model is obtained by linearly regressing known values of $E_b$ *versus* known solute partition coefficients for a particular polymer and obtaining the coefficients in eqn. 5.

A typical equilibrium interaction model (VA–VC copolymer) is shown in Fig. 1 and regression coefficients are given in Table II. An excellent correlation between $E_b$ and the partition coefficients is obtained for the three materials studied. As shown by the relative magnitude of the $P_{o\text{–}w}$ and $P_{h\text{–}w}$ coefficients,

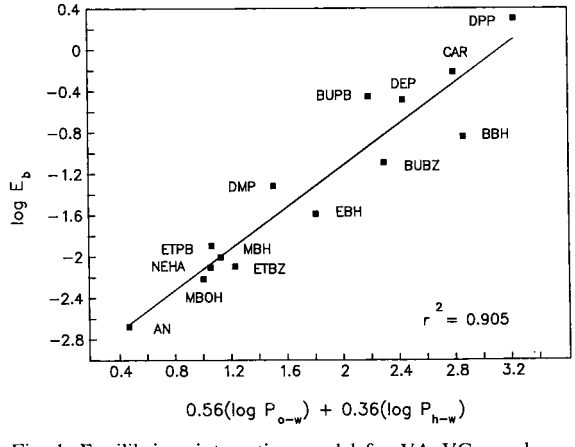


Fig. 1. Equilibrium interaction model for VA–VC copolymer. Plot of log $E_b$ (from shake-flask methods) *versus* the linear combination of the octanol–water (o–w) and hexane–water (h–w) partition coefficients.

TABLE II

VARIOUS CURVE FIT PARAMETERS

Equilibrium interaction model constants[a], eqn. 5

| Constant | PVC | VA–VC | PP |
|---|---|---|---|
| $a$ | 0.46 (0.09) | 0.56 (0.13) | 0.26 (0.19) |
| $b$ | 0.30 (0.07) | 0.36 (0.11) | 0.61 (0.12) |
| $c$ | −2.80 (0.20) | −3.23 (0.30) | −3.41 (0.27) |
| $r^2$ | 0.940 | 0.905 | 0.925 |

Dynamic interaction model constants[a], $\log D_b = a(\log P_{o-w}) + b(\log P_{h-w}) + c$

| Constant | PVC[b] | VA–VC[b] | VA–VC[c] | PP[d] |
|---|---|---|---|---|
| $a$ | 0.66 (0.12) | 0.65 (0.12) | 0.65 (0.11) | −0.01 (0.19) |
| $b$ | 0.35 (0.10) | 0.21 (0.10) | 0.27 (0.10) | 0.63 (0.11) |
| $c$ | −5.9 (0.28) | −5.47 (0.28) | −5.34 (0.26) | −5.30 (0.27) |
| $r^2$ | 0.929 | 0.904 | 0.926 | 0.904 |

Curve fit parameters[a], $\log D_b = a(\log E_b) + b$

| Parameter | PVC | VA–VC[c] | PP[c] |
|---|---|---|---|
| $a$ | 1.28 (0.90) | 0.94 (0.06) | 0.83 (0.09) |
| $b$ | −2.23 (0.23) | −2.14 (0.20) | −2.99 (0.26) |
| $r^2$ | 0.949 | 0.952 | 0.898 |

[a] Numbers in parentheses are the standard errors.
[b] 25°C, knotted column.
[c] 25°C, column with beads.
[d] 45°C, knotted column.

the VA–VC copolymer and PVC possess mixed interaction characteristics (classical lipophilic interaction plus hydrogen bonding) while the PP blend is dominantly hexane-like and possesses little hydrogen bonding ability.

When a model solute is injected onto the polymer column, two distinct effects are observed. For all but the most hydrophilic solutes, both peak shape and size (total area) are affected as the solute passes through the polymeric column. As the solute lipophilicity increases, the total peak response decreases and the peak develops a pronounced tail. While both peak response and shape could be related to the polymer's binding ability, peak area is used here as it is most easily and reproducibly measured.

*Dynamic binding constants and models*

Dynamic binding constants for a variety of different tubing configurations are listed in Table III. For several of the materials, $D_b$ data are not available for every solute. This illustrates a practical disadvantage of the dynamic binding approach, its limited dynamic range. As the determination of $D_b$ rests on a differential measurement of solute elution between an inert and polymer column, it is constrained by either the ability to measure a difference between two peak areas or, in the case of a strongly interacting solute, to measure any peak response at all with the polymeric column.

Dynamic binding constant models for the three materials evaluated are illustrated in Figs. 2–4 and the regression constants are summarized in Table II. Although in general adequate correlations can

TABLE III

EQUILIBRIUM AND DYNAMIC BINDING CONSTANTS

| Solute | PVC[a] | | VA–VC[b] | | PP[c] | |
|---|---|---|---|---|---|---|
| | Log $E_b$ | Log $D_b$ | Log $E_b$ | Log $D_b$ | Log $E_b$ | Log $D_b$ |
| DMP | −1.56 | −4.28 | −1.32 | −3.62 | −2.56 | −5.11 |
| DEP | −0.53 | −3.16 | −0.49 | −2.65 | −1.73 | −4.31 |
| DPP | 0.05 | −2.14 | 0.30 | −2.08 | −0.83 | −3.30 |
| NEHA | −[d] | – | −2.11 | −4.20 | – | – |
| MBH | −1.87 | −4.36 | −2.01 | −4.00 | −3.24 | −5.51 |
| EBH | −1.33 | −4.22 | −1.59 | −3.43 | −2.10 | −4.84 |
| BBH | −0.93 | −3.20 | −0.85 | −2.62 | −1.14 | −4.30 |
| AN | −2.41 | −5.37 | −2.68 | −4.50 | – | – |
| MBOH | −2.1 | −4.80 | −2.22 | −4.45 | – | – |
| CAR | −0.4 | −2.65 | −0.02 | −2.20 | −1.06 | −3.60 |
| ETBZ | −1.82 | −4.88 | −2.10 | −4.21 | −2.25 | −4.99 |
| BUBZ | −0.85 | −3.57 | −1.10 | −2.96 | −1.54 | −4.70 |
| ETPB | −1.76 | −4.49 | −1.69 | −3.92 | −3.46 | −5.84 |
| BUPB | −0.95 | −3.11 | −0.46 | −2.36 | −2.55 | −5.20 |

[a] 25°C, knotted column.
[b] 25°C, knotted column with beads.
[c] 45°C, knotted column.
[d] – = Not measurable.

be obtained between $D_b$ and the solvent–solvent partition coefficients of a solute, the correlations obtained with the dynamic binding constant are not as good as those obtained using the equilibrium interaction constants. However, the correlation between $D_b$ and the partition coefficients are sufficiently strong that the dynamic binding models could be used to semi-quantitatively assess the relative behaviors of several polymeric materials.

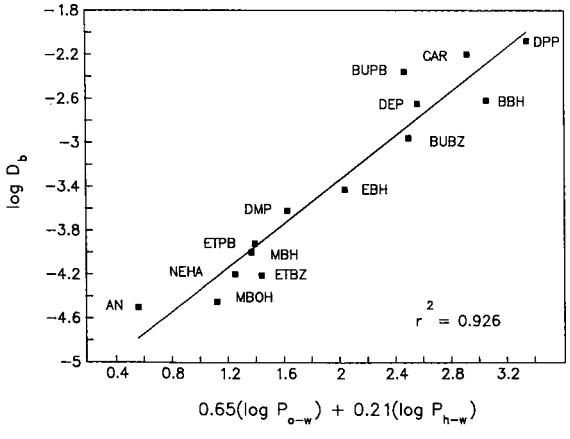


Fig. 2. Dynamic binding model for the VA–VC copolymer. Plot of log $D_b$ (from the column experiments) *versus* the linear combination of the octanol–water (o–w) and hexane–water (h–w) partition coefficients of the solute at 25°C. The data were obtained with the knotted column.

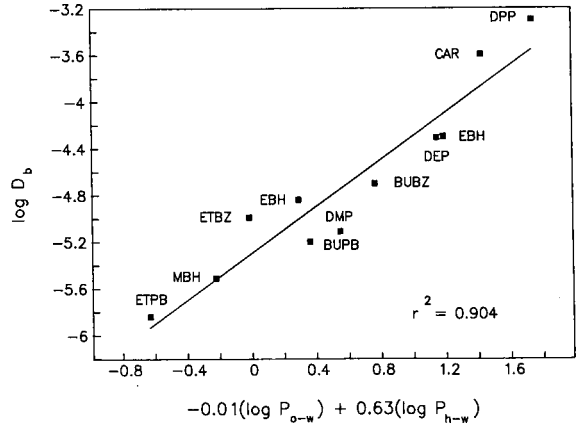


Fig. 3. Dynamic binding model for the polypropylene blend. Plot of log $D_b$ (from the column experiments) *versus* the linear combination of the octanol–water (o–w) and hexane–water (h–w) partition coefficients of the solute at 45°C. The data were obtained with the knotted column.

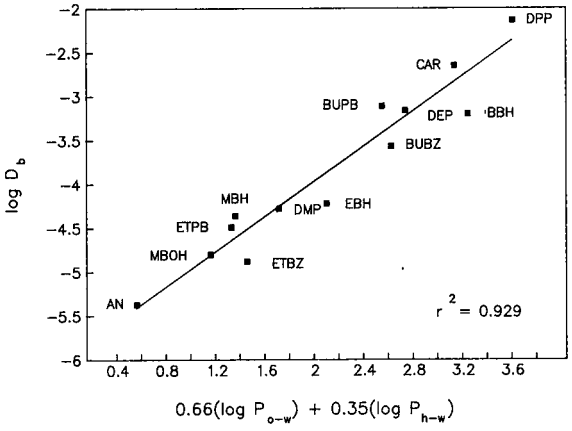


Fig. 4. Dynamic binding model for PVC. Plot of log $D_b$ (from the column experiments) *versus* the linear combination of the octanol–water (o–w) and hexane–water (h–w) partition coefficients of the solute at 25°C. The data were obtained with the knotted column.

*Factors influencing the magnitude of the dynamic binding constant*

The dynamic binding process is not reversibly chromatographic in the sense of producing varying retention times as a function of column material and solute identity. Rather, the dynamic binding process is essentially an "on-the-fly" approximation of the equilibrium polymer–solute interaction, wherein a fraction of the solute is irreversibly bound to the polymeric stationary phase. The absolute amount of a solute which will partition irreversibly on to the binding column will be impacted by factors that control the length of time the solute is in the column (*e.g.*, flow-rate and column length), by factors that promote turbulent mixing in the column (and thus promote column–solute interactions, *e.g.*, column geometry) and by factors that influence the rate of diffusion of the solute into the column (*e.g.*, temperature).

The mobile phase flow-rate directly affects the magnitude of solute absorption by the binding column. As the flow-rate decreases, the amount bound by the column increases and in general the peak shape becomes more skewed. The 0.3 ml/min flow-rate applied used here represents the practical lower limit for the polymeric materials and solutes used. Even at this flow-rate, it takes nearly 20 min for the baseline to become re-established after a strongly bound solute is injected into the system.

In many respects, the polymer binding column is similar to a post-column reactor used in HPLC detection. For such reactors, the effect of reactor geometry (*e.g.*, coiled, knotted, knitted) on the efficiency of mixing and the turbulence of the flow within the reactor is well established (*e.g.*, ref. 17). As the polymer binding columns used have large inner diameters, any column configuration which promotes turbulent flow will maximize solute–wall interactions and thus the amount of solute bound by the column. By inducing turbulent flow (knotting the column) and reducing the inner void volume of the column (by filling the column with inert glass beads), one dramatically improves the column's solute binding efficiency. For the more efficient columns, the solute peak is smaller and less skewed.

While changing the column geometry will change the absolute magnitude of $D_b$, the effect should be similar for all solutes. Thus, while the absolute value of $D_b$ would be different for two different column configurations, the regression constants for $D_b$ interaction models for the same column material in two different column configurations should be comparable. Dynamic binding models generated with knotted VA–VC columns either empty or filled with inert glass beads are statistically identical (Fig. 5). The unit slope of the best fit line relating $D_b$ obtained from both column configurations confirms that the column configuration does not impact the

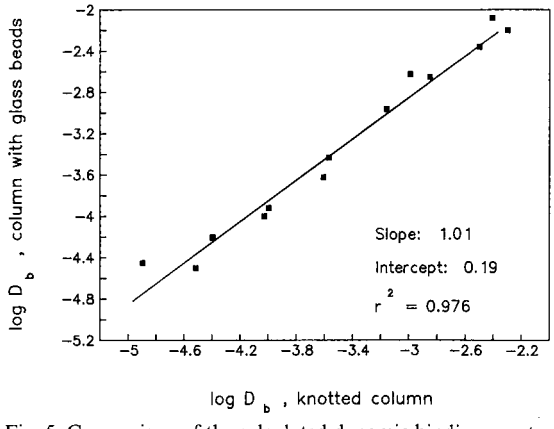


Fig. 5. Comparison of the calculated dynamic binding constants obtained on two different column configurations from the same material. The material used was the VA–VC copolymer and the experiment was performed at a column temperature of 25°C.

trend observed in $D_b$ as a function of solute identity. As shown by the non-zero intercept, the column configuration merely impacts the absolute magnitude of the $D_b$ constant.

Temperature impacts the ability of the solute of diffuse to the surface of the polymer column through the mobile phase and to diffuse into the polymeric material and thus be irreversible bound by the polymer column. One would expect that an increase in column temperature would result in a larger measured $D_b$. As shown in Fig. 6, an increased column temperature results in a reproducible increase in the measured $D_b$.

As the polymeric "column" irreversibly binds a fraction of the solute with each injection, one would expect that after a certain period of time the polymer would become saturated and additional solute binding would cease. Repetitive injections of high concentration sample did not cause a change in the solute's elution response. Replicate injections of one solute, separated by the injection of other solutes, were equivalent in terms of shape and response. Thus column saturation was not observed in this research.

*Relationship between equilibrium and dynamic interaction constants*

The most useful application of $D_b$ would be to provide a rapid estimate of $E_b$, which in turn is a parameter critical to polymer–solute interaction calculations. While the two factors are defined in a similar manner, one suspects that they will not be numerically equivalent because the solution volumes associated with both types of experiments are radically different. Whereas in the case of a shake-flask experiment used to determine $E_b$ the solution interaction volume is known and fixed, in the case of $D_b$ the assignment of the column void volume as the interaction volume is more a matter of convenience (providing internal consistency for $D_b$) than a matter of strict theoretical correctness. This difference between $E_b$ and $D_b$, being a matter of definition, should be species independent and constant and would be reflected as a non-zero intercept in a plot of log $D_b$ *versus* log $E_b$.

Another reason why $E_b$ and $D_b$ might be different is the variable uptake rates of the model solutes themselves. In the dynamic experiment, the solute is in contact with any given portion of the column for a relatively short period of time. For especially the more lipophilic solutes, one could envision a scenario in which there was insufficient interaction time at any given plate to allow for an instantaneous equilibrium between the solution and the column material in the plate to be established. If equilibrium is not established at each plate within the column, then $D_b$ will be inherently less than $E_b$. As one would expect that this effect would be most prevalent for the highly bound, lipophilic solutes, one would expect that a log $D_b$ *versus* log $E_b$ plot would have a slope of less than unity.

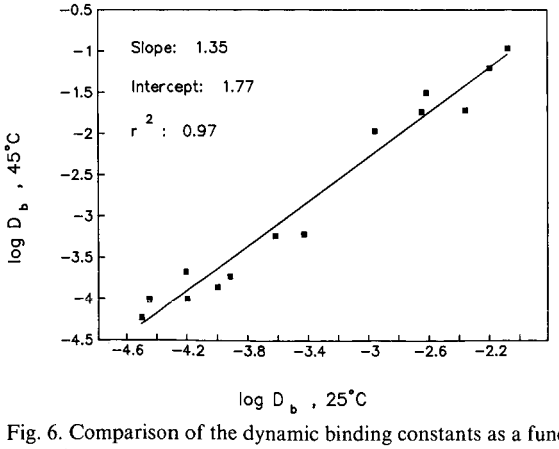


Fig. 6. Comparison of the dynamic binding constants as a function of column temperature. The column used was the knotted configuration of the VA–VC copolymer.

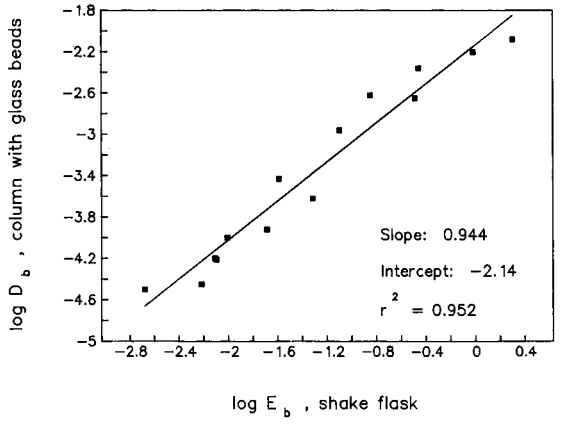


Fig. 7. Comparison of the equilibrium interaction constants and dynamic binding constants for the VA–VC copolymer. The column used was knotted with beads and the experiment was performed at 25°C.

A typical plot of log $D_b$ *versus* log $E_b$ for the three polymers studied is shown in Fig. 7. For all three, the two interaction constants can be linearly related with a modest degree of accuracy. Curve fit parameters are given in Table II. In all instances, the intercept of the best fit line is negative, indicating that $E_b$ tends to be larger than $D_b$. This results was anticipated in the previous discussion. Slopes of the best fit line were less than 1 for the VA–VC and PP materials (although the standard error is sufficiently large that the confidence interval for the slope includes 1.0). For PVC, however, the slope is significantly larger than 1. No explanation for this behavior is apparent.

## CONCLUSIONS

Dynamic interaction constants can be reproducibly determined for various model solutes via a chromatographic method involving a column made from capillaries of polymeric materials. The method requires the comparison of peak sizes when the solute is injected on to a "column" of an inert material and a "column" made from the polymer of interest. The magnitude of the measured $D_b$ is influenced by the conditions employed during the experiment (*e.g.*, column length, flow-rate, column geometry, temperature) but is relatively insensitive to solute concentration over the range 5–50 ppm. Thus, although $D_b$ may change as a function of changing operating conditions, it has proved to be reproducible when the operating conditions are rigidly controlled.

A material's $D_b$ can be linearly correlated with its equilibrium binding constant, thus establishing the dynamic binding approach as a rapid means of determining $E_b$. Once $E_b$ has been determined, one can directly determine the magnitude of a solute–polymer interaction, for example, in a typical container configuration.

## REFERENCES

1 M. S. Mirrlees, S. J. Moulton, C. T. Murphy and P. J. Taylor, *J. Med. Chem.*, 19 (1976) 615–619.
2 T. Yamana, A. Tsuji, E. Miyamota and O. Kubo, *J. Pharm. Sci.*, 66 (1977) 747–749.
3 M. L. Bieganowska, *J. Liq. Chromatogr.*, 5 (1982) 39–48.
4 P. J. Carillo, S. G. Gilbert and H. Daun, *J. Food Sci.*, 53 (1988) 1199–1203.
5 U. Coelho, J. Miltz and S. G. Gilbert, *Macromolecules*, 12 (1988) 1226–1230.
6 J. E. Guillet, M. Romansky, G. J. Price and R. Van der Mark, *ACS Symp. Ser.*, 391 (1989) 20–32.
7 P. Munk, P. Hattam, Q. Du, A. Abdel-Azim, *J. Appl. Polym. Sci., Appl. Polym. Symp.*, 45 (1990), 289–316.
8 G. Schomburg *Trends Anal. Chem.*, 10 (1991) 163–169.
9 A. L. Khurana and C. Ho, *J. Liq. Chromatogr.*, 12 (1989) 1679–1686.
10 J. E. Garst and W. C. Wilson, *J. Pharm. Sci.*, 73 (1984) 1616–1929.
11 A. Bechalany, T. Rothlisberger, N. El Tayar and B. Testa, *J. Chromatogr.*, 473 (1989) 115–124.
12 C. Yamagami, T. Ogura and N. Takao, *J. Chromatogr.*, 514 (1990) 123–136.
13 D. R. Jenke, D. S. Hayward and R. A. Kenly, *J. Chromatogr. Sci.*, 28 (1990) 609–612.
14 L. Illum, H. Bundgaard and S. S. Davis, *Int. J. Pharm.*, 17 (1983) 183–192.
15 C. G. Pitt, Y. T. Bao, A. L. Andrady and P. N. K. Samuel, *Int. J. Pharm.*, 45 (1988) 1–11.
16 D. S. Hayward, R. A. Kenley and D. R. Jenke, *Int. J. Pharm.*, 59 (1990) 245–253.
17 B. Lillig and H. Engelhardt, in I. S. Krull (Editor), *Reaction Detection in Liquid Chromatography*, Marcel Dekker, New York, 1986, pp. 1–61.

*Journal of Chromatography*, 594 (1992) 37–43
Elsevier Science Publishers B.V., Amsterdam

CHROM. 23 865

# Retention behavior of β-cyclodextrin complexes of anthracene and pyrene using reversed-phase liquid chromatography

## The effects of *tert.*-butanol and cyclopentanol

Vincent C. Anigbogu☆, Arsenio Muñoz de la Peña☆☆, Thilivhali T. Ndou and Isiah M. Warner*

*Department of Chemistry, Emory University, Atlanta, GA 30322 (USA)*

(First received July 30th, 1991; revised manuscript received November 8th, 1991)

ABSTRACT

The effects of *tert.*-butanol and cyclopentanol on the formation of β-cyclodextrin (β-CD)–anthracene and β-CD–pyrene complexes have been studied using reversed-phase liquid chromatography. The retention times of anthracene and pyrene were monitored when eluted in a $C_{18}$ column with mobile phase mixtures consisting of methanol, water, β-CD, and a small amount of *tert.*-butanol or cyclopentanol. Plots of capacity factor of anthracene *versus* concentration of β-CD in the mobile phase in methanol–water mixtures and in mixtures containing 1% (v/v) cyclopentanol or *tert.*-butanol as secondary modifiers showed very similar trends. This suggests that anthracene forms weak complexes with β-CD, and that the presence of these secondary mobile phase modifiers have little effect on the β-CD–anthracene inclusion reaction. In contrast, pyrene showed no discernable change in retention time with increases in β-CD concentration. However, in the presence of 1% (v/v) *tert.*-butanol or cyclopentanol, capacity factor of pyrene decreased drastically, more in 1% (v/v) cyclopentanol than in 1% (v/v) *tert.*-butanol. Formation of a ternary β-CD–pyrene–alcohol complex has been proposed to explain the effects.

## INTRODUCTION

It is well established that α-, β- and γ-cyclodextrins (CDs) readily form stable inclusion complexes with a variety of organic and inorganic molecules and ions [1]. The CD-inclusion phenomenon has found applications in pharmaceutics [2] and chromatography [3–9]. Applications in chromatography have mostly centered on the improved resolution of isomers [3–5]. Improvement in resolution results from differences in the retention behavior of the free and complexed solute species in the column. The degree of inclusion of the guest is determined by several factors including cavity size of the CD, the polarity of the solute, the nature and position of substituents on the solute, and the nature and concentration of concomitants in the solution medium.

The effects of concomitant species on the inclusion phenomenon of β-CD have been reported. Hamai [10] has reported on the quenching of fluorescence signal of pyrene- and 1-pyrenesulfonate complexes of β-CD by anilines. Others [11,12] have also shown that there are changes in the chemical behavior of inclusion complexes of CDs in

☆ Present address: Department of Chemistry, Austin Peay State University, Clarksville, TN 37044, USA.
☆☆ Present address: Department of Analytical Chemistry, University of Extremadura, Badajoz 06071, Spain.

0021-9673/92/$05.00 

the presence of surfactants as third components. Ueno *et al.* [13] and Nelson and Warner [14] reported on the concomitant effect of alcohols on the inclusion complexes of cyclodextrins with some guest molecules. Fluorescence studies in our laboratory of the effects of alcohol size on the stoichiometry and formation constants of β-CD and γ-CD complexes of pyrene were recently published [15–167]. The results show that in the presence of small amounts of alcohols as modifiers, ternary complexes of stoichiometry 2:1:2 are formed for β-CD–pyrene–alcohol and 1:1:1 (depending on the size of the alcohol) for γ-CD–pyrene–alcohol, respectively. In the case of β-CD–pyrene–alcohol complexes, the explanation for the observed results is that the *tert.*-butanol or cyclopentanol molecules are positioned at the open ends of the cyclodextrin cavities [15]. In this case, the geometry and molecular volume of the alcohols play important roles in the formation of the ternary complexes with β-CD. In contrast, there does not appear to be a correlation between the size and volume of the alcohols in the formation of γ-CD–pyrene–alcohol complexes. The alcohols are postulated to fill the void inside the γ-CD cavity; thus, the alcohols act as space regulators inside the larger γ-CD cavity.

The use of spectroscopic techniques to study the mechanisms of the inclusion complexes of the CDs has its advantages and disadvantages. The major advantages includes high sensitivity and short analysis time. A major disadvantage is the fact that not all CD inclusion phenomenon would be accompanied by significant changes in spectroscopic signals. Several reports have appeared in the literature on the use of liquid chromatography to study the concomitant effects of alcohols and other compounds on the formation of β-CD complexes. Tarr *et al.* [18] investigated the influence of 1% (v/v) *tert.*-butanol as a secondary organic mobile phase modifier on the retention behavior of 1-methyl-, 2-methyl-, 1,3-dimethyl-, 1,4-dimethylnaphthalenes, and acenaphthylene in a β-CD bonded column. Lamparczyk *et al.* [19] and others [7,8] have examined the effects of molecular structure and the nature and position of substituents on the formation of β-CD complexes in methanol–water mixtures. This paper re-examines fluorescence studies of the effects of *tert.*-butanol and cyclopentanol on the formation of anthracene–β-CD–pyrene complexes using reversed-phase high-performance liquid chromatography (RP-HPLC). Pyrene and anthracene were used as probe molecules in keeping with the experimental conditions of the fluorescence studies [15–17]. The enhanced β-CD solubility in aqueous solutions of methanol and other analytical implications of these effects are discussed.

## EXPERIMENTAL

### *Apparatus*

The liquid chromatographic system consisted of a Beckman Model 114 solvent delivery system equipped with a Rheodyne Model 7010 sample injector with a 20-μl sample loop (Rheodyne, Berkeley, CA, USA) and a Beckman Model 160 variable-wavelength UV absorbance detector set at 255 nm. The column used was a Bondclone $C_{18}$ column (300 mm × 3.9 mm) purchased from Phenomenex (Torrance, CA, USA). The column temperature was maintained at 22 ± 1°C using a Brinkman (Westbury, NY, USA) Model Lauda RM3 constant-temperature bath connected to an Alltech (Deerfield, IL, USA) column water jacket. The Hewlett-Packard (Avondale, PA, USA) Model 3399A integrator was used to acquire and analyze the chromatograms.

### *Reagents*

The primary organic modifier (methanol) and water used were HPLC grade purchased from B&J (Baxter, McGraw Park, IL, USA) and Fisher (Fair Lawn, NJ, USA), respectively. The *tert.*-butanol and the cyclopentanol (secondary organic modifiers), the pyrene (99 + %) and anthracene (99 + %), were all purchased from Aldrich (Milwaukee, WI. USA). These reagents were used as received. The β-cyclodextrin was obtained from American Maize-Products (Hammond, IN, USA) and was also used as received. The column void volume was determined using reagent-grade potassium nitrite purchased from Mallinckrodt (Paris, KY, USA).

### *Procedure for the preparation of samples*

Appropriate amounts of anthracene and pyrene required to make about 0.10 m*M* solution of each were accurately weighed (to the nearest 0.1 mg) into a 250-ml volumetric flask. About 200 ml of methanol were added to the flask; the contents were

sonicated for 10 min and *ca.* 0.5 g of $KNO_2$ added to the flask before diluting to the mark with methanol. Different mobile phase mixtures were prepared by initially making about 4 l of the desired methanol–modifier–water mixtures, which were allowed to equilibrate overnight. A series of solutions from each mixture, containing from 0 to 6 m*M* β-CD, were prepared by weighing appropriate amounts of β-CD into a 1 l HPLC solvent reservoir, adding 500 ml of the solvent mixture and sonicating the mixture at 40°C for 1–3 h. The dissolution time depended on the amount of β-CD and the solution mixture. For example, mixtures with low methanol concentration (<60% (v/v) methanol in water) and those with 1% (v/v) *tert.*-butanol or 1% (v/v) cyclopentanol, dissolved readily within an hour. The mixture solutions containing various β-CD concentrations were allowed to sit overnight before use. It was noticed that higher concentrations of β-CD (>4 m*M*) in methanol–water mixtures, though fully dissolved during the preparation step and stable many hours after, showed some precipitation after they were allowed to stand overnight. Consequently the solutions containing 5 m*M* and 6 m*M* β-CD in methanol–water mobile phase mixtures were discarded. On the other hand, β-CD solutions in mobile phase mixtures containing 1–2% (v/v) *tert.*-butanol or cyclopentanol were stable for several days.

*Procedure for the liquid chromatographic runs*

Mobile phase mixtures were purged with helium for *ca.* 10 min prior to being used to elute the solutes at 1 ml/min. Whenever the mobile phase solution was changed, the column was conditioned for at least 30 min with the new mixture. The solutions containing different concentrations of β-CD were run randomly in an attempt to minimize the effect of drift. For runs with reasonable retention times (less than 45 min), two runs were averaged. Otherwise, one run was made. However, preliminary evaluation showed that retention times were reproducible within 2% in the best and 5% in the worst cases. The column pressure varied from 800 to 2300 p.s.i. and depended on the mobile phase mixture; for a given mixture, it remained constant throughout the run time. This suggests that β-CD was not precipitating in the column as was initially feared, particularly for the methanol–water mixtures containing high concentrations of β-CD. At the end of each set of runs, which usually lasted over 8 h, water was pumped through the column for about 1 h, methanol–water (55:45, v/v) for 10 min, and methanol overnight at a flow-rate of 0.3 ml/min.

## RESULTS AND DISCUSSION

*Effects of organic modifier and β-CD on retention behavior of pyrene and anthracene*

The choice of primary organic modifier and its concentration in the mobile phase mixtures was governed by several factors including short analysis time, adequate solubility of β-CD in the resultant mobile phase mixture, and low formation constant for the β-CD–primary organic modifier in order to minimize competition with the solute molecules for the β-CD cavity. Of the most commonly used polar organic solvents in RP-HPLC, namely acetonitrile, methanol and tetrahydrofuran, methanol forms the weakest complex with β-CD [8]; hence, it was chosen as the primary organic modifier.

As would be expected, the retention times of anthracene and pyrene are very sensitive to the concentration of methanol in the mobile phase. Fig. 1 shows the typical linear relationship between log $k'$ and methanol concentration in the mobile phase, suggestive of a hydrophobic-type interaction between the solute molecules and the stationary phase. The concentration of methanol in the mobile phase is very critical if the interaction between β-CD, the secondary organic modifier, and the solute mole-

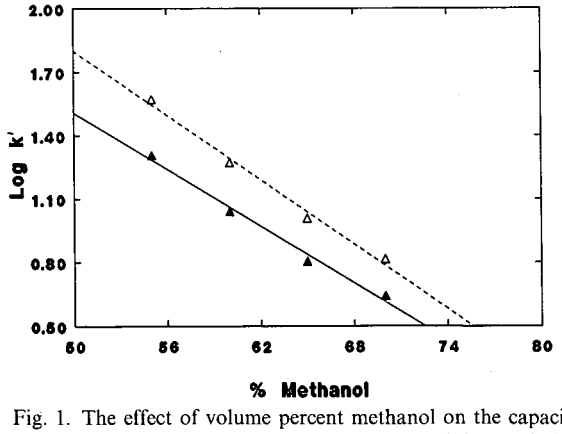


Fig. 1. The effect of volume percent methanol on the capacity factors ($k'$), of anthracene (▲) and pyrene (△) in a solution containing 3.0 m*M* β-CD.

TABLE I

RETENTION TIMES OF ANTHRACENE AND PYRENE IN METHANOL–WATER MOBILE PHASE MIXTURES

| Methanol (%) | Retention time (min) | |
|---|---|---|
| | Anthracene | Pyrene |
| 80 | 7.79 | 9.66 |
| 75 | 12.91 | 18.03 |
| 70 | 18.46 | 25.49 |
| 65 | 24.76 | 36.39 |
| 60 | 43.42 | 65.53 |
| 55 | 66.12 | 125 |

cules is to be observed at reasonable retention times. For example, Table I shows that the retention times of anthracene and pyrene were about 66 and 125 min, respectively, when eluted with methanol–water (55:45, v/v) mixture, and about 18 and 25 min, respectively, with methanol–water (70:30, v/v) mixture. At methanol–water (55-45, v/v), the retention time of pyrene is over 2 h resulting in severely broadened chromatographic peaks. At high concentration of methanol, not only does the solubility of β-CD decreases drastically, but the competitive equilibria between methanol and β-CD molecules are dramatically enhanced. Matsui and Mochida [23] and Buvari *et al.* [24] have independently estimated the apparent formation constants of the β-CD–methanol complex to be 0.32 and 0.40 $M^{-1}$, respectively. Although these numbers suggest that methanol forms very weak complexes with β-CD, it effectively impairs or even precludes the inclusion of many solutes such as pyrene at high concentrations. Consequently, 55, 60 and 65% (v/v) methanol concentrations in water were chosen, in keeping with the three foregoing considerations, as the initial test solutions. Moreover, extreme sensitivity of the retention times of anthracene and pyrene to the methanol concentration in the mobile phase required that extra care be exercised in preparing the mobile phase mixtures. The approach described in the *Procedure for the preparation of samples* section was found satisfactory in maintaining a uniform methanol concentration for a given set of runs.

The effects of β-CD concentration on the capacity factors of anthracene when eluted with different

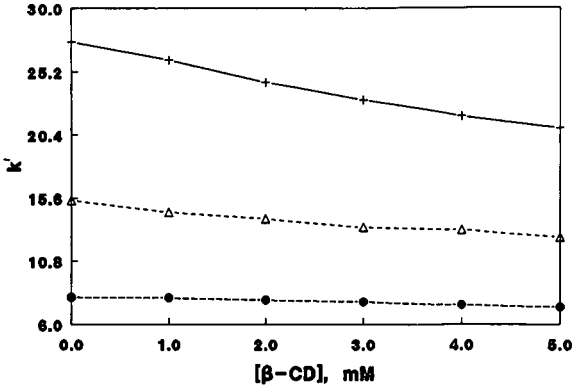


Fig. 2. Plots of $k'$ *vs.* [β-CD] for anthracene in mobile phase mixtures containing 55% (v/v) methanol (+), 60% (v/v) methanol (△) or 65% (v/v) methanol (○).

methanol–water mobile phase mixtures are shown in Fig. 2. Anthracene exhibited the expected decrease in capacity factor with increasing β-CD concentration as the associated molecules interact less with the stationary phase than the free molecules in solution. Also, for a given β-CD concentration, the capacity factor of anthracene decreased with increasing methanol concentration from 55 to 60% (v/v). In contrast, the capacity factors of pyrene (Fig. 3) did not show the expected trend in all methanol–water mixtures (in the absence of co-modifiers). It should be mentioned that both anthracene and pyrene include readily in β-CD in highly aqueous systems [15,16]. A possible explanation for minimal inclu-

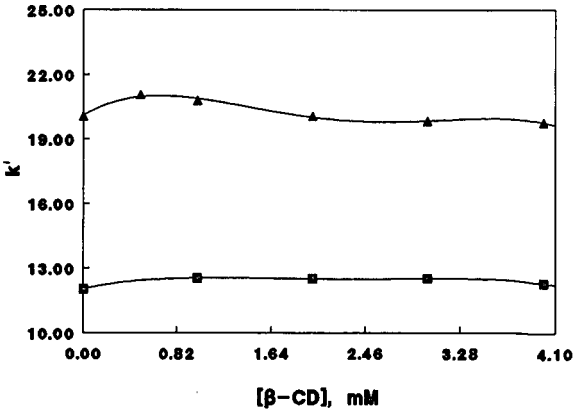


Fig. 3. Plots of $k'$ *vs.* [β-CD] for pyrene in mobile phase mixtures containing 60% (v/v) methanol (▲) and 65% (v/v) methanol (■).

sion of these solutes in these high methanol (> 55% v/v) solutions is the competitive equilibria between the methanol an the solute molecules for the concentration-limited β-CD. It should be reiterated that methanol–water mixtures did not sustain β-CD concentrations above 4 m*M*.

*The effects of secondary organic modifier in the mobile phase on the capacity factor of anthracene and pyrene*

Warner and co-workers [15,16] recently reported their extensive studies of β-CD– and γ-CD–pyrene complexes, in the presence of various alcohols using steady-state fluorescence spectroscopy. In these studies, the apparent formation constants of β- and γ-CD–pyrene complexes were determined by monitoring the variations in the I/III fluorescence vibronic band ratio of pyrene [20–22] with increasing β-CD concentration. In the case of β-CD–pyrene complexes, and 1% (v/v) alcohol concentration in water, all the alcohols investigated showed an enhancement effect (increase in apparent formation constant, $K_f$). The largest increases in β-CD–pyrene $K_f$ values were observed in the presence of *tert.*-butanol (for the straight chain) and cyclopentanol (for the cyclic chain). This observation was attributed to the formation of a ternary complex of β-CD–pyrene–alcohol. The influence of 1% (v/v) *tert.*-butanol as a secondary organic mobile phase modifier on the retention behavior of 1-methyl-, 2-methyl-, 1,3-dimethyl- and 1,4-dimethylnaphthalenes, and acenaphthylene using a bonded β-CD stationary phase has been reported by Tarr *et al.* [18]. The results show that the 1-methyl-, 1,4-dimethylnaphthalenes and acenaphthylene exhibited the largest increases in retention times in the presence of 1% (v/v) *tert.*-butanol. We investigated the effect of the addition of 1% (v/v) *tert.*-butanol and cyclopentanol, as secondary modifiers, on the formation of β-CD–pyrene and β-CD–anthracene complexes especially since we did not discern any complexation of pyrene in mobile phase mixtures of 55, 60 and 65% (v/v) methanol in water mixtures. These effects, if any, would be manifested as decreases in the retention times of these solutes with increasing amounts of β-CD concentration in the mobile phase.

The effects of the secondary modifier on the capacity factor of anthracene, eluted with methanol–modifier–water (54:1:45, v/v/v) and methanol–modifier–water (59:1:40, v/v/v), are shown in Fig. 4. The secondary modifiers seem to have little or no influence on the β-CD–anthracene complex formation. However, as Fig. 5 shows, the capacity factor of pyrene decreased remarkably in the presence of 1% (v/v) *tert.*-butanol or cyclopentanol in the mobile phase. This clearly suggests that these alcohols participate, directly or indirectly, in the formation of the inclusion complexes of pyrene. It should

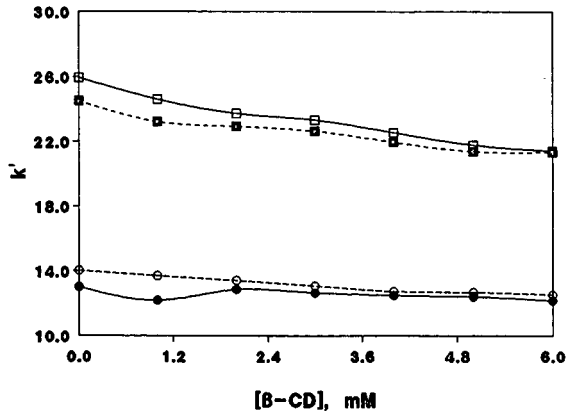


Fig. 4. Plots of *k'* *vs.* [β-CD] for anthracene in mobile phase mixtures methanol–*tert.*-butanol–water (54:1:45, v/v/v) (□), methanol–cyclopentanol–water (54:1:45, v/v/v) (■), methanol–*tert.*-butanol–water (59:1:40, v/v/v) (○) and methanol–cyclopentanol–water (59:1:40, v/v/v) (●).

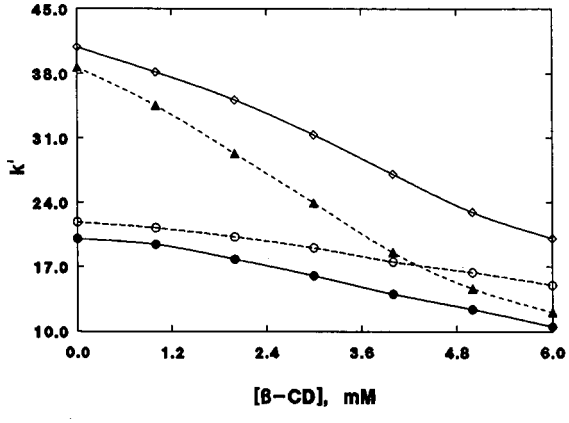


Fig. 5. Plots of *k'* *vs.* [β-CD] for pyrene in mobile phase mixtures methanol–*tert.*-butanol–water (54:1:45, v/v/v) (◇), methanol–cyclopentanol–water (54:1:45, v/v/v) (▲), methanol–*tert.*-butanol–water (59:1:40, v/v/v) (○) and methanol–cyclopentanol–water (59:1:40, v/v/v) (●).

be noted that the effects are more pronounced in aqueous solutions than in the mixtures examined here [9,15,16]. Again, the formation of a ternary complex of β-CD–pyrene–cyclopentanol of 2:1:2 stoichiometric ratio has been postulated to explain these effects [15].

*The effects of secondary modifiers on the selectivity factor*

The decrease in capacity factor of pyrene with increasing β-CD concentration imply that a mobile phase comprised of appropriate concentrations of β-CD and organic modifiers, could be used to enhance both the selectivity and the efficiency of separation by reversed-phase liquid chromatography. For example, the selectivity enhancement is illustrated in Fig. 6 where the separation factor, α, is plotted against total β-CD concentration for different mobile phase mixtures. In the absence of β-CD, the retention time of pyrene is about 1.5 times that of anthracene in all mobile phase mixtures. However, as the concentration of β-CD increases, the retention time of pyrene decreases faster than that of anthracene. This effect is so profound in mixtures containing cyclopentanol that, at 6.0 m*M* β-CD, the retention time of pyrene in methanol–water–cyclopentanol (54:45:1, v/v/v) is about 1.5 times less than that of anthracene. This is a complete reversal of their initial retention times, reducing the separation time by one-third. This observation predicts that at even lower methanol concentration than 55% (v/v), the retention time of pyrene would be further reduced at 6 m*M* β-CD. Another potential application of the modifier effects is their use to improve the solubility and stability of β-cyclodextrin in solutions of high methanol composition. As previously stated in the *Procedure for the preparation of samples* section, high concentrations of β-CD (>4 m*M*) solutions were stable in the presence of *tert.*-butanol or cyclopentanol but not in methanol–water mixtures.

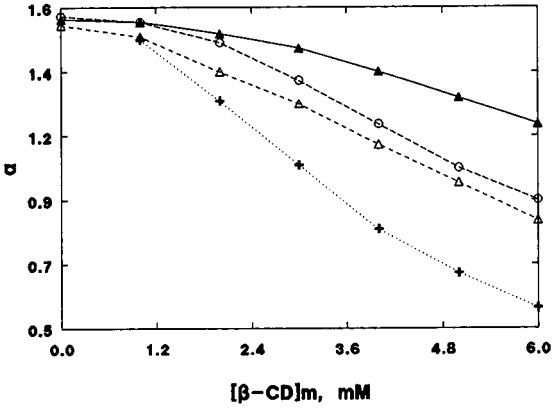


Fig. 6. Plots of selectivity factors, α, as the ratio of $k'$ of pyrene to anthracene, *vs.* [β-CD] in mobile phase mixtures methanol–*tert.*-butanol–water (59:1:40, v/v/v) (▲), methanol–cyclopentanol–water (59:1:40, v/v/v) (○), methanol–*tert.*-butanol–water (54:1:45, v/v/v) (△) and methanol–cyclopentanol–water (54:1:45, v/v/v) (+).

## CONCLUSIONS

The results presented show that the addition of 1% (v/v) *tert.*-butanol or cyclopentanol in methanol–water mobile phase mixtures enhances the complexation of pyrene molecules by β-CD which is in keeping with fluorescence results [9]. In the case of cyclopentanol–methanol–water (1:55:45, v/v/v) this resulted in almost 70% reduction in the retention time of pyrene as its capacity factor changed from 38 to 12, and β-CD concentration changed from 0 to 6.0 m*M*, respectively. The modifier effects could also be used to improve solubility of β-CD in aqueous solutions of polar organic solvents. For example we have been able to prepare 10 m*M* β-CD in methanol–water–cyclopentanol (62:35:3, v/v/v). A full scale study of the solubility effect is already in effect. Another potential use of the ternary forming concomitants is to improve resolution in liquid chromatography or selective extraction of ternary-forming solutes in a mixture. These latter techniques would be applicable to environmental analysis.

It is highly unlikely that pyrene would be the only species that forms ternary complex with β-CD. Other large molecules can be encapsulated partly or fully by one or more β-CD molecules, and the process can further be enhanced by a third component such as alcohols. As previously discussed, both molecular geometry, volume, and polarity influence the degree of β-CD–guest formation. Molecules such as perylene, 1,2,3,6,7,8-hexahydropyrene and 4H-cyclopenta[*def*]phenanthrene, have similar molecular volume and geometry comparable to pyrene, and are being studied by RP-HPLC in an attempt to understand structural relationships, if any, to the ternary complex formation. Obviously,

full exploitation of the β-CD inclusion phenomenon in developing pharmaceutical, spectroscopic, chromatographic and other methodologies depends on some or full knowledge of these kinds of interactions. Our results suggests that liquid chromatography will continue to play a major role in comparative studies of cyclodextrin complexes under various conditions.

## ACKNOWLEDGEMENT

This work was supported by the National Science Foundation (CHE-9001412). A.M.P. acknowledges support from D.G.I.C.Y.T. of the Ministry of Education and Science of Spain for the grant that made possible his research in Professor Warner's Laboratory. The authors are also grateful to G. A. Reed of American Maize Products for providing the β-cyclodextrin used in this study.

## REFERENCES

1 J. Szejtli, *Cyclodextrins and their Inclusion Complexes*, Akademiai Kiado, Budapest, 1982.
2 M. Kurihara, F. Hirayama, K. Uekama and M. Yamasaki, *J. Incl. Phenom.*, 8 (1990) 363.
3 W. L. Hinze and D. W. Armstrong, *Anal. Lett.*, 13 (1980) 1093.
4 D. Sybliska, J. Zukowski and J. Bojarski, *J. Liq. Chromatogr.*, 9 (1986) 591.
5 D. W. Armstrong, *Anal. Chem.*, 59 (1987) 84A.
6 L. A. Blyshak, K. Y. Dobson, G. Patonay, I. M. Warner and N. E. May, *Anal. Chem.*, 61 (1989) 955.
7 R. M. Mohseni and R. J. Hurtubise, *J. Chromatogr.*, 499 (1990) 395.
8 K. Fujimura, T. Ueda, K. Masashi, H. Takayanagi and T. Ando, *Anal. Chem.*, 58 (1986) 2668.
9 V. Anigbogu, A. Muñoz de la Peña, T. T. Ndou and I. M. Warner, *Anal. Chem.*, (1991) in press.
10 S. Hamai, *Bull. Chem. Soc. Jpn.*, 55 (1982) 2721.
11 H. E. Edwards and J. K. Thomas, *Carbohydr. Res.*, 65 (1978) 173.
12 G. Nelson and I. M. Warner, *Carbohydr. Res.*, 192 (1989) 305.
13 A. Ueno, K. Takahashi, Y. Hino and T. Osa, *J. Chem. Soc., Chem. Commun.*, (1981) 194.
14 G. Nelson and I. M. Warner, *J. Phys. Chem.*, 94 (1990) 576.
15 J. B. Zung, A. Muñoz de la Peña, T. T. Ndou and I. M. Warner, *J. Phys. Chem.*, 95 (1991) 6701.
16 A. Muñoz de la Peña, T. T. Ndou, J. B. Zung, K. L. Greene, D. H. Live and I. M. Warner, *J. Am. Chem. Soc.*, 113 (1991) 1572.
17 A. Muñoz de la Peña, T. T. Ndou, V. C. Anigbogu and I. M. Warner, *Anal. Chem.*, 63 (1991) 1018.
18 M. A. Tarr, G. Nelson, G. Patonay and I. M. Warner, *Anal. Lett.*, 21 (1988) 843.
19 H. Lamparczyk, P. Zarzycki, R. J. Ochocka and D. Sybilska, *Chromatographia*, 30 (1990) 91.
20 A. Nakajima, *Spectrochim. Acta*, 39A (1983) 913.
21 S. Hashimoto and J. K. Thomas, *J. Am. Chem. Soc.*, 107 (1985) 4655.
22 J. B. Zung, T. T. Ndou and I. M. Warner, *Appl. Spectrosc.*, 44 (1990) 1491.
23 Y. Matsui and K. Mochida, *Bull. Chem. Soc. Jpn.*, 52 (1979) 2808.
24 A. Buvari, J. Szejtli and I. Barcza, *J. Incl. Phenom.*, 1 (1983) 151.

*Journal of Chromatography*, 594 (1992) 45–64
Elsevier Science Publishers B.V., Amsterdam

CHROM. 23 856

# Selection of robust combinations of extraction liquid composition and internal standard

# Monte Carlo simulation of improvement of assay methods with liquid–liquid extraction prior to high-performance liquid chromatography

J. Wieling*,☆

**Pharma Bio-Research International BV, P.O. Box 200, NL-9470 AE Zuidlaren, and Chemometrics Research Group, Department of Analytical Chemistry and Toxicology, University of Groningen, Antonius Deusinglaan 2, NL-9713 AW Groningen (Netherlands)*

P. M. J. Coenegracht

*Chemometrics Research Group, Department of Analytical Chemistry and Toxicology, University of Groningen, Antonius Deusinglaan 2, NL-9713 AW Groningen (Netherlands)*

C. K. Mensink and J. H. G. Jonkman

*Pharma Bio-Research International BV, P.O. Box 200, NL-9470 AE Zuidlaren (Netherlands)*

D. A. Doornbos

*Chemometrics Research Group, Department of Analytical Chemistry and Toxicology, University of Groningen, Antonius Deusinglaan 2, NL-9713 AW Groningen (Netherlands)*

(First received September 4th, 1991; revised manuscript received October 31st, 1991)

ABSTRACT

The liquid–liquid extraction of a mixture of sulphonamides was achieved to examine the correlation between the experimental errors in the recoveries. Also, the impact of the composition of the extraction liquid was investigated. Six sulphonamides were repeatedly extracted simultaneously with ten different extraction liquids and determined with a reversed-phase high-performance liquid chromatographic (HPLC) system. The means, standard deviations and covariances (or correlations) of the recoveries were calculated. These data showed that correlation between the extraction of two or more structurally related compounds depends strongly on the extraction liquid composition used: the selection of an appropriate extraction liquid is very important for the development of accurate and reproducible assay methods. Selection of improper extraction liquids may introduce errors in internal standard calibration that are larger than the errors in external standard calibration. The selection of a suitable internal standard is also very important for the development of accurate and reproducible assay methods. Even compounds that are structurally related to the analyte may demonstrate completely different extraction behaviour. Selection of a proper internal standard and an accurate extraction liquid increases the

☆ Present address: TNO, IMW, Department of Analytical Chemistry, P.O. Box 6011, NL-2600 JA Delft, Netherlands.

0021-9673/92/$05.00 

accuracy and precision of the method. To investigate the influence on routine analysis, the data were used to simulate 50 analytical runs (calibration graphs with quality control samples) for each sulphonamide separately with external and internal standard calibration. In the latter option the other five sulphonamides were all tested as internal standards. This was done for all extraction liquids used. The results of these simulations demonstrate great differences between different extraction liquid compositions and internal standards for a given analyte. Also the calibration method (internal or external calibration) was found to be very important. Circumstances have been observed where external standard calibration gives better analysis results than internal standard calibration. The method described here can be applied for the selection of a suitable internal standard and extraction liquid for sample preparation by liquid–liquid extraction prior to HPLC.

## INTRODUCTION

In bioanalytical methods, calibration graphs constructed from standard assays in relevant biological media are always required. The goal of method development is to develop accurate measurements, through improvement of procedures, precision and calibration. In biopharmaceutical analysis, three methods of calibration are commonly used: external and internal standard methods and standard addition methods. A detailed discussion of the three methods was given by Smith and Stewart [1]. A variant of the external standard technique, the deferred standard technique, was introduced by Guillemin *et al.* [2]. In this method, the compound to be analysed is injected in pure solution, some time after injection but during the chromatographic run of the real sample.

External standard methods have the disadvantage, as compared with internal standard assays, that each step must be controlled regularly. For example, in liquid–liquid extractions followed by evaporation of part of the organic phase, the partial volume of the organic phase has to be maintained constant during an analytical run or it should be weighed for each standard and each sample. The use of an internal standard through the complete procedure eliminates these problems, as the ratio of analyte and internal standard are considered.

The standard addition method is very well suited for samples with analyte concentrations near the sensitivity limit. The method has the drawback of being a one-point determination; each sample has to be analysed at least twice. If only a few samples are to be measured, the method is well suited, but multiple-sample analytical runs may be more economically analysed using internal standard methods.

The use of internal standard techniques in bioanalytical assay methods with chromatographic determination is common practice. A number of reasons can be given for the importance of the use of internal standards. First, internal standards are used for the correction of injection volume in the case of manual high-performance liquid chromatographic (HPLC) injections and partial loop fillings. Haefelfinger [3] demonstrated that under such circumstances the precision of the volume of injection may be the limiting factor for method reproducibility and that the internal standard technique improves the reproducibility; the imprecision due to the variance of the injection volume can largely be eliminated by use of an internal standard. Haefelfinger also concluded that the use of an internal standard with automated injection with complete loop filling does not improve the precision of chromatographic methods. In fact, he stated that it was better not to use an internal standard under such conditions.

Kelly *et al.* [4] introduced a method for internal standard selection with the use of an internal standard data base and a marker solution. The place of the internal standard peak in the chromatogram was the selection criterion. The approach applies to aqueous acetonitrile eluents and is essentially independent of column manufacturer.

A second argument for the use of an internal standard in chromatographic assays is the interception of chromatographic instability and measurement variability, especially when peak heights are measured in the calibration procedure. Addition of an internal standard compensates for variance in peak heights due to retention time instability or column efficiency variance, as these variances influence both the analyte and internal standard. In assays with chromatographic system instability as the only source of imprecision, addition of internal standards prior to sample preparation is not necessary and addition of an internal standard after sample preparation but prior to injection in the chromatographic system suffices. An example of

addition of internal standard after sample preparation was given by Banno *et al.* [5]. To protect the stability of their HPLC system, Wieling *et al.* [6] developed a computer program that monitors the characteristics of the internal standard such as retention time and the peak area during an analytical run. In this manner, system instabilities can be detected. Sample preparation and injection of extracts into the system are discontinued until the adverse influences have been corrected.

This guarding routine by Wieling *et al.* also monitors the operation of the (robotic) sample preparation, being the third and probably most important basis for the use of internal standards: control of sample preparation and corrections for variances in sample preparation (variance in recovery, adsorption on glassware or variances in evaporation volumes).

Summarizing, an internal standard in chromatographic assays should meet the following requirements: its chromatographic peak is completely resolved, it elutes close to the analyte, its behaviour in any sample preparation procedure is the same as that of the analyte, it is detectable under the same conditions as the analyte, it is not present in original samples and it is stable and not subjected to any reaction except for sample preparation procedures. Usually, a compound structurally as similar as possible and with similar physico-chemical properties is selected.

This paper examines the correlation of the experimental errors of simultaneously extracted sulphonamides and introduces a method for the selection of a suitable internal standard and extraction liquid in sample preparation with liquid–liquid extraction. The recoveries of a mixture of six sulphonamides after replicated liquid–liquid extractions were determined, including the statistical parameters. These results were used to simulate calibration graphs for sulphonamides with external standard calibration and with internal standard calibration by Monte Carlo methods. In Monte Carlo methods, computer-generated observations are easily obtained as independent realizations from the theoretical population distribution, using computer random generators. The mean and the variance of a sample are estimates of the population distributions and are calculated from replicated measurements. Computer simulations can be used to make analytical predictions, including variability. The algorithms for generating recoveries and peak responses after liquid–liquid extraction prior to HPLC determination are discussed in the next section.

The extractions and simulations were done with ten ternary mixtures of three extraction solvents ($\equiv$ ten extraction liquids). The composition of the extraction liquid was the only parameter changed in the liquid–liquid extraction step. In the internal standard alternative, the remaining five sulphonamides were used as internal standards. For each sulphonamide, an internal standard and extraction liquid can be selected that give the best values for the validation criteria preferred.

## THEORY

In the literature, examples were found where the investigation of the characteristics of the recovery of the internal standard was ignored [7] or where the internal standard was added to the extract after the actual extraction and before the instrumental measurement [5]. In the first example the development of the method is not complete. We think that if an internal standard is used for assay control, the properties of this compound (recovery, variance of recovery, covariance of recovery with recoveries of other compounds, retention times, resolutions, etc.) should be investigated in the same way as those of the analyte, with respect to both sample preparation and chromatography. The method in the second example can only be rationalized when the sample preparation is completely under control or when no proper internal standard has been found. A paper by Osman *et al.* [8] described the use of different internal standards for different sample matrices.

In the internal standard method applied for correction of imprecision due to sample preparation, it is generally difficult to select an internal standard that meets all the necessary requirements. These requirements find their origin in both sample preparation and determination as mentioned above: a good internal standard will correct the assay for losses of the compound of interest in the isolation steps and improve the precision of the results by compensating for random errors associated with adsorption losses, extraction yield, aliquot taking, extent of derivatization, decomposition of analyte and instrumental performance. Ideally, the sample

preparation yield of the internal standard and the compound of interest should have a constant ratio throughout the isolation and preparation steps. Therefore, the variance of recoveries of both analyte and internal standard should be completely correlated. This should also be the case in the extraction of a drug with one or more metabolites. It is economically advantageous to determine drug and metabolites within one assay method instead of analysing each compound separately, and therefore it is necessary to find suitable conditions.

In sample preparation using liquid–liquid extraction and internal standard calibration, two quantities determine the quality of the real extraction step of a compound: first, the extraction yield of the analyte (and to a lesser extent that of the internal standard) is important, as high recoveries guarantee more sensitive methods. Second, a robust ratio of the extraction yields of the analyte and the internal standard has a considerable effect on the precision and accuracy of the method (robust with respect to varying random conditions). In cases where several analytes are extracted in one extraction step (*e.g.*, a drug with several metabolites or co-drugs), all recoveries should be maximized and the robustness of all ratios of recoveries should be optimized. If the recovery of a compound is *ca.* 100%, then it can be expected that the variation in recovery will be small. However, if recoveries of 100% cannot be obtained, then one should try to optimize the variance in the recovery and in the extraction ratio, if an internal standard is used.

According to Curry and Whelpton [9] the probability that the internal standard will adversely affect the data is significant and should be considered. This can occur in a number of ways according to Curry and Whelpton: first, if an error can arise in the extraction of the analyte, then it can arise just as easily in extraction of the internal standard; second, if calibration is non-linear (*e.g.*, in gas chromatographic assays with electron-capture detection), then a variance in the internal standard response will inevitably cause, rather than correct, an error in the response to the analyte.

The first argument by Curry and Whelpton can be rejected in many instances for the following reason: if two compounds are extracted simultaneously, they are both subjected to a number of random variables that are not under control of the analyst: small variances in room temperature, small variances in the sample matrix used, small variances in glassware, etc. However, we expect that these variances will have more or less the same effect on the amount of analyte and internal standard extracted into the organic phase if their physico-chemical properties and structures are similar. In other words, the variances in the recoveries of both compounds are more or less correlated. This leads to the conclusion that, even if analyte and internal standard recoveries have large variances, an assay may be good if these variances in the recoveries of both compounds are highly correlated, that is, if random variables have identical effects on both compounds. It is the responsibility of the analytical chemist to find a suitable internal standard and a suitable composition of the extraction liquid. The combination of these two elements should provide a constant extraction ratio of internal standard and analyte. The second argument of Curry and Whelpton (non-linearity) is not a problem arising during sample preparation, but is a detection problem that can be solved by proper selection of calibration experiments and/or calibration models.

A problem in sample preparation using liquid–liquid extraction that demands the use of internal standard may be the different extraction behaviours of the internal standard and analyte with respect to variance in random conditions (room temperature, time of extraction and intensity of extraction). This may introduce errors larger than the errors in the external standard calibration. Indeed, in these instances the internal standard should be removed from the procedure, substituted by a different compound or the complete liquid–liquid extraction procedure should be modified/changed (other extraction liquid, etc.).

In two papers [10,11], Snyder and Van der Wal discussed the sources of imprecision that can affect assays based on solvent extraction and HPLC analysis. An example was given that demonstrates an increase in assay imprecision with decrease in analyte recovery. Snyder and Van der Wal also explained why internal standard calibration does not guarantee an improvement in assay precision: precision may sometimes even be worse for internal standard calibration, because the number of measurements in internal standard calibration is double that in external standard calibration. The overall

precision of assay methods may therefore sometimes be negatively affected if the imprecision in the double measurements is larger than the imprecision of external standard calibration, where no correction is made for procedure variance.

The mean recovery, $R_a$, and the variance of this recovery, $S_a^2$, of an analyte depend strongly on the sample matrix and on the composition of the extraction liquid [12–16]. Introduction of an internal standard introduces two new quantities, $R_i$ and $S_i^2$. The ratio of the recoveries $Q$ and its variance $S_Q^2$ are determined by the recoveries $R_a$ and $R_i$ of both compounds, the variances in the recoveries $S_a^2$ and $S_i^2$ and the covariance $S_{a,i}^2$ between the recoveries of both compounds when they are extracted simultaneously.

The ratio of the recoveries of two compounds is expressed by the ratio of the two recoveries:

$$Q = R_a/R_i \tag{1}$$

The rules for error propagation give an expression for the variance of the ratio of the recoveries:

$$S_Q^2 = S_a^2\left(\frac{\partial Q}{\partial R_a}\right)^2 + S_i^2\left(\frac{\partial Q}{\partial R_i}\right)^2 + 2S_{a,i}^2\left(\frac{\partial Q}{\partial R_a}\cdot\frac{\partial Q}{\partial R_i}\right)$$

$$= Q^2\left[\left(\frac{S_a}{R_a}\right)^2 + \left(\frac{S_i}{R_i}\right)^2 - 2\cdot\frac{S_{a,i}^2}{R_aR_i}\right] \tag{2}$$

The partial derivatives provide an estimate of the change in the overall response variable $Q$ with a change in one of the component variables ($R_a$ and $R_i$) while the other component variable is held constant.

When the variables $R_a$ and $R_i$ are completely independent of each other (*i.e.*, uncorrelated) the covariance $S_{a,i}^2$ is zero and the variance of the ratio is

$$S_Q^2 = Q^2\left[\left(\frac{S_a}{R_a}\right)^2 + \left(\frac{S_i}{R_i}\right)^2\right] = \frac{S_a^2}{R_i^2} + Q^2\cdot\frac{S_i^2}{R_i^2} \tag{3}$$

The covariance can be calculated from $n$ replicate measurements of the recoveries of both compounds:

$$S_{a,i}^2 = \frac{\sum_{j=1}^{n}(R_{a_j} - \bar{R}_a)(R_{i_j} - \bar{R}_i)}{n-1} \tag{4}$$

The correlation coefficient $\rho$ is a measure of the correlation between the two variances of the recovery of each compound:

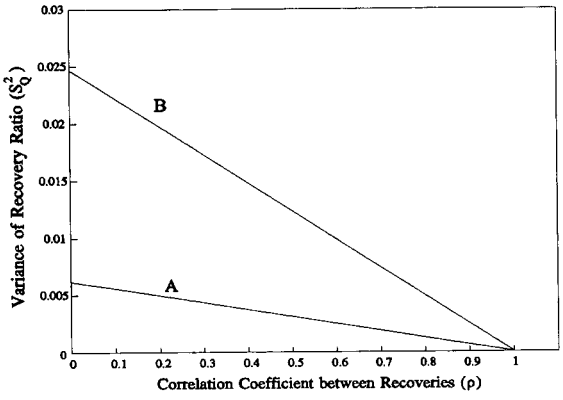


Fig. 1. Variance of the ratio of the recovery of analyte and internal standard as a function of their correlation. [$R_i = R_a = 90\%$; $S_i = S_a$ = (A) 5% and (B) 10%].

$$\rho = S_{a,i}^2/S_aS_i \tag{5}$$

A detailed discussion on error propagation was given by Ku [17] and Balke [18].

In conclusion, the variance of the ratio of the recovery of two compounds is a function of the ratio $Q$, the recoveries of the compounds $R_a$ and $R_i$, the variances of the recoveries of both compounds $S_a^2$ and $S_i^2$ and the correlations between those variances $\rho$. Figs. 1 and 2 describe the influence of the variances and the correlation coefficient on the variance of the ratio $Q$ ($S_Q^2$). In Fig. 1, the recoveries of both compounds are assumed to be 90% ($Q = 1$) and their standard deviations are both 5% in situation A and both 10% in situation B. The variance in the ratio of the recoveries is plotted against the correlation coefficient between the experimental errors. There is a linear relationship between correlation coefficient and the variance of the recovery ratio (Fig. 1). In Fig. 2, the variance in the ratio is plotted against the variance in the recoveries of both compounds (the S.D.s for both compounds are equal) for different correlation coefficients between the experimental errors in the recovery. There is a linear relationship between the variance in the recoveries of the analytes and the variance in the recovery ratio (Fig. 2), which can also be understood from eqn. 2. Figs. 1 and 2 and eqn. 2 show that not only the correlation of experimental errors is important for method quality, it is also important that the individual experimental errors are not too large.

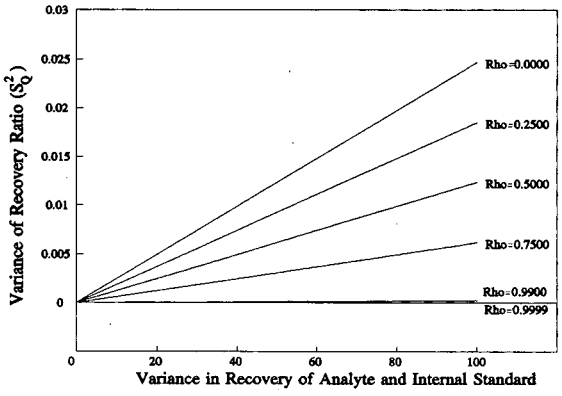


Fig. 2. Variance of the ratio of the recovery of analyte and internal standard as a function of their individual variances ($S_i = S_a$) at different correlation coefficients ($R_i = R_a = 90\%$).

## EXPERIMENTAL

### *Instruments and instrumental conditions*

The assay was performed with an HPLC system consisting of a Spectra-Physics (San Jose, CA, USA) SP8700 solvent-delivery system at a flow-rate of 1.0 ml $min^{-1}$ and a Kratos (Ramsey, NJ, USA) Model 757 UV detector, wavelength 260 nm, range 0.005 a.u.f.s., rise time 1 s. The injections of extracts into a Zymark (Zymark, Hopkinton, MA, USA) Z 310 HPLC injection station, equipped with an electrically controlled Rheodyne valve and a 20-$\mu$l sample loop, were performed by a Zymate II robot system. The Zymark Z 310 Analytical Instrument Interface was used to control the HPLC injection station. Data analysis was performed by means of a Spectra-Physics Chromjet SP4400 computing integrator. The analytical column was a Microsphere 3-$\mu$m $C_{18}$ cartridge system (100 × 4.6 mm I.D.) (Chrompack, Middelburg, Netherlands).

Mixing was performed on a Type VF2 vortex mixer (Janke und Kunkel, Staufen, Germany), shaking of the extraction container was performed on a Heidolph (Kelheim, Germany) Reax-2S shaker and a Labofuge GL (Heraeus-Christ, Osterode am Harz, Germany) was used for centrifugation.

Simulations and calculations were performed on an IBM PS/2 Model 80-A31 computer using a laboratory-made software package written in Pascal under MS-DOS 3.3.

### *Chemicals and reagents*

The sulphonamides sulphisomidine (SOMI), sulphathiazole (THIA), sulphapyridine (PYRI), sulphamerazine (MERA), sulphamethoxypyridazine (MEPY) and sulphachloropyridazine (CLPY) were supplied by Sigma (St. Louis, MO, USA). The structural formulae are given in Fig. 3. Acetonitrile (ACN), tetrahydrofuran (THF), dichloromethane (DCM) and methanol (MeOH) were supplied by Labscan (Dublin, Ireland) and were of HPLC grade. Chloroform (ChromAR) (Clf) was of analytical-reagent grade and supplied by Malinckrodt (Promochem, Wesel, Germany). Acetic acid (100%) (HAc), triethylamine (TEA), phosphoric acid (85%), potassium dihydrogenphosphate ($KH_2PO_4$) and ammonium acetate were all of analytical-reagent grade and supplied by Merck (Darmstadt, Germany). Methyl *tert.*-butyl ether (Uvasol) (tBME) was also supplied by Merck. Water was purified by using a Milli-RO-4 and a Milli-Q water purification system

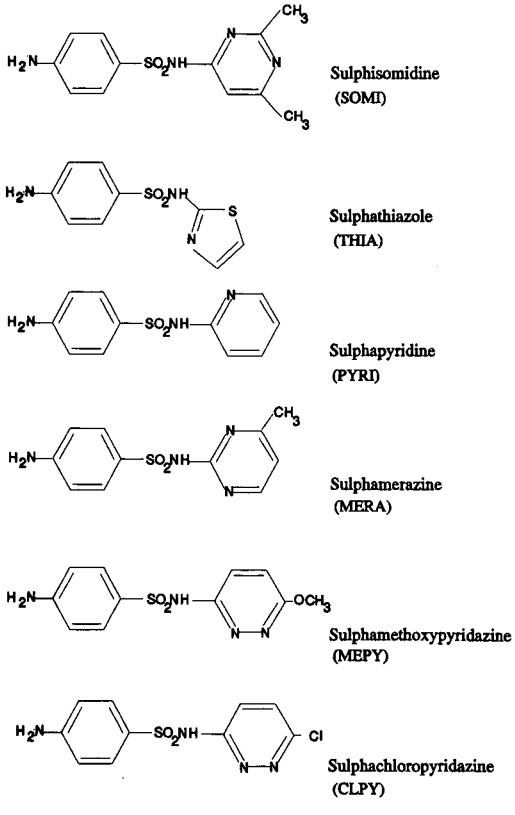


Fig. 3. Structural formulae of the sulphonamides investigated.

TABLE I

EXTRACTION LIQUID COMPOSITIONS INVESTIGATED FOR THE SIMULTANEOUS EXTRACTION OF SIX SULPHONAMIDES

| No. | Fraction DCM | Fraction Clf | Fraction tBME |
|---|---|---|---|
| 1 | 1.000 | 0.000 | 0.000 |
| 2 | 0.000 | 1.000 | 0.000 |
| 3 | 0.000 | 0.000 | 1.000 |
| 4 | 0.500 | 0.500 | 0.000 |
| 5 | 0.500 | 0.000 | 0.500 |
| 6 | 0.000 | 0.500 | 0.500 |
| 7 | 0.333 | 0.333 | 0.333 |
| 8 | 0.666 | 0.167 | 0.167 |
| 9 | 0.167 | 0.666 | 0.167 |
| 10 | 0.167 | 0.167 | 0.666 |

(Millipore, Bedford, MA, USA). Unless stated otherwise, Milli-Q-water was used.

Dichloromethane, chloroform and methyl *tert.*-butyl ether were used to prepare ten pure, binary and ternary extraction liquids in accordance with Table I and Fig. 4. These three solvents are commonly used extraction solvents and were selected from the solvent selectivity theory according to Rohrschneider [19] and Snyder [20]. The solvents selected were similar to those which Glajch *et al.* [21] used for normal-phase liquid chromatography. Methyl *tert.*-butyl ether was selected instead of diethyl ether as it is less volatile.

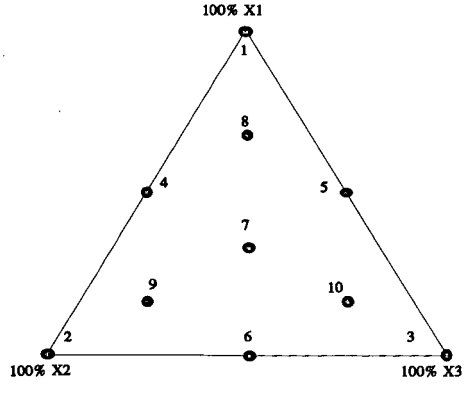


Fig. 4. Extraction liquid compositions where the recoveries of six sulphonamides have been measured prior to simulation. X1 = Dichloromethane; X2 = chloroform; X3 = methyl *tert.*-butyl ether.

An acetate buffer (pH 5.0; 0.5 *M*) was prepared by dissolving 3.85 g of ammonium acetate in 100 ml of water. pH adjustment was performed using concentrated acetic acid.

A phosphate buffer (pH 3.0; 0.05 *M*) was prepared by dissolving 6.80 g of $KH_2PO_4$ in 1000 ml of water. pH adjustment was performed using concentrated phosphoric acid. To this buffer 4.15 ml of TEA and 10 ml of acetic acid were added.

The mobile phase was optimized using the POEM (Predicting Optimal Eluent Mixtures) computer optimization package [22]. A description of the optimization of the mobile phase was given by Wieling *et al.* [23]. The mobile phase was prepared by mixing 1 ml of acetonitrile, 5 ml of THF and 140 ml of methanol and adding phosphate buffer (pH 3.0; 0.05 *M*) to 1000 ml.

The stock solutions of sulphonamides were prepared by dissolving 100 mg of the compounds in 100 ml of methanol. These solutions were stored at 4°C and were used to prepare a standard solution (1 mg $l^{-1}$ in water) used for the extraction studies containing all six sulphonamides. This solution was stored at 4°C.

*Analytical procedure*

A 250-µl aliquot of blank human plasma, 250 µl of the standard solution and 250 µl of acetate buffer solution were pipetted in a 11.5-ml glass tube and mixed for 10 s on a vortex mixer. An aliquot of 9 ml of extraction liquid were added and the tubes were extracted for 5 min with a Heidolph tumble mixer at 20 rpm.

After centrifugation at 4000 rpm (2755 *g*) for 10 min, the organic layer was transferred to another 11.5-ml glass tube and evaporated to dryness under a gentle stream of nitrogen at 55°C. The residue of the sample was reconstituted in 1 ml of 50% methanol and 20 µl were injected into the HPLC system. Extractions were repeated five times. Peak areas were measured as the response criterion.

For the determination of the absolute analytical recovery of the sulphonamides, the peak areas of prepared samples were compared with peak areas measured by injecting directly seven times the standard solution into the HPLC system.

*Calibration graph simulation*

*Internal standard calibration simulation.* For each

composition of the extraction liquid the mean and standard deviation of the recoveries of the six sulphonamides were determined with the procedure outlined above. Also, the covariances and the correlations between the variances of the recoveries of each pair of sulphonamides were determined.

These data were used to simulate calibration graphs with eight different concentrations of analyte of 10, 20, 50, 100, 200, 500, 800 and 1000 concentration units $l^{-1}$. One sulphonamide was selected as the analyte, while the five other sulphonamides were successively used as internal standards. In turn each sulphonamide was selected as the analyte. The simulation of a calibration graph was always accompanied by simulation of four quality control samples (duplicates at two concentration levels, 15.00 and 900.0 concentration units $l^{-1}$).

Simulation of standards was done with the following procedure, which demonstrates the simulation of a calibration graph for an assay method using liquid–liquid extraction as the sample clean-up step. One particular analyte, one particular internal standard and one particular extraction liquid were used in the procedure.

Recoveries and peak areas were simulated with an algorithm that produces random data of the recoveries of internal standard according to a gaussian distribution [24] as follows.

(1) For a particular extraction liquid composition: simulate an observation of the recovery of the analyte $R_a$ by adding a random error component $S_a$ to the "true" value of the recovery of the analyte $\bar{R}_a$:

$$R_a = \bar{R}_a + S_a \cos[2\pi random(0\ldots1)]\{\sqrt{-2\ln[random(0\ldots1)]}\}$$

or

$$R_a = \bar{R}_a + S_a \sin[2\pi random(0\ldots1)]\{\sqrt{-2\ln[random(0\ldots1)]}\}$$

Both equations are needed alternately to obtain random results.

(2) For the same extraction liquid composition, simulate an observation of the recovery of the selected internal standard $R_i$ by adding a random error component $S_i$ to the "true" value of the recovery of the internal standard $\bar{R}_i$ using the correlation $\rho_{a,i}$ between the variances of the recoveries of analyte and internal standard:

$$R_i = \rho_{a,i} \cdot \frac{S_i}{S_a}(R_a - \bar{R}_a) + \bar{R}_i + \sqrt{S_i(1-\rho_{a,i}^2)} \cdot \cos[2\pi random(0\ldots1)]\{\sqrt{-2\ln[random(0\ldots1)]}\}$$

or

$$R_i = \rho_{a,i} \cdot \frac{S_i}{S_a}(R_a - \bar{R}_a) + \bar{R}_i + \sqrt{S_i(1-\rho_{a,i}^2)} \cdot \sin[2\pi random(0\ldots1)]\{\sqrt{-2\ln[random(0\ldots1)]}\}$$

Both equations are needed alternately to obtain random results.

(3) Generate a peak area for the analyte from the simulated observation $R_a$. If the recovery of the analyte is 100% a peak area of 100 000 was generated for the highest standard. For the lower concentration levels a peak area was generated of 100 000 times a concentration factor:

$$\textit{peak area standard} = 100\,000R_a \cdot \frac{\textit{concentration units standard}}{\textit{concentration units highest standard}}$$

(4) Generate a peak area for the internal standard from the simulated observation $R_i$. For the internal standard a peak area of 50 000 was generated in the case of 100% recovery:

$$\textit{peak area internal standard} = 50\,000R_i$$

(5) Repeat steps 1–4 for each concentration level of the analyte to obtain the complete calibration graph (= eight times).

(6) Simulate four quality control samples (duplicates at two concentration levels, 15.00 and 900.0 concentration units $l^{-1}$) using steps 1–4.

In this way, a calibration graph consisting of eight points is obtained, together with two quality control samples in duplicate. In turn each sulphonamide is considered as being the analyte; the other five sulphonamides are successively observed as being the internal standard for each extraction liquid composition in Fig. 4. The ratio of the peak area of the analyte to that of the internal standard is used as the response factor (Fig. 5).

This total procedure (steps 1–6) is repeated 50 times for each combination of analyte, internal standard and extraction liquid (= 50 analytical runs).

The procedure above denotes that the magnitude and the variance in the recovery of the analyte in this

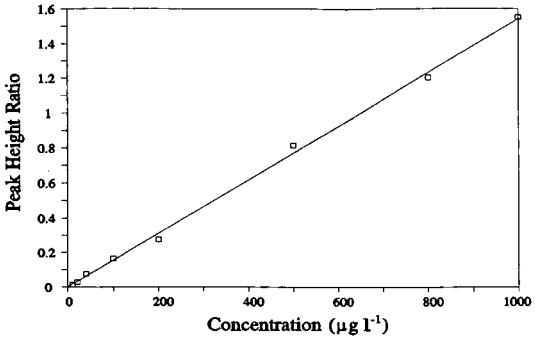


Fig. 5. Example of a simulated calibration graph at eight concentration levels.

simulation experiment are not affected by the concentration of the analyte (the relative standard deviation of the recovery is constant; no concentration effect on recovery is simulated). As a consequence, the standard deviation of the peak area ratio is proportional to concentration.

*External standard calibration simulation.* A similar procedure was followed for the external standard calibration, in which the simulation of internal standard recoveries and internal standard peak areas was omitted. The correlation coefficients between the experimental errors of the recoveries of two solutes were not required: steps 2 and 4 in the procedure described above are omitted. Here, the response used for calculating calibration models was the peak area of the analyte.

*Procedure summary*

Recovery data for the replicate extraction of a mixture of sulphonamides in ten different extraction liquid compositions were obtained. The recovery data were used to select robust combinations of internal standard and extraction liquid composition for a particular analyte. The differences in the quality of the different methods were predicted and demonstrated by Monte Carlo simulation of assay methods using liquid–liquid extraction prior to HPLC for the given analyte, internal standard and extraction liquid. Alternatively, if external standard calibration may give better quality control data, the internal standard was omitted.

It is also possible to use the method for the selection of an extraction liquid composition that gives the most robust results for all recoveries and recovery ratios after extraction of several analytes.

TABLE II

RECOVERIES AND STANDARD DEVIATIONS OF THE SULPHONAMIDES FOR THE DIFFERENT COMPOSITIONS OF THE EXTRACTION LIQUID

| Fractional composition of extraction liquid | | | Sulphonamide | | | | | | |
|---|---|---|---|---|---|---|---|---|---|
| DCM | Clf | tBME | SOMI | THIA | PYRI | MERA | MEPY | CLPY | C.V. (%)[a] |
| 1.000 | 0.000 | 0.000 | 0.759 (0.016) | 0.755 (0.020) | 0.931 (0.017) | 0.962 (0.019) | 0.940 (0.012) | 0.950 (0.022) | 2.0 |
| 0.000 | 1.000 | 0.000 | 0.741 (0.027) | 0.551 (0.022) | 0.885 (0.032) | 0.950 (0.031) | 0.931 (0.028) | 0.923 (0.029) | 3.4 |
| 0.000 | 0.000 | 1.000 | 0.694 (0.032) | 0.684 (0.030) | 0.890 (0.032) | 0.910 (0.034) | 0.894 (0.039) | 0.945 (0.047) | 4.3 |
| 0.500 | 0.500 | 0.000 | 0.746 (0.013) | 0.710 (0.011) | 0.954 (0.008) | 0.985 (0.012) | 0.972 (0.007) | 0.944 (0.017) | 1.3 |
| 0.500 | 0.000 | 0.500 | 0.796 (0.015) | 0.799 (0.019) | 0.891 (0.017) | 0.911 (0.020) | 0.876 (0.018) | 0.900 (0.023) | 2.2 |
| 0.000 | 0.500 | 0.500 | 0.676 (0.017) | 0.666 (0.024) | 0.848 (0.026) | 0.911 (0.029) | 0.882 (0.030) | 0.904 (0.027) | 3.1 |
| 0.333 | 0.333 | 0.333 | 0.726 (0.017) | 0.739 (0.021) | 0.887 (0.022) | 0.902 (0.021) | 0.885 (0.023) | 0.875 (0.033) | 2.7 |
| 0.666 | 0.167 | 0.167 | 0.767 (0.016) | 0.841 (0.015) | 0.949 (0.015) | 0.961 (0.016) | 0.951 (0.012) | 0.932 (0.020) | 1.8 |
| 0.167 | 0.666 | 0.167 | 0.728 (0.032) | 0.743 (0.028) | 0.908 (0.033) | 0.943 (0.036) | 0.922 (0.028) | 0.889 (0.028) | 3.6 |
| 0.167 | 0.167 | 0.666 | 0.693 (0.008) | 0.779 (0.016) | 0.901 (0.020) | 0.921 (0.026) | 0.897 (0.024) | 0.901 (0.026) | 2.3 |
| C.V. (%)[b] | | | 2.6 | 2.9 | 2.5 | 2.6 | 2.4 | 3.0 | 2.7 |

[a] Mean of six coefficients of variation for one extraction liquid.
[b] Mean of ten coefficients of variation for one solute.

TABLE III

CORRELATIONS BETWEEN THE MEASUREMENT ERRORS OF THE RECOVERIES OF EACH PAIR OF SULPHONAMIDES FOR TEN DIFFERENT COMPOSITIONS OF THE EXTRACTION LIQUID

| Fractional composition of extraction liquid | | | Sulphonamide pair | | | | | |
|---|---|---|---|---|---|---|---|---|
| DCM | Clf | tBME | SOMI THIA | SOMI PYRI | SOMI MERA | SOMI MEPY | SOMI CLPY | THIA PYRI |
| 1.000 | 0.000 | 0.000 | 0.9171 | 0.9333 | 0.9462 | 0.7501 | 0.9312 | 0.9868 |
| 0.000 | 1.000 | 0.000 | 0.9932 | *0.9785* | 0.9694 | 0.8728 | 0.8756 | 0.9530 |
| 0.000 | 0.000 | 1.000 | 0.9880 | 0.9772 | 0.9784 | *0.9681* | 0.9763 | *0.9973* |
| 0.500 | 0.500 | 0.000 | 0.8170 | 0.6643 | **−0.1801** | 0.2627 | 0.3584 | 0.8720 |
| 0.500 | 0.000 | 0.500 | *0.9974* | 0.9713 | *0.9971* | 0.8299 | 0.6775 | 0.9731 |
| 0.000 | 0.500 | 0.500 | 0.9558 | 0.9550 | 0.9531 | 0.9177 | 0.8871 | 0.9943 |
| 0.333 | 0.333 | 0.333 | 0.9501 | 0.9013 | 0.9151 | 0.9537 | *0.9898* | 0.9291 |
| 0.666 | 0.167 | 0.167 | **0.4097** | 0.7716 | 0.7348 | 0.6188 | 0.4885 | **0.5801** |
| 0.167 | 0.666 | 0.167 | 0.9559 | 0.9517 | 0.9509 | 0.8969 | 0.7154 | 0.9899 |
| 0.167 | 0.167 | 0.666 | 0.6877 | **0.1562** | 0.1186 | **−0.2302** | **−0.4712** | 0.8138 |
| **Minimum correlation** | | | 0.4097 | 0.1562 | −0.1801 | −0.2302 | −0.4712 | 0.5801 |
| *Maximum correlation* | | | 0.9974 | 0.9785 | 0.9971 | 0.9681 | 0.9898 | 0.9973 |

TABLE IV

RATIOS OF THE RECOVERIES ($Q$) AND THEIR STANDARD DEVIATIONS ($S_Q$) OF EACH PAIR OF SULPHONAMIDES FOR TEN DIFFERENT COMPOSITIONS OF THE EXTRACTION LIQUID

| Fractional composition of extraction liquid | | | Sulphonamide pair | | | | | |
|---|---|---|---|---|---|---|---|---|
| DCM | Clf | tBME | SOMI THIA | SOMI PYRI | SOMI MERA | SOMI MEPY | SOMI CLPY | THIA PYRI |
| 1.000 | 0.000 | 0.000 | 1.006 | 0.816 | 0.789 | 0.808 | 0.799 | 0.811 |
| | | | (0.011) | (0.007) | (0.006) | (0.012) | (0.007) | (0.007) |
| 0.000 | 1.000 | 0.000 | 1.344 | 0.837 | 0.780 | 0.795 | 0.802 | 0.623 |
| | | | (0.008) | (0.006) | (0.007) | (0.014) | (0.014) | (0.008) |
| 0.000 | 0.000 | 1.000 | 1.015 | 0.780 | 0.763 | 0.777 | 0.734 | 0.768 |
| | | | (0.007) | (0.010) | (0.009) | (0.009) | (0.008) | (0.007) |
| 0.500 | 0.500 | 0.000 | 1.052 | 0.782 | 0.758 | 0.768 | 0.790 | 0.744 |
| | | | (0.010) | (0.010) | (0.017) | (0.013) | (0.015) | (0.007) |
| 0.500 | 0.000 | 0.500 | 0.997 | 0.894 | 0.874 | 0.909 | 0.885 | 0.897 |
| | | | (0.005) | (0.004) | (0.004) | (0.011) | (0.016) | (0.006) |
| 0.000 | 0.500 | 0.500 | 1.014 | 0.797 | 0.742 | 0.766 | 0.748 | 0.786 |
| | | | (0.015) | (0.008) | (0.008) | (0.011) | (0.010) | (0.006) |
| 0.333 | 0.333 | 0.333 | 0.982 | 0.818 | 0.804 | 0.820 | 0.830 | 0.833 |
| | | | (0.010) | (0.009) | (0.008) | (0.006) | (0.012) | (0.009) |
| 0.666 | 0.167 | 0.167 | 0.912 | 0.808 | 0.798 | 0.807 | 0.823 | 0.886 |
| | | | (0.020) | (0.011) | (0.012) | (0.014) | (0.018) | (0.014) |
| 0.167 | 0.666 | 0.167 | 0.979 | 0.802 | 0.772 | 0.789 | 0.819 | 0.819 |
| | | | (0.013) | (0.012) | (0.011) | (0.017) | (0.025) | (0.004) |
| 0.167 | 0.167 | 0.666 | 0.890 | 0.769 | 0.752 | 0.773 | 0.769 | 0.864 |
| | | | (0.013) | (0.018) | (0.021) | (0.024) | (0.028) | (0.011) |
| C.V. (%)[b] | | | 1.1 | 1.2 | 1.3 | 1.6 | 1.9 | 1.0 |

[a] Means of the coefficient of variation of the ratio of the recoveries of two compounds of fifteen combinations of two compounds in one particular extraction liquid composition.

[b] Means of the coefficient of variation of the ratio of the recoveries of two compounds in ten different extraction liquid compositions.

| THIA MERA | THIA MEPY | THIA CLPY | PYRI MERA | PYRI MEPY | PYRI CLPY | MERA MEPY | MERA CLPY | MEPY CLPY |
|---|---|---|---|---|---|---|---|---|
| 0.9773 | 0.9457 | 0.7661 | 0.9825 | 0.8989 | 0.8308 | 0.8652 | 0.8082 | 0.5517 |
| 0.9375 | 0.8368 | 0.8179 | 0.9884 | 0.9214 | 0.9207 | 0.8709 | 0.9624 | 0.8040 |
| 0.9910 | 0.9800 | *0.9971* | 0.9820 | 0.9674 | *0.9952* | *0.9952* | *0.9949* | *0.9853* |
| **0.3039** | **0.5341** | 0.8129 | **0.5762** | **0.7582** | 0.8554 | **0.5049** | **0.7164** | 0.7760 |
| 0.9951 | 0.8497 | 0.6560 | 0.9760 | 0.8168 | 0.7467 | 0.7969 | 0.7222 | **0.2270** |
| **0.9966** | *0.9845* | 0.8186 | 0.9915 | *0.9937* | 0.8669 | 0.9789 | 0.8216 | 0.8451 |
| 0.9477 | 0.9533 | 0.9138 | 0.9975 | 0.9838 | 0.9138 | 0.9907 | 0.9197 | 0.9581 |
| 0.5385 | 0.5582 | 0.7356 | 0.9955 | 0.9537 | 0.9008 | 0.9736 | 0.8918 | 0.8786 |
| *0.9991* | 0.9627 | 0.8889 | 0.9943 | 0.9879 | 0.8673 | 0.9732 | 0.8933 | 0.8843 |
| 0.7905 | 0.5437 | **0.2890** | *0.9992* | 0.9235 | **0.7045** | 0.9367 | 0.7227 | 0.8969 |
| 0.3039 | 0.5341 | 0.2890 | 0.5762 | 0.7582 | 0.7045 | 0.5049 | 0.7164 | 0.2270 |
| 0.9991 | 0.9845 | 0.9971 | 0.9992 | 0.9937 | 0.9952 | 0.9952 | 0.9949 | 0.9853 |

| THIA MERA | THIA MEPY | THIA CLPY | PYRI MERA | PYRI MEPY | PYRI CLPY | MERA MEPY | MERA CLPY | MEPY CLPY | C.V. (%)[a] |
|---|---|---|---|---|---|---|---|---|---|
| 0.784 | 0.803 | 0.795 | 0.967 | 0.990 | 0.980 | 1.024 | 1.013 | 0.990 | |
| (0.006) | (0.012) | (0.014) | (0.004) | (0.009) | (0.013) | (0.011) | (0.014) | (0.019) | 1.1 |
| 0.580 | 0.592 | 0.597 | 0.931 | 0.950 | 0.958 | 1.020 | 1.029 | 1.008 | |
| (0.009) | (0.013) | (0.014) | (0.006) | (0.014) | (0.014) | (0.016) | (0.009) | (0.019) | 1.4 |
| 0.752 | 0.765 | 0.724 | 0.978 | 0.996 | 0.942 | 1.018 | 0.963 | 0.946 | |
| (0.007) | (0.007) | (0.005) | (0.007) | (0.012) | (0.014) | (0.007) | (0.013) | (0.010) | 1.0 |
| 0.720 | 0.730 | 0.752 | 0.968 | 0.981 | 1.010 | 1.013 | 1.043 | 1.030 | |
| (0.012) | (0.010) | (0.008) | (0.010) | (0.005) | (0.011) | (0.011) | (0.013) | (0.013) | 1.3 |
| 0.877 | 0.912 | 0.888 | 0.978 | 1.017 | 0.990 | 1.039 | 1.012 | 0.974 | |
| (0.002) | (0.012) | (0.018) | (0.005) | (0.012) | (0.017) | (0.015) | (0.018) | (0.028) | 1.2 |
| 0.731 | 0.755 | 0.737 | 0.931 | 0.962 | 0.938 | 1.033 | 1.008 | 0.976 | |
| (0.004) | (0.005) | (0.016) | (0.004) | (0.005) | (0.015) | (0.007) | (0.019) | (0.018) | 1.2 |
| 0.819 | 0.835 | 0.845 | 0.983 | 1.003 | 1.015 | 1.020 | 1.032 | 1.012 | |
| (0.008) | (0.008) | (0.013) | (0.002) | (0.005) | (0.018) | (0.004) | (0.019) | (0.014) | 1.1 |
| 0.875 | 0.884 | 0.903 | 0.987 | 0.998 | 1.019 | 1.011 | 1.032 | 1.021 | |
| (0.015) | (0.014) | (0.013) | (0.002) | (0.005) | (0.010) | (0.005) | (0.010) | (0.012) | 1.3 |
| 0.788 | 0.806 | 0.836 | 0.963 | 0.984 | 1.022 | 1.022 | 1.061 | 1.038 | |
| (0.001) | (0.009) | (0.015) | (0.004) | (0.008) | (0.018) | (0.011) | (0.018) | (0.015) | 1.3 |
| 0.845 | 0.868 | 0.864 | 0.978 | 1.005 | 1.000 | 1.027 | 1.022 | 0.995 | |
| (0.014) | (0.020) | (0.026) | (0.005) | (0.010) | (0.021) | (0.010) | (0.021) | (0.013) | 2.0 |
| 1.0 | 1.4 | 1.8 | 0.5 | 0.9 | 1.5 | 0.9 | 1.5 | 1.6 | 1.3 |

## RESULTS AND DISCUSSION

### *Results of the extraction*

The recoveries of the sulphonamides and their standard deviations after extraction into the ten extraction liquids are given in Table II. Also, mean coefficients of variation (C.V.) are given for each extraction liquid composition, demonstrating the differences between the variance of extraction of each composition. As the extractions were repeated five times, there is some uncertainty in the resulting variance and covariance estimates. A discussion on confidence limits for population variance was given by Box *et al.* [25]. We assume that the recoveries measured ($R_1, R_2, \ldots, R_n$) are independent, normally distributed random variables having mean $\mu$ and variance $\sigma^2$. The standardized sum of squares, $\sum z_j^2$, of deviations from the population means has a chi-squared distribution with $n$ degrees of freedom:

$$\sum z_j^2 = \frac{\sum (R_j - \mu)^2}{\sigma^2} \sim \chi^2$$

For very precise estimation of a population variance many observations are needed. This is beyond the scope of this paper; here, it is important to obtain a first estimate of variances and covariances.

The influence of the extraction liquid composition (C.V. = 1.3–4.3%) on the variance of the extraction of individual compounds is far more significant than the influence of the solute (C.V. = 2.4–3.0%). A Bartlett test [26] indicated that the variance in the direction of extraction liquid compositions was significantly different from the variance in the direction of solutes. The correlations between the experimental errors of the recoveries of each pair of sulphonamides in each extraction liquid are given in Table III. The highest values for the standard deviations in the recoveries are measured in pure chloroform and methyl *tert.*-butyl ether (Table II). However, especially in pure methyl *tert.*-butyl ether, correlations between the experimental errors are very high. This high correlation reduces the standard deviation of the ratio of the recoveries in this extraction liquid composition. Small variance in the recoveries is measured in binary (50:50) mixtures of dichloromethane and chloroform. However, here the correlations are significantly lower than those for the previous extraction liquids. Table IV gives the values for $Q$ and $S_Q$ for all pairs of sulphonamides. The differences in the variance of the extraction of the compounds that could be seen in the direction of extraction liquids (Table II) are considerably reduced when it concerns ratios of recoveries. Table IV shows that in the direction of compounds (C.V. = 0.9–1.9%) and in the direction of extraction liquids (C.V. = 1.0–2.0%), the robustness is approximately equal. The overall mean coefficient of variation of ratios of recoveries is 1.3%, which is less than 50% of that of separate recovery data (overall mean coefficient of variation = 2.7%). Hence, generally, ratios of the extraction yield of two compounds are more robust than individual recovery data. A clear exception to this statement is presented by sulphisomidine and sulphachloropyridazine in extraction liquid 10: the coefficients of variation of individual recoveries are 1.2% and 2.9%, respectively, whereas the coefficient of variation of their ratio is 3.6%. From Table IV, the differences between the use of different extraction liquid compositions is clear: in the extraction of sulphisomidine with sulphamerazine used as the internal standard, the coefficient of variation in the ratios of the recoveries are as follows:

extraction liquid 2: C.V. = 0.007/0.780 · 100 = 0.9%

extraction liquid 3: C.V. = 0.009/0.763 · 100 = 1.2%

extraction liquid 4: C.V. = 0.017/0.758 · 100 = 2.2%

extraction liquid 10: C.V. = 0.021/0.752 · 100 = 2.8%

From all tables, a clear effect of the composition of the extraction liquid can be seen. Recoveries and standard deviations of recoveries and correlations of the recoveries of pairs of sulphonamides vary with the extraction liquid composition.

The combination of analyte and internal standard with the largest range between the minimum and maximum correlation between the experimental errors of the recoveries over the different extraction liquids is the combination of sulphisomidine with sulphachloropyridazine. This combination also demonstrates the worst correlation of all combinations (−0.4712 in extraction liquid composition 10, Table III). Under these conditions, the standard deviation of the ratio of the recoveries is 3.6% (0.028/0.769 · 100%). Sulphapyridine and sulpha-

methoxypyridazine demonstrate the smallest range. The best correlation is demonstrated by the recoveries of sulphapyridine and sulphamerazine with a ternary mixture (extraction liquid 10). Under these conditions, the coefficients of variation of the recoveries of these sulphonamides are 2.2% and 2.9%, respectively. The C.V. of their ratio is small, 0.5%. Most stable values for the C.V. of the ratio of recoveries are measured for sulphapyridine and sulphamerazine in extraction liquids 7 and 8 (0.2%). From the results discussed above, it can be concluded that optimization of extraction liquid composition in addition to the choice of the internal standard is possible.

*Monte Carlo simulation of routine analysis of sulphisomidine*

As the results for sulphisomidine and sulphachloropyridazine show the largest differences, this pair is used to demonstrate the internal standard and extraction liquid composition selection procedure by means of routine analysis simulation with Monte

TABLE V

SUMMARY OF SIMULATED CALIBRATION GRAPHS FOR SULPHISOMIDINE WITH EXTERNAL STANDARD CALIBRATION AND WITH SULPHACHLOROPYRIDAZINE AS THE INTERNAL STANDARD FOR DIFFERENT EXTRACTION LIQUIDS

$\mu(x_1) = 15.00$; $\mu(x_2) = 900.0$; $n = 50$.

| Extraction liquid composition[a] | $\bar{r}$[b] (range) | $\bar{x}_1$[c] (range) | C.V. (%) (range) | $\bar{x}_2$[c] (range) | C.V. (%) (range) |
|---|---|---|---|---|---|
| 1[d] | 0.99971 | 14.44 | 1.8 | 899.1 | 1.5 |
| | 0.99886–1.0000 | 10.56–18.50 | 0.2–5.4 | 861.0–940.2 | 0.1–5.4 |
| 1 | 0.99996 | 15.08 | 0.6 | 898.5 | 0.7 |
| | 0.99980–1.0000 | 13.58–16.82 | 0.0–2.5 | 881.7–913.8 | 0.0–2.1 |
| 2[d] | 0.99931 | 15.44 | 3.1 | 899.8 | 3.0 |
| | 0.99806–0.99998 | 4.26–23.88 | 0.0–9.4 | 809.0–992.7 | 0.0–9.1 |
| 2 | 0.99986 | 15.37 | 1.2 | 895.28 | 1.3 |
| | 0.99947–0.99999 | 11.92–18.10 | 0.0–4.3 | 869.2–924.8 | 0.0–3.4 |
| 3[d] | 0.99887 | 16.05 | 4.0 | 897.77 | 4.4 |
| | 0.99291–0.99995 | 3.81–23.83 | 0.1–23.8 | 830.2–986.1 | 0.1–11.7 |
| 3 | 0.99993 | 14.90 | 1.0 | 898.30 | 0.9 |
| | 0.99966–0.99999 | 13.33–16.42 | 0.0–2.5 | 881.3–923.5 | 0.1–2.4 |
| 4 | 0.99978 | 15.08 | 1.4 | 901.12 | 1.5 |
| | 0.99906–0.99999 | 9.42–19.72 | 0.0–4.6 | 861.2–948.6 | 0.0–4.8 |
| 5 | 0.99982 | 15.12 | 1.6 | 898.96 | 1.4 |
| | 0.99878–0.99999 | 10.15–18.95 | 0.2–4.2 | 869.2–933.9 | 0.0–3.5 |
| 6 | 0.99990 | 14.90 | 1.2 | 900.30 | 1.0 |
| | 0.99949–1.0000 | 11.81–17.56 | 0.1–3.7 | 872.0–923.6 | 0.0–4.5 |
| 7 | 0.99985 | 15.12 | 1.2 | 896.31 | 1.1 |
| | 0.99941–0.99999 | 12.07–18.19 | 0.0–4.2 | 876.8–923.8 | 0.0–3.3 |
| 8 | 0.99981 | 15.14 | 1.8 | 901.36 | 2.0 |
| | 0.99927–1.0000 | 10.24–19.02 | 0.1–5.0 | 866.5–947.3 | 0.0–5.5 |
| 9 | 0.99946 | 15.20 | 2.7 | 899.89 | 2.9 |
| | 0.99788–0.99999 | 9.91–22.88 | 0.0–8.6 | 860.2–992.5 | 0.0–8.4 |
| 10[d] | 0.99992 | 15.03 | 1.0 | 899.58 | 0.9 |
| | 0.99959–1.00000 | 12.89–18.05 | 0.0–3.0 | 876.4–922.2 | 0.1–3.0 |
| 10 | 0.99935 | 15.40 | 2.7 | 899.5 | 3.3 |
| | 0.99750–0.99994 | 7.01–20.49 | 0.0–9.7 | 829.1–963.4 | 0.0–8.0 |

[a] For compositions, see Table I.
[b] $r$ = Correlation coefficient of the calibration graph simulated.
[c] $\bar{x}_i$ = Mean concentration of a quality control sample analysed in duplicate with a coefficient of variation C.V. (%).
[d] Simulation of external standard calibration.

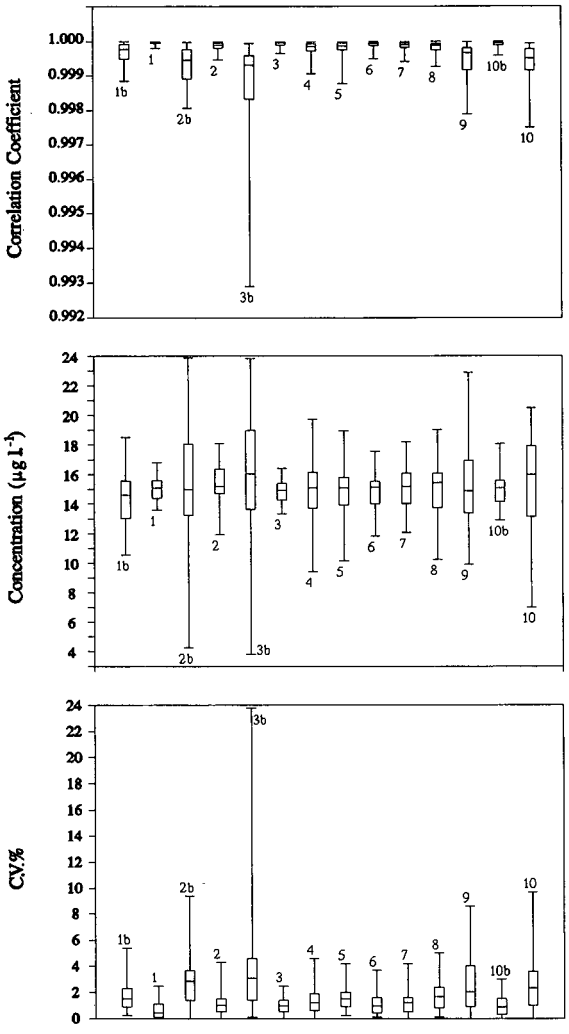


Fig. 6. Box-and-whisker plots for the correlation coefficients of the calibration graphs, the mean of quality control sample ($\mu$ = 15.00 $\mu$g $l^{-1}$) and the coefficient of variation of the duplicate quality control samples ($\mu$ = 15.00 $\mu$g $l^{-1}$) after simulation of the extraction of sulphisomidine with internal and external standard calibration using different extraction liquid compositions (data in Table V).

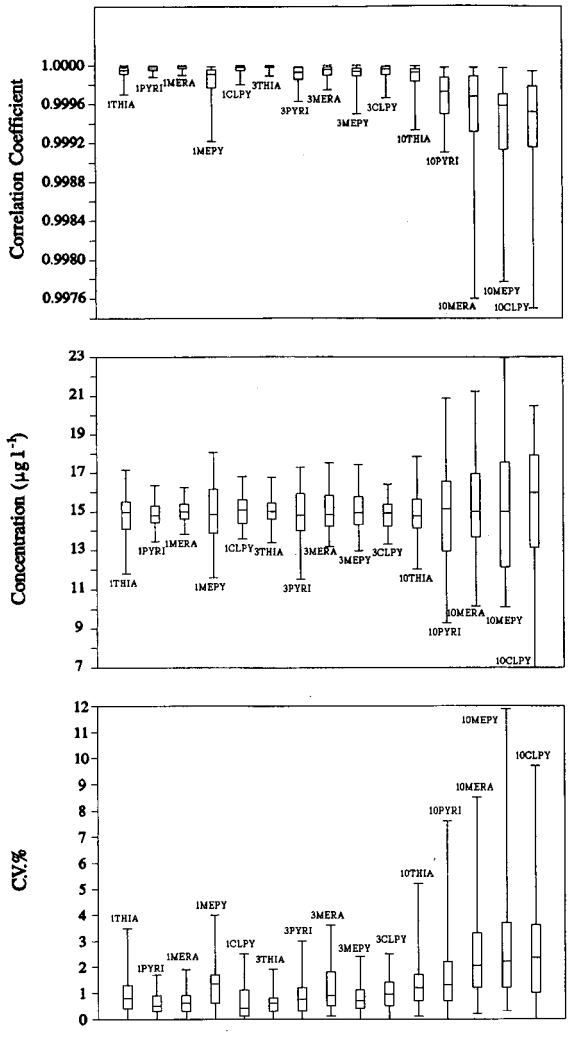


Fig. 7. Box-and-whisker plots for the correlation coefficients of the calibration graphs, the mean of quality control sample ($\mu$ = 15.00 $\mu$g $l^{-1}$) and the coefficient of variation of the duplicate quality control samples ($\mu$ = 15.00 $\mu$g $l^{-1}$) after simulation of the extraction of sulphisomidine with different extraction liquid compositions and different internal standards (data in Table VI).

Carlo methods. A summary of the calibration graphs simulated for sulphisomidine and sulphachloropyridazine with different extraction liquids is given in Table V. The data in this table are also plotted as box-and-whisker plots in Fig. 6 to illustrate the differences graphically. The central boxes in the plots cover the middle 50% of the data values, between the lower and upper quartiles. The whiskers extend out to the minimum and maximum values, while the central lines are at the medians. Table VI and the box-and-whisker plots in Fig. 7 show the simulation results of liquid–liquid extraction of sulphisomidine with five internal standards in three extraction liquids. These tables and figures demon-

TABLE VI

SUMMARY OF SIMULATED CALIBRATION GRAPHS FOR SULPHISOMIDINE WITH FIVE OTHER SULPHONAMIDES AS INTERNAL STANDARD AND WITH THREE DIFFERENT EXTRACTION LIQUIDS

$\mu(x_1) = 15.00$; $\mu(x_2) = 900.0$; $n = 50$.

| Extraction liquid[a] | Internal standard | $\bar{r}^b$ (range) | $\bar{x}_1{}^c$ (range) | C.V. (%) (range) | $\bar{x}_2{}^c$ (range) | C.V. (%) (range) |
|---|---|---|---|---|---|---|
| 1 | THIA | 0.99993 | 14.79 | 1.0 | 901.00 | 0.9 |
| | | 0.99970–1.0000 | 11.81–17.19 | 0.0–3.5 | 879.8–919.8 | 0.0–3.0 |
| | PYRI | 0.99997 | 14.86 | 0.6 | 899.70 | 0.6 |
| | | 0.99988–1.00000 | 13.46–16.35 | 0.0–1.7 | 884.9–915.9 | 0.0–1.9 |
| | MERA | 0.99998 | 15.03 | 0.6 | 899.36 | 0.7 |
| | | 0.99990–1.0000 | 13.83–16.26 | 0.0–1.9 | 886.5–913.3 | 0.0–2.4 |
| | MEPY | 0.99984 | 14.97 | 1.4 | 901.87 | 1.3 |
| | | 0.99922–0.99999 | 11.61–18.09 | 0.0–4.0 | 885.9–928.7 | 0.0–3.9 |
| | CLPY | 0.99996 | 15.08 | 0.6 | 898.5 | 0.7 |
| | | 0.99980–1.0000 | 13.58–16.82 | 0.0–2.5 | 881.7–913.8 | 0.0–2.1 |
| 3 | THIA | 0.99998 | 15.01 | 0.6 | 900.54 | 0.6 |
| | | 0.99989–1.0000 | 13.41–16.80 | 0.0–1.9 | 884.6–913.9 | 0.0–1.9 |
| | PYRI | 0.99989 | 14.93 | 1.0 | 898.86 | 0.9 |
| | | 0.99963–0.99999 | 11.54–17.30 | 0.0–3.0 | 876.2–928.9 | 0.0–2.5 |
| | MERA | 0.99994 | 15.11 | 1.2 | 899.06 | 0.9 |
| | | 0.99975–1.0000 | 13.20–17.54 | 0.1–3.6 | 867.2–922.9 | 0.0–2.9 |
| | MEPY | 0.99990 | 15.12 | 0.8 | 898.69 | 1.0 |
| | | 0.99950–1.0000 | 12.99–17.46 | 0.0–2.4 | 878.9–919.3 | 0.0–2.5 |
| | CLPY | 0.99993 | 14.90 | 1.0 | 898.30 | 0.9 |
| | | 0.99966–0.99999 | 13.33–16.42 | 0.0–2.5 | 881.3–923.5 | 0.1–2.4 |
| 10 | THIA | 0.99985 | 14.85 | 1.4 | 900.00 | 1.1 |
| | | 0.99933–0.99999 | 12.05–17.88 | 0.1–5.2 | 870.1–926.2 | 0.1–3.0 |
| | PYRI | 0.99966 | 15.02 | 1.6 | 897.11 | 1.6 |
| | | 0.99910–0.99997 | 9.31–20.89 | 0.0–7.6 | 849.4–944.5 | 0.0–4.9 |
| | MERA | 0.99948 | 15.16 | 2.5 | 896.17 | 2.7 |
| | | 0.99760–0.99997 | 10.16–21.24 | 0.2–8.5 | 822.6–944.2 | 0.0–8.2 |
| | MEPY | 0.99940 | 14.98 | 2.9 | 896.67 | 2.5 |
| | | 0.99777–0.99997 | 10.12–22.96 | 0.3–11.9 | 847.4–958.0 | 0.0–7.5 |
| | CLPY | 0.99935 | 15.40 | 2.7 | 899.5 | 3.3 |
| | | 0.99750–0.99994 | 7.01–20.49 | 0.0–9.7 | 829.1–963.4 | 0.0–8.0 |

[a] For compositions, see Table I.

[b] $r$ = Correlation coefficient of the calibration graph simulated.

[c] $\bar{x}_i$ = Mean concentration of a quality control sample analysed in duplicate with a coefficient of variation C.V. (%).

strate that the quality of a method can be improved by selection of the proper internal standard and with extraction by a suitable extraction liquid. Criteria to judge these improvements here are the predictive qualities of the calibration model (concentration of control samples) and reproducibility (C.V.) of the concentrations of control samples and the linearity of the simulated calibration graphs (correlation coefficient $r$).

The results in Tables V and VI are based on recovery data. Errors arising during phase separation, evaporation, injection, etc., are not taken into account in this simulation experiment: they are assumed to be equal for all extraction liquid compositions. Concluding, the only source of variation assumed here that causes variation in experimental error and in covariation of experimental errors is the extraction liquid composition and the potential internal standard selected. The results of the simulations (especially with external standard calibration)

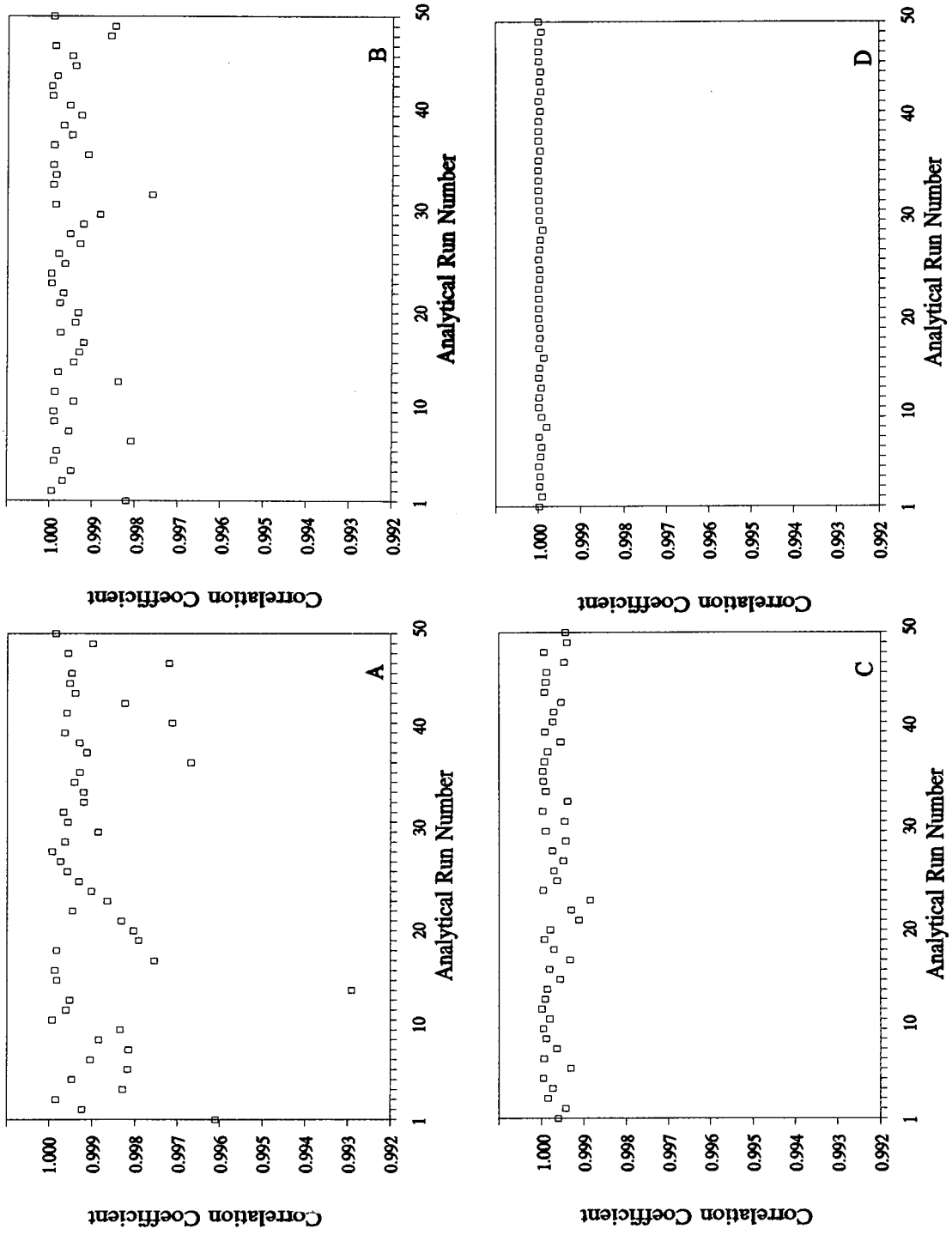


Fig. 8. Quality control chart of linearity of 50 simulated calibration graphs using four different combinations of internal standard and extraction liquid. For description of methods A, B, C and D, see Results and Discussion.

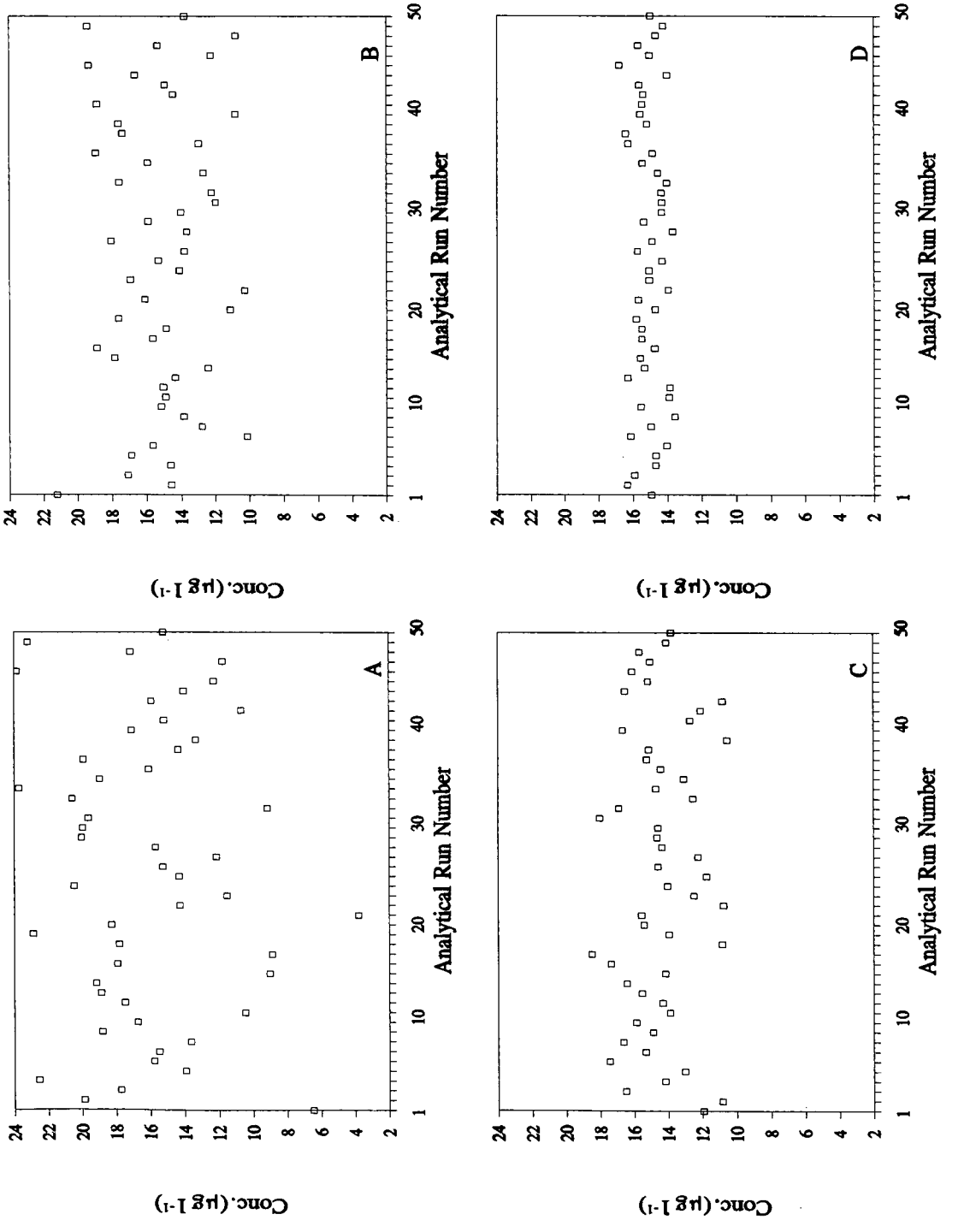


Fig. 9. Quality control chart of control samples (concentrations; $n = 2$) during 50 simulated analytical runs using four different combinations of internal standard and extraction liquid ($\mu = 15.00\ \mu g\ l^{-1}$). For description of methods A, B, C and D, see Results and Discussion.

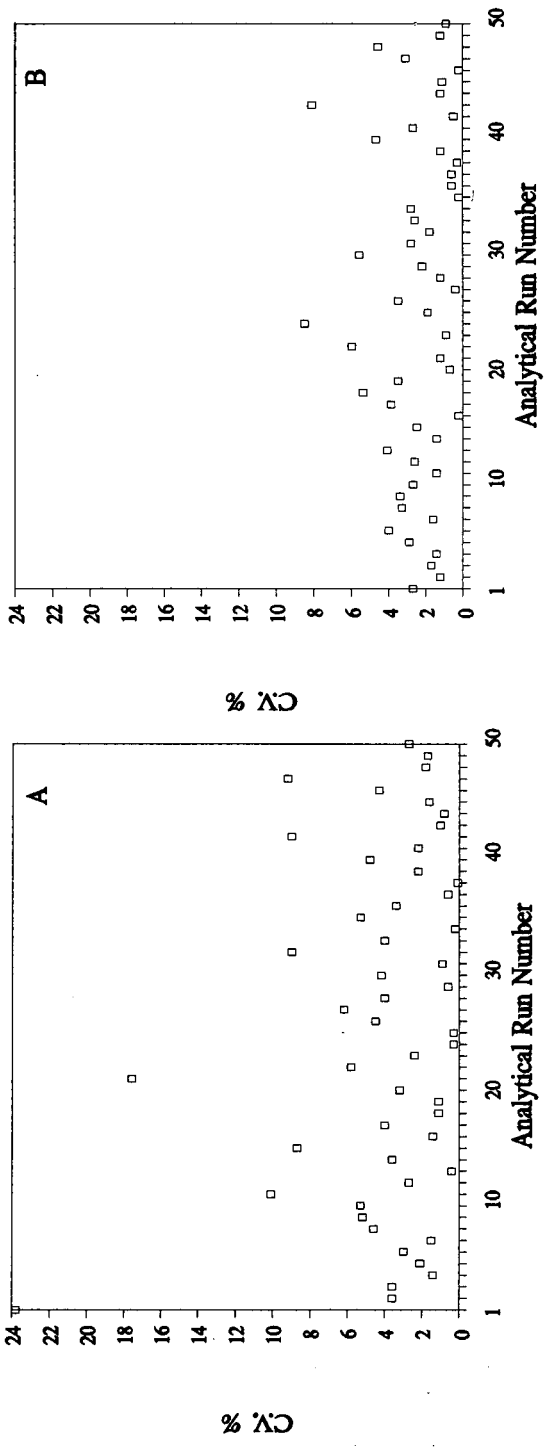


Fig. 10. Quality control chart of control samples (coefficient of variation of duplicates of $\mu = 15.00\ \mu g\ l^{-1}$) during 50 simulated analytical runs using four different combinations of internal standard and extraction liquid. For description of methods A, B, C and D, see Results and Discussion.

may be slightly optimistic as compared with the results one might obtain during the actual routine analysis: there may be small concentration effects, especially when low concentrations are used. However, the results of the routine analysis simulation give a good initial estimate of the behaviour under laboratory circumstances.

From Table V, it can be observed that there is a very large difference between external and internal standard calibration, especially for extraction into extraction liquid 3. An exception to this statement is extraction liquid composition 10. If sulphisomidine is being extracted with this composition it is better not to use the internal standard method, as better results are obtained with external standard calibration: none of the sulphonamides used in this investigation is suitable as an internal standard with extraction liquid composition 10 (Table VI). Figs. 8–10 demonstrate the simulated routine analysis (50 analytical runs) of sulphisomidine under four different conditions. These figures illustrate the difference that may arise between different methods with respect to calibration method, internal standard selected and extraction liquid composition selected. Situation (A) represents analysis with external standard calibration using extraction liquid composition 3. Situation (B) represents analysis with internal standard (sulphamerazine) calibration using extraction liquid composition 10. Situation (C) represents analysis with external standard using extraction liquid composition 1. Situation (D) represents analysis with internal standard (sulphachloropyridazine) using extraction liquid composition 1. It is clear that situation (A) is inferior to situation (D) for the analysis of sulphisomidine: linearity of the calibration graphs, C.V. of the duplicate quality control samples and predicted mean concentrations of duplicate quality control samples are much better. External standard calibration in extraction liquid composition 1 (C) is better than internal calibration with sulphamerazine in extraction liquid composition 10 (B).

Table II demonstrates that the standard deviation of the recoveries are relatively small (maximum C.V. *ca.* 5%). Much greater variances of the ratios of recoveries may be obtained from extractions with relatively large S.D. values.

The extraction procedure of the mixture of sulphonamides from plasma by replicate measurements from ten different extraction liquid compositions is accomplished within 24 h. The simulation of each combination of analyte, internal standard and extraction liquid composition takes *ca.* 12 h of calculation on the IBM PS/2 Model 80-A31 computer.

It can be calculated that this simulation includes 18 000 analytical runs, *i.e.*, 216 000 analyses. This represents *ca.* 15 years of experimental work [5 days per week, five analytical runs = $(5 \cdot 8) + (5 \cdot 4) = 60$ analyses in 24 h], which is impossible to accomplish.

## CONCLUSIONS

Experimental errors in the recoveries of structurally related compounds are more or less correlated. However, the extraction liquid chosen greatly affects the correlation between the errors in the recovery of analyte and internal standard. The selection of an appropriate extraction liquid is very important for the development of accurate and reproducible assay methods. Selection of unsuitable extraction liquids may introduce errors in internal standard calibration that are larger than errors in external standard calibration.

Also, the choice of the internal standard is very important: even compounds that are structurally related to the analyte may demonstrate a dissimilar extraction behaviour. It is well reasoned to select as the internal standard a stucturally related compound that demonstrates an extraction behaviour in the selected extraction liquid which is most similar.

Generally, internal standard calibration gives better results for liquid–liquid extraction than external standard calibration. However, circumstances can be indicated where external standard calibration is better.

A method has been developed for the selection of an extraction liquid and/or an internal standard in liquid–liquid extraction sample preparation prior to HPLC analysis. The quality of routine analysis is used as a selection criterion. This quality is approximated by simulation of 50 analytical runs under different conditions (extraction liquid composition and calibration method, Figs. 8–10). The quality control results under these conditions are compared to give optimum extraction conditions.

The method developed may also be very useful for the selection of the composition of an extraction

liquid that gives the most robust results for all recoveries and recovery ratios after extraction of several analytes.

ACKNOWLEDGEMENT

The authors thank the Dutch Technology Foundation (Stichting voor de Technische Wetenschappen, STW) for their support of this project.

REFERENCES

1 R. V. Smith and J. T. Stewart, *Textbook of Biopharmaceutic Analysis, a Description of Methods for the Determination of Drugs in Biological Fluids*, Lea & Febiger, Philadelphia, PA, 1981, pp. 107–112.
2 C. Guillemin, J. Gressin and M. Caude, *J. High Resolut. Chromatogr. Chromatogr. Commun.*, 3 (1982) 128.
3 P. Haefelfinger, *J. Chromatogr.*, 218 (1981) 73.
4 N. E. Kelly, S. W. Barr and A. P. Zelinko, *J. Chromatogr.*, 535 (1990) 199.
5 K. Banno, M. Matsuoka, S. Horimoto and J. Kato, *J. Chromatogr.*, 525 (1990) 255.
6 J. Wieling, J. Hempenius, H. J. Jeuring, J. H. G. Jonkman, P. M. J. Coenegracht and D. A. Doornbos, *J. Pharm. Biomed. Anal.*, 8 (1990) 577.
7 T. P. Davis, S. K. Veggeberg, S. R. Hameroff and K. L. Watts, *J. Chromatogr.*, 273 (1983) 436.
8 M. A. Osman, L. K. Dunning, V. P. Bhavnagri and L. K. Cheng, *J. Chromatogr.*, 496 (1989) 478.
9 S. H. Curry and R. Whelpton, in E. Reid (Editor), *Blood Drugs and Other Analytical Challenges*, Ellis Horwood, Chichester, 1978, pp. 29–41.
10 L. R. Snyder and Sj. van der Wal, *Anal. Chem.*, 53 (1981) 877.
11 Sj. van der Wal and L. R. Snyder, *Clin. Chem.*, 27 (1981) 1233.
12 D. N. Bailey and M. Kelner, *J. Anal. Toxicol.*, 8 (1984) 26.
13 S. M. Lampluch, *J. Chromatogr.*, 273 (1983) 442.
14 L. B. Nilsson, *J. Chromatogr.*, 431 (1988) 113.
15 A. S. Gross, B. Borstel and M. Eichelbaum, *J. Chromatogr.*, 525 (1990) 183.
16 Y. Soeishi, M. Kobori, S.-I. Kobayashi and S. Higuchi, *J. Chromatogr.*, 531 (1990) 291.
17 H. H. Ku, *J. Res. Natl. Bur. Stand., Sect. C*, 70 (1966) 263.
18 S. T. Balke, *Quantitative Column Liquid Chromatography, a Survey of Chemometric Methods*, Elsevier, Amsterdam, 1984, pp. 38–45.
19 L. Rohrschneider, *Anal. Chem.*, 45 (1973) 1241.
20 L. R. Snyder, *J. Chromatogr. Sci.*, 16 (1978) 223.
21 J. L. Glajch, J. J. Kirkland, K. M. Squire and J. M. Minor, *J. Chromatogr.*, 199 (1980) 57.
22 P. M. J. Coenegracht, A. K. Smilde, H. J. Metting and D. A. Doornbos, *J. Chromatogr.*, 485 (1989) 195.
23 J. Wieling, J. Schepers, J. Hempenius, C. K. Mensink and J. H. G. Jonkman, *J. Chromatogr.*, 545 (1991) 101.
24 J. Mandel, *The Statistical Analysis of Experimental Data*, Wiley, New York, 1964, p. 48.
25 G. E. P. Box, W. G. Hunter and J. S. Hunter, *Statistics for Experimenters, an Introduction to Design, Data Analysis and Model Building*, Wiley, New York, 1978, pp. 118–120.
26 D. L. Massart, B. G. M. Vandeginste, S. N. Deming, Y. Michotte and L. Kaufman, *Data Handling in Science and Technology, Vol. 2, Chemometrics: a Textbook*, Elsevier, Amsterdam, 1988, p. 70.

*Journal of Chromatography*, 594 (1992) 65–73
Elsevier Science Publishers B.V., Amsterdam

CHROM. 23 881

# Computer simulation as a tool for the rapid optimization of the high-performance liquid chromatographic separation of a tryptic digest of human growth hormone

Rosanne C. Chloupek* and William S. Hancock

*Genentech, Inc., 460 Point San Bruno Blvd., South San Francisco, CA 94080 (USA)*

Lloyd R. Snyder

*LC Resources Inc., 2930 Camino Diablo, Suite 110, Walnut Creek, CA 94596 (USA)*

(First received September 5th, 1991; revised manuscript received November 14th, 1991)

ABSTRACT

Computer simulation was used to optimize the separation of a tryptic digest of recombinant human growth hormone using reversed-phase high-performance liquid chromatography in a gradient mode. DryLab G/plus software modelled the retention behavior of the complex tryptic digest mixture as a function of gradient conditions, based on data from two experimental gradient runs. The theoretical optimum separation conditions were rapidly obtained and reproduced experimentally. Resolution did not simply increase as gradient steepness was decreased, rather, an intermediate gradient time provided maximum sample resolution. The simulation results also indicate that the method is reasonably rugged, with little change in the separation expected for different high-performance liquid chromatography systems, and changes in the separation can be compensated by a change in the gradient steepness. Computer simulation can also be useful to quickly reoptimize conditions for a new column, if it fails to provide the same separation.

## INTRODUCTION

Peptide mapping by reversed-phase high-performance liquid chromatography (RP-HPLC) has become an important method for the characterization of recombinant DNA-derived proteins [1–4]. In this procedure, the protein is cleaved by a proteolytic enzyme, such as trypsin, to a number of peptides which are then separated by RP-HPLC. It has been shown in a variety of studies [5,6] that amino acid substitutions result in a substantial shift in the retention time of a given peptide. The map has been used to detect mistranslation events that result in the substitution of norleucine for methionine and to detect degradative processes such as deamidation, oxidation, and proteolysis [6,7]. Thus, reversed-phase peptide mapping is used for both the characterization of a novel protein product [8] as well as in quality control for the release of different production lots [2]. For these applications, it is important that the map is optimized so that the analyst is able to detect amino acid substitutions with a high probability [9].

The identification of minor new peptides is complicated by the fact that protein digests typically comprise a large number of "primary" peptides, plus a significant number of other reaction products present at lower concentrations. It is not unusual to see 50–100 distinct peaks in the final tryptic map chromatogram. The presence of lower level peptides can be related either to fragmentation of the enzyme during the digestion or to secondary cleavages of the primary peptides. The resolution of the primary peptides in such mixtures is usually a major consideration, but other peaks in the chromatogram are often of interest. For instance, the sep-

0021-9673/92/$05.00 

aration of protein digests can be used to detect the presence of protein variants [3] usually at levels of 0.5 to 5%.

The complexity of protein digests and the variety of separation conditions that can be developed for HPLC in a gradient mode complicates the development of an optimized separation. A further problem is caused by changes in elution order that can occur with different gradient slopes, so that a longer gradient may give worse rather than improved resolution. A large number of experimental runs may be required before an acceptable chromatogram is obtained and during this time changes in column performance are common. The result is a considerable expenditure of time, materials and sample, with possible uncertainty in the final results. It is therefore rare that a final HPLC procedure has been "optimized" with respect to the goals of the separation (resolution, run time, etc.). The possibility that peaks of potential interest remain unresolved (and undetected) is also a concern.

An alternative to this traditional approach to HPLC method development for reversed-phase gradient elution is the use of computer simulation [10]. With this technique the data from two or three experimental runs are entered into a personal computer (PC), and separation can then be predicted as a function of gradient conditions. Further iterations via computer simulation are used to eventually arrive at an optimized separation, while minimizing the problems of trial-and-error experimentation.

Computer simulation has been applied previously for the HPLC separation of both peptides [10] and proteins [11–14] with the primary objective of resolving the major components of the sample. In the present study we have shown that the optimization of the tryptic map of recombinant DNA-derived human growth hormone (rhGH) is a complex task and that computer simulation can greatly aid this process. Another commonly encountered problem is a change in the separation when different operators or equipment are involved in a quality control program. This study explores the use of computer simulation to correct for changes in mobile phase composition, column-to-column variations and alterations in dwell volume. Computer simulation can also be used to readily reoptimize the separation for a given peptide, a feature which is particularly useful in the characterization of a protein variant.

## EXPERIMENTAL

### *Equipment and materials*

HPLC separations were carried out on an HP 1090 with autosampler (Hewlett-Packard, Palo Alto, CA, USA) and a diode array detector; the dwell volume was determined equal to 2.3 ml [15]. All solvents were of HPLC grade.

### *Procedure*

Gradient separations were carried out using 0.1% trifluoroacetic acid (TFA)–water as solvent A and 0.08% TFA–acetonitrile as solvent B at a flow-rate of 1.0 ml/min. The column temperature was 40°C and 100 $\mu$l of 1.0 mg/ml sample was injected. Two 15 × 0.46 cm I.D., 5-$\mu$m Nucleosil $C_{18}$ columns with 100-Å pores (Alltech, Deerfield, IL, USA) from different manufacturing lots were used.

### *Sample*

*Tryptic digestion.* A sample of rhGH (Genentech) South San Fransisco, CA, USA) was exchanged into 100 m*M* sodium acetate–10 m*M* Tris–1 m*M* calcium chloride, pH 8.3 with a final concentration of approximately 1 mg/ml. Samples were incubated at 37°C for a total of 4 h with the addition of trypsin (1:100 ratio by weight of trypsin to substrate) at time $t = 0$ and $t = 2$ h. The digest was stopped by the addition of phosphoric acid to a final pH of 2–3. The sample was stored at 2–8°C.

Digestion of rhGH by trypsin results in the release of 21 peptides. These peptides are sequentially numbered from the N-terminus (T1) through to the C-terminus (T21).

### *Software*

The computer simulation software used in the present study is DryLab G/plus from LC Resources (Walnut Creek, CA, USA). It requires an IBM-compatible PC with 640K of RAM memory; a math coprocessor was used for fast computation.

## RESULTS AND DISCUSSION

Previous work [10,16] has shown that the separation of protein digests by reversed-phase gradient elution can be quite sensitive to gradient conditions. In this study the least resolved pair of peaks in a given separation will be defined as a "critical

peak pair". A resolution factor ($R_s$) equal to 1.5 would result in baseline resolution of a peak pair. A change in gradient slope can often be used to alter the peak spacing within the chromatogram, leading to major improvements in the resolution of critical peak pairs. By varying gradient steepness for different parts of the chromatogram (multi-segment gradients), it may be possible to achieve a separation that is better than any linear (single-segment) gradient [11–14].

*Resolution of major components in the hGH digest*

Gradient separations were initially carried out from 0–60 % B in 30 and 120 min, in order to obtain the necessary data for computer simulation. These chromatograms are shown in Fig. 1.

*Peak tracking*. It is necessary to match the peaks between the two chromatograms (referred to as peak tracking [17]) before beginning computer simulation, as summarized in Table I for all peaks with areas >0.5% of the total sample. In Table I the peak areas show that there are three unresolved doublets in the 30-min run, and peaks 9 and 10 are reversed in the 120-min run. The assignment of the various peaks is indicated in Table I, including two minor "unknown" peaks. Peak tracking as in Table I can be done manually, but we have also used recently developed software to accomplish this by computer [18]. The ease of peak tracking for protein digests is very much dependent on the reproducibility of peak areas from run to run (about ±5% in the runs of Table I), which in turn depends on the quality of the baseline (*i.e.*, blank gradient). A complete digestion of the protein with minimum formation of artifacts, such as non-specific cleavages or contamination with fragments of the protease, is also desirable.

Inaccurate peak matching or a failure to account for all the peaks of interest can occur for chromatograms as complex as those of Fig. 1. In order to insure that errors of this kind have been avoided, a third experimental run with an intermediate gradient time (*e.g.*, 60 min) was carried out. Comparison of the resulting chromatogram with that predicted by computer simulation can uncover certain errors. As seen in Table II and Fig. 2, all major

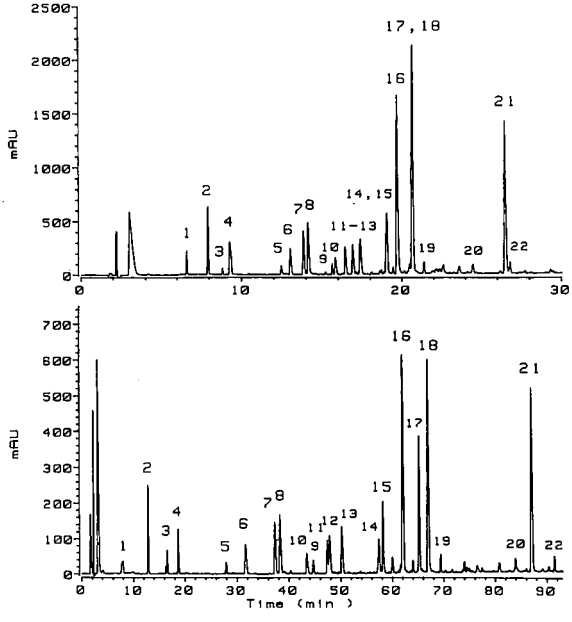


Fig. 1. The experimental separations of the tryptic digest of rhGH used as input for computer simulation. These were performed on a 5-$\mu$m Nucleosil $C_{18}$ column (15 × 0.46 cm I.D.) with a mobile phase A of 0.1% TFA–water and a mobile phase B of 0.08% TFA–acetonitrile. The flow-rate was 1 ml/min and the column temperature was 40°C. The 100-$\mu$g samples were loaded in 100-$\mu$l of digest buffer and monitored at 220 nm. One separation (top) was a linear gradient from 0–60% B in 30 min and the other separation (bottom) was a linear gradient from 0–60% B in 120 min.

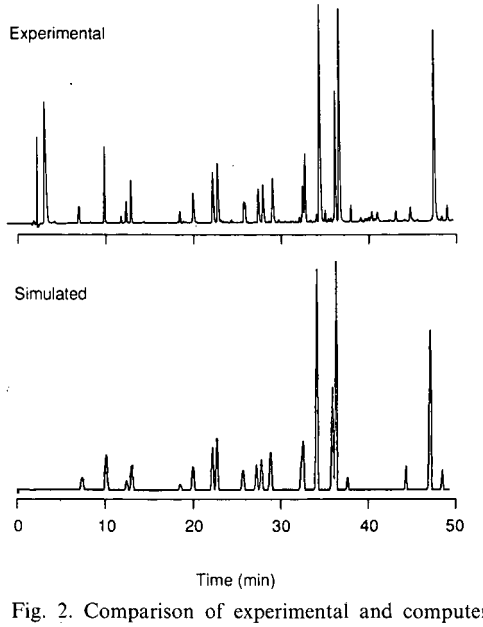


Fig. 2. Comparison of experimental and computer-simulated rhGH tryptic digest separations for 0–60% B in 60 min. Other conditions as in Fig. 1.

TABLE I

TRACKING OF THE MAJOR PEAKS IN THE TWO RUNS OF FIG. 1

| Compound[a] | Run 1 (30 min) | | Run 2 (120 min) | |
|---|---|---|---|---|
| | Retention time (min) | Area | Retention (min) | Area |
| 1 T7 | 6.6 | 87 | 7.9 | 93 |
| 2 T14 | 7.9 | 245 | 12.8 | 238 |
| 3 T14c | 9.3 | 225[b] | 16.5 | 68 |
| 4 T12 | 9.3 | 225[b] | 18.7 | 151 |
| 5 T10a | 12.5 | 47 | 27.9 | 44 |
| 6 T13 | 13.0 | 152 | 31.6 | 164 |
| 7 T20–21 | 13.8 | 247 | 37.2 | 242 |
| 8 T15 | 14.1 | 304 | 38.2 | 306 |
| 9 T8 | 15.6 | 46 | 44.6 | 49 |
| 10 T17–18–19 | 15.8 | 99 | 43.4 | 99 |
| 11 T2 | 16.5 | 159 | 47.3 | 148 |
| 12 T18–19 | 16.9 | 186 | 47.8 | 199 |
| 13 T1 | 17.4 | 236 | 50.1 | 241 |
| 14 T10bc | 19.1 | 429[b] | 57.3 | 163 |
| 15 T11 | 19.1 | 429[b] | 58.1 | 269 |
| 16 T4 | 19.7 | 1113 | 61.9 | 1131 |
| 17 T10 | 20.2 | 1527[b] | 65.1 | 562 |
| 18 T6–16 | 20.2 | 1527[b] | 66.8 | 1040 |
| 19 T6–16c | 21.4 | 63 | 69.3 | 58 |
| 20 Unknown | 24.5 | 72 | 83.9 | 80 |
| 21 T9 | 26.5 | 951 | 86.9 | 990 |
| 22 Unknown | 26.8 | 73 | 91.3 | 87 |

[a] The tryptic peptides are numbered from the amino terminus so that T1 contains residues 1 to 7. The letters a, b and c refer to peptide fragment [8]. The numbers refer to the peak assignment in Fig. 1.

[b] These peaks were not resolved and the total peak area was recorded.

peaks are accounted for, and the predicted retention times match those for the 60-min gradient within an average error of ±0.1 min (±0.3%). We can therefore assume that no errors in peak matching have occurred in the assignments of Table I.

*Optimizing gradient steepness.* Computer simulation requires entry into the computer of the run conditions, retention times and peak areas from the experiments of Fig. 1. Correction for differences in column plate number can also be made by entering the actual resolution of a peak pair for a specific gradient time. Peak pair 11/12, ($R_s$ = 0.87 in the 120-min run), was selected in this case and the resulting average plate number for the present separations of the rhGH digest was $N$ = 3600. The adjusted column plate number allows the simulation of chromatograms which will closely match experimental runs.

The next step is to generate a resolution map, as shown in Fig. 3 for the present sample. Here the resolution ($R_s$) of the most-overlapped or critical peak pair is plotted against gradient time for a starting mobile phase of 0% B. The numbering on the plot in Fig. 3 identifies the critical peak pair for each value of % B/min, and it is seen that different peaks become "critical" for a change in gradient time. For example, for gradient times between 40 and 200 min, the critical peak pairs are 9/10, 11/12, and 14/15. Segments of simulated chromatograms illustrating the critical peak pairs at several gradient times in the resolution map are shown in Fig. 4. An examination of Figs. 3 and 4 shows that sample resolution does not simply increase as gradient steepness (time) is decreased. Peaks 9 and 10, for example, co-elute ($R_s$ = 0) for a gradient time of 45 min, with peak 10 eluting first for shorter gradient times and peak 9 eluting first for longer gradient times (see Fig. 4). Alternatively, peaks 11 and 12 are found to be well resolved at shorter gradient times and actually decrease in resolution with increasing gradient time, until they co-elute at a 180-min gradient time. In most cases, there will be an intermediate gradient time that provides maximum resolution of the initial peak pair.

Maximum resolution is indicated for a gradient time of 74 min ($R_s$ = 1.3, %B/min = 0.6) or 330 min ($R_s$ = 2.0, %B/min = 0.1). Normally the steeper gradient would be preferred (0.6% B/min, 74 min), because of the considerably shorter run time and narrower peaks for easier detection. The predicted and experimental chromatograms for the optimal linear gradient are shown in Fig. 5. The experimental retention times match predicted values within an average error of ±0.2 min (±0.7%). The observed resolution for the critical peak pairs 11/12 and 14/15 was $R_s$ = 1.1 *vs.* 1.3 predicted. The slightly lower experimental resolution can be attributed to a decrease in the column plate number during the one month that elapsed between the runs of Fig. 1 and the run of Fig. 5. This emphasized the fact that changes in performance can be expected during continued use of the column (see later discussion).

*Initial mobile phase composition (%B).* Often it is found that the maximum possible resolution is de-

TABLE II

CONFIRMING THE PEAK ASSIGNMENTS OF TABLE I

Experimental and predicted retention times for a 0–60% B gradient in 60 min.

| Band | Retention times (min) | | |
|---|---|---|---|
| | Calc. | Expt. | Difference |
| 1 | 7.3 | 7.0 | 0.3 |
| 2 | 10.1 | 9.8 | 0.3 |
| 3 | 12.4 | 12.3 | 0.1 |
| 4 | 13.0 | 12.8 | 0.2 |
| 5 | 18.5 | 18.4 | 0.1 |
| 6 | 20.0 | 19.9 | 0.1 |
| 7 | 22.2 | 22.2 | 0.0 |
| 8 | 22.7 | 22.7 | 0.0 |
| 9 | 25.7 | 25.7 | 0.0 |
| 10 | 25.8 | 25.8 | 0.0 |
| 11 | 27.3 | 27.3 | 0.0 |
| 12 | 27.9 | 27.9 | 0.0 |
| 13 | 29.0 | 29.0 | 0.0 |
| 14 | 32.4 | 32.4 | 0.0 |
| 15 | 32.6 | 32.7 | −0.1 |
| 16 | 34.2 | 34.3 | −0.1 |
| 17 | 36.0 | 36.1 | −0.1 |
| 18 | 36.4 | 36.5 | −0.1 |
| 19 | 37.8 | 37.9 | −0.1 |
| 20 | 44.5 | 44.6 | −0.1 |
| 21 | 47.3 | 47.3 | 0.0 |
| 22 | 48.7 | 48.8 | −0.1 |
| Av. error | | ±0.1 min (±0.3%) | |

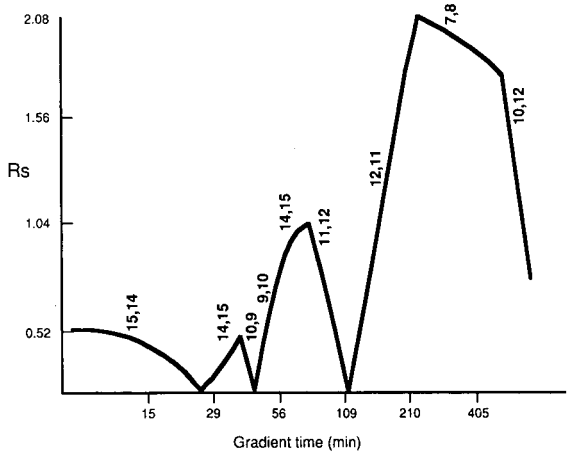


Fig. 3. The relative resolution map generated using the retention time data from the chromatograms in Fig. 1. The resolution ($R_s$) of the predicted critical peak pair is plotted *vs.* gradient time. The identity of the critical peak pair is indicated by numbers above the line. The column used in this separation had an $N$ = 3600.

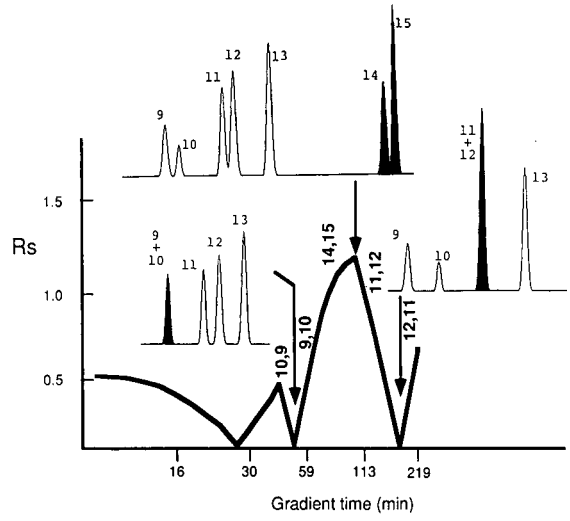


Fig. 4. The relative resolution map with critical peak pairs illustrated at several gradient times by relevant segments of simulated chromatograms. An $R_s > 1$ for 14, 15 at a gradient time between 70 and 110 min results in good resolution of the critical peak pair and indicates a region in the resolution map where the gradient time would be optimal for good resolution of all the peptide peaks.

pendent on the choice of the initial mobile phase %B (see Figs. 4–6 of ref. 19).

The best choice of the initial mobile phase is easily addressed via computer simulation. Resolution maps were generated for 2, 5, and 7.5% B as starting mobile phase, similar to the map of Fig. 5 for 0% B. The maximum possible resolution for run times of less than 5 h was found to vary from $R_s$ = 1.25 to 1.28 between 0 and 5% B ($R_s < 0.7$ for 7.5% B). These data make it clear that the initial mobile phase concentration should be $\leqslant$5% B, but resolution is essentially the same for 0–5% B. Run time decreases from 74 min for 0% B to 65 min for 5% B, favoring a higher value of %B. Changes in the retention of early peaks are shown in Fig. 6 as a function of %B, with experimental chromatograms shown for comparison. These data suggest that beginning the gradient with 2% B will avoid any problems with the early elution of initial peptide peaks, since in comparative mapping applications it is important that the polar peptides are retained sufficiently for separation, so that any alteration in these peptides can be detected. These conditions could also be an advantage because the time required for column equilibration is often less when the initial

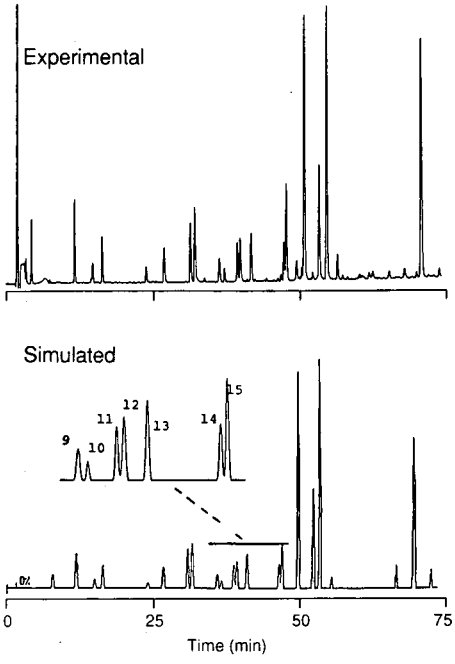


Fig. 5. A comparison of the predicted optimal linear gradient in a minimum run time *vs.* the experimental run. Conditions: 0–47% B in 74 min; other conditions as in Fig. 1.

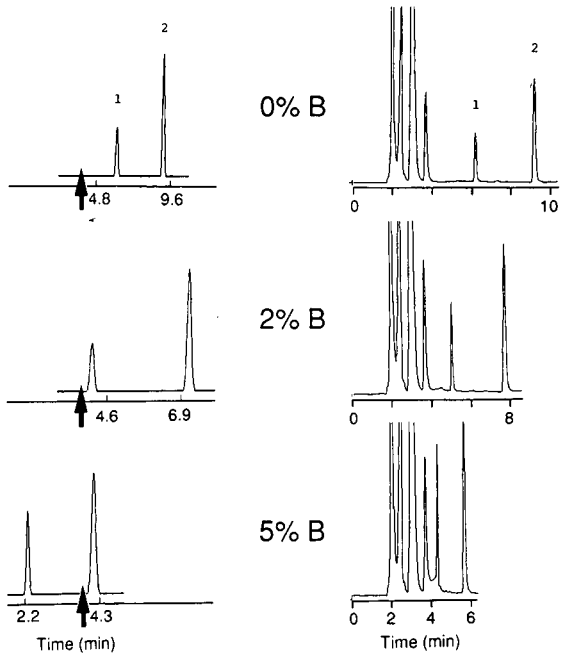


Fig. 6. The effect of starting mobile phase composition of the separation of early rhGH tryptic peptide peaks. The arrows on the simulated chromatograms (left) indicate the minimum retention time for peaks before the void peaks in the experimental runs (right) would interfere with detection. Other conditions as in Fig. 2.

mobile phase contains some organic solvent (*e.g.*, 2% B *vs.* 0% B).

*Use of segmented gradients.* The run time for the separation in Fig. 5 can be further shortened by noting that peaks eluting after the last critical pair (14/15) are all well resolved. This suggests the use of a steeper gradient after the elution of the latter peaks at 48 min. Computer simulation allows the evaluation of a number of 2-segment gradients, with an improved separation shown in Fig. 7. The run time is reduced from 74 min in Fig. 5 to 53 min. The experimental chromatogram (top) compares well with the predicted separation (bottom), and retention times agree within ±0.2 min or ±0.7% (average error). The total effort required for the development of an optimized separation such as this should be about two days for experimental runs plus a few hours of computer simulation.

Other workers have shown [20] that changes in the column, mobile phase pH and/or concentration of an ion-pair reagent, etc. may provide greater control over the separation of polar peptide mixtures compared to the variation of gradient steepness. This may be true for some samples, but changes in gradient conditions, especially when guided by computer simulation, will usually provide adequate separation of all but the most polar peptides. Hydrophobic ion-pairing reagents can be used in such cases [21].

*Correction for changes in separation*

The use of silica-based columns with low-pH mobile phases can lead to a loss of bonded phase and changes in sample retention [22]. Differences in the reversed-phase retention of peptide and protein samples are also found for columns from different production batches [11–13]. Once an optimized separation has been developed for a given sample (as in Fig. 7), it is not uncommon to find a loss of resolution for one or more critical peak pairs at some later time.

*Column-to-column variations.* These were studied by using an identical column (see Experimental) from a different manufacturing lot. Runs were car-

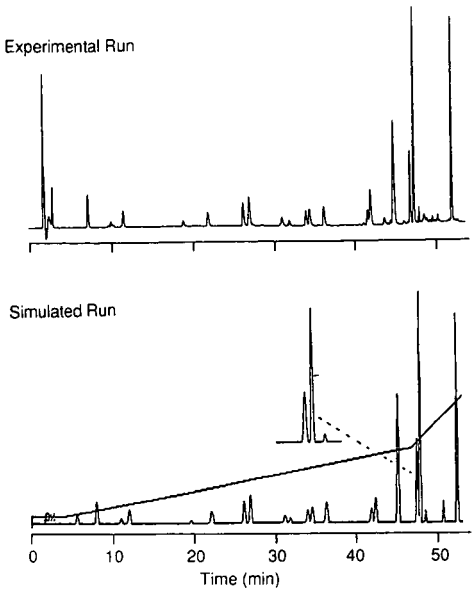


Fig. 7. The total run time of the optimal separation of rhGH tryptic peptides in Fig. 5 was reduced to 53 min by a segmented gradient of 2–32% B in 48 min, then 32–47% B in 5 min. The predicted chromatogram is compared to the actual run.

ried out from 0–60% B in gradient times of 60 and 240 min. It was found that the new column was slightly more efficient ($N$ = 5000 *vs.* 3600 for the previous column), so a somewhat better separation was expected–other factors being equal. Confirmatory runs at 30 and 120 min were also made, with a average agreement between experimental and predicted retention times of ±0.2–0.3% (data not shown).

The resolution map of an hGH digest for the new column showed the same essential features as before, but minor differences existed which had a significant effect on separation. This is illustrated in Fig. 8, where the separation of peaks 7 through 15 are compared by computer simulations for the two columns. Fig. 8A shows the separation of the sample on the original column with the optimized conditions of Fig. 5. Under the same separation conditions as (A) it is apparent that the resolution of peaks 11 and 12 is not as good ($R_s$ = 0.9 *vs.* 1.3) for the new column (B). The higher $N$-value of the new column tends to hide part of these differences in the two columns, as illustrated in Fig. 8C which shows the theoretical separation on the original column if the column had the same selectivity but with $N$ = 5000 ($R_s$ for bands 11/12 = 1.5). That is, the differences in the separations are due to differences in selectivity for the two columns.

Computer simulation can be repeated with a new column so as to reoptimize the separtion. When this was attempted with the new column, it was found that a minor change in the original gradient (2–28% B in 37 min, then 28–46% B in 13 min *vs.* 2–32% B in 48 min, then 32–47% B in 5 min) increased the resolution of the critical pair to $R_s$ = 1.1 *vs.* $R_s$ = 0.9. This is somewhat less than found for the original column ($R_s$ = 1.3), but is probably adequate for the present application.

*Separation using a different HPLC system*

The use of different HPLC equipment can result in a change in separation when using gradient elution [23,24]. Therefore, a procedure that is intended for use by others should be evaluated for system dependence as a part of method development. The primary cause of system-to-system differences in

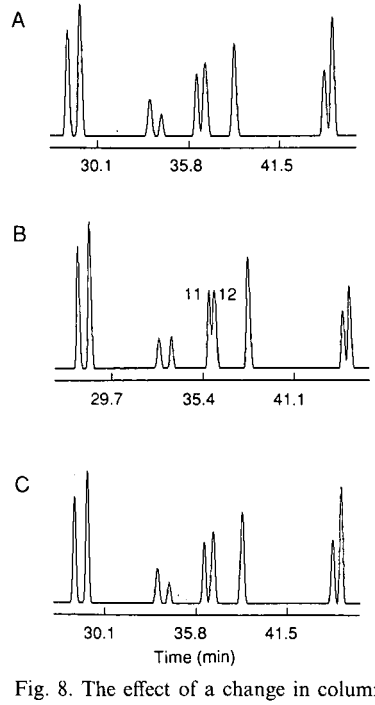


Fig. 8. The effect of a change in column efficiency on the separation of rhGH tryptic peptides. Computer simulations show: A, an optimized separation of peaks 7–15 using the first column and $N$ = 3600 (conditions, Fig. 5); B, the same separation with a second column and $N$ = 3600; C, the same separation with a first column and $N$ = 5000.

gradient separation is a difference in *dwell volume* ($V_D$) (the volume from the gradient mixer to the column inlet). The effect of a change in dwell volume is usually to shift all peaks in the chromatogram to higher or lower retention times, in some cases with a change in relative retention. This can lead to two kinds of problems: (a) loss in resolution for early-eluting peaks and (b) confusion as to the identity of various peaks in the chromatogram.

Computer simulation can be used to evaluate system-to-system reproducibility, as illustrated in Fig. 9. The chromatogram labeled "$V_D$ = 2.3 ml" corresponds to our optimized separation (Fig. 7) carried out on the present HPLC system (HP 1090 with autosampler, $V_D$ = 2.3 ml). Other HPLC systems can often have dwell volumes as large as 10 ml [23], depending on the system components. Fig. 9 also shows a computer simulation for a system having a much larger dwell volume ($V_D$ = 10 ml). The data of Fig. 9 demonstrate that an increase in $V_D$ results in the later elution (by 2–8 min) of all peaks, and peaks 1–4 are more spread out for $V_D$ = 10 ml. However the relative retention of peaks 5–22 is unchanged, and the resolution of critical peak-pairs (9/10, 11/12, 14/15) remains the same. These predictions are confirmed in the experimental runs on two different HPLC systems, where the dwell volumes have been adjusted to match those of Fig. 9 (data not shown).

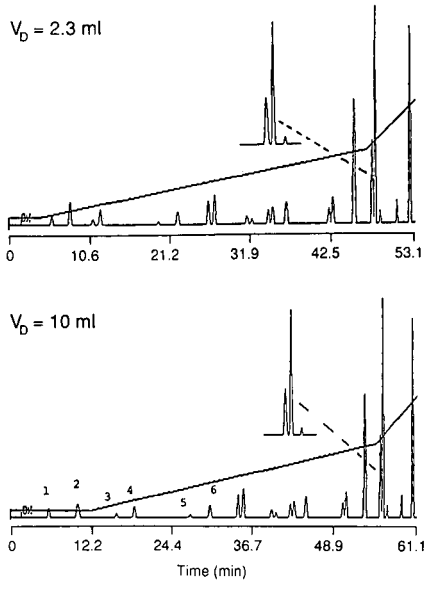


Fig. 9. A simulation of the effect of equipment dwell volume ($V_D$) on the optimized separation (as shown in Fig. 7) of the rhGH tryptic digest.

*Optimization of the separation of a specific peptide*

Computer simulation lends itself to a variety of other separation goals, such as maximizing the resolution of a given peak in the chromatogram for subsequent preparative isolation. Computer simulation can be used to explore such possibilities, as illustrated by peak 11 of the rhGH digest. The separation of Fig. 5 and 7 has been optimized in terms of a maximum resolution for the poorest-resolved peak pair in the sample. As a result, the resolution of peak 11 is $R_s$ = 1.3. If peak 11 is the only component of interest, however, its separation from adjacent peaks can be considerably improved. In this case it is useful to generate a *partial resolution map*, where the resolution of peak 11 from adjacent peaks is plotted *vs.* gradient time (Fig. 10, above). The latter map shows that a resolution of $R_s$ = 2.2 can be achieved for peak 11 in a run time of only 25 min. The predicted separation in Fig. 10, (below) shows that it is possible to greatly improve the separation of peak 11 when other components of the sample can be ignored. Advance knowledge of the appearance of the chromatogram by computer simulation will also greatly aid in the isolation of the correct peak(s) in a preparative run.

## CONCLUSIONS

Computer simulation was used to optimize gradient conditions for the RP-HPLC separation of a tryptic digest of human growth hormone. Twenty two major bands were resolved almost to baseline ($R_s$ = 1.3) in a run time of 53 min. The effort required for method development was relatively minor: four experimental runs plus a few hours of computer time.

Changes in separation due to a change in column or HPLC equipment were also studied via computer simulation. It was found possible to correct for column-to-column differences so as to maintain acceptable separation. Even less time was required for reoptimization because the validity of the computer simulation had already been established. Similarly, computer simulation indicated that the present separation should be consistent when using different

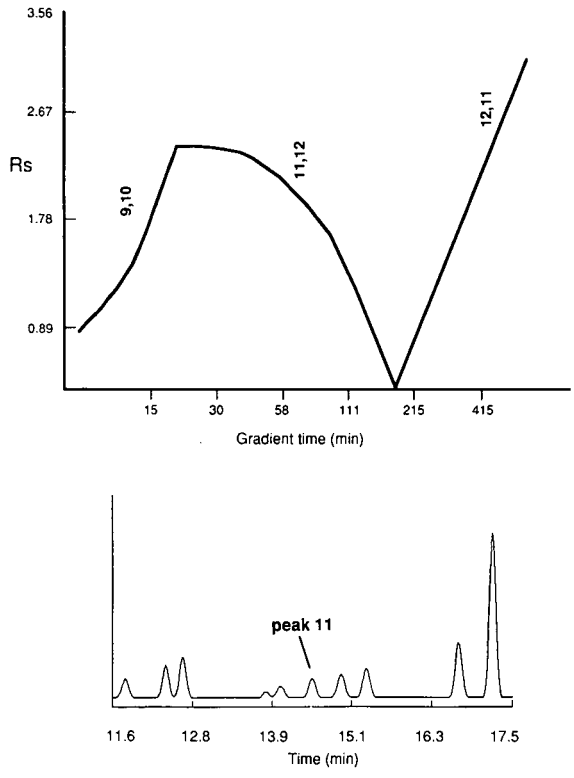


Fig. 10. The optimized separation of peak 11 of the rhGH tryptic digest sample. The partial resolution map for peak 11 is shown above and the predicted separation for 0–60% B in 25 min is shown below. Other conditions as in Fig. 1.

HPLC systems. This was verified experimentally. Computer simulation can also be used to optimize the separation of a single sample component, prior to its isolation or purification from other peaks in the chromatogram.

## REFERENCES


1 W. S. Hancock, *Chromatogr. Forum*, 1 (1986) 57.
2 R. L. Garnick, N. J. Solli and P. A. Papa, *Anal. Chem.*, 60 (1988) 2546.
3 D. G. Burstyn, *BioPharm –The Technology and Business of Biopharmaceuticals*, Feb. (1991) 22.
4 C. T. Mant and R. S. Hodges, in K. M. Gooding and F. E. Regnier (Editors), *HPLC of Biological Macromolecules*, Marcel Dekker, New York, 1990, Ch. 11.
5 R. S. Hodges and C. T. Mant, in C. T. Mant and R. S. Hodges (Editors), *HPLC of Peptides and Proteins: Separation, Analysis and Conformation*, CRC Press, Boca Raton, FL, 1991, pp. 3–9.
6 R. M. Riggin, G. K. Dorulla and D. J. Miner, *Anal. Biochem.*, 167 (1987) 199.
7 W. S. Hancock, E. Canova-Davis, R. C. Chloupek, S.-L. Wu, I. P. Baldonado, J. E. Battersby, M. W. Spellman, L. J. Basa and J. A. Chakel, in D. R. Marshak and D. T. Liu (Editors), *Therapeutic Peptides and Proteins: Assessing the New Technologies, Banbury Report 29*, Cold Spring Harbor Laboratory, Cold Spring Harbor, NY, 1988, pp. 95–117.
8 W. F. Bennett, R. Chloupek, R. Harris, E. Canova-Davis, R. Keck, J. Chakel, W. S. Hancock, P. Gellefors and B. Pavlu, in E. E. Miller, D. Cocchi and V. Locatelli (Editors), *Advances in Growth Hormone and Growth Factor Research*, Pythagora Press, Rome, Milan and Springer, Berlin, Heidelberg, 1989, pp. 29–50.
9 W. S. Hancock, E. Canova-Davis, J. E. Battersby and R. Chloupek, in J. L. Guerigan, V. Fattorusso and D. Poggioline (Editors), *Biotechnologically-Derived Medical Agents: the Scientific Basis of their Regulation*, Raven Press, New York, 1988, p. 29–49.
10 J. W. Dolan, D. C. Lommen and L. R. Snyder, *J. Chromatogr.*, 485 (1989) 91.
11 B. F. D. Ghrist, B. S. Cooperman and L. R. Snyder, *J. Chromatogr.*, 459 (1988) 1.
12 B. F. D. Ghrist and L. R. Snyder, *J. Chromatogr.*, 459 (1988) 25.
13 B. F. D. Ghrist and L. R. Snyder, *J. Chromatogr.*, 459 (1988) 43.
14 B. F. D. Ghrist, L. R. Snyder and B. S. Cooperman, in K. M. Gooding and F. E. Regnier (Editors), *HPLC of Biological Macromolecules*, Marcel Dekker, New York, 1990, Ch. 15.
15 L. R. Snyder and J. W. Dolan, *LC · GC*, 7 (1990) 524.
16 J. L. Glajch, M. A. Quarry, J. F. Vasta and L. R. Snyder, *Anal. Chem.*, 58 (1986) 280.
17 H. A. H. Billiet and L. de Galan, *J. Chromatogr.*, 485 (1989) 27.
18 J. W. Dolan and L. R. Snyder, presented at the *14th International Symposium on Column Liquid Chromatography Boston, MA, May 20–25, 1990.*
19 P. Jandera and M. Spacek, *J. Chromatogr.*, 366 (1986) 107.
20 P. M. Young and T. E. Wheat, *J. Chromatogr.*, 512 (1990) 273.
21 W. S. Hancock, C. A. Bishop, L. J. Meyer, D. R. K. Harding and M. T. W. Hearn, *J. Chromatogr.*, 161 (1978) 291.
22 J. J. Kirkland, J. L. Glajch and R. D. Farlee, *Anal. Chem.*, 61 (1989) 2.
23 P. Jandera and J. Churacek, in P. Jandera (Editor), *Gradient Elution in Column Liquid Chromatography*, Elsevier, Amsterdam, 1985, Ch. 8.
24 L. R. Snyder and J. W. Dolan, *LC · GC*, 8 (1990) 524.

*Journal of Chromatography*, 594 (1992) 75–86
Elsevier Science Publishers B.V., Amsterdam

CHROM. 23 826

# Mixed-mode hydrophilic and ionic interaction chromatography rivals reversed-phase liquid chromatography for the separation of peptides

Bing-Yan Zhu, Colin T. Mant and Robert S. Hodges*

*The Medical Research Council of Canada Group in Protein Structure and Function, Department of Biochemistry, University of Alberta, Edmonton, Alberta T6G 2H7 (Canada)*

(First received July 24th, 1991; revised manuscript received October 22nd, 1991)

ABSTRACT

Peptide separations based upon mixed-mode hydrophilic and ionic interactions with a strong cation-exchange column have been investigated. The peptide separations were generally achieved by utilizing a linear increasing salt (sodium perchlorate) gradient in the presence of acetonitrile (20–90%, v/v) at pH 7. The presence of acetonitrile in the mobile phase promotes hydrophilic interactions with the hydrophilic stationary phase, these hydrophilic interactions becoming increasingly important to the separation process as the acetonitrile concentration is increased. At acetonitrile concentrations of 20–50% (v/v) in the mobile phase, the peptides utilized in this study were eluted in order of increasing net positive charge, indicating that ionic interactions were dominating the separation process. Peptides with the same net positive charge were also well resolved by an hydrophilic interaction mechanism, being eluted in order of increasing hydrophilicity (decreasing hydrophobicity). At higher acetonitrile concentrations (70–90%, v/v), column selectivity was changed dramatically, with hydrophilic interactions now dominating the separation process. Under these conditions, specific peptides may be eluted earlier or later than less highly charged peptides, depending upon their hydrophilic/hydrophobic character. This mixed-mode methodology was compared to reversed-phase liquid chromatography of the peptides at pH 2 and pH 7. The results of this comparison suggested that mixed-mode hydrophilic-ion-exchange chromatography on a strong cation-exchange column rivals reversed-phase liquid chromatography for peptide separations.

## INTRODUCTION

The utility of ion-exchange chromatography (IEC) for peptide separations has been somewhat overshadowed in the past by the extensive employment of reversed-phase liquid chromatography (RPLC) for such applications. The major advantages of the latter technique, apart from its powerful resolving capability, include the availability of volatile mobile phases, aqueous trifluoroacetic acid (TFA)–acetonitrile systems being the most frequently employed [1]. Such volatile mobile phases avoid the need for sample desalting, frequently an important consideration for subsequent peptide characterization or use. Thus, although IEC has been successfully applied to peptide mixtures [1–8], occasionally as one part of a multi-step protocol (*e.g.*, IEC followed by RPLC for a final desalting/purification step) [1,2,7], its use to date has certainly not rivalled that of RPLC.

Although the major process governing peptide retention behaviour on ion-exchange columns involves ionic interactions between the column matrix and the peptide solutes, all ion-exchange packings have, in our hands, also exhibited some hydrophobic character leading to long peptide retention times and peak broadening [1,8]. Most researchers prefer to avoid separations based upon such mixed-mode ionic-hydrophobic column behaviour. Thus, an organic solvent, such as acetonitrile, is frequently added to the mobile phase buffers to suppress any such hydrophobic packing characteristics [1,8]. Recently, this laboratory demonstrated that manipulation of the acetonitrile concentration (20–50%) in the mobile phase buffers enabled considerable flexi-

0021-9673/92/$05.00 

bility in the separation of basic peptides on a PolySulfoethyl A strong cation-exchange column [9]. Thus, at lower levels of acetonitrile, with hydrophobic interactions suppressed, the peptides were separated by an ionic mechanism only, *i.e.*, peptides were eluted in order of increasing net positive charge. However, as the level of acetonitrile was raised, while ionic interactions were still the chief separation mechanism (*i.e.*, peptides were still eluted in order of increasing net positive charge), hydrophilic interactions between the peptides and the column also came into play. Such a mixed-mode mechanism allowed the efficient resolution of peptides containing the same number of positively charged residues, with these identically charged peptides being eluted with excellent peak shape in order of increasing peptide hydrophilicity (or decreasing peptide hydrophobicity). The term hydrophilic interaction chromatography (HILIC) has been recently coined to describe separations based on solute hydrophilicity [10]. HILIC effects were more pronounced on the cation-exchange column in comparison to the HILIC column [9].

The present study extends our investigation of strong cation-exchange chromatography operated under controlled conditions favouring a mixed-mode hydrophilic-ionic interaction mechanism for peptide applications. By comparing the retention behaviour of a series of model peptides in this mixed-mode hydrophilic-ionic chromatography with that of their retention behaviour during RPLC, we have been able to draw some extremely positive conclusions concerning the potential of this novel cation-exchange approach to peptide separations.

## EXPERIMENTAL

### *Materials*

HPLC-grade water and acetonitrile and reagent-grade sodium perchlorate ($NaClO_4$) were obtained from J. T. Baker (Phillipsburg, NJ, USA). HPLC-grade trifluoroacetic acid (TFA) was obtained from Pierce (Rockford, IL, USA) and ACS-grade orthophosphoric acid ($H_3PO_4$) from Anachemia (Toronto, Canada). Synthetic model peptides were obtained from Synthetic Peptides (University of Alberta, Edmonton, Canada).

### *Instrumentation*

The high-performance liquid chromatographic (HPLC) system consisted of a Spectra-Physics (San José, CA, USA) SP8700 solvent-delivery system, SP8750 organizer coupled to an Hewlett-Packard (Avondale, PA, USA) HP 1040A detection system, HP 3390A integrator, HP 85 computer, HP 9121 disc drive and HP 7470 plotter.

### *Columns*

Peptides were separated on two columns: (1) a Zorbax SB-300 $C_8$ reversed-phase column, 150 × 4.6 mm I.D., 6 μm particle size, 250 Å pore size (Rockland Technologies, West Chester, PA, USA); and (2) a polysulfoethylaspartamide (PolySulfoethyl A) strong cation-exchange column, 200 × 4.6 mm I.D., 5 μm, 300 Å (PolyLC, Columbia, MD, USA).

## RESULTS AND DISCUSSION

### *Synthetic model peptides*

The relevant properties of the model peptides employed in this study are shown in Table I. Peptide pairs a–e, b–f, c–g and d–h possess identical amino acid sequences, the only difference being that peptides a, b, c and d contain a free N-terminal α-amino group, while peptides e, f, g and h are acetylated (*i.e.*, blocked) at their N-terminals.

Peptides i, j, k and l are commercially available as standards for monitoring cation-exchange column performance.

All of the peptides contain only basic (*i.e.*, potentially positively charged) residues (Lys, Arg, α-amino group), with no acidic residues (*i.e.*, potentially negatively charged) present, thus simplifying interpretation of results. In Figs. 2–5, the peptides are denoted by a number in addition to their letter. The number denotes the number of potentially positively charged groups a particular peptide contains, *e.g.*, k3 denotes that peptide k has three potentially positively charged groups. The presence of tyrosine in peptides d, h, j and l permits detection of these peptides at 280 nm in addition to peptide bond absorbance at 210 nm.

### *Reversed-phase liquid chromatography of model peptides*

In order to determine the overall hydrophobicity/

TABLE I

PROPERTIES OF SYNTHETIC PEPTIDES USED IN THIS STUDY

| Peptide | Peptide sequence[a] | No. of potentially positively charged residues[b] | Relative hydrophobicity[c] | |
|---|---|---|---|---|
| | | | pH 2 | pH 7 |
| a | *$NH_2$-*Arg-Gly-**Gly-Gly**-Gly-Leu-Gly-Leu-Gly-*Lys-amide | 3 | 16.4 | 20.6 |
| b | *$NH_2$-*Arg-Gly-**Ala-Gly**-Gly-Leu-Gly-Leu-Gly-*Lys-amide | 3 | 17.1 | 21.4 |
| c | *$NH_2$-*Arg-Gly-**Val-Gly**-Gly-Leu-Gly-Leu-Gly-*Lys-amide | 3 | 19.6 | 24.2 |
| d | *$NH_2$-*Arg-Gly-**Val-Tyr**-Gly-Leu-Gly-Leu-Gly-*Lys-amide | 3 | 22.3 | 27.2 |
| e | Ac-*Arg-Gly-**Gly-Gly**-Gly-Leu-Gly-Leu-Gly-*Lys-amide | 2 | 17.5 | 20.9 |
| f | Ac-*Arg-Gly-**Ala-Gly**-Gly-Leu-Gly-Leu-Gly-*Lys-amide | 2 | 18.3 | 21.8 |
| g | Ac-*Arg-Gly-**Val-Gly**-Gly-Leu-Gly-Leu-Gly-*Lys-amide | 2 | 20.8 | 24.4 |
| h | Ac-*Arg-Gly-**Val-Tyr**-Gly-Leu-Gly-Leu-Gly-*Lys-amide | 2 | 23.7 | 27.5 |
| i | Ac-Gly-Gly-Gly-Leu-Gly-Gly-Ala-Gly-Gly-Leu-*Lys-amide | 1 | 17.7 | 19.2 |
| j | Ac-*Lys-Tyr-Gly-Leu-Gly-Gly-Ala-Gly-Gly-Leu-*Lys-amide | 2 | 20.4 | 23.2 |
| k | Ac-Gly-Gly-Ala-Leu-*Lys-Ala-Leu-*Lys-Gly-Leu-*Lys-amide | 3 | 26.0 | 31.7 |
| l | Ac-*Lys-Tyr-Ala-Leu-*Lys-Ala-Leu-*Lys-Gly-Leu-*Lys-amide | 4 | 27.1 | 35.0 |

[a] Ac = $N^{\alpha}$-Acetyl; amide = $C^{\alpha}$-amide. Variations in the composition of peptides a–h are shown in bold.
[b] Potentially positively charged residues (Lys, Arg, free α-$NH_2$ group) are denoted*.
[c] Relative peptide hydrophobicity is represented by their reversed-phase retention times, as described in Fig. 1.

hydrophilicity of the model peptides at pH 2 and pH 7, they were subjected to RPLC. Fig. 1A and D shows the elution profiles of peptides a to h and i to l, respectively, on a $C_8$ column following application of a linear gradient (1% B/min at a flow-rate of 1 ml/min), where eluent A was 0.1% aqueous TFA and eluent B was 0.1% TFA in acetonitrile. At the pH of this commonly employed mobile phase system (pH 2), all of the potentially positively charged groups in the peptides (Table I) possess a full positive charge. Thus, peptides a to d each exhibit a net charge of +3; peptides e to h each exhibit a net charge of +2; peptides i, j, k and l exhibit net charges of +1, +2, +3 and +4, respectively. The retention times of the peptides under these conditions represent their relative hydrophobicities/hydrophilicities at pH 2 (Table I). From Fig. 1A, it can be seen that for peptide pairs of identical sequence (a–e, b–f, c–g, d–h), the analogues containing a free α-amino group (peptides a, b, c and d) were always eluted prior to their acetylated versions (peptides e, f, g and h). This was not surprising, considering the hydrophilic nature of the full positive charge on the α-amino groups.

Fig. 1B and E shows the RPLC elution profiles of peptides a to h (Fig. 1B) and i to l (Fig. 1E) obtained under the same conditions as Fig. 1A and D, save for the substitution of 0.1% $H_3PO_4$ for 0.1% TFA. The pH of the two acidic mobile phases remains the same (pH 2). The elution profiles of the peptides under the $H_3PO_4$ system are markedly different from those obtained with the TFA system. Not only are all peptides eluted earlier on the $H_3PO_4$ system, but the relative elution order of peptides was occasionally changed. Thus, from Fig. 1B (compare to 1A), peptide c is now eluted prior to peptide f and peptide d is eluted prior to peptide g (the latter pair forming a doublet); from Fig. 1E (compare 1D), peptide l is now eluted with peptide k. The decrease in peptide elution times and the changes in peptide elution order in the $H_3PO_4$ system compared to the TFA system can be rationalized by considering the relative hydrophobicities/hydrophilicities of the anionic (*i.e.*, negatively charged) trifluoroacetate and phosphate counterions. Ion-pairing reagents such as $H_3PO_4$ and TFA effect changes in peptide retention time solely through interaction with positively charged groups on a peptide [1,11]. Since, the phosphate ion of $H_3PO_4$ is a significantly more hydrophilic counterion than the trifluoroacetate

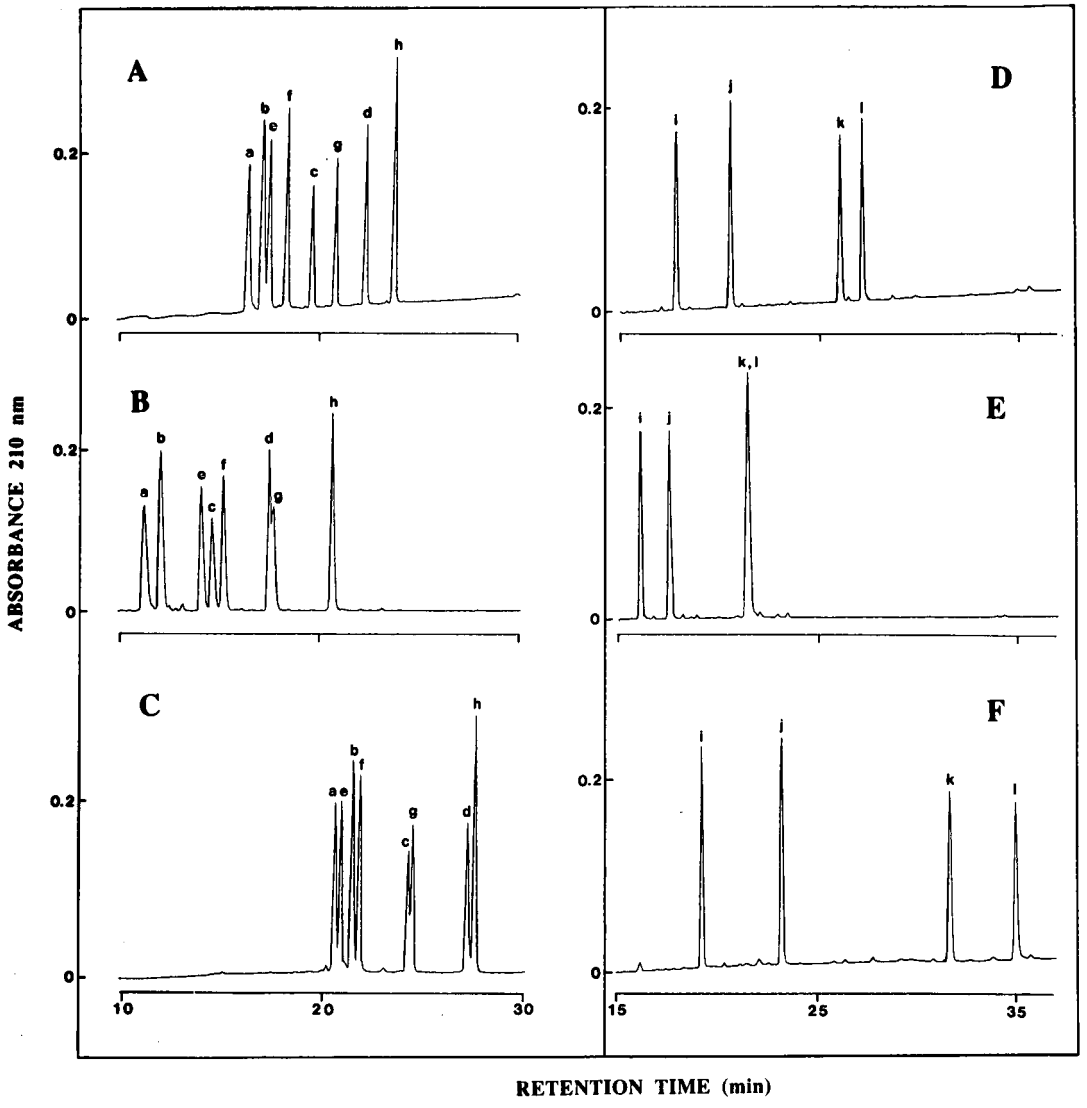


Fig. 1. Separation of mixtures of positively charged peptides by RPLC. Column, Zorbax SB-300 $C_8$ (150 × 4.6 mm I.D.). Mobile phase: panels A and D, linear A–B increasing acetonitrile gradient (1% B/min, starting with 100% A) at a flow-rate of 1 ml/min, where A is 0.1% aqueous TFA and B is 0.1% TFA in acetonitrile; panels B and E, linear A–B increasing acetonitrile gradient (1% B/min, starting with 100% A) at a flow-rate of 1 ml/min, where A is 0.1% aqueous $H_3PO_4$ and B is 0.1% $H_3PO_4$ in acetonitrile; panels C and F, linear A–B increasing acetonitrile gradient (2% B/min, equivalent to 1% acetonitrile/min,starting with 100% A) at a flow-rate of 1 ml/min, where A is 10 m*M* aqueous $(NH_4)_2HPO_4$, pH 7, and B is 50% aqueous acetonitrile containing 10 m*M* $(NH_4)_2HPO_4$, pH 7, both A and B also containing 200 m*M* $NaClO_4$. Temperature, 26°C.

ion, all 12 basic (*i.e.*, potentially positively charged) peptides shown in Table I would be expected to be eluted earlier in the presence of the phosphate ion compared to the trifluoroacetate ion, as was, indeed, the case. In addition, the magnitude of the effect on a particular peptide of changing from a more hydrophobic (less hydrophilic) ion-pairing reagent such as TFA to a less hydrophobic (more hydrophilic) ion-pairing reagent such as $H_3PO_4$ will depend on the number of positive charges the peptide contains —the greater the number of positive charges on a peptide, the greater the effect of increasing counter-

ion hydrophilicity, *i.e.*, the larger the decrease in retention time on substituting $H_3PO_4$ for TFA. Thus, comparing Fig. 1A and B, peptides with net charges of +3 (peptides a to d) exhibited an average decrease in retention time of *ca.* 5 min on substituting $H_3PO_4$ (Fig. 1B) for TFA (Fig. 1A); in contrast, peptides with net charges of +2 (peptides e to h) exhibited an average decrease in retention time of only *ca.* 3 min. Comparing Fig. 1D and E, the retention times of the four peptides decreased in the $H_3PO_4$ system (Fig. 1E) from that of the TFA system (Fig. 1D) by values of 1.8 min (peptide i; +1 net charge), 3 min (peptide j; +2), 4.5 min (peptide k; +3) and 5.6 min (peptide l; +4).

Fig. 1C and F shows the elution profiles of the peptides at pH 7. These elution profiles were obtained under linear gradient conditions (1% acetonitrile/min at a flow-rate of 1 ml/min), where the mobile phase pH 7 buffers also contained 0.2 *M* sodium perchlorate ($NaClO_4$). The addition of perchlorate was necessary for the suppression of ionic interactions between the positively charged peptides and negatively charged free silanols ($pK_a$ *ca.* 4) present on the silica-based stationary phase. Such undesirable interactions, if unsuppressed, may lead to significant band broadening and peak tailing of basic solutes. The addition of perchlorate was not necessary for the TFA and $H_3PO_4$ systems, since silanol ionization is effectively suppressed at pH 2 on this column. From Fig. 1C and F, the retention times of all 12 peptides have increased in the pH 7 system compared to the TFA system (Fig. 1A and D). The dramatic change in elution orders and increase in retention times at pH 7 are probably due to a combination of effects. The high salt concentration in the mobile phase (200 m*M* sodium perchlorate) is possibly promoting hydrophobic interactions of the peptides with the stationary phase by increasing the hydrophilicity of the mobile phase, leading to a general increase in peptide retention times over those observed at pH 2. In addition, the high concentration of the negatively charged hydrophilic perchlorate counterion could decrease the hydrophilicity of the peptides by ion-pair formation with the positively charged groups in the peptides. This effect was previously demonstrated with the negatively charged trifluoroacetate counterion which, on increasing the counterion concentration, increased peptide hydrophobicity through ion-pair formation with positively charged residues [11]. Interestingly, the peptides having identical sequence are eluted in pairs (a–e, b–f, c–g and d–h) where peptides e, f, g and h are the peptides with their N-terminals acetylated while peptides a, b, c, and d have free α-amino groups. These results suggest that the α-amino groups at pH 7 are not fully charged and therefore the acetylated and non-acetylated peptides of the same sequence have similar overall hydrophobicities at pH 7 when compared to pH 2 (the differences in elution times of the peptide pairs in panel A varies from 1.1 to 1.4 min compared to 0.2 to 0.4 min in panel C). The $pK_a$ of an α-amino group in free amino acids is generally in the range of 9 to 10, but may be lowered significantly in peptides and proteins, depending on the microenvironment created by the N-terminal residue side-chain. Hence, deprotonation of the α-amino group may occur at pH values around neutrality. This laboratory has demonstrated (unpublished results) that this effect is not limited to basic residues (such as the N-terminal arginine residues of peptides a–h), but occurs to a greater or lesser extent with all 20 amino acids. The different counterions and pH values were chosen for RPLC to allow for a better comparison of RPLC with the mixed-mode hydrophilic–cation-exchange chromatography.

*Mixed-mode chromatography of peptides on a cation-exchange column*

While the major separation mechanism of IEC is electrostatic in nature, ion-exchange packings may also exhibit significant hydrophobic characteristics, giving rise to mixed-mode contributions to solute separations. Fig. 2A and C shows elution profiles of peptides a3, d3, e2 and h2 (Fig. 2A) and peptides i1, j2, k3 and l4 (Fig. 2B) on the PolySulfoethyl A strong cation-exchange column. The peptides were eluted by a linear gradient (5 m*M* salt/min at a flow-rate of 1 ml/min) of $NaClO_4$ in triethylammonium phosphate (TEAP) buffer at pH 7. As would be expected, the major peptide separation mechanism was electrostatic in nature with the more highly charged a3 and d3 being eluted later than the lesser charged e2 and h2. Similarly, peptides i1, j2 and k3 (+1, +2 and +3 net charge, respectively) were eluted in order of increasing net positive charge. However, it is clear that a secondary hydrophobic separation mechanism is also present, with the more

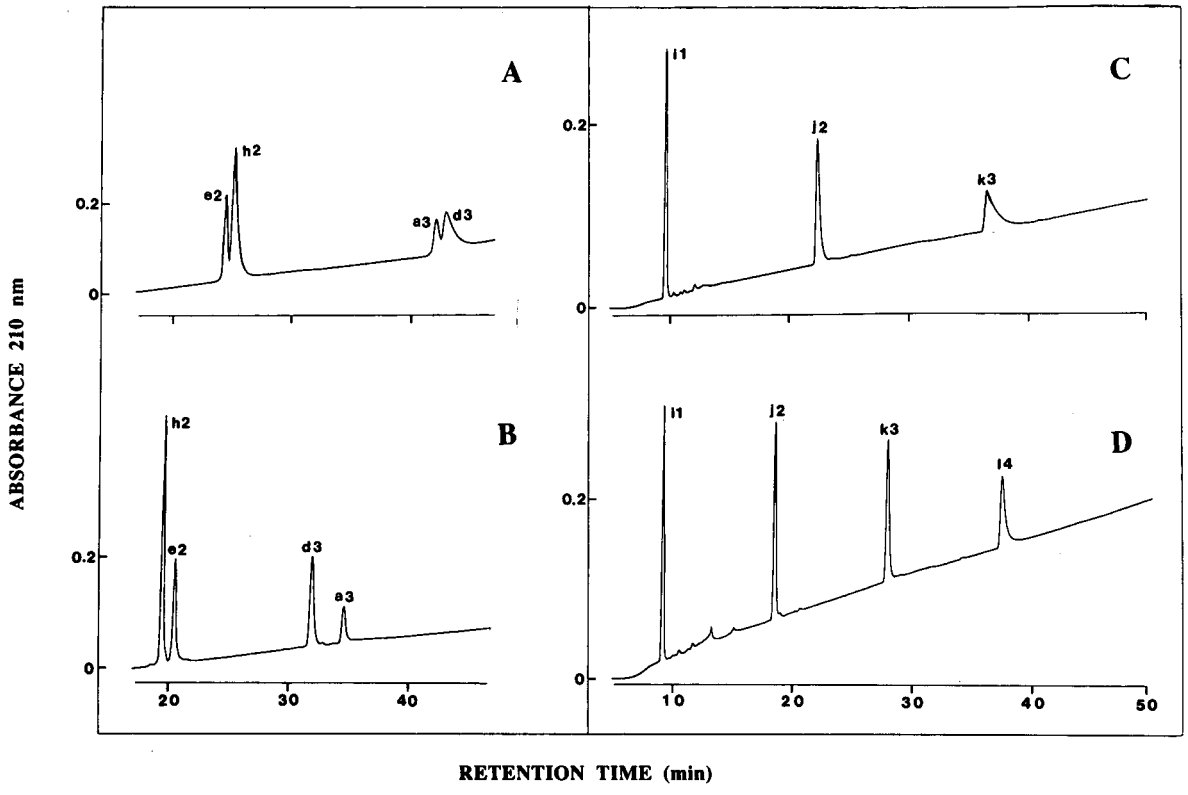


Fig. 2. Demonstration of hydrophobic and hydrophilic interactions between positively charged peptides and the stationary phase during strong cation-exchange chromatography. Column, PolySulfoethyl A strong cation-exchange column (200 × 4.6 mm I.D.). Mobile phase: panels A and C, linear A–B increasing salt gradient (2% B/min, equivalent to 5 m*M* $NaClO_4$/min, starting with 100% A) at a flow-rate of 1 ml/min, where A is 5 m*M* aqueous TEAP, pH 7, and B is A plus 0.25 *M* $NaClO_4$, pH 7; panels B and D, linear A–B increasing salt gradient (2% B/min, equivalent to 5 m*M* $NaClO_4$/min, starting with 100% A) at a flow-rate of 1 ml/min, where A is 5 m*M* aqueous TEAP, pH 7, and B is A plus 0.25 *M* $NaClO_4$, pH 7, both A and B containing 15% (v/v) acetonitrile. Temperature, 26°C. Peptides are denoted by both a letter and a number, with the number denoting the number of potentially positively charged groups a particular peptide contains, *e.g.*, d3 denotes that peptide d has three potentially positively charged groups. The sequences of the peptides are shown in Table I.

hydrophobic h2 and d3 being eluted after the less hydrophobic e2 and a3, respectively (Fig. 2A). Also, peptide l4 (+4 net charge and the most hydrophobic peptide employed in this study; Table I) was not even eluted from the column under these conditions.

Fig. 2B and D shows elution profiles of the same peptide mixtures under the same run conditions, save for the addition of 15% (v/v) acetonitrile to the mobile phase to overcome hydrophobic interactions. The excellent solubility of TEAP and $NaClO_4$ in such aqueous acetonitrile solutions recommended their employment in the present study. From Fig. 2B and D, the peptides (including l4) were eluted earlier, and with generally improved peak shape, compared to the elution profiles obtained in the absence of acetonitrile (Fig. 2A and C). In addition, when comparing Fig. 2B with A, it can also be seen that like-charged peptide pairs e2–h2 and a3–d3 have reversed their elution orders in the presence of 15% acetonitrile (Fig. 2B) compared to those observed in its absence (Fig. 2A). Thus, the peptides are now eluted in order of increasing hydrophilicity with e2 being eluted after h2, and a3 being eluted after d3. Hence, following suppression of hydrophobic interactions by the addition of acetonitrile, the peptide separation mechanism has become based upon

mixed-mode ionic and hydrophilic interactions (Fig. 2B), compared to the mixed-mode ionic and hydrophobic interactions apparent in the absence of acetonitrile (Fig. 2A). This mixed-mode hydrophilic-cation-exchange chromatography (HILIC-CEC) separation resulted in an excellent separation of identically charged peptides, with good peak shape and baseline resolution.

*Effect of acetonitrile concentration on HILIC-CEC of peptides*

The results shown in Fig. 2, concerning the induction of a mixed hydrophilic ionic mode of chromatography in the presence of acetonitrile, prompted a more thorough investigation of the effect of increasing acetonitrile concentration (up to 90%, v/v) on peptide elution profiles during HILIC-CEC. Fig. 3 shows the elution profiles of peptides a to h (Table I) obtained on the PolySulfoethyl A column under the same gradient elution conditions as Fig. 2, save for the presence of 80% (Fig. 3A), 70% (Fig. 3B), 30% (Fig. 3C) or 15% (Fig. 3D) (v/v) acetonitrile in the mobile phase.

From Fig. 3, hydrophilic interactions between the peptides and the stationary phase generally increased with increasing acetonitrile concentration. This is apparent from the progressively improved resolution of the identically charged peptides as the acetonitrile concentration was raised. Thus, at a level of 15% acetonitrile (Fig. 3D), each set of four peptides of like charge (a3 to d3; e2 to h2) were not completely resolved. In contrast, at acetonitrile concentrations of 70% (Fig. 3B) and 80% (Fig. 3A), all eight peptides are resolved to baseline with good peak shape and no tailing. At all levels of acetonitrile shown in Fig. 3, peptides of like charge were eluted in order of increasing hydrophilicity.

The increasing importance of an hydrophilic mechanism in the mixed-mode chromatography illustrated in Fig. 3 is also highlighted by considering the elution behaviour of peptides e2 and d3. Although more highly charged, d3 is considerably more hydrophobic (less hydrophilic) relative to e2 from Table I, d3 and e2 exhibited RPLC retention times of 27.2 min and 20.9 min, respectively, at pH 7. If the peptides were being separated solely by an hydrophilic mechanism, d3 would be eluted prior to e2, which is clearly not the case in Fig. 3. From Fig. 3, since the hydrophilic separation mechanism is

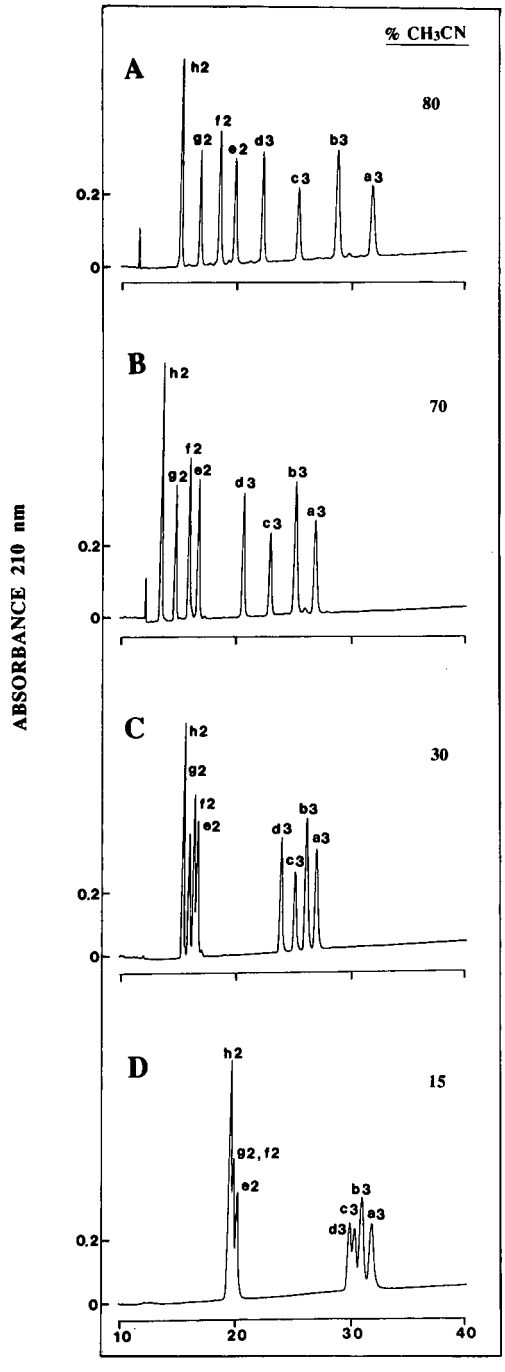


Fig. 3. Effect of acetonitrile concentration on peptide separations during strong cation-exchange chromatography. Column, same as Fig. 2. Mobile phase, linear A–B increasing salt gradient (2% B/min, equivalent to 5 m*M* $NaClO_4$/min, starting with 100% A) at a flow-rate of 1 ml/min, where A is 5 m*M* aqueous TEAP, pH 7, and B is A plus 0.25 *M* $NaClO_4$, pH 7, both A and B containing 80% (panel A), 70% (panel B), 30% (panel C) or 15% (panel D) (v/v) acetonitrile. Temperature, 26°C. The sequences of the peptides are shown in Table I. For peptide denotion, see Fig. 2.

secondary to that of the ionic interactions, particularly at the lower acetonitrile concentrations, d3 is eluted after e2. However, as the acetonitrile concentration is increased, the difference in retention times of these two peptides decreased. Thus, at an acetonitrile concentration of 20%, the retention time difference ($\Delta t$) between these two peptides was 10 min, decreasing to 6.5 min, 1.8 min and 0.6 min at acetonitrile concentrations of 50%, 80% and 90%, respectively, underscoring the increasing influence of hydrophilic interactions in the separation process.

Also from Fig. 3, acetonitrile concentration has little effect on the retention time difference between peptides of similar hydrophobicity/hydrophilicity. For example, $\Delta t$ for h2 and d3 (RPLC retention times of 27.5 min and 27.2 min, respectively, at pH 7; Table I) was 12 min at acetonitrile concentrations of both 20% and 90%.

Fig. 4 summarizes the effect of acetonitrile concentration on the mixed-mode retention behaviour of peptides a3, d3, e2 and h2 on the cation-exchange column. From Fig. 4 (and Fig. 3), as the acetonitrile concentrtion in the mobile phase was raised from 0% to 20%, peptide retention times decreased as hydrophobic interactions were suppressed. Note the reversal in elution order of peptides a3 and d3, and e2 and h2 at 10% acetonitrile as hydrophilic interactions come into play. As the acetonitrile concentration was raised further to 70%, little effect on peptide retention times was observed, save for a slow decrease in retention time of d3 and h2. A further

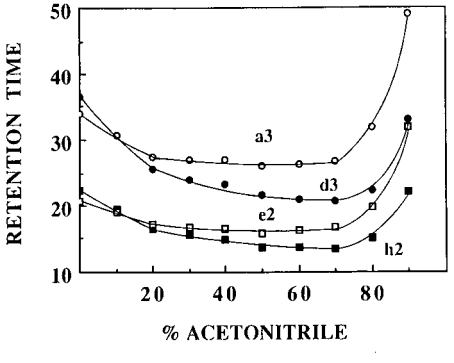


Fig. 4. Plot of peptide retention time *versus* acetonitrile concentration (v/v) in the mobile phase during strong cation-exchange chromatography. Column and mobile phase, same as Fig. 3. The sequences of peptides a3, d3, e2 and h2 are shown in Table I. For peptide denotion, see Fig. 2.

increase in the acetonitrile level up to 90% produced a marked increase in peptide retention times, probably due to an increase in hydrophilic interactions with increasing levels of acetonitrile, until such interactions may possibly be dominating the mixed-mode separation mechanism (note, as mentioned above, how peptides d3 and e2 are almost coeluted in the presence of 90% acetonitrile).

*Effect of acetonitrile concentration on cation-exchange column selectivity*

The possibility, suggested by the results of Figs. 3 and 4, that an hydrophilic interaction mechanism may be the dominant separation process during HILIC–CEC in the high acetonitrile concentrations was now further investigated. To this end, all 12 peptides in Table I were subjected to HILIC-CEC under the same gradient elution conditions, with varying acetonitrile levels in the mobile phase, as those employed for Figs. 2, 3 and 4. It was felt that, if hydrophilic interactions were to become dominant in the mixed-mode separation process (*i.e.*, no longer secondary to ionic interactions), then a peptide of higher net positive charge could be eluted earlier than a peptide of lower net positive charge if the overall hydrophilicity of the latter (expressed as RPLC retention time at pH 7; Table I) was greater than that of the former, *i.e.*, perhaps column selectivity could be dramatically changed for charged peptides depending upon the acetonitrile concentration [12]. From the results of Fig. 5, it can be seen that this was indeed achieved with certain peptides. Thus, at a level of 90% acetonitrile (Fig. 5A) peptide i1 (19.2 min RPLC retention time at pH 7) was eluted after the less hydrophilic peptide h2 (RPLC; 27.5 min). Similarly, e2 (RPLC; 20.9 min) was eluted after the much less hydrophilic k3 (RPLC; 31.7 min). Most dramatically, peptide l4 (RPLC; 35.0 min) was eluted before the more hydrophilic c3, b3 and a3 (RPLC; 24.2 min, 21.4 min, 20.6 min, respectively).

Fig. 5B demonstrates how dominant hydrophilic (over ionic) interactions may be maintained while reducing analysis time but retaining good column selectivity. This was achieved by employment of an increasing salt gradient combined with a decreasing acetonitrile gradient. The lower level of acetonitrile in buffer B (50% as against 90% in buffer A) led to a decrease in peptide retention relative to that effected by maintaining 90% acetonitrile in both mobile

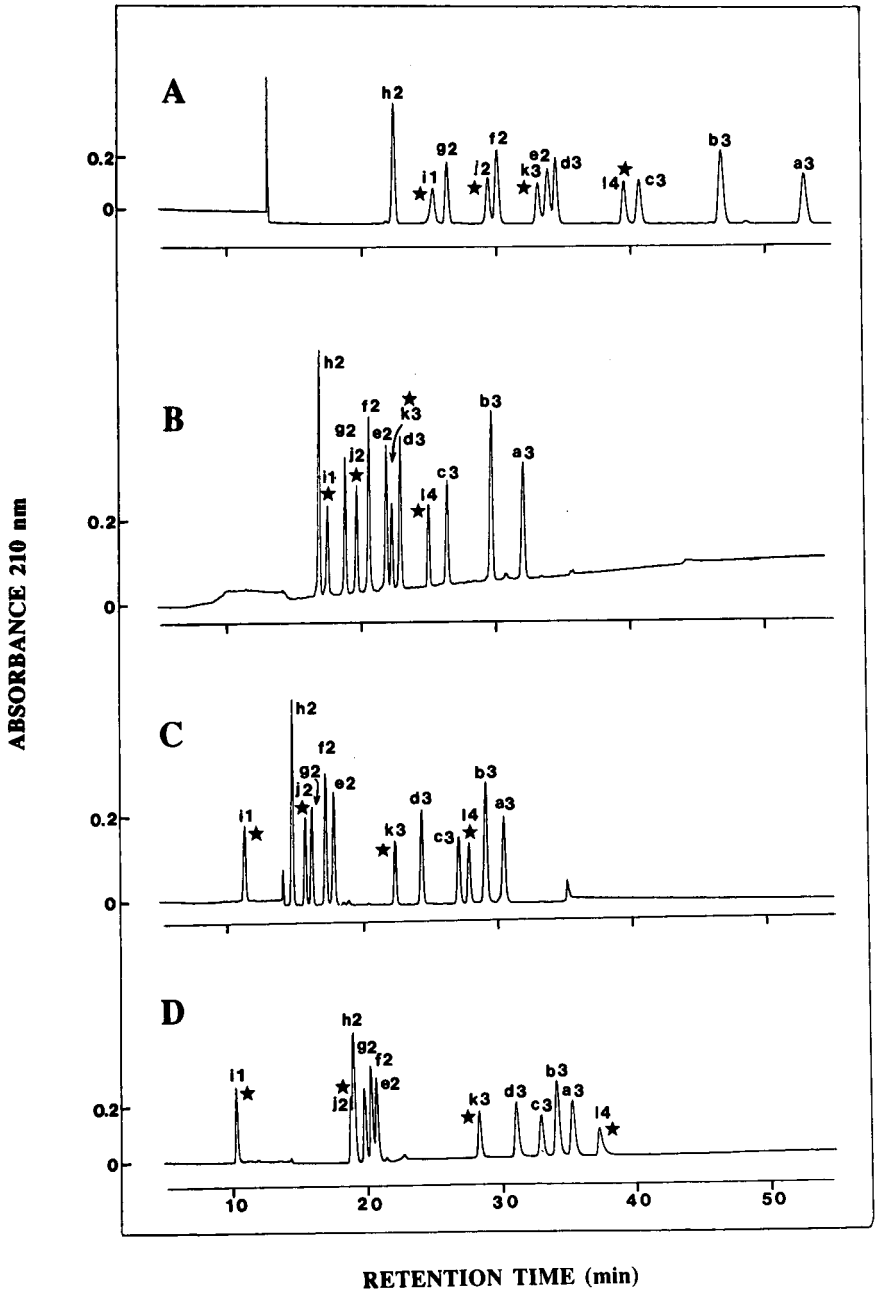


Fig. 5. Effect of acetonitrile concentration on column selectivity during HILIC-CEC of peptides. Column, same as Fig. 2. Mobile phase: panels A, C and D, linear A–B increasing salt gradient (2% B/min, equivalent to 5 m*M* $NaClO_4$/min, starting with 100% A) at a flow-rate of 1 ml/min, where A is 5 m*M* aqueous TEAP, pH 7, and B is A plus 0.25 *M* $NaClO_4$, pH 7, both A and B containing 90% (panel A), 50% (panel C) or 20% (panel D) (v/v) acetonitrile; panel B, linear A–B gradient (2% B/min, equivalent to a linear increasing salt gradient of 5 m*M* $NaClO_4$/min and a linear decreasing acetonitrile gradient of 0.8% acetonitrile/min, starting with 100% A) at a flow-rate of 1 ml/min, where A is 5 m*M* aqueous TEAP, pH 7, containing 90% (v/v) acetonitrile and B is 5 m*M* aqueous TEAP, pH 7, containing 0.25 M $NaClO_4$ and 50% (v/v) acetonitrile. Temperature, 26°C. The sequences of the peptides are shown in Table I. The stars denote the positions of peptides i1, j2, k3 and l4 (+1 to +4 net charge, respectively) relative to the non-acetylated (a to d) and acetylated (e to h) peptide analogues. For peptide denotion, see Fig. 2.

phase buffers (Fig. 5A). The peptide elution order obtained with this combined salt and acetonitrile gradient (Fig. 5B) was almost identical (save for a reversal of e2 and k3) to that shown in Fig. 5A, but was obtained in about 2/3 of the time and with sharper peptide peaks.

As the concentration of acetonitrile in the mobile phase was decreased to 50% (Fig. 5C), peptides were generally eluted in order of increasing net positive charge, except for l4 (RPLC retention time of 35.0 min at pH 7.0; Table I) which was still eluted earlier than the lesser charged a3 and b3 (RPLC retention times of 20.6 min and 21.4 min, respectively). Thus, even at relatively lower acetonitrile concentrations (*e.g.*, 50% as opposed to 90%), more highly charged peptides may still be eluted prior to less highly charged peptides if the latter are significantly more hydrophilic than the former.

At a concentration of 20% acetonitrile in the mobile phase (Fig. 5D), the overall elution order of all 12 peptides was based on increasing net positive charge, *i.e.*, ionic interactions are dominating the separation process.

An interesting anomaly of Fig. 5 is the retention behaviour of peptide j2 relative to peptides e2 to h2. All five of these peptides possess a net charge of +2. The elution order of e2 to h2 remains constant through all levels of acetonitrile concentrations employed in Fig. 5, *i.e.*, in order of increasing peptide hydrophilicity h2 < g2 < f2 < e2. However, j2, which may be expected to be eluted between f2 and g2 (see Table I for RPLC retention times at

TABLE II

COMPARISON OF RPLC AND MIXED-MODE CEC FOR PEPTIDE SEPARATIONS

| Peptides[a] | $\Delta t(R_s)$[d] | | | | | | | | | | | |
|---|---|---|---|---|---|---|---|---|---|---|---|---|
| | RPLC[b], pH 2 | | RPLC, pH 7 | | CEC[c] 50/50 | | CEC 80/80 | | CEC 90/90 | | CEC 90/50 | |
| *A. Peptides with different net positive charges* | | | | | | | | | | | | |
| a–e | −1.1 | (3.8) | −0.3 | (1.3) | 12.6 | (33.7) | 15.4 | (31.3) | 19.1 | (26.7) | 10.2 | (29.2) |
| b–f | −1.2 | (4.6) | −0.4 | (1.5) | 11.9 | (33.3) | 12.9 | (28.1) | 16.7 | (25.8) | 9.1 | (28.9) |
| c–g | −1.2 | (5.0) | −0.2 | (0.9) | 10.9 | (32.9) | 10.3 | (30.9) | 14.3 | (26.8) | 7.6 | (26.3) |
| d–h | −1.4 | (6.4) | −0.4 | (1.4) | 9.6 | (31.4) | 8.5 | (24.8) | 12.1 | (24.5) | 6.0 | (22.9) |
| e–b | 0.3 | (1.3) | −0.6 | (2.4) | −11.3 | (30.8) | −11.2 | (23.9) | −12.9 | (19.0) | −7.8 | (24.1) |
| c–f | 1.3 | (5.3) | 2.4 | (10.1) | 9.9 | (29.1) | 7.9 | (22.7) | 10.6 | (18.1) | 5.8 | (19.6) |
| g–d | −1.5 | (6.7) | −2.7 | (10.6) | −8.2 | (25.3) | −5.8 | (16.3) | −8.1 | (15.9) | −4.1 | (15.1) |
| *B. Peptides with +3 net charge only* | | | | | | | | | | | | |
| a–b | −0.7 | (2.3) | −0.9 | (3.3) | 1.4 | (3.1) | 4.2 | (7.0) | 6.2 | (8.3) | 2.4 | (6.2) |
| b–c | −2.5 | (8.8) | −2.8 | (10.9) | 2.0 | (4.9) | 5.0 | (10.7) | 6.1 | (9.2) | 3.3 | (9.6) |
| c–d | −2.7 | (11.2) | −2.9 | (11.5) | 2.8 | (7.2) | 4.4 | (11.6) | 6.2 | (10.6) | 3.5 | (11.4) |
| k–d | 3.7 | (15.5) | 4.6 | (17.4) | −2.0 | (5.7) | −0.3 | (0.8) | −1.4 | (2.4) | −0.6 | (2.4) |
| *C. Peptides with +2 net charge only* | | | | | | | | | | | | |
| e–f | −0.9 | (3.8) | −0.9 | (3.9) | 0.6 | (2.1) | 1.8 | (5.0) | 3.8 | (6.3) | 1.3 | (4.6) |
| f–g | −2.4 | (11.0) | −2.6 | (11.1) | 1.0 | (3.7) | 2.4 | (7.3) | 3.7 | (7.3) | 1.8 | (6.7) |
| g–h | −2.9 | (13.1) | −3.1 | (12.9) | 1.4 | (5.6) | 2.6 | (9.1) | 4.0 | (9.0) | 1.9 | (7.8) |
| e–j | −3.0 | (12.9) | −2.4 | (10.7) | 2.1 | (8.0) | 3.4 | (9.9) | 4.5 | (7.4) | 2.2 | (8.1) |
| g–j | 0.3 | (1.5) | 1.2 | (5.3) | 0.5 | (1.8) | −0.8 | (2.4) | −3.0 | (5.9) | −0.9 | (3.2) |

[a] The letters denote the peptides listed in Table I.

[b] The chromatographic conditions for RPLC at pH 2 (TFA system) and pH 7 are shown in Fig. 1.

[c] The chromatographic conditions for CEC are shown in Fig. 5. The values 50/50, 80/80, 90/90 and 90/50 denote the acetonitrile concentrations (%, v/v) in buffers A and B, respectively, used in linear AB gradients.

[d] $\Delta t$ denotes the difference in retention time between two peptides. For example, "a–e" (RPLC, pH 2) denotes the retention time of peptide a minus the retention time of peptide e: 16.4 min–17.5 min = −1.1 min. Resolution ($R_s$) was calculated from the equation $R_s = 1.176\,\Delta t/(w_1 + w_2)$, where $\Delta t$ is the retention time difference between two peptides and $w_1$ and $w_2$ are the peak widths at half height.

pH 7), exhibited a varying elution position relative to the other four peptides as the acetonitrile concentration is varied. Thus, from being eluted just prior to peptide f2, and well after peptides h2 and g2 at a concentration of 90% acetonitrile (Fig. 5A), peptide j2 gradually moved through the elution order as the acetonitrile concentration was decreased until, at a level of 20% acetonitrile (Fig. 5D), it was eluted prior to all four peptides possessing a net charge of +2. It is known that aqueous solutions of acetonitrile may affect the conformation of peptides, *e.g.*, the induction of α-helical structure in potentially helical peptides. The anomalous behaviour of peptide j2 relative to the other four like-charged peptides may be due to such conformational changes at different acetonitrile concentrations.

*Comparison of RPLC and HILIC-CEC for peptide separations*

Table II shows the resolution of selected peptide pairs following RPLC and HILIC-CEC of all 12 peptides in Table I. The aqueous TFA–acetonitrile, pH 2, RPLC mobile phase represents the run conditions employed by the great majority of researchers for peptide applications. The pH 7 run serves as a comparison. The HILIC-CEC results represent peptide separations obtained by a range of run conditions designed to manipulate the separation process. Thus, the peptide mixture was resolved by a separation process where ionic interactions were dominant (50/50, *i.e.*, 50% acetonitrile, v/v, in both buffers) or a separation process where hydrophilic interactions become increasingly more important as the acetonitrile concentration was raised.

For peptides with different net positive charges (and close relative hydrophobicities at pH 2), the selectivity advantage of HILIC-CEC over that of RPLC at either pH 2 or pH 7 is quite clear. During RPLC at pH 2, the resolution of peptide pairs ranged from 1.3 (e–b) to 6.7 (g–d); in contrast, HILIC-CEC (50/50) achieved resolution values ranging from 25.3 (g–d) to 33.7 (a–e).

From Table IIB and C, it can be seen that even instances where RPLC proved to be superior to that of HILIC-CEC for separating peptides of the same net charge, separations based on the latter approach were still excellent. In fact, depending on the conditions of HILIC-CEC, this approach frequently produced superior separation of such peptide pairs compared to that of RPLC at pH 2. For instance, for peptides of +3 net charge only, the resolution obtained by HILIC-CEC (80/80 and 90/50) was superior for three out of four peptide pairs, k–d being the exception. Similarly, for peptide pairs e–f and g–j (peptides with +2 net charge only), the resolution achieved by HILIC-CEC at the higher acetonitrile concentrations (80–90%) were superior to that obtained by RPLC at pH 2. Resolution of the other three peptide pairs in Table IIC by HILIC-CEC in the presence of the higher acetonitrile concentration also compared well with the RPLC results. It is difficult to make a meaningful comparison of peak capacity between the RPLC and HILIC-CEC approaches to peptide separations, since the two separation modes are so different mechanistically. Thus, we compared the effectiveness of the two HPLC approaches for resolving all 12 peptides in Table I by applying the equation, $\Delta t/W_{1/2}$, where $\Delta t$ is the retention time difference between the first and last eluted peptide and $W_{1/2}$ is the average peak width of all 12 peptides. Representative values obtained were 75 (RPLC at pH 2), 88 (HILIC-CEC 90/90; Fig. 5A) and 98 (HILIC-CEC 50/50; Fig. 5C), indicating that the excellent selectivity of the HILIC-CEC approach is being achieved without any serious concomitant band broadening.

## CONCLUSIONS

Mixed-mode hydrophilic and ionic interaction chromatography (HILIC-IEC) combines the most advantageous aspects of two widely different separation mechanisms: a separation based upon hydrophilicity/hydrophobicity differences between peptides and the large selectivity advantages of ion-exchange chromatography on the separation of peptides of varying net charge. Peptide separations were generally achieved by utilizing a linear increasing salt (sodium perchlorate) gradient in the presence of acetonitrile (20% to 90%, v/v) at pH 7. The presence of acetonitrile promotes hydrophilic interactions with the hydrophilic stationary phase, these hydrophilic interactions becoming increasingly important to the separation process as the acetonitrile concentration was increased. This mixed-mode methodology on a strong CEC column was compared to reversed-phase chromatography of

positively charged peptides at pH 2 and pH 7. The results of this comparison suggested that, although the mobile phases employed for HILIC-IEC in this study are somewhat less convenient than the volatile mobile phases characteristic of RPLC, HILIC-IEC may rival RPLC for peptide separations.

ACKNOWLEDGEMENTS

This work was supported by the Medical Research Council of Canada and equipment grants from the Alberta Heritage Foundation for Medical Research.

REFERENCES

1 C. T. Mant and R. S. Hodges, *HPLC of Peptides and Proteins: Separation, Analysis and Conformation*, CRC Press, Boca Raton, FL, 1991.
2 C. T. Mant and R. S. Hodges, *J. Chromatogr.*, 326 (1985) 349.
3 C. T. Mant and R. S. Hodges, *J. Chromatogr.*, 327 (1985) 147.
4 A. J. Alpert and P. C. Andrews, *J. Chromatogr.*, 443 (1988) 85.
5 D. L. Crimmins, J. Gorka, R. S. Thoma and B. D. Schwartz, *J. Chromatogr.*, 443 (1988) 63.
6 P. C. Andrews, *Pept. Res.*, 1 (1988) 93.
7 C. T. Mant and R. S. Hodges, *J. Liq. Chromatogr.*, 12 (1989) 139.
8 T. W. L. Burke, C. T. Mant, J. A. Black and R. S. Hodges, *J. Chromatogr.*, 476 (1989) 377.
9 B.-Y. Zhu, C. T. Mant and R. S. Hodges, *J. Chromatogr.*, 548 (1991) 13.
10 A. J. Alpert, *J. Chromatogr.*, 499 (1990) 177.
11 D. Guo, C. T. Mant and R. S. Hodges, *J. Chromatogr.*, 386 (1987) 205.
12 G. B. Cox and R. W. Stout, *J. Chromatogr.*, 384 (1987) 315.

*Journal of Chromatography*, 594 (1992) 87–96
Elsevier Science Publishers B.V., Amsterdam

CHROM. 23 939

# Suppression of the effect of metal impurities in alkylsilylated silica packing materials

Kazuhiro Kimata, Nobuo Tanaka* and Takeo Araki

*Kyoto Institute of Technology, Department of Polymer Science and Engineering, Matsugasaki, Sakyo-ku, Kyoto 606 (Japan)*

(First received October 11th, 1991; revised manuscript received December 9th, 1991)

ABSTRACT

Octadecylsilylated silica packing materials prepared from octadecyltrichlorosilane showed much better performance than those prepared from octadecyldimethylchlorosilane for chelating compounds that can interact with metal impurities in the silica support. Stationary phases containing an ether linkage in the alkyl group also showed improved performance. The presence of polar groups and the increased hydrophilicity of such stationary phases can account for the results based on the better accessibility of metal sites in a hydrophobic stationary phase. Similar results were obtained with carboxylic acids and phenols. Packing materials prepared from high-purity silica gel showed good performance for all the solutes studied, regardless of the functionality of the silylating reagents.

## INTRODUCTION

The retention of a solute in reversed-phase liquid chromatography (RPLC) is primarily determined by the interactions between the solute and aqueous–organic solvents in the mobile phase and between the solute and the alkylsilyl groups on silica surfaces containing solvent molecules extracted from the mobile phase [1–4]. In addition to these essential constituents of RPLC systems, surface silanols and metal impurities are known to participate in the retention of solutes.

The sources of undesirable secondary retention processes which cause peak tailing in RPLC were accessible silanols, surface acidity and metal impurities [5–14]. The binary metal oxide structures provided by the presence of metals other than silicon in the silica skeleton seem to provide surface acidity as in silica–alumina acidic catalysts [14–16]. The metal impurities also participate in the interaction with chelating reagents [14,17].

Much effort has been made to eliminate these secondary retention processes from silica-based packing materials. Trimethylsilylation (end-capping of silanols) proved to be effective for reducing the effect of hydrogen bonding between silanols and proton acceptors. Extensive alkylsilylation, however, was not totally successful in eliminating tailing associated with amines and chelates, and sometimes showed adverse effects for carboxylic acids and phenols [18].

The effects of isolated silanols can be minimized by hydrating the silica surface by using hydrofluoric acid and other bases [5]. The effects of surface acidity caused by metal impurities on the elution of amines can be suppressed by the use of mobile phase additives or by treating silica gel with hydrochloric acid or nitric acid prior to alkylsilylation [11,13]. The acid treatment reduces the metal content of the silica gel. This treatment, however, was insufficiently complete to eliminate the effect of metal impurities on the elution of chelating reagents.

The use of high-purity silica gel as a support, particularly in combination with polymer coating, has been shown to be very effective in eliminating all the secondary retention processes related to metal impurities in silica [13,14,19,20]. However, the availability of high-purity silica gel is relatively limited at present. The polymer coating cannot be readily carried out in common laboratories. More practical

0021-9673/92/$05.00 

ways to eliminate the secondary retention processes related to metals would be valuable in this respect.

We report here that the extent of the undesirable secondary retention process related to metal impurities is strongly dependent on the hydrophobic property of the stationary phase, and that RPLC packing materials containing some hydrophilic groups can perform much better with metal-interacting solutes even in the presence of metal impurities. Such hydrophilic groups can be easily introduced into the stationary phase by using octadecyltrichlorosilane or an alkylsilane containing an ether linkage in the alkyl group. These stationary phases are easy to prepare, not requiring high-purity silica gel, and can provide a practical solution for reducing the secondary retention process for chelating compounds, carboxylic acids and phenol derivatives.

## EXPERIMENTAL

### *Materials*

Two types of silica gel particles [Develosil, 5 $\mu$m, 330 $m^2/g$ (Nomura Chemicals, Seto, Japan) and Kromasil, 5 $\mu$m, 340 $m^2/g$ (Eka Nobel, Surte, Sweden)] were used to prepare $C_{18}$ packing materials with octadecyldimethylchlorosilane (I), octadecylmethyldichlorosilane (II) and octadecyltrichlorosilane (III), with end-capping (designated as T) or without. The silica gels were treated with 6 *M* hydrochloric acid (10 ml/g silica) under reflux for 2 h. This process was repeated three times. The alkylsilylation was carried out in dry toluene and dry pyridine as described previously [21]. Octadecylsilylation was repeated twice to ensure maximum surface coverage with octadecyl groups.

Octadecylsilylating and trimethylsilylating reagents were purchased from Petrarch Systems (Bristol, PA, USA). Tetradecyloxypropyldimethylchlorosilane [E: $C_{14}H_{29}O(CH_2)_3Si(CH_3)_2Cl$] was prepared by the reaction of allyl tetradecyl ether with dimethylchlorosilane in the presence of platinum catalyst. Other chemicals were of analytical-reagent grade obtained from Nacalai Tesque (Kyoto, Japan).

For the study of the effect of highly acidic silanols, heat treatment of silica particles was carried out at 700°C for 7 h in a ceramic pot. Thermally treated silica was cooled, then refluxed in 6 *M* HCl for 2 h to rehydrate the surface. Thermal treatment is designated as H and the subsequent acid treatment as A in the designation of the stationary phases. The silica gels were subjected to Fourier transform IR analysis (FIRIS 100; Fuji Electric, Tokyo, Japan) for the surface hydroxyl groups. Metal analysis of silica particles was carried out by inductively coupled plasma atomic emission spectrometry (ICPS-1000 plasma spectrometer; Shimadzu, Kyoto, Japan), following dissolution of silica gel in 50% aqueous hydrofluoric acid.

### *Equipment*

The high-performance liquid chromatographic (HPLC) system consisted of an LC-6A pump, SPD-6A variable-wavelength UV detector and C-R5A data processor (all from Shimadzu). Chromatographic measurements were carried out at 30°C by immersing the column in a thermostated water-bath.

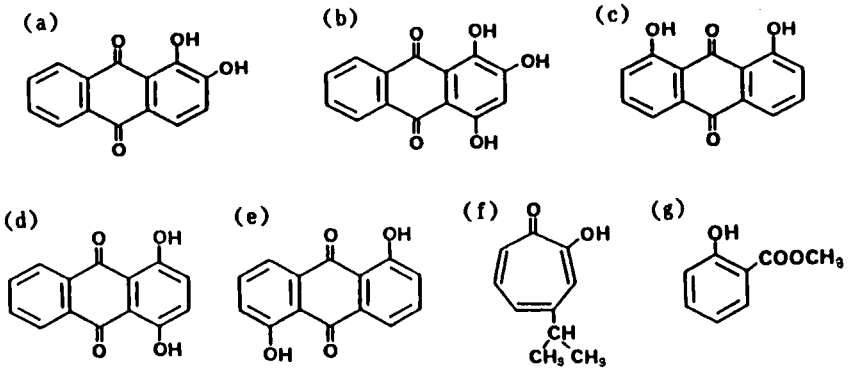


Fig. 1. Structures of chelating reagents. (a) Alizarin; (b) purpurin; (c) chrysazin; (d) quinizarin; (e) anthrarufin; (f) hinokitiol; (g) methyl salicylate.

TABLE I

METAL ANALYSIS OF SILICA GEL PARTICLES

| Silica | Metal content (ppm) | | | | | | | |
|---|---|---|---|---|---|---|---|---|
| | Al | Ca | Fe | K | Mg | Na | Ti | Zr |
| Develosil | 54 | 215 | <0.2[a] | <0.5[a] | 51 | 25 | 38 | 5 |
| Kromasil | <1[a] | <1[a] | <0.2[a] | <0.5[a] | <0.1[a] | 25 | 2 | <0.2[a] |

[a] Lower than the detection limit indicated.

## RESULTS AND DISCUSSION

$C_{18}$ phases with and without end-capping were prepared from the two types of silica gels with different metal contents. The silica gel particles were treated with acid prior to octadecylsilylation to remove as much metal impurities as possible. Table I lists the metal contents of the two silica gels after acid treatment. Kromasil is one of the few high-purity silica gels available at present (high-purity silica gels can also be obtained from other manufacturers, including Rockland Technologies and Separations Group, and from others as chemically bonded phases).

The alkylsilylation was carried out under conditions that would allow maximum surface coverage. Table II shows that the $C_{18}$ packing materials prepared from the trifunctional silane, D-$C_{18}$(III)

TABLE II

SURFACE COVERAGE AND HYDROPHOBIC PROPERTIES OF $C_{18}$ PACKING MATERIALS

D = Develosil; K = Kromasil; $C_{18}$(I) = prepared with octadecyldimethylchlorosilane; $C_{18}$(II) = from dichlorosilane; $C_{18}$(III) = from trichlorosilane; $C_{18}$(E) = from tetradecyloxypropylsilane; T = trimethylsilylation; H = heat treatment; A = acid treatment.

| Stationary phase | Carbon content (%) | Surface coverage ($\mu$mol/m$^2$) | Selectivity | | $N^c$ |
|---|---|---|---|---|---|
| | | | $\alpha(CH_2)^a$ | $\alpha(CO)^b$ | |
| D-$C_{18}$(I) | 15.92 | 2.53 | 1.500 | 0.332 | 9930 |
| D-$C_{18}$(I)-T | 15.99 | – | 1.511 | 0.321 | 10900 |
| D-$C_{18}$(II) | 17.57 | 3.08 | 1.495 | 0.324 | 11790 |
| D-$C_{18}$(II)-T | 17.81 | – | 1.500 | 0.315 | 11140 |
| D-$C_{18}$(III) | 17.31 | 3.25 | 1.469 | 0.368 | 10420 |
| D-$C_{18}$(III)-T | 17.69 | – | 1.488 | 0.327 | 10440 |
| K-$C_{18}$(I) | 14.42 | 2.46 | 1.510 | 0.316 | 9670 |
| K-$C_{18}$(I)-T | 14.64 | – | 1.523 | 0.300 | 8830 |
| K-$C_{18}$(II) | 15.12 | 2.79 | 1.497 | 0.325 | 8780 |
| K-$C_{18}$(II)-T | 15.63 | – | 1.507 | 0.308 | 7270 |
| K-$C_{18}$(III) | 15.01 | 2.97 | 1.474 | 0.380 | 6570 |
| K-$C_{18}$(III)-T | 15.85 | – | 1.496 | 0.315 | 7610 |
| D-$C_{18}$(E) | 11.77 | 1.86 | 1.428 | 0.379 | 9210 |
| D-$C_{18}$(E)-T | 12.14 | – | 1.434 | 0.373 | 8850 |
| D-H-$C_{18}$(I) | 11.87 | 1.77 | 1.425 | 0.464 | 10930 |
| D-H-A-$C_{18}$(I) | 15.01 | 2.35 | 1.485 | 0.370 | 7290 |
| D-H-A-$C_{18}$(III) | 13.56 | 2.37 | 1.468 | 0.357 | 6740 |
| D-H-A-$C_{18}$(E) | 11.96 | 1.90 | 1.378 | 0.429 | 8810 |

[a] $k'$(amylbenzene)/$k'$(butylbenzene), 80% methanol.

[b] $k'$(butyl phenyl ketone)/$k'$(butylbenzene), 80% methanol.

[c] Number of theoretical plates for amylbenzene, 80% methanol. 15 cm × 4.6 mm I.D. column.

and K-$C_{18}$(III) with or without end-capping, are less hydrophobic that those prepared from the monochlorosilane, D-$C_{18}$(I) and K-$C_{18}$(I), respectively, as determined by comparison of the retention increase with the addition of one methylene group to the solute structure, $\alpha(CH_2)$ [13]. The $\alpha(CH_2)$ values (1.51–1.52) found with D-$C_{18}$(I) and K-$C_{18}$(I) are the maximum obtainable with $C_{18}$ packing materials, as shown previously [13]. (The retention increase due to one methylene group is a convenient measure of the hydrophobicity of stationary phase, because it can be related to the free energy change associated with the transfer of a methylene group from the mobile phase to the stationary phase.) Stationary phases prepared from trichlorosilane and also that containing an ether linkage showed a greater $\alpha(C=O)$ together with a smaller $\alpha(CH_2)$, indicating either reduced hydrophobicity or the contribution of silanols.

Among the secondary retention processes in RP–LC, the effect of neutral silanols on hydrogen bonding can be reduced by trimethylsilylation of a $C_{18}$ phase. The effect of surface acidity on peak tailing of amines at acidic pH caused by metal impurities was reduced by acid treatment of silica particles prior to the bonding process that removed the extraneous metals from silica surface [11,13,22]. These methods have been utilized in the preparation of many currently available packing materials. However, it was not possible to obtain good peak shapes for chelating compounds if these preparation methods were used with silicas containing substantial metal impurities. The use of high-purity silica gel in combination with polymer coating was shown to

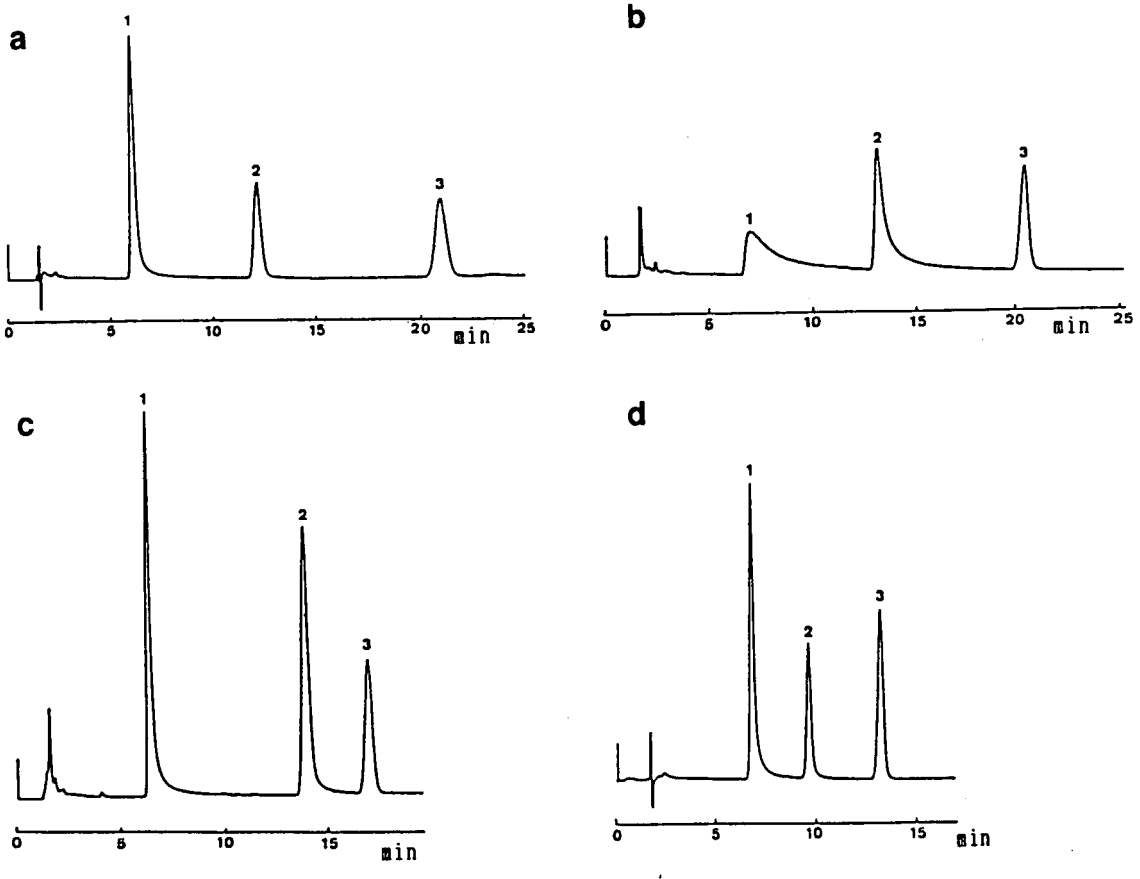


Fig. 2. Chromatograms of chelating reagents on (a) K-$C_{18}$(I)-T, (b) D-$C_{18}$(I)-T, (c) D-$C_{18}$(III)-T and (d) D-$C_{18}$(E)-T. Mobile phase: 75% methanol-0.02 *M* phosphate (pH 3). Solutes: (1) purpurin, (2) quinizarin and (3) amylbenzene.

be one way to prepare a stationary phase free from the secondary retention process related to metals [14]. Hence the most rigorous test for silica $C_{18}$ packing materials with respect to the contribution of the secondary retention mechanism is the elution of chelating compounds, such as those in Fig. 1.

Fig. 2a and b show the chromatograms obtained for 1,2,4-trihydroxy-9,10-anthracenedione (purpurin) and 1,4-dihydroxy-9,10-anthracenedione (alizarin) on stationary phases prepared from the two silicas, Kromasil and Develosil, by using octadecyldimethylchlorosilane followed by trimethylsilylation, K-$C_{18}$(I)-T and D-$C_{18}$(I)-T. In each instance, the peak shape should be compared with that of amylbenzene. The stationary phase prepared from the high-purity silica gel with any silylating reagent showed little effect of the metal on the elution of hydroxyanthraquinones. The peaks of these chelating compounds, however, were severely distorted on the stationary phase prepared from the silica gel containing some metal impurities, D-$C_{18}$(I)-T.

Table III shows the performances of various stationary phases prepared from Develosil. The data indicate that D-$C_{18}$(I) and D-$C_{18}$(II) showed a poor performance for all the chelating reagents. Trimethylsilylation of the $C_{18}$ bonded phase was not effective, and sometimes worked adversely. Table III also indicates that the effect of metal chelate formation is reduced by the addition of phosphoric acid or acetylacetone to the mobile phase. Some very effective chelating reagents, such as hinokitiol and 8-quinolinol, cannot be eluted from stationary phases prepared from metal-containing silicas with octadecyldimethylchlorosilane.

Fig. 2c and 2d show how to overcome the effect of metals. The stationary phases bonded with a trifunctional silane, D-$C_{18}$(III)-T, gave comparable results to K-$C_{18}$(I)-T for the hydroxyanthraquinones. The stationary phases prepared from tetradecyloxypropyldimethylchlorosilane containing an ether linkage, D-$C_{18}$(E)-T, also showed much better results than D-$C_{18}$(I)-T. As shown in Table III, better performance of a stationary phase prepared from trichlorosilane than that from monochlorosilane was also noted when the silica gel was used without acid treatment.

TABLE III

PERFORMANCE FOR CHELATING COMPOUNDS

Mobile phase: 75% methanol–0.02 *M* phosphate buffer (pH 3).

| Stationary phase[a] | Column efficiency[b] | | | | | |
|---|---|---|---|---|---|---|
| | Alizarin | Purpurin | Chrysazin | Quinizarin | Anthrarufin | Hinokitiol |
| $C_{18}$(I) | 0.32 | 0.01 | 0.81 | 0.22 | 0.48 | NE[c] |
| $C_{18}$(I)-T | 0.32 | 0.02 | 0.75 | 0.23 | 0.40 | NE |
| $C_{18}$(II) | 0.37 | 0.05 | 0.80 | 0.42 | 0.59 | NE |
| $C_{18}$(II)-T | 0.38 | 0.06 | 0.79 | 0.35 | 0.49 | NE |
| $C_{18}$(III) | 0.47 | 0.30 | 0.85 | 0.71 | 0.77 | 0.013 |
| $C_{18}$(III)-T | 0.53 | 0.36 | 0.84 | 0.73 | 0.68 | 0.026 |
| $C_{18}$(E) | 0.77 | 0.49 | 0.86 | 0.91 | 0.78 | 0.002 |
| $C_{18}$(E)-T | 0.75 | 0.49 | 0.92 | 0.88 | 0.73 | NE |
| $C_{18}$(I)[d] | 0.94 | 0.64 | 1.36 | 1.29 | 1.16 | 0.014 |
| $C_{18}$(I)-T[d] | 1.00 | 0.80 | 1.45 | 1.38 | 1.34 | NE |
| $C_{18}$(I)[e] | 0.01 | —[f] | 0.29 | 0.01 | 0.06 | NE |
| $C_{18}$(III)[e] | 0.27 | 0.01 | 0.67 | 0.13 | 0.18 | NE |

[a] All stationary phases were prepared from Develosil. $C_{18}$(I), prepared with octadecyldimethylchlorosilane; $C_{18}$(II), from dichlorosilane; $C_{18}$(III), from trichlorosilane; $C_{18}$(E), from tetradecyloxypropylsilane; T, trimethylsilylation.

[b] Number of theoretical plates for the chelating compound divided by that for propylbenzene.

[c] Not eluted.

[d] Mobile phase containing 1 m*M* acetylacetone.

[e] Stationary phases were prepared without acid treatment of silica gel prior to bonding.

[f] Peak was barely detectable.

TABLE IV

PERFORMANCE FOR ISOAMYL SALICYLATE

| Stationary phase[a] | Column efficiency[b] | | | |
|---|---|---|---|---|
| | 80% $CH_3OH$ | 70% $CH_3CN$ | 70% $CH_3CN$–$H_3PO_4$[c] | 70% $CH_3CN$–acetylacetone[d] |
| $C_{18}$(I) | 0.549 | 0.381 | 0.860 | 1.108 |
| $C_{18}$(I)-T | 0.624 | 0.416 | 0.907 | 1.177 |
| $C_{18}$(II) | 0.684 | 0.523 | 0.879 | 1.135 |
| $C_{18}$(II)-T | 0.637 | 0.573 | 0.781 | 1.085 |
| $C_{18}$(III) | 0.874 | 0.831 | 0.831 | 1.051 |
| $C_{18}$(III)-T | 0.858 | 0.845 | 0.925 | 1.139 |

[a] All stationary phases were prepared from Develosil.
[b] Number of theoretical plates for isoamyl salicylate divided by that for butylbenzene.
[c] 0.02 *M* phosphate buffer (pH 3).
[d] 1 m*M* acetylacetone was added.

The shielding of metal sites on the silica surface by a polymeric structure formed from trichlorosilane [23,24] does not seem to be the major reason for the improvement. D-$C_{18}$(E) phase showed good performance without such a contribution. A higher surface coverage by end-capping had no improving effect, and was actually disadvantageous.

A plausible explanation for the improved performance is the association of metal sites with polar functionalities such as silanols or ether oxygen in bonded alkylsilyl groups, or water or methanol brought into the stationary phase from the mobile phase by the presence of the hydrophilic groups. Solvents in the mobile phase are known to be extracted into the stationary phase, and considerably alter the environment of the alkyl chains [3,4]. The presence of competing groups for the metal sites in the more hydrophilic stationary phase permits the easier displacement of ligands or faster equilibration, and explains the results, as was proposed for the silanophilic retention of amines [25]. Slower flow-rates improved the results, whereas reduced sample size did not effect any improvement.

The undesirable effects of metal impurities were also observed with isoamyl salicylate (Table IV). The use of acetonitrile in the mobile made the results

TABLE V

PERFORMANCE FOR CARBOXYLIC ACIDS

Mobile phase: 30% acetonitrile–0.02 *M* phosphate buffer.

| Stationary phase[a] | Column efficiency[b] | | | | | | | |
|---|---|---|---|---|---|---|---|---|
| | pH 2.28 | | pH 3.19 | | pH 3.84 | | pH 4.26 | |
| | B | T | B | T | B | T | B | T |
| $C_{18}$(I) | 0.90 | 0.95 | 0.65 | 0.78 | 0.62 | 0.61 | 0.54 | 0.53 |
| $C_{18}$(I)-T | 0.54 | 0.61 | 0.40 | 0.31 | 0.27 | 0.20 | 0.19 | 0.06 |
| $C_{18}$(III) | 0.80 | 0.88 | 0.60 | 0.75 | 0.76 | 0.82 | 0.31 | 0.73 |
| $C_{18}$(III)-T | 0.71 | 0.69 | 0.64 | 0.59 | 0.60 | 0.60 | 0.53 | 0.56 |

[a] All stationary phases were prepared from Develosil.
[b] Number of theoretical plates for (B) benzoic acid or (T) *p*-toluic acid divided by that for 3-phenylpropanol.

worse. The addition of phosphoric acid or acetylacetone [17], which are metal complexing agents, improved the results considerably.

Table V shows the effect of pH and the method of preparation of the stationary phase on the performance for carboxylic acids with an acetonitrile–phosphate buffer mobile phase. Trimethylsilylated packing materials prepared from monochlorosilane showed tailing for carboxylic acids, especially at pH values near their $pK_a$ values. As shown in Fig. 3, a similar packing material from Kromasil and less hydrophobic D-$C_{18}$(III)-T and D-$C_{18}$(E)-T showed better performances. The improvement with the addition of acetylacetone suggests that the poor performance seen with D-$C_{18}$(I)-T phase is related to metals [26].

The retention of an acid in the ionization control mode is expressed by the equation [27]

$$k' = \frac{k'_{AH}}{1 + K_a/[H_3O^+]} + \frac{k'_{A^-} \cdot K_a/[H_3O^+]}{1 + K_a/[H_3O^+]} \quad (1)$$

where $k'_{AH}$ and $k'_{A^-}$ are the $k'$ values of the neutral and ionized form of the acid, respectively. Hence the retention of a carboxylic acid is the sum of the retention of the neutral form and that of the ionized form at a particular pH. The retention is most sensitive to the variation of elution conditions around the $pK_a$ of the acid, where poor performance was seen with $C_{18}$(I). The source of tailing seems to be the interaction between metals and the ionized form of the acids.

The results indicate that the effect of metal impurities is emphasized with greater hydrophobic properties of the stationary phase, which lead to poor accessibility of competing polar groups to the metal sites, as is the case with chelating reagents. The undesirable effect on D-$C_{18}$(I)-T was reduced by the use of acetate buffer instead of phosphate, by methanol instead of acetonitrile or by the addition of reagents masking the metals. In some instances, however, mobile phase additives such as EDTA, acetylacetone or sodium octanoate [18,28] caused a

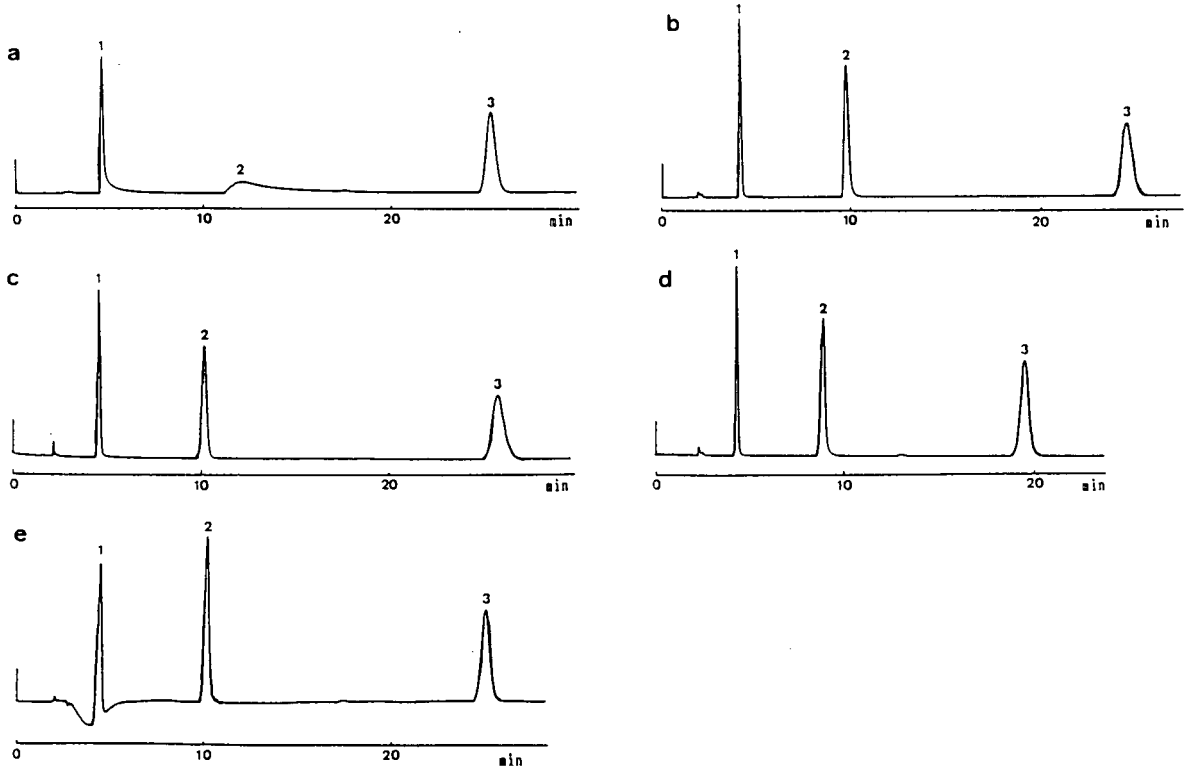


Fig. 3. Chromatograms obtained for carboxylic acids on (a) D-$C_{18}$(I)-T, (b) K-$C_{18}$(I)-T, (c) D-$C_{18}$(III)-T and (d) D-$C_{18}$(E)-T. Mobile phase: 20% acetonitrile–0.05 *M* phosphate (pH 4.8). Solutes: (1) benzoic acid, (2) *p*-toluic acid and (3) 3-phenylpropanol. (e) D-$C_{18}$(I)-T, 1 m*M* acetylacetone added to the mobile phase.

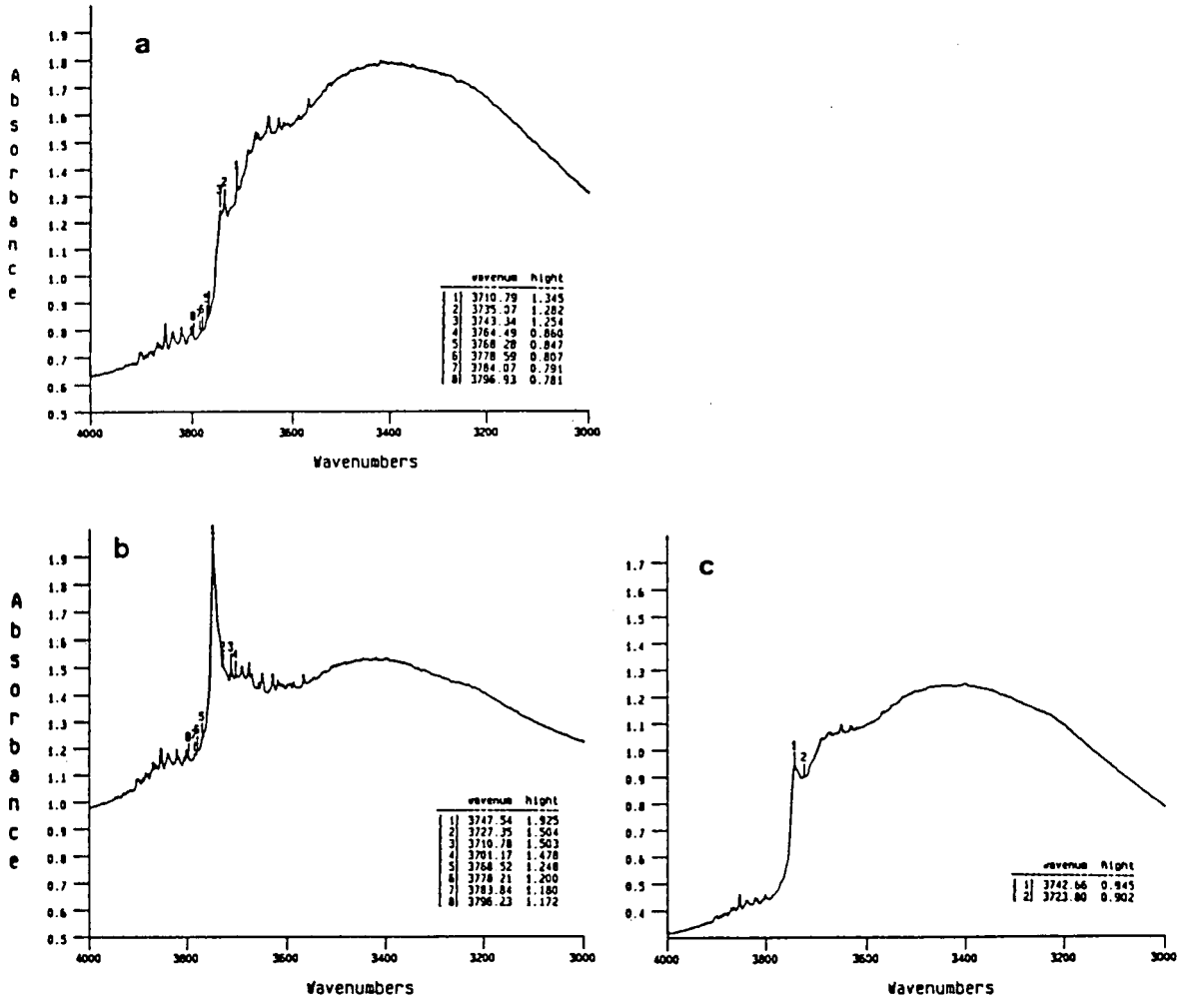


Fig. 4. Fourier transform IR spectra of silica gel. (a) Develosil after the initial acid treatment; (b) Develosil after thermal treatment (D-H); (c) Develosil after acid treatment following the thermal treatment (D-H-A).

noisy baseline or a prolonged equilibration time of the chromatographic system, and hence were unsatisfactory [18].

Another interesting observation is the effect of the hydrophilicity of the stationary phase on the appearance of the effect of hydrogen bonding caused by silanol in the stationary phase. When silicas were heated to high temperatures, dehydration caused the silanols to condense to form siloxanes, leaving isolated silanols [29]. The remaining silanols possess higher acidity than the usual silanols hydrogen bonded to each other [5]. The acid treatment with hydrochloric acid rehydrated the surface to some extent, but not completely [22]. Fig. 4 shows the variation of the type and amounts of silanols on silica gel after each treatment. Some isolated silanols remained after the second acid treatment following the thermal treatment.

$C_{18}$ phase prepared from heat-treated silica [D-H-$C_{18}$(I)] possesses a low surface coverage owing to the scarcity of silanols, and showed a small retention of phenol, in agreement with the low carbon content. However, D-H-$C_{18}$(I) showed a longer retention for caffeine than D-$C_{18}$(I), which possesses a higher carbon content, indicating the effect of hydrogen bonding, as shown in Fig. 5.

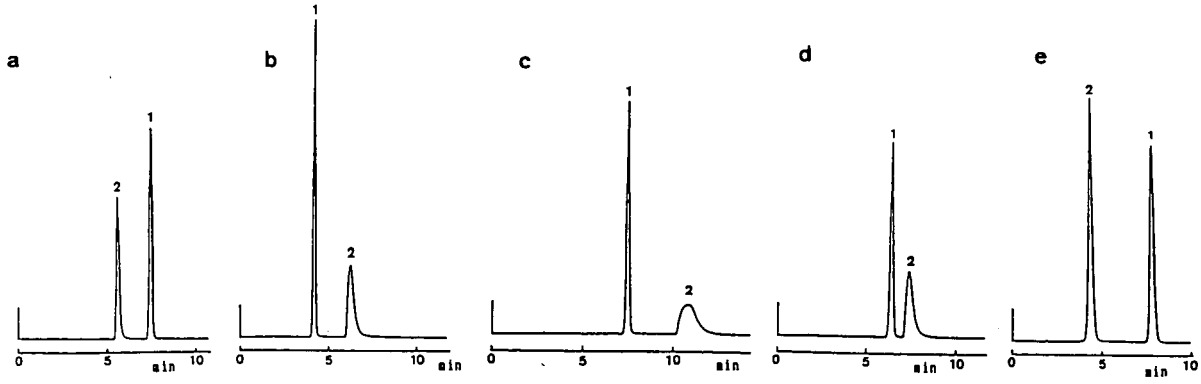


Fig. 5. Chromatograms obtained for caffeine (peak 2) and phenol (peak 1) on (a) D-$C_{18}$(I), (b) D-H-$C_{18}$(I), (c) D-H-A-$C_{18}$(I), (d) D-H-A-$C_{18}$(III) and (e) D-H-A-$C_{18}$(E). Mobile phase: 30% methanol.

Caffeine is known to undergo interaction with silanols [13,30].

$C_{18}$ phase prepared from acid-treated silica following thermal treatment (D-H-A) showed a normal retention for phenol, but a much longer retention for caffeine with a poor peak shape. The incomplete rehydration left some acidic silanols, which participate in more effective hydrogen bonding in the hydrophobic environment provided by the higher surface coverage. Interestingly, D-H-A-$C_{18}$(III) showed a better performance, resulting in a smaller $k'$ value for caffeine in spite of the larger amount of silanols on this stationary phase than D-H-A-$C_{18}$(I). D-H-A-$C_{18}$(E) also showed a much better performance for caffeine with a smaller retention. The results indicate that the acidic, isolated silanols created by thermal treatment become less detrimental when associated with the polar functionality in alkylsilyl groups or polar solvents.

These results may be of little practical importance, because the hydrogen bonding effect can be suppressed by trimethylsilylation. Nonetheless, the present results are interesting in that hydrophilic stationary phases with more silanols showed a better performance for solutes suffering from the hydrogen bonding effect of the silanols. It should be noted that the acidic silanols should be minimized by appropriate treatment of silica gel or by a suitable bonding method to avoid the problems of chemical stability associated with trimethylsilyl-bonded phases.

The results indicate the importance of the presence of competing polar functionalities in stationary phases prepared from metal-containing silica gel for faster equilibration with respect to the silanols and metals which participate in the secondary retention processes.

This study clearly indicates the advantages of the use of high-purity silica gel as a support for RPLC packing materials. It can be stated that stationary phases prepared from metal-containing silica gels with trichlorosilane may not be as good as those prepared from high-purity silica gel, but they are at least much better than comparable stationary phases obtained from monochlorosilane. They are easy to prepare from the usual silica gels and show adequate performance for many chelating compounds, hydroxybenzenes and carboxylic acids. Although most of the newer commercial $C_{18}$ packing materials are prepared from monochlorosilane for better reproducibility and better performance for silanophilic solutes, those prepared with trichlorosilane can provide a solution to one of the most difficult problems in packing materials for RPLC.

## ACKNOWLEDGEMENT

This work was supported in part by the Monbusho International Joint Research Program (No. 03044089), funded by the Ministry of Education.

## REFERENCES

1 Cs. Horváth, W. Melander and I. Molnár, *J. Chromatogr.*, 125 (1976) 129.
2 N. Tanaka and E. R. Thornton, *J. Am. Chem. Soc.*, 99 (1977) 7300.
3 N. Tanaka, H. Goodell and B. L. Karger, *J. Chromatogr.*, 158 (1978) 233.

4 R. McCormick and B. L. Karger, *J. Chromatogr.*, 199 (1980) 259.
5 J. Kohler, D. B. Chase, R. D. Farlee, A. J. Vega and J. J. Kirkland, *J. Chromatogr.*, 352 (1986) 275.
6 J. Kohler and J. J. Kirkland, *J. Chromatogr.*, 385 (1987) 125.
7 J. Nawrocki and B. Buszewski, *J. Chromatogr.*, 449 (1988) 1.
8 J. Nawrocki, *J. Chromatogr.*, 407 (1987) 171.
9 S. G. Weber and W. G. Tramposch, *Anal. Chem.*, 55 (1983) 1771.
10 P. C. Sadek, P. W. Carr and L. W. Bowers, *J. Liq. Chromatogr.*, 8 (1985) 2369.
11 P. C. Sadek, C. J. Koester and L. D. Bowers, *J. Chromatogr. Sci.*, 25 (1987) 489.
12 M. Verzele, M. De Potter and J. Ghysels, *J. High Resolut. Chromatogr. Chromatogr. Commun.*, 2 (1979) 151.
13 K. Kimata, K. Iwaguchi, S. Onishi, K. Jinno, R. Eksteen, K. Hosoya, M. Araki and N. Tanaka, *J. Chromatogr. Sci.*, 27 (1989) 721.
14 Y. Ohtsu, Y. Shiojima, T. Okumura, J. Koyama, K. Nakamura, O. Nakata, K. Kimata and N. Tanaka, *J. Chromatogr.*, 481 (1989) 147.
15 C. L. Thomas, *Ind. Eng. Chem.*, 41 (1949) 2564.
16 K. Tanabe, T. Sumiyoshi, K. Shibata, T. Kiyoura and J. Kitagawa, *Bull. Chem. Soc. Jpn.*, 47 (1974) 1064.
17 M. Verzele and C. Dewaele, *Chromatographia*, 18 (1984) 84.
18 N. Tanaka, A. Yamaguchi, K. Hashizume, M. Araki, A. Wada and K. Kimata, *J. High Resolut. Chromatogr. Chromatogr. Commun.*, 9 (1986) 683.
19 Y. Ohtsu, H. Fukui, T. Kanda, K. Nakamura, M. Nakano, O. Nakata and Y. Fujiyama, *Chromatographia*, 24 (1987) 380.
20 H. Figge, A. Deege, J. Kohler and G. Schomburg, *J. Chromatogr.*, 351 (1986) 393.
21 K. Jinno, S. Shimura, N. Tanaka, K. Kimata, J. C. Fetzer and W. R. Biggs, *Chromatographia*, 27 (1989) 285.
22 K. K. Unger, K. D. Lork, B. Pfleiderer, K. Albert and E. Bayer, *J. Chromatogr.*, 556 (1991) 395.
23 D. W. Sindorf and G. E. Maciel, *J. Am. Chem. Soc.*, 103 (1981) 4263.
24 D. W. Sindorf and G. E. Maciel, *J. Am. Chem. Soc.*, 105 (1983) 3767.
25 B. A. Bidlingmeyer, J. K. Del Rios and J. Korpi, *Anal. Chem.*, 54 (1982) 442.
26 M. Verzele and C. Dewaele, *J. Chromatogr.*, 217 (1981) 399.
27 B. L. Karger, J. LePage and N. Tanaka, in C. Horváth (Editor), *High Performance Liquid Chromatography*, Academic Press, New York, 1980, p. 113.
28 N. Tanaka, K. Hosoya, K. Nomura, T. Yoshimura, T. Ohki, R. Yamaoka, K. Kimata and M. Araki, *Nature (London)*, 341 (1989) 727.
29 K. K. Unger, *Porous Silica*, Elsevier, Amsterdam, 1979, Ch. 3.
30 G. B. Cox and R. W. Stout, *J. Chromatogr.*, 384 (1987) 315.

*Journal of Chromatography*, 594 (1992) 97–103
Elsevier Science Publishers B.V., Amsterdam

CHROM. 23 831

# Ligand–receptor interactions in affinity cell partitioning

# Studies with transferrin covalently linked to monomethoxypoly(ethylene glycol) and rat reticulocytes

Cristina Delgado*,☆, Pilar Sancho, Jesus Mendieta and Jose Luque

*Departamento de Bioquimica y Biologia Molecular, Universidad de Alcala, 28871 Alcala de Henares, Madrid (Spain)*

(First received July 17th, 1991; revised manuscript received October 29th, 1991)

ABSTRACT

The partitioning of rat reticulocytes in poly(ethylene glycol) (PEG)–dextran two-phase systems increases into the PEG-rich top phase when the cells are incubated with transferrin covalently modified with monomethoxy-PEG (MPEG–transferrin) prior to partitioning. Two observations support the suggestion that such an increase in top-phase partitioning is due to the specific interaction of the MPEG–transferrin conjugate with the transferrin receptor on the surface of the reticulocyte: first, the MPEG–transferrin conjugate competes with [$^{125}$I]transferrin for the transferrin receptor on reticulocytes ($K_a = 6.28 \cdot 10^6$ l mol$^{-1}$); and second, the MPEG-modified transferrin is unable to change the partitioning of rat erythrocytes, cells lacking the transferrin receptor. This example illustrates the feasibility of manipulating the partitioning of a selected cell population when ligand–receptor interactions are exploited. The increase in the partitioning of the reticulocytes takes place within a narrow range of MPEG–transferrin bound per cell, *viz.*, 10.2–11.3 fg per cell. The latter range corresponds to *ca.* 80 000–89 000 molecules of MPEG–transferrin bound per cell.

## INTRODUCTION

The partitioning of cells in poly(ethylene glycol) (PEG)–dextran aqueous two-phase systems can be specifically directed towards one of the phases by coating the cells with a ligand which partitions into that phase [1–3]. Several examples have demonstrated the feasibility of this affinity partitioning methodology for the extraction of a selected cell population into the PEG-rich top phase of a biphasic system in which the bulk cells partition into the interface [4–9]. Complete separation of artificial mixtures of red blood cells from two species has been achieved by multiple extractions with the counter-current distribution procedure [4–6]. This affinity cell partitioning technique has been demonstrated to distinguish cells on the basis of the expression of the target protein on their surface [7]. Strategies for isolating cells present at low abundance (1%) have been identified [9]. In all these examples the ligands were antibodies raised against one or several proteins on the surface of the targets cells. The antibodies were covalently linked to monomethoxy-PEG (MPEG) to produce MPEG–antibody conjugates with high partitioning into the PEG-rich phase. More recently, soluble metal–chelate–PEG conjugates have been used to increase the partitioning of erythrocytes from different species [10].

Ligand–receptor interactions, however, have not been exploited to manipulate the partitioning behaviour of a selected cell population. A positive selection of cells in the top phase of the biphasic system by using a natural ligand might have advan-

☆ Present address: Molecular Cell Pathology Laboratory, Royal Free Hospital School of Medicine, Rowland Hill Street, London NW3 2PF, UK.

tages over the immunoaffinity approach where antibodies, either polyclonal or monoclonal, have to be produced for each single antigen.

Two experimental approaches have been used to apply immunoaffinity cell partitioning. In the first the cells are partitioned in a biphasic system containing the MPEG–antibody conjugate, *i.e.*, the cell–antibody interaction and the partitioning occur simultaneously [5,7]. In the second approach the cells are first incubated with the MPEG–antibody conjugate, to allow cell–antibody interaction, and then the cells are recovered and introduced into the biphasic system for partitioning [4,6,8,9]. In most of the examples the MPEG–antibody conjugate has to be isolated from the non-physiological reaction mixture (excess of activated MPEG and phosphate–borate buffer) prior to use [4–7]. A simplified version of the second approach uses MPEG activated with tresyl chloride (TMPEG), which can be linked to the protein in phosphate-buffered saline (PBS) at pH 7.5, the excess of TMPEG being quenched by reaction with bovine serum albumin, leading to a reaction mixture suitable for direct incubation with the cells [8,9].

We have examined the feasibility of ligand–receptor interactions to manipulate the partitioning of a cell population using transferrin as the ligand and rat reticulocytes as the target cells. MPEG is first covalently linked to transferrin using TMPEG to produce a MPEG–transferrin conjugate with increased partitioning into the PEG-rich top phase. The feasibility of the MPEG–transferrin conjugate as an affinity ligand was studied by examining the partitioning of rat reticulocytes. To test the specificity of the MPEG–transferrin conjugate for the transferrin receptor, two independent approaches were undertaken. Erythrocytes, a related cell type lacking the relevant receptor [11,12], were subjected to the same process. Second, the affinity of the MPEG–transferrin conjugate for the transferrin receptor on rat reticulocytes was addressed. Finally, the value for the association constant ($K_a$) of MPEG–transferrin for the transferrin receptor was used to establish mathematically the number of MPEG–transferrin molecules required to be bound per cell to produce an increase in the partitioning.

## EXPERIMENTAL

### *Chemicals*

PEG (relative molecular mass, $M_r$ = 6000) was obtained from Serva (Heidelberg, Germany), dextran T-500 (lot NK 05164) from Pharmacia (Uppsala, Sweden), MPEG ($M_r$ 5000) (record 398) from Union Carbide (New York, USA), 2,2,2-trifluoroethanesulphonyl (tresyl) chloride from Fluka (Buchs, Switzerland), iodine-125 (sodium salt) from Amersham (Amersham, UK) and human transferrin (iron saturated) and bovine serum albumin (globulin free) from Sigma (St. Louis, MO, USA). All other chemicals were from Merck (Darmstadt, Germany).

### *Preparation of rat reticulocytes and erythrocytes*

Male Wistar rats of weight 175 g received an intraperitoneal injection of phenylhydrazine (30 mg $kg^{-1}$) during five consecutive days to produce lysis of the erythrocytes. Two days after the final injection the blood with a content of more than 95% reticulocytes [13] was taken over heparin, plasma separated by centrifugation and the pellet of reticulocytes washed twice with 0.15 *M* sodium chloride and finally resuspended in Hank's balanced salt solution (HBSS). Erythrocytes were obtained similarly from the blood of untreated rats.

### *Affinity cell partitioning*

The procedure for affinity cell partitioning includes two major stages: first, modification of the transferrin with MPEG and neutralization of the excess of activated MPEG and second, incubation of the cells with the MPEG–transferrin and partitioning. A similar experimental protocol has been used previously for immunoaffinity cell partitioning [8,9].

The activated (tresylated) MPEG (TMPEG) is obtained by reaction of MPEG with tresyl chloride in anhydrous dichloromethane with pyridine as acid scavenger as reported previously [14]. To produce the MPEG–transferrin conjugate, TMPEG is made up in PBS [0.05 *M* sodium phosphate buffer (pH 7.5) in 0.125 *M* sodium chloride] to a concentration of 216 mg $ml^{-1}$ and mixed with 3 mg $ml^{-1}$ transferrin in PBS, in a 1:1 volume ratio. An excess of 20 mol of TMPEG per mole of lysine residues in the transferrin is used to obtain a high degree of substitution of the protein with TMPEG. The solution is gently

stirred for 2 h at room temperature. An aliquot of this preparation is then removed to measure the partition coefficient of the MPEG–transferrin conjugate. To neutralize the excess of TMPEG, 90 mg $ml^{-1}$ BSA in PBS is added at a 1:1 volume ratio and the solution is gently strirred for a further 2 h at room temperature. The BSA is added in a molar excess of four lysine residues per active group in TMPEG. This strategy has been used previously for immunoaffinity cell partitioning [8,9], as the unreacted TMPEG reacts with proteins on the surface of the cells leading to non-specific increases in their partitioning [15]. To calculate the molar ratio of TMPEG to lysine residues in transferrin and BSA, molecular weights of 76 500 and 60 000 are used, respectively. Transferrin has been described as a protein having 50 lysine residues per molecule whereas BSA has 60 lysine residues per molecule [16]. The concentration of MPEG–transferrin is always expressed as weight of transferrin per unit volume.

To proceed with the incubation of the cells with the MPEG–ligand, the solution containing the MPEG–transferrin is first diluted with PBS to the required concentration in a volume of 400 $\mu$l and then 100 $\mu$l of HBSS containing the appropriate number of cells (see figure captions) are added. The incubation is carried out at 4°C in a rotary mixer for 2 h, after which the cells are recovered by centrifugation. The supernatant is discarded and the pelleted cells resuspended in 1 ml of top phase. This top phase is sampled to determine the number of cells added to the biphasic system. Then 0.8 ml of top phase containing cells is mixed with 0.8 ml of fresh bottom phase by gentle inversions. The system is allowed to settle for 20 min at 4°C into the top and bottom phases and then the top phase is sampled to determine the number of cells recovered. Partitioning is expressed as the percentage of cells which distribute to the top phase. Determination of cell numbers is done by impedance cell counting with a Coulter Counter Model ZBI.

*Preparation of the biphasic system for cell partitioning*

The two-phase system consisting of 4.75% PEG, 4.75% dextran, 0.01 *M* sodium phosphate and 0.15 *M* sodium chloride (non-charged system) is prepared at a total of 250 g from the following stock solutions: 40% (w/w) PEG, *ca.* 20% (w/w) dextran (the exact concentration of the stock solution is determined by polarimetry), 0.44 *M* sodium phosphate buffer (pH 6.8) and 0.6 *M* sodium chloride. The total weight is achieved by addition of distilled water. The system is mixed and then allowed to settle into the top PEG-rich and the bottom dextran-rich phases at 4°C for 4–6 h. The top and bottom phases are then separated and stored at 4°C until required. For cell partitioning, the biphasic system is reconstituted by mixing top and bottom phases in a 1:1 volume ratio.

*Association constant of transferrin and MPEG-modified transferrin for the transferrin receptor*

A competition assay with $^{125}$I-labelled transferrin is used. [$^{125}$I]Transferrin with a specific activity of $1.56 \cdot 10^7$ cpm $\mu g^{-1}$ is obtained as described previously [13]. Reticulocytes ($1 \cdot 10^8$) were resuspended in 0.5 ml of HBSS containing 1% BSA, 0.06 $\mu$g $ml^{-1}$ [$^{125}$I]transferrin and increasing concentrations of either transferrin or MPEG–transferrin conjugate (0.1–200 $\mu g\ ml^{-1}$). Before sealing the tubes, the air is purged with oxygen–carbon dioxide (95:5, v/v) (gas cylinder supplied by SEO, Spain) and the incubation is carried out at 4°C with constant shaking for 90 min. Reticulocytes are then washed three times in ice-cold PBS. The amount of bound [$^{125}$I]transferrin is determined in the last pellet of cells (500 *g*, 10 min, 4°C) by using a gamma counter. Bound [$^{125}$I]transferrin is expressed as a percentage of the amount bound in the absence of transferrin or MPEG–transferrin.

The association constant of the MPEG–transferrin conjugate for the transferrin receptor is calculated from the association constant of transferrin ($2 \cdot 10^8$ l $mol^{-1}$ [13]) and the concentrations of transferrin and MPEG–transferrin conjugate required to displace 50% of the [$^{125}$I]transferrin form the receptor. This approach has been described by Koteman [17].

The saturation curve of the transferrin receptor with MPEG–transferrin conjugate is simulated by solving the equation for the binding equilibrium and considering a value of 100 000 binding sites per reticulocyte [13].

*Partition coefficient of transferrin and MPEG–transferrin*

Two-phase systems consisting of 4.75% PEG-6000, 4.75% dextran T-500, 0.15 *M* sodium chloride and 0.01 *M* sodium phosphate buffer (pH 6.8) (non-charged system) are prepared on a weight for weight basis (1 g total) from stock solutions of 40% (w/w) PEG, 20% (w/w) dextran, 0.44 *M* sodium phosphate buffer (pH 6.8), 0.6 *M* sodium chloride, distilled water and 0.1 g of solutions of either the native transferrin or the MPEG–modified transferrin in PBS. After inversion 30–40 times, the mixture is left to settle at room temperature until complete separation of the phases is observed (15–20 min). Aliquots from the top and bottom phases are then analysed for protein concentration by the Coomassie Brilliant Blue assay [18]. The partition coefficient is defined as the ratio between the protein concentrations in the top and the bottom phases.

## RESULTS

In order to use transferrin as an affinity ligand to change the partitioning of a cell population towards the PEG-rich top phase of a PEG–dextran biphasic system, the protein requires at least two features (a) high partitioning into the PEG-top phase and (b) affinity for the receptor on the surface of the cells with maintenance of the ligand–receptor interaction in the biphasic system.

Transferrin in its native form favours the dextran-rich bottom phase of a non-charged two-phase system of 4.75% PEG, 4.75% dextran, as shown by its low partition coefficient of 0.6 ± 0.05 [mean ± standard error of the mean (S.E.M.) of three observations]. However, as a result of a 2-h incubation of the protein with TMPEG, the partition coefficient of the tansferrin increases to 6.1 ± 0.5 (mean ± S.E.M. of three observations). Hence, the incubation with TMPEG produces a transferrin that favours the PEG-rich top phase of the system, therefore fulfilling one of the requirements for affinity partitioning purposes.

To evaluate the feasibility of the MPEG–transferrin conjugate for affinity partitioning, rat reticulocytes were used as a model system (Fig. 1). A constant concentration of MPEG–transferrin (75 $\mu$g ml$^{-1}$) was first used and the number of cells per incubation was varied from 7.5 · 10$^7$ to 2.5 · 10$^7$ cells

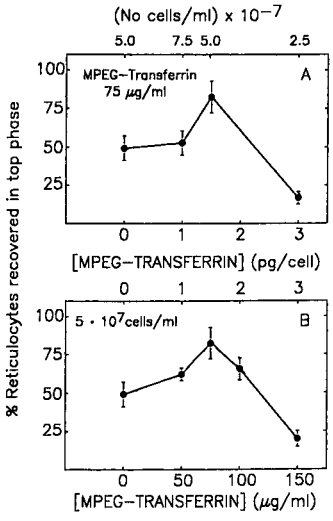


Fig. 1. Partitioning of rat reticulocytes after incubation with the MPEG–transferrin preparation: influence of the concentrations of cells and MPEG–transferrin conjugate. (a) Constant concentration of MPEG–transferrin (75 $\mu$g ml$^{-1}$) and decreasing number of cells and (b) constant number of cells (5 · 10$^7$ cells ml$^{-1}$) and increasing concentration of MPEG–transferrin. Data are means ± S.E.M. of three experiments.

ml$^{-1}$ (Fig. 1A). A maximum in the partition coefficient, far above that of resting reticulocytes, is observed for the incubation with 5 · 10$^7$ cells ml$^{-1}$. When the number of cells was reduced to 2.5 · 10$^7$ cells ml$^{-1}$ the partitioning of the reticulocytes was below that of the resting cells (Fig. 1A). The influence of increasing concentrations of MPEG–transferrin was then studied using the optimum concentration of cells (Fig. 1B). The partitioning of reticulocytes increased with increasing concentration of MPEG–transferrin to a maximum for a ratio of 1.5 pg per cell. Higher concentrations of the MPEG–transferrin preparation led to reductions in the partition coefficient of the reticulocytes, which decreased below that of the resting reticulocytes for a ratio of MPEG–transferrin of 3 pg per cell (Fig. 1B).

To demonstrate that the increased partitioning of reticulocytes was due to a specific interaction of the MPEG–transferrin conjugate with the transferrin receptor, two approaches were used. First the partitioning of rat erythrocytes (cells lacking the transferrin receptor) was studied under conditions leading to increased reticulocyte partitioning. Second, compe-

tition studies between MPEG–transferrin and [$^{125}$I]-transferrin for the receptor were carried out.

The partitioning of resting erythrocytes (48.4 ± 3.2, mean ± S.E.M., $n$ = 6) did not change on incubation with MPEG–transferrin at concentrations of 0.75 pg per cell (48.8 ± 1.2, mean ± S.E.M., $n$ = 3) or 2 pg per cell (42.5 ± 3.7, mean ± S.E.M., $n$ = 3). These observations exclude coating of the cell surface with any of the components in the MPEG–transferrin preparation.

Fig. 2 shows the displacement of [$^{125}$I]transferrin from the transferrin receptor on reticulocytes by increasing concentrations of either native transferrin or MPEG–transferrin. Both ligands compete similarly for the transferrin receptor (as shown by the parallel slopes), although MPEG–transferrin shows a lower affinity.

The interaction of the MPEG–transferrin preparation with the transferrin receptor and the lack of effect on erythrocyte partitioning strongly support the suggestion that the increased partitioning of reticulocytes is a result of specific coating of the cells with MPEG via binding of the MPEG–transferrin conjugates to the transferrin receptor.

The association constant for the MPEG–transferrin conjugates is $6 \cdot 10^6$ l mol$^{-1}$, two orders of magnitude below that of unmodified transferrin ($2 \cdot 10^8$ l mol$^{-1}$ [13]). Knowing the association constant for the MPEG–transferrin conjugates and the number of binding sites on the reticulocyte, the curve for the saturation of the receptor with MPEG–transferrin is easily simulated (Fig. 3). This allows us to interpolate the values for MPEG–transferrin bound per cell under those incubation conditions leading to increased partitioning of reticulocytes (Fig. 3). The number of MPEG–transferrin molecules bound per cell with the corresponding amounts of MPEG–transferrin bound per cell are summarized in Table I.

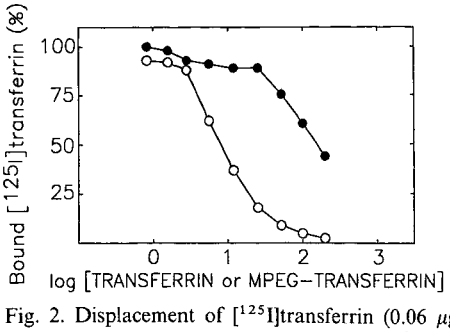


Fig. 2. Displacement of [$^{125}$I]transferrin (0.06 μg ml$^{-1}$) from transferrin receptor on rat reticulocytes ($2 \cdot 10^8$ cells ml$^{-1}$) by (○) transferrin and (●) MPEG-modified transferrin.

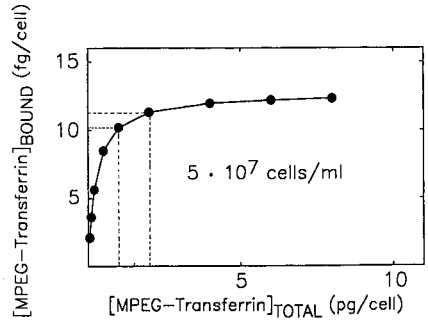


Fig. 3. Simulation of the saturation of the transferrin receptor with MPEG–transferrin in an incubation with $5 \cdot 10^7$ reticulocytes ml$^{-1}$.

## DISCUSSION

Transferrin covalently linked to MPEG has been successfully applied as an affinity ligand for affinity cell partitioning. The covalent linkage of MPEG to transferrin is demonstrated by the increase in the partition coefficient in PEG–dextran aqueous two-phase systems and presumably takes place via the ε-amino groups of lysine residues in the protein. Such attachment has been demonstrated previously for BSA [14].

The MPEG–transferrin conjugate is a suitable ligand for affinity cell partitioning, as shown by its ability to increase the partitioning of rat reticulocytes. Such an increase is due to a specific interaction of the MPEG–transferrin conjugate with the trans-

TABLE I

MPEG–TRANSFERRIN BOUND TO TRANSFERRIN RECEPTOR AFTER INCUBATION WITH RAT RETICULOCYTES ($5 \cdot 10^7$ CELLS ml$^{-1}$): INFLUENCE OF THE TOTAL CONCENTRATION OF MPEG–TRANSFERRIN

| MPEG–transferrin in incubation (pg per cell) | MPEG–transferrin bound (fg per cell) | MPEG–transferrin bound (molecules per cell) |
|---|---|---|
| 1.0 | 10.2 | 80 217 |
| 1.5 | 10.9 | 85 884 |
| 2.0 | 11.3 | 89 034 |

ferrin receptor because first, the increased partitioning only takes place with the cells expressing the receptor, and second, the MPEG–transferrin conjugate retains affinity for the receptor.

The reduced affinity of the MPEG–transferrin conjugate for the transferrin receptor was not unexpected, although its molecular basis is unclear. It is well established that the covalently linkage of MPEG to enzymes leads to a severe reduction in their activity, presumably by preventing the formation of the substrate–enzyme complex owing to steric hindrance [19–21]. It is also known that the apparent binding activity of a monoclonal anti-rabbit Fc fragment antibody is considerably decreased when PEG-1900 is covalently attached to the molecule [22], but this is the first study in which the affinity of the protein for its receptor after covalent linkage of MPEG is reported.

Although these results demonstrate the principle of affinity cell partitioning, the experimental approach adopted here does not provide the spectacular increase in partitioning observed when MPEG–antibodies were used instead of MPEG–transferrin [9]. In addition, with MPEG–antibodies the increased partitioning did not decrease at high concentrations of the ligand [9]. The BSA added in a large excess to quench the unreacted TMPEG might be responsible for the reduction in partitioning of rat reticulocytes at concentrations of MPEG–transferrin of 2 pg per cell or higher. It is known that BSA partitions into the bottom phase of the biphasic system used in this study [14]. The cells coated with the BSA will then partition towards the bottom phase, thereby opposing the affinity effect of the MPEG–transferrin. A decrease in the partitioning of liposomes with MPEG covalently linked to their surface has been observed when the liposomes were exposed to plasma, and this effect has been attributed to absorption of albumin to the lipid bilayer [23]. The number of transferrin receptors per reticulocyte is much lower than the number of antigenic determinants per erythrocyte used for the immunoaffinity approach [9]. This difference might explain why the negative effect of BSA was not seen in the latter.

The immediate alternative to quenching with BSA is the isolation of the MPEG–ligand from the excess of activated TMPEG. However, this is not a trivial issue, as the MPEG in the mixture interferes with the resolution of chromatographic techniques such as gel filtration [24,25]. In addition, despite the low molecular weight of the MPEG, its exclusion radius is substantially greater than that of proteins of even greater molecular weight [26] and this complicates the use of other conventional molecular sieve methods such as dialysis or ultrafiltration. Quenching with other small nucleophiles rather than BSA will affect the osmolarity of the preparation and then again isolation of the PEG–ligand conjugate will be required. These problems have not yet been resolved. New chromatographic media incorporating PEG in the matrix [27] might help to isolate the PEG–transferrin conjugate from the reaction mixture (and this might increase the effectiveness of the ligand for affinity cell partitioning).

To summarize, we have shown the feasibility of taking advantage of ligand–receptor interactions for affinity cell partitioning. Despite the drastic reduction in the affinity of the MPEG–transferrin for the transferrin receptor, the MPEG–transferrin conjugate can efficiently increase the partitioning of the reticulocyte. This model system has demonstrated the feasibility of using affinity cell partitioning to change the partitioning of a cell when about 80 000 molecules of the PEG–ligand are attached to the surface. To optimize affinity cell partitioning further, suitable methodologies to produce individual MPEG–ligand conjugates free of spent TMPEG or quenching agent will be required.

ACKNOWLEDGEMENTS

This work was supported by a grant awarded by the Ministerio de Educacion y Ciencia to C.D. and by grants from the Comision Interministerial de Ciencia y Tecnologia (Spain). The authors thank Dr. Angel Herraez for critical reading of the manuscript.

REFERENCES

1 P. A. Albertsson, *Partitioning of Cell Particles and Macromolecules*, Wiley-Interscience, New York, 3rd ed., 1986.
2 H. Walter, D. E. Brooks and D. Fisher (Editors), *Partitioning in Aqueous Two-Phase Systems —Theory, Methods, Uses and Applications to Biotechnology*, Academic Press, New York, 1985.
3 D. Fisher and I. A. Sutherland (Editors), *Separations Using Aqueous Phase Systems —Applications in Cell Biology and Biotechnology*, Plenum Press, London, 1989.

4 L. J. Karr, S. G. Shafer, J. M. Harris, J. M. Van Alstine and R. S. Snyder, *J. Chromatogr.*, 354 (1986) 269.
5 K. A. Sharp, M. Yalpani, S. J. Howard and D. E. Brooks, *Anal. Biochem.*, 154 (1986) 110.
6 L. J. Karr, J. M. Van Alstine, R. S. Snyder, S. G. Shafer and J. M. Harris, *J. Chromatogr.*, 442 (1988) 219.
7 S. J. Stocks and D. E. Brooks, *Anal. Biochem.*, 173 (1988) 86.
8 C. Delgado, G. E. Francis and D. Fisher, *Biochem. Soc. Trans.*, 16 (1988) 968.
9 C. Delgado, R. J. Anderson, G. E. Francis and D. Fisher, *Anal. Biochem.*, 192 (1991) 322.
10 H. G. Botros, G. Birkenmeier, A. Otto, G. Kopperschlager and M. A. Vijayalakshmi, *Biochim. Biophys. Acta*, 1074 (1991) 69.
11 F. M. Van Bockxmeer and E. H. Morgan, *Biochim. Biophys. Acta*, 584 (1979) 76.
12 R. M. Johnstone, M. Adam and B. T. Pan, *Can. J. Biochem. Cell. Biol.*, 62 (1984) 1246.
13 J. Mendieta, A. Herraez, P. Sancho and J. Luque, *Biosci. Rep.*, 9 (1989) 541.
14 C. Delgado, J. N. Patel, G. E. Francis and D. Fisher, *Biotechnol. Appl. Biochem.*, 12 (1990) 119.
15 C. Delgado, G. E. Francis and D. Fisher, in D. Fisher and I. A. Sutherland (Editors), *Separations Using Aqueous Phase Systems —Applications in Cell Biology and Biotechnology*, Plenum Press, London, 1989, p. 211.
16 F. W. Putnam (Editor), *The Plasma Proteins*, Vol. 1, Academic Press, New York, 2nd ed., 1975, Ch. 6.
17 S. Koteman, *Methods Enzymol.*, 36 (1975) 49.
18 M. N. Bradford, *Anal. Biochem.*, 72 (1976) 248.
19 Y. K. Park, A. Abuchowski, S. Davis and F. Davis, *Anticancer Res.*, 1 (1981) 373.
20 C. O. Beauchamp, S. L. Gonias, D. P. Menapace and S. V. Pizzo, *Anal. Biochem.*, 131 (1983) 25.
21 J. M. Harris, K. Yoshinaga, M. S. Paley and M. R. Herati, in D. Fisher and I. A. Sutherland (Editors), *Separations Using Aqueous Phase Systems —Applications in Cell Biology and Biotechnology*, Plenum Press, London, 1989, p. 203.
22 S. J. Stocks and D. E. Brooks, in D. Fisher and I. A. Sutherland (Editors), *Separations Using Aqueous Phase Systems —Applications in Cell Biology and Biotechnology*, Plenum Press, London, 1989, p. 183.
23 J. Senior, C. Delgado, D. Fisher, C. Tilcock and G. Gregoriadis, *Biochim. Biophys. Acta*, 1062 (1991) 77.
24 T. Arakawa, *Anal. Biochem.*, 144 (1985) 267.
25 S. B. Yan, D. A. Tuason, V. B. Tuason and W. H. Frey, II, *Anal. Biochem.*, 138 (1984) 137.
26 T. F. Busby and K. C. Ingham, *Vox Sang.*, 39 (1980) 93.
27 J.-P. Chang, Z. El Rassi and Cs. Horváth, *J. Chromatogr.*, 319 (1985) 396.

*Journal of Chromatography*, 594 (1992) 105–109
Elsevier Science Publishers B.V., Amsterdam

CHROM. 23 818

# Liquid chromatographic separation of all-carbon molecules $C_{60}$ and $C_{70}$ with multi-legged phenyl group bonded silica phases

Kiyokatsu Jinno*, Kunihiko Yamamoto, Takanori Ueda, Hideo Nagashima and Kenji Itoh

*School of Materials Science, Toyohashi University of Technology, Toyohashi 441 (Japan)*

John C. Fetzer and Wilt R. Biggs

*Chevron Research and Technology Company, Richmond, CA 94802 (USA)*

(First received September 10th, 1991; revised manuscript received October 23rd, 1991)

ABSTRACT

The separation of $C_{60}$ and $C_{70}$ all-carbon compounds has been examined using new multi-legged phenyl group bonded silicas as the stationary phase in liquid chromatography. Two-legged biphenyl bonded silica gave the best separation because this phase offers the most suitable cavity-like structure to retain the $C_{70}$ molecule, and this provides good separation between $C_{60}$ and $C_{70}$.

## INTRODUCTION

The most attractive and interesting compounds in organic chemistry today are all-carbon molecules, called "buckminsterfullerenes" or "fullerenes" for short, which are produced in large quantities in the vaporization of graphite or in soot extracts. The major species have been identified as molecular $C_{60}$ and $C_{70}$ by NMR, mass spectrometry (MS) and other spectroscopic tools [1–4]. To isolate these interesting compounds, it is important to separate both compounds by chromatographic techniques, especially liquid chromatography (LC). The technique could be used on the preparative scale for the mass production of the compounds. There have been some studies using LC techniques in which both compounds have been separated. Taylor *et al.* [5] used an alumina column, and Ajie *et al.* [6] and Allemand *et al.* [7] used silica gel as the stationary phase. However, the separation was incomplete in those cases.

Cox *et al.* [8] discussed the chromatographic characteristics of $C_{60}$ and $C_{70}$, which should closely resemble planar molecules with the corresponding "molecular footprints". They used nitroanilinopropyl silica (DNAP) as the stationary phase with an *n*-hexane to 50% dichloromethane gradient as the mobile phase. And they found that the retention of $C_{60}$ on the DNAP phase is very similar to that of triphenylene, a $C_{18}$ planar molecule, while the $C_{70}$ retention lies somewhere between the five-ring benzo[*a*]pyrene and the six-ring coronene compounds. Thus they assumed that $C_{60}$ may be considered an extreme example of the effect of non-planarity on retention time, which has been well documented with smaller polycyclic aromatic hydrocarbons in reversed-phase LC by several authors [9–11]. Therefore, it is reasonable to consider that stationary phases which can offer non-planarity recognition capability for these polycyclic aromatic hydrocarbons should be the best choice for the purpose of separation of $C_{60}$ and $C_{70}$.

0021-9673/92/$05.00 

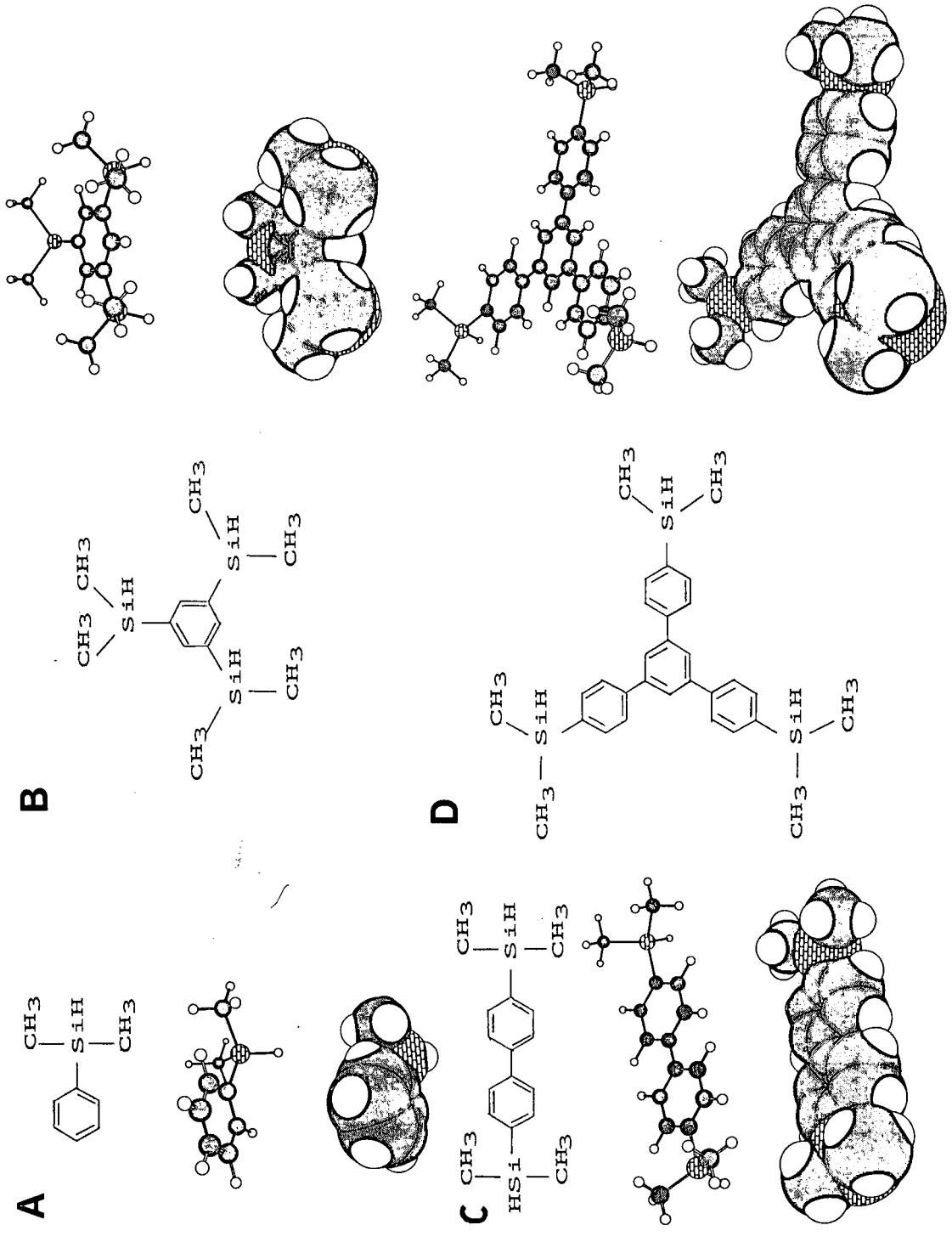


Fig. 1. Multi-legged phenyl group bonded phases used in this work. (A) P, (B) TP, (C) BP, (D) QP.

Hawkins *et al.* [12] thought that a stationary support containing $\pi$-acids might increase the retention and promote the discrimination of these $\pi$-basic aromatic clusters. They found that Pircle's phenylglycine-based LC column, which was originally designed for the separation of enantiomers by interactions that include the attraction between $\pi$-basic aromatic groups on substrates and $\pi$-acidic dinitrobenzamide groups on the stationary support, was useful for separating $C_{60}$ and $C_{70}$ [12].

In the above-mentioned situation of the problem of separating $C_{60}$ and $C_{70}$, one would expect "multi-legged" phenyl group bonded silica phases [13] to be useful. These phases have a different cavity-like space size formed by the methyl and phenyl groups, and the separation is based on molecular–molecular interactions between the phenyl ring(s) and the methyl groups of the stationary phase and the solutes [13]. As the separation factor between *o*-terphenyl (non-planar) and triphenylene (planar) can be useful for indicating the molecular planarity recognition capability of stationary phases in reversed-phase LC mode, the phases were evaluated on this point. For example, typical octadecylsilica (ODS) phases (both polymeric and monomeric types) have planarity recognition capability, and therefore triphenylene elutes later than *o*-terphenyl with those phases. However, in a previous work [13], it was found that the typical multi-legged phase 1,3,5-tris(dimethylphenyl) (TP) as shown in Fig. 1B elutes *o*-terphenyl later than triphenylene. Therefore, it appeared that this phase has strong molecular non-planarity recognition capability based on the molecular–molecular interaction between the phase and the solutes. In this work, we will describe the preliminary experimental results of the separation of $C_{60}$ and $C_{70}$ by the novel multi-legged phenyl group bonded phases which use a different space cavity to recognize differences in the size and shape of $C_{60}$ and $C_{70}$.

## EXPERIMENTAL

The LC system consisted of a JEOL CAP-G03 intelligent cascade pump (Tokyo, Japan) with a Model GAP G02 control unit, a Kontron capillary LC detector 433 (Amsterdam, Netherlands) and a Rheodyne injector 7513 (Cotati, CA, USA) of 0.5 $\mu$l volume.

The multi-legged phenyl group bonded phases were synthesized using reactions developed in our laboratory [13]. Base silica was obtained from Shiseido (Yokohama, Japan). The particle diameter is *ca.* 5 $\mu$m and very few metal impurities are present. The surface area of the silica is *ca.* 270 $m^2/g$. These new materials are *p*-bis(dimethyldiphenyl) (BP); TP; and 1,1′,1″-tris(dimethylquarternaryphenyl) (QP) bonded silicas.

For comparison, polymeric ODS (Vydac 201 TPB5 [10,11], Separations Groups, Hesperia, CA, USA), which is considered to have a strong molecular planarity recognition capability, was also evaluated. Because of its polymeric nature, the "slot-adsorption" model proposed by Wise and Sander [9] is rationalized, and because fullerenes such as $C_{60}$ and $C_{70}$ are sterically bulky, non-planar compounds the separation of $C_{60}$ and $C_{70}$ on the Vydac column is not expected to be better than on monomeric ODS phases and on the "multi-legged" phases. A monomeric-type ODS phase, Develosil-ODS, was also evaluated.

The synthesized phases were evaluated by cross-polarization magic angle spinning (CP-MAS) solid-state NMR spectroscopic measurements and Fourier-transform IR measurements. As shown in Fig. 1, TP, BP and QP phases have a unique structure which covers the silica surface horizontally, while the ODS phase is attached vertically to the silica surface by siloxane bonding.

All the phases were packed into fused-silica capillaries of 100–150 mm × 0.53 mm I.D. by a slurry technique. The mobile phase system was *n*-hexane. The sample probe $C_{60}$ and $C_{70}$ were obtained from a soot extract.

## RESULTS AND DISCUSSION

The molecular sizes of $C_{60}$ and $C_{70}$ are approximately 8 Å × 8 Å with the carbon atoms arranged like a soccer ball and 10 Å × 7 Å like a rugby ball, respectively, as shown in Fig. 2. Therefore, one would expect that the space size of the TP phase (the size of the space is *ca.* 5 Å × 5 Å), in which methyl groups and one phenyl ring form the cavity, would not be able to accept either solute, and thus the retention behaviour should be almost similar for both. The experimental results clearly agree with this hypothesis. With the BP phase, in contrast, the size

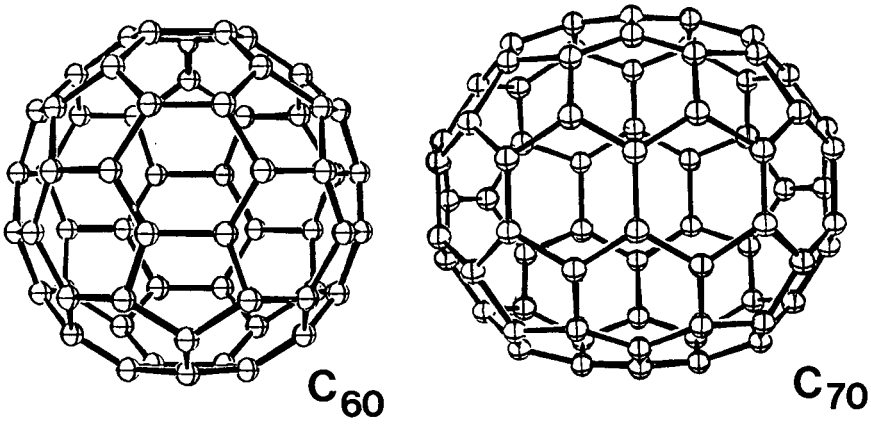


Fig. 2. Structures of $C_{60}$ and $C_{70}$.

of $C_{70}$ fits well into the pan-like space of the phase, while $C_{60}$ is not large enough to fit well in the space, because the BP phase has *ca.* 11 Å between the methyl groups bonded to both silicon atoms. Therefore, $C_{70}$ should have a longer retention than $C_{60}$ with the BP phase. The result shown in Fig. 3A indicates excellently that this expectation is true. Also, as both solutes are retained because of the interaction between the BP phase and the solutes in the sense of molecular recognition, the BP phase clearly offers a large relative retention of the solutes and large capacity factors for both solutes. The interpretation of these results also means that the concept of this molecular–molecular interaction is useful in the design of new stationary phases which offer specific and/or selective separation of other fullerenes such as $C_{76}$, $C_{78}$ and others which are thought to exist in soot extracts. In addition to those two phases, the QP phase was also tested. However, the space in this phase is too large to catch both solutes on its flat phenyl ring surface and, therefore, the phase cannot retain and recognize well the size difference between $C_{60}$ and $C_{70}$. The experimental result with the QP phase shown in Table I suggests that this mechanism is present, although Cox *et al.* [9] and Hawkins *et al.* [12] suggested that a $\pi$–$\pi$ interaction mechanism should be useful for the separation of $C_{60}$ and $C_{70}$.

In Table I, the retention data obtained by various separation systems are summarized. It is apparent that the BP phase gave very high separation factor values with an *n*-hexane mobile phase system. With the polymeric ODS phase, although high separation factor values can be obtained, the absolute retention value is not large enough for a good separation. As expected, monomeric ODS, Develosil, offered a

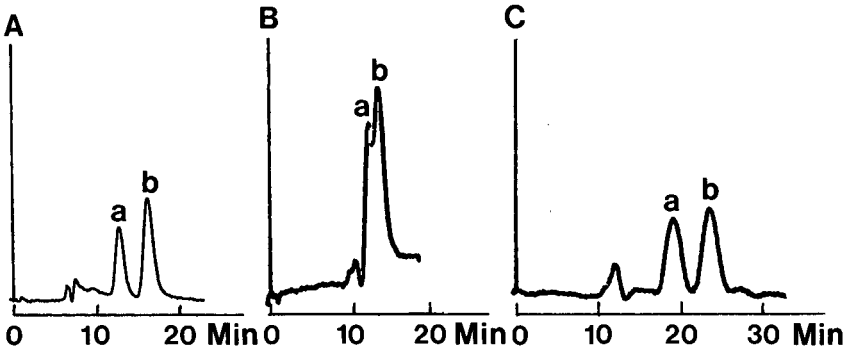


Fig. 3. Chromatograms for the separation of $C_{60}$ and $C_{70}$. (A) BP, (B) Vydac, (C) Develosil. Mobile phase: *n*-hexane, 2 μl/min. Peaks: a = $C_{60}$; b = $C_{70}$.

TABLE I

CAPACITY FACTORS AND SEPARATION FACTORS FOR $C_{60}$ AND $C_{70}$ WITH VARIOUS STATIONARY PHASES

Mobile phase: *n*-hexane at room temperature.

| Stationary phase | Capacity factor | | Separation factor |
|---|---|---|---|
| | $C_{60}$ | $C_{70}$ | |
| P | 0.302 | 0.396 | 1.31 |
| TP | 0.107 | 0.126 | 1.18 |
| BP | 0.752 | 1.223 | 1.63 |
| QP | No retention | | |
| Vydac | 0.171 | 0.284 | 1.66 |
| Develosil | 0.585 | 0.962 | 1.65 |

better separation factor than Vydac with larger capacity factors. Therefore, it is also possible to conclude that if one would like to use ODS phases for the separation of fullerenes, monomeric ODS should be a more feasible and better stationary phase. It should be mentioned here that the Vydac phase is a very powerful stationary phase for the separation of polycyclic aromatic hydrocarbons based on its high molecular planarity recognition capability [10,11]. Fig. 3 compares the separation of $C_{60}$ and $C_{70}$ with the BP phase (Fig. 3A), Vydac (Fig. 3B) and Develosil (Fig. 3C) with *n*-hexane as the mobile phase. The separation with Vydac is not very good because of the low retention of the compounds. However, this is not because of the low surface area of this phase.

It should also be mentioned here that separation of actual soot extracts yielded a number of fullerenes larger than $C_{70}$, and the identification of those compounds is in progress.

In conclusion, the molecular–molecular interaction mechanism with multi-legged phenyl group bonded phases can achieve higher separation capability for these all-carbon compounds. Although the separation obtained with the BP phase is not better than those reported phases discussed in the first part of this article, it has been shown that the BP phase can be useful as the stationary phase for preparative work because it offers larger retention and separation factor for $C_{60}$ and $C_{70}$. For the separation of larger fullerenes such as $C_{76}$, $C_{78}$, $C_{84}$ one can use the concept of the multi-legged phases to design more suitable stationary phases which have an appropriate cavity size to catch the fullerenes once the size and shape of those compounds are found by computer calculations. Such work is under way in our laboratory.

REFERENCES


1 W. Kratschmer, L. D. Lamb, K. Fostiropoulos and D. R. Huffman, *Nature (London)*, 347 (1990) 354.
2 W. Kratschmer, L. D. Lamb, K. Fostiropoulos and D. R. Huffman, *Chem. Phys. Lett.*, 170 (1990) 160.
3 H. W. Kroto, J. R. Heath, S. C. O'Brien, R. F. Curl and R. E. Smalley, *Nature (London)*, 318 (1985) 162.
4 W. Welther, Jr. and R. J. Van Zee, *Chem. Rev.*, 89 (1989) 1713.
5 R. Taylor, J. P. Hare, A. K. Abdul-Safa and H. W. Kroto, *J. Chem. Soc., Chem. Commun.*, 20 (1990) 1423.
6 H. Ajie, H. M. Alvarez, S. J. Anz, R. D. Beck, F. Diederich, K. Fostiropoulos, D. R. Huffman, W. Kratschmer, Y. Rubin, K. E. Schriver, D. Sensharma and R. L. Whetten, *J. Phys. Chem.*, 94 (1990) 8630.
7 P. M. Allemand, A. Koch and F. Wudl, *J. Am. Chem. Soc.*, 113 (1991) 1050.
8 D. M. Cox, S. Behal, M. Disko, S. M. Gorun, M. Greaney, C. S. Hsu, E. B. Kollin, J. Millar, R. D. Robbins, R. D. Sherwood and P. Tindall, *J. Am. Chem. Soc.*, 113 (1991) 2940.
9 S. A. Wise and L. C. Sander, *J. High Resolut. Chromatogr. Chromatogr. Commun.*, 8 (1985) 248.
10 K. Jinno, T. Nagoshi, N. Tanaka, M. Okamoto, J. C. Fetzer and W. R. Biggs, *J. Chromatogr.*, 392 (1987) 75.
11 K. Jinno, T. Ibuki, N. Tanaka, M. Okamoto, J. C. Fetzer, W. R. Biggs, P. R. Griffiths and J. M. Olinger, *J. Chromatogr.*, 461 (1989) 209.
12 J. M. Hawkins, T. A. Lewis, S. D. Loren, A. Meyer, J. R. Heath, Y. Shibato and R. J. Saykally, *J. Org. Chem.*, 55 (1990) 6250.
13 K. Jinno, K. Yamamoto, H. Nagashima, T. Ueda and K. Itoh, *J. Chromatogr.*, 517 (1990) 193.

*Journal of Chromatography*, 594 (1992) 111–115
Elsevier Science Publishers B.V., Amsterdam

CHROM. 23 823

# Liquid chromatographic isolation and structural elucidation of methoxymethylene dimethyl dodecatrienes catalytically synthesized from methanol and three moles of isoprene

Christof Tröltzsch* and Rüdiger Berger

*Ernst-Moritz-Arndt-Universität FB Chemie, Soldtmannstrasse 16, O-2200 Greifswald (Germany)*

Manfred Michalik

*Institut für Organische Katalyseforschung, Buchbinderstrasse 5-6, O-2500 Rostock (Germany)*

(First received July 23rd, 1991; revised manuscript received October 21st, 1991)

ABSTRACT

The palladium-catalysed reaction of isoprene with methanol yields methoxy dimethyl octadienes ("methoxy dimers") and dimers of isoprene. To obtain additional information about the mechanism of catalysis this paper is aimed at identifying the higher boiling side-products of this reaction. After distillation in high vacuum the residue of the reaction was separated by analytical and preparative reversed-phase and normal-phase high-performance liquid chromatography, yielding at least six compounds with the formula $C_{16}H_{28}O$ ("methoxy trimers") plus trimers and tetramers of isoprene, all proven by mass spectra. The structure of two methoxy trimers was elucidated by $^{1}H$ and $^{13}C$ NMR spectra. Up until now they have not been described in the literature and they show an unexpected position of the methoxy group.

## INTRODUCTION

Palladium complex compounds catalyse the dimerization of isoprene in the presence of phosphines. Protic nucleophiles used as a co-catalyst can be added to the dimer with the elimination of one double bond. For example, in the presence of methanol and by means of palladium acetylacetonate and triphenylphosphine about 60% methoxy dimethyl octadienes (called methoxy dimers hereafter) plus isoprene dimers are obtained from isoprene at 80°C as well as at room temperature [1,2]. Isoprene is almost completely converted.

About 5 l of methoxy dimers per gram of palladium used can be obtained before the catalyst becomes ineffective [2]. 1-Methoxy-2,6-dimethyl-octa-2,7-diene (40%) and 1-methoxy-2,7-dimethyl-octa-2,7-diene (20%) are formed at room temperature [1]. Similar mixtures are obtained when using tri-*n*-butylphosphine [3,4]. In each case, however, the formation of higher boiling products was observed, which could not be analysed by gas chromatography up to 200°C [1,3,5].

The present paper is aimed at studying this higher boiling residue and answering the following questions:

(1) Do isoprene trimers form during the above catalysis?

(2) Does the reaction result in the formation of addition compounds of methanol to trimers of isoprene (called methoxy trimers hereafter, molecular empirical formula $C_{16}H_{28}O$)?

(3) What can be stated about the structure of these methoxy trimers?

0021-9673/92/$05.00 

Up until now only 1-methoxy-1-vinyl-1,5,9-trimethyl-deca-4,8-diene [6], *i.e.*, nerolidole methyl ether, has been known beside 1-methoxy-3,7,11-trimethyl-dodeca-2,6,10-triene (farnesyl methyl ether), which is often mentioned in the literature.

## EXPERIMENTAL

### *Reaction of isoprene with methanol for obtaining the starting mixture [1]*

Under exclusion of oxygen and moisture 0.745 g of triphenylphosphine, 0.761 g of palladium acetylacetonate, 50 ml of isoprene and 80 ml of methanol were mixed and stirred. After allowing to stand at room temperature for 20 h in intervals of 2 h each, the following substances were added: two portions each of 150 ml of isoprene, one portion of 150 ml of isoprene and 100 ml of methanol, two portions each of 100 ml of isoprene and one portion of 70 ml of isoprene (total volumes 770 ml of isoprene and 180 ml of methanol, both free of moisture and oxygen and freshly distilled). After allowing to stand overnight and refluxing for 1 h, distillation yielded 381 g of methoxy dimers, b.p. 46–58°C at 270 Pa.

After taking two intermediate fractions at 58–95°C/270–470 Pa and 63–68°C/27–33 Pa, 7.45 g of crude mixture were obtained at 68–110°C/20–33 Pa. A 0.351-g amount of this high-vacuum distillate yielded 0.152 g of a mixture of methoxy trimers after the first liquid chromatographic group separation (see below). Therefore the yield of methoxy trimers is 0.53% relative to isoprene used. In repeated preparations the yields ranged from 0.5 to 2%.

### *Chemicals*

Octadecyl silica gel for the preparative column was prepared according to ref. 7, but with the following modification: 61 g (0.176 mol) of *n*-octadecyl dimethyl chlorosilane (prepared from *n*-octadecyl magnesium bromide and dimethyldichlorosilane) were dissolved in 350 ml of *n*-hexane, and 50 ml of dry gaseous dimethylamine were introduced. After separation of the solid dimethylamine hydrochloride by filtration, the resulting solution was directly reacted (16 h at 50°C in hexane and 8 h at 80°C hexane-free) with 94.7 g of spherical ES silica gel (previously dried at 150°C for 30 h) from VEB Leuna Werke (particle size, $d_p$, 10 $\mu$m, 331 $m^2/g$; with 7.8 $\mu$mol SiOH/$m^2$ = 0.2445 mol SiOH). After washing with toluene and methanol and drying *in vacuo* at 80°C, 123.5 g of octadecyl silica gel were obtained. Elementary analysis resulted in 17.55% carbon and 3.85% hydrogen. According to ref. 8, 3.64 $\mu$mol of octadecyl groups per $m^2$ can be calculated.

All eluents were purified and regenerated by means of fractional distillation using a Vigreux column. The mixtures of the eluents were prepared by weighing in the constituents and degassing the mixtures by ultrasound and *in vacuo*.

### *High-performance liquid chromatographic (HPLC) separations*

The first group separation was made in a self-constructed apparatus by means of preparative reversed-phase (RP) chromatography. The apparatus consisted of an MC 300 micropump with a low-dead-volume filter and an L pump head (Mikrotechna, Prague, Czechoslovakia); PTFE tubing of 1.0 mm I.D. and 2.0 mm O.D. as an overpressure safety device; a manometer measuring up to 160 bar with a Bourdon tube —reconstructed to allow permanent passage of the eluent; a 1-m stainless-steel capillary of about 0.3 mm I.D. and 0.7 mm O.D.; a self-constructed six-way valve of stainless-steel and PTFE with a sample loop of 1.85 ml volume and about 1 mm I.D.; a self-constructed stainless-steel preparative column 400 × 22 mm I.D. (column A), filled with a slurry of the prepared octadecyl silica gel in 1,2-dichloroethane at about 200 bar by means of a Haskel pump (Haskel-Burbanks)[a] with a filling tube of 2000 × 22 mm I.D., an RIDK 101 differential refractometer (Laboratorni Přistroje, Prague, Czechoslovakia), the reference cell of which was passed by pure eluent by means of gravity flow, combined with a K201 recorder (VEB Carl Zeiss, Jena, Germany); and a 8300 Uvicord II UV detector (LKB, Sweden) with a 100-$\mu$l measuring cell (about 2.5 mm optical pathway), combined with an MK motor compensator (VEB Messgeraetewerk, Magdeburg, Germany).

Preparative samples were introduced into column A via the sample loop. All other injections were made directly into the column bed by means of the

[a] For the possibility of filling column A, we would like to thank Dr. Beerbaum, Amt für Atomsicherheit und Strahlenschutz, Berlin-Friedrichshagen, Germany.

stop-flow method. The fractions were collected manually.

In the following separations the MMC minipump with the 2 D pump head (Mikrotechna) was used and the Uvicord II UV detector was substituted by a Dukol UD UV detector (VEB Carl Zeiss). For recording the UV and refractive index (RI) signals the TZ 4620 line recorder (double line recorder) (Laboratorni Přistroje) was used.

The semipreparative separation of the methoxy trimer fraction from column A was carried out in a self-constructed column of 308 × 7.5 mm I.D. on LiChrospher SI 100 (Merck), $d_p$ 10 μm (column B), filled in as a slurry in cyclohexanol at 200 bar using an SK 15 pump (Orlita, Giessen, Germany) and rinsing with *n*-heptane afterwards. This semipreparative separation was repeated 15 times. The fractions (1–3, Fig. 3) obtained in this way were separately rechromatographed in 5–8 portions of 2.5–5 μl after removing the eluent on a 15-cm Vigreux column and finally with a water jet pump.

The fractions were analysed in a self-constructed column 250 × 4 mm I.D. on RP-18 silica gel (Merck), $d_p$ 10 μm (column C), and in a self-constructed column, 300 × 4.5 mm I.D., on LiChrospher SI 100, $d_p$ 10 μm (column D), both being filled in as a slurry in cyclohexanol at about 250 bar and subsequently rinsed with methanol and heptane, respectively.

The dead volumes ($V_0$) were determined with deuterated methanol ($CH_3O^2H$) in methanol-containing eluents and with pentane in hexane-containing eluents (column A 90.1 ml, B 9.25 ml, C 1.93 ml, D 3.05 ml).

*NMR*

The $^1H$ and $^{13}C$ NMR spectra were recorded with a Varian XL-300 spectrometer in [$^2H$]chloroform solution. The $\delta$ values are referred to tetramethylsilane as standard. The assignments of the $^{13}C$ NMR signals to the primary, secondary, tertiary and quaternary carbon atoms were verified by means of the distortionless enhancement by polarisation transfer (DEPT) spectra [9].

## RESULTS AND DISCUSSION

Using octadecyl silica gel (column A) and pure methanol a rapid group separation of the high-

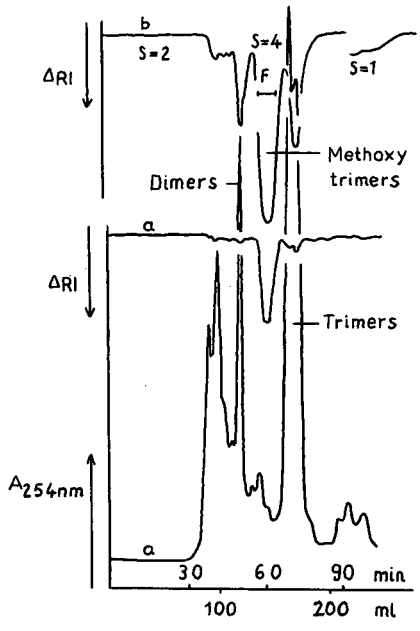


Fig. 1. Group separation of the high-vacuum distillate on 400 × 22 mm octadecyl silica gel (column A) in pure methanol. Pressure about 15 bar. (a) Sample of 40 μl. Detectors: RIDK 101, sensitivity 1, and Uvicord II. Injection into the column bed. (b) Sample of 500 μl + 500 μl of methanol. Detector: RIDK 101, sensitivity (S) 2, 4 and 1. Injection via sample loop. Retention volume of methoxy trimers 153 ml.

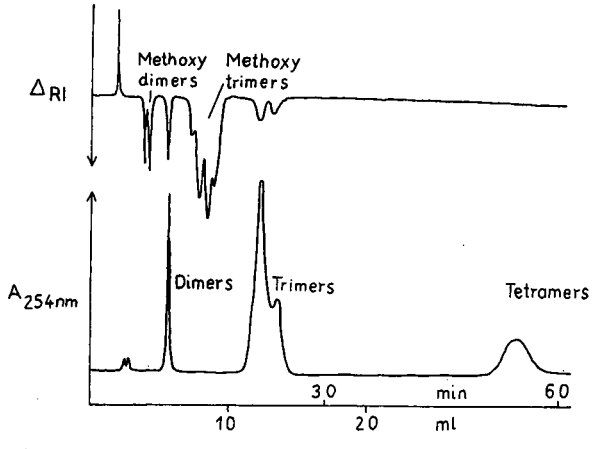


Fig. 2. Analytical separation of a synthetic mixture of appropriate amounts of methoxy dimers, methoxy trimers, dimers, trimers and tetramers of isoprene on 250 × 4 mm RP-18 silica gel (Merck), $d_p$ 10 μm (column C), in methanol–water (85:15, w/w). Detectors: RIDK 101, sensitivity 1, and Dukol UD. Flow-rate 34.28 ml/h. Pressure about 20 bar.

vacuum distillate into dimers, methoxy trimers, trimers and tetramers of isoprene is possible (Fig. 1). At first the fractions were analysed on octadecyl silica gel (column C) with methanol–water (85:15, w/w) (Fig. 2).

The assignments of the peaks resulted from the molecular mass determined by mass spectrometry. It is advantageous that, unlike the methoxy compounds, the oligomers of isoprene contain a conjugated double bond and show intensive signals at 254 nm, while unlike the oligomers the methoxy compounds in the eluents employed show intensive signals in the differential refractometer.

As anticipated, the methoxy trimer fraction could be separated into distinct structural isomers more easily by adsorption chromatography than by RP chromatography. Therefore this fraction was first analytically separated on LiChrospher SI 100 with hexane–diethyl ether (99:1, w/w) (column D) and then preparatively (column B, Fig. 3).

Fractions 1, 2 and 3 (Fig. 3) were concentrated and then again purified on column B. Fraction 1 (compound I) could be shown to be a methoxy trimer (mass number 236) by mass spectrometry.

To elucidate the structure of compounds II (fraction 2) and III (fraction 3) the $^1H$ and $^{13}C$ NMR spectra were recorded. The interpretation of the $^1H$ spectra resulted in the following signal assignments:

Compound II: $\delta$ = 5.68 (m, 1 CH=); 5.40 (m, 1 CH=); 4.94 (m, 2 CH=); 4.69 (m, 2 CH=); 3.81 (s, 1 $CH_2O$); 3.21 (s, 1 $CH_3O$); 2.00 (m, 3 $CH_2$, 1 CH); 1.73 (s, 1 $CH_3$–C=); 1.52 (m, 1 $CH_2$); 1.35 (m, 1 $CH_2$); 0.98 (d, J = 6.5 Hz, 1 $CH_3$–CH=).

Compound III: $\delta$ = 5.93 (t, 1 CH=); 4.71 (m, 4 CH=); 3.81 (s, 1 $CH_2O$); 3.26 (s, 1 $CH_3O$); 2.01 (m, 4 $CH_2$); 1.71, 1.62 (2s, 2 $CH_3$–C=); 1.53 (m, 2 $CH_2$).

In the $^{13}C$ NMR spectra the following signals were found:

Compound II: $\delta$ = 145.8, 136.0 (2 C=); 144.7, 129.1 (2 CH=); 112.7, 109.9 (2 $CH_2$=); 76.9 ($CH_2O$); 57.4 ($CH_3O$); 37.5 (CH); 37.8, 36.6, 27.7, 26.3, 25.2 (5 $CH_2$); 22.4, 20.2 (2 $CH_3$).

Compound III: $\delta$ = 149.6, 145.9, 132.3 (3 C=); 128.2 (1 CH=); 109.9, 109.0 (2 $CH_2$=); 78.8 ($CH_2O$); 54.4 ($CH_3O$); 37.6, 35.8, 35.8, 27.7, 27.4, 25.9 (6 $CH_2$); 22.4, 13.8 (2 $CH_3$).

The NMR spectra of both substances prove the existence of the following structural elements:

Three C=C double bonds.

One $CH_3$–O–$CH_2$ group.

Five $CH_2$ groups (compound II), 6 $CH_2$ groups (compound III).

Two $CH_3$ groups.

In the case of II the structural element $CH_3$–CH– is unambiguously present.

On principle, several isomeric structures must be taken into consideration regarding the possible course of the reaction. From the NMR data, especially the $^{13}C$ chemical shifts, the structures in Fig. 4 can be assumed to be most likely for compounds II and III.

The $^{13}C$ chemical shifts of the olefinic carbon atoms are especially representative of the elucidation of the structure. By comparison with literature data of compounds containing similar structural

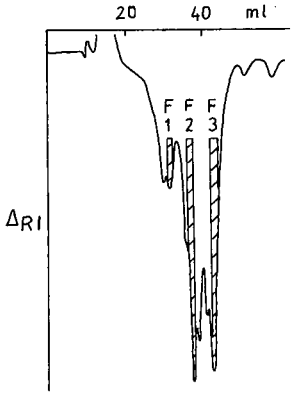


Fig. 3. Preparative separation of 25 µl of the fraction of methoxy trimers of Fig. 1 on a 308 × 7.5 mm LiChrospher SI 100 column (Merck), $d_p$ 10 µm (column B), in hexane–diethyl ether (99:1, w/w). Detector: RIDK 101, sensitivity 4. Flow-rate 119.7 ml/h. Pressure about 18 bar. [F1, capacity factor ($k'$) = 2.45; F2, $k'$ = 3.0; F3, $k'$ = 3.7].

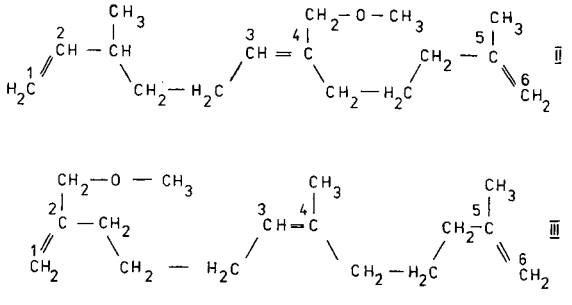

Fig. 4. Proposed structures for compounds II and III.

TABLE I

ASSIGNMENTS OF THE $^{13}C$ NMR SIGNALS TO THE OLEFINIC CARBON ATOMS

| | C-1 | C-2 | C-3 | C-4 | C-5 | C-6 |
|---|---|---|---|---|---|---|
| II | 109.9 | 144.7 | 129.1 | 136.0 | 145.8 | 109.0 |
| III | 109.9 | 149.6 | 128.2 | 132.3 | 145.9 | 109.0 |

elements [10,11], an assignment of the signals can be made as shown in Table I.

The proposed structures for II and III are also in accordance with the elution behaviour of both substances, because III, with the methoxyl at the end-position, should be more strongly retained on a polar stationary phase than II. It should be pointed out that, beside the structures given here, one alternative structure for both II and III is also possible, in which the substituents at the central double bond ($CH_3OCH_2$ in II, $CH_3$ in III) would be positioned at carbon-3. It should be difficult to distinguish between them.

These data support the idea that all substances eluted between fractions 1, 2 and 3 (Fig. 3) are also methoxy trimers. This leads to the conclusion that in the above-mentioned reaction at least six different methoxy trimers with the formula $C_{16}H_{28}O$ (including *Z–E* isomers) are formed beside dimers, trimers and tetramers of isoprene and methoxy dimers. The position of the methoxy group is unexpected and important for elucidating the mechanism of the catalysis.

ACKNOWLEDGEMENT

The authors are indebted to Dr. Basner, Institut für Gasentladung, Greifswald, and Dr. U. Vollert, Vereinigte Sächsische Olefinwerke, Boehlen, for making mass spectra. They thank Ing. Witt, Greifswald, for valuable assistance and not least Professor Dr. Gaube, Greifswald, for kindly posing the problem.

REFERENCES

1 R. Berger, H. Stegemann and W. Gaube, *Miltitzer Berichte*, (1981) 7.
2 W. Gaube and R. Berger, *Mittbl. Chem. Ges. DDR*, 34 (1987) 6122.
3 W. Gaube and H. Stegemann, *J. Prakt. Chem.*, 326 (1984) 729.
4 W. Gaube and H. Stegemann, *J. Prakt. Chem.*, 326 (1984) 947.
5 H. Stegemann, *Dissertation A*, Ernst-Moritz-Arndt Universität, Greifswald, 1983.
6 L. J. Colaianni and M. L. Tanzer/F. Hoffmann-La Roche & Co., *US Pat.*, 2 841 620; *C.A.*, 53 (1959) 2090c; *Ger. Pat.*, 1 080 098; *C.A.*, 55 (1961) 24566.
7 K. Szabo, N. L. Ha, P. Schneider, P. Zeltner and E. sz. Kováts, *Helv. Chim. Acta*, 67 (1984) 2128.
8 C. E. Berendsen and L. de Galan, *J. Liq. Chromatogr.*, 1 (1978) 561.
9 H. Kessler, M. Gehrke and C. Greisinger, *Angew. Chem.*, 100 (1988) 507.
10 E. Breitmaier and W. Voelter, *$^{13}C$-NMR-Spectroscopy*, Verlag Chemie, Weinheim, 1974, p. 195.
11 H.-O. Kalinowski, S. Berger and S. Braun, *$^{13}C$-NMR-Spektroskopie*, Georg Thieme, Stuttgart, New York, 1984, p. 115.

*Journal of Chromatography*, 594 (1992) 117–123
Elsevier Science Publishers B.V., Amsterdam

CHROM. 23 836

# Identification of the constituent flavanoid units in sainfoin proanthocyanidins by reversed-phase high-performance liquid chromatography

Mohammed R. Koupai-Abyazani*, John McCallum and Bruce A. Bohm

*Department of Botany, University of British Columbia, 6270 University Boulevard, Vancouver, B.C. V6T 1Z4 (Canada)*

(First received September 16th, 1991; revised manuscript received October 30th, 1991)

ABSTRACT

A rapid and sensitive method for the separation and identification of flavan-3-ols and their phloroglucinol adducts using reversed-phase high-performance liquid chromatography is reported. The application of the method is demonstrated for the analysis of the degradation products of sainfoin leaf proanthocyanidins. The results showed that the extension and terminal units in this sample are catechin, epicatechin, gallocatechin and epigallocatechin.

## INTRODUCTION

Proanthocyanidins (condensed tannins) are a group of phenolic polymers which are widely distributed in the plant kingdom particularly in plants with a woody growth habit [1–4]. These compounds consist of flavan-3-ol (Fig. 1) units, linked together through C-4–C-6 or C-4–C-8 bonds [5]. Structural variation of proanthocyanidins ranges from dimers and trimers to more complex oligomers and polymers depending on the nature of the interflavanoid linkage, hydroxylation pattern and stereochemistry at the three chiral centers (carbons 2, 3 and 4) of the C-ring [4,6,7]. These polymers are found in numerous gymnosperms and angiosperms in large amounts [8] and have an important defensive function in many plants against micro organisms and predators [9]. In fruits and seed coats, considerable quantities of these compounds make an important contribution to the quality, colour and taste of the fruit and products derived from them [2,10,11] and play a major role in the preservation of beers [12].

Proanthocyanidins have been shown to have an important role in non-bloating forage crops because they bind with excess protein in the rumen and prevent the development of a gas trapping stable foam [13–15]. In the course of investigations aimed at the identification of proanthocyanidins in sainfoin leaves, we have examined the application of reversed-phase high-performance liquid chromatography (RP-HPLC) for the separation and identification of flavan-3-ol units in the proanthocyanidins of this species.

Degradation of proanthocyanidins is essential for the determination of their structural units [16]. Several methods have been used to analyze the degradation products of these compounds of which the most common are column chromatography [17], thin-layer chromatography (TLC), two-dimensional (2D) TLC [16,18,19] and spectroscopic methods [20–22]. However, these methods are time consuming, limited in separation power or require purified samples.

In this paper we report a rapid and sensitive method for the separation and identification of flavan-3-ols and their phloroglucinol adducts in proanthocyanidins by RP-HPLC. The application of the method is demonstrated for the analysis of degradation products of sainfoin proanthocyanidins.

0021-9673/92/$05.00 

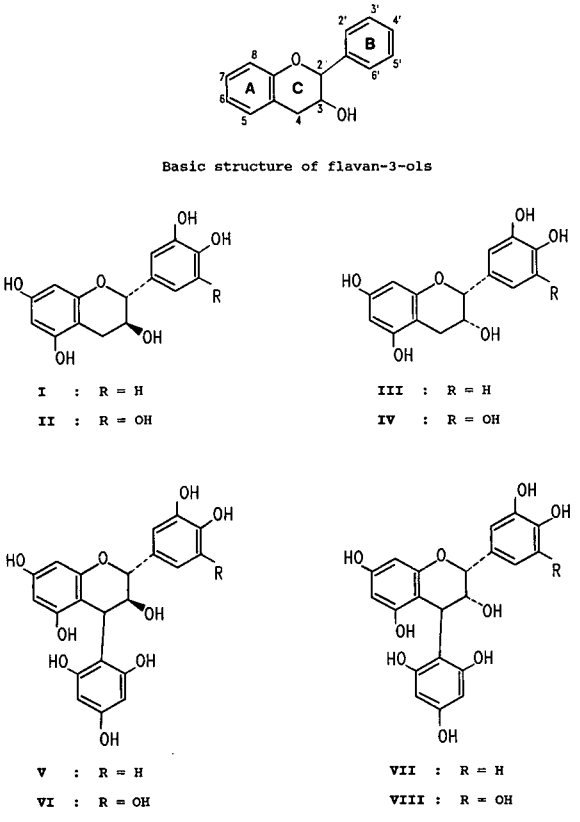


Fig. 1. Structures of flavan-3-ols and their phloroglucinol adducts used for the HPLC analysis.

## EXPERIMENTAL

### *Apparatus*

The high-performance liquid chromatograph was a Millipore-Waters (Milford, MA, USA) equipped with a Model 600E multisolvent delivery system and a Model 994 programmable photodiode array detector. A prepacked analytical column (25 cm × 4 mm I.D.) of LiChrospher 100 RP-18 (5 $\mu$m) (E. Merck, Darmstadt, Germany) was used for all experiments. The guard column (4 mm × 4 mm I.D.) was packed with the same material.

### *Elution*

Two solvents were used: A = 1% aqueous acetic acid; B = methanol. The elution system was: 0–30 min, 0–15% B in A (linear gradient); 30–45 min, 15–60% B in A (linear gradient); 45–50 min, 60% B in A (isocratic). The column temperature was ambient and the flow-rate was set at 1 ml $min^{-1}$.

### *Detection*

The photodiode array detector was set to monitor the chromatograms at 280 nm and acquire the UV spectra between 200–400 nm.

### *Materials*

The solvents chloroform (Fisher Scientific, Ottawa, Canada), acetone and ethyl acetate (BDH, Toronto, Canada) were of analytical grade. The methanol (BDH) used for the analysis was of HPLC grade. Sainfoin leaves, *Onobrychis viciifolia* Scop. (var. Melrose), were supplied by Agriculture Canada, Saskatoon. Phloroglucinol was obtained from Aldrich (Milwaukee, WI, USA) and recrystallized before use. (−)-Epigallocatechin was purchased from Apin Chemicals (Abingdon, UK). (−)-Epicatechin and (+)-catechin were obtained from Sigma (St. Louis, MO, USA). (+)-Gallocatechin and (+)-gallocatechin-, (−)-epigallocatechin-, (−)-epicatechin- and (+)-catechin-4-phloroglucinol adduct standards were kindly supplied by L. Y. Foo (DSIR, Petone, New Zealand). Some of these compounds contained impurities, but all consisted of one major component. These compounds were used without further purification.

### *Isolation and purification of sainfoin leaf proanthocyanidins*

A sample of finely ground sainfoin leaves (200 g, dry weight) was extracted with 4 × 250 ml 75% aqueous acetone containing 0.1% ascorbic acid according to the method of Foo and Porter [23]. The acetone was removed under reduced pressure at $\leqslant$30°C. The aqueous solution was filtered through a plug of glasswool. The filtrate was then extracted with 3 × 300 ml chloroform. The chloroform extract was discarded and the aqueous phase was filtered through a plug of glasswool. The filtrate was extracted with 3 × 1000 ml ethyl acetate. The ethyl acetate-soluble fractions were combined and stored at 4°C for further analysis. The aqueous fraction was mixed with the same volume of methanol and chromatographed on Sephadex LH-20 column (15 cm × 4 cm I.D.). The column was washed with 50% aqueous methanol (600 ml) and proanthocyanidins were then eluted with 75% aqueous acetone

(500 ml). A brown solid (3.65 g) was obtained following the removal of acetone and freeze-drying the aqueous fraction.

*Preparation of the phloroglucinol adducts of sainfoin proanthocyanidins*

A sample of sainfoin proanthocyanidins (12 mg) together with 8 mg of phloroglucinol were dissolved in 100 μl 1% HCl in ethanol. The mixture was shaken vigorously and allowed to stand at room temperature for 2 h. The solvent was evaporated by a stream of dry nitrogen and the residue was dissolved in 50 μl distilled water. The latter was extracted with 2 × 100 μl ethyl acetate. The ethyl acetate extracts were combined and evaporated to dryness by a stream of dry nitrogen. The residue was dissolved in 50 μl of 70% aqueous methanol. This solution was used for injection onto the HPLC column.

*Analysis of ethyl acetate-soluble fraction*

The ethyl acetate-soluble fraction was evaporated to obtain a concentrated solution which was applied to a LH-20 column (30 cm × 3.5 cm I.D.). The elution was initiated with 1000 ml ethanol (five fractions, 1–5, were collected) and followed by ethanol–acetone (19:1, v/v) [22] which yielded one fraction (6). Each fraction was evaporated and the residue was dissolved in 100 μl 70% aqueous methanol and tested for flavan-3-ols and di- or trimeric proanthocyanidins by 2D-TLC and HPLC.

*2D-TLC procedure*

The preliminary detection of dimeric proanthocyanidins, flavan-3-ols and their phloroglucinol adducts was carried out using the standard method of two-dimensional cellulose TLC [3,16]. The chromatograms were developed in *tert.*-butanol–acetic acid–water (3:1:1, v/v/v) in the first direction and 6% acetic acid in the second direction. Compounds were visualized by spraying the chromatograms with freshly prepared 4% vanillin in methanol-conc. HCl (4:1, v/v). Red or purplish-red spots were produced after spraying and warming.

*Preparation of standard samples*

All standards were prepared at 1 mg $ml^{-1}$ concentration in 70% aqueous methanol.

## RESULTS AND DISCUSSION

The retention times, $t_R$, for some typical flavan-3-ols and their phloroglucinol adducts (Fig. 1) are given in Table I. These results demonstrate the potential of HPLC as an alternative to the other chromatographic methods for such separations reported by other workers [16–19]. Fig. 2 shows the chromatogram obtained for a mixture of these compounds. All the peaks are well resolved except for (−)-epicatechin-4-phloroglucinol (**VII**) and (+)-catechin-4-phloroglucinol (**V**) which form a critical pair. However, under the conditions reported here a sufficient separation of these two peaks was

TABLE I

RETENTION TIMES OF SOME FLAVAN-3-OLS AND THEIR PHLOROGLUCINOL ADDUCTS

HPLC conditions: column, LiChrospher 100 RP-18 (25 cm × 4 mm, I.D., 5 μm); flow-rate, 1 ml $min^{-1}$; column temperature, ambient; detection, 280 nm.

| No. | Compound | OH Position | Absolute configuration | $t_R$ (min) |
|---|---|---|---|---|
| **I** | (+)-Catechin | 3,5,7,3′,4′ | 2*R*:3*S* | 39.56 |
| **II** | (+)-Gallocatechin | 3,5,7,3′,4′,5′ | 2*R*:3*S* | 23.06 |
| **III** | (−)-Epicatechin | 3,5,7,3′,4′ | 2*R*:3*R* | 44.68 |
| **IV** | (−)-Epigallocatechin | 3,5,7,3′,4′,5′ | 2*R*:3*R* | 38.49 |
| **V** | (+)-Catechin-4-phloroglucinol | 3,5,7,3′,4′ | 2*R*:3*S* | 26.47 |
| **VI** | (+)-Gallocatechin-4-phloroglucinol | 3,5,7,3′,4′,5′ | 2*R*:3*S* | 13.61 |
| **VII** | (−)-Epicatechin-4-phloroglucinol | 3,5,7,3′,4′ | 2*R*:3*R* | 25.83 |
| **VIII** | (−)-Epigallocatechin-4-phloroglucinol | 3,5,7,3′,4′,5′ | 2*R*:3*R* | 16.74 |

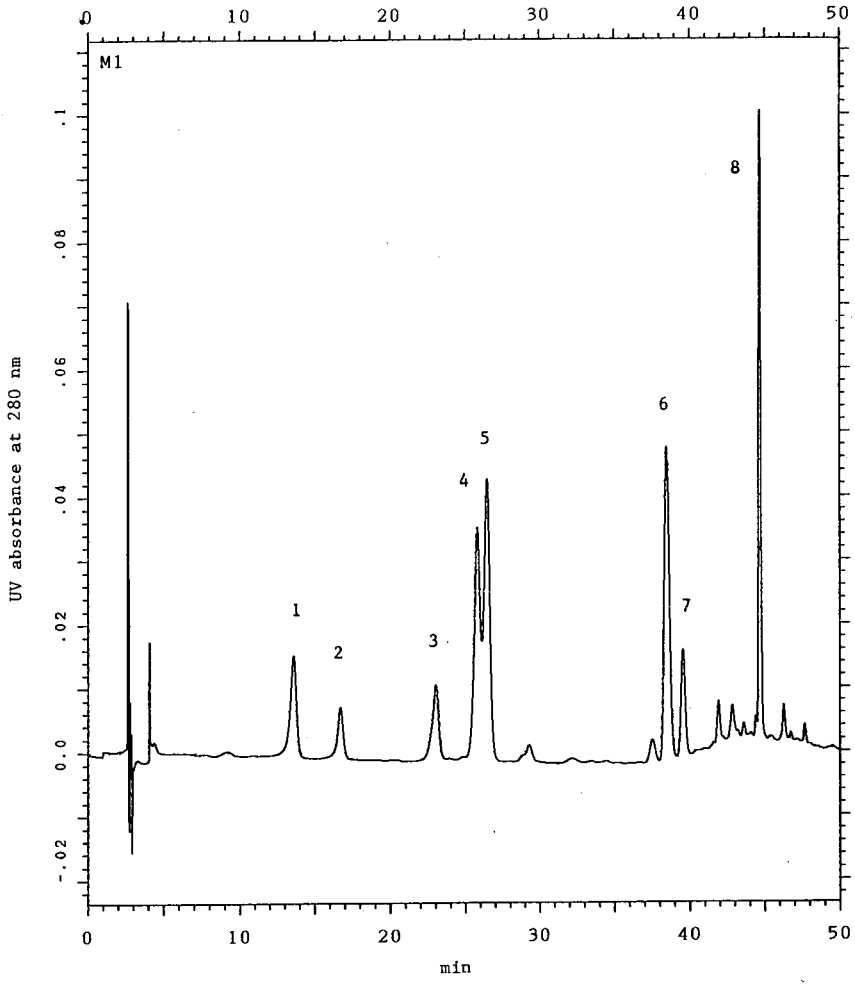


Fig. 2. HPLC of a standard mixture of flavan-3-ols and their phloroglucinol adducts using a LiChrospher 100 RP-18 column (25 cm × 4 mm I.D., 5 μm) at a flow-rate of 1 ml $min^{-1}$. For the elution system see Experimental. Peaks: 1 = (+)-gallocatechin-4-phloroglucinol; 2 = (−)-epigallocatechin-4-phloroglucinol; 3 = (+)-gallocatechin; 4 = (−)-epicatechin-4-phloroglucinol; 5 = (+)-catechin-4-phloroglucinol; 6 = (−)-epigallocatechin; 7 = (+)-catechin; 8 = (−)-epicatechin.

achieved (Fig. 2). Since the structures of these two compounds (**V** and **VII**) differ only in the stereochemistry at C-3, a better separation may be obtained using a chiral HPLC column [24]. As a general rule, the substitution pattern of the B-ring is an important factor in the elution order of these compounds.

The retention times of the compounds with three hydroxyl groups on the B-ring (*i.e.* compounds with pyrogallol group) are shorter than those of the corresponding compounds with two hydroxyl groups (*i.e.* compounds with cathechol group). Thus the elution order for flavan-3-ols is: (+)-gallocatechin (**II**) < (−)-epigallocatechin (**IV**) < (+)-catechin (**I**) < (−)-epicatechin (**III**). This is true in the case of phloroglucinol adducts as well, since (+)-gallocatechin-4-phloroglucinol (**VI**, 13.61 min) and (−)-epigallocatechin-4-phloroglucinol (**VIII**, 16.74 min) are eluted before (−)-epicatechin-4-phloroglucinol (**VII**, 25.83 min) and (+)-catechin-4-phloroglucinol (**V**, 26.47 min). As expected, all the phloroglucinol adducts (compounds **V–VIII**) are eluted faster than their corresponding flavan-3-ols (compound **I–IV**). This can be attributed to the polarity of these compounds which is greater than the corresponding flavan-3-ols due to the substitution of a phlorogluci-

nol group at the C-4 positions resulting in the formation of stronger hydrogen bonds with the mobile phase. In addition to the substitution pattern of the B-ring and the polarity of the compounds, the stereochemistry at the C-3 (*i.e.* the stereochemical position of the OH group at this position) also influences the elution order. For example, (+)-catechin (**I**) with 2*R*:3*S* configuration has a shorter retention time than (−)-epicatechin (**III**) with 2*R*:3*R* configuration (39.56 min and 44.68 min, respectively). In the same way, (+)-gallocatechin, **II** (2*R*:3*S*) eluted before (−)-epigallocatechin, **IV** (2*R*:3*R*) at the retention times of 23.06 min and 38.49 min, respectively.

Identification of the constituent flavanoid units in sainfoin proanthocyanidins was carried out by degradation of these compounds using acid hydrolysis in the presence of phloroglucinol. Degradation of these compounds with acids in the presence of various nucleophiles is a well known method since the stereochemistry at C-2 and C-3 positions is preserved [16]. Although acid-catalyzed thiolysis has been used by many workers [22,25,26], it requires a long procedure and has an offensive odour. However, the use of phloroglucinol as the nucleophile is more convenient and offers a better separation of the degradation products when using different chromatographic systems [16]. The results obtained

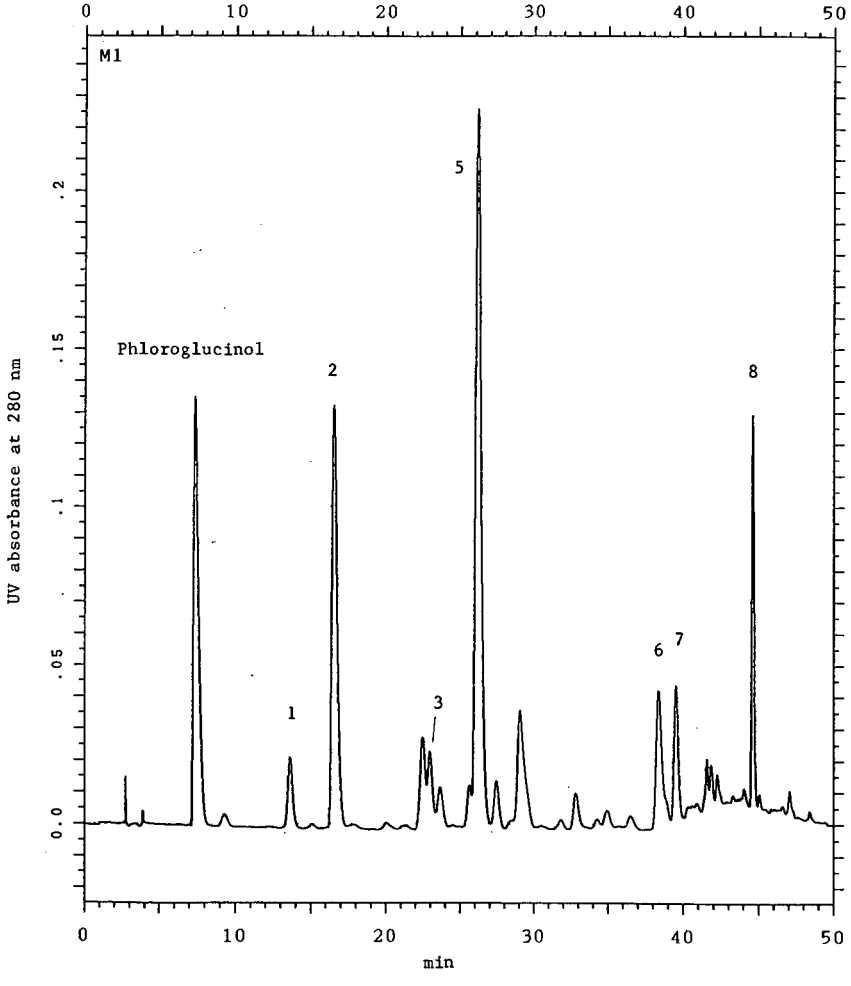


Fig. 3. HPLC of the degradation products of sainfoin leaf proanthocyanidins. HPLC conditions and peak identification as for Fig. 2.

from the time course studies of sainfoin proanthocyanidin hydrolysis in present work indicated that a total of 2 h time was sufficient for the completion of hydrolysis.

The flavan-3-ols and their phloroglucinol adducts discussed below were identified by the comparison of their retention times and in some cases UV spectra with those of authentic standards. Analysis of the degradation products of sainfoin leaf proanthocyanidins by RP-HPLC, showed that (+)-catechin (**I**), (+)-gallocatechin (**II**), (−)-epicatechin (**III**), (−)-epigallocatechin (**IV**) and (+)-catechin-, (+)-gallocatechin- and (−)-epigallocatechin-4-phloroglucinol adducts (compounds **V**, **VI** and **VIII**, respectively) are present in sainfoin sample (Fig. 3). The extension and terminal units in sainfoin proanthocyanidins, therefore, are catechin, gallocatechin, and epigallocatechin, while epicatechin appears to be terminal unit only.

The ethyl acetate-soluble fraction of sainfoin leaves (see Experimental) was also tested for the detection of any low molecular weight proanthocyanidins (dimers and trimers) and/or flavan-3-ols, if present. This sample was applied to a LH-20 column and eluted with ethanol and ethanol–acetone (19:1, v/v) which yielded six fractions. All the fractions were monitored by 2D-TLC [3,16] of which fractions 5 and 6 showed four and two purple spots, respectively indicating the presence of flavan-3-ols or low-molecular-weight proanthocyanidins. Application of the HPLC method proposed in this paper, showed that the major component in fraction 5 was (−)-epicatechin (**III**) while traces of (+)-catechin (**I**), (+)-gallocatechin (**II**) and (−)-epigallocatechin (**IV**) were also detected. Two purple spots in the 2D-TLC of fraction 6 were tentatively identified as (−)-epigallocatechin (**IV**) and a dimer by comparison with data from literature [3,16]. Isolation and purification of these two compounds by preparative HPLC and further analysis, confirmed the result obtained from 2D-TLC that one of the compounds is (−)-epigallocatechin (**IV**). Degradation of the dimer followed by HPLC analysis showed only two peaks in the chromatogram. Comparison of the retention times of these peaks with those of standards (Table I) showed that they are (−)-epicatechin (**III**) and its phloroglucinol adduct (**VII**). These results indicate that the dimer could be (−)-epicatechin-(4$\beta$-8)-epicatechin (**IX**) as the extension and terminal units are both epicatechin.

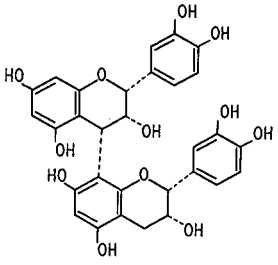


(IX)

RP-HPLC analysis of the degradation products of proanthocyanidins offers an attractive method for the rapid and sensitive separation and identification of structural units in these compounds. The adoption of this technique provides greater resolution, better sensitivity than other chromatographic methods and requires only a small amount of the proanthocyanidins. This method is currently being used for the structural and biosynthetic studies of sainfoin leaf proanthocyanidins in our laboratory.

ACKNOWLEDGEMENTS

This research was supported by a Strategic Grant from the Natural Sciences and Engineering Research Council (Canada). We would like to thank the Forage Section in Agriculture Canada (Saskatoon) and L. Y. Foo (DSIR, New Zealand) for the gift of samples.

REFERENCES

1 K. Weinges, *Phytochemistry*, 3 (1964) 263.
2 R. S. Thompson, D. Jacques, E. Haslam and R. J. N. Tanner, *J. Chem. Soc., Perkin Trans. 1*, (1972) 1387.
3 L. J. Porter, in P. M. Dey and J. B. Harborne (Editors), *Methods in Plant Biochemistry*, Vol. 1, Academic Press, London, 1989, p. 389.
4 N. G. Lewis and E. Yamamoto, in R. W. Hemingway and J. J. Karchesy (Editors), *Chemistry and Significance of Condensed Tannins*, Plenum Press, New York, 1989, p. 23.
5 Z. Czochanska, L. Y. Foo, R. H. Newman and L. J. Porter, *J. Chem. Soc., Perkin Trans. 1*, (1980) 2278.
6 R. W. Hemingway, in R. W. Hemingway and J. J. Karchesy (Editors), *Chemistry and Significance of Condensed Tannins*, Plenum Press, New York, 1989, p. 83.
7 L. J. Porter, in J. B. Harborne (Editor), *The Flavonoids—Advances in Research Since 1980*, Chapman & Hall, London, 1988, p. 21.
8 H. A. Stafford and H. L. Lester, *Plant Physiol.*, 66 (1980) 1085.

9 T. Swain, in G. A. Rothenthal and D. H. Jaryen (Editors), *Herbivores and Their Interaction With Secondary Plant Metabolites, Tannins and Lignins*, Academic Press, New York, 1979.
10 J. R. Ramirez-Martinez, A. Levi, H. Padua and A. Bakal, *J. Food Sci.*, 42 (1977) 1201.
11 A. G. H. Lea and G. M. Arnold, *J. Sci. Food Agric.*, 29 (1978) 478.
12 J. A. Delcour and G. M. Tuytens, *J. Inst. Brew.*, 90 (1984) 153.
13 T. N. Barry and T. R. Manley, *J. Sci. Food Agric.*, 37 (1986) 248.
14 W. T. Jones and J. L. Mangan, *J. Sci. Food Agric.*, 28 (1977) 126.
15 W. T. Jones and J. W. Lyttleton, *N. Z. J. Agric. Res.*, 14 (1971) 101.
16 R. W. Hemingway, in R. W. Hemingway and J. J. Karchesy (Editors), *Chemistry And Significance of Condensed Tannins*, Plenum Press, New York, 1989, p. 265.
17 S. Morimoto, G. I. Nonaka and I. Nishioka, *Chem. Pharm. Bull.*, 34 (1986) 633.
18 R. W. Hemingway and G. M. McGraw, *J. Wood Chem. Technol.*, 3 (1983) 421.
19 A. G. H. Lea, P. Bridle, C. F. Timberlake and V. L. Singleton, *Am. J. Enol. Vitic.*, 30 (1979) 289.
20 L. J. Porter, R. H. Newman, L. Y. Foo, H. Wong and R. W. Hemingway, *J. Chem. Soc., Perkin Trans. 1*, (1982) 1217.
21 R. H. Newman, L. J. Porter, L. Y. Foo, S. R. Jones and R. I. Willing, *Mag. Res. Chem.*, 25 (1987) 118.
22 Y. Cai, F. J. Evans, M. F. Roberts, J. D. Phillipson, M. H. Zenk and Y. Y. Gleba, *Phytochemistry*, 30 (1991) 2033.
23 L. Y. Foo and L. J. Porter, *J. Chem. Soc., Perkin Trans. 1*, (1978) 1186.
24 T. Ozawa and A. Okamoto, *Bull. Soc. Group Polyphenols*, 14 (1988) 134.
25 M. J. Betts, B. R. Brown, P. E. Brown and W. T. Pike, *J. Chem. Soc., Chem. Commun.*, (1967) 1110.
26 R. W. Hemingway, L. Y. Foo and L. J. Porter, *J. Chem. Soc., Perkin Trans. 1*, (1982) 1209.

*Journal of Chromatography*, 594 (1992) 125–130
Elsevier Science Publishers B.V., Amsterdam

CHROM. 23 858

# Chromatographic separation of polyols by ligand exchange

# Effects of the ion-exchange resin cross-linking and size

H. Caruel, P. Phemius, L. Rigal* and A. Gaset

*Laboratoire de Chimie des Agroressources, École Nationale Supérieure de Chimie de Toulouse, 118 Route de Narbonne, 31077 Toulouse Cedex (France)*

(First received July 16th, 1991; revised manuscript received November 7th, 1991)

ABSTRACT

The influence of the degree of ion-exchange resin cross-linking and size on the resolution and purity of products separated by ligand-exchange liquid chromatography was studied with mannitol–sorbitol and arabitol–xylitol mixtures. The experiment was carried out with seven calcium resins. The best results (90% recovery of pure mannitol and sorbitol and 80% recovery of pure arabitol and xylitol) were obtained with an average size of 25 μm and 7% cross-linking.

## INTRODUCTION

Extraction by water diffusion, hydrolysis or pressing of plant materials produces sugar mixtures. Catalytic [1] or enzymatic [2] hydrogenation of these mixtures yields polyol mixtures. Chromatography using cation-exchange resins and water as the eluent makes it possible to separate different components of these mixtures and therefore, favours their utilization. The separations depend on the complex-formation equilibria between carbohydrates and the resin counter-ions. In this case chromatography is called ligand exchange. Many works deal with this topic, such as those by Angyal *et al.* [3] and Goulding [4]. Apart from the chemical equilibria involved in the formation of sugar–cation complexes, for which the choice of the resin counter-ion is important [5], many parameters influence the efficiency of a chromatographic separation:

(i) The accessibility of the resin sites for ligand exchange. This depends on the pore size of the support. In the case of gel ion-exchange resins, accessibility will depend on the degree of cross-linking of the polymer matrix expressed as a weight percentage of divinylbenzene (DVB).

(ii) The dispersion of molecules to be separated in relation to the path differences in the chromatographic column. The dispersion depends on how the column is packed and on the particle size.

In order to optimize the chromatographic separation of two industrial mixtures on a ion-exchange resin in the calcium form, the influence of the degree of cross-linking and size of the support were studied. The two mixtures tested were:

Mannitol–sorbitol obtained from the catalytic hydrogenation of fructose [6],

Arabitol–xylitol obtained from the hydrogenation of fibre plant hydrolysates [7].

Although various models have been used to predict the effects of different factors (dispersion in the eluting phase, external resistance to mass transfer around particles, internal diffusion in the stationary phase) [8–10], none presents a direct and simple correlation with the support characteristics.

0021-9673/92/$05.00 

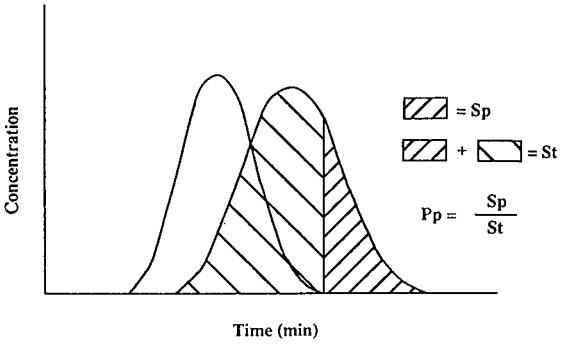


Fig. 1. Definition of recoverable pure product.

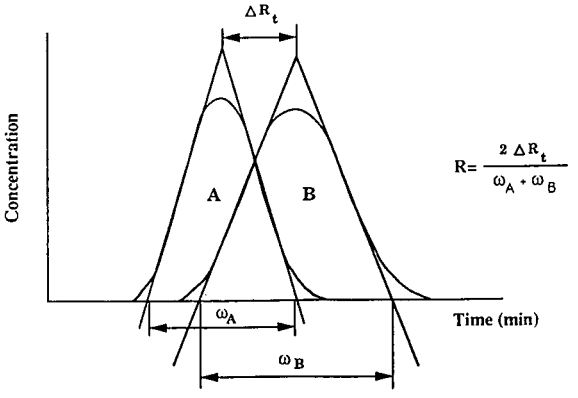


Fig. 2. Definition of resolution.

The experimental design set-up allows the determination of a polynomial correlation involving reticulation, resin average size and separation efficiency. This efficiency is controlled through yields of recovered pure products, $P_p$ (Fig. 1), and resolution, $R$ (Fig. 2).

## EXPERIMENTAL

A 200 cm × 1.67 cm I.D. glass column maintained at 50°C by fluid circulation in the jacket was packed with calcium Purolite resin (PCR) a chosen size and degree of cross-linking by progressive water sedimentation. The characteristics of the gel resins are shown in Table I. Products used to reconstitute polyol mixtures to be separated were commercial products from Fluka (mannitol, xylitol), Aldrich (sorbitol) and Extrasynthese (arabitol). Mixtures were recombined in deionized water (resistivity above 10 MΩ cm). The concentration of each constituent of the mixture was 50 g/l. A 1.5-cm$^3$ volume of the solution to be separated was directly injected onto the resins at the top of the column. To prevent the injected solution from being diluted, water elution was only started when the total solution had penetrated the resin. A Gilson Minipul se 2 peristaltic pump fed the system with eluent (deionized water) at 50°C. A Gilson MTDC automa tic fraction collector recovered the effluent at the column outlet. At the end of the separation, the collected fractions were analysed by high performan ce liquid chromatography (HPLC) on an LDC Milton Roy III device coupled with a refractometric detector equipped with a data base. These analyses made it possible to draw the chromatogram for the separation obtained at the column outlet.

TABLE I

CHARACTERISTICS OF GEL RESINS

| PCR | DVB (%) | Total capacity (equiv./l $H^+$) | Humidity (% $H^+$) | Particle size ($\mu$m) | |
|---|---|---|---|---|---|
| | | | | Mean | Range (90%) |
| 833 | 7.6 | 1.80 | 51–55 | 225 ± 25 | 150–300 |
| 853 | 7.6 | 1.55 | 57–61 | 350 ± 25 | 275–425 |
| 453 | 4.7 | 1.20 | 64–67 | 350 ± 25 | 275–425 |
| 433 | 4.7 | 1.55 | 57–61 | 225 ± 25 | 150–300 |
| 593 | 5.9 | 1.20 | 64–67 | 525 ± 25 | 150–300 |
| 533 | 5.9 | 1.80 | 51–55 | 225 ± 25 | 275–425 |
| 553 | 5.9 | 1.55 | 57–61 | 350 ± 25 | 450–600 |

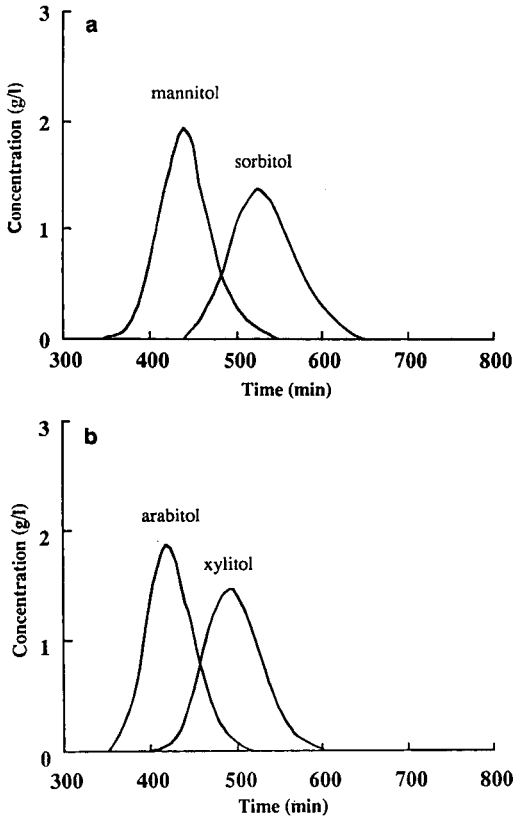


Fig. 3. (a) Separation of mannitol–sorbitol on PCR 593 Ca. Flow-rate: 0.95 ml/min. (b) Separation of arabitol–xylitol on PCR 593 Ca. Flow-rate: 1.0 ml/min.

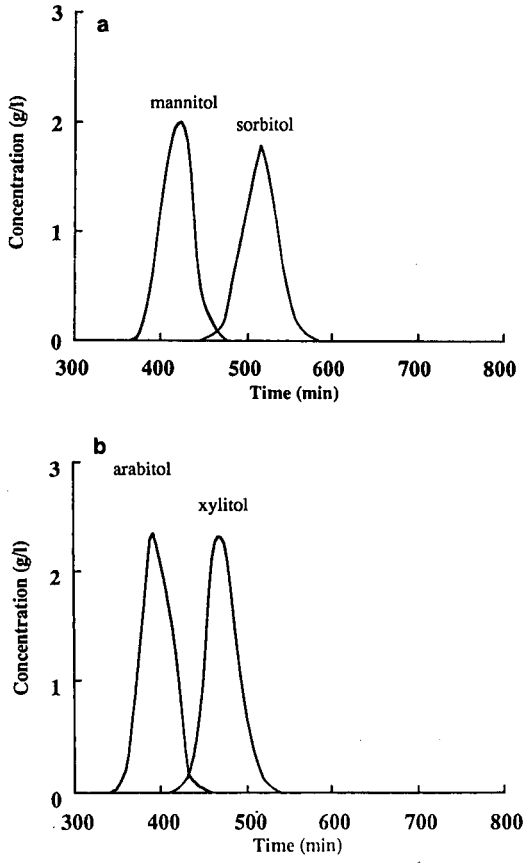


Fig. 4. (a) Separation of mannitol–sorbitol on PCR 533 Ca. Flow-rate: 1.0 ml/min. (b) Separation of arabitol–xylitol on PCR 533 Ca. Flow-rate: 1.0 ml/min.

TABLE II

EXPERIMENTAL RESULTS OF THE TWO STUDIED RESPONSES

| PCR | [a] $R_{MOH-SOH}$ | [b] $R_{XOH-AOH}$ | [c] $P_{p\,MOH}$ (%) | [d] $P_{p\,SOH}$ (%) | [e] $P_{p\,AOH}$ (%) | [f] $P_{p\,XOH}$ (%) |
|---|---|---|---|---|---|---|
| 833 | 1.01 | 1.00 | 94 | 82 | 83 | 75 |
| 853 | 0.78 | 0.68 | 24 | 28 | 20 | 28 |
| 453 | 1.09 | 0.93 | 75 | 43 | 54 | 34 |
| 433 | 0.73 | 0.47 | 46 | 42 | 21 | 22 |
| 593 | 0.67 | 0.60 | 11 | 31 | 22 | 20 |
| 533 | 1.30 | 1.05 | 91 | 87 | 69 | 72 |
| 553 | 0.85 | 0.69 | 58 | 63 | 41 | 64 |

[a] Resolution of mannitol–sorbitol separation.
[b] Resolution of arabitol–xylitol separation.
[c] Pure mannitol recoverable.
[d] Pure sorbitol recoverable.
[e] Pure arabitol recoverable.
[f] Pure xylitol recoverable.

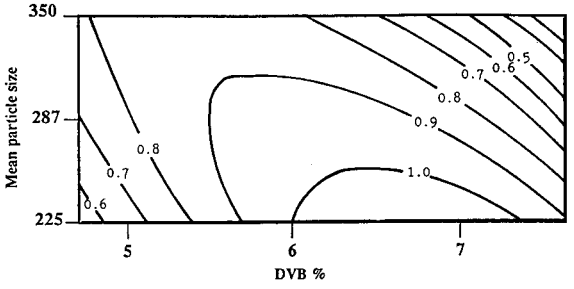


Fig. 5. Isoresponse curves of the resolution of mannitol–sorbitol separation as a function of degree of cross-linking and resin particle size (in $\mu$m).

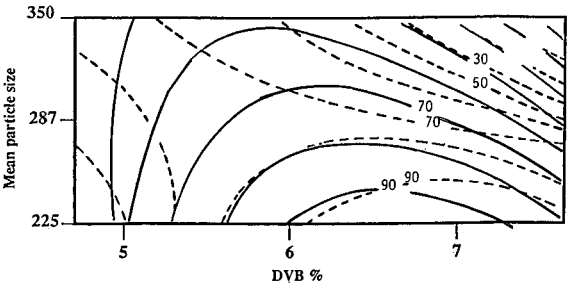


Fig. 7. Isoresponse curves of pure mannitol (broken lines) and sorbitol (solid lines) yield. Mean particle size in $\mu$m.

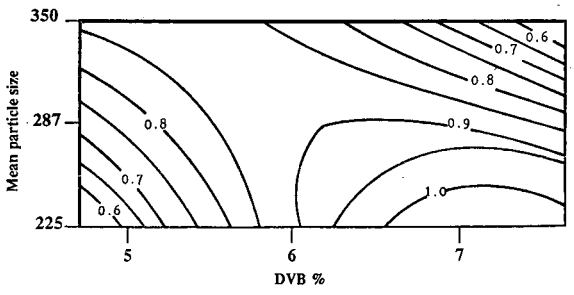


Fig. 6. Isoresponse curves of the resolution of arabitol–xylitol separation as a function of degree of cross-linking and resin particle size (in $\mu$m).

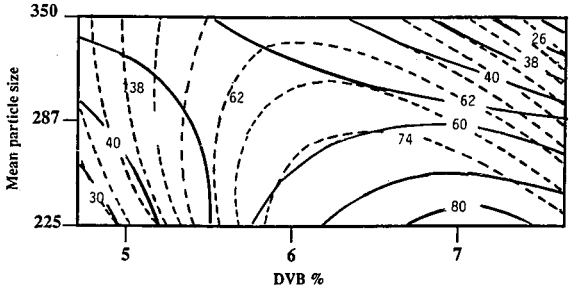


Fig. 8. Isoresponse curves of pure arabitol (solid lines) and xylitol (broken lines) yield. Mean particle size in $\mu$m.

## RESULTS AND DISCUSSION

Separation chromatograms (Figs. 3 and 4) obtained with each resin allow calculation of the two responses studied (Table II). The analysis of isoresponse curves, drawn by calculating coefficients of the second-degree polynomial model [11], indicates that:

(i) With a degree of cross-linking averaging 5%, an increase in the resin size favours resolution (Figs. 5, 6) and higher yields of pure products. This has been already noted in the separation of glucose–fructose with the same type of resins [12].

(ii) With high degrees of cross-linking (>6% DVB), a decrease in the resin size favours resolution. Such results have already been noted in xylose–mannose separations [13] using Duolite resins C 204 in the $Pb^{2+}$ form with a 5.5–6.5% DVB cross-linking. The best yields of pure products, 90% mannitol and sorbitol and 80% arabitol and xylitol, were achieved with a degree of cross-linking averaging 7 DVB and an average size of 225 $\mu$m (Figs. 7 and 8).

These results show how complex is the effect of cross-linking on the phenomena involved in a separation.

An increase in the degree of cross-linking results in an increase in the capacity of the chromatographic column. This should lead to an improvement in capacity factors ($k'$) and, therefore, a better separation. However, after calculating $k'$, no systematic correlation could be determined (Figs. 9 and 10). Indeed, increased in cross-linking corresponds to decreased humidity, which leads to reduced resin swelling. Penetration of molecules to be separated inside the resin, towards complexing sites, is then favoured. Likewise, depending on the nature of the molecules and cross-linking, this restriction could be more or less important than the positive effect of an increase in capacity.

Models reported up until now do not take into account variations in the resin swelling during the passage of substrate. Variations in the height of the

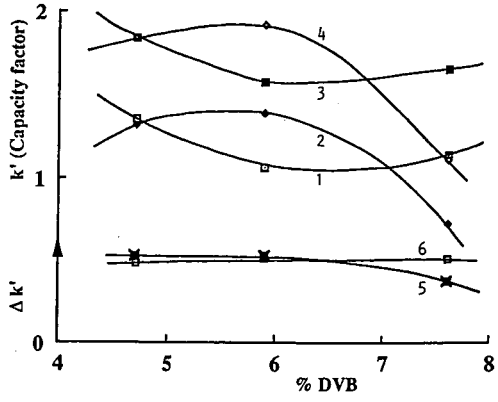


Fig. 9. Influence of the degree of cross-linking on the capacity factor of mannitol and sorbitol. Curves: 1 = $k'$ mannitol 350; 2 = $k'$ mannitol 225; 3 = $k'$ sorbitol 350; 4 = $k'$ sorbitol 225; 5 = $\Delta k'$ sorbitol − manitol 225; 6 = $\Delta k'$ sorbitol − mannitol 350. The values 350 and 225 indicate the mean particle size ($\mu$m) (Table I).

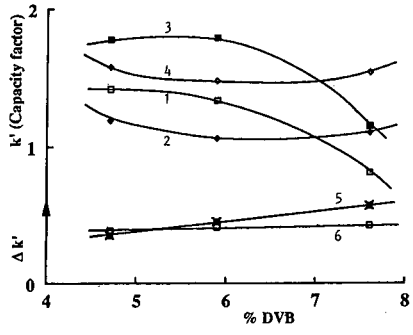


Fig. 10. Influence of the degree of cross-linking on the capacity factor of arabitol and xylitol. Curves: 1 = $k'$ arabitol 225; 2 = $k'$ arabitol 350; 3 = $k'$ xylitol 225; 4 = $k'$ xylitol 350; 5 = $\Delta k'$ xylitol − arabitol 225; 6 = $\Delta k'$ xylitol − arabitol 350. The values 350 and 225 indicate the mean particle size ($\mu$m) (Table I).

chromatographic column bed have been experimentally observed. These variations may be responsible for the larger dispersion, resulting in peak widening and a lower resolution.

The positive effect of an increase in degree of cross-linking could be explained by a lower sensitivity of the resin towards swelling phenomena.

## CONCLUSIONS

It is clear that the effect of the degree of cross-linking is hard to determine. Indeed, its increase leads to:

(i) A higher capacity through a larger number of complex sites on an equally sized column.

(ii) A restricted dispersion of molecules to be separated through a lower swelling sensitivity when substrates pass down the columns.

However these two positive effects are restricted by the diffusion of molecules into the resin.

The influence of the resin size seems to be linked to that of the degree of cross-linking since isoresponse curves indicate that there are two opposite ways of improving separation.

According to these results and those of Welstein and Sauer [12], the selection of the support characteristics should depend on yield and purity of expected products. In the case of polyols, a small-sized resin (225 $\mu$m) with 7% DVB should be selected, whereas a larger sized resin (about 400 $\mu$m) with a 6% DVB cross-linking should be used to separate glucose–fructose mixtures.

TABLE III

CAPACITY FACTORS ($k'$) FOR THE DIFFERENT COMPONENTS SEPARATED ON PUROLITE RESINS ELUTING WITH WATER

| PCR | DVB | Particle | $k'$ arabitol | $k'$ xylitol | $\Delta k'_1$ | $k'$ mannitol | $k'$ sorbitol | $\Delta k'_2$ |
|---|---|---|---|---|---|---|---|---|
| 833 | 7.6 | 225 | 1.32 | 1.90 | 0.58 | 0.73 | 1.11 | 0.38 |
| 853 | 7.6 | 350 | 1.11 | 1.55 | 0.44 | 1.14 | 1.66 | 0.52 |
| 453 | 4.7 | 350 | 1.19 | 1.58 | 0.39 | 1.35 | 1.84 | 0.49 |
| 433 | 4.7 | 225 | 1.42 | 1.78 | 0.36 | 1.31 | 1.84 | 0.53 |
| 593 | 5.9 | 525 | 1.40 | 1.84 | 0.44 | 1.38 | 1.89 | 0.51 |
| 551 | 5.9 | 350 | 1.15 | 1.59 | 0.44 | 1.38 | 1.92 | 0.54 |
| 553 | 5.9 | 350 | 1.06 | 1.48 | 0.42 | 1.06 | 1.58 | 0.52 |
| 533 | 5.9 | 225 | 1.34 | 1.80 | 0.46 | 1.39 | 1.92 | 0.53 |

ACKNOWLEDGEMENTS

The authors acknowledge the Purolite International (France) Company for providing samples of ion-exchange resins and the Applexion Company (France) for their collaboration.

REFERENCES

1 G. M. Jaffe, W. Szkrybalo and H. Weinert, *U.S. Pat.*, 3 784 408 (1974).
2 S. Nagai, N. Nishio, M. Mayashi and K. Ikeda, *Jpn. Pat.*, 62/104588 (1987).
3 S. J. Angyal, G. S. Bethell and R. J. Beveridge, *Carbohydr. Res.*, 73 (1979) 9–18.
4 R. W. Goulding, *J. Chromatogr.*, 103 (1975) 229–239.
5 H. Caruel, L. Rigal and A. Gaset, *J. Chromatogr.*, 558 (1991) 89.
6 A. P. G. Kieboom and H. Van Bekkum, *Starch Conversion Technology*, Marcel Dekker, New York, 1985, pp. 278–280.
7 M. L. Dupuy and P. Strehaiano, *Eur. Pat.*, 89 00209 (1989).
8 A. M. Wilhelm, G. Casamatta, T. Carillon, L. Rigal and A. Gaset, *Bioprocess Eng.*, 4 (1989) 147–151.
9 V. Viard and M. L. Lameloise, *2nd French Congress on Process Engineering, Toulouse, France, September 5–7, 1989*, Vol. 3, No. 8.
10 E. Suwondo, A. M. Wilhelm, L. Pibouleau and S. Domenech, presented at the *5th Mediterranean Congress on Chemical Engineering, Barcelona, Spain, November, 5–7, 1990.*
11 D. Mathieu, R. Phan Tan Luu, *Software N.E.M.R.O.D., L.P.R.A.I.*, Aix Marseille University, 1982.
12 H. Welstein and C. Sauer, in D. Naden and M. Streat (Editors), *Ion Exchange Technology*, Horwood, Chichester, 1984, pp. 463–471.
13 T. Carillon, *Ph.D. Thesis No. 423*, INP Toulouse, Toulouse, 1987.

*Journal of Chromatography*, 594 (1992) 131–135
Elsevier Science Publishers B.V., Amsterdam

CHROM. 23 841

# Determination of the norlignan glucosides of Hypoxidaceae by high-performance liquid chromatography

P. Betto*, R. Gabriele and C. Galeffi

*Istituto Superiore di Sanita', Viale Regina Elena 299, 00161 Rome (Italy)*

(First received August 12th, 1991; revised manuscript received October 31st, 1991)

ABSTRACT

A reversed-phase high-performance liquid chromatography system with UV detection is proposed for the qualitative and quantitative determination of norlignan glucosides isolated from some African Hypoxidaceae used in traditional medicine and, more recently, for pharmaceutical preparations. The analysis indicated the occurrence of these compounds, the aglucones of which are characterized by the rare $C_6H_5$–$C_5$–$C_6H_5$ skeleton type, in other Hypoxidaceae of different geographical origin.

## INTRODUCTION

Hypoxidaceae were first considered as distinct from Amaryllidaceae in 1814 [1] and after some hesitation were eventually identified as a separate family in 1964 [2]. The family includes many genera such as *Hypoxis, Curculigo, Pauridia, Molinera, Spiloxene, Empodium, Rhodohypoxis, Campynema* and *Capynemanthe*, which are found in the southern hemisphere and in southern Africa in particular. According to the tradition of the local medicine, the rhizomes of the genus *Hypoxis* are prescribed for prostatic hypertrophy and internal cancer [3]. The former indication, for which a phytopharmaceutical is marketed in Germany [4], has been associated with chemically non-defined steroid glucosides, whereas the latter (structures presented in Fig. 1) is related to glucosides of unsaturated aglucones which, on the basis of structural evidence and biogenetic considerations, can be considered as norlignans. These compounds have the rare skeleton type $C_6H_5$–$C_5$–$C_6H_5$, 1,3- or 1,5-diphenylpentane. To the latter series belong the first diglucoside isolated, hypoxoside, **1** [5], the two monoglucosides of its aglucone, rooperol (**2**),obtuside A (**3**) and obtuside B (**4**) [6], isolated from *Hypoxis obtusa* of Mozambique, and nyasicoside (**5**), isolated from *Hypoxis nyasica* of Malawi [7] and *Curculigo recurvata* of Zaire [8]. Interjectin (**6**), a complex diglucoside of nyasicol, the aglucone of nyasicoside, has recently been isolated from *Hypoxis interjecta* and *Hypoxis multiceps* of South Africa [9]. Two other glucosides, curculigine and hypoxine, isolated from *Curculigo recurvata* and *Hyposix obtusa,* respectively, from Mozambique are currently under study.

Nyasoside (**7**) [3], the two monoglucosides of its aglucone, mononyasine A (**8**) and mononyasine B (**9**) [10] and the triglucoside nyaside (**10**) [11], isolated with hypoxoside and nyasicoside from *Hypoxis nyasica* of Malawi belong to the 1,3-diphenylpentane series. The aglucone of nyasoside, nyasol (**11**), was isolated from *Hypoxis angustifolia* from Zimbabwe [12].

As a result of the promising cytotoxic and antitumour activities of these compounds, some of which have been patented [13,14], research on the *in vitro* propagation of rhizomes and unopened flower buds is in progress [15,16]; the seeds are not capable of vegetal propagation.

The two main glucosides, hypoxoside and nyaso-

0021-9673/92/$05.00 

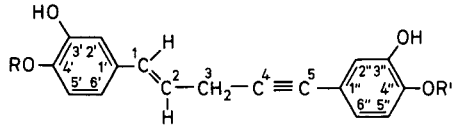

| | R | R' | |
|---|---|---|---|
| 1 | Gl | Gl | hypoxoside |
| 2 | H | H | rooperol |
| 3 | Gl | H | obtuside A |
| 4 | H | Gl | obtuside B |

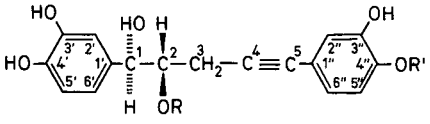

| | R | R' | |
|---|---|---|---|
| 5 | Gl | H | nyasicoside |
| 6 | p-hydroxycinnamoyl →2-Gl | Gl | interjectin |

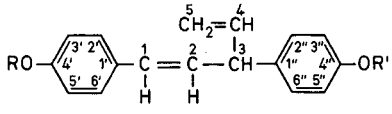

| | R | R' | |
|---|---|---|---|
| 7 | Gl | Gl | nyasoside |
| 8 | H | Gl | mononyasine A |
| 9 | Gl | H | mononyasine B |
| 10 | Gl | Ap→6-Gl | nyaside |
| 11 | H | H | nyasol |

Fig. 1. Structures of nortignan glucosides of nypoxidaceae.

side, can be separated with difficulty by countercurrent distribution, thin-layer chromatography [3] and by high-performance liquid chromatography (HPLC) [16]. The method proposed here can separate all known glucosides except the isomer monoglucosides **3**, **4**, **8** and **9**, using a reversed-phase column with an acidic eluent (pH 3.0). It is useful for monitoring production in tissue cultures and for establishing the presence of these norlignan glucosides, which can be of taxonomical relevance for the genus *Hypoxis* and other genera of Hypoxidaceae.

## EXPERIMENTAL

### *Plant material*

The samples examined were: rhizomes of *Hypoxis obtusa* Burch from Maputo (Mozambique); rhizomes of *Hypoxis obtusa* Burch-complex supplied by Dr. S. Sibanda, Harare (Zimbabwe) and by Dr. E. Nyandat, Nairobi (Kenya); rhizomes of *Hypoxis angustifolia* Lam. supplied by Dr. P. Rasoanaivo, Antananarivo (Madagascar) and by Dr. S. Sibanda, Harare (Zimbabwe); rhizomes of *Hypoxis dubumbens* Lin. supplied by Dr. A. Chiappeta, Pernanbuco (Brazil); rhizomes of *Hypoxis nyasica* Bak. supplied by Professor J. D. Msonthi, Zomba (Malawi); rhizomes of *Hypoxis interjecta* Nel, Pretoria (South Africa), *Hypoxis multiceps* Buching ex Krauss, Pretoria (South Africa), *Hypoxis argentea*, Pretoria (South Africa) and *Campynema lineare*, Tasmania, obtained from Professor P. Raven (Director of the Missouri Botanical Garden); and rhizomes and flowers of *Curculigo recurvata* Dryand obtained from Dr. Chifundera Kusamba (Zaire).

### *Reagents*

The chemicals used were of analytical reagent-grade. The acetonitrile used was of HPLC grade. Water was purified by a Milli-Q water purification system (Millipore, Bedford, MA, USA).

TABLE I

RETENTION TIMES AND CAPACITY FACTORS

| Compound | Retention time (min) | Capacity factor |
|---|---|---|
| Curculigine | 13.28 | 2.30 |
| **5** | 14.43 | 2.58 |
| Hypoxine | 18.02 | 3.44 |
| **6** | 18.57 | 3.61 |
| **1** | 22.37 | 4.55 |
| **10** | 22.98 | 4.70 |
| **7** | 23.96 | 4.96 |
| **3** and **4** | 25.12 | 5.24 |
| **2** | 27.97 | 5.94 |
| **8** and **9** | 29.67 | 6.36 |
| **11** | 35.62 | 7.84 |

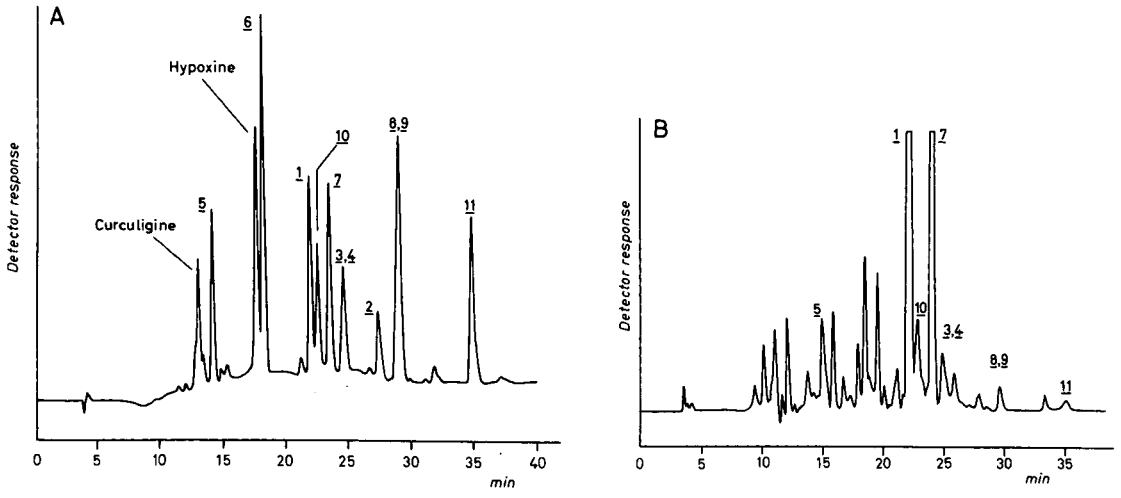


Fig. 2. (A) Chromatogram of a mixture of reference compounds. Peaks: curculigine; 5 = nyasicoside; hypoxine; 6 = interjectin; 1 = hypoxoside; 10 = nyaside; 7 = nyasoside; 3 = obtuside A; 4 = obtuside B; 2 = rooperol; 8 = mononyasine A; 9 = mononyasine B; 11 = nyasol. (B) Chromatogram of the methanol extract from *Hypoxis obtusa* rhizomes of Zimbabwe. The chromatographic conditions are given under Experimental.

*Instrumentation*

The HPLC analyses were performed on a Perkin-Elmer system (Norwalk, CT, USA) equipped with a Series 3 liquid chromatograph connected to an LC-75 spectrophotometric detector. The samples were introduced with an injection valve Rheodyne 7125 (Berkeley, CA, USA) with a 100-$\mu$l loop. Chromatograms were recorded on a Perkin-Elmer Sigma 10 B chromatography data station. The column was 250 × 4.6 mm I.D. (5 $\mu$m particle size) Spherisorb ODS-2 (Phase Separations, Queensferry, UK).

*High-performance liquid chromatography*

The separations were achieved using a linear gradient of acetonitrile (solvent A) and 0.05 *M* phosphate buffer at pH 3.0 (solvent B), increasing from 20% solvent A at time $t$ = 0 min to 70% solvent A at $t$ = 30 min with a constant flow-rate of 0.8 ml/min at room temperature. The eluent was monitored at 260 nm.

*Preparation of natural standards*

Hypoxoxide, nyasoside, obtusides A and B, mononyasines A and B, nyaside, nyasicoside, inter-

TABLE II

LINEARITY RESPONSE AS A FUNCTION OF CONCENTRATION

$y$ = peak area; $x$ = amount ($\mu$g per injection).

| Compound | Range tested ($\mu$g) | Regression equation | Correlation coefficient |
|---|---|---|---|
| **5** | 0.88–7.04 | $y = 1.182x - 0.263$ | 0.9989 |
| **6** | 0.30–4.80 | $y = 0.978x - 0.082$ | 0.9997 |
| **1** | 0.15–2.32 | $y = 4.732x - 0.078$ | 0.9998 |
| **10** | 0.60–9.60 | $y = 1.497x - 0.008$ | 0.9979 |
| **7** | 0.55–8.80 | $y = 1.312x - 0.018$ | 0.9996 |
| **3** and **4** | 0.90–14.40 | $y = 2.744x - 0.013$ | 0.9987 |
| **2** | 0.46–7.36 | $y = 2.499x - 0.037$ | 0.9993 |
| **8** and **9** | 0.17–2.72 | $y = 5.634x - 0.090$ | 0.9992 |
| **11** | 0.20–8.00 | $y = 1.786x - 0.025$ | 0.9997 |

TABLE III

QUALITATIVE AND QUANTITATIVE ANALYSIS OF THE METHANOLIC EXTRACTS

| Plant material | Country of origin | Concentration in dried plant material (g/100 g) | | | | | | | | | | |
|---|---|---|---|---|---|---|---|---|---|---|---|---|
| | | Curculigine | **5** | Hypoxine | **6** | **1** | **10** | **7** | **3** and **4** | **2** | **8** and **9** | **11** |
| *Hypoxis obtusa* complex rhizomes | Zimbabwe Kenya | – | 0.33 | – | – | 2.90 | 0.17 | 1.55 | 0.14 | – | 0.10 | 0.06 |
| *Hypoxis obtusa* rhizomes | Mozambique | – | – | 0.12 | – | 3.71 | – | – | 0.48 | – | – | – |
| *Hypoxis angustifolia* rhizomes | Zimbabwe | – | – | – | – | 0.07 | 0.09 | 1.56 | 0.01 | – | 0.12 | 0.03 |
| *Hypoxis angustifolia* rhizomes | Madagascar | – | 0.08 | – | – | – | – | – | – | – | – | |
| *Hypoxis decumbens* rhizomes | Brazil | – | 0.17 | – | – | – | 0.17 | – | – | – | – | – |
| *Curculigo recurvata* rhizomes | Zaire | 0.18 | 0.25 | – | – | – | – | – | – | – | – | – |
| *Curculigo recurvata* flowers | Zaire | 0.04 | 0.07 | – | – | – | – | – | – | – | – | – |
| *Hypoxis interjecta* rhizomes | South Africa | – | – | – | 0.45 | 4.37 | 0.22 | 0.26 | 0.19 | – | – | – |
| *Hypoxis multiceps* rhizomes | South Africa | – | – | – | 0.41 | 3.98 | 0.18 | 0.27 | 0.29 | – | – | – |
| *Hypoxis argentea* rhizomes | South Africa | – | – | – | 0.23 | – | – | – | – | – | – | – |
| *Campynema lineare* rhizomes | Tasmania | – | – | – | – | 0.91 | – | 0.46 | 0.32 | – | – | – |
| *Hypoxis nyasica* rhizomes | Malawi | – | 0.16 | – | – | 5.40 | 0.15 | 3.12 | 0.29 | – | 0.03 | – |

jectin, curculigine, hypoxine, rooperol and nyasol were obtained as described. Fig. 1 shows the chemical structures of compounds **1–11**. The purity of these compounds was tested by HPLC.

*Preparation of crude extracts*

The botanical material was homogenized and extracted with methanol for 24 h. After centrifugation and rinsing with methanol, the solvent was evaporated under vacuum at 40°C. A small aliquot of the residue was dissolved in methanol, passed through a Millipore filter and 2–10 $\mu$l of the solution were directly injected into the chromatographic system.

## RESULTS AND DISCUSSION

Table I gives the retention times and capacity factors of all the compounds isolated. The results show that the polarity, both as sugar units and as phenolic hydroxy groups, plays an important part in the determination of the retention times.

Fig. 2 gives the chromatograms of a standard solution containing all the tested compounds and of the extract of *Hypoxis obtusa* from Zimbabwe. The peak identification was performed on the basis of the chromatographic retention time and by the simultaneous injection of a standard.

To verify the linearity of the detector response, suitable amounts of the substances were weighed and dissolved in calibrated flasks. Measured volumes of the solutions were injected and chromatographed. The data were plotted to show the relationship between the amount injected and the corresponding peak area. The regression equations and their correlation coefficients are listed in Table II. The minimum limit of detection is 10 $\mu$g/g of plant material for hypoxoside, nyasoside, mononyasine A, mononyasine B and nyasol, and 30 $\mu$g/g of plant material for nyasicoside, nyaside, obtuside A, obtuside B and rooperol at a signal-to-noise ratio of 3. Repeated analyses of the methanol extract samples spiked with standards at three different concentrations gave within-assay relative standard deviations (R.S.D.) ranging from 3.5 to 8.3%. The between-assay R.S.D. ranged from 4.5 to 9.6%.

Table III gives the analytical results for the plant materials examined.

## REFERENCES


1 R. Brown, in Flinders, *A Voyage to Terra Australensis*, Vol. 2, 1814.
2 H. Melchior, *Engler's Syllabus der Pflanzenfamilien*, Vol. 2, Gebrüder Borntraeyr, Berlin, 12th ed., 1964, p. 531.
3 G. B. Marini-Bettolo, M. Nicoletti, I. Messana, C. Galeffi, J. D. Msonthi and W. A. Chapya, *Tetrahedron*, 41 (1985) 665.
4 V. E. Tyler, *Econ. Bot.*, 40 (1986) 279.
5 G. B. Marini-Bettolo, M. Patamia, M. Nicoletti, C. Galeffi and I. Messana, *Tetrahedron*, 38 (1982) 1683.
6 C. Galeffi, G. Multari, Y. De Vincente, I. Messana, M. Nicoletti and G. B. Marini-Bettolo, *Planta Med.*, 55 (1989) 318.
7 C. Galeffi, G. Multari, J. D. Msonthi, M. Nicoletti and G. B. Marini-Bettolo, *Tetrahedron*, 43 (1987) 3519.
8 K. Chifundera, I. Messana, C. Galeffi and Y. De Vincente, *Tetrahedron*, 47 (1991) 4369.
9 G. B. Marini-Bettolo, C. Galeffi, G. Multari, G. Palazzino and I. Messana, *Tetrahedron*, 47 (1991) 6717.
10 I. Messana, J. D. Msonthi, Y. De Vincente, G. Multari and C. Galeffi, *Phytochemistry*, 28 (1989) 2807.
11 C. Galeffi, Y. De Vincente, M. Nicoletti and G. B. Marini-Bettolo, *Gazz. Chim. Ital.* 119 (1989) 565.
12 S. Sibanda, O. Ntabeni, M. Nicoletti and C. Galeffi, *Biochem. Syst. Ecol.*, 18 (1990) 481.
13 S. Drewes and R. W. Liebenberg, *UK Pat Appl.*, GB 8211293, 2120650A (1982).
14 G. B. Marini-Bettolo, J. D. Msonthi, C. Galeffi, I. Messana and M. Nicoletti, *Ital. Pat. Appl.*, A/83 49561 (1983).
15 Y. M. Page and J. van Staden, *S. Afr. J. Bot.*, 52 (1986) 261.
16 P. Vinesi, M. Serafini, M. Nicoletti, L. Spano' and P. Betto, *J. Nat. Prod.*, 53 (1990) 196.

*Journal of Chromatography*, 594 (1992) 137–144
Elsevier Science Publishers B.V., Amsterdam

CHROM. 23 835

# High-performance liquid chromatography of okadaic acid and free fatty acids in mussels

Fabio Zonta*

*Istituto di Studi Aziendali, Università di Trento, Via Inama 1, 38100 Trento (Italy)*

Bruno Stancher, Paolo Bogoni and Paola Masotti

*Dipartimento di Economia e Merceologia delle Risorse Naturali e della produzione, Università di Trieste, Via Valerio 6, 34127 Trieste (Italy)*

(First received August 1st, 1991; revised manuscript received October 30th, 1991)

ABSTRACT

A high-performance liquid chromatographic method developed for the determination of both okadaic acid (OA) and free fatty acids (FFA) was used for analysing mussel samples collected in the Gulf of Trieste. OA and FFA extracted from mussel hepatopancreas were derivatized prior to their chromatographic separation and spectrofluorimetric detection. 9-Chloromethylanthracene (CA) was used as a fluorescent labelling agent. The presence of toxic fatty acids (*e.g.*, linolenic acid), which may interfere with the bioassay of diarrhoetic shellfish poisoning (DSP) toxins, in the lipidic fraction of the extract was observed, whereas no OA was detected in the analysed samples.

## INTRODUCTION

Diarrhoetic shellfish poisoning (DSP) toxins were recognized for the first time as human pathogenic agents in Japanese seafood by Yasumoto *et al.* in 1978 [1]. Further research led to the elucidation of the structural formulae of the toxins, which are mainly constituted by okadaic acid (OA) and its derivatives [2–4], to the development of biological [1,5] and high-performance liquid chromatographic (HPLC) [6] methods of analysis and to the understanding of the toxicological and tumour-promoting activities of DSP toxins [7,8].

During 1989 and 1990, mussels farmed in the Adriatic Sea appeared to be contaminated (for long periods, related to algal blooms) by DSP toxins; as a consequence, the Italian hygiene authorities prohibited the sale of mussels, with severe economic consequences for the fishing industry [9].

In Italy, the official method of analysis for DSP toxins has been modified several times; currently a mouse bioassay test based on that developed by Yasumoto *et al.* [1], but with a modified threshold limit, is used [10]. The inter-laboratory repeatability of this biological method is very poor [11]. Further, in a previous paper, Lee *et al.* [6] pointed out the disadvantages of the mouse bioassay test and the possible interference (false-positive results) of free fatty acids (FFA). The toxicity of FFA in the biotest when mice are injected intraperitoneally (i.p.) with the liposoluble fraction extracted from mussels was also reported by Cassais and Perez [12], who listed the most toxic FFA in mussels.

As far as we know, previous papers on the HPLC analysis of DSP toxins refer to mussel samples collected in France, Spain, Norway and Japan [4,6,13,14], and the method has never been tested in Italy.

In this paper we describe the development and application of an HPLC method for OA, modified with respect to that formerly published by Lee *et al.* [6], and further integrated with the detection of the

0021-9673/92/$05.00 

FFA present in the samples. This integration may possibly represent a key factor for understanding the discrepancies between the results given by the mouse bioassay and the HPLC test for DSP toxins.

## EXPERIMENTAL

### *Apparatus*

The chromatographic apparatus consisted of a pump module (Series 3 liquid chromatograph), a spectrofluorimetric detector (LS30) and a data processor (LCI-100) (all from Perkin-Elmer, Norwalk, CT, USA).

### *Reagents and samples*

Pure (>97% by HPLC) okadaic acid (OA) [isolated from *Prorocentrum lima*, delivered in sealed vials, dissolved in dimethylformamide (DMF), 100 ± 5 μg/ml] was purchased from Moana BioProducts (Honolulu, HI, USA).

9-Anthryldiazomethane (ADAM) was obtained from Serva (Heidelberg, Germany) and used in methanol solution (0.1%, w/v); 9-chloromethylanthracene (CA), from Fluka (Buchs, Switzerland), was used in dimethylformamide solution (0.1%, w/v). Tetramethylammonium hydroxide (TMA) [25% (w/v) solution in methanol] was purchased from Aldrich (Steinheim, Germany) and was used diluted (1:500, v/v) in dimethylformamide. Acetone (analytical-reagent grade) and methanol, acetonitrile, chloroform and *n*-hexane (HPLC grade) were obtained from E. Merck (Darmstadt, Germany).

Light petroleum (b.p. 30–40°C) (AnalaR; BDH, Poole, UK) and anhydrous sodium sulphate (Carlo Erba, Milan, Italy) were also used.

Mussels were provided by a mussel farm in the Gulf of Trieste, and were all collected at the same site (approximately latitude 45°46′N, longitude 13°36′E) every 10 days during the winter and spring, 1990–91. The hepatopancreas (HP) of the mussels were excised from the fresh shellfish, homogenized and extracted (see Fig. 1).

Disposable cartridge column chromatography for sample purification was accomplished by using Sep-Pak Classic Cartridges (Waters-Millipore, Milford, MA, USA), packed either with silica (690 mg per cartridge) or $C_{18}$ material (360 mg per cartridge).

### *Methods*

Three different methods of sample preparation were tested. A schematic diagram of the three methods, for comparison, is reported in Fig. 1.

*Method 1.* The method described by Lee *et al.* [6] was followed.

*Method 2.* The Italian official mouse bioassay [10] was followed up to the final evaporation of the extract, which was redissolved in DMF for purification and subsequent chromatographic injection instead of being dissolved in Tween as required for i.p. injections into mice.

*Method 3.* This method uses two parallel routes of sample extraction and purification for either OA (method 3a) or FFA (method 3b) analysis.

For OA analysis (method 3a), steps similar to those in method 1 were followed, but for the derivatization of the extract CA was used instead of ADAM. An aliquot of 1 ml (from the total extracted volume of 10 ml) was evaporated under nitrogen and 200 μl of CA plus 100 μl of TMA solutions were added to the residue; the mixture was left to react, in a capped vial, in a thermostated water-bath at 75°C for 30 min, following a procedure similar to that used by Kaneda *et al.* [15]. After re-evaporation, the residue was submitted to a modified clean-up procedure similar to that suggested by Stabell *et al.* [16]. As our silica cartridges were packed with 0.69 g of phase instead of the 0.1 g used by Stabell *et al.*, the solvent volumes used in the clean-up procedure were proportionally modified.

For FFA analysis (method 3b), steps similar to those in method 2 were intitially followed; the volumes of the extraction solvents (acetone and diethyl ether) were reduced proportionally to those used in method 2 (as 1 g instead of 20 g of mussel hepatopancreas was extracted). The evaporated extract was redissolved in 2 ml of DMF, and an aliquot of 0.5 ml was derivatized by adding 1 ml of CA and 0.5 ml of TMA solutions [15]. A 500-μl volume of the derivatized mixture was loaded on a $C_{18}$ Sep-Pak column (conditioned with DMF) and eluted using 10 ml of acetone. After evaporation, the volume was again adjusted to 500 μl using DMF and the solution was used for chromatographic injections (injection volume 4 μl).

According to method 1, an injection of 10 μl corresponds to 1/400th of the extract from 1 g of mussel hepatopancreas [6]. Method 3a uses an

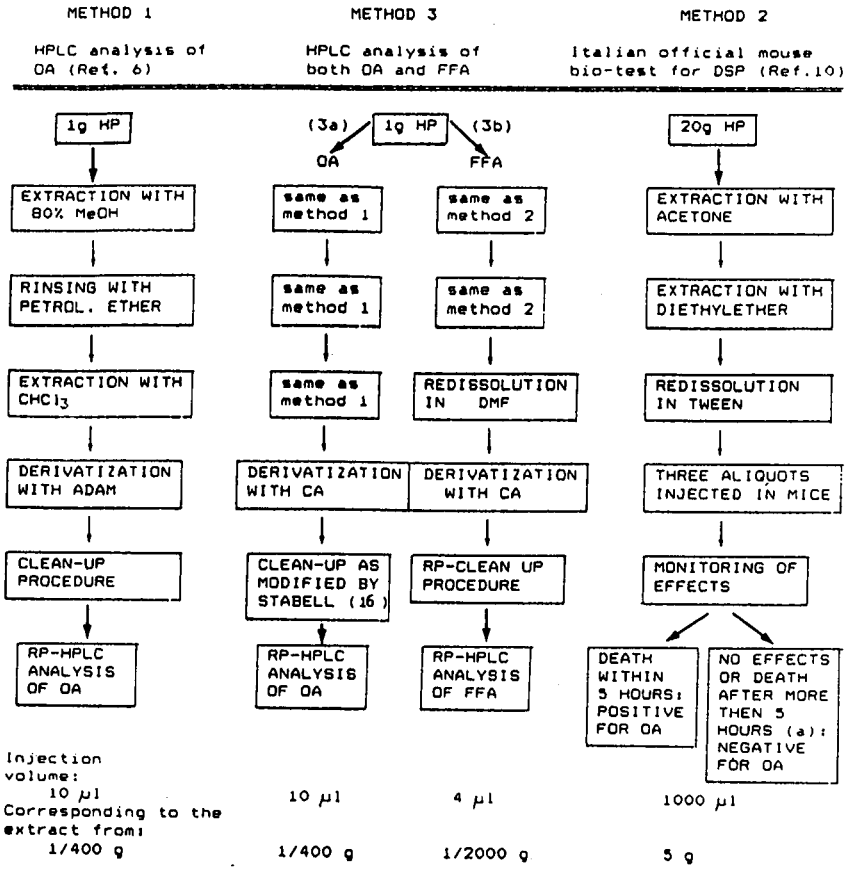


Fig. 1. Schematic diagram of analytical methods for DSP toxins. According to Italian law [10] the mouse biotest is positive when the average death time (three mice) is less than 5 h.

injection of the same volume (10 µl) and the same amount of extract, whereas in method 3b for FFA analysis the volume injected (4 µl) contains 1/2000th of the extract from 1 g of mussel hepatopancreas.

In method 2, as the weight of the dry extract from 5 g (corresponding to the dose used for injecting i.p. a 20-g mouse) was found to be about 100 mg, the dose used in the biotest is about 5000 mg/kg, which is very high.

*Chromatographic conditions*

The developed chromatographic conditions were as follows. Solvent A was acetone and solvent B was acetonitrile–water (50%, v/v), the solvent programme being 55% of A, isocratic for 6.5 min, then a linear gradient up to 95% of A in 26.5 min (total time), followed by 5 min of purging (98% of A) and 10 min of column re-equilibration. The solvent flow-rate was 1 ml/min. The column used was an Hibar LiChrosorb RP-8 (body porous, 5 µm) (25 × 0.4 cm I.D.) (E. Merck), equipped with a precolumn (4 × 0.4 cm I.D.) filled with a $C_{18}$ phase (pellicular, 15 µm) (E. Merck). The chromatograms were recorded with the excitation and emission wavelengths of the spectrofluorimetric detector set at 366 and 404 nm, respectively.

## RESULTS AND DISCUSSION

To enhance the detection sensitivity of very small amounts (ng) of OA, a derivatization reaction with ADAM as fluorescent labelling reagent was used [6]. A similar derivatization reaction occurs when CA is used instead of ADAM; recent applications of these

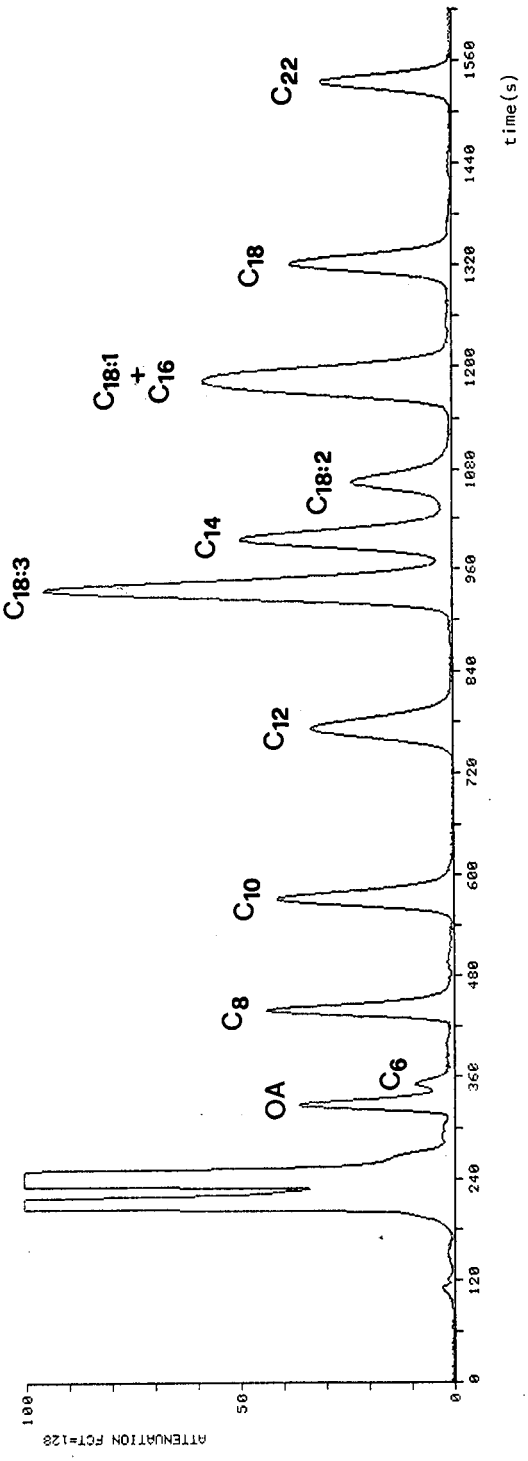


Fig. 2. Chromatogram of a mixture of OA and FFA derivatized with CA and injected without purification. Spectrofluorimetric detection with $\lambda_{ex}$ 366 nm and $\lambda_{em}$ 404 nm. Injection volume, 10 $\mu$l. The mixture shown was not prepared for quantitative analysis; the peaks correspond to about 80 ng of OA and to various amounts (from 20 to 100 ng) of FA.

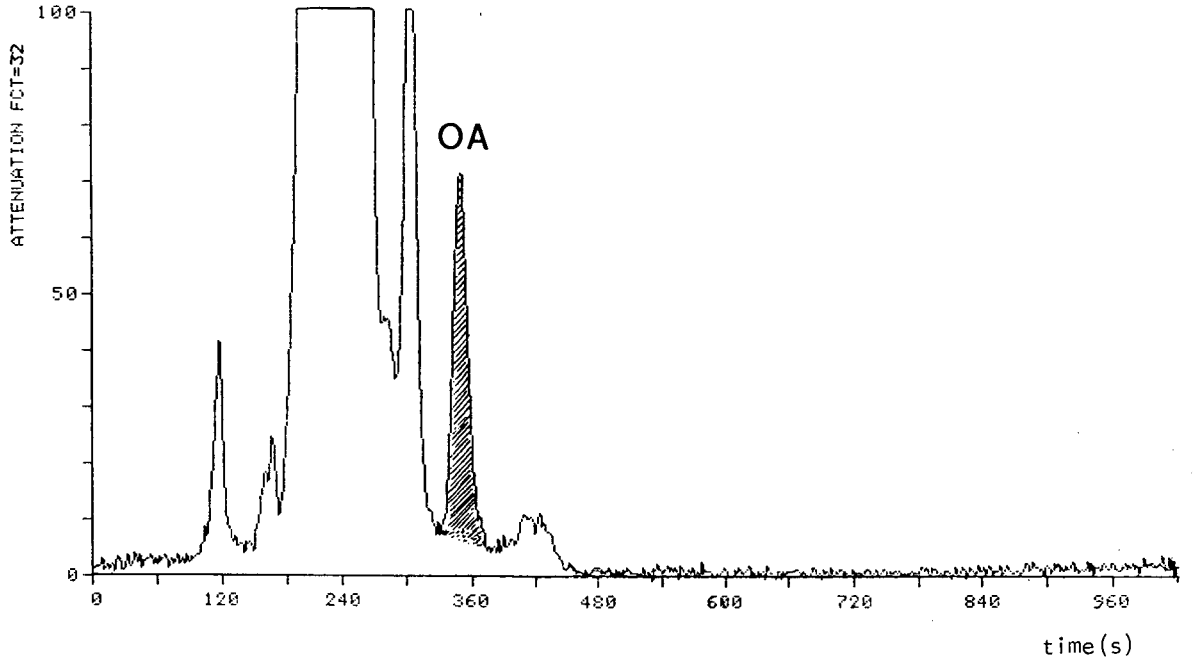


Fig. 3. Chromatogram of a mussel sample spiked with OA to obtain the recovery graph. The sample injected (10 μl) was prepared using method 3a and the OA peak corresponds to 40 ng.

derivatization reactions have been published relating to the HPLC determination of FFA in human serum (derivatized with ADAM) [17] and in beer (derivatized with CA) [15].

In the extract of mussel hepatopancreas, OA and FFA may both be present, and we developed a chromatographic system that allows for their simultaneous separation in an artificial standard mixture (Fig. 2). This separation cannot be obtained with mussel extracts, owing to the separate methods (3a and 3b) of sample preparation.

In our hands, method 1 failed to yield reproducible results; similar problems, with large inter-laboratory variations, were recently reported [16]. The method was therefore modified, changing the derivatization agent from ADAM to CA, and adopting the sample clean-up procedure suggested by Stabell *et al.* [16]. CA was chosen instead of ADAM for labelling the analytes because of the instability of ADAM. Fig. 3 shows the chromatogram obtained from a mussel sample spiked with OA, extracted, derivatized and purified according to method 3a.

The calibration (c) and recovery (r) graphs of OA, obtained from standard solutions and from spiked samples, respectively, are described by the following equations:

(c) $y = 0.400 \cdot 10^6 + 1.410 \cdot 10^6 x$ ($R^2 = 0.99994$)

(r) $y = -0.200 \cdot 10^6 + 1.313 \cdot 10^6 x$ ($R^2 = 0.99798$)

The accuracy of the method relates to the recovery of OA from spiked samples; the recovery, calculated as the ratio between the slope of the recovery graph and that of the calibration graph, was 93.1 ± 3.2% ($n = 5$). The resulting precision (relative standard deviation) was 3.4%. These values are close to those reported by Edebo *et al.* [13].

Japanese law sets the maximum level for DSP in shellfish hepatopancreas (HP) at 0.5 MU/g HP (MU = mouse units), that is, 2 μg OA/g HP [6]; in Norway the maximum tolerable level was set at 24 μg OA per 100 g of shellfish meat [16]. These concentrations are almost equivalents. As far as the Italian law is concerned, the tolerable level of OA (which must be determined using the mouse biotest with a recently modified threshold limit) can hardly be expressed as a weight concentration value. It may anyway be assumed that the tolerated concentration

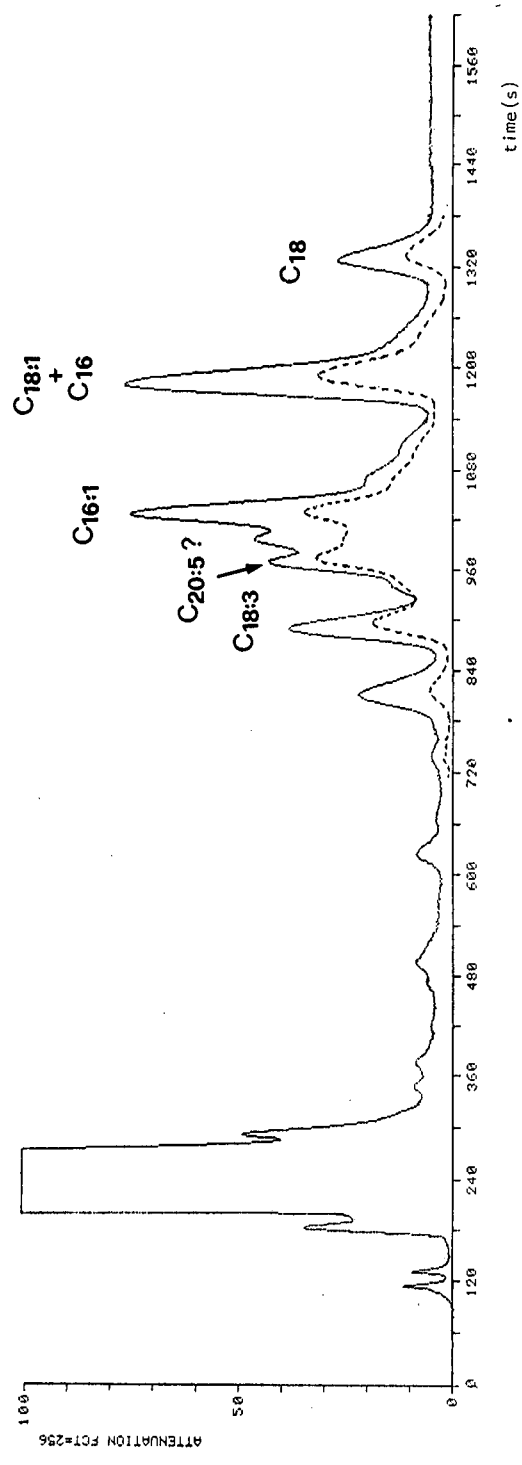


Fig. 4. Chromatograms of FFA of mussel hepatopancreas. The samples were prepared according to method 3b. The continuous and dashed lines refer to samples collected on March 18th and May 21st, 1991, respectively. Injection volume, 4 $\mu$l.

of OA is similar to or slightly higher than the above-cited values (2–2.5 μg OA/g HP).

The detection limit of OA using the HPLC method was reported to be 0.4 μg/g [6]; our detection limit, at a signal-to-noise ratio of 3, is higher, 1 μg/g, but good enough to detect OA levels well within the limits of the cited laws. In the mussel samples analysed so far to test the method, no OA was found, or its concentration was below the detection limit.

The analytical methods for DSP toxins which use the mouse biotest suffer from variability problems. As the toxicity of the FFA (when injected i.p. in the mouse biotest) present in the extract was well known [6,12], we developed a parallel route (method 3b) for determining the FFA present in the same sample as tested for OA. In this instance, the extraction was performed according to the Italian official biotest, to produce comparable samples.

Fig. 4 shows the chromatograms obtained from two different mussel samples following method 3b. The chromatogram drawn with the continuous line refers to a sample collected on March 18th 1991, whereas that drawn with the dashed line refers to a sample collected on May 21st 1991. The FFA distribution is similar, but the total amount is higher in the sample collected in March. The different concentrations of FFA found in mussel HP are linked to the biological cycle and reflect similar differences observed in mussel meat [18]. Comparing the peak retention times and by using the standard addition technique, some of the FFA (including C18:3) were identified, as listed. Our tentative assignment of one peak of the chromatogram, attributed to C20:5, was deduced from its expected elution order. The use of a more complex FFA standard mixture (including more polyunsaturated FA and possibly all of those listed [12] as the most toxic, *viz.*, linolenic, C18:3; araquidonic, C20:4; and eicosapentaenoic, C20:5) is planned for future studies.

A calibration and a recovery graph of palmitoleic acid (C16:1), used as a standard, was obtained. The same recovery value (95%) and the same fluorescence response were attributed to all FFA, and the area sum of all peaks was used to obtain the total amount of FFA in mussel HP. The FFA concentrations found in the two samples were 136 and 360 μg/g HP (these are only rough figures because different FA may give slightly different fluorescence responses). These concentrations are far from the dose (12 mg per mouse) reported as effective in causing death in mice [12], but the differences could explain the large variability of the results obtained by means of the mouse biotest. If and when future incidents of mussel contamination with DSP toxins occur, a systematic application of the present instrumental method, coupled with the official biomethod, should prove very useful for a more detailed interpretation of the results.

ACKNOWLEDGEMENTS

We acknowledge the courtesy of Professor T. Yasumoto, who sent us reprints of his papers on DSP toxins and provided valuable information about the availability of OA standard. We also thank Mr. M. Minca for providing mussel samples and M. Franco Orel for his skilled technical assistance.

REFERENCES

1 T. Yasumoto, Y. Oshima and M. Yamaguchi, *Bull. Jpn. Soc. Sci. Fish.*, 44 (1978) 1249.
2 M. Murata, M. Shimatani, H. Sugitani, Y. Oshima and T. Yasumoto, *Bull. Jpn. Soc. Sci. Fish.*, 48 (1982) 549.
3 M. Kumagai, T. Yanagi, M. Murata, T. Yasumoto, M. Kat, P. Lassus and J. A. Rodriguez-Vazquez, *Agric. Biol. Chem.*, 50 (1986) 2853.
4 J. Lee, K. Tangen, E. Dahl, P. Hovgaard and T. Yasumoto, *Nippon Suisan Gakkaishi*, 54 (1988) 1953.
5 Ministry of Health and Welfare, Japan, *Food Sanit. Res.*, 31 (1981) 565.
6 J. Lee, T. Yanagi, R. Kenma and T. Yasumoto, *Agric. Biol. Chem.*, 51 (1987) 877.
7 K. Terao, E. Ito, T. Yanagi and T. Yasumoto, *Toxicon*, 24 (1986) 1141.
8 H. Fujiki, M. Suganuma, H. Suguri, S. Yoshizawa, K. Takagi, N. Uda, K. Wakamatsu, K. Yamada, M. Murata, T. Yasumoto and T. Sugimura, *Jpn. J. Cancer Res.*, 79 (1988) 1089.
9 B. Stancher and F. Zonta, in *Atti XIV Congresso Nazionale di Merceologia, Pescara, 27–30 Settembre 1990*, in press.
10 Decreti Ministeriali 1/8/90 n. 256 e 257, *Gazzetta Ufficiale*, 10/9/90, and *Circolare Ministero della Sanità*, 29/5/90.
11 M. Bussani, *Federazione Italiana Maricoltori*, personal communication.
12 C. Cassais and R. Perez, *Rev. Lationoam. Quim.*, 19 (1988) 67.
13 L. Edebo, S. Lange, X. P. Li, S. Allenmark, K. Lindgren and R. Thompson, *APMIS*, 96 (1988) 1036.
14 C. Marcaillou-Le Baut and P. Masselin, in E. Graneli, B. Sundström, L. Edler and D. M. Anderson (Editors), *Toxic Marine Phytoplankton*, Elsevier, Amsterdam, 1990, p. 487.

15 H. Kaneda, Y. Kano, M. Kamimura, T. Osawa and S. Kawakishi, *J. Agric. Food Chem.*, 38 (1990) 1363.
16 O. B. Stabell, V. Hormazabal, I. Steffenak and K. Pedersen, *Toxicon*, 29 (1991) 21.
17 G. Kargas, T. Rudy, T. Spennetta, K. Takayama, N. Querishi and E. Shrago, *J. Chromatogr.*, 526 (1990) 331.
18 C. Calzolari, E. Cerma and B. Stancher, *Riv. Ital. Sostanze Grasse*, 48 (1971) 605.

*Journal of Chromatography*, 594 (1992) 145–151
Elsevier Science Publishers B.V., Amsterdam

CHROM. 23 860

# Isolation of aristolochic acids $HA_sI$ and $HA_sII$ by preparative liquid chromatography

Bogumiła Makuch* and Krystyna Gazda

*Institute of Inorganic Chemistry and Technology and Corrosion, Technical University of Gdańsk, 80-952 Gdańsk (Poland)*

Wojciech Cisowski

*Department of Pharmacognosy, Medical Academy of Gdańsk, Gdańsk (Poland)*

(First received August 14th, 1991; revised manuscript received November 8th, 1991)

ABSTRACT

To isolate the aristolochic acids $HA_sI$ and $HA_sII$ from a crude extract of the *Aristolochia clematitis* L. roots, preparative liquid chromatography was used. A system of reversed phases was applied with a methanol–water–acetic acid mobile phase. Conditions for the extraction of the acids with chloroform from the eluate were also elaborated. The production rate of the chromatographic separation depending on the mobile phase composition was evaluated.

## INTRODUCTION

Aristolochic acids, derivatives of 3,4-methylenedioxy-10-nitro-1-carboxyphenanthrene, belong, in addition to chloramphenicol and a few other natural compounds, to substances rarely found in nature that contain a nitro-group. Owing to their biological action [1–5] and their capability of potentiating leukocyte phagocytosis, they are used in the therapy of infectious diseases, although they also have some toxic properties [4,5]. Compounds of this group are difficult to separate, so a mixture of the aristolochic acids is used in therapy.

*Aristolochia clematitis* L. roots contain six acids of very similar structure [6,7]; $HA_sI$ and $HA_sII$ are prevalent and the remaining four acids are found only in insignificant amounts. They can be isolated by a standard method consisting of methyl esterification followed by separation of the esters on alumina and de-esterification to the free acids. The yield of the de-esterification process is very low, within the range 5–15% [8,9]. Partial degradation occurs, probably owing to the known sensitivity of aromatic nitro compounds to alkalis. Kupchan and Wermser [7] separated a crude mixture of acids and their esters by chromatography using a column packed with silicic acid–Celite (4:1) and a mobile phase of chloroform–ethanol mixtures in various proportions. We failed to reproduce their experiments.

In the method described here, we used high-efficiency preparative reversed-phase liquid chromatography to isolate $HA_sI$ and $HA_sII$ from a mixture of crude acids. A preliminary choice of the mobile phase for the preparative system was made with the use of an analytical system described elsewhere [10].

In the last decade, many studies dealing with optimization of the experimental conditions of preparative elution chromatography have been reported, and general rules were established relating throughput or production rate with the various chromatographic parameters [11–16]. An understanding of these rules diminishes considerably the number of necessary trial-and-error runs, but does not eliminate them completely. The equations given in the literature can be used for the rough estimation of the parameters rather than for their accurate

0021-9673/92/$05.00 

calculation. For the latter, an accurate determination of the equilibrium isotherms is necessary. Moreover, the determination of the optimum injection conditions is complicated with samples that are sparingly soluble in the mobile phase [17].

## EXPERIMENTAL

### *Solvents*

Methanol, tetrahydrofuran (THF), acetic acid and chloroform of analytical-reagent grade were obtained from POCH (Gliwice, Poland). All solvents were distilled before use. Water was distilled twice.

### *Apparatus*

The apparatus employed for preparative-scale liquid chromatography was equipped with a pump of output up to 270 $cm^3$/min and a UV detector (254 nm) with a flow cell of 10 $mm^3$ capacity. A 250 × 13 mm I.D. column was slurry-packed with bonded-phase octadecylsilica, particle size $d_p$ = 10 $\mu$m. Approximately 23 g of the material were packed in each column. The surface area of the packing material was 360 $m^2$/g. Before packing, a final capping with trimethylchlorosilane was performed to minimize the available silanol groups. This material was prepared in the Department of Organic Chemistry, Technical University of Gdańsk.

Sampling the substance was performed by means of a valve with loops of different volumes.

Fraction purity was checked using a Merck–Hitachi liquid chromatograph equipped with a Model L 4250 UV detector, Model L 6200 pump, Model D 2500 integrator and a column (125 × 4.6 mm I.D.) packed with LiChrosorb RP-18, $d_p$ = 5 $\mu$m.

### *Preparation of crude aristolochic acids mixture from plant material*

A 1000-g amount of crushed *A. clematitis* L. roots was macerated for 18 h in 10% aqueous formic acid solution. The macerated material was then extracted at room temperature with dichloromethane. The extract thus obtained was filtered and shaken with

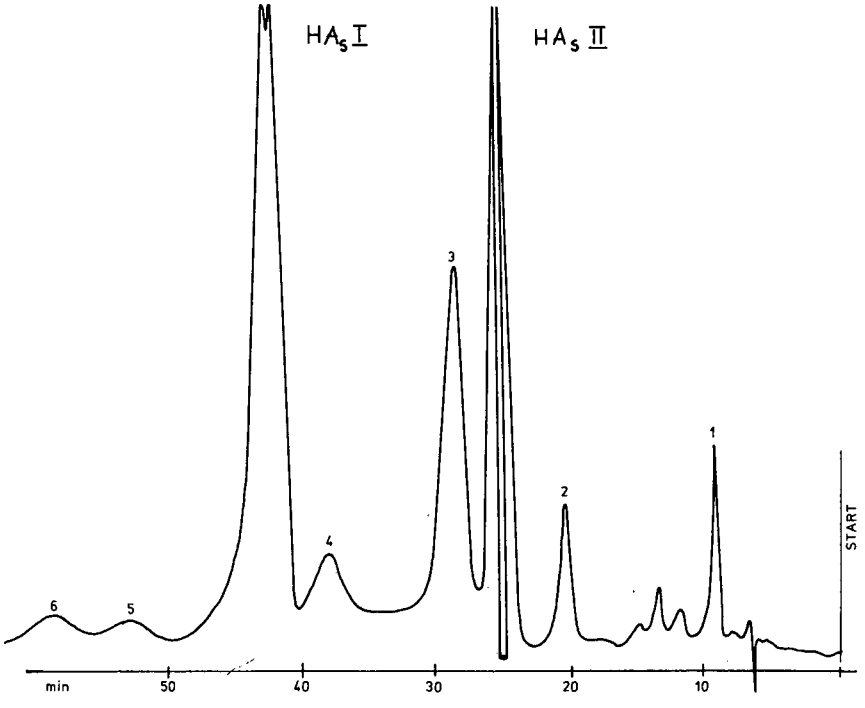


Fig. 1. Analytical chromatogram. Sample, crude mixture of acids; column, 250 × 13 mm I.D., octadecylsilica, $d_p$ = 10 $\mu$m; mobile phase, methanol–water–acetic acid (55:45:1, v/v/v); flow-rate, 5.3 $cm^3$/min; loading, 2 · $10^{-5}$ mg/g. Detection, UV at 254 nm; sensitivity, 0.08 a.u.f.s.

15% $NaHCO_3$ in the distributer. The aqueous layer was separated and acidified with hydrochloric acid to pH *ca.* 3 and the yellow precipitate was filtered and washed with water until neutral and then dried. The $HA_sI$ and $HA_sII$ content in the crude mixture was up to 24% and 68%, respectively.

*Chromatographic procedure*

Conditions for preparative separation were chosen on the basis of data obtained for the analytical columns. Comparability of the two systems was obtained by using identical packings in the analytical and preparative separations. The crude mixture of acids dissolves well in THF but hardly at all in methanol and water. A sample was dissolved in THF–methanol (1:1, v/v) with an acid concentration of 20 mg/cm$^3$ and loaded on to a column. It was confirmed in tests that introducing the sample in drops into the mobile phase did not cause precipitation of components. The column was loaded with amounts of sample from $2 \cdot 10^{-5}$ to 2.8 mg/g. Fractions were manually collected by monitoring the recorder output from the UV detector. They were collected in batches of 10 cm$^3$ each.

Typical analytical and preparative chromatograms are shown in Figs. 1 and 2. The number of fractions collected depended on the composition of the mobile phase. Substances with retentions higher than that of $HA_sI$ were eluted from the column with methanol (80–120 cm$^3$). The fractions were successively analysed by the analytical liquid chromatography method using the methanol–water–acetic acid (65:35:1, v/v/v) as the mobile phase. Fractions with concentrations of the isolated components ($HA_sI$ and $HA_sII$) not lower than 96% were collected, the others being evaporated and rechromatographed. When the column was loaded with a sample amount of 1.3 mg/g, a crystalline lamella-shaped orange precipitate appeared in fractions 11–14 and an amorphous light-yellow precipitate in fractions 20–24 (see Fig. 2).

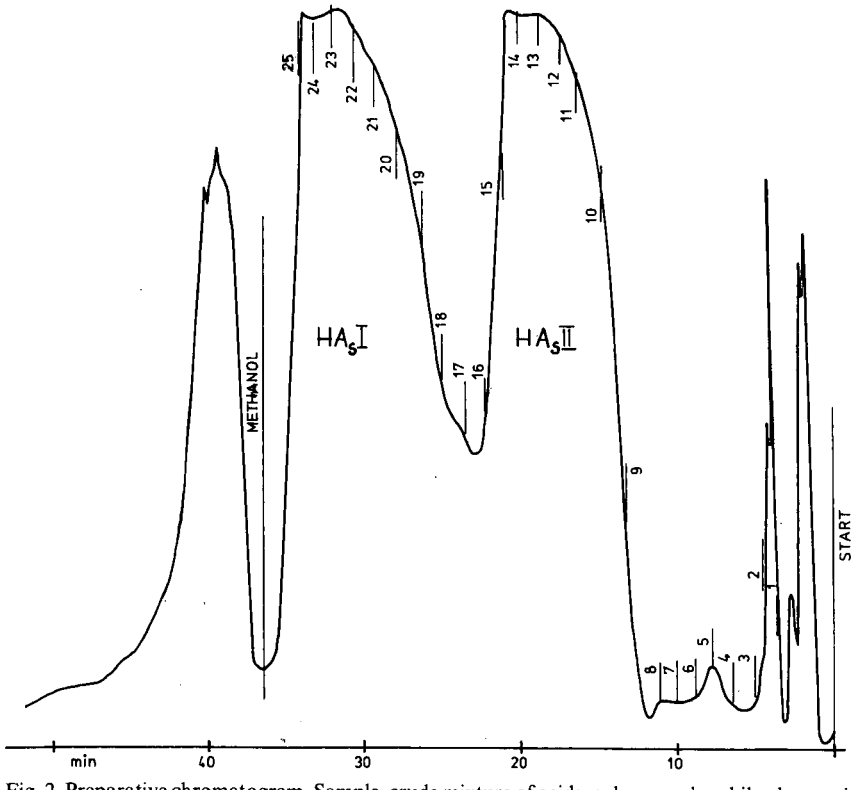


Fig. 2. Preparative chromatogram. Sample, crude mixture of acids; column and mobile phase as in Fig. 1; 25 fractions collected; loading, 1.3 mg/g; flow-rate, 8.3 cm$^3$/min; sensitivity, 1.28 a.u.f.s.

## RESULTS AND DISCUSSION

### *Selection of mobile phase*

The components of the mixture differed considerably with respect to polarity, which renders the selection of an appropriate preparative system difficult, so numerous systems were tested [10]. It has been found that changing the methanol concentration has a substantial effect on retention and selectivity. The values of some retention parameters obtained for various mobile phases are given in Table I. For the most important pairs of substances, *i.e.*, peak 2 and $HA_sII$, and peak 4 and $HA_sI$ (see Fig. 1), the $\alpha$ factor has the maximum value for mobile phase 2 and one may expect the highest production rate when using this phase.

### *Selection of sample size*

The aim of this work was to obtain multigram amounts of $HA_sI$ and $HA_sII$. A column of dimensions 250 × 13 mm I.D. ($n = 4000$) was applied for this purpose. The number of theoretical plates is large enough to ensure preparative resolution using mobile phases 2 and 3. The required number of plates, estimated according to eqn. 5 in ref. 16, for the $HA_sI$–peak 4 pair was 1200 for mobile phase 2 and about 1800 for mobile phase 3. As the $d_p^2/L$ ratio was fixed, only the amount of sample and the flow-rate of the mobile phase could be chosen. Unfortunately, principles for the choice of the sample size presented elsewhere [11–16] appeared to be unsuitable here owing to the very low solubility of the sample in the mobile phase. Taking into consideration Cox and Snyder's simplifying assumption [16], the maximum sample mass would be 17 mg of $HA_sII$ and 12 mg of $HA_sI$ (mobile phase 3). It was tested experimentally that the solubility of $HA_sII$ in this mobile phase was 0.3 mg/cm$^3$. The total sample volume should not exceed 17 cm$^3$, so only a small amount of the solute could be injected. Other mobile phases, containing less methanol, dissolve the acids even worse. Therefore, we injected the sample in a solvent stronger than the mobile phase but in which the sample was readily soluble. The problems resulting from this method of injection are known [18–21], but sometimes the results are reasonable.

Changing the volume of the injected sample solution in THF–methanol within the range 0.6–3.0 cm$^3$, the optimum sample size for mobile phase 3 was found to be 30 mg. An increase in the volume of the sample at the same concentration above 1.5 cm$^3$ caused a considerable decrease in resolution and hence the throughput of the acids in the required purity decreased. A sample volume of 1.5 cm$^3$ was arbitrarily taken as adequate for mobile phases 1 and 2.

Examples of the chromatograms obtained for various column loads are presented in Fig. 3. Table II shows the results achieved with three mobile phases. The aim of these experiments was to check whether a change in the mobile phase strength (in addition to the solubility) does not lead to peak distortion, which could result in deterioration of the resolution.

The production rate was calculated from $P_i = r_i Q_i / t_c A_c$, where $r_i = Q_r/Q_i$ is the recovery, $Q_r$ is the substance mass obtained and $Q_i$ is the substance mass injected in one separation cycle, $t_c$ is duration

TABLE I

CAPACITY FACTORS ($k'$) AND SELECTIVITY COEFFICIENTS ($\alpha$) FOR SELECTED PAIRS OF SUBSTANCES ACCORDING TO THE ORDER OF THEIR ELUTION OBTAINED FOR MOBILE PHASES CONTAINING VARIOUS AMOUNTS OF METHANOL

| Mobile phase: methanol–water–acetic acid (v/v/v) | $k'$[a] | | | | | | | | $\alpha$[a] | |
|---|---|---|---|---|---|---|---|---|---|---|
| | 1 | 2 | $HA_sII$ | 3 | 4 | $HA_sI$ | 5 | 6 | $HA_sII$–2 | $HA_sI$–4 |
| (1) 50:50:1 | 1.0 | 5.8 | 7.5 | 8.5 | 13.1 | 14.1 | 16.2 | 18.0 | 1.29 | 1.08 |
| (2) 53:47:1 | 0.8 | 4.3 | 6.2 | 6.5 | 8.4 | 10.8 | 11.4 | 13.2 | 1.44 | 1.28 |
| (3) 55:45:1 | 0.8 | 3.1 | 4.0 | 4.8 | 6.5 | 8.0 | 9.0 | 10.6 | 1.29 | 1.23 |

[a] Nos. 1–6 refer to peak numbers in Fig. 1.

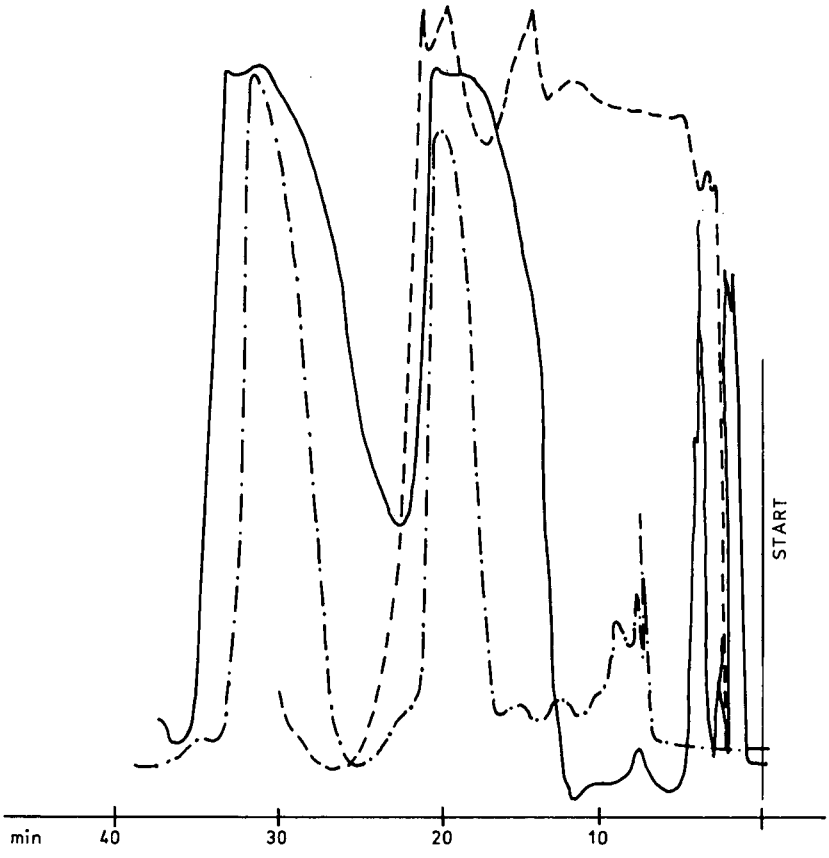


Fig. 3. Preparative chromatogram obtained for various sample volumes: –·–, 0.6 $cm^3$; ——, 1.5 $cm^3$; – – –, 3.0 $cm^3$. Sample concentration, 20 $mg/cm^3$; sensitivity, 1.28 a.u.f.s. Other conditions as in Fig. 2.

of the separation cycle, $A_c = \pi d_c^2/4$ and $d_c$ is column diameter. The results in Table II lead to the conclusion that the production rate depends, as usual, on $\alpha$ and $k'$, that is, it increases while $\alpha$ increases and $k'$ decreases.

Important parameters are the volume of fractions collected and the total elution volume. When mobile phase 3 was used, the volume of the fraction containing $HA_sI$ decreased by 50% and the total elution volume decreased by a factor of 1.7.

We also examined the mobile phase flow-rate, which influences the process production rate. Fig. 4

TABLE II

PRODUCTION RATES OF ACIDS AT VARIOUS MOBILE PHASE COMPOSITIONS

| Mobile phase: methanol–water–acetic acid (v/v/v) | $k'_{anal}$ | | Flow-rate ($cm^3$/min) | Total elution volume ($cm^3$) | Recovery (%) | | Fraction volume ($cm^3$) | | Production rate, $P_i$ ($mg/cm^2 \cdot min$) | |
|---|---|---|---|---|---|---|---|---|---|---|
| | $HA_sII$ | $HA_sI$ | | | $HA_sII$ | $HA_sI$ | $HA_sII$ | $HA_sI$ | $HA_sII$ | $HA_sI$ |
| (1) 50:50:1 | 7.5 | 14.1 | 8.3 | 448 | 36 | 42 | 30 | 80 | 0.10 | 0.04 |
| (2) 53:47:1 | 6.2 | 10.8 | 8.3 | 370 | 45 | 40 | 40 | 60 | 0.16 | 0.05 |
| (3) 55:45:1 | 4.0 | 8.0 | 8.3 | 260 | 32 | 40 | 40 | 40 | 0.16 | 0.07 |

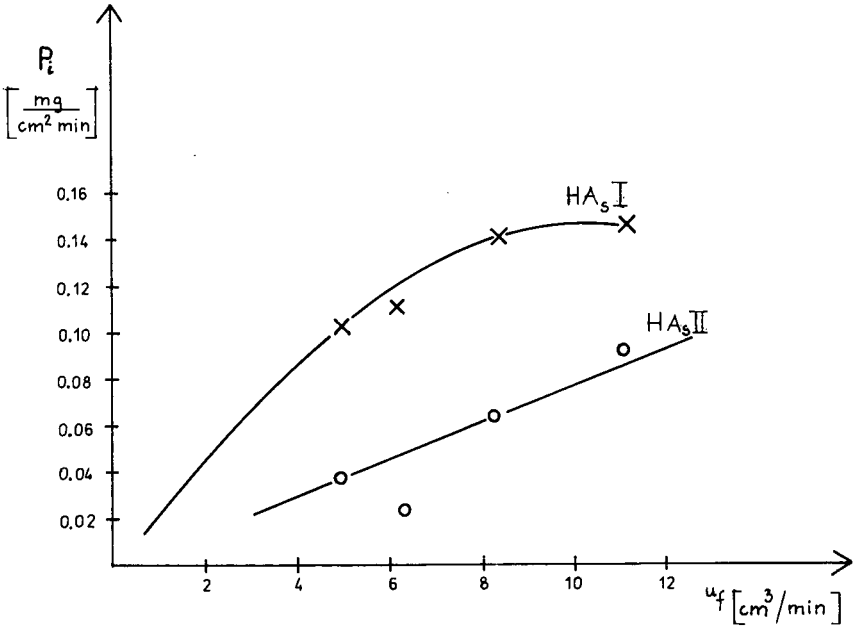


Fig. 4. Dependence of production rate, $P_i$, on flow-rate. Column and mobile phase as in Fig. 1.

shows the changes in the production rate of $HA_sI$ and $HA_sII$. The production rate of purified $HA_sI$ is low and it would be profitable to increase the flow-rate. Our conclusions are similar to those in refs. 22 and 23. Unfortunately, technical problems limited the flow-rate of the mobile phase in further experiments to 8.3 $cm^3$/min. The procedure was repeated ten times with mobile phase 3 and 28 mg of $HA_sI$ and 65 mg of $HA_sII$ were obtained.

As was mentioned before, the solutes began to crystallize from the collected eluates after a few minutes. The crystallization process might be speeded up by cooling, but the crystals formed are very fine and considerable amounts of substances, particularly $HA_sII$, remain in the filtrate. It is possible to evaporate the solvent using a vacuum evaporator but this takes a long time as the mobile phase contains much water. In addition, the evaporation must be carried out carefully because the acids are surface-active substances and cause excessive foaming. To avoid these difficulties, the acids were extracted from the eluate using various solvents. The best results were achieved with chloroform; 3 × 5 $cm^3$ were sufficient for complete extraction. This made it possible to diminish the volume of the solvent to be evaporated threefold and the evaporation process was much easier than with methanol–water–acetic acid mobile phase.

In conclusion, it is possible to purify aristolochic acids by liquid chromatography. The low solubility of the sample in the mobile phase might be a substantial difficulty, but this problem was overcome by dissolving the sample in a solvent stronger than the mobile phase. A sample of volume 1.5 $cm^3$ in a solvent considerably stronger than the mobile phase did not decrease the resolution so much that it would not be possible to obtain acids of the required purity.

REFERENCES

1 J. R. Möse, *Arzneim.-Forsch.*, 16 (1966) 118.
2 M. Białecki, T. Wroński and S. Szwemin, *Herba Pol.*, 19 (1973) 370.
3 S. M. Kupchan and R. W. Doscoth, *J. Med. Pharm. Chem.*, 5 (1962) 657.
4 J. Hociung, *Stud. Cercet. Chim.*, 22 (1974) 215.
5 P. Górecki and H. Otta, *Herba Pol.*, 21 (1975) 148.
6 M. Pailer, P. Bergthaller and G. Schafen, *Monatsch. Chem.*, 96 (1965) 863.
7 S. M. Kupchan and H. C. Wermser, *J. Org. Chem.*, 30 (1965) 3792.

8 W. Cisowski, H. Rządkowska-Bodalska and J. Lutomski, *Rocz. Chem.*, 51 (1977) 2115.
9 J. Benz, I. Fischer and W. Rüdiger, *Phytochemistry*, 22 (1983) 2801.
10 B. Makuch, W. Cisowski and J. S. Kowalczyk, *Chem. Anal. (Warsaw)*, (1992) in press.
11 J. H. Knox and H. M. Pyper, *J. Chromatogr.*, 363 (1986) 1.
12 L. R. Snyder, G. B. Cox and P. E. Antle, *Chromatographia*, 24 (1987) 82.
13 K. Jones, *Chromatographia*, 25 (1988) 547.
14 G. B. Cox and L. R. Snyder, presented at the *2nd International Symposium on Preparative and Up-Scale Liquid Chromatography, Baden-Baden, February 1988.*
15 S. Golshan-Shirazi and G. Guiochon, *Anal. Chem.*, 61 (1989) 1368.
16 G. B. Cox and L. R. Snyder, *LC · GC*, 6 (1988) 894.
17 G. Cretier and J. L. Rocca, *Sep. Sci. Technol.*, 22 (1987) 1881.
18 J. J. DeStefano and J. J. Kirkland, *Anal. Chem.*, 47 (1975) 1193A.
19 R. A. Wall, *J. Liq. Chromatogr.*, 2 (1979) 775.
20 K. Gazda and B. Makuch, *J. Chromatogr.*, 357 (1986) 371.
21 M. Kamiński and J. F. Reusch, *J. Chromatogr.*, 436 (1988) 367.
22 N. M. Cantwell, R. Calderone and M. Sienko, *J. Chromatogr.*, 316 (1984) 130.
23 M. Kamiński, B. Sledzińska and J. Klawiter, *J. Chromatogr.*, 367 (1986) 45.

*Journal of Chromatography*, 594 (1992) 153–158
Elsevier Science Publishers B.V., Amsterdam

CHROM. 23 837

# Determination of taxol by high-performance liquid chromatography–thermospray mass spectrometry

Seppo O. K. Auriola*, Anna-Maija Lepistö and Toivo Naaranlahti

*Department of Pharmaceutical Chemistry, University of Kuopio, P.O. Box 1627, SF-70211 Kuopio (Finland)*

Seppo P. Lapinjoki

*VTT-Biotechnology, Technological Research Centre of Finland, P.O. Box 1627, SF-70211 Kuopio (Finland)*

(First received September 9th, 1991; revised manuscript received October 30th, 1991)

ABSTRACT

A high-performance liquid chromatography–thermospray mass spectrometry method has been developed for the determination of taxol, found in the *Taxus* species. The compound is chromatographed by isocratic elution in 14 min and is quantitated by selected-ion recording of the protonated molecule. The method is linear over the range 1–1000 ng (1.2 pmol–1.2 nmol) of taxol per injection. The standard deviation of replicate bark samples ($n$ = 6) was 12.8%.

## INTRODUCTION

Taxol is a diterpene (Fig. 1), which has been shown to have important anti-neoplastic activity in preclinical and clinical studies [1]. The most common source of the chemical is the bark of the western yew, *Taxus brevifolia* Nutt. (Taxaceae), but it is also found in other *Taxus* spp., including *T. baccata* L., *T. media* Rehder and *T. cuspidata* Sieb. et Zucc. The taxol content of the plant materials is low, varying from 0.00003 to 0.069% dry weight [2–4]. Taxol has also been produced in a cell suspension culture of *T. brevifolia*, with a yield of 1–3 mg/l [5].

High-performance liquid chromatography (HPLC) with UV detection has been used for the determination of taxol in plant materials [3–5] and in pharmacokinetic studies [6]. Optimal separation of taxol and related compounds has been achieved using cyano- or phenyl-phase columns with gradient elution [4], and the strong absorbance at 235 nm allows their detection at concentrations of 50 pmol [7].

The identity and purity of the peaks detected is always a problem when HPLC samples are derived from complex biological matrices. This is a particular problem when new production methods and the metabolism of a drug are investigated, as new and unpredictable compounds are often present. As HPLC–thermospray mass spectrometry (TSP-MS) has been effectively used to overcome these problems [8], its suitability for the determination of taxol was studied. A method using a reversed-phase cyano-phase column and selected-ion recording (SIR) of the $MH^+$ ion was developed for the verification of the HPLC peak and for the quantitation of taxol in bark and needle samples of *T. cuspidata*.

## EXPERIMENTAL

The *T. cuspidata* samples were obtained from the Botanical Garden of the University of Kuopio. The bark and needle samples were freeze-dried and ground in a mortar. The samples (240 mg) were extracted with 3 ml of methanol for 24 h at 4°C. The samples were sonicated for 30 min and centrifuged

0021-9673/92/$05.00 

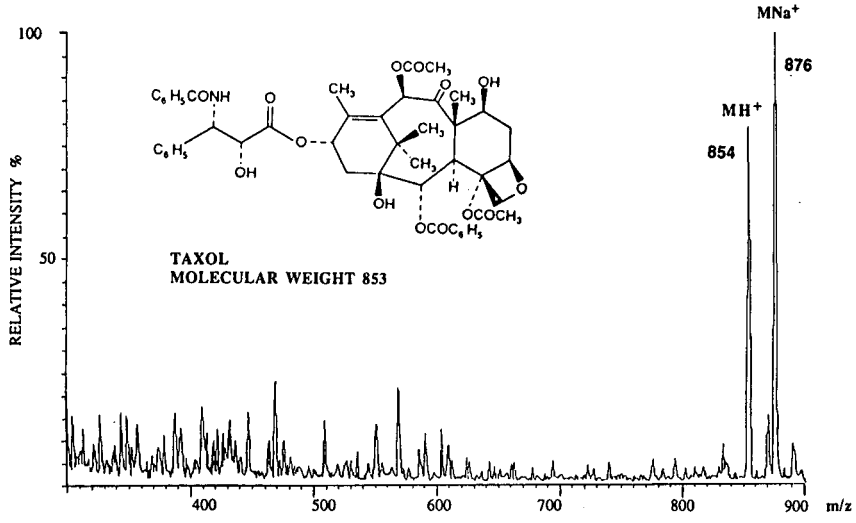


Fig. 1. Molecular structure and thermospray mass spectrum of taxol. Conditions: 50% methanol–water, flow-rate 1 ml/min, capillary temperature 200°C, ion source temperature 200°C. A 100-ng amount of taxol was injected via a loop.

for 10 min (500 *g*) with an FP-510 centrifuge (Labsystems, Finland). The supernatant was collected. The sonification and centrifugation were repeated three times with 1 ml of methanol and the supernatants were combined and evaporated to dryness in a stream of nitrogen. The residue was dissolved in 1.5 ml of methanol–water (30:70).

The solid-phase extraction procedure described by Vidensek *et al.* [3] was modified to purify the crude plant extracts. The extraction cartridges (Bond-Elut $C_{18}$, 1 ml, Analytichem, Harbor City, CA, USA) were conditioned with 1 ml of methanol and 1 ml of methanol–water (30:70). The sample was added and the columns were washed once with 1 ml of water and twice with 1 ml of acetonitrile–water (30:70). Taxol was eluted from the column with 0.5 ml of methanol. Pure standard taxol (NSC-12973), supplied by the Drug Synthesis and Chemistry Branch, Division of Cancer Treatment, National Cancer Institute (Bethesda, MD, USA) was used to optimize the extraction and HPLC procedures.

*HPLC conditions*

The HPLC pump used with the mass spectrometer was a Model 2900-0374 solvent delivery system (Applied Biosystems, USA). The injector was a Rheodyne Model 7125 instrument with a 20-$\mu$l loop (Rheodyne, Cotati, CA, USA). The cyano-phase HPLC column was Zorbax CN (25 cm × 4.6 mm, 5 $\mu$m) (DuPont, Wilmington, DE, USA). The isocratic eluent system was acetonitrile–methanol–0.1 *M* ammonium acetate buffer (pH 5) (26.5:26.5:47).

*Mass spectrometry*

The HPLC–MS system used was a VG thermospray–plasmaspray probe coupled to a VG Trio-2 quadrupole mass spectrometer (VG Masslab, Manchester, UK). The measurements were carried out using the TSP mode. Tuning of the mass spectrometer and the eluent composition experiments were performed with triplicate injections of 100 ng of taxol via a loop.

The vaporizer orifice was adjusted by crimping with wire cutters to obtain a 25–30 bar back-pressure at a 1 ml/min flow-rate without heating, as described by Robins and Crow [9]. The original back-pressure was 11 bar. The capillary temperature of the TSP probe was optimized by increasing the temperature from 180 to 230°C in 10°C steps using a constant ion source temperature of 200°C. The capillary temperature was then set at 220°C and the source temperature was tested at 150, 200 and 227°C. The ion repeller potential of the TSP probe was optimized by increasing the voltage from 180 to 340 V in 30-V steps.

The effect of the eluent pH on ionization was

studied with methanol–water (50:50) using an ion source temperature of 200°C and a capillary temperature of 220°C. The pH was adjusted with trifluoroacetic acid, acetic acid or ammonium hydroxide to 2.1, 4.1, 6.0, 8.0 or 9.9.

The effect of the ammonium acetate concentration on the spectrum was studied with methanol mixed with buffer solution at 0.001, 0.01 and 0.1 *M* concentrations (50%). The pH was adjusted to 5.1.

The intensities and signal-to-noise ratios of the protonated molecular ion at *m/z* 854 and the sodium adduct ion at *m/z* 876 were observed by SIR.

For the determination of taxol in the *T. cuspidata* samples the ion source temperature was set to 200°C, the capillary temperature to 190°C, the solvent flow-rate to 1 ml/min, and the ion repeller voltage to 290 V. The mass spectrum of taxol was recorded by injecting 100 ng of taxol via a loop. Taxol was quantitated by SIR of the $MH^+$ and $MNa^+$ ions. The external standard method was used. The calibration graphs were created by using 1, 10, 100 and 1000 ng of taxol per injection (duplicate injections). Linear regression analysis was used to calculate the curve parameters. The precision of the TSP-MS system was determined by analysing one needle sample six times and the inter-day precision was tested by analysing one bark and one needle sample on six different days. The precision of the whole analytical method was tested by extracting and analysing six replicate bark samples.

## RESULTS AND DISCUSSION

The primary process for the production of ions in a TSP ion source in the absence of external ionization is considered to be gas-phase ionization by the ammonium ion originated from the volatile ammonium acetate buffer [10]. The direct-ion evaporation process in the TSP source is dependent on the type and relative amount of ionic species and the pH in solution. Typical ions for the ion evaporation spectra are the adduct ions of organic compounds and alkali metal cations originated from the residual salts in most solvents [11]. The efficiency of ionization by the TSP source is dependent on the solvent composition, the proton affinity of the analyte and the conditions in the vaporizer capillary and ion source [12–14]. As the mass spectrum of taxol (Fig. 1) showed an abundant protonated molecule at *m/z* 854 and a sodium adduct ion at *m/z* 876 suitable for the identification and quantitation of the chromatographic peak, SIR of these ions was used to tune the instrument and optimize the solvent compositions.

The restriction of the capillary increased the peak area of the $MH^+$ and $MNa^+$ ions and the signal-to-noise ratio by more than five times. This is presumably due to the smaller droplets produced, which resulted in a greater charge-to-surface area ratio and an enhanced ion evaporation process [9,15]. However, the restriction prevented the use of capillary temperatures above 230°C, which caused too high a back-pressure (over 350 bar) for the HPLC pump.

The best response in ionization by a TSP source is achieved with capillary temperatures at which nearly complete vaporization occurs. Strong heating of the TSP ion source further enhances the vaporization of the droplets in the jet and improves the sensitivity for less volatile compounds [16]. As shown in Fig. 2, the intensities of the $MH^+$ and $MNa^+$ ions of taxol remained stable at capillary temperatures between 180 and 200°C and then increased with temperature from 200 to 230°C. When the source temperature was increased from the initial 200 to 227°C to enhance the desolvatation of the droplets, the response of these two ions could be further increased

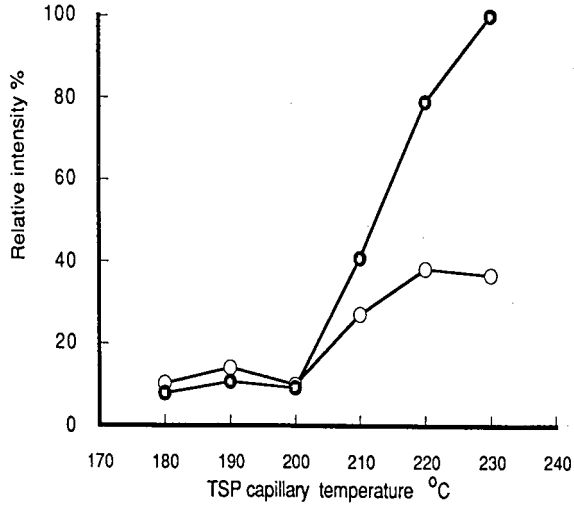


Fig. 2. Relative amounts of $MH^+$ (○) and $MNa^+$ (●) ions produced at different thermospray capillary temperatures. Other conditions as in Fig. 1.

two-fold. The temperature of 227°C was the maximum for the ion source of this instrument. For the analytical method, a capillary temperature of 190°C was chosen to prevent small changes from affecting the response and the source temperature was set to 200°C to conserve the heater wire.

The use of a high repeller electrode voltage has been observed to improve the sensitivity of ionization by a TSP source, especially at high masses (near $m/z$ 1000). The presence of the electrostatic field may increase the evaporation of ions from equilibrated droplets [9,17] and it may increase the extraction efficiency of high mass ions with a higher kinetic energy [15]. The increase in the repeller potential from 160 to 340 V increased the response of the $MNa^+$ ion more than the response of the $MH^+$ ion (Fig. 3). This indicates that in addition to increasing the sampling efficiency of the ions, by increasing the ion mobility in the source, the evaporation ionization process is also affected, possibly by inducing expulsion of the ions from the droplets.

The effect of pH on the response was studied with a methanol–water eluent between pH 2 and 10. As shown in Fig. 4, the responses of the $MH^+$ and $MNa^+$ ions were good between pH 4 and 8, but decreased sharply beyond these. At pH 2.1 the adduct ion $MNa^+$ could no longer be seen. This indicates that the solvent pH affects the spectra, and that the ion evaporation process is responsible for the ionization. The use of 0.001, 0.01 or 0.1 *M* ammonium acetate buffer only slightly affected the $MH^+/MNa^+$ ratio (Fig. 5). This is much less than the decrease of one or two orders of magnitude in the $MNa^+$ ion intensity observed for nucleosides by Voyksner [11]. With buffer concentrations of 0.01 and 0.1 *M* the background was higher, but the

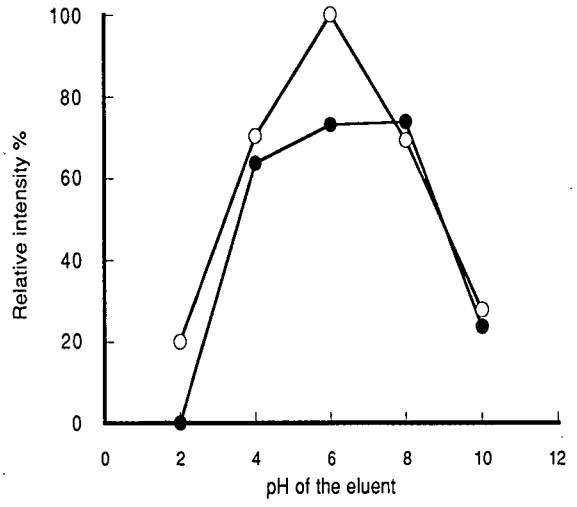


Fig. 4. Effect of the eluent pH on the amount of $MH^+$ (○) and $MNa^+$ (●) ions. Conditions as in Fig. 1, but the capillary temperature was set to 220°C.

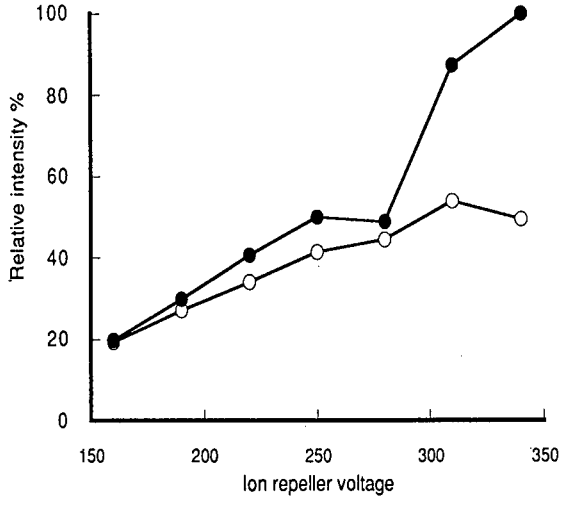


Fig. 3. Effect of the thermospray ion repeller potential on the amount of $MH^+$ (○) and $MNa^+$ (●) ions.

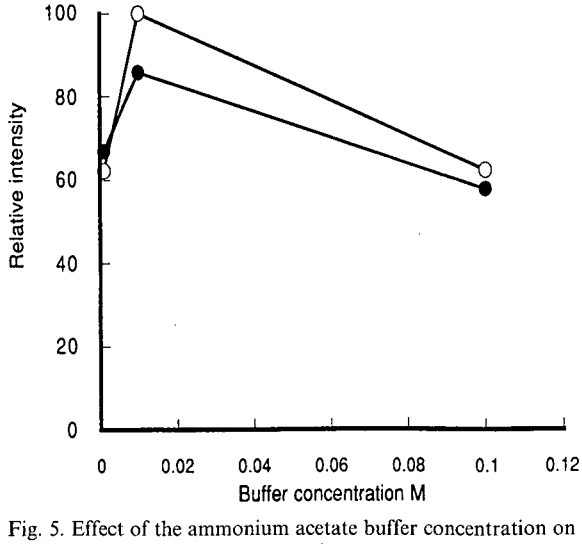


Fig. 5. Effect of the ammonium acetate buffer concentration on the amount of $MH^+$ (○) and $MNa^+$ (●) ions. The pH was set to 5.1; other conditions as in Fig. 4.

signal-to-noise ratio was as good as without the buffer.

SIR of the $MH^+$ ion at $m/z$ 854 was used for the quantitation of taxol in plant extracts and the sodium adduct ion at $m/z$ 876 was also monitored to confirm the identity of the peak (Fig. 6). Taxol was chromatographed in 14 min using an isocratic solvent system, and baseline separation was achieved for taxol on both channels. The abundant peak eluting at 11 min is probably a related compound, cephalomannin (molecular weight 831 dalton). In the cyano-phase columns, cephalomannin elutes before taxol when acetonitrile–methanol–water is used as the eluent [4]. The calibration graphs were determined by plotting the chromatographic peak areas ($y$) against the amount of taxol per injection ($x$) (1, 10, 100 and 1000 ng). When the $MNa^+$ ion was recorded, the regression equation of the linear relationships was $y = 0.9953x + 5.51$ ($r = 1.00$); the confidence limits of the slope and intercept were $0.9953 \pm 0.069$ and $5.51 \pm 34.7$ ($p = 0.05$), respectively. When $MH^+$ was recorded the regression equation of the linear relationships was $y = x + 2.17$ ($r = 1.00$) for the range 10–1000 ng; the confidence limits of the slope and intercept were $1 \pm 0.044$ and $2.16 \pm 25.4$ ($p = 0.05$), respectively. Although the response of the method is almost linear for a wide concentration range, calibration graphs for narrower concentration ranges should be determined to obtain the optimum results, especially at low analyte concentrations.

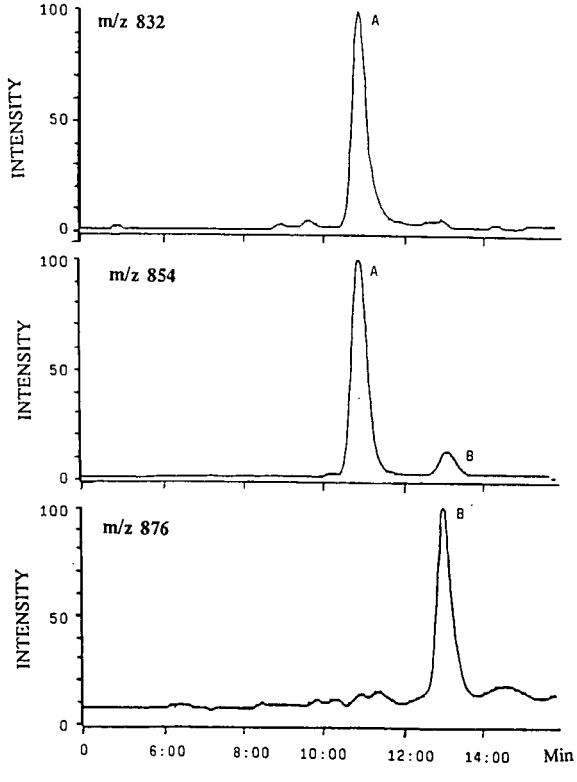


Fig. 6. Selected ion chromatograms of a *Taxus cuspidata* needle sample. Compounds monitored: peak (B) is taxol, $MH^+$ at $m/z$ 854 and $MNa^+$ at $m/z$ 876; peak (A) is probably cephalomannin, $MH^+$ at $m/z$ 832 and $MNa^+$ at $m/z$ 854. Conditions: acetonitrile–methanol–0.1 $M$ ammonium acetate (26.5:26.5:47), flow-rate 1 ml/min, capillary temperature 190°C, source temperature 200°C, repeller voltage 290 V.

The precision of the TSP system was tested by analysing six needle samples in parallel (approximately 715 ng per injection). When the $MH^+$ ion was recorded, the relative standard deviation (R.S.D.) was 6.8%; it was 11.2% when the sodium adduct ion was used for quantitation. However, as changes in the capillary or ion source parameters may considerably change the response, the performance must be evaluated daily.

The precision of the whole assay method was determined by analysing six replicate bark samples (280 ng). The R.S.D. was 12.8%. The inter-day precision was tested by analysing one needle sample (607 ng) and one bark sample (260 ng) on six days. The R.S.D. values were 10.8 and 7.4%, respectively.

The amount of taxol in the bark samples of *T. cuspidata* grown in Finland varied from 0.0027 to 0.0049% and in the needle samples from 0.0048 to 0.0061%. These values are comparable with the results of Vidensek *et al.* [3].

## CONCLUSIONS

These results show that ion evaporation is at least partly responsible for the ionization of taxol by a TSP source, as the mass spectrum of the compound showed abundant $MH^+$ and $MNa^+$ ions in the absence of ammonium acetate buffer. The presence of the $MNa^+$ ion and the dependence of the ionization on the eluent pH indicate that the ions are formed in solution. These processes made it possible to use HPLC–TSP-MS and SIR of the $MH^+$ ion for the determination of taxol. The selectivity and sensitivity of the method is needed as taxol is only a

minor component in the *Taxus* species. The precision of the method is adequate for screening the taxol content of plant extracts.

ACKNOWLEDGEMENTS

The work was supported by the Provincial Government of Kuopio. The authors thank Mr. Jari Kaipio for advice about the statistics.

REFERENCES

1 W. J. Slichenmyer and D. D. Von Hoff, *J. Clin. Pharmacol.*, 30 (1990) 770.
2 M. C. Wani, H. I. Taylor, M. E. Wall, P. Coggon and A. T. McPhail, *J. Am. Chem. Soc.*, 93 (1971) 2325.
3 N. Vidensek, P. Lim, A. Campbell and C. Carlson, *J. Nat. Prod.*, 53 (1990) 1609.
4 K. M. Witherup, S. A. Look, M. W. Stasko, T. G. McCloud, H. J. Issaq and G. M. Muschik, *J. Liq. Chromatogr.*, 12 (1989) 2117.
5 A. A. Christen, J. Bland and D. M. Gibson, *Proc. Am. Assoc. Cancer Res.*, 30 (1989) 566.
6 S. M. Longnecker, R. C. Donehower, A. E. Cates, Tiang-Ling Chen, E. E. Brundrett, L. B. Grochow, D. S. Ettinger and M. Colvin, *Cancer Treat. Rep.*, 71 (1987) 53.
7 B. Monsarrat, E. Mariel, S. Cros, M. Gares, D. Guénard, F. Guéritte-Voegelein and M. Wright, *Drug Metab. Dispos.*, 18 (1990) 895.
8 A. L. Yergey, C. G. Edmonds, I. A. S. Lewis and M. L. Vestal, *Liquid Chromatography/Mass Spectrometry, Techniques and Applications*, Plenum Press, New York, 1990.
9 R. H. Robins and F. W. Crow, *Rapid Commun. Mass Spectrom.*, 2 (1988) 30.
10 A. J. Alexander and P. Kebarle, *Anal. Chem.*, 58 (1986) 471.
11 R. D. Voyksner, *Org. Mass Spectrom.*, 22 (1987) 513.
12 R. D. Voyksner and C. A. Haney, *Anal. Chem.*, 57 (1985) 991.
13 D. J. Liberato and A. L. Yergey, *Anal. Chem.*, 58 (1986) 6.
14 M. M. Bursey, C. E. Parker, R. W. Smith and S. J. Gaskell, *Anal. Chem.*, 57 (1985) 2597.
15 S. W. Fink and R. B. Freas, *Anal. Chem.*, 61 (1989) 2050.
16 M. L. Vestal and G. J. Fergusson, *Anal. Chem.*, 57 (1985) 2373.
17 M. A. McLean, M. L. Vestal, C. H. Vestal, M. H. Allen and F. A. Field, *Proceedings of the 38th ASMS Conference on Mass Spectrometry and Allied Topics, Tucson, AZ, June 3–8, 1990*, p. 1138.

*Journal of Chromatography*, 594 (1992) 159–163
Elsevier Science Publishers B.V., Amsterdam

CHROM. 23 810

# Reversed-phase liquid chromatographic behaviour of alkylamines with amperometric detection and its application to trace analysis

Masao Maruyama* and Takayuki Nagayoshi

*Faculty of Science and Engineering, Chuo University, Kasuga, Bunkyo-ku, Tokyo 112 (Japan)*

(First received August 13th, 1991; revised manuscript received October 11th, 1991)

ABSTRACT

The reversed-phase liquid chromatographic behaviour of tri- and dialkylamines with amperometric detection was studied. Peak retention and peak shape can be improved by the addition of ammonium ion (as competing base) to the mobile phase. The retention behaviour of alkylamines can be explained by both ion and solvophobic interactions. This method can be applied to the selective and sensitive determination of trace amounts of tri- and dialkylamines. In air samples the limit of determination of trimethylamine is a few μg/l and in water samples (direct injection) a few tenths of 1 mg/l.

## INTRODUCTION

Amines have been separated by high-performance liquid chromatography with UV detection [1–3] and also by cation-exchange chromatography [4] and ion-pair chromatography [5]. Most aliphatic amines do not absorb in the ultraviolet region and it is difficult to monitor aliphatic amines directly by high-performance liquid chromatography (HPLC) with UV detection. Chemical derivatization techniques are often used to increase UV detectability. For example, aliphatic and aromatic amines were derivatized to N,N′-disubstituted ureas with phenyl isocyanate [1] and aliphatic amines to 2,4-dinitrophenyl derivatives with 2,4-dinitrofluorobenzene [6] and prior to HPLC.

The amperometric detector is one of the most sensitive and the most specific detectors available and responds to substances that are either oxidizable or reducible. Benzidine and its analogues [7] and aminophenyl isomers [8] have been determined by reversed-phase HPLC with amperometric detection.

In this paper, the reversed-phase HPLC behaviour of tri- and dialkylamines with amperometric detection and its application to trace analysis is described.

## EXPERIMENTAL

### *Apparatus*

Chromatograms were measured with a Yanagimoto (Kyoto, Japan) Model L-3200 HPLC system equipped with an amperometric detector. The amperometric detector contained a three-electrode cell, with a glassy carbon working electrode, platinum auxiliary electrode and Ag/AgCl reference electrode. Semi-differential voltammetric measurements were performed with a Yanagimoto Model VMA-010 cyclic voltammetric analyser. The column was 75 mm × 4.6 mm I.D. stainless steel, packed with Nucleosil $C_{18}$ (Macherey-Nagel, Düren, Germany) of 3-μm particle size.

### *Chemicals*

Alkylamines were purchased from Tokyo Kasei (Tokyo, Japan). Acetonitrile was of HPLC grade. All other chemicals and solvents were of analytical-

0021-9673/92/$05.00 

reagent grade and used as received.

Stock solutions (1000 mg/l) of alkylamines were prepared in fresh glass-distilled water. The concentration of the stock solution was checked by acidimetry. Working standard solutions used for normalization and for the fortification of recovery samples were prepared by dilution of the stock solutions.

*Chromatographic conditions*

The mobile phase was acetonitrile–phosphate buffer (pH 7.0) (40:60, v/v) containing 0.05 *M* ammonium acetate. The flow-rate of mobile phase through the analytical column was 1.0 ml/min. All experiments were carried out at 25°C. The eluate was monitored with the amperometric detector. Measurements were made at as low a voltage as possible because it is difficult to use a high voltage routinely owing to increased background noise and a lack of stability. For monitoring trimethylamine, an applied voltage of 1000 mV *vs.* Ag/AgCl was selected.

## RESULTS AND DISCUSSION

*Cyclic voltammograms of alkylamines and applied voltages*

Cyclic voltammograms of trialkylamines in acetonitrile–phosphate buffer (pH 7.0) (20:80, v/v) containing 0.1 *M* ammonium acetate were measured at potentials between 0 and 1500 mV *vs.* Ag/AgCl with a scan rate of 80 mV/s. A typical voltammogram of trialkylamines is shown in Fig. 1.

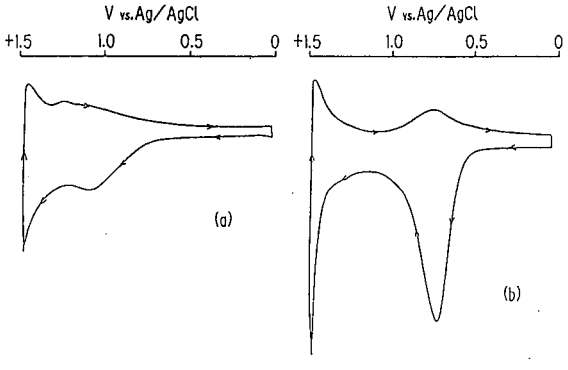


Fig. 1. Cyclic voltammograms of trialkylamines. Concentration, $1 \times 10^{-3}$ *M*; medium, acetonitrile–phosphate buffer (pH 7.0) (40:60, v/v) + 0.1 *M* ammonium acetate; scan rate, 80 mV/s. (a) Trimethylamine; (b) tri-*n*-propylamine.

An oxidation peak due to one-electron oxidation to produce the cation radical was observed at a potential of about 700–1100 mV *vs.* Ag/AgCl. The peak potentials of trialkylamines are given in Table I. The optimum oxidation applied voltage was selected according to which trialkylamines were being measured. The cyclic voltammograms of dialkylamines were also measured under the same conditions as trialkylamines and the peak potentials are given in Table I.

Trialkylamines are more easily oxidized than dialkylamines and their peak potentials decrease with increasing size of the alkyl group owing to the stronger electron-donating power. The oxidation process of monoalkylamines is very different and more complex and they cannot be oxidized under the conditions mentioned above.

*Chromatography of alkylamines*

A typical chromatogram of trialkylamines measured under the conditions mentioned above is shown in Fig. 2. The compounds were clearly separated in order of increasing length of the alkyl group. In this chromatogram, the peak of tri-*n*-propylamine is broad with a low column efficiency, but a sharp peak can be obtained by increasing the concentration of acetonitrile in the mobile phase (Fig. 3). Fig. 3 shows a typical chromatogram of di- and tri-*n*-propylamine at an applied voltage of 1100 mV *vs.* Ag/AgCl.

*Linearity and detection limit*

The relationship between sample size and peak height was linear over the range 3–30 ng under the conditions mentioned above. The minimum detectable amount of trialkylamines was found to be a few nanograms based on a signal-to-noise ratio of $\geqslant 3$. This method is very sensitive and good repro-

TABLE I

PEAK POTENTIALS OF DI- AND TRIALKYLAMINES

| Alkylamine | Peak potential (mV *vs.* Ag/AgCl) | | | |
|---|---|---|---|---|
| | Methyl | Ethyl | *n*-Propyl | *n*-Butyl |
| Di- | 1280 | 1300 | 1230 | 1210 |
| Tri- | 1100 | 820 | 720 | 700 |

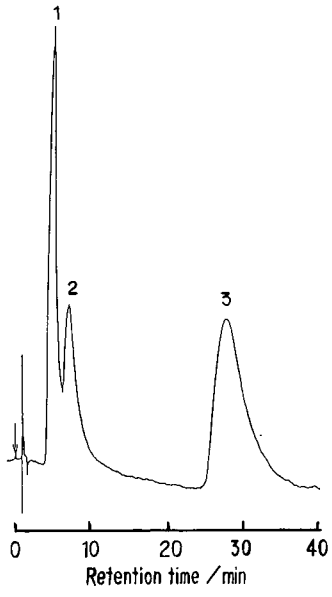


Fig. 2. Typical chromatogram of trialkylamines. Mobile phase, acetonitrile–phosphate buffer (pH 7.3) (20:80, v/v) + 50 m*M* ammonium acetate; flow-rate, 1 ml/min; applied voltage, 1000 mV *vs.* Ag/AgCl; temperature, 25°C. Peaks: 1 = trimethylamine (50 ng); 2 = triethylamine (50 ng); 3 = tri-*n*-propylamine (100 ng).

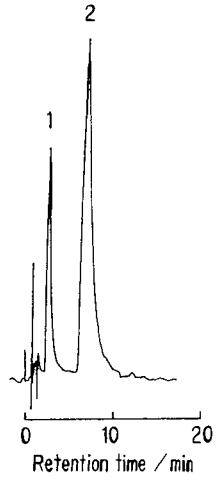


Fig. 3. Typical chromatogram of di- and tri-*n*-propylamine. Mobile phase, acetonitrile–phosphate buffer (pH 7.0) (40:60, v/v) + 50 m*M* ammonium acetate; flow-rate, 1 ml/min; applied voltage, 1100 mV *vs.* Ag/AgCl; temperature, 25°C. Peaks: 1 = di-*n*-propylamine (30 ng); 2 = tri-*n*-propylamine (100 ng).

ducibility was obtained for repeated injections [trimethylamine: sample size, 10 ng; relative standard deviation ($n$ = 5) = 3.5%]. With dialkylamines, linearity was observed under almost the same conditions as for trialkylamines. The minimum detectable amount of dialkylamines was found to be *ca.* 10 ng.

*Effect of the concentration of acetonitrile in the mobile phase on the retention of trialkylamines*

The retention times of trialkylamines altered with variation of the concentration of acetonitrile in the mobile phase. Some results are given in Table II.

For trimethylamine, the retention time increased with increase in the concentration of acetonitrile, for tri-*n*-propyl- and tri-*n*-butylamine it decreased and for triethylamine it scarcely changed. These results indicate that the elution order of trialkylamines can be reversed by increasing the concentration of acetonitrile in the mobile phase. This elution behaviour is not the same as that in ordinary reversed-phase liquid chromatography.

*Retention mechanism of tri- and dialkylamines*

Many workers have observed cation-exchange characteristics during the reversed-phase chromatography of cations on silica-based column [9–15], but the retention mechanism of reversed-phase ion-pair liquid chromatography is not yet clearly established.

In the present instance, the retention mechanism can be explained as follows. There are two processes involved: ion interaction (silanophilic) and solvophobic interactions. For more hydrophobic solutes, such as tripropyl- and tributylamines, solvophobic interactions predominate, whereas for the less hydrophobic trimethylamine silanophibic interactions dominate.

Ammonium acetate added as a supporting electrolyte plays an important role as a competing base. Increasing the ammonium ion concentration in the eluent can improve the peak retention and peak shape (Fig. 4). This change can be explained as follows: because of its relatively high concentration, ammonium ion is preferentially adsorbed by the silanol groups, thus minimizing the adsorption of amine. However, concentrations of ammonium ion in the eluent above 50 m*M* do not improve the peak retention and peak shape further.

TABLE II

RETENTION TIMES OF TRIALKYLAMINES (min)

| $R_3N$ | Acetonitrile: buffer solution | | | | |
|---|---|---|---|---|---|
| | 7:3 (pH 7.76)[a] | 6:4 (pH 7.74)[a] | 5:5 (pH 7.74)[a] | 3:7 (pH 7.50)[a] | 2:8 (pH 7.42)[a] |
| Methyl | 5.3 | 4.4 | 4.2 | 2.4 | 2.2 |
| Ethyl | 3.5 | 3.3 | 3.6 | 2.8 | 3.2 |
| *n*-Propyl | 3.2 | 4.0 | 5.2 | 8.8 | 13.0 |
| *n*-Butyl | 3.8 | 6.1 | 10.8 | – | – |

[a] Apparent pH.

*Application to trace analysis*

Small amounts of trimethylamine in air and water were determined by this HPLC method as a demonstration of its application to trace analysis.

*Determination of small amounts of trimethylamine in air.* A Sep-Pak $C_{18}$ cartridge was used for the trace determination of trimethylamine in air. A Sep-Pak $C_{18}$ cartridge was washed with 5 ml of acetonitrile, then dried by passing a stream of dry nitrogen at 80–100 ml/min for 30 min. The collection efficiency of trimethylamine was investigated by using two Sep-Pak $C_{18}$ cartridges in series. All the trimethylamine was recovered on the first cartridge.

The sampling and analytical procedure was as follows. A 2–100-l air sample was passed through the Sep-Pak $C_{18}$ cartridge with a stream of dry nitrogen at 0.5–1.5 l/min. The trimethylamine adsorbed on the cartridge was extracted with a few millilitres of acetonitrile–water (30:70, v/v) containing 50 m*M* ammonium acetate. The eluate was diluted to 10 ml with acetonitrile. A 10–50-$\mu$l aliquot of the solution was injected into the liquid chromatograph and the eluate was monitored with the amperometric detector at an applied voltage of 1000 mV *vs.* Ag/AgCl. The minimum detectable amount of trimethylamine was found to be 1 ng.

Synthetic air samples fortified with trimethylamine were prepared in a 2-l gas sampling bottle. The recoveries of trimethylamine are given in Table III; in each instance, 75–90% recoveries were achieved. The limit of determination is a few $\mu$g/l. This method can easily be used for the selective and

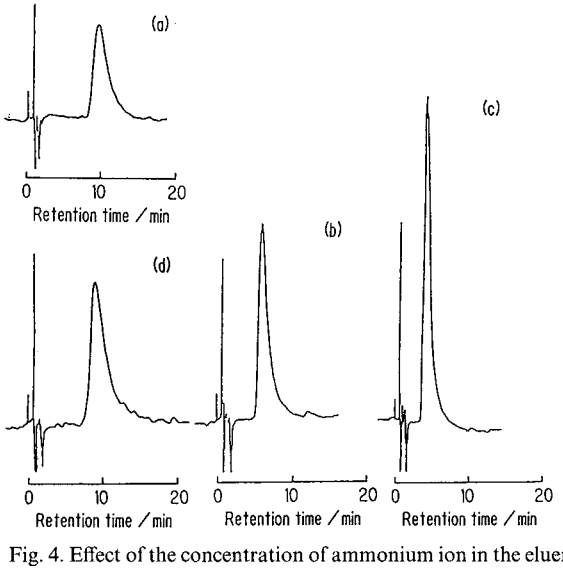


Fig. 4. Effect of the concentration of ammonium ion in the eluent on the chromatogram of trimethylamine. Mobile phase: (a) acetonitrile–phosphate buffer (pH 7.0) (40:60, v/v); (b) (a) + 30 m*M* ammonium acetate; (c) (a) + 50 m*M* ammonium acetate; (d) (a) + 50 m*M* sodium acetate. Amount of trimethylamine, 30 ng; flow-rate, 1 ml/min; applied voltage, 1000 mV *vs.* Ag/AgCl; temperature, 25°C.

TABLE III

RECOVERIES OF TRIMETHYLAMINE IN AIR

| Trimethylamine ($\mu$g) | | Recovery (%) |
|---|---|---|
| Taken | Found | |
| 5 | 3.8 | 76 |
| 10 | 8.5 | 85 |
| 20 | 17.6 | 88 |
| 40 | 35.1 | 86 |

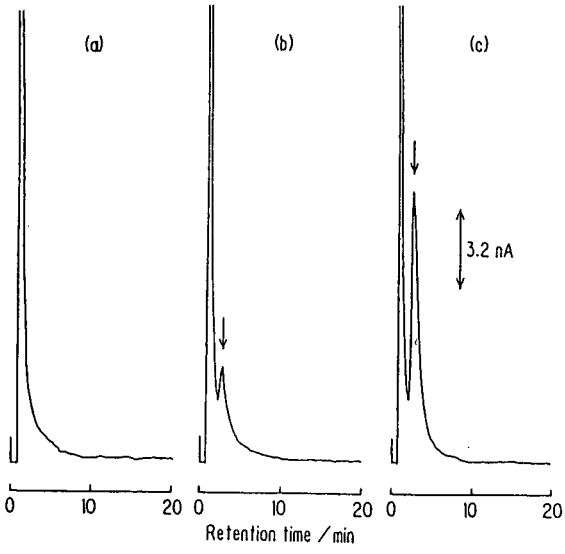


Fig. 5. Typical chromatogram of trimethylamine in water. Concentration of trimethylamine: (a) blank (river water); (b) 0.5 mg/l; (c) 2.0 mg/l. For chromatographic conditions, see the text.

sensitive determination of trace amounts of trimethylamine in air.

*Determination of small amounts of trimethylamine in water.* A 10-$\mu$l sample of water fortified with trimethylamine was injected directly into the chromatograph through a membrane filter (0.45 $\mu$m). The eluate was monitored with the amperometric detector at an applied voltage of 1000 mV *vs.* Ag/AgCl. Fig. 5 shows typical chromatograms of trimethylamine in water (Tama River, Japan) at fortification levels of 0.5 and 2.0 mg/l.

The limit of determination is 0.2 mg/l. For ultra-trace analysis, trimethylamine is transferred from the aqueous to the vapour phase by bubbling a stream of nitrogen through the water sample (the pH of the water sample has to be taken into consideration) and the vapour obtained is swept through a Sep-Pak $C_{18}$ cartridge to collect the trimethylamine.

## CONCLUSIONS

The retention behaviour of tri- and dimethylamines here is different to that in ordinary reversed-phase liquid chromatography. Ammonium acetate added as a supporting electrolyte plays an important role as a competing base. This behaviour can be explained by both ion and solvophobic interactions.

This method can be used for the simple determination of small amounts of trimethylamine in environmental samples.

## REFERENCES

1 B. Bjorkqvist, *J. Chromatogr.*, 204 (1981) 109.
2 F. K. Chow and E. Grushka, *Anal. Chem.*, 49 (1977) 1756.
3 A. S. Narang, D. R. Choudhury and A. Richards, *J. Chromatogr. Sci.*, 20 (1982) 235.
4 I. Kifune and K. Oikawa, *Bunseki Kagaku*, 28 (1979) 587.
5 R. C. Simpson, H. Y. Mohanmmed and H. Veening, *J. Liq. Chromatogr.*, 5 (1982) 245.
6 Y. Suzuki and R. Miyagawa, *Bunseki Kagaku*, 30 (1981) 81.
7 J. R. Rice and P. T. Kissinger, *Environ. Sci. Technol.*, 16 (1982) 263.
8 M. Maruyama and M. Kakemoto, *Nippon Kagaku Kaishi*, (1978) 1646.
9 D. Westerland and A. Theodorson, *J. Chromatogr.*, 144 (1977) 27.
10 B. A. Bidlingmeyer, S. N. Deming, W. P. Price, Jr., B. Sachok and N. Petrusek, *J. Chromatogr.*, 186 (1979) 419.
11 W. R. Melander and Cs. Horváth, *J. Chromatogr.*, 201 (1980) 211.
12 K. E. Bij, Cs. Horváth, W. R. Melander and A. Nahum, *J. Chromatogr.*, 203 (1981) 65.
13 J. H. Knox and R. A. Hartwick, *J. Chromatogr.*, 204 (1981) 3.
14 G. B. Cox and R. W. Stout, *J. Chromatogr.*, 384 (1987) 315.
15 N. E. Hoffman and J. C. Liao, *J. Chromatogr. Sci.*, 28 (1990) 428.

*Journal of Chromatography*, 594 (1992) 165–171
Elsevier Science Publishers B.V., Amsterdam

CHROM. 23 780

# Chromatography of 99 amino acids and other ninhydrin-reactive compounds in the Pickering lithium gradient system

John A. Grunau* and John M. Swiader

*Horticulture Department, University of Illinois, 1707 South Orchard Street, Urbana, IL 61801 (USA)*

(Received September 10th, 1991 )

ABSTRACT

High-performance liquid chromatographic systems can be adapted to the high-resolution determination of free amino acids with hardware and reagents from Pickering Labs. The lithium-based eluent gradients used allow good separations to be achieved isothermally in 2 h. Although the overall elution pattern correlates strongly with those of established automated methods, the differences can be large, and are numerous enough that one type of system cannot serve as a predictor for the other. Relative retention times in the Pickering system were determined for 99 ninhydrin-positive compounds: imino acids, ureides, amino sugars, amino acids and derivatives, with emphasis on those occurring in plants.

## INTRODUCTION

Automated analyses of the amino acids derived from proteins, based on cation-exchange chromatography with post-colum ninhydrin derivatization [1], found widespread application with a variety of instruments dedicated to that purpose. Many commercial amino acid analyzers have been produced worldwide, including, in the USA, those from Technicon (Tarrytown, NY, USA), Beckman Instrument (Fullerton, CA, USA), Durrum Instruments (Palo Alto, CA, USA) and Phoenix Precision Instruments (Philadelphia, PA, USA). Run times were usually several hours, and for the much more difficult separations of so-called physiological amino acids (the highly complex mixtures of free amino acids and related compounds found in both animal and plant materials) could range up to 25 h. These systems used automated changes of eluent buffers, stepwise or gradient, and automated changes in column temperature, to achieve critical separations [2]. The advent of higher performance resins and lithium-based eluents facilitated such separations in much shorter run times [3].

Further developments included greater sensitivity from postcolumn reagents allowing fluorescence detection, the rapid derivatizations at ambient temperature encouraging the use of non-dedicated high-performance liquid chromatographic (HPLC) equipment [4]. In addition, the introduction of several precolumn reagents yielding relatively hydrophobic derivatives allowed the entirely different chromatographic principles of reversed-phase HPLC to be exploited [4]. Rapid high-resolution separations thus became attainable, although not without drawbacks. Some reagents yield unstable derivatives; others may produce artefactual peaks and/or multiple peaks from single amino acids; most do not react with secondary amines; and the complex matrices of physiological mixtures can interfere with smooth derivatization [5,6]. More importantly, matrix variation can lead to considerable uncertainty in elution times [7].

In contrast, ion exchange is relatively insensitive to matrix components other than easily removed proteins. The ion-exchange columns and postcolumn hardware developed by Pickering Labs. permit the adaptation of suitable (*i.e.*, rapid-pulse or essen-

0021-9673/92/$05.00 

tially pulseless) HPLC systems to the high-resolution determination of free, non-derivatized amino acids. For physiological amino acids (lithium system) the eluent gradients employed permit good separations to be achieved isothermally in a 2 h run to arginine. We adopted this system for the dual purpose of determining the basic amino acid S-methylmethionine in corn [8] and the free amino acids in plant roots. Ninhydrin was the reagent of choice because it reacts with a wide range of compounds, including secondary amines, and can provide valuable structural information when absorbance is measured at more than one wavelength.

With the Pickering system, despite the overall similarities, there are many substantial differences in elution order compared with automated sodium-based eluent methods, stepwise or gradient [9–11]. The points of difference with a lithium gradient technique [12] are fewer, but still significant. We present here the results of a chromatographic survey of 99 amino acids and related compounds, most chosen because they occur in plants or are known metabolic inhibitors [13–15].

## EXPERIMENTAL

### *Biochemicals*

Forty-four compounds are present in the solution (Amino Acid Calibration Standard) provided by Pickering Labs. (Mountain View, CA, USA) for their lithium Physiologic Fluid columns. The remainder were purchased from Sigma (St. Louis, MO, USA), except for the two dimethylated arginines ($N^{G1}$Me,$N^{G2}$Me; $N^{G1}$diMe), which were gifts from Pickering.

### *Chromatography*

The compounds were separated by the lithium system for physiological fluids, the Pickering 150 × 3 mm I.D., 5-μm column ("high efficiency", formerly "fast run") being used. This system was combined with an HP1090 liquid chromatograph (Hewlett-Packard, Palo Alto, CA, USA), modified by dead-heading the pressure transducer to prevent its corrosion by the lithium citrate–chloride eluents [8]. The detector was an Altex/Hitachi Model 100-10 spectrophotometer (Beckman Instruments, Fullerton, CA, USA) and the integrator/recorder was a Shimadzu (Columbia, MD, USA) Model CR3A. Li280 and Li750 eluents (eluents A and B), RG003 regenerant (lithium hydroxide–chloride, eluent C), diluent and ninhydrin reagent were all from Pickering.

The chromatographic conditions were as follows. The column temperature was 42°C and the gradient program was as shown in Table I. This is the standard Pickering program modified slightly to improve some separations, plus an extension to remove homoarginine and to clean the column with 100% (or 99.6%) regenerant between runs. The latter, plus a more essential *ca.* 10-min regenerant wash prior to the first run of the day, was found to be necessary to eliminate ghost peaks. The 99.6% regenerant was used rather than 100% solely because the controlling HP 85B computer cannot handle gradients between eluents B and C alone, *i.e.*, with 0% A. Therefore, 0.4% A was the minimum used. Each regenerant wash was followed by equilibration with eluent A for 25–30 min prior to injection. Injected mixtures were in pH 2.2 diluent and the loop size was 10 μl. The eluent flow-rate was 0.30 ml/min, ninhydrin flow-rate *ca.* 0.3 ml/min and post column reaction temperature 130°C. The monitored wavelength was 570 nm throughout. (Multi-wavelength monitoring with the HP 1040A diode-array detector proved impossible. The system's software prevents the use of this instrument, at any wavelength, when the liquid phase absorbs very strongly in the ultraviolet region, as does the ninhydrin reagent.)

TABLE I

GRADIENT PROGRAM

| Time (min) | Eluent A (Li280) (%) | Eluent B (Li750) (%) | Eluent C (RG003) (%) |
|---|---|---|---|
| 0.0 | 100.0 | 0.0 | 0.0 |
| 9.0 | 100.0 | 0.0 | 0.0 |
| 21.0 | 90.5 | 9.5 | 0.0 |
| 33.0 | 80.0 | 20.0 | 0.0 |
| 49.0 | 65.0 | 35.0 | 0.0 |
| 88.0 | 0.4 | 99.6 | 0.0 |
| 94.6 | 0.4 | 99.6 | 0.0 |
| 120.0 | 0.4 | 93.6 | 6.0 |
| 120.5 | 0.4 | 93.6 | 6.0 |
| 126.5 | 0.4 | 0.0 | 99.6 |
| 134.5 | 0.4 | 0.0 | 99.6 |
| 135.0 | 100.0 | 0.0 | 0.0 |

## RESULTS AND DISCUSSION

The results are given in Table II. The twenty protein amino acids are designated by their standard single-letter symbols, the remaining compounds by number in order of elution. The precise retention times may vary slightly from one run to another, one influence being length of preinjection equilibration, and some differences would be expected with other HPLC configurations. However, these retention times will be good indicators of *relative* positions under the stated conditions. In this regard, however, it should be noted that this project was begun with one kind of column and finished with another, packed with resin from a newly acquired source. This resin's properties were sufficiently different that the composition of eluent A, previously designated Li275, was changed to compensate. The new designation became Li280, although both eluents A were actually of pH 2.75 [16]. Differences in relative retention times between the two columns were minor in most instances, one such resulting in a poorer proline–glycine separation. However, all three amino sugars eluted from the new column 3 min earlier in relation to adjacent amino acids (suggesting a higher degree of cross-linking in the new resin [10]). The retention times and profiles presented here were all obtained with the latter column and Li280.

Of the 99 compounds surveyed, 62 elute in the first one-third of the profile. Therefore, to illustrate peak positions and shapes, the compounds were split between three different runs, shown in Figs. 1–3. As markers for profile 2, the following from profile 1 were added: glutamic acid (E), valine (V), $\beta$-alanine (67), $\delta$-hydroxylysines (77) and canavanine (91). For profile 3, the markers were aspartic acid (D), proline (P), valine and $\beta$-alanine. Included in Table II but not in these profiles were homoglutamine (31), oxidized glutathione (33) and selenomethionine (58). In profile 1 the amount of each compound injected was *ca.* 2 nmol, except for creatinine (80), 20 nmol, and dimethylarginine (95), unknown. In profile 2 each was at 2 nmol except for $N^{G1}$-methyl, $N^{G2}$-methylarginine (96), unknown (the two dimethylarginines were provided by Pickering as solutions of unstated concentration). Some oxidation of homocysteine (51) to homocystine (69) was apparent. In profile 3 the following components, which react weakly with ninhydrin and/or yield derivatives that absorb sub-optimally at 570 nm, were at 20 nmol: allantoic acid (4), allantoin (7), hydroxyproline (16), aminooxyacetic acid (20), 5-hydroxypipecolic acid (30), proline, pipecolic acid (49) and 1-aminocyclopropane-1-carboxylic acid (55). The remainder were at 2 nmol. The urea (11) in profile 3 was derived from the breakdown of allantoic acid, which is markedly unstable under these conditions. Carbamyl phosphate (1) and argininosuccinic acid (61) are also unstable at pH 2.2, the latter giving rise to an additional unidentified peak (X) at 57.8 min.

N-Acetylglutamic acid and N-acetylglutamine, eluting at 2.80 and 2.88 min, respectively, react with ninhydrin at only *ca.* $1 \cdot 10^{-4}$ and $3 \cdot 10^{-4}$ times the rates of the corresponding non-acetylated compounds, and are not included in Table II or the profiles. Similarly, N-acetylglucosamine and adenosine-5′-monophosphate also were chromatographed but did not react significantly with ninhydrin under these conditions, as monitored at 570 nm; nor did cytidine-5′-monophosphate, even though the oxidative deamination of cytosine is known to occur in DNA as a long-established pathway of spontaneous mutation [17]. The chromatography of octopine [N-(D-1-carboxyethyl)arginine], widely distributed in plants, yielded a detectable peak only in the position of free arginine.

With regard to the lack of matrix influence on the behavior of amino acids in ion exchange chromatography, our work confirms that such influences appear to be very minor. The only noticeable matrix effects so far have been on aspartic acid. From extracts of both corn kernels [8] and pumpkin roots (unpublished work) made with 3.5% sulfosalicylic acid, ultrafiltered through a membrane with a 5000 molecular weight cut-off, adjusted to pH 2.2 and diluted 1:1 with diluent prior to injection, aspartic acid eluted 1 min *later* than usual. In addition, as a comparison of Figs. 1 and 3 shows, the sharpness, though not the retention time, of the aspartic acid peak can be affected by other amino acids in the mixture. In Fig. 1 the aspartic acid and valine peaks are of similar height, but in the mixture in Fig. 3 the aspartic acid peak (now off-scale) is reproducibly about 60% taller.

The resolving power, speed, matrix indifference and cost of the Pickering system appear to present a

TABLE II

ORDER OF ELUTION

| Retention time (min) | Symbol/No. | Compound | Described in plants (P) |
|---|---|---|---|
| 2.25 | 1 | Carbamyl phosphate | P |
| 2.28 | 2 | L-Cysteic acid | |
| 2.42 | 3 | O-Phospho-DL-serine | P |
| 2.95 | 4 | Allantoic acid | P |
| 3.2 | 5 | D-Glucosamine-6-phosphate | |
| 3.4 | 6 | Taurine (2-aminoethanesulfonic acid) | P |
| 3.6 | 7 | Allantoin | P |
| 3.7 | 8 | DL-*threo*-β-Hydroxyaspartic acid | |
| 3.9 | 9 | O-Phosphoethanolamine | P |
| 4.5 | 10 | Mannopine [$N^{\alpha}$-(1-D-mannityl)-L-glutamine] | |
| 5.1 | 11 | Urea | P |
| 6.3 | 12 | β-Cyano-L-alanine | P |
| 6.5 | 13 | N-Methyl-L-aspartic acid | |
| 8.8 | 14 | Glutathione (reduced form) | P |
| 9.4 | D | L-Aspartic acid | P |
| 10.5 | 16 | L-Hydroxyproline | P |
| 10.7 | 17 | O-Acetyl-L-serine | P |
| 12.5,13.0 | 18 | L-Methionine sulfoxides | |
| 13.0 | T | L-Threonine | P |
| 13.3 | 20 | Aminooxyacetic acid | |
| 13.7 | S | L-Serine | P |
| 14.9 | N | L-Asparagine | P |
| 15.8 | E | L-Glutamic acid | P |
| 16.1 | 24 | L-Azetidine-2-carboxylic acid | P |
| 16.9 | Q | L-Glutamine | P |
| 17.4 | 26 | DL-β-Hydroxynorvaline | |
| 17.5 | 27 | L-Homoserine | P |
| 17.5+ | 28 | L-Albizziine | P |
| 19.4 | 29 | Sarcosine | P |
| 19.5 | 30 | 5-Hydroxy-L-pipecolic acid | P |
| 19.6 | 31 | L-Homoglutamine | |
| 19.9 | 32 | γ-Methylene-DL-glutamic acid | P |
| 20.5B | 33 | Glutathione (oxidized) | P |
| 21.2 | 34 | DL-α-Aminoadipic acid | P |
| 21.6 | C | L-Cysteine | P |
| 22.5 | 36 | S-Methyl-L-cysteine | P |
| 25.2 | P | L-Proline | P |
| 25.8 | G | Glycine | P |
| 25.9 | 39 | D-Glucosamine | P |
| 27.3 | A | L-Alanine | P |
| 27.4B | 41 | D-Mannosamine | P |
| 27.9 | 42 | L-Citrulline | P |
| 28.8B | 43 | D-Galactosamine | P |
| 29.1 | 44 | $N^{\varepsilon}$-Acetyl-L-lysine | P |
| 29.5 | 45 | L-α-Aminobutyric acid | P |
| 31.1 | V | L-Valine | P |
| 32.8 | 47 | L-Cystine | P |
| 33.3 | 48 | L-Saccharopine [$N^{\varepsilon}$-(L-glutar-2-yl)-L-lysine] | P |
| 33.7 | 49 | L-Pipecolic acid | P |
| 34.7 | 50 | α-Methyl-DL-methionine | |
| 34.8 | 51 | DL-Homocysteine | P |

TABLE II (*continued*)

| Retention time (min) | Symbol/No. | Compound | Described in plants (P) |
|---|---|---|---|
| 35.8 | M | L-Methionine | P |
| 36.6 | 53 | Glycylglycine | |
| 37.4 | 54 | L-Cystathionine | P |
| 38.3 | 55 | 1-Aminocyclopropane-1-carboxylic acid | P |
| 38.7 | 56 | $N^{\alpha}$-Acetyl-L-ornithine | |
| 38.8 | I | L-Isoleucine | P |
| 40.3 | 58 | L-Selenomethionine | P |
| 40.4 | L | L-Leucine | P |
| 40.6 | 60 | DL-α,ε-Diaminopimelic acid | P |
| 40.9 | 61 | Argininosuccinic acid[b] | P |
| 42.3 | 62 | L-Norleucine | |
| 44.2 | Y | L-Tyrosine | P |
| 44.2 | 64 | L-Methionine sulfoximine | |
| 47.1 | F | L-Phenylalanine | P |
| 47.2 | 66 | L-Glutamic acid amide (isoglutamine) | |
| 51.1 | 67 | β-Alanine | P |
| 53.9 | 68 | DL-β-Aminoisobutyric acid | P |
| 55.8 | 69 | DL-Homocystine | P |
| 56.9 | 70 | δ-Aminolevulinic acid | P |
| 61.4B | 71 | 5-Hydroxy-L-tryptophan | P |
| 62.9 | 72 | γ-Aminobutyric acid | P |
| 64.1 | 73 | DL-Kynurenine | P |
| 64.3 | 74 | 3-Hydroxy-DL-kynurenine | |
| 72.5B | W | L-Tryptophan | P |
| 76.5 | 76 | Ethanolamine | P |
| 80.0,81.3 | 77 | δ-Hydroxylysines (DL- and DL-*allo*-) | P |
| 82.4 | 78 | Ammonia | P |
| 84.4 | 79 | ε-Amino-*n*-caproic acid | |
| 85.8 | 80 | Creatinine | P |
| 90.1 | 81 | L-Ornithine | P |
| 90.2 | 82 | L-α,γ-Diaminobutyric acid | P |
| 93.3 | K | L-Lysine | P |
| 96.3 | H | L-Histidine | P |
| 98.2 | 85 | 3-Methyl-L-histidine (τ-methyl-L-histidine) | P |
| 99.3 | 86 | $N^{\varepsilon}$-Methyl-L-lysine | P |
| 100.1 | 87 | 1-Methyl-L-histidine (π-methyl-L-histidine) | |
| 102.4 | 88 | L-Homocarnosine (γ-aminobutyryl-L-histidine) | |
| 102.7 | 89 | L-Carnosine (β-alanyl-L-histidine) | |
| 104.3 | 90 | L-Anserine (β-alanyl-1-methyl-L-histidine) | |
| 107.1 | 91 | L-Canavanine | P |
| 108.0 | 92 | S-Methyl-DL-methionine | P |
| 108.5 | 93 | L-α-Amino-β-guanidinopropionic acid | |
| 109.4 | 94 | L-Leucinamide | |
| 116.8 | 95 | $N^{G1}$-Dimethyl-L-arginine | |
| 117.3 | 96 | $N^{G1}$-Methyl,$N^{G2}$-methyl-L-arginine | |
| 120.4 | 97 | $N^{G}$-Methyl-L-arginine | |
| 120.6 | R | L-Arginine | P |
| 128.1 | 99 | L-Homoarginine | P |

[a] B denotes broad peak (ratio of height to width at half-height $\leq 10$, with the chromatography and chart parameters used here).
[b] Isomeric constitution unknown.

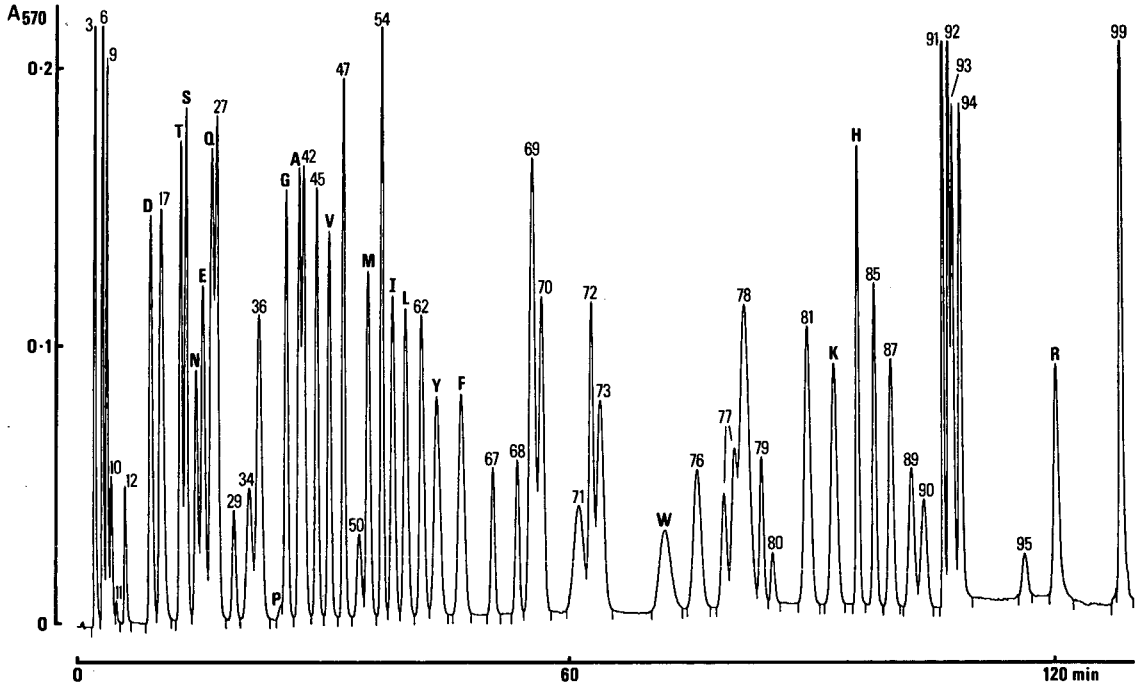


Fig. 1. Chromatographic profile of 59 amino acids and related compounds. Gradient program as in Table I. Injected amounts *ca.* 2 nmol except for 80 (20 nmol) and 95 (not determined).

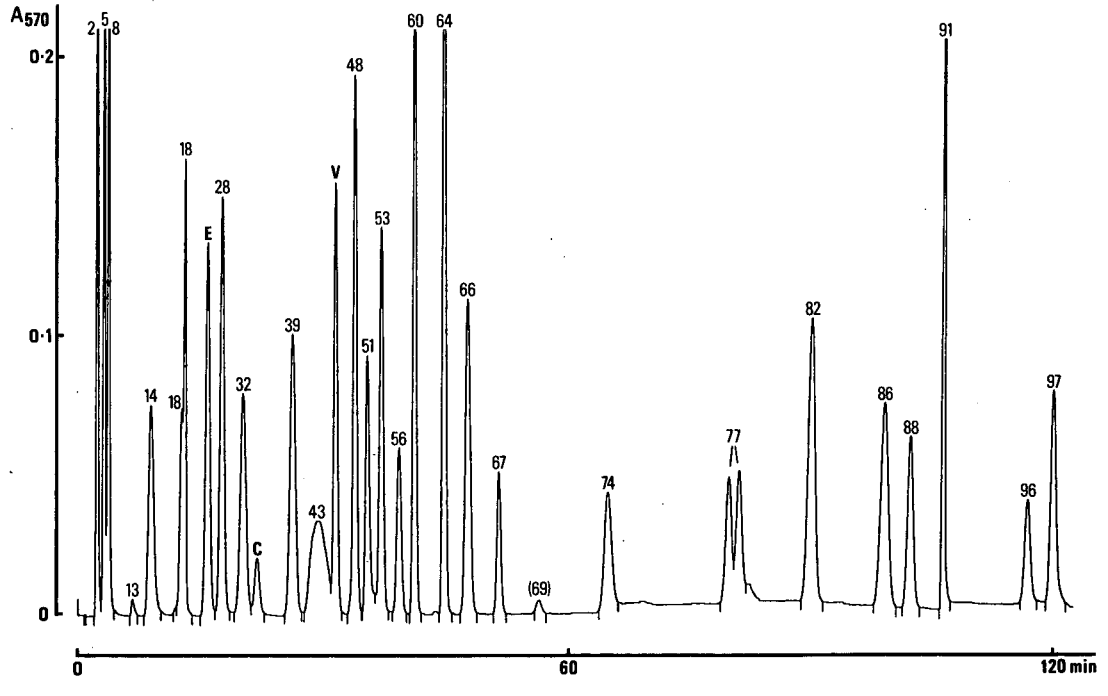


Fig. 2. As for Fig. 1, for 29 compounds. All at 2 nmol except for 96 (not determined). Peak 69: oxidation product of 51.

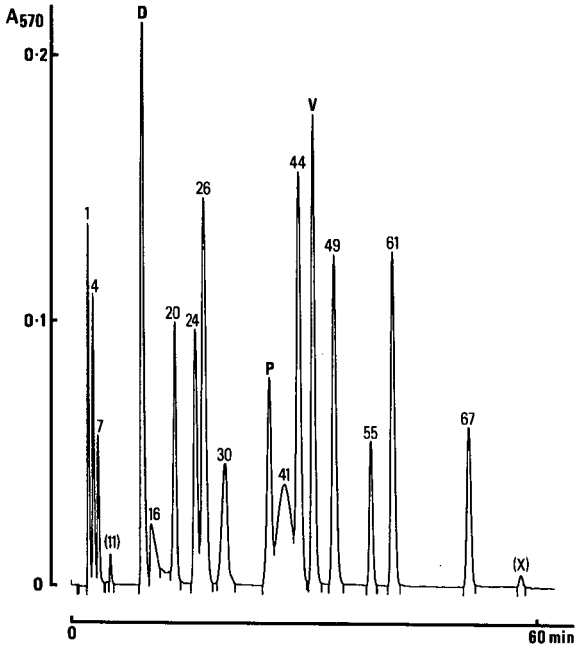


Fig. 3. As for Fig. 1, for 17 compounds. Peaks D, V, 1, 24, 26, 41, 44, 61 and 67 injected at 2 nmol, the remainder at 20 nmol. Peak 11: breakdown product of 4. Peak X: unidentified breakdown product of 61.

relatively favorable combination. Also, because of the first two factors, almost all amino acids elute within small volumes of eluent, 0.2–0.6 ml for the nanomolar amounts employed in this study. This suggests that the most challenging separation problems, those likely to be encountered in the often crowded first 40 min of a profile, especially when concentrations of neighboring components differ widely, could profitably be attacked in the following way. Rather than stretch the profile by using shallower gradients, a more promising approach would be first to apply this system, minus ninhydrin, in order to collect selected narrow bands of the eluate, then, after suitable derivatization in this now-simple matrix, to take advantage of the different separation principles of reversed-phase HPLC. Conceivably, the same piece of HPLC equipment could be utilized for both modes.

ACKNOWLEDGEMENTS

This research was supported by Project 65-332 of the Illinois Agricultural Experiment Station, University of Illinois at Urbana–Champaign. We thank Dr. Gary L. Salmon, Illinois State Geological Survey, for the generous loan of a Hewlett-Packard ChemStation computer that facilitated the completion of this work.

REFERENCES

1 D. H. Spackman, W. H. Stein and S. Moore, *Anal. Chem.*, 30 (1958) 1190.
2 J. V. Benson, Jr., and J. A. Patterson, in A. Niederwieser and G. Pataki (Editors), *New Techniques in Amino Acid, Peptide and Protein Analysis*, Ann Arbor Sci. Publ., Ann Arbor, MI, 1971, Ch. 1, p. 1.
3 J.V. Benson, Jr., M. J. Gordon and J. A. Patterson, *Anal. Biochem.*, 18 (1967) 228.
4 R. E. Pfeiffer and D. W. Hill, *Adv. Chromatogr.*, 22 (1983) 37.
5 R. Bongiovanni, A. R. Glass and T. M. Boehm, in G. L. Hawk (Editor), *Biological/Biomedical Applications of Liquid Chromatography III*, Marcel Dekker, New York, 1981, p. 211.
6 A. Oaks, I. L. Boesel, V. J. Goodfellow and M. J. Winspear, in H. Lambers, J. J. Neeteson and I. Stulen (Editors), *Fundamental, Ecological and Agricultural Aspects of Nitrogen Metabolism in Higher Plants*, Martinus Nijhoff, Dordrecht, 1986, p. 197.
7 M. V. Pickering, *LC · GC*, 7 (1989) 484.
8 J. A. Grunau and J. M. Swiader, *Commun. Soil Sci. Plant Anal.*, 22 (1991) 1873.
9 R. M. Zacharius and E. A. Talley, *Anal. Chem.*, 34 (1962) 1551.
10 P. B. Hamilton, *Anal. Chem.*, 35 (1963) 2055.
11 Y. Mardens, M. van Sande and J. Caers, *Anal. Lett.*, 4 (1971) 285.
12 P. Adriaens, B. Meesschaert, W. Wuyts, H.Vanderhaeghe and H. Eyssen, *J. Chromatogr.*, 140 (1977) 103.
13 G. A. Rosenthal, *Plant Nonprotein Amino and Imino Acids*, Academic Press, New York, 1982.
14 T. Robinson, *The Organic Constituents of Higher Plants*, Cordus Press, North Amherst, MA, 5th ed., 1983.
15 *The Merck Index*, Merck, Rahway, NJ, 11th ed. 1989.
16 M. V. Pickering, personal communication.
17 C. Coulondre, J. H. Miller, P. J. Farabaugh and W. Gilbert, *Nature (London)*, 274 (1978) 775.

*Journal of Chromatography*, 594 (1992) 173–178
Elsevier Science Publishers B.V., Amsterdam

CHROM. 23 857

# Determination of glutamine, glutamic acid and pyroglutamic acids using high-performance liquid chromatography on dynamically modified silica

B. Polanuer*, A. Sholin, N. Demina and N. Rumiantseva

*Institute for Genetics of Industrial Microorganisms, Dorozny pr. 1, 113545 Moscow (Russia)*

(First received July 3rd, 1991; revised manuscript received November 7th, 1991)

ABSTRACT

For the determination of glutamine and the products of its degradation, glutamic and pyroglutamic acids, in fermentation broth and other biotechnological samples, a rapid and convenient high-performance liquid chromatographic method is proposed. The method is based on the separation of these compounds on silica dynamically modified with Cu(II) ions. Modification is obtained by the addition of copper sulphate to the mobile phase. The copper complexes of amino acids, including pyroglutamic acid, are easily formed in the column and are detected by UV absorption at 235 nm. If it is necessary to improve the separation, an ion-pairing reagent (sodium dodecyl sulphate) is added to the mobile phase. Using this method, the levels of glutamine and related compounds are determined in fermentation media of industrial strains and other biotechnological samples. The total time of analysis is less then 10 min with a detection limit of 0.1 g/l.

## INTRODUCTION

Glutamine is used as a medicine and as a component of tissue culture media. It has been demonstrated that glutamine is unstable and is easily converted into glutamic acid and pyroglutamic (5-oxoproline, 2-pyrrolidone-5-carboxylic) acid.

In our study of glutamine and glutamic acid production by biotechnological methods, a simple and sensitive technique for the determination of glutamine and related products in technological solutions is necessary. The aim of this work was to develop such a method suitable for the simultaneous determination of glutamine, glutamic acid and pyroglutamic acid in biotechnological samples.

Analysis of amino acids is a routine task in biochemistry, medicine, biotechnology and another fields, and different approaches have been proposed. Ion-exchange chromatography with post-column derivatization, pre-column derivatization and reversed-phase chromatography are the most widely used methods [1]. Usually such techniques are developed for the analysis of protein amino acids and are suitable for the determination of glutamine and glutamic acid. However, pyroglutamic acid has a tertiary nitrogen atom which does not participate in the conventional reactions used to form detectable amino acid derivatives.

Several gas chromatographic methods have been proposed for glutamine analysis. These methods are suitable for the determination of pyroglutamic acid but include the complex and time-consuming production of volatile derivatives [2,3].

For the determination of pyroglutamic and glutamic acids in glutamine preparations, it has been proposed to use high-performance liquid chromatographic (HPLC) separation on an ion-exchange column with UV detection at 210 nm. The total time of the analysis is about 20 min [4]. It has also been recommended to determine pyroglutamic acid using reversed-phase chromatography with UV detection at 200 nm. Glutamine and glutamic acid have been determined as *o*-phthalaldehyde derivatives by chromatography, but this technique was very time

0021-9673/92/$05.00 

consuming [5]. Neither approach was selective enough for the analysis of fermentation media, which usually contain many organic acid, carbohydrates and other compounds that strongly adsorb in the range 200–210 nm.

Another approach to the separation and detection of amino acids is based on its ability to form a complexes with Cu(II) ions. Such complexes are detectable in the range 230–235 nm. The influence of the chromatographic conditions on such separations has been intensively studied. It was demonstrated that under isocratic conditions all the protein amino acids can be separated on a reversed-phase column using eluents containing ion-pair reagents [6,7]. This approach was recently used for the determination of proline in urine [8]. Modification of this method based on the column switching technique has also been described [9]. The method proposed have for the determination of glutamine and its degradation products in biotechnological samples is based on these studies.

## EXPERIMENTAL

Standard samples of glutamine, glutamic acid and pyroglutamic acid were purchased from Sigma, isopropanol (HPLC grade), sulphuric acid and sodium hydroxide (ACS grade) from Aldrich, sodium dodecyl sulphate from Serva and $CuSO_4 \cdot 10H_2O$ (analytical-reagent grade) from Soyuzchimreactiv HPLC-grade water was produced using a Milli-Q system (Millipore).

Stock standard solutions of glutamine, glutamic acid and pyroglutamic acid and samples of fermentation media were stored at −20°C and diluted just before use.

UV spectra of the copper(II) complexes of glutamine, glutamic acid and pyroglutamic acid were obtained using a Spectronic Model 2000 scanning spectrophotometer (Bauseh and Lomb).

All analyses were carried out using an LKB isocratic HPLC system consisting of a Model 2150 HPLC pump and a Model 2151 variable-wavelength monitor operated at 235 nm. Samples were injected using a Model 7410 injector with a 1-$\mu$l internal sample loop (Rheodyne). Stainless-steel columns (250 × 4 mm I.D.) packed with unmodified silica (5 $\mu$m) were obtained from Labor-MIM. Columns were thermostated at 40°C using a water jacket and Model U1 circulating thermostat. Chromatograms were recorded with a C-R1B computing integrator (Shimadzu) and calculated using the external standard method.

The eluent consisted of 0.01 *M* sodium dodecyl sulphate, 0.001 *M* copper(II) sulphate and up to 10% (v/v) of isopropanol. The flow-rate was 0.5 ml/min. Before analysis, the column was thermostated and equilibrated in the eluent for 1 h. At the end of the working period the column and detector

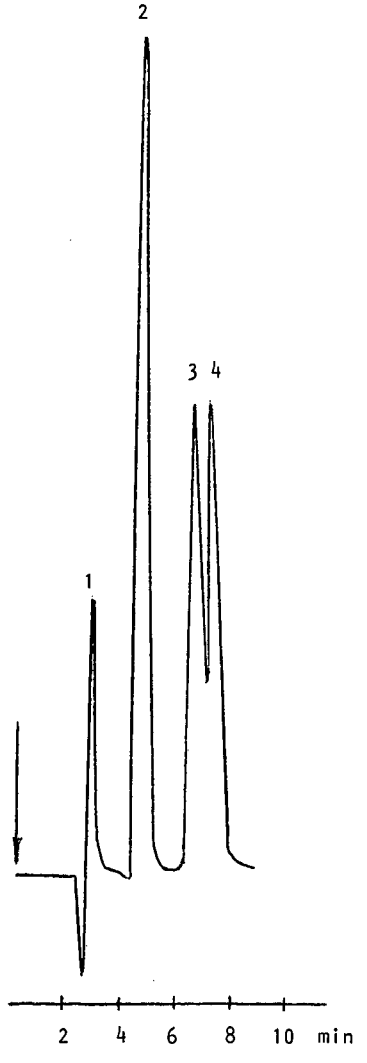


Fig. 1. Typical chromatogram of model mixture. Eluent, 0.001 *M* copper(II) sulphate–2.5% isopropanol; flow-rate, 0.5 ml/min; detection, UV at 235 nm. Peaks: 1 = pyroglutamic acid; 2 = glutamine; 3 = glutamic acid; 4 = proline. Concentrations, 0.5 g/l.

TABLE I

REGRESSION EQUATIONS AND CALIBRATION COEFFICIENTS OF CALIBRATION GRAPHS FOR THE SEPARATION OF GLUTAMINE AND RELATED COMPOUNDS WITH COPPER(II)-CONTAINING MOBILE PHASE

Concentration range, 0.1–100 g/l.

| Compound | Regression equation[a] | | Correlation coefficient ($r^2$) |
|---|---|---|---|
| | Slope | Intercept | |
| Pyroglutamic acid | 341.2 | −158.6 | 0.996 |
| Glutamic acid | 2325.6 | −2545.1 | 0.998 |
| Glutamine | 2683.3 | −1278.0 | 0.998 |

[a] Peak area = intercept + slope × concentration (g/l).

flow cell were cleaned with 200 ml of 40% aqueous isopropanol.

Fermentation media of glutamine- and glutamic acid-producing strains of *Corinebacterium glutamicum* were used for analysis. A typical sample contained up to 40 g/l of glutamine, 40 g/l of glutamic and 20 g/l of pyroglutamic acid. Cells were separated by centrifugation at 13 000 *g* for 3 min and the supernatant was diluted 50-fold and used for analysis without additional pretreatment.

To study the influence of pH on the stability of glutamine, the pH of the samples of the fermentation broth was adjusted with sodium hydroxide or sulphuric acid. Test-tubes with fermentation media were thermostated in a water-bath at 60°C.

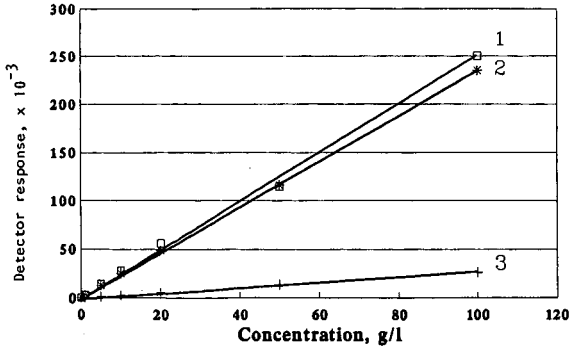


Fig. 2. Linearity of HPLC determination of glutamine, glutamic acid and pyroglutamic acids. Column, 5-μm silica (250 × 4 mm I.D.). Chromatographic conditions as in Fig. 1. The calculated areas are in arbitrary units. Lines: 1 = Glutamic acid; 2 = glutamine; 3 = pyroglutamic acid.

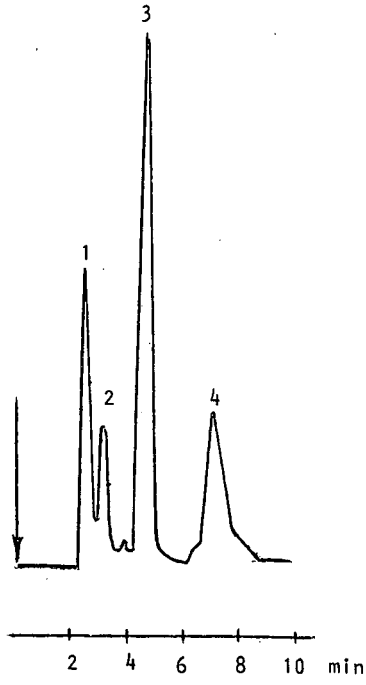


Fig. 3. Typical chromatogram of model mixture. Eluent, 0.001 *M* copper(II) sulphate–2.5% isopropanol–0.01 *M* sodium dodecyl sulphate; flow-rate, 0.5 ml/min; detection, UV at 235 nm. Peaks: 1 = ammonium sulphate; 2 = pyroglutamic acid; 3 = glutamic acid; 4 = glutamine.

## RESULTS AND DISCUSSION

Pyroglutamic acid also forms a complex with Cu(II) with an absorbance maximum at 226 nm. Therefore, such a complex can be determined using a conventional UV detector. Considering the ability of some keto acids to absorb at 210–220 nm, we decided to carry out the detection at the highest wavelength, 235 nm. The sensitivity to pyroglutamic acid under these conditions decreases about five-fold, but the selectivity increases. Therefore it is possible to determine glutamine, glutamic acid and pyroglutamic acid simultaneously as their copper complexes.

Analysis was carried out using silica dynamically modified with Cu(II) ions. Owing to the low ability of silica to undergo dispersive interactions, the retention time under such conditions is lower than on reversed-phase sorbents. Under the selected chromatographic conditions it is possible to separate all the studied compounds in model mixtures within 8

TABLE II

REGRESSION EQUATIONS AND CALIBRATION COEFFICIENTS OF CALIBRATION GRAPHS FOR THE SEPARATION OF GLUTAMINE AND RELATED COMPOUNDS WITH COPPER(II)–SODIUM DODECYL SULPHATE-CONTAINING MOBILE PHASE

Concentration range, 0.1–100 g/l.

| Compound | Regression equation[a] | | Correlation coefficient ($r^2$) |
|---|---|---|---|
| | Slope | Intercept | |
| Ammonium sulphate | 1016.4 | −85.5 | 0.998 |
| Pyroglutamic acid | 260.3 | −172.3 | 0.996 |
| Glutamic acid | 2334.7 | 991.5 | 0.998 |
| Glutamine | 2447.0 | 1600.1 | 0.998 |

[a] Peak area = intercept + slope × concentration (g/l).

min (Fig. 1). The calibration graphs for all compounds are linear in the concentration range 1–100 g/l (Table I, Fig. 2). Hence this approach is suitable for the determination of glutamine and related compounds during separation and purification.

During the analysis of fermentation media it was found that ammonia, which is often present in such samples also forms a complex with Cu(II). This complex elutes too close to the copper complex of pyroglutamic acid. To improve the separation of these compounds we used sodium dodecyl sulphate as an ion-pair reagent. In this instance a nearly baseline separation of the ammonia–pyroglutamic acid pair was achieved (Fig. 3).

Under these chromatographic conditions the cali-

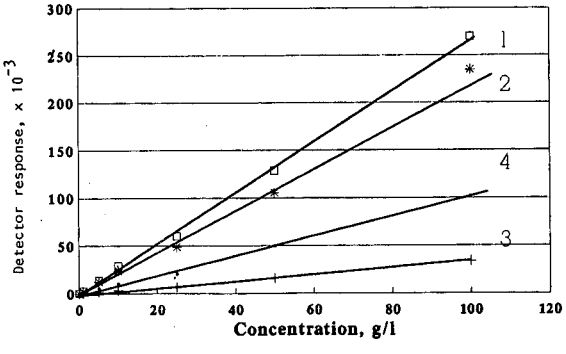


Fig. 4. Linearity of HPLC determination of glutamine, glutamic acid and pyroglutamic acid. Column, 5-μm silica (250 × 4 mm I.D.). Chromatographic conditions as in Fig. 3. The calculated areas are in arbitrary units. Lines: 1 = glutamic acid; 2 = glutamine; 3 = pyroglutamic acid; 4 = ammonium sulphate.

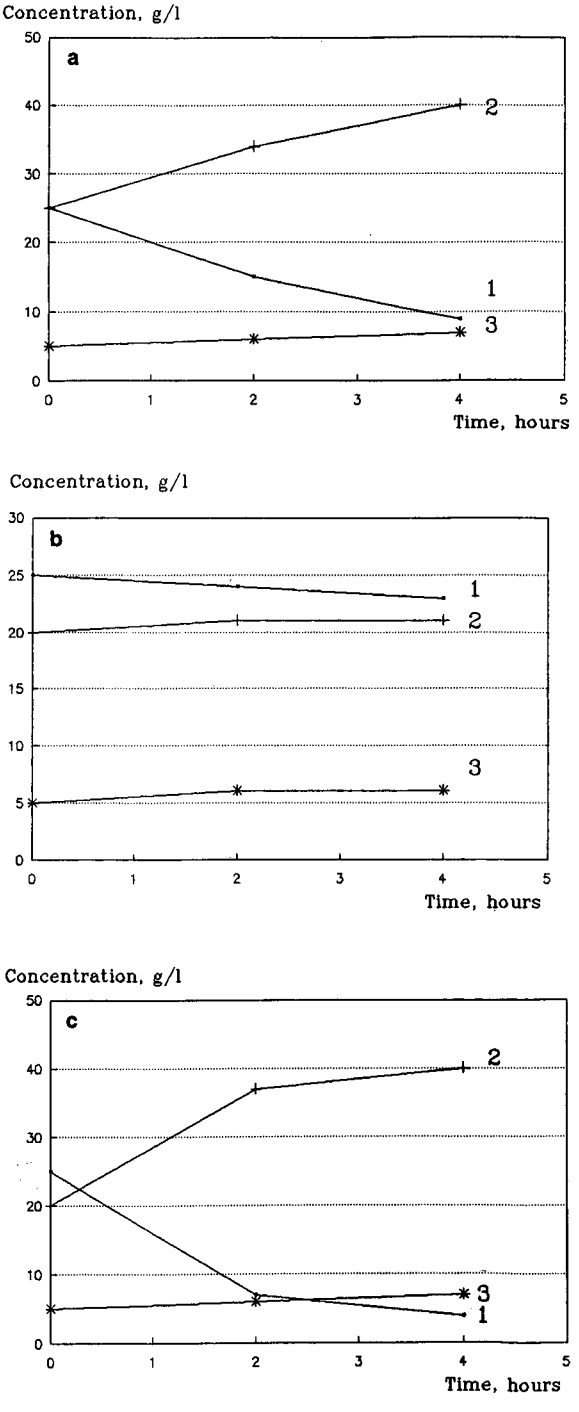


Fig. 5. Degradation of glutamine in fermentation media at 60°C and different pH values: (a) pH 1.5; (b) pH 5.5; (c) pH 10.5. Curves: 1 = glutamine; 2 = pyroglutamic acid; 3 = glutamic acid.

bration graphs were linear within the range 1–100 g/l (Table II, Fig. 4).

Consequently, for the determination of glutamine and glutamic acid it is possible to use the chromatographic conditions as in Fig. 1. The same conditions are suitable for the determination of pyroglutamic acid in model solutions. If it is necessary to determine pyroglutamic acid in samples containing salts of ammonia, *e.g.* in fermentation media, the addition of an ion-pair reagent is recommended.

This technique was used to study the stability of glutamine during its separation from fermentation broth and purification [10]. Previously it was reported that degradation of glutamine to glutamic and pyroglutamic acids in model mixtures may be influenced by temperature, pH, the presence of anions, etc. [5]. Our study demonstrated that at high and low pH values glutamine in model solutions and fermentation media is easly converted into these products (Fig. 5).

At 60°C and pH 1.5 and 10.5, 80% degradation of glutamine occurred in 3 h (Fig. 5a and c, respectively). At the same temperature and at pH 5.5 glutamine is more stable (Fig. 5b).

This technique was also used for the rapid control of glutamine and glutamic acid accumulation in the fermentation media of industrial strains (Figs. 6 and 7). The precision of quantitative analysis was confirmed by techniques such as amino acid analysis and planar chromatography. It was found that owing to the simple sample pretreatment, the possibility of carrying out HPLC analysis under the isocratic conditions and the short time of analysis, the method developed here is suitable for routine appli-

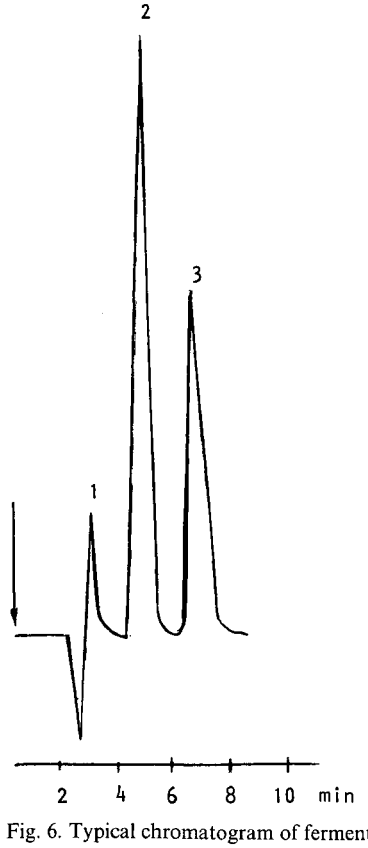


Fig. 6. Typical chromatogram of fermentation media of *Corinebacterium glutamicum*. Dilution, 1:50. Peaks: 1 = pyroglutamic acid; 2 = glutamic acid; 3 = glutamine. Analytical conditions as in Fig. 1.

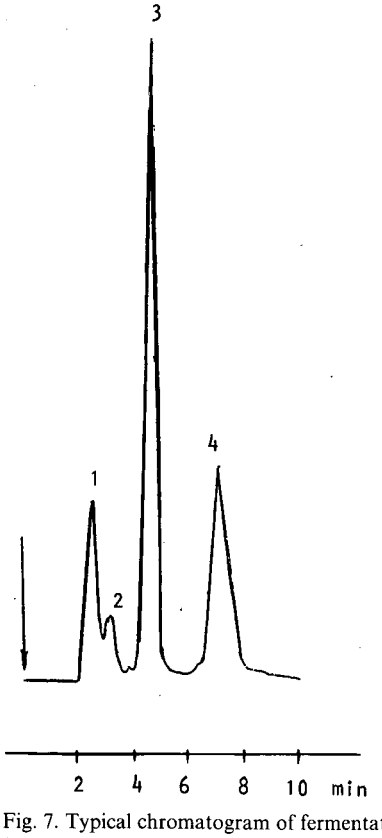


Fig. 7. Typical chromatogram of fermentation media of *Corinebacterium glutamicum*. Dilution, 1:50. Peaks: 1 = ammonium sulphate; 2 = pyroglutamic acid; 3 = glutamic acid; 4 = glutamine. Analytical conditions as in Fig. 2.

cation. The unmodified silica column demonstrates very good stability. After the analysis of more than 500 samples, its chromatographic properties had not changed.

REFERENCES

1 Z. Deyl, J. Hyanek and M. Horakova, *J. Chromatogr.*, 379 (1986) 177.
2 L. W. Anderson, D. W. Zaharevitz and J. M. Strong, *Anal. Biochem.*, 163 (1987) 358.
3 H. J. Chaves das Neves and A. P. M. Vasconelos, *J. Chromatogr.*, 392 (1987) 249.
4 N. Nishimoto, Y. Mitani and S. Hayashi, *J. Chromatogr.*, 176 (1979) 448.
5 F. F. Shih, *J. Chromatogr.*, 322 (1985) 248.
6 E. Grushka and S. Levin, *J. Chromatogr.*, 235 (1982) 401.
7 S. Levin and E. Grushka, *Anal. Chem.*, 57 (1985) 1830.
8 I. Z. Atamna, G. M. Muschik and H. J. Issaq, *J. Liq. Chromatogr.*, 12 (1989) 1085.
9 M. Hirukawa and T. Hanai, *J. Liq. Chromatogr.*, 11 (1988) 1741.
10 N. G. Demina, B. M. Polanuer, N. F. Rumiantseva and A. F. Sholin, *Biotekhnologiya*, in press.

*Journal of Chromatography*, 594 (1992) 179–185
Elsevier Science Publishers B.V., Amsterdam

CHROM. 23 840

# High-performance gel permeation chromatographic analysis of immunoglobulin M produced by hybridoma cell culture

Nathalie Chauret*

*Merck Frosst Canada, P.O. Box 1005, Pointe-Claire-Dorval, Quebec H4R 4P8 (Canada)*

Johanne Côté, Jean Archambault and Gérald André

*Biotechnology Research Institute, National Research Council Canada, 6100 Royalmount Avenue, Montreal H4P 2R2 (Canada)*

(First received August 19th, 1991; revised manuscript received October 31st, 1991)

ABSTRACT

A high-performance gel permeation chromatographic (HPGPC) method, using TSK-Gel $SW_{XL}$ 3000 and TSK-Gel $SW_{XL}$ 4000 columns installed in series, was developed for the analysis of immunoglobulin M (IgM) produced by hybridoma cell culture. The detection of this protein was achieved using ultraviolet absorption at 225 nm, yielding a detection limit of *ca.* 0.3 $\mu g\ ml^{-1}$. IgM-containing samples obtained from different culture systems (T-flask, roller bottle, spinner flask, bioreactor operated in batch, fed-batch or perfusion modes) and media (Dulbecco's Modified Eagle Medium or Protein-Free Hybridoma Medium) were evaluated by this chromatographic technique and also by conventional enzyme-linked immunosorbent assay (ELISA). Concentrations of IgM in culture samples determined by both techniques were always in the same range (± 10%). The main advantages of HPGPC over ELISA included improved reproducibility (relative average deviation of 1–3% compared with 10–20% for ELISA), high linearity range between the signal and the concentration [at least three decades (0.3–500 $\mu g\ ml^{-1}$) compared with one decade for ELISA (25–200 $ng\ ml^{-1}$)] and ease of operation.

## INTRODUCTION

Monoclonal antibodies are used routinely for blood typing and have considerably improved our understanding of the various structures expressed at the surface of human erythrocytes [1]. Hybridoma cell culture represents the most interesting alternative for the production of monoclonal antibodies (MAbs). The technology being developed in our laboratory for the large-scale production of an immunoglobulin M (IgM) directed against a human blood type antigen required a simple, efficient and sensitive method for MAb quantification. Hemagglutination is often used as a rapid method for the determination of the titer of a given MAb in a solution. Erythrocyte aggregates are formed and detected by subjective visual inspection. Other commonly used procedures for detecting and quantify MAb include highly specific immunoassays and especially enzyme-linked immunosorbent assay (ELISA) [2,3]. However, these techniques, based on antigen–antibody interactions, are known for their poor reproducibility [4,5]. The development of large-scale MAb production processes requires accurate and reproducible methods to assess their performance. Semi-quantitative tests such as hemagglutination or ELISA do not allow a proper evaluation of the effect of culture conditions on MAb production. Chromatography, which represents a more reliable technique, was evaluated for this purpose. Among the chromatographic techniques available, high-performance gel permeation chromatography

0021-9673/92/$05.00 

(HPGPC) for protein separation appeared to be a valuable approach because of its easy of operation and the information that it provided on the relative molecular weight (MW) of the proteins analyzed. Since the introduction of silica-based GPC columns that allowed efficient and rapid separation of large molecules, several studies have been published on the separation of small immunoglobulins, including IgG and IgA [6,7]. The main problem with large IgM immunoglobulins is that they are excluded from the packing of most of the silica-based columns available. Flapper *et al.* [8] recently presented a separation methodology for serum proteins using HPGPC. In comparing the elution behaviours of IgM, macroglobulin, IgG and albumin on three different column systems (TSK-Gel SW, Zorbax and Sepharose), they concluded that the best separation was achieved using TSK-Gel SW columns. However, their work, which emphasized the theoretical aspects of the elution behavior of the different proteins, did not report quantitative statistical analyses of actual culture samples.

This work addresses the development and characterization, in terms of detection limit, linearity range, reproducibility and selectivity, of an HPGPC method for the quantification of a specific IgM protein produced by hybridoma cell culture. The analysis was achieved using TSK-Gel $SW_{XL}$ columns installed in series and ultraviolet detection. These columns were preferred to TSK-Gel SW columns, as they were found to yield better separations of proteins [9]. Culture samples obtained from different hybridoma culture systems were analyzed by HPGPC and compared with the highly specific ELISA analysis.

## EXPERIMENTAL

### *Hybridoma cell culture*

Mouse × mouse hybridoma cell lines secreting an IgM against the human blood type antigen Lewis b were kindly provided by Chembiomed (Edmonton, Canada). Cell lines were cultured in Dulbecco's Modified Eagle Medium (DMEM) (Sigma, St.-Louis, MO, USA) supplemented with 1% (v/v) fetal bovine serum (FBS) (Flow Labs., Mississauga, Canada) or in Protein-Free Hybridoma Medium (PFHM II) (Gibco, Burlington, Canada) at 37°C and under appropriate carbon dioxide partial pressure. Cells were grown in various systems [T-flasks, roller bottles, spinner flasks or bioreactors (2.4 l)] under different culture modes (batch, fed-batch and perfusion).

### *Sample preparation*

Samples obtained from the different cultures were used as the experimental source of IgM. Samples of various culture ages were collected and centrifuged at 8 800 *g* for 2 min and the supernatants were frozen at −80°C for further analyses by HPGPC and ELISA.

### *HPGPC system*

The HPGPC system used (Waters Assoc., Bedford, MA, USA) included a pump (Model 590), a manual injector (Model U6K) or an automatic sampler (WISP, Model 710) and a UV detector (Model 481) connected to a chart recorded (Model 2210, LKB, Gaithersburg, MD, USA). The protein separation was achieved using a TSK-Gel 4000 $SW_{XL}$ column connected in series to a TSK-Gel 3000 $SW_{XL}$ column (Toyo Soda, Tokyo, Japan). A filter (0.45 μm) was placed on-line before the two columns. The mobile phase was a phosphate-buffered saline (PBS) aqueous solution (0.2 *M* sodium chloride–0.2 *M* sodium phosphate) (Anachemia, Montreal, Canada) of pH 6.8. The flow-rate and inlet pressure were 0.5 ml $min^{-1}$ and *ca.* 35 bar, respectively. A volume of 50 μl supernatant was injected directly into the HPGPC system.

A protein standard mixture made of five globular proteins of known molecular weight [thyroglobulin (670 000 dalton), IgG (158 000 dalton), ovalbumin (44 000 dalton), myoglobin (17 000 dalton) and cyanocobalamin (1300 dalton) was purchased from Bio-Rad Labs. (Richmond, CA, USA) (catalog No. 151–1901) and was used to evaluate protein separation. The presence of IgM in samples was determined by comparison with the retention time of an IgM standard which was an affinity purified antibody solution [1 mg $ml^{-1}$ in PBS + 1% BSA (lot No. 8PLB-0002)] kindly provided by Chembiomed. This same standard was also used for ELISA calibration. The IgM was quantified from its peak height on UV detection at 225 nm. The peak width was constant for the range of concentrations studied (1–500 μg $ml^{-1}$).

*ELISA*

A PBS solution of pH 7.2 was prepared using 1.11 g $l^{-1}$ sodium phosphate dibasic (Anachemia), 0.30 g $l^{-1}$ potassium phosphate monobasic (Anachemia), 9.0 g $l^{-1}$ sodium chloride (Anachemia) and 0.1 m*M* thimerosal (Sigma) in deionized water. A washing buffer solution (WB) was prepared by adding 0.1% (v/v) of Tween 20 (Bio-Rad Labs.) to the PBS. An antibody diluting buffer solution (DB) was prepared by adding 1.0% (w/v) bovine serum albumin (BSA) and 1.0% (v/v) Tween 20 to the PBS. The enzyme-substrate solution was made of 4.67 g $l^{-1}$ sodium citrate (Fisher, Montreal, Canada), 7.90 g $l^{-1}$ sodium phosphate monobasic (Sigma) of pH 5.5 and, prior to use, 3 mg $ml^{-1}$ *o*-phenylenediamine (OPD) (Sigma) and 0.67 $\mu$l $ml^{-1}$ 30% hydrogen peroxide (Sigma). A Dulbecco's PBS solution (D-PBS) (Gibco) was used to prepare the antigen solution. A purified Lewis b antigen supplemented with BSA was used for the plate coating for ELISA at a concentration of 0.5 $\mu$g $ml^{-1}$ in D-PBS. An enzyme immunoassay (EIA)-grade affinity purified goat anti-mouse IgG horseradish peroxidase conjugate (HRP) (Bio-Rad Labs.) was diluted 1:8000 in the DB.

Microtitration plates with 96 flat-bottomed wells (Flow Labs.) were coated with the antigen by dispensing 100 $\mu$l per well of the antigen solution. These plates were incubated at room temperature overnight, washed six times with the WB using an automatic microplate washer (Titertek, Flow Labs.) and stored at 4°C. The affinity purified antibody used as standard was diluted with the DB in the 25–200 ng $ml^{-1}$ concentration range for calibration. Culture samples were diluted (1:200 to 1:1000) to reach the same range of concentrations. The WB solution was aspirated from wells and a 100-$\mu$l volume of the diluted standard or sample solution was distributed in each well. Four wells were used for each dilution and three different dilutions were prepared for each sample tested. The plates were covered and incubated at room temperature for 1 h before rinsing six times with the WB. A 100-$\mu$l volume of goat anti-mouse HRP conjugate was dispensed in each well. The plates were incubated and rinsed as above. A 100-$\mu$l volume of the enzyme substrate solution was distributed in each well. The plates were covered with aluminum foil for 10–20 min. Thereafter, the absorbances of the 96 wells were read rapidly at a wavelength of 450 nm using a microplate reader (Titertek Multiskan, MCC, Flow Labs.). The results were transferred to a microcomputer for calculations.

## RESULTS AND DISCUSSION

*Performance of the HPGPC system*

The separation characteristics of the TSK columns were determined using the standard protein mixture described in the previous section. As shown in Fig. 1, each protein eluted as a single, symmetrical peak and was resolved under the conditions of

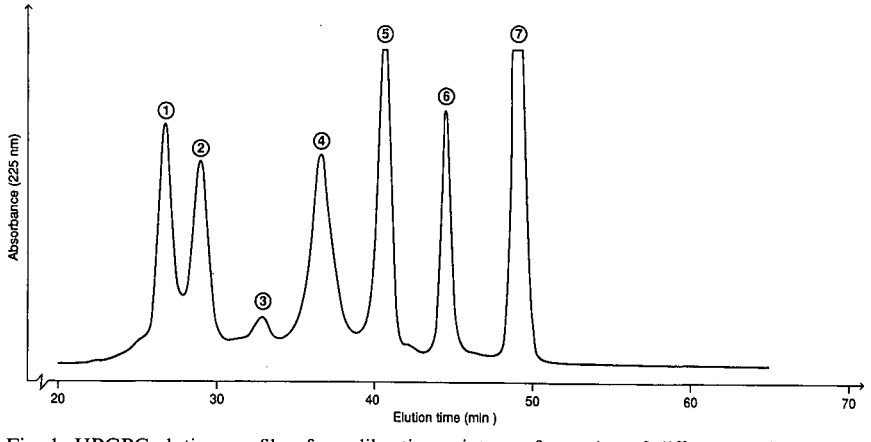


Fig. 1. HPGPC elution profile of a calibration mixture of proteins of different molecular weights with TSK-Gel 3000 $SW_{XL}$ and TSK-Gel 4000 $SW_{XL}$ columns connected in series. Conditions as described in the text (0.02 a.u.f.s.). Peaks: 1 = IgM (950 000 dalton); 2 = thyroglobulin (670 000 dalton); 3 = impurity; 4 = IgG (158 000 dalton); 5 = ovalbumin (44 000 dalton); 6 = myoglobin (17 000 dalton); 7 = cyanocobalamin (1300 dalton).

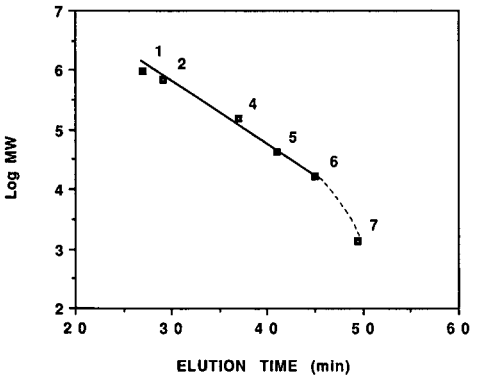


Fig. 2. Calibration graph: correlation between molecular weight (MW) and elution time obtained for TSK-Gel 3000 $SW_{XL}$ and TSK-Gel 4000 $SW_{XL}$ HPGPC columns connected in series. Peaks as in Fig. 1.

separation used. The elution time of these proteins as a function of their relative MW indicated that there is a linear relationship (Fig. 2) between log MW and elution time $t_e$ (reported in min) for MW ranging from 17 000 to 950 000 dalton (correlation coefficient = 0.99):

$$\log MW = -0.0947\, t_e + 8.57 \quad (1)$$

Similar results were reported by Flapper *et al.* [8] using TSK Gel 3000 SW and TSK Gel 4000 SW columns. Cyanocobalamin (1300 dalton) eluted at the total volume of the columns (24.5 ml) and was not in the linear range of the calibration graph as expected from the lower MW limits given by the manufacturer for these columns (fractioning ranges of TSK gel 3000 $SW_{XL}$ = 10 000–500 000 dalton and TSK Gel 4000 $SW_{XL}$ = 20 000–$10^7$ dalton).

The detection limit of this technique evaluated at twice the noise level was 0.3 $\mu g\ ml^{-1}$. A linear relationship (correlation coefficient 0.99) between peak height $h$ (reported in absorbance units) and IgM concentration $c$ (expressed in $\mu g\ ml^{-1}$) was obtained for various IgM standards with concentrations varying from 1 to 500 $\mu g\ ml^{-1}$:

$$h = (1.52c + 1) \cdot 10^{-4} \quad (2)$$

The reproducibility of the analysis, defined as the relative standard deviation (R.S.D.) for five injections of the same IgM standard solution at 100 $\mu g\ ml^{-1}$, was 3% of the average value on manual injection and 1% on automatic injection.

*GPC analysis of culture samples*

Fresh DMEM medium contains known concentrations of salts, amino acids, vitamins and carbohydrates. Generally, this medium is supplemented with FBS. PFHM II medium is an unpublished formulation. In order to evaluate any interferences of the culture medium components with IgM determination, fresh samples of the medium were analyzed by HPGPC. The chromatograms obtained for serum-free DMEM, a 1% FBS solution in PBS and PFHM II are presented in Fig. 3a, b and c, respectively. These chromatograms showed several peaks at 50–60 min which exceeded the total volume of the columns. These small molecules may have penetrated the small pores of the gel phase and interacted with the residual silanol groups present, which caused their excessive retention in the columns [10]. The injection of a mixture of amino acids and a mixture of vitamins showed that some of these compounds eluted also after the total volume of the columns. The 1% FBS solution showed peaks at 29, 37 and 41 min (Fig. 3b). These peaks correspond to 660 000-, 168 000- and 68 000-dalton species and probably to thyroglobulin, IgG and albumin, three proteins usually found in FBS. As expected (Fig. 3c), the chromatogram of PFHM II showed no peak before 44 min (*i.e.*, MW > 17 000 dalton). Consequently, these analyses indicated that IgM determination should not be affected by compounds present in the medium used to grow hybridomas. This was confirmed by co-injection of IgM standard with different medium samples.

Fig. 4 illustrates typical chromatograms of actual culture supernatants. For DMEM 1% FBS supplemented samples, the IgM peak (26.5 min) was symmetrical and well resolved from the other peak at 29 min originating from 1% FBS solution (Fig. 3b). The peak pattern in the 45–65 min range of low-MW DMEM components was different from that obtained for a fresh sample of medium (Fig. 3a), indicating changes in the composition of the medium, probably as a result of nutrient consumption and cell metabolism. Similar results were obtained for PFHM II culture samples (Fig. 4b). In this instance, however, the IgM peak was sometimes slightly asymmetric, indicating co-elution of other

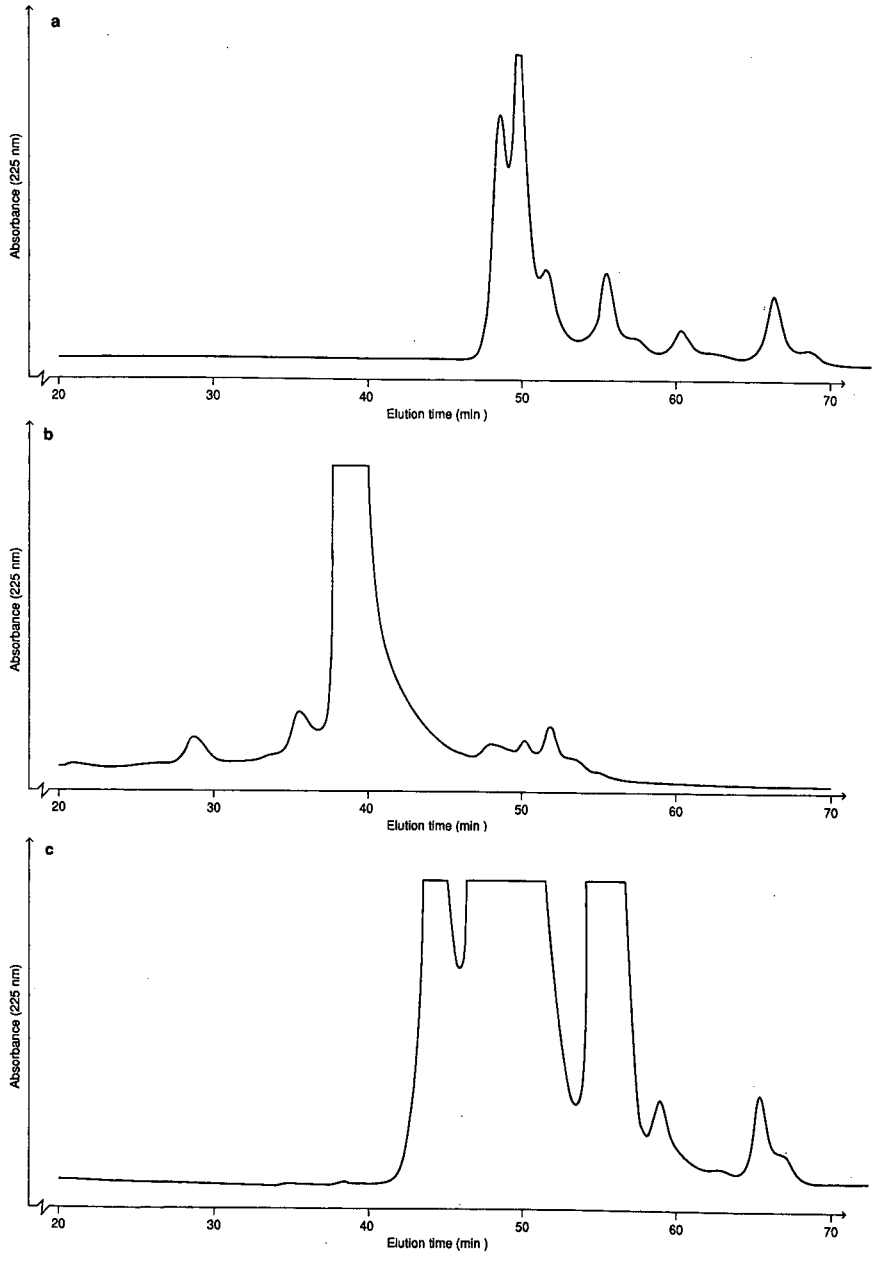


Fig. 3. HPGPC elution profiles of culture media and additives: (a) fresh DMEM (0.05 a.u.f.s.) (b) 1% FBS solution in PBS buffer (0.01 a.u.f.s.); (c) fresh PFHM II (0.01 a.u.f.s.). For experimental conditions, see text.

high-MW proteins or adsorption of the IgM molecule on the column. Previous injection of the IgM standard diluted in fresh PFHM II medium did not result in a similar asymmetric peak, indicating that the fresh medium does not contain compounds causing adsorption of the IgM molecule onto the columns. Future experiments will involve the characterization of the origin of this phenomenon.

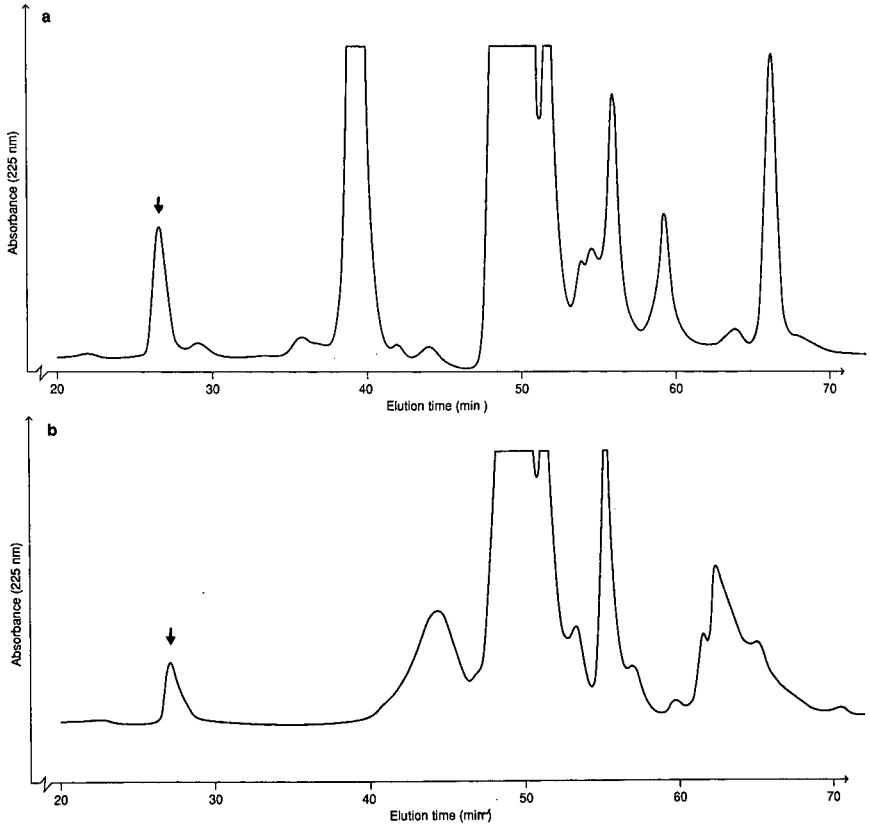


Fig. 4. Typical HPGPC elution profiles of IgM-containing samples from cell culture supernatants: (a) 40 $\mu$g ml$^{-1}$ IgM produced in DMEM with 1% FBS (0.02 a.u.f.s.) and (b) 62 $\mu$g ml$^{-1}$ IgM produced in PFHM-II (0.05 a.u.f.s.). For experimental conditions, see text.

*Comparison of HPGPC and ELISA techniques*

Results of the analysis of various IgM-containing samples produced using DMEM + 1% FBS and PFHM II media are presented in Table I. Both techniques measured similar concentrations of IgM in these samples. However, for 7 out of 22 samples (PFHM 4, 9, 11 and 12; DMEM + 1% FBS 4, 7 and 9) a significant difference (higher-to-lower average values *ca.* 20–50%) was observed between both methods, which decreased to 0–10% on taking into account the total spread of the data. As these differences were observed for the whole range of concentrations studied, and appeared randomly, they may be attributed to experimental errors. The HPGPC technique showed better reproducibility (relative average deviation *ca.* 1–2%) than the ELISA method (relative average deviation *ca.* 10–20%), which involves numerous steps and serial dilution, all contributing to the high variability of the results obtained.

The good agreement observed beween the two methods, based on molecular size exclusion and immuno-specific interaction, respectively, suggests that HPGPC is selective enough and represents a valuable quantitative technique for measuring IgM products obtained from protein-free and serum-containing cultures. It is now used to evaluate rapidly off-line, and eventually on-line, the performance of various culture processes. However, it remains a complementary technique to ELISA and hemagglutination, which allow the assesment of the quality and specificity of the MAbs produced.

## CONCLUSION

The results clearly indicate that HPGPC is a reliable technique for the quantification of IgM contained in cell culture supernatants originating from either protein-free or serum-containing media. This

TABLE I

COMPARISON OF HPGPC AND ELISA MEASUREMENT FOR IgM CONTAINED IN DIFFERENT HYBRIDOMA CELL CULTURE SAMPLES

Average deviations (± values) calculated for 3–4 (ELISA) and 2–3 (HPGPC) independent measurements.

| Culture medium | Sample No. | IgM concentration ($\mu g\ ml^{-1}$) | |
|---|---|---|---|
| | | ELISA | HPGPC |
| PFHM II | 1 | 3 ± 1 | 2.7 ± 0.3 |
| | 2 | 5 ± 1 | 6.0 ± 0.1 |
| | 3 | 9 ± 1 | 8.7 ± 0.2 |
| | 4 | 35 ± 6 | 27.8 ± 0.3 |
| | 5 | 24 ± 2 | 26.1 ± 0.2 |
| | 6 | 48 ± 2 | 54 ± 0 |
| | 7 | 115 ± 8 | 118 ± 2 |
| | 8 | 117 ± 23 | 115 ± 1 |
| | 9 | 128 ± 11 | 106 ± 1 |
| | 10 | 194 ± 23 | 211 ± 7 |
| | 11 | 287 ± 58 | 212 ± 7 |
| | 12 | 290 ± 58 | 220 ± 2 |
| DMEM + 1% FBS | 1 | 24 ± 5 | 27.2 ± 0.3 |
| | 2 | 27 ± 7 | 23.0 ± 0.9 |
| | 3 | 31 ± 2 | 33.4 ± 0.7 |
| | 4 | 22 ± 1 | 27.4 ± 0.3 |
| | 5 | 32 ± 4 | 34.0 ± 0.3 |
| | 6 | 35 ± 5 | 38.8 ± 0.7 |
| | 7 | 20 ± 10 | 33.0 ± 0.7 |
| | 8 | 32 ± 3 | 36.6 ± 0.4 |
| | 9 | 49 ± 2 | 40 ± 1 |
| | 10 | 54 ± 10 | 57 ± 1 |

method can be used to obtain reliable results in order to optimize culture processes for the production of IgM. It allows a rapid off-line analysis, which was not possible with ELISA because of its long and laborious protocol.

ACKNOWLEDGEMENTS

The authors thank S. Mercille, M. Johnson, S. Meyer and L. Tremblay for providing the different cell samples and performing the ELISA test. The active collaboration of Barbara Allen of Supelco Canada is greatly acknowledged.

REFERENCES

1 L. Choucane, J. Breyer, A. van Spronsen, J. L. Guillaume, D. Goossens, Ph. Rouger and A. D. Strosberg, *Dev. Biol. Stand.*, 71 (1990) 9.
2 A. M. Campbell, in R. H. Burdon and P. H. Knippenberg, (Editors), *Monoclonal Antibody Technology*, Elsevier, New York, 1984, p. 33.
3 E. Harlow and D. Lane, *Antibodies—a Laboratory Manual*, Cold Spring Harbor Laboratoy, Cold Spring Harbor, 1988, p. 560.
4 J. D. Macmillan, D. Velez, L. Miller and S. Reuveny, in B. K. Lyderson (Editor), *Large-Scale Cell Culture Technology*, Hanser, New York, 1987, p. 25.
5 B. C. Batt, R. H. Davis and D. S. Kompala, *Biotechnol. Prog.*, 6 (1990) 458.
6 H. Suomela, J. J. Himberg and T. Kuronen, *J. Chromatogr.*, 297 (1984) 369.
7 G. Sam, G. Schneider, S. Locke and H. W. Doerr, *J. Chromatogr.*, 59 (1983) 121.
8 W. Flapper, A. G. M. Theeuwes, J. T. G. Kierkels, J. Steenbergen and H. J. Hoenders, *J. Chromatogr.*, 533 (1990) 47.
9 Y. Kato, Y. Yamasaki, H. Moriyama, K. Tokunaga and T. Hashimoto, *J. Chromatogr.*, 404 (1987) 333.
10 H. Watanabe, M. Umino and T. Sasagawa, *Toyo Soda Kenkyu Hokoku*, 28 (1984) 3.

*Journal of Chromatography*, 594 (1992) 187–194
Elsevier Science Publishers B.V., Amsterdam

CHROM. 23 790

# Determination of ascorbic and dehydroascorbic acid in potatoes (*Solanum tuberosum*) and strawberries using ion-exclusion chromatography

William D. Graham and Donald Annette

*Food and Agricultural Chemistry Research Division, Department of Agriculture for Northern Ireland, Newforge Lane, Belfast BT9 5PX (UK)*

(First received May 13th, 1991; revised manuscript received October 4th, 1991)

ABSTRACT

A high-performance liquid chromatographic method has been developed for determination of ascorbic and dehydroascorbic acid. Samples were extracted with 62.5 m*M* metaphosphoric acid and ascorbic acid determined using an ion-exclusion column with detection at 245 nm. Dehydroascorbic acid was determined after reduction to ascorbic acid. The use of ion-exclusion chromatography enables ascorbic acid to be completely resolved from co-extracted material in both raw and cooked foods. Completeness of separation was confirmed using a photodiode-array detector.

## INTRODUCTION

Vitamin C is an important micronutrient and plays many physiological roles [1,2]. Fruits and vegetables constitute the major sources in most human diets; it occurs as *l*-ascorbic acid (AA) and *l*-dehydroascorbic acid (DHAA), its oxidized form, both of which are biologically active. Any analysis for vitamin C activity must take this into consideration since a proportion of AA may be oxidized to DHAA in some foods upon storage or processing.

Numerous methods for the analysis of vitamin C acitivity have been described [3]. Chemical methods remain widely used but the presence of interfering compounds in the complex matrices of foods has resulted in these traditional approaches being replaced by high-performance liquid chromatographic (HPLC) methods which are more selective and sensitive. The wide range of HPLC methods available for viamin C determination have been reviewed by Polesello and Rizzolo [4].

The most common modes of separation are reversed phase, reversed phase with ion pairing, and weak anion exchange with $NH_2$-bonded phases. Procedures vary in the type of column, elution conditions, detection systems and the extraction technique but in most published methods AA elutes very close to the void volume; this may lead to errors.

The importance of the extracting media and stabilizing solutions for AA and DHAA to prevent oxidative changes has been emphasized by Nicolson *et al.* [5], and Margolis and Black [6]. The well established extractant and stabilizer, metaphosphoric acid (MPA), was critical in determining the HPLC method used. The work described in this paper was carried out because of the problems encountered when different combinations of extractants and stabilizers have been used with silica-based packing materials [7,8]. The use of amino-bonded columns and reversed-phase $C_{18}$ columns with and without ion-pairing was investigated. When the amino-bonded column procedure of Rose and Nahrwold [9] was used good resolution of AA in the extracts of uncooked foods was possible. However with the extracts of cooked potatoes, resolution was poor and the AA peak on spectral examination proved to be contaminated with a co-eluting component from the extract. The column was quickly poisoned most

0021-9673/92/$05.00 

probably by carbohydrates *e.g.* starch, as reported by Churms [10]. The ion-pairing method of Augustin *et al.* [11] was not satisfactory. Examination of the AA peak spectrum showed that it was not a single-component peak. Similarly in a reversed-phase mode without the use of an ion-pair reagent, column poisoning occurred. It was not possible to use precipitation of the starch with ethanol since the addition of homocysteine to the ethanol supernatant to reduce DHAA to AA caused the formation of a gel.

Ashoor *et al.* [12] used ion-exclusion chromatography to determine ascorbic acid in fruits, fruit juices and vegetables. When this was investigated it was found that their sample extraction procedure led to imcomplete reduction of DHAA to AA, only 80% being achieved. Ascorbic acid was eluted as part of a large tailing peak during chromatography of the extracts of strawberries, raw and cooked potatoes (Fig. 1). For this reason an ion-exclusion chromatographic separation using polystyrene–divinylbenzene packing materials was developed which was capable of determining total AA quantitatively in strawberries, raw and cooked potatoes.

## EXPERIMENTAL

### *Apparatus*

A Hewlett-Packard 1090M liquid chromatograph with integral photodiode-array detector, autosampler and autoinjector and a Hewlett-Packard 9000 series 320 datastation with 9153 disc-drive unit from Hewlett-Packard (Winnersh, Wokingham, UK) was used. A Bio-Rad Aminex HPX-87H, 300 mm × 7.8 mm I.D. ion-exclusion column, particle size 9 μm, packed with sulphonated styrene–divinylbenzene copolymer resin, 8% cross-linked, from Bio-Rad Labs. (Watford, UK) was employed. A Micro-Guard cation $H^+$ cartridge was installed in front of the analytical column to maintain column performance and prolong column lifetime.

### *Reagents*

Chemicals and standard materials used were of the highest purity available. Metaphosphoric acid and dipotassium hydrogenphosphate were from BDH (Poole, UK), *l*-ascorbic acid from Sigma (Poole, Dorset, UK), *dl*-homocysteine from Aldrich (Poole, UK) and sulphuric acid from May and Baker (Manchester, UK).

All solutions, including the mobile phase 4.5 m*M* sulphuric acid, were prepared with high purity water obtained using an Elgastat UHQ water purifier from Elga (High Wycombe, UK) which incorporates reversed osmosis, adsorption, deionization, microfiltration and photooxidation processes.

### *Ascorbic acid standard solutions*

A stock solution of AA (200 μg/ml) was prepared by dissolving 20 mg AA in 100 ml of 62.5 m*M* metaphosphoric acid. The stock solution was stored at 5 ± 1°C. Fresh standard solutions were prepared by diluting the stock solution to appropriate concentrations with 62.5 m*M* metaphosphoric acid.

### *Sample preparation*

Potatoes and fresh strawberries were purchased from a local store and extracted on the day of purchase. Samples of potato skin and flesh (30 g) were obtained by subsampling 16 pooled cores (diameter 7 mm) taken from four tubers. A 10-g sample of fresh strawberries was obtained by cutting four strawberries into sections and subsampling. An amount of 80 g of 62.5 m*M* metaphosphoric acid was added immediately to the samples and blended for 3 min in a Waring blender. The weight of ho-

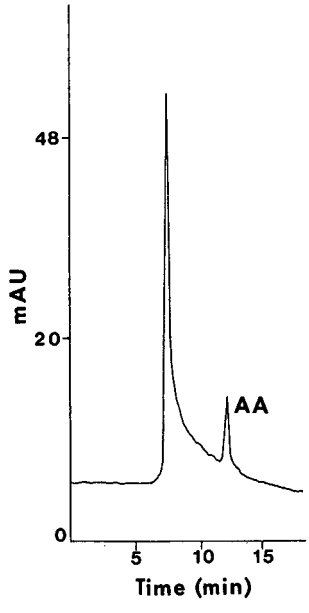


Fig. 1. Chromatogram obtained using method of Ashoor *et al.* [12].

mogenate plus washings was adjusted to 150 g with metaphosphoric acid solution, centrifuged at 6500 *g* for 15 min and filtered (Whatman 541). A quantitative amount of filtrate sufficient to give between 5 and 20 μg/ml of AA in the final volume was diluted to 20 ml with 62.5 m*M* metaphosphoric acid. All extracts were stored in amber vials at 5 ± 1°C. Mass rather than volume adjustments during blending were necessary to overcome problems caused by frothing.

Boiled potatoes were obtained by boiling 1.25 kg of raw tubers in 1.2 l water for 30 min. Baked potatoes were obtained by microwaving raw tubers at 650 W for 15 min. Sampling and extraction were carried out in the same way as for the raw tubers.

The extracting procedures were replicated four times using a total of sixteen tubers or strawberries in order to determine the overall variability of extraction. This includes both sample and extraction variability.

*HPLC analysis*

AA was determined by injecting 10 μl of the standard solutions or sample extracts into the HPLC system and eluting the ion-exclusion column with 4.5 m*M* sulphuric acid at a flow-rate of 0.5 ml/min. Column temperature was maintained at ambient and column back pressure was 90 ± 1 bar. Analysis was completed in 20 min which included a post-column elution time of 5 min. Spectral data from the photodiode-array detector were collected over the wavelength range 210–400 nm. AA was monitored at 245 nm.

*Reduction of DHAA*

DHAA was determined as the difference between total AA after DHAA reduction and AA content of the original sample. The reduction of DHAA to AA was accomplished using a minor modification of the method proposed by Hughes [13]. To 3 ml of extract were added 0.5 ml of 30 m*M* *dl*-homocysteine solution and the pH adjusted to 6.8–7.0 by slow addition of 1.5 ml of 2.6 *M* dipotassium hydrogenphosphate. After 30 min reduction was stopped by addition of 1 ml 6.25 *M* metaphosphoric acid.

## RESULTS AND DISCUSSION

Typical chromatograms of AA standard, reduced DHAA, strawberry extract and raw, boiled and baked potato extracts are presented in Fig. 2a–f. Under the described chromatographic conditions, AA eluted at 12.10 ± 0.02 min. Chromatograms of strawberries and potatoes produced extra peaks due to the presence of co-extracted material but these did not interfere with the separation of AA.

The peak area associated with AA, measured at 245 nm, against concentration was linear over the range 1 to 20 ng/μl and the correlation coefficient ($r^2$) was 1.00. Thus a single point calibration can be used for determination of AA. The detection limit for AA is 1 ng/μl, with a 10-μl injection.

Retention times and peak areas for ten consecutive injections over a 3.5-h period, from both 5 and 20 ng/μl AA standards (Table I) show the method has excellent reproducibility and stability. The results of five consecutive injections of sample extracts prepared from fresh strawberries and raw, boiled and baked potatoes (Table II) also confirm this for these extracts.

The results of the four separate extracts prepared from the samples (Table III) indicate the variability in the vitamin content of these foodstuffs. The mean values obtained are in agreement with those presented elsewhere [14].

When the standards of 20 and 5 ng/μl AA were subdivided into a series of HPLC vials, sealed and stored at 5 ± 1°C, the AA solutions were stable for up to 5 days (Table IV). Similarly, vitamin loss from

TABLE I

REPRODUCIBILITY OF CHROMATOGRAPHIC SYSTEM FOR AA STANDARDS

S.D. = Standard deviation; R.S.D. = relative standard deviation.

| | AA | | | |
|---|---|---|---|---|
| | 20 ng/μl AA standard | | 5 ng/μl AA standard | |
| | Retention time (min) | Peak area | Retention time (min) | Peak area |
| Mean | 12.1 | 637 | 12.1 | 152 |
| S.D. ($n$ = 10) | 0.01 | 4.0 | 0.02 | 6.3 |
| R.S.D. (%) | 0.08 | 0.6 | 0.2 | 4.1 |

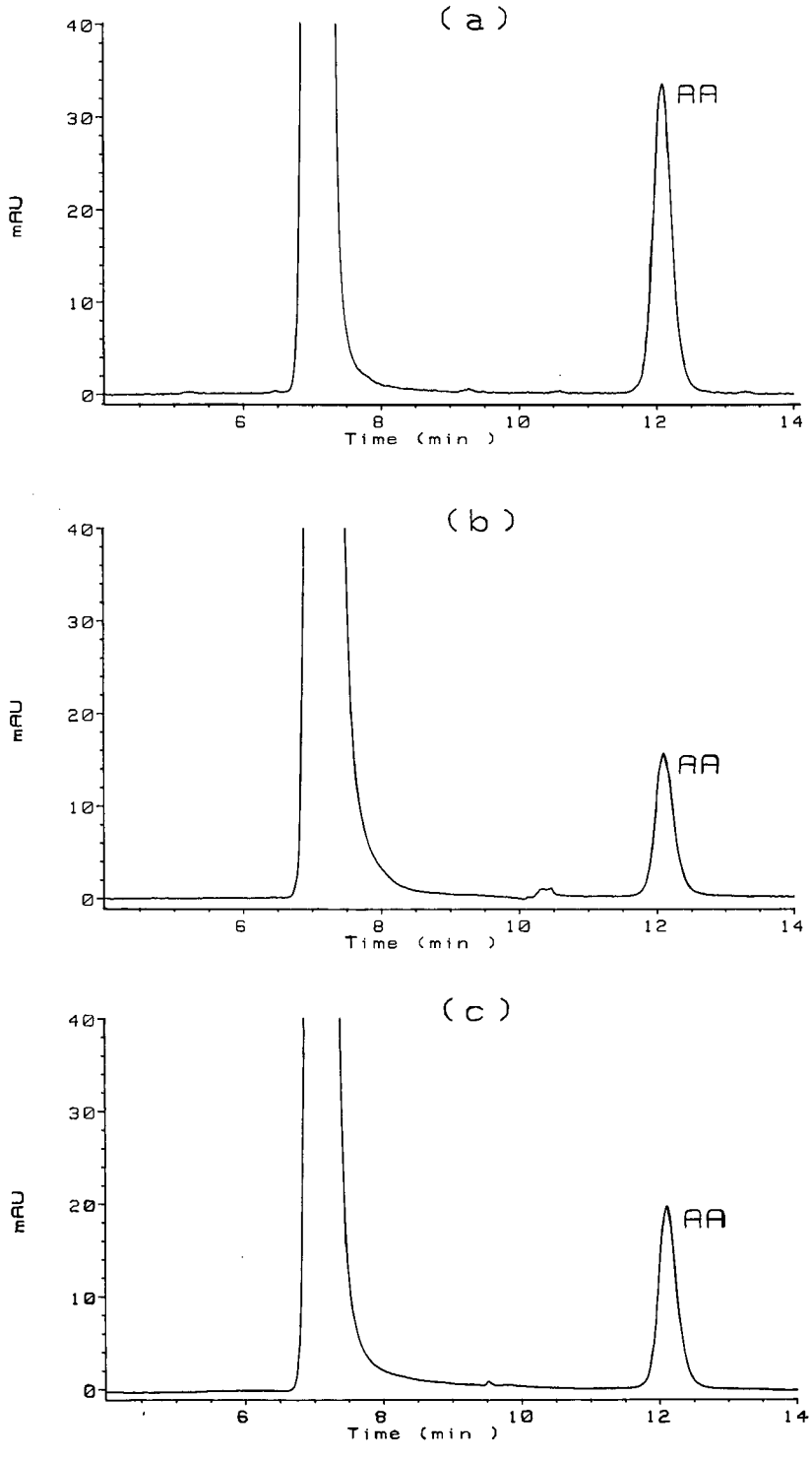
(a)
AA
mAU
40
30
20
10
0
6
8
10
12
14
Time (min)
(b)
AA
mAU
40
30
20
10
0
6
8
10
12
14
Time (min)
(c)
AA
mAU
40
30
20
10
0
6
8
10
12
14
Time (min)

Fig. 2.

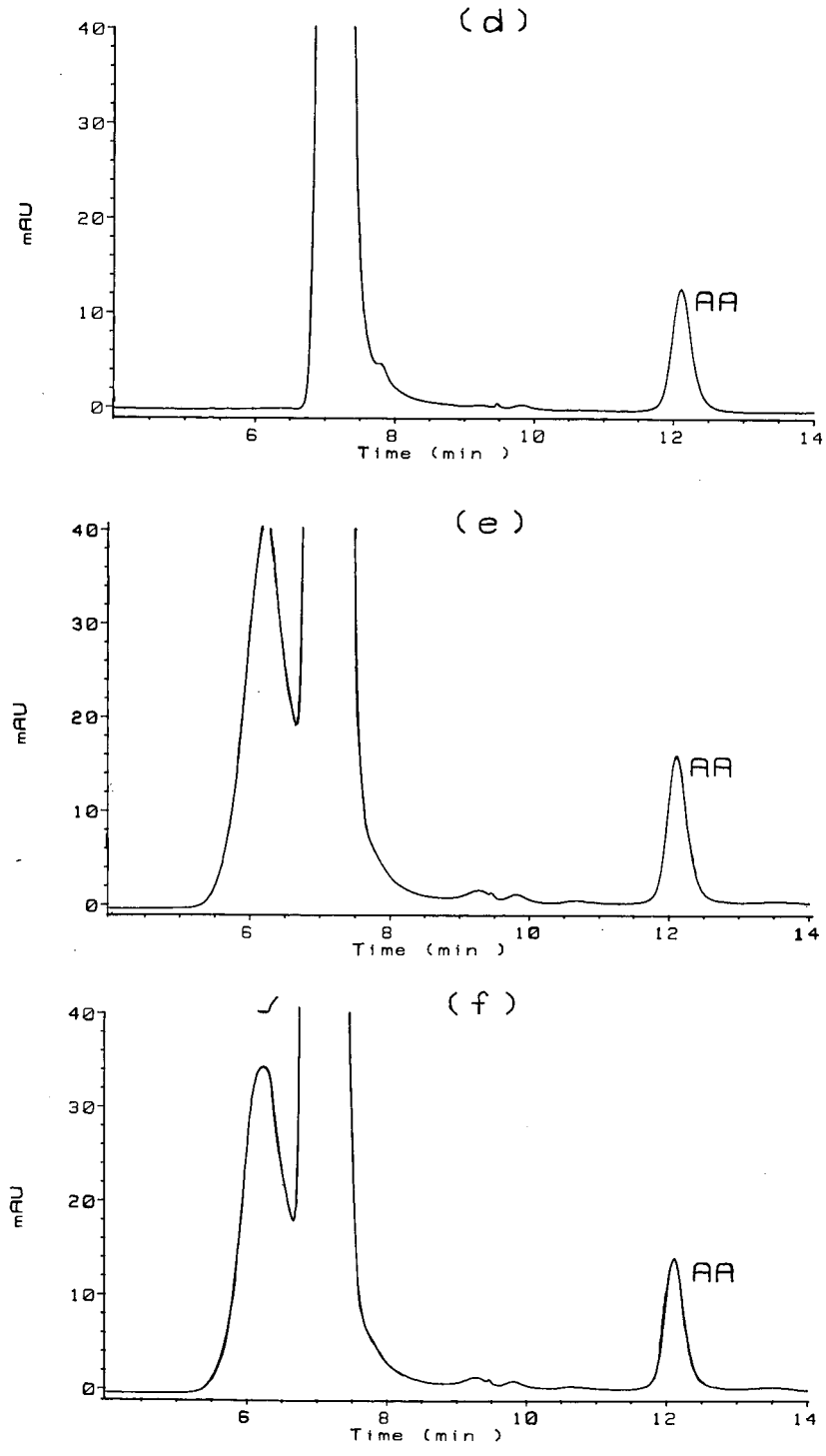


Fig. 2. Typical chromatograms of (a) 20 ng/$\mu$l AA standard, (b) reduced DHAA, (c) strawberry extract, (d) raw potato extract, (e) boiled potato extract and (f) baked potato extract.

TABLE II

REPRODUCIBILITY OF CHROMATOGRAPHIC SYSTEM FOR FOOD SAMPLE EXTRACTS

| | AA | | | | | | | |
|---|---|---|---|---|---|---|---|---|
| | Strawberry | | Potato | | | | | |
| | Retention time (min) | peak area | Raw | | Boiled | | Baked | |
| | | | Retention time (min) | Peak area | Retention time (min) | Peak area | Retention time (min) | Peak area |
| Mean | 12.1 | 357 | 12.1 | 261 | 12.1 | 258 | 12.1 | 305 |
| S.D. ($n$ = 5) | 0.01 | 2.9 | 0.01 | 2.5 | 0.02 | 7.4 | 0.0 | 3.17 |
| R.S.D. (%) | 0.08 | 0.82 | 0.07 | 0.96 | 0.19 | 2.85 | 0.23 | 5.50 |

TABLE III

VITAMIN C LEVELS OBTAINED BY THE PRESCRIBED METHOD

| | Vitamin C (mg/100 g fresh weight) | | | | | | | |
|---|---|---|---|---|---|---|---|---|
| | Strawberry | | Potato | | | | | |
| | TAA[a] | AA | Raw | | Boiled | | Baked | |
| | | | TAA | AA | TAA | AA | TAA | AA |
| Mean | 68.7 | 67.3 | 13.7 | 11.7 | 10.2 | 8.3 | 7.8 | 7.3 |
| S.D. ($n$ = 4) | 5.26 | 5.65 | 1.63 | 0.74 | 1.53 | 0.38 | 1.49 | 1.33 |
| R.S.D. (%) | 7.66 | 8.40 | 11.90 | 6.32 | 15.00 | 4.58 | 19.10 | 18.22 |

[a] TAA = total ascorbic acid.

TABLE IV

STABILITY OF AA STANDARDS AND OF AA IN FOOD SAMPLE EXTRACTS

Values are mean of two samples. S.E.M. = Standard error of the mean.

| Sample | AA (ng/$\mu$l) | | | | | | | |
|---|---|---|---|---|---|---|---|---|
| | Storage (days) | | | | | | | S.E.M. |
| | 0 | 1 | 2 | 3 | 4 | 5 | 10 | |
| Standards | | | | | | | | |
| 20 ng/$\mu$l | 20.00 | 20.12 | 19.62 | 19.95 | 19.94 | 19.92 | 17.70 | 0.115 |
| 5 ng/$\mu$l | 5.00 | 4.95 | 4.97 | 4.69 | 4.57 | 4.73 | 3.46 | 0.083 |
| Strawberry | | | | | | | | |
| fresh | 13.76 | 13.26 | 13.43 | 13.32 | 13.46 | 13.43 | 10.45 | 0.380 |
| Potato | | | | | | | | |
| Raw | 6.64 | 6.61 | 5.77 | 6.14 | 6.08 | 5.99 | 2.25 | 0.126 |
| Boiled | 6.74 | 6.50 | 6.30 | 5.85 | 5.80 | 5.87 | 1.71 | 0.158 |
| Baked | 4.32 | 4.19 | 3.44 | 3.58 | 4.13 | 3.99 | 1.49 | 0.095 |

TABLE V

PERCENT RECOVERY OF AA ADDED (a) PRIOR TO BLENDING, (b) TO THE FINAL EXTRACT

| Sample | Recovery of AA (%) ± S.D. ($n$ = 4) | |
|---|---|---|
| | a | b |
| Strawberry | | |
| fresh | 97.3 ± 3.25 | 99.3 ± 0.97 |
| Potato | | |
| Raw | 99.3 ± 0.97 | 94.8 ± 0.64 |
| Boiled | 96.2 ± 1.89 | 99.7 ± 1.47 |
| Baked | 98.6 ± 1.95 | 99.6 ± 2.11 |

extracts of strawberries and potatoes over this same period was minimal (Table IV).

Recovery of AA, added either prior to blending or to the final extract exceeded 94% in all cases (Table V). The identity of the AA peaks was further characterised by their UV spectra (Fig. 3) obtained using diode array detection (DAD). Purity was confirmed by analysis of the upslope, apex and downslope of the spectra of each sample.

DHAA prepared by quantitative oxidation of AA [9] had a retention time of 10.5 min using the same chromatographic conditions. The absorption maximum for DHAA was 230 nm. Thus this system could be used to detect both AA and DHAA simultaneously, since AA also absorbs strongly at 230 nm. However, the ability to do so depends on the concentration of DHAA since the minimum detection level is 100 ng/$\mu$l with a 10-$\mu$l injection. In the present study, the concentrations of DHAA in strawberries and potatoes were low and it was necessary to quantify DHAA by reduction to AA using the modified Hughes method referred to previously.

The values obtained for the oxidation of 20 and 5 ng ng/$\mu$l AA standards to DHAA and its subsequent reduction by *dl*-homocysteine were 96 and 94%, respectively, which are in agreement with those of Rose and Nahrwold [9].

To date some 1500 samples have been analysed using one column with no detectable loss of resolution or column deterioration.

## CONCLUSION

The HPLC procedure described provides a simple, rapid and sensitive method for determination of AA, DHAA and hence the total vitamin C content of strawberries and potatoes. Although not tested, ion-exclusion chromatography may provide a quantitative method for the determination of total ascorbic acid in the complex matrices of other raw and cooked foods.

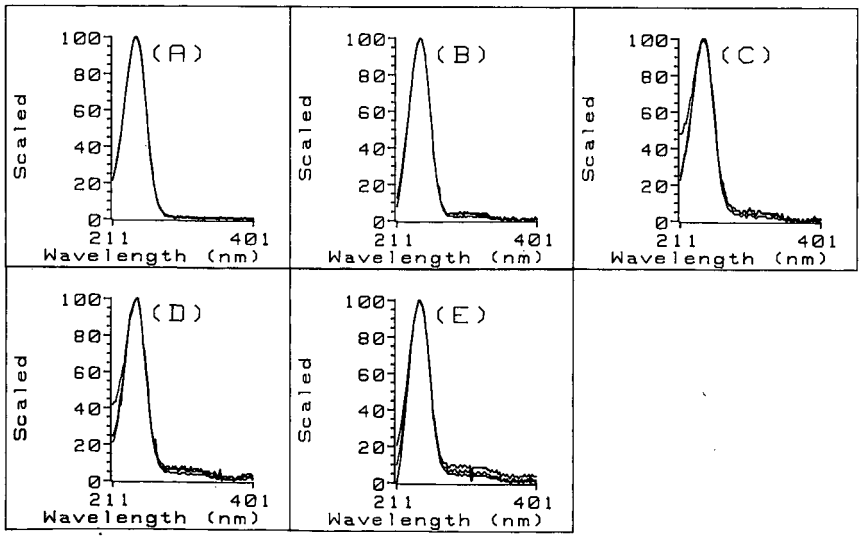


Fig. 3. Spectra obtained using DAD for: (A) AA standard, (B) strawberry extract, (C) raw potato extract, (D) boiled potato extract, (E) baked potato extract.

ACKNOWLEDGEMENT

The authors wish to thank Dr. D. J. Kilpatrick for statistical analyses.

REFERENCES

1 A. Bendich, *Food Technol.*, 11 (1987) 112.
2 B. Borenstein, *Food Technol.*, 11 (1987) 98.
3 L. A. Pachla, D. L. Reynolds and P. T. Kissinger, *J. Assoc. Off. Anal. Chem.*, 68 (1985) 1.
4 A. Polesello and A. Rizzolo, *J. Micronutr. Anal.*, 2 (1986) 153.
5 I. A. Nicolson, R. Macrae and D. P. Richardson, *Analyst, (London)*, 109 (1984) 267.
6 S. A. Margolis and I. Black, *J. Assoc. Off. Anal. Chem.*, 70 (1987) 806.
7 L. F. Russel, *J. Food Sci.*, 51 (1986) 1567.
8 P. Wimalasiri and R. B. H. Wills, *J. Chromatogr.*, 256 (1983) 368.
9 R. C. Rose and D. L. Nahrwold, *Anal. Biochem.*, 114 (1981) 140.
10 S. C. Churms, *J. Chromatogr.*, 500 (1990) 555.
11 J. Augustin, C. Beck and G. I. Marousek, *J. Food Sci.*, 46 (1981) 312.
12 S. H. Ashoor, W. C. Monte, and J. Welty, *J. Assoc. Off. Anal. Chem.*, 67 (1984) 78.
13 R. E. Hughes, *Biochem. J.*, 64 (1956) 203.
14 A. A. Paul and D. A. T. Southgate, *McCance and Widdowsons The Composition of Foods*, H.M.S.O., London, 4th ed., 1978.

*Journal of Chromatography*, 594 (1992) 195–201
Elsevier Science Publishers B.V., Amsterdam

CHROM. 23 825

# Solvent degradation of cloxacillin *in vitro*

# Tentative identification of degradation products using thermospray liquid chromatography–mass spectrometry

Krystyna L. Tyczkowska*

*Clinical Pharmacology Unit, Department of Anatomy, Physiology Sciences and Radiology, College of Veterinary Medicine, North Carolina State University, 4700 Hillsborough Street, Raleigh, NC 27606 (USA)*

Robert D. Voyksner

*Analytical and Chemical Sciences, Research Triangle Institute, P.O. Box 12194, Research Triangle Park, NC 27709 (USA)*

Arthur L. Aronson

*Clinical Pharmacology Unit, Department of Anatomy, Physiology Sciences and Radiology, College of Veterinary Medicine, North Carolina State University, 4700 Hillsborough Street, Raleigh, NC 27606 (USA)*

(First received July 2nd, 1991; revised manuscript received October 21st, 1991)

ABSTRACT

The determination of cloxacillin and the other penicillin antibiotics at trace levels in pharmaceutical samples and biological fluids and tissues is difficult. Degradation of penicillins occurs during exposure to chemicals and solvents used in sample extraction, storage of extracts and chemical analysis. One of the most important factors for the determination of cloxacillin in bovine milk and tissues is the choice of solvent used for extraction. Cloxacillin stored in different solutions underwent two types of degradation: hydrolysis with decarboxylation to yield cloxacillinpenilloic acids when water or aqueous solutions of acetonitrile or 2-propanol were used, and alcoholysis to form cloxacillinpenicilloic acid ester when methanol or ethanol was used. Cloxacillin stored in aqueous methanol or acetonitrile solution underwent faster degradation when stored in water or aqueous solutions of 2-propanol or ethanol. The solvent combinations that resulted in minimum sample degradation of cloxacillin were acetonitrile–ethanol–water (25:25:50) or ethanol–water (50:50). Degradation of cloxacillin was faster at the lower levels (500 and 50 ng/ml) of the antibiotic for all solvents tested. Nearly complete degradation of cloxacillin was observed at the 50 ng/ml level after 2 h at 20°C. Degradation was nearly non-existent at the 1 mg/ml level of the antibiotic in each solvent.

## INTRODUCTION

The determination of β-lactam antibiotics in pharmaceutical samples, biological fluids or tissues is difficult owing to solvent degradation occurring during sample extraction, storage and chemical analysis. Degradation of β-lactam in the presence of methanol has been reported [1] and solvents used in sample preparation or storage of extracted samples could account for some degradation products reported for penicillins [2–13]. Degradation in common solvents used in β-lactam analysis, such as methanol or acetonitrile [14–20], could prevent their determination at part per billion (ppb) levels. Further, under these circumstances, the determination of penicillins at ppb levels may be based on the

0021-9673/92/$05.00 

detection of degradation products with nearly identical retention times in the absence of a specific liquid chromatographic (LC) detector. In order to achieve ppb determinations of β-lactams, the stability of these antibiotics in various solvents used for sample extraction from milk or tissue and LC analysis must be studied. This paper reports the extent of degradation observed for cloxacillin in various solvents and identified the major degradation products formed.

## EXPERIMENTAL

### *Materials and reagents*

A 100 μg/ml cloxacillin (Sigma, St. Louis, MO, USA) solution was prepared in the following solvents: acetonitrile–water (50:50), acetonitrile, methanol–water (50:50), methanol, water, ethanol–water (50:50), 2-propanol–water (50:50), acetonitrile–0.2% aqueous phosphoric acid (50:50), acetonitrile–acetic acid–0.1 *M* aqueous ammonium acetate (50:2:48) and acetonitrile–ethanol–water.

Acetonitrile, methanol, ethanol and 2-propanol were of high-performance liquid chromatographic (HPLC) grade (American Burdick and Jackson, Muskegon, MI, USA), water was obtained from Hydro Services and Supplies (Research Triangle Park, NC, USA) and ammonium acetate was of HPLC grade (Fisher Scientific, Raleigh, NC, USA). The cloxacillin solutions were stored in amber-glass vials for up to 8 weeks at −20°C. Every 1–2 weeks the samples were analyzed by liquid chromatography–ultraviolet detection (LC–UV). The sample solutions of cloxacillin were analyzed by thermospray LC–mass spectrometry (MS) at the 4–8-week point in the stability study to identify degradation products formed.

The correlation between degradation rate and concentration of cloxacillin was also investigated from the 1 mg/ml–50 ng/ml levels. Solutions of 1000, 100 and 0.5 μg/ml and 50 ng/ml of cloxacillin in acetonitrile–water (50:50), methanol–water (50:50), ethanol–water (50:50), isopropanol–water (50:50) and water were stored in amber-glass vials for three weeks at −20 or 20°C (room temperature). The stored samples were analyzed weekly by LC–UV to determine the extent of degradation.

### *Liquid chromatography–ultraviolet detection*

The LC–UV equipment consisted of a Waters Model W 600 solvent-delivery system coupled to a Model 900 UV–VIS photodiode-array detector (Waters Chromatography Division, Milford, MA, USA). The LC separation was conducted using a mobile phase consisting of acetonitrile–water (30:70, v/v) containing 5 m*M* dodecanesulfonate (Regis, Morton Grove, IL, USA) and 0.1% (v/v) 85% phosphoric acid at a flow-rate of 0.5–0.7 ml/min. The separation of the degradation product was accomplished on an Ultremex phenyl 3-μm analytical column 150 × 4.6 mm I.D.) (Phenomenex, Torrance, CA, USA). The UV–VIS photodiode-array detector was set to a wavelength range of 200–310 nm at 0.01–0.3 a.u.f.s.

### *Liquid chromatography–mass spectrometry*

Thermospray LC–MS was applied under the following conditions. The LC mobile phase was isopropanol–acetic acid–0.25 *M* aqueous ammonium acetate solution (12:2.5:85.5) at a flow-rate of 1 ml/min and an Ultremex phenyl 3-μm analytical column (150 × 4.6 mm I.D.) was used for the separation. The thermospray interface (Finnigan MAT, San Jose, CA, USA) was operated with source and vaporizer temperatures of 300 and 130°C, respectively. The thermospray interface was mounted on a Finnigan MAT 4800 quadrupole mass spectrometer. The mass spectrometer was operated in the positive-ion detection mode, scanning from 150 to 600 u in 2 s.

## RESULTS AND DISCUSSION

The major aim of this study was to determine the degradation products formed when cloxacillin was exposed to solvents commonly used in sample preparation. To verify the purity of cloxacillin and demonstrate that no artifact signals originating from the analysis method were present, a newly prepared aqueous solution of cloxacillin (structure I, Fig. 1) was analyzed by thermospray LC–MS. This analysis indicated that no impurities were present in the standard and no degradation products were formed in the LC–MS analysis (Fig. 2). The thermospray mass spectrum of this standard exhibited an $[M + H]^+$ ion at $m/z$ 436 and several protonated fragment ions at $m/z$ 410, 277 and 160. All protonated frag-

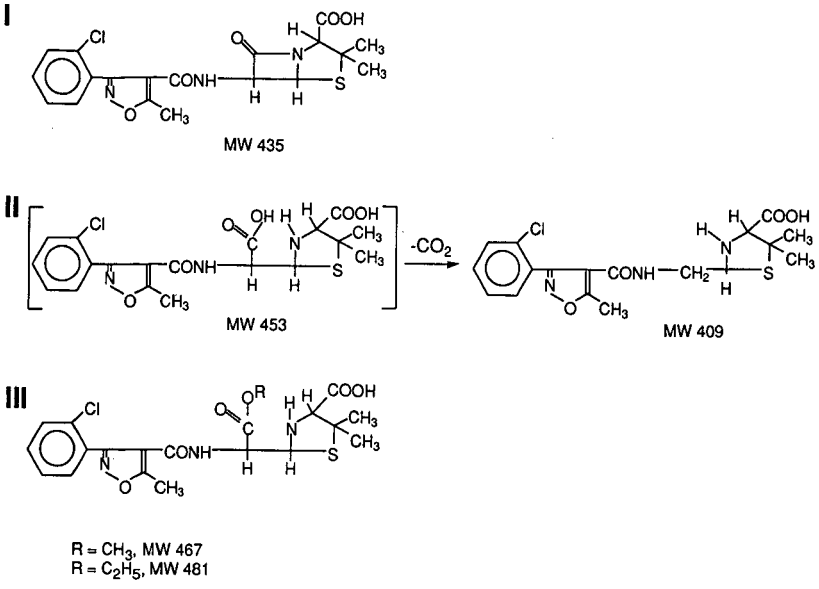


Fig. 1. Structures of (I) cloxacillin, (II) cloxacillinpenicilloic acid (left) and cloxacillinpenilloic acid (right) and (III) cloxacillinpenicilloic acid methyl and ethyl esters. MW = Molecular weight.

ment ions of cloxacillin involve ring opening and cleavage of the $\beta$-lactam ring. The ion at $m/z$ 160 is representative of all penicillin antibiotics and the ion at $m/z$ 410 formed as a result of thermal degradation of cloxacillin [21].

The storage of cloxacillin in water or in acetonitrile–water (50:50) for 2–4 weeks at −20°C resulted in sample degradation. LC–UV indicated the presence of three components in acetonitrile–water (50:50) (Fig. 3). Water resulted in a similar chromatogram, showing only differences in the relative intensities of the three peaks. The first peak (1) produced the thermospray mass spectrum shown in Fig. 4. This spectrum was interpreted as being clox-

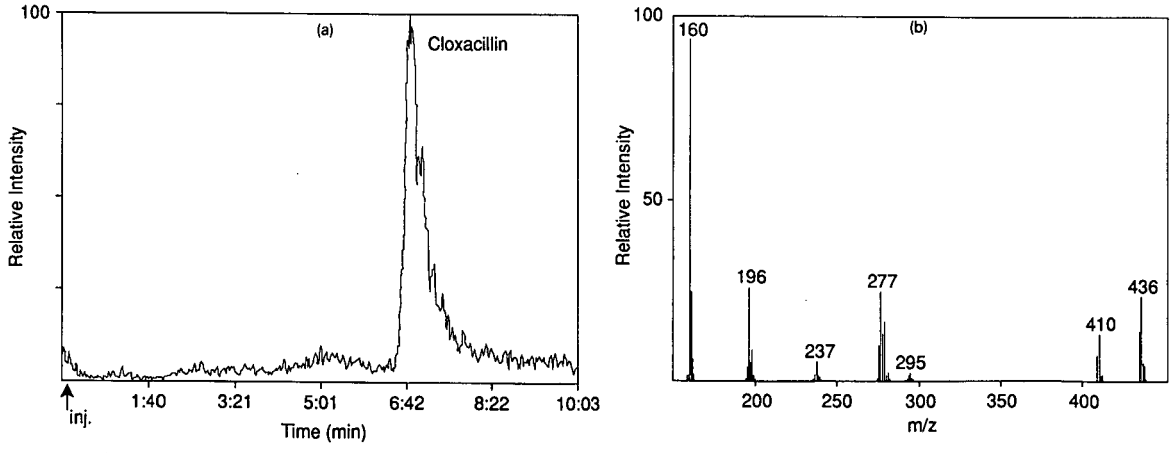


Fig. 2. Analysis of a newly prepared cloxacillin in water solution by thermospray LC–MS. (a) Chromatogram; (b) mass spectrum of cloxacillin.

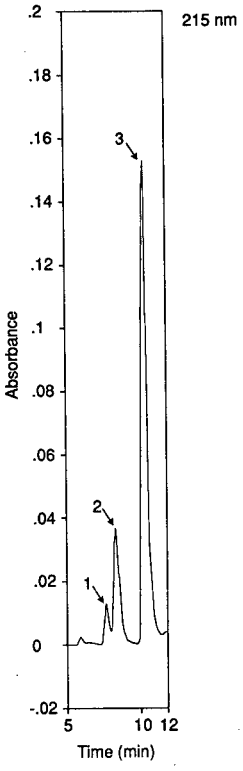


Fig. 3. LC–UV of cloxacillin (100 μg/ml) after 2 weeks in acetonitrile–water (50:50). Peak 1 is the β-epimer, peak 2 is the α-epimer of cloxacillinpenilloic acid and peak 3 is cloxacillin.

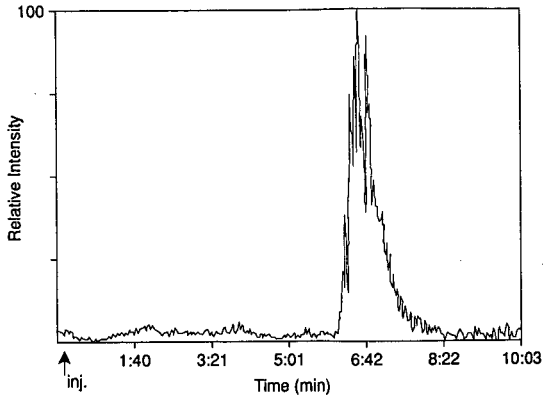


Fig. 5. Thermospray LC–MS chromatogram obtained after 4 weeks of storage of cloxacillin in methanol–water (50:50). This resulted in 100% conversion into its methyl ester.

acillin-β-penilloic acid (structure II, right, Fig. 1). The spectrum exhibited an $[M + H]^+$ ion at $m/z$ 410 and several protonated fragment ions at $m/z$ 279, 237 and 196. As the β-lactam ring was opened in the formation of the cloxacillin-β-penilloic acid, the ion at $m/z$ 160 (characteristic of β-lactams) was absent. The second peak (2) in the chromatogram exhibited the identical thermospray mass spectrum to Fig. 4 and showed the same UV spectral curve as the β-penilloic acid. Based on this information it was postulated that these two peaks were epimers (cloxacillin-α- and β-penilloic acids). Further investigation showed that peak 1 was converted into peak 2 with time in both solutions. This conversion

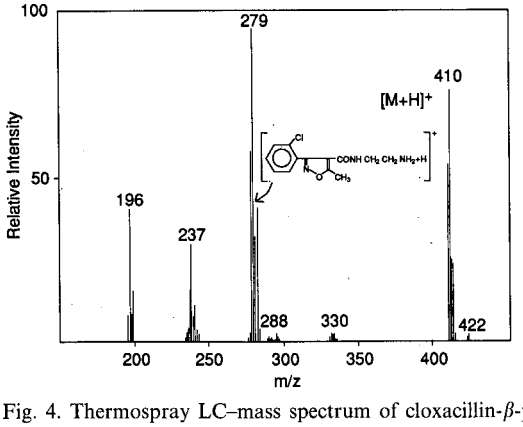


Fig. 4. Thermospray LC–mass spectrum of cloxacillin-β-penilloic acid in acetonitrile–water (50:50). The spectrum for the compound in pure water was identical.

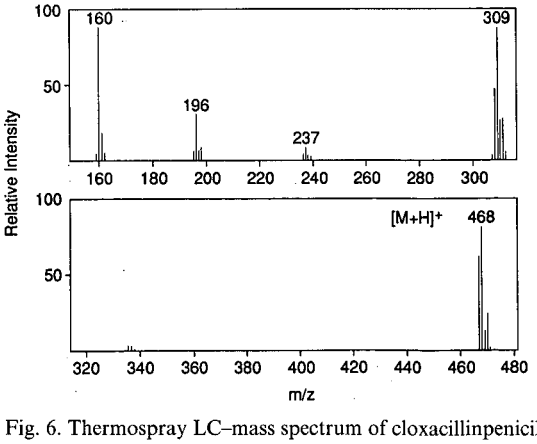


Fig. 6. Thermospray LC–mass spectrum of cloxacillinpenicilloic acid methyl ester stored in methanol–water (50:50) for 2 weeks.

was consistent with a report in the literature that indicated cloxacillin-$\beta$-penilloic acid is converted into cloxacillin-$\alpha$-penilloic acid [3]. The last peak in the chromatogram (3) was cloxacillin. This peak showed a thermospray mass spectrum that was identical with that in Fig. 2b for cloxacillin in both solutions.

The storage of cloxacillin in methanol solution resulted in the formation of different degradation products. Thermospray LC–MS analysis of cloxacillin stored in methanol for 4 weeks exhibited only one peak, the retention time of which was slightly longer than that of cloxacillin (Fig. 5). This peak was identified as the methyl ester of cloxacillin (structure III, Fig. 1). The thermospray mass spectrum of the peak (Fig. 6) showed an $[M + H]^+$ ion at $m/z$ 468 and protonated fragment ions at $m/z$ 309, 196 and 160. The fragmentation of the methyl ester is similar to that for cloxacillin. The ion at $m/z$ 160 results from fragmentation after methanolysis instead of thermal opening of the ring. The ion at $m/z$ 309 is the methyl ester of the ion observed at $m/z$ 277 for cloxacillin.

The use of other common longer chain alcohols such as ethanol and 2-propanol also exhibited degradation of cloxacillin. The storage of cloxacillin in ethanol resulted in the formation of the cloxacillin ethyl ester (Fig. 7). The thermospray LC–MS mass spectrum exhibited an $[M + H]^+$ ion at $m/z$ 482 and two characteristic protonated fragment ions at $m/z$ 323 and 160. The use of 2-propanol did not result in formation of a propyl ester, but rather the cloxacillin-$\alpha$- and $\beta$-penilloic acid epimers were detected. The thermospray mass spectrum of the $\alpha$-epimer exhibited a spectrum nearly identical with the $\beta$-epimer spectrum shown in Fig. 4.

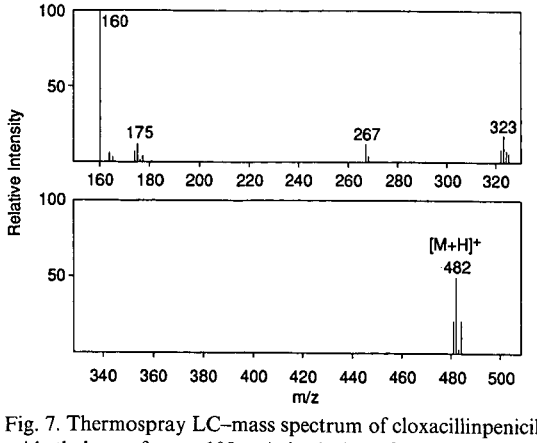


Fig. 7. Thermospray LC–mass spectrum of cloxacillinpenicilloic acid ethyl ester from a 100 $\mu$g/ml solution of cloxacillin stored in ethanol–water (50:50) for 6 weeks.

The storage of cloxacillin (100 $\mu$g/ml) in various solutions (Fig. 8) indicated that there was a wide range of degradation rates. Methanol resulted in the most rapid degradation of this antibiotic whereas acetonitrile–ethanol–water (25:25:50) resulted in the least degradation. After 2 weeks of storage in methanol–water (50:50) or methanol, cloxacillin was entirely converted into its methyl ester. Ethanol–water (50:50) resulted in a slower alcoholysis of cloxacillin compared with methanol. When cloxacillin was stored in 2-propanol–water (50:50), degradation initially occurred quickly, then slowed significantly over the 8-week study.

Cloxacillin underwent slower hydrolysis in water than in many organic or organic–water solutions. After 4 weeks of storage in water only 14% of cloxacillin had been converted into its degradation products. The storage of cloxacillin in acetonitrile for 4 weeks resulted in 25% degradation. The addition of 0.2 % of phosphoric acid or 2% of acetic acid in 0.1 *M* ammonium acetate (mobile phase for LC–UV or thermospray LC–MS) further increased the degradation rate. It was interesting that after 2 weeks further hydrolysis was not detected for the solutions containing phosphoric acid or acetic acid and ammonium acetate. Ethanol–acetonitrile–water (25:25:50) showed the least degradation, with only a 5% loss of cloxacillin after 4 weeks.

Most important, the degradation rate of cloxacillin was dependent on concentration. Lower concentrations of cloxacillin underwent faster degradation than higher concentrations. The storage of 0.5 $\mu$g/ml cloxacillin in methanol-water (50:50), 2-propanol–water (50:50), acetonitrile–water (50:50) and ethanol–water (50:50) resulted in 100%, 87%, 47% and 73% degradation, respectively of the antibiotic after 1 week. Cloxacilin completely degraded in the 0.5 $\mu$g/ml solution after 3 weeks of storage. Cloxacillin solutions stored in water resulted in 78% degradation in 1 week and 82% degradation in 3 weeks. The degradation rates for the five solutions evaluated at 0.5 $\mu$g/ml were significantly higher than those at the 100 $\mu$g/ml level as shown in Fig. 8.

Degradation of cloxacillin at the 50 ppb level occurred in a matter of hours at room temperature or

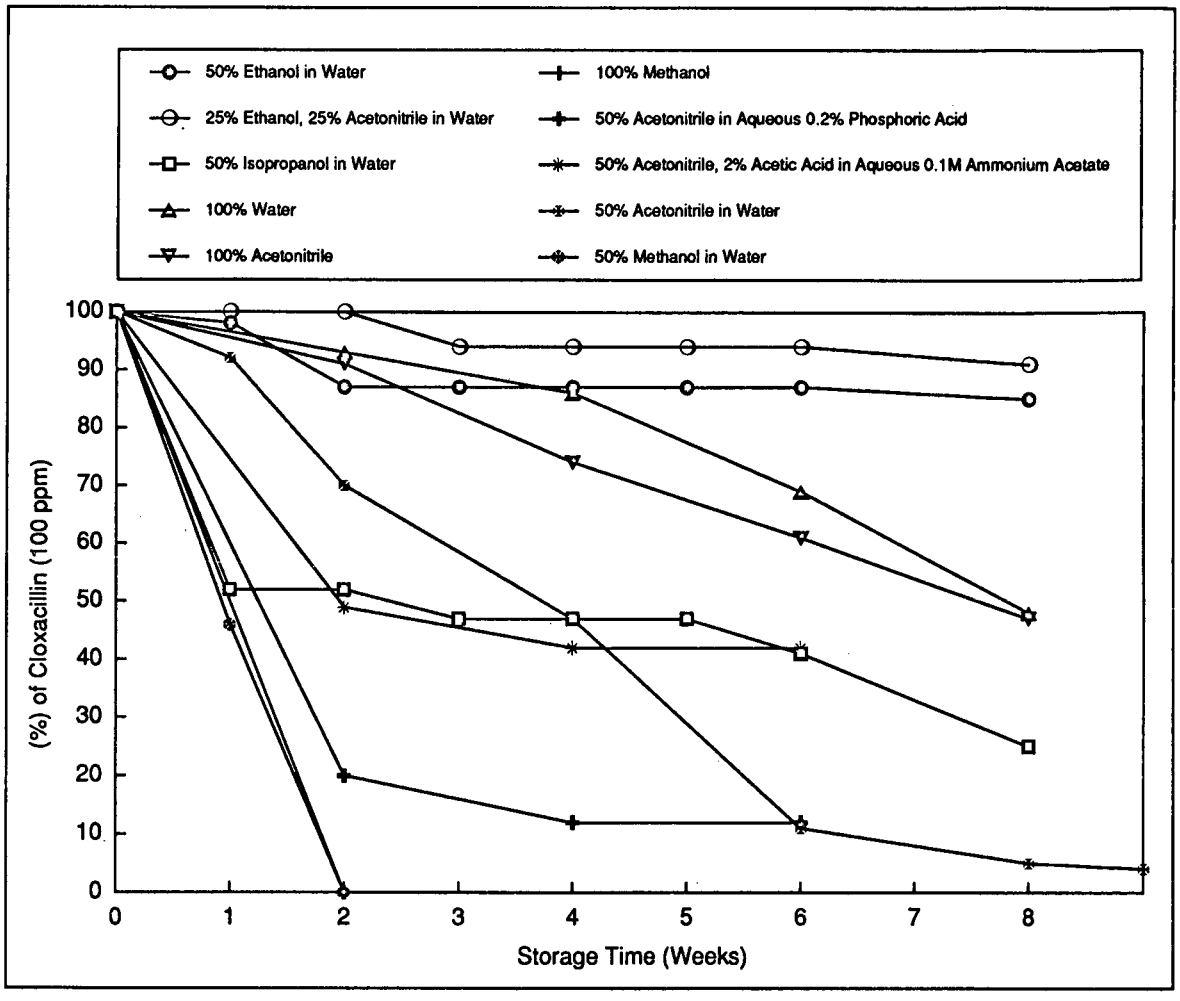


Fig. 8. Degradation of a 100 μg/ml solution of cloxacillin in different solvents during storage for up to 8 weeks at −20°C. This simulates the storage of sample extracts before LC analysis.

at −20°C. After storage of 50 ng/ml of cloxacillin in any organic-containing solvent for 2 h resulted in complete degradation. Degradation was slightly less at lower temperature (−20°C). It is obvious that these fast degradation rates can drastically alter the measurement of penicillin during extraction, storage of the extract before analysis and even during LC analysis. Water resulted in the least degradation for cloxacillin at the 50 ng/ml level, resulting in only about 18% degradation in 1 day and complete degradation within 3 weeks. On the other hand, cloxacillin stored in the same solvents at the 1000 μg/ml level did not undergo detectable degradation through the 3-week stability evaluation.

## CONCLUSIONS

Degradation of trace (low ppb) levels of penicillins can occur in a matter of hours. Exposure of penicilins to organic solvents that are necessary for extraction or chromatography can lead to the formation of degradation products. Storage of a penicillin extract for analysis at −20°C in an organic-containing solvent used for extraction can result in complete degradation in as little as 2–4 h (for methanol). Cloxacillin stored in various solutions underwent two types of degradation: hydrolysis with decarboxylation in the presence of water, acetonitrile and 2-propanol and alcoholysis when methanol or

ethanol was present. As the methanolysis products form at a faster rate, methanol cannot be used in any step of an analytical procedure. With strict control of the analytical procedure, ethanol–water (50:50) or acetonitrile–ethanol–water (25:25:50) can be utilized for extraction from biological fluids or tissue and for the chromatographic separation of penicillins. If the extracts cannot be analyzed immediately, the samples should be stored dry or only in the presence of water at −20°C or lower temperatures to minimize degradation. Further, care must be taken in the determination of penicillins by LC in the absence of specific detectors, as some of the degradation products have very similar retention times to the undegraded antibiotic, possibly leading to misidentification.

ACKNOWLEDGEMENT

This research was supported by the Food and Drug Administration under Cooperative Agreement No. FD-U-000589.

REFERENCES

1 K. L. Tyczkowska, R. D. Voyksner and A. L. Aronson, *J. Vet. Pharmacol. Ther.*, 14 (1991) 51.
2 P. E. Manni, R. A. Lipper, J. M. Blaha and S. L. Hem, *J. Chromatogr.*, 76 (1978) 512.
3 G. W. K. Fong, R. N. Johnson and B. T. Kho, *J. Chromatogr.*, 225 (1983) 199.
4 J. Hoogmartens, E. Roets, G. Jansen and V. Vanderhaeghe, *J. Chromatogr.*, 244 (1982) 299.
5 W. A. Vadino, T. E. Sugita, R. L. Schnaare, H. Y. Ando and P. J. Niebergall, *J. Pharma. Sci.*, 68 (1979) 1316.
6 J. M. Blaha, A. M. Knevel and S. L. Hem, *J. Pharm. Sci.*, 64 (1975) 1384.
7 A. H. Thomas and R. A. Broadbridge, *Analyst (London)*, 95 (1970) 459.
8 F. Nachtmann, *Chromatographia*, 12 (1979) 380.
9 G. W. K. Fong, D. T. Martin, R. N. Johnson and B. T. Kho, *J. Chromatogr.*, 298 (1984) 459.
10 I. Ghebre-Sellassie, S. L. Hem and A. M. Knevel, *J. Pharm. Sci.*, 71 (1982) 351.
11 L. Koprivc, E. Polla and J. Hranilovic, *Acta Pharm. Suec.*, 13 (1976) 421.
12 P. O. Roksvaag, H. I. Brummeneaes and T. Waaler, *Pharm. Acta Helv.*, 54 (1979) 180.
13 A. E. Bird, E. A. Cutmore, K. R. Jennings and A. C. Marshal, *J. Pharm. Pharmacol.*, 35 (1983) 138.
14 H. Terrada and Y. Sakabe, *J. Chromatogr.*, 348 (1985) 379.
15 M. J. Lebelle, W. L. Wilson and G. Lauriault, *J. Chromatogr.*, 202 (1980) 144.
16 C. M. Moore, K. Sato, H. Hattori and Y. Katsumata, *Clin. Chim. Acta*, 190 (1990) 121.
17 D. E. Holt, J. de Louvois, R. Hurley and D. Harvey, *J. Antimicrob. Chemother.*, 26 (1990) 107.
18 K. Tyczkowska, R. D. Voyksner and A. L. Aronson, *J. Chromatogr.*, 490 (1989) 101.
19 W. A. Mopats, *J. Chromatogr.*, 507 (1990) 177.
20 J. Carlqvist and D. Westerlund, *J. Chromatogr.*, 344 (1985) 285.
21 M. M. Siegel, R. K. Isensee and D. J. Beck, *Anal. Chem.*, 59 (1987) 989.

*Journal of Chromatography*, 594 (1992) 203–208
Elsevier Science Publishers B.V., Amsterdam

CHROM. 23 871

# Determination of dirithromycin purity and related substances by high-performance liquid chromatography

B. A. Olsen*, J. D. Stafford and D. E. Reed

*Lilly Research Laboratories, Eli Lilly and Company, P.O. Box 685, Lafayette, IN 47902 (USA)*

(First received August 27th, 1991; revised manuscript received November 4th, 1991)

ABSTRACT

High-performance liquid chromatographic methods for the characterization of dirithromycin, a macrolide antibiotic derived from erythromycin, are described. Chromatography is performed on a Hypersil ODS column using a mobile phase consisting of acetonitrile–methanol–50 m*M* potassium phosphate buffer, pH 7.5 (44:19:37) with ultraviolet detection at 205 nm. The strength of the phosphate buffer can be used to control the selectivity of the separation of dirithromycin and related substances, especially the separation of erythromycylamine. The addition of methanol to the mobile phase improves peak shapes for the compounds of interest. Validation data for purity and related substances methods are described.

## INTRODUCTION

Dirithromycin, an oxazine derivative of erythromycin, is a new gram-positive macrolide antibiotic currently undergoing clinical evaluation. Accurate, well-characterized methods for the determination of dirithromycin purity and related substances are necessary for development and quality control of the bulk drug production process and assessment of bulk drug stability. The purity method must be free from interference by process-related impurities and degradation products. The related substances method must be able to detect and quantify these same impurities.

High-performance liquid chromatography (HPLC) has been widely used for the analysis of erythromycin and related macrolides because of its ability to separate closely related compounds arising from biosynthetic, synthetic, or metabolic processes [1–16]. Methods for biological fluid analysis have been designed primarily for quantification of the drug itself rather than low levels of related impurities [11–16]. The emphasis of methods for quality control has been separation of the main component from stucturally similar impurities and adequate quantification of these impurities [1–9]. Common problems encountered with methods for erythromycin and derivatives include peak tailing, poor resolution of impurities, and short column life due to the use of high-pH mobile phases and/or high column temperature [1–4,6,9,10]. A dependence of separation on column history or conditioning has also been observed [1,10].

The structures of dirithromycin and related substances are given in Fig. 1. Dirithromycin B is produced from the corresponding erythromycin B factor present in the starting material. Erythromycin hydrazone and erythromycylamine are precursors in the synthesis of dirithromycin and may be present at low levels in samples. Erythromycylamine may also arise from hydrolysis of dirithromycin in neutral or slightly acidic solution. Dirithromycin forms an equilibrium amount of epi-dirithromycin in solution with epimerization accelerated under acidic conditions [17].

The determination of dirithromycin and related substances represents a distinct challenge because of the lack of a UV chromophore in the molecule, the tendency to produce tailing peaks, and the instability of dirithromycin under neutral or slightly acidic

0021-9673/92/$05.00 

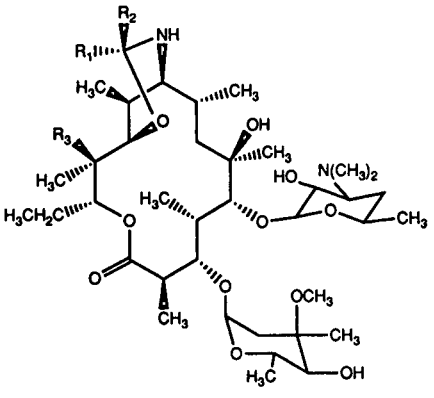

| Compound | R1 | R2 | R3 |
|---|---|---|---|
| Dirithromcyin | $CH_3OCH_2CH_2OCH_2$ | H | OH |
| Epi-dirithromycin | H | $CH_3OCH_2CH_2OCH_2$ | OH |
| Dirithromycin B | $CH_3OCH_2CH_2OCH_2$ | H | H |

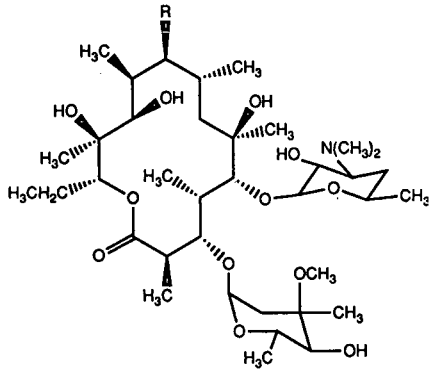

| Compound | R |
|---|---|
| Erythromycylamine | $NH_2$ |
| Erythromycin hydrazone | $NNH_2$ |

Fig. 1. Structures of dirithromycin and related substances.

conditions. Although dirithromycin has been determined by HPLC with electrochemical detection [12], this detection mode is not as easily established in quality control laboratories as UV detection. Ultraviolet detection at low wavelengths limits the mobile phase modifiers that can be used to enhance selectivity and peak shape. Also, the need to use a relatively high-pH mobile phase results in concerns about column life and method performance over time. This report describes methods for dealing with the above problems to provide suitable assay procedures for the determination of dirithromycin and related substances in the bulk drug.

## EXPERIMENTAL

### *Reagents*

HPLC-grade acetonitrile and methanol were obtained from EM Science (Gibbstown, NJ, USA). Buffer solutions were prepared using appropriate concentrations of potassium phosphate, mono and dibasic, also from EM Science. Water for mobile phase and sample solutions was purified with a Milli-Q system from Millipore (Milford, MA, USA).

Dirithromycin and the related substances shown in Fig. 1 were prepared at Eli Lilly. Sample solutions were prepared as described in the text.

### *Apparatus*

The chromatographic system consisted of a Model 600 pump with column heater (Waters, Bedford, MA, USA), a Model 728 autoinjector (Alcott, Norcross, GA, USA) with a 10-$\mu$l fixed-loop injection valve (Valco, Houston, TX, USA), and a Model 787 UV detector set at 205 nm (Applied Biosystems, Ramsey, NJ, USA). Chromatograms were recorded using an in-house data aquisition system. The column temperature was maintained at 40°C, except during temperature effect studies. The flow-rate was 2.0 ml/min. The following columns were investigated: Hypersil ODS (Jones Chromatography, Littleton, CO, USA), YMC Basic and YMC ODS (YMC, Morris Plains, NJ, USA), Capcell Pak $C_{18}$ (Dychrom, Sunnyvale, CA, USA), Zorbax RX and Zorbax ODS (MacMod Analytical, Chadds Ford, PA, USA), Supelcosil LC-18-DB (Supelco, Bellefonte, PA, USA), Ultrasphere ODS (Beckman, San Ramon, CA, USA), Asahipak ODP-50 (Advanced Separation Technologies, Whippany, NJ, USA), ACT-1, 150 mm × 4.6 mm I.D. (Anspec, Ann Arbor, MI, USA), and Unisphere-PDB, 8 $\mu$m particle size (Biotage, Charlottesville, VA, USA). Unless indicated otherwise, all column dimensions were 250 mm × 4.6 mm I.D. with 5-$\mu$m particles.

## RESULTS AND DISCUSSION

### *Column choice*

Initial assay development indicated that a mobile

phase pH greater than 7.0 and elevated column temperature were necessary to achieve adequate separation and peak shape. These conditions, however, promoted short column life and associated reproducibility problems. Polymer columns with greater stability to high-pH eluents (Asahipak ODP-50, ACT-1) were investigated, but poor resolution and peak shape similar to that observed by Kibwage *et al.* [4], for erythromycins was obtained. A polymer-coated column (Capcell Pak $C_{18}$) was investigated using a pH 8.0 mobile phase. It provided acceptable resolution initially, but retention times drifted and selectivity was lost in 2–3 d. A polybutadiene-coated alumina column (Unisphere-PBD) was also used without success.

Efforts were then focussed on identification of silica-based reversed-phase columns that would provide the necessary selectivity with good stability. Columns investigated include the following: Zorbax ODS, Zorbax RX, YMC ODS, YMC Basic, Supelcosil LC-18-DB, Ultrasphere ODS, and Hypersil ODS. Of these, the Ultrasphere ODS and Hypersil ODS columns provided the best combination of selectivity and stability. These two columns displayed similar selectivity for the compounds of interest. The Hypersil ODS column provided longer column life, so it was used for further optimization.

*Organic modifier*

It was possible to control the retention of dirithromycin using acetonitrile to adjust eluent solvent strength, but badly tailing peaks were obtained. The retention and peak shape of dirithromycin and related substances were investigated as methanol was added to the mobile phase. Toluene was also included in the component mixture as a possible impurity from the production process. Fig. 2 shows chromatograms obtained as the methanol content was increased at the expense of the phosphate buffer. The peak shape of the macrolides improved dramatically with increases in methanol and, unexpectedly, their retention times remained almost constant. Plots of ln $k'$ (capacity factor) *vs.* % organic modifier are shown in Fig. 3. A linear plot with negative slope was obtained for toluene, indicating normal behavior for a simple hydrophobic retention mechanism. In contrast, the plots for the macrolides were almost flat. The phosphate buffer and methanol have roughly equal eluting strength

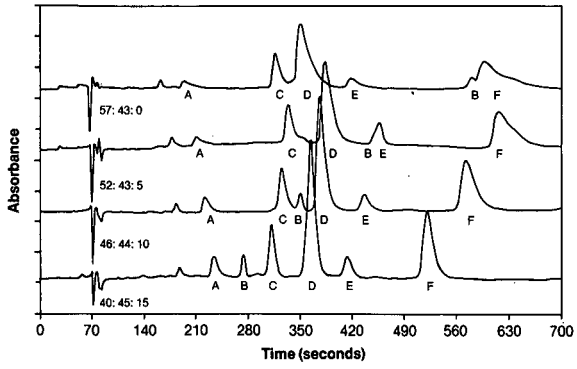


Fig. 2. Effect of methanol on separation and peak shape of dirithromycin and related substances. Mobile phase: 50 m*M* potassium phosphate, pH 7.3–acetonitrile–methanol in the ratios indicated; A = erythromycylamine (4 μg), B = toluene (0.02 μg), C = erythromycin hydrazone (2 μg), D = dirithromycin (20 μg), E = epidirithromycin (4 μg), F = unknown.

for dirithromycin and related substances, suggesting that retention for these compounds is controlled by a combination of hydrophobic and ion-exchange mechanisms.

*Buffer concentration*

The buffer concentration was also found to be a key parameter in controlling the separation of

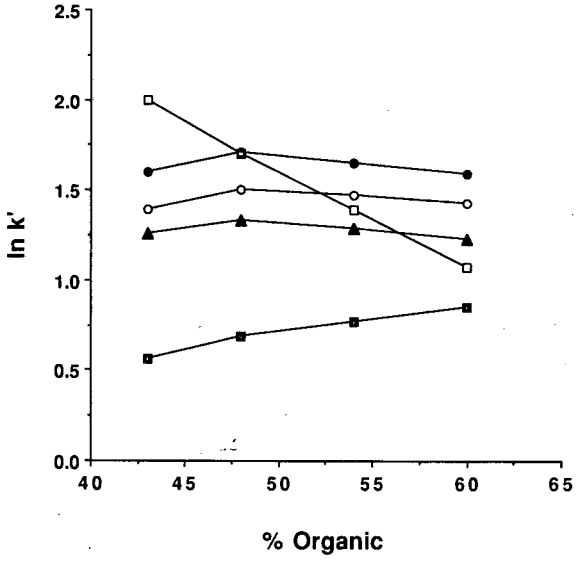


Fig. 3. Ln $k'$ *vs.* % organic solvent in mobile phase: □ = toluene, ■ = erythromycylamine, ▲ = erythromycin hydrazone, ○ = dirithromycin, ● = epidirithromycin.

dirithromycin and related substances. This is consistent with the influence of the aqueous portion of the eluent described above. Capacity factors are plotted as a function of buffer concentration in Fig. 4. While increases in buffer concentration produced slight decreases in retention for most sample components, the retention of erythromycylamine was dramatically affected. As evident in Fig. 4, the buffer concentration could be adjusted to elute erythromycylamine in the desired position relative to the other components.

*pH*

The pH dependence of the separation is illustrated by the plot of *k' vs.* pH at constant buffer concentration in Fig. 5. Mobile phase pH values greater than 7.0 were necessary for optimum resolution and peak shape. As has been observed with other macrolides, increases in pH produced longer retention and better resolution [14,15]. Better peak shape was also observed at higher pH for dirithromycin and related substances. As expected, pH had no effect on toluene retention. Another concern about the mobile phase pH was on-column epimerization of dirithromycin. This would be manifested as a distortion in the trailing side of the dirithromycin peak,

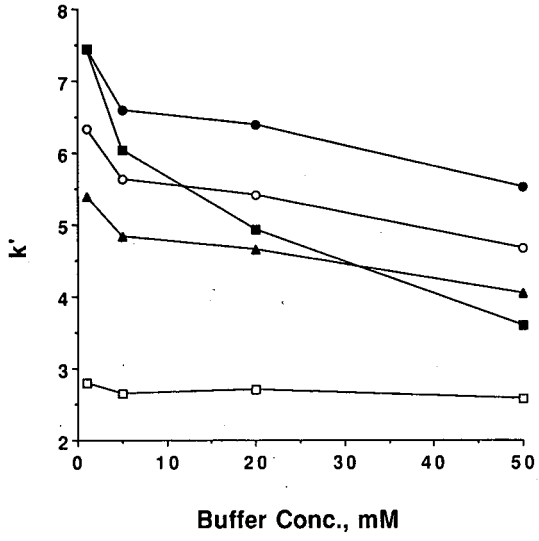


Fig. 4. Effect of buffer concentration on retention of dirithromycin and related substances. Buffer = potassium phosphate, pH 8.0; mobile phase = buffer–acetonitrile–methanol (36:50:14); column temperature = 45°C; symbols as in Fig. 3.

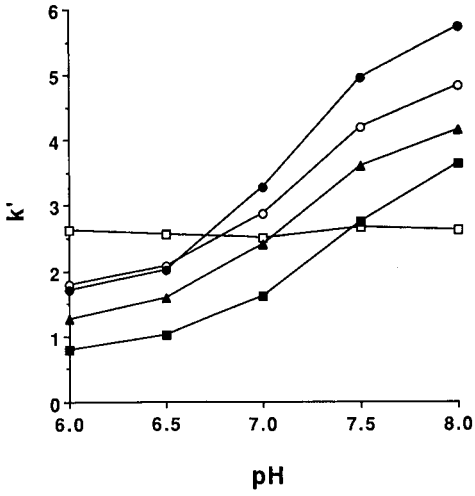


Fig. 5. Effect of pH on retention of dirithromycin and related substances. Mobile phase = 50 m*M* potassium phosphate–acetonitrile–methanol (36:50:14); column temperature = 45°C; symbols as in Fig. 3.

since the epimer was eluted closely after. No significant distortion was observed, indicating that little epimerization occurred during the time between injection and exit from the column at a flow-rate of 2.0 ml/min.

*Temperature*

Column temperature also affected dirithromycin retention, although not as significantly as other parameters. Retention times increased slightly with increases in temperature rather than decreased as might normally be expected. This inverse temperature dependence of retention has been observed for other erythromycin derivatives [1] and tylosin, another macrolide [18].

*Final conditions*

A number of factors were considered when choosing the final conditions for dirithromycin analysis. Although high mobile phase pH and high column temperature gave the best separations, the conditions led to short column life. Values of 7.5 for pH and 40°C for column temperature were chosen as a compromise between column lifetime and resolution. Acceptable resolution was obtained and columns could normally be used for over 300 h.

A mobile phase composition of 50 m*M* phosphate

buffer, pH 7.5–acetonitrile–methanol (37:44:19) was chosen to provide the best separation and peak shape for dirithromycin and known impurities. As shown in Fig. 6, these conditions gave good selectivity and peak shape. Erythromycylamine was of particular concern since it is a degradation product as well as a process-related impurity. Under the conditions chosen, it was separated from other known and unknown impurities that appeared in most samples.

*Other considerations*

It is often impractical or impossible to use reference standards to quantify each related substance in a sample such as dirithromycin, so a common practice is to determine related substances relative to a diluted standard of the main component [2,19]. Consideration of the response of the related substance relative to the main component is important when using this approach. A relative response factor, if significantly different from 1.0, can be applied to correct for differences in absorptivity at the detection wavelength. This was necessary if toluene or erythromycin hydrazone were observed in dirithromycin samples. They absorb much more strongly than dirithromycin as indicated by relative response factors of 64 and 4.1, respectively. Normally, these impurities were not observed in samples. All other impurities were determined relative to a dilute dirithromycin standard with no response correction.

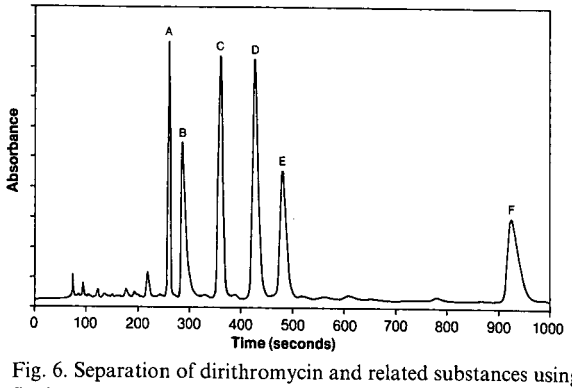


Fig. 6. Separation of dirithromycin and related substances using final assay conditions. Mobile phase = 50 m*M* potassium phosphate buffer, pH 7.5–acetonitrile–methanol (37:44:19); A = toluene (0.1 μg), B = erythromycylamine (10 μg), C = erythromycin hydrazone (4 μg), D = dirithromycin (20 μg), E = epidirithromycin (10 μg), F = dirithromycin B (10 μg).

Sample concentration and injection volume were chosen to provide adequate response without overloading the column and degrading resolution. Concentrations of 2 mg/ml and 10 mg/ml were used for the purity and related substances methods, respectively. A 10-μl injection was used for both methods. Higher concentration or larger injection volume for the related substances method caused loss of resolution between the main peak and components that were eluted just before it.

The stability of sample solutions before injection was investigated. Sample solution stability was greatly dependent on the diluent employed. Epimerization was sufficiently rapid in aqueous buffer/organic diluents to preclude predissolution of samples for automated analysis. Stability of these solutions was increased using a refrigerated autoinjector at 4°C, but epimerization was still observed in less than 4 h. Solutions were stable for 4 h at room temperature, however, in a completely organic diluent composed of acetonitrile–methanol (70:30). Methanol was necessary for adequate solubility of the sample. Adverse effects on the chromatography, such as distorted peak shape, were not observed even though this diluent has a greater solvent strength than the mobile phase. Peaks were broadened only slightly compared to samples dissolved in mobile phase. For automated analysis, stability considerations outweighed the marginal loss of column efficiency, so the completely organic diluent was used.

*Method validation*

Linearity of the purity method was evaluated over a concentration range of 1.66–2.70 mg/ml which encompasses the nominal assay concentration of 2 mg/ml. A coefficient of determination of 0.9996, a relative standard deviation (R.S.D.) of 0.4%, and a log–log slope of 1.00 were obtained.

The reproducibility of the purity method was determined by repeated analysis of a control sample over a period of 6 months. During this time, the analysis was performed by three analysts, on four instruments, using seven columns. An R.S.D. ($n$ = 40) of 0.47% was obtained for the average of duplicate analyses done each day. This demonstrates excellent intralaboratory precision over a number of variables known to affect assay performance.

Linearity of the related substances method was evaluated at the low and high concentration ranges. Dilute standards of dirithromycin over a range of 0.01–0.2 mg/ml provided a coefficient of determination of 0.9996, an R.S.D. of 2.7%, and a log–log slope of 1.03. This range corresponds to 0.1–2.0% related substances in the sample solution. The linearity of total peak area for related substances in sample solutions over a range of 5–15 mg/ml was also determined. A coefficient of determination of 0.9926, an R.S.D. of 4.0%, and a log–log slope of 1.02 were obtained. The above data demonstrate the linearity of response for the standard and sample solutions used in the related substances method.

Reproducibility for related substances was also determined with a control sample. As with the purity method, this measure of precision incorporated variability due to different days, analysts, instruments, and columns. For a sample containing 1.9% related substances, the R.S.D. ($n$ = 29) over a 5-month period was 8%. As expected, the within-day R.S.D. of 2.4% was much lower because it was not affected by as many variables.

*System suitability*

Dirithromycin reacts in mobile phase solution to form epidirithromycin and erythromycylamine. These compounds provide an excellent means of checking the suitability of the chromatographic system each time the method is performed. The system suitability solution was prepared by allowing a 2.5 mg/ml solution of dirithromycin in mobile phase to stand at room temperature for 24 h. After this time, the relative concentrations of the three compounds remained constant for at least 1 month. Dirithromycin peak tailing and resolution from the degradation products were established as meaningful system suitability parameters. Based on data collected over a period of six months ($n$ = 149), criteria for an acceptable system were dirithromycin peak tailing of less than 2.0, resolution between dirithromycin and erythromycylamine of at least 5.0, and resolution between dirithromycin and epidirithromycin of at least 2.0. When these criteria were not met, the mobile phase was adjusted slightly or the column was replaced.

## CONCLUSIONS

A mobile phase consisting of methanol, acetonitrile and phosphate buffer with a Hypersil ODS column was shown to provide separation of dirithromycin and related substances. Methanol reduced peak tailing and the phosphate buffer concentration could be adjusted to control the retention of erythromycylamine relative to the other macrolides studied. The methods described for purity and related substances provided good precision and are suitable for quality control of the bulk drug substance.

## REFERENCES

1 Th. Cachet, I. O. Kibwage, E. Roets, J. Hoogmartens and H. Vanderhaeghe, *J. Chromatogr.*, 409 (1987) 91.
2 D. Morgan, P. Cugier, B. Marello, C. Sarocka, D. Stroz and A. Plasz, *J. Chromatogr.*, 502 (1990) 351.
3 K. Tsuji and M. P. Kane, *J. Pharm. Sci.*, 71 (1982) 1160.
4 I. O. Kibwage, E. Roets, J. Hoogmartens and H. Vanderhaeghe, *J. Chromatogr.*, 330 (1985) 275.
5 T. Geria, W. Hong and R. E. Daly, *J. Chromatogr.*, 396 (1987) 191.
6 N. Kovacic-Bosnjak, J. Marincel, N. Lopotar and G. Kobrehel, *Chromatographia*, 25 (1988) 999.
7 K. Tsuji and J. F. Goetz, *J. Chromatogr.*, 157 (1978) 185.
8 C. Stubbs and I. Kanfer, *Int. J. Pharm.*, 63 (1990) 113.
9 K. Tsuji and J. F. Goetz, *J. Chromatogr.*, 147 (1978) 359.
10 G. Pellegatta, G. P. Carugati and G. Coppi, *J. Chromatogr.*, 269 (1983) 33.
11 C. Stubbs, J. M. Haigh and I. Kanfer, *J. Pharm. Sci.*, 74 (1985) 1126.
12 G. W. Whitaker and T. D. Lindstrom, *J. Liq. Chromatogr.*, 11 (1988) 3011.
13 C. Stubbs and I. Kanfer, *J. Chromatogr.*, 427 (1988) 93.
14 D. Croteau, F. Vallee, M. G. Bergeron and M. LeBel, *J. Chromatogr.*, 419 (1987) 205.
15 F. M. Demotes-Mainaird, G. A. Vincon, C. H. Jarry and H. C. Albin, *J. Chromatogr.*, 490 (1989) 115.
16 G. S. Duthu, *J. Liq. Chromatogr.*, 7 (1984) 1023.
17 J. Firl, A. Prox, P. Luger, R. Maier, E. Woitun and K. Daneck, *J. Antibiotics*, 43 (1990) 1271.
18 J. H. Kennedy, *J. Chromatogr.*, 281 (1983) 288.
19 E. L. Inman and H. J. Tenbarge, *J. Chromatogr. Sci.*, 26 (1988) 89.

*Journal of Chromatography*, 594 (1992) 209–216
Elsevier Science Publishers B.V., Amsterdam

CHROM. 23 820

# Development of stability indicating assay methods for the determination of hydroxamic acids in topical formulations☆

James E. DiNunzio* and R. Rao Gadde

*Bristol-Myers Squibb Company, Pharmaceutical Research Institute, 100 Forest Avenue, Buffalo, NY 14213 (USA)*

(First received May 23rd, 1991; revised manuscript received October 22nd, 1991)

ABSTRACT

This paper reports on the development of high-performance liquid chromatographic methods for the determination of hydroxamic acids in topical formulations. A poly(styrene–divinylbenzene) copolymer stationary phase with a mobile phase of acetonitrile and pH 6 phosphate buffer at a flow-rate of 1.0 ml/min was used. Analyte detection was at 254 nm. This system is capable of the separation of phenylalkylhydroxamic acids and benzohydroxamic acids.

Excellent quantitative results were obtained. The recoveries from both cream and gel formulations were >99% with <1% relative standard deviation. Linearity of over one order of magnitude was obtained.

The selectivity of the method using the polymeric stationary phase was investigated. Variation of the mobile phase composition and pH showed that the selectivity of the method could be easily changed by changing mobile phase pH. The method selectivity was demonstrated by forced degradation of selected acids and separation of the analyte from the products. Decomposition to the corresponding carboxylic acid was found to be a major pathway for degradation of these compounds.

The separation of the hydroxamic acids on silica bonded phases was also investigated. It was found that the poor chromatography observed on these phases resulted from the presence of metal impurities in the silica support.

## INTRODUCTION

Hydroxamic acids are known to possess biological activity [1]. They are capable of both *in vitro* and *in vivo* enzyme inhibition, and have been shown to possess anti-inflammatory and analgesic properties. The bioactivity of hydroxamic acids makes them potential candidates for drug product development, and there are a few products on the market containing hydroxamic acids.

Hydroxamic acids also possess properties which make them difficult to separate. They are thermally unstable and their strong chelate formation makes many separation schemes unsuitable. However, a few methods for their separation have been reported [2–7]. Desferoxamine, a naturally occurring trihydroxamic acid was determined by reversed-phase chromatography [2]. Purging the column with the analyte along with the addition of EDTA to the mobile phase was required in order to eliminate the interference of traces of iron in the chromatographic system. Aromatic hydroxamic acids were separated by reversed-phase chromatography employing a methanol phosphate buffer eluent system [3]. While it was found that peak symmetry was improved by the use of the buffer, severe tailing was still observed for some of the hydroxamic acids. A procedure for the extraction and quantitation of cyclic hydroxamic acids in grains employed reversed-phase chromatography with a methanol–1% acetic acid eluent and gradient elution [4]. Good peak symmetry was obtained for the compounds determined since the cyclic hydroxamic acid group is not available for interactions with metals or residual silanol groups

☆ Presented at the *Fifth Annual Meeting and Exposition of the American Association of Pharmaceutical Scientists, Las Vegas, NV, 1990.*

on the stationay phase. Recoveries ranged from 78 to 106%. The separation of N-arylhydroxamic acids was performed by reversed-phase chromatography in a methanolic eluent containing 0.01% desferal mesylate [5]. This trihydroxamate was used to improve peak symmetry of the analytes. This reagent was also used for an improved assay of desferoxamine [6]. In a similar manner ferric chloride was added to the eluent for the separation of hydroxamic acids [7].

Recently, the biochemical and anti-inflammatory activity of a new topical anti-inflammatory hydroxamic acid was described [8,9]. It was reported that this compound was capable of inhibition of cyclooxygenase and lipoxygenase, and thus could be a potent anti-inflammatory agent. This compound was identified as a result of the investigation of the bioacitvity of a variety of hydroxamic acids. The data presented here describes the analytical method development work performed to support this investigation.

## EXPERIMENTAL

### *Apparatus*

A Hewlett-Packard Model 1090 high-performance liquid chromatography (HPLC) apparatus with a diode array detector was used for method development. Routine analyses were performed on a Waters Assoc. Model 204 HPLC system with a Model M6000 pump, a Model 440 absorbance detector at 254 nm, and a Model 712B WISP autoinjector. Data collection was performed on a Hewlett-Packard HP-3350A LAS computer. A Waters $\mu$Bondapak $C_{18}$ column (30 cm × 3.9 mm I.D., 10 $\mu$m packing), a Whatman 10 ODS-3 column (25 cm × 4.6 mm I.D., 10 $\mu$m packing) and a Hamilton PRP-1 column (15 cm × 4.6 mm, 5 $\mu$m packing) were used.

### *Reagents*

Series of phenylalkylhydroxamic acids and benzohydroxamic acids, the structures of which are shown in Fig. 1, were prepared in-house [9] for use in this study. The following phenylalkylhydroxamic acids were used: 6-phenylhexanohydroxamic acid, 8-phenyloctanohydroxamic acid, 9-phenylnonanohydroxamic acid, and 10-phenyldecanohydroxamic acid. The following benzohydroxamic acids were used: 3-chlorobenzohydroxamic acid, 2,4-dichlorobenzohydroxamic acid, 4-methylbenzohydroxamic acid and 4-methoxybenzohydroxamic acid.

For development and validation of the topical product assays two compounds were selected: 3-chlorobenzohydroxamic acid (3CBHA) and 9-phenylnonanohydroxamic acid (9PNHA). For product analysis 2,4-dichlorobenzohydroxamic acid and 8-phenyloctanohydroxamic acid were used as internal standards for 3CBHA and 9PNHA, respectively.

The carboxylic acids corresponding to the individual hydroxamic acids were obtained from Aldrich (Milwaukee, WI, USA). HPCL grade acetonitrile, HPLC grade tetrahydrofuran (THF) and reagent grade sodium phosphate salts and phosphoric acid were obtained from Fisher Scientific (Springfield, NJ, USA). Solvents and samples were filtered through type HVLP membrane filters (0.45 $\mu$m) (Millipore, Bedford, MA, USA).

### *Procedure*

*Effect of eluent pH.* The effect of eluent pH on the selectivity of the method was determined by measuring the change in retention time with the change in the apparent pH of the eluent. The apparent pH was determined by measuring the pH of the eluent, which was collected at the detector outlet, using a

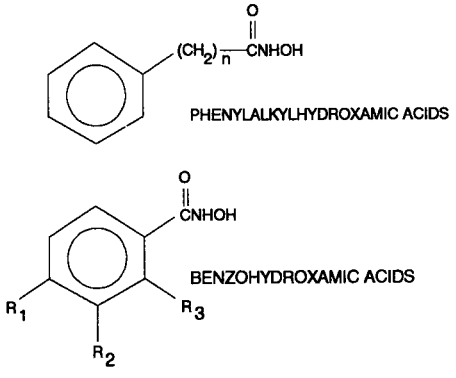


Fig. 1. Structures of test hydroxamic acids. 6-Phenylhexanohydroxamic acid, $n$ = 6; 8-phenyloctanohydroxamic acid, $n$ = 8; 9-phenylnonanohydroxamic acid, $n$ = 9; 10-phenyldecanohydroxamic acid, $n$ = 10; 3-chlorobenzohydroxamic acid, $R_1$ = $R_3$ = H, $R_2$ = Cl; 2,4-dichlorobenzohydroxamic acid, $R_2$ = H, $R_1$ = $R_3$ = Cl; 4-methylbenzohydroxamic acid, $R_2$ = $R_3$ = H, $R_1$ = $CH_3$; and 4-methoxybenzohydroxamic acid, $R_2$ = $R_3$ = H, $R_1$ = $OCH_3$.

glass electrode conditioned and calibrated with pure aqueous buffers.

The $pK_a$ values of 9-phenylnonanoic acid and 3-chlorobenzoic acid were determined by potentiometric titration of the acids in acetonitrile–water. The volume ratios for the acids were 40:60 and 15:85, respectively.

*Sample preparation.* Standard and internal standard stock solutions were prepared by accurately weighing known amounts of the reagents and dissolving in acetonitrile. Working standard solutions were prepared for analysis by pipetting aliquots of these stock solutions into volumetric flasks and adding the appropriate amounts of acetonitrile and aqueous sodium phosphate solution so that the final solution was identical to the mobile phase.

A variety of sodium phosphate solutions at different pH were used in this study. Unless stated otherwise they were prepared as follows. The appropriate weight of either dibasic or tribasic sodium phosphate equivalent to 0.1 moles was accurately weighed into a 1-l beaker. This was dissolved in 900 ml of water and adjusted to the required pH with phosphoric acid. The solution was quantitatively transferred to a 1-l volumetric flask and diluted to volume with water.

Both cream and gel formulations were assayed. Gel samples were prepared by accurately weighing 2 g of gel product into a 50-ml volumetric flask. This was dispersed in 10 ml of THF and about 25 ml of acetonitrile was added. The sample was mixed well and diluted to volume with acetonitrile. Aliquots of 5 ml of this solution and 5 ml of the internal standard stock solution were pipetted into a 50-ml volumetric flask. Acetonitrile (12 ml) was added and the sample diluted to volume with aqueous sodium phosphate solution.

Cream samples were prepared by accurately weighing 1 g of product into a 100-ml volumetric flask. This was dispersed in 15 ml of aqueous sodium phosphate solution and diluted to volume with acetonitrile. After mixing an aliquot was centrifuged, 5 ml of the clear solution and 5 ml of the internal standard stock solution were pipetted into a 50 ml volumetric flask. This was then diluted to volume with aqueous sodium phosphate solution.

Both the cream and gel sample final solutions were filtered through 0.45-$\mu$m membrane filters prior to injection. Between 30 and 50 $\mu$l of sample were injected.

## RESULTS AND DISCUSSION

### *Method development*

The major obstacle in the development of separation methods for hydroxamic acids is the strong chelating ability of these compounds. This leads to broad asymmetric bands in the chromatograms of

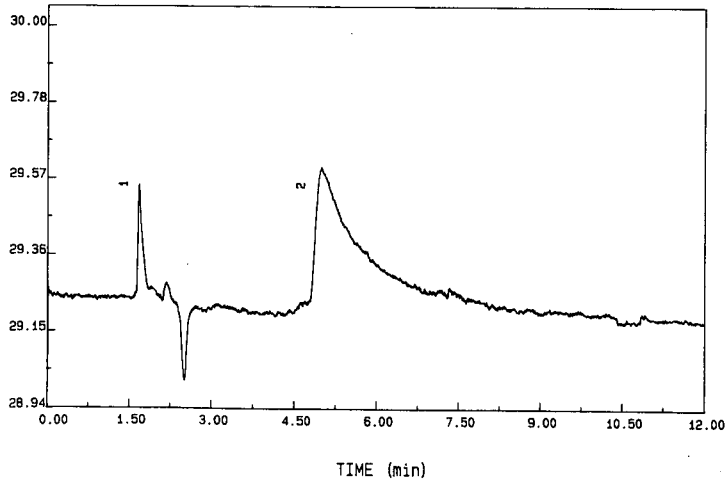


Fig. 2. Chromatogram of 9-phenylnonanohydroxamic acid on a silica bonded phase. Column, $\mu$Bondapak $C_{18}$; eluent, acetonitrile–aqueous sodium phosphate (pH 6) (60:40, v/v). Identification: 1 = solvent; 2 = 9-phenylnonanohydroxamic acid. The values on the $y$-axis are arbitrary units.

hydroxamic acids [2–6]. Fig. 2 shows a typical chromatogram obtained for the separation of 9PNHA on a reversed-phase system. The broad asymmetric peak is typical of those obtained for the hydroxamic acids investigated in this work.

The severity of the band broadening problem depends on several factors including the degree of surface coverage of the stationary phase, the amount of free metal ion in the chromatographic system, and the substitution of the hydroxamic acid functional group. Based on our results band broadening appeared to be more severe for the unsubstituted hydroxamic acids than that reported previously [4,5] for substituted acids.

Several different chromatographic systems were tested in order to improve the peak shape of the hydroxamic acids. These results are summarized in Table I which shows a comparison of the peak tailing factor [10] for 9 PNHA under the different chromatographic conditions.

Comparison of the first two entries in Table I shows the effect of addition of EDTA to the eluent. The addition of competing chelating agents has been shown to improve the peak symmetry of hydroxamic acids [2,6]. The addition of 0.01 M EDTA for the seaparation of 9PNHA reduced the tailing factor on the Waters $C_{18}$ column from 8.7 to 5.7. However, the peak symmetry is not improved enough to use this system for analysis.

In order to determine the effect of unreacted silanol groups in the stationary phase on the chromatography of these hydroxamic acids, a comparison of end-capped *vs.* non end-capped phases (Whatman 10 ODS-3 *vs.* Waters μBondapak $C_{18}$ was made. Some improvement with the end-capped phase was observed, but the peak symmetry was still poor.

TABLE I

PEAK TAILING ON SELECTED STATIONARY PHASES

Eluent: acetonitrile–aqueous sodium phosphate solution pH 6.

| Column type | Tailing factor |
|---|---|
| Waters μBondapak | 8.7 |
| Waters μBondapak | 5.7[a] |
| Whatman 10 ODS-3 | 4.3 |
| Hamilton PRP-1 | 1.3 |

[a] Eluent contained 0.01 *M* EDTA.

The use of the polymeric stationary phase (Hamilton PRP-1) resulted in excellent peak shape, as indicated by the tailing factor listed in Table I. The nearly symmetrical peaks obtained with the polymeric phase produces good resolution and improved sensitivity. This makes this system suitable for analytical purposes.

Peak asymmetry of hydroxamic acids could result from chelation of the hydroxamic acids with metal impurities in the stationary phase [5], trace metals, particularly Fe(III), in the chromatographic system, or residual silanol groups on the bonded stationary phase. No studies have attempted to differentiate between these causes. The data presented here supports the theory that metal impurities in the silica support cause band broadening of the acids. The facts that EDTA and the use of a stationary phase with low residual silanol groups resulted in only a marginal improvement in chromatography, along with the fact that replacing the silica-based column with the polymeric column on the same chromatographic system resulted in very good peak shape, indicate that neither trace metals in the chromatographic system nor residual silanol interactions are the main cause of peak asymmetry. Therefore, the loss in efficiency when using the silica-based stationary phases must be due to metals in the silica support. Since the polymeric stationary phase is essentially free of trace metals band broadening is significantly reduced compared to the silica supports.

The influence of metal impurities in the bonded stationary phase on chromatographic retention processes has been investigated [11–13] and has been shown to be important for some classes of compounds. Chromatographic grade silica gel has been found to contain more than 1000 ppm of metal impurities (not including Group I metals) [14]. This high content has been shown to produce broad asymmetric peaks, similar to those observed here for the hydroxamic acids. The use of the polymeric stationary phase results in superior chromatography for the hydroxamic acids because of the much lower level of metal impurities. Analysis of this material found no detectable heavy metals [15]. Since this stationary phase has a significantly lower level of metal impurities which can influence the chromatographic retention process, its use results in the improved peak shapes observed.

TABLE II

EFFECT OF MOBILE PHASE COMPOSITION ON RETENTION TIME

Mobile phase: acetonitrile–aqueous sodium phosphate solution pH 6. Column: Hamilton PRP-1.

| Acetonitrile (%, v/v) | Retention time (min) | |
|---|---|---|
| | 3CBHA | 9PNHA |
| 46 | – | 5.8 |
| 40 | 1.8 | 12.2 |
| 35 | – | 23.1 |
| 30 | – | 55.9 |
| 20 | 4.1 | – |
| 15 | 7.2 | – |
| 13.5 | 9.1 | – |
| 12 | 11.5 | – |

Initial experiments to optimize the eluent showed that the test compounds behave as would be expected in a reversed-phase system. As the amount of acetonitrile increased the retention time decreased. This is shown by the data in Table II. These data reflect the difference in polarity of the two classes of acids in that the more hydrophobic phenylalkylhydroxamic acids required more organic solvent to be eluted than the hydrophilic benzohydroxamic acids.

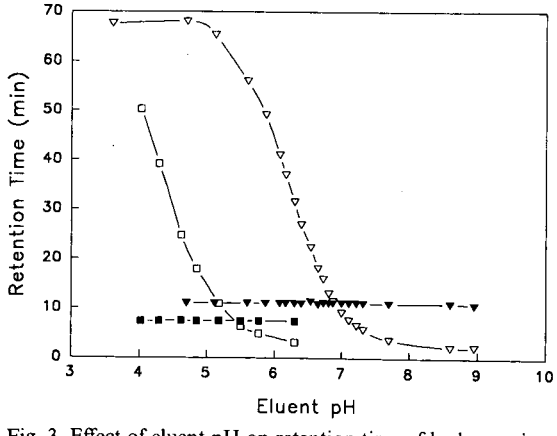


Fig. 3. Effect of eluent pH on retention time of hydroxamic and carboxylic acids. Column, Hamilton PRP-1; eluent, acetonitrile–aqueous sodium phosphate (40:60, v/v for ▽ and ▼), (15:85, v/v for □ and ■). Identification: ▽ = 9-phenylnonanoic acid; □ = 3-chlorobenzoic acid; ▼ = 9-phenylnonanohydroxamic acid; ■ = 3-chlorobenzohydroxamic acid.

In order to develop a stability indicating assay method which can be used to support pharmaceutical product development it is necessary to be able to separate the analyte from its degradation products. Although two classes of hydroxamic acids were investigated they can be expected to form analogous degradation products. Our work demonstrated that hydrolysis to the parent carboxylic acid is a main mechanism for degradation of these compounds in solution. Therefore, any stability indicating method must be able to separate both the hydroxamic and carboxylic acids.

The effect of pH on the separation of test hydroxamic acids and their corresponding carboxylic acids is shown in Fig. 3. These data show that the separation of the hydroxamic acids and their main degradation product, the carboxylic acid, can be controlled by controlling the pH of the eluent. The data is consistent with the ionization of these acids. The carboxylic acids, which are stronger than the hydroxamic acids ionize at a lower pH. Therefore, their retention times begin to decrease at a lower pH. At very high pH both acids can be completely dissociated. Experiments performed at pH 11.5 showed that both the hydroxamic acid and the corresponding carboxylic acid co-eluted due to their like charge.

From the data in Fig. 3 an interesting observation can be made regarding the effect of acetonitrile on the dissociation of the carboxylic acids. The data for these acids is essentially the titration curve for the acids in the mixed solvent system. At the inflection point then the pH of the eluent is equal to the $pK_a$ of the acid. For 9-phenylnonanoic acid this occurs at a pH of about 6.2. The $pK_a$ of this carboxylic acid in water is about 4.8. This difference is due to the suppressed dissociation of the acid in the mixed solvent. In a similar, but less dramatic manner the $pK_a$ of 3-chlorobenzoic acid shifted from 3.82 [16] in aqueous solution to about 4.2 in a mixed solvent containing 15% acetonitrile. These values are in excellent agreement with the $pK_a$ values determined in our laboratory for these compounds by potentiometric titration in mixed acetonitrile and water. Clearly, the suppression of dissociation of ionizable species due to the presence of organic modifiers in the eluent must be considered when developing an HPLC separation for these types of compounds.

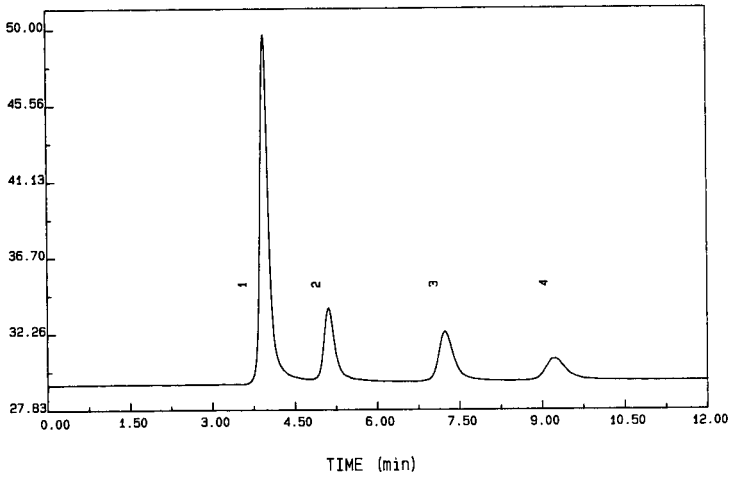


Fig. 4. Separation of benzohydroxamic acids. Column, Hamilton PRP-1; eluent, acetonitrile–aqueous sodium phosphate (pH 6) (15:85, v/v). Peaks 1 = 4-methoxybenzohydroxamic acid; 2 = 4-methylbenzohydroxamic acid; 3 = 3-chlorobenzohydroxamic acid; 4 = 2,4-dichlorobenzohydroxamic acid. *y*-Axis in arbitrary units.

Figs. 4 and 5 show chromatograms for the series of benzohydroxamic and phenylalkylhydroxamic acids, respectively. Good peak shape and resolution were obtained for each class of hydroxamic acid. Based on these separations an eluent of acetonitrile–aqueous sodium phosphate solution (pH 6) (15:85) was used for analysis of the benzohydroxamic acids, and acetonitrile–aqueous sodium phosphate solution (pH 6) (43:57) was used for the phenylalkylhydroxamic acids.

*Method validation*

In order to demonstrate that an assay method is stability indicating, it is necessary to demonstrate

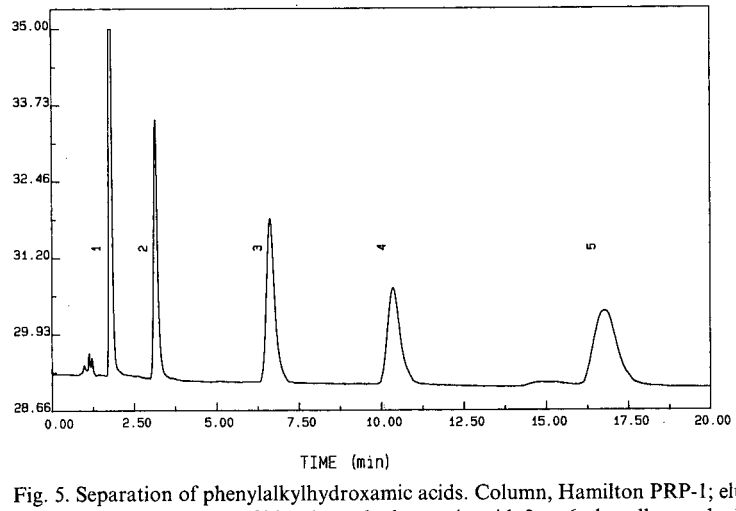


Fig. 5. Separation of phenylalkylhydroxamic acids. Column, Hamilton PRP-1; eluent, acetonitrile–aqueous sodium phosphate (pH 6) (40:60, v/v). Peaks: 1 = 3-Chlorobenzohydroxamic acid; 2 = 6-phenylhexanohydroxamic acid; 3 = 8-phenyloctanohydroxamic acid; 4 = 9-phenylnonanohydroxamic acid; 5 = 10-phenyldecanohydroxamic acid. *y*-Axis in arbitrary units.

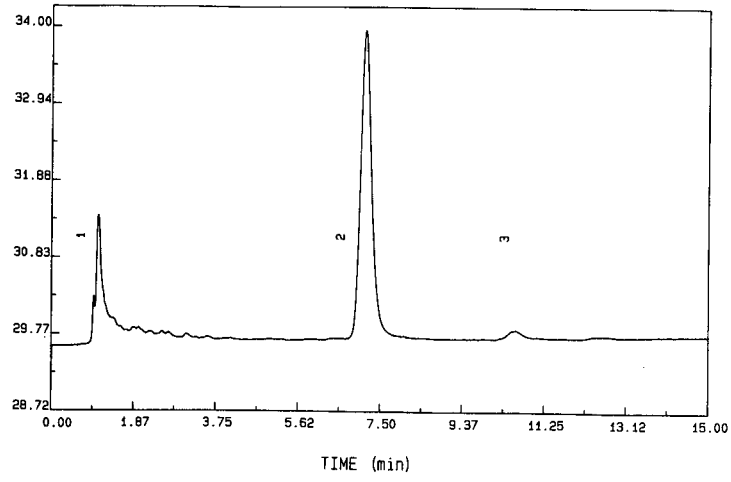


Fig. 6. Chromatogram of light-degraded 9-phenylnonanohydroxamic acid. Column, Hamilton PRP-1; eluent, acetonitrile–aqueous sodium phosphate (pH 6) (43:57, v/v). Peaks: 1 = solvent; 2 = 9-phenylnonanohydroxamic acid; 3 = 9-phenylnonanoic acid. *y*-Axis in arbitrary units.

that the active and an internal standard, if used, can be separated from potential degradation products which could form during the life of the product. This was demonstrated by separating forced degraded solutions of the test compounds. These were degraded by exposure to light or by hydrolysis in basic solution. Absorbance spectra were collected using a diode array detector. From these data absorbance ratio plots of the active from the degraded samples were made to verify that no co-eluting degradation products were present in the chromatograms.

Fig. 6 shows the separation obtained for 9PNHA which had been forced degraded by exposure to UV radiation. A number of small peaks are seen from the degradation of the active. These include the parent carboxylic acid at a retention time of about 10.5 min, and several unidentified products eluting before the active. Absorbance ratio plots showed that no detectable co-eluting products could be ob-

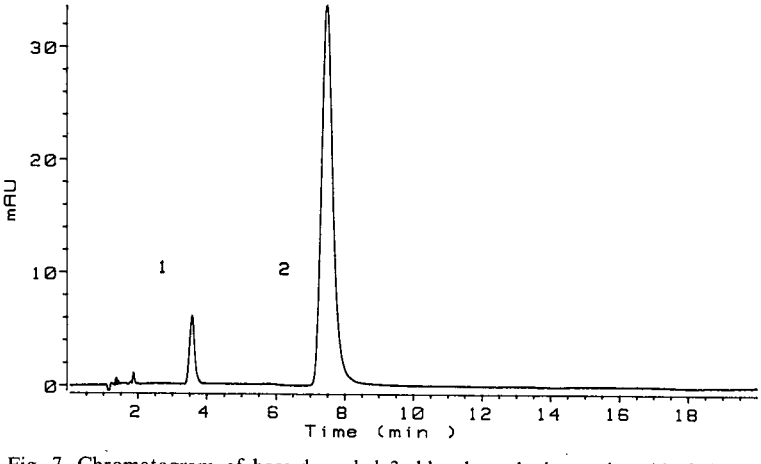


Fig. 7. Chromatogram of base-degraded 3-chlorobenzohydroxamic acid. Column, Hamilton PRP-1; eluent, acetonitrile–aqueous sodium phosphate (pH 6) (15:85, v/v). Peaks: 1 = 3-chlorobenzoic acid; 2 = 3-chlorobenzohydroxamic acid.

served. Similar results were obtained for the separation of 3CBHA and its photodegradation products.

Fig. 7 shows the separation obtained for 3CBHA which has been forced degraded in basic solution at elevated temperature. The parent carboxylic acid is seen as the major degradation product. Absorbance ratio plots showed that no co-eluting products could be observed. Similar results were obtained for the separation of 9PHHA and its base degradation products.

The method was validated for assay of topical creams and gels by determining the response linearity, precision and accuracy for the determination of 9PNHA and 3CBHA. For both analytes excellent linearity ($r > 0.999$) of over one order of magnitude was obtained. The linear range tested was from 0.3% (w/w) to 13.5% (w/w) of the drug in product.

The precision of the method was determined by the analysis of replicate samples of the products. The precision for the determination of 3CBHA in a cream formulation determined on 11 replicate assays was ± 0.5% relative standard deviation. The precision for the determination of 9PNHA in a gel formulation determined on 6 replicate assays was ± 0.4% relative standard deviation.

The accuracy for the determination of hydroxamic acids in topical formulations was determined by the analysis of synthetic samples prepared by spiking product placebos with solutions of the analytes. The recovery of 3CBHA for 9 replicate assays of the cream formulation was 100.0 ± 0.2%. The recovery of 9PNHA for 18 replicate assays of the gel formulation was 99.4 ± 0.5%.

## CONCLUSIONS

The method described is precise and accurate when used to determine hydroxamic acids in topical formulations. This method has been used for routine analysis with good success.

The use of the polymeric stationary phase allows the separation of these hydroxamic acids which could not be achieved using the silica-bonded phases.

## ACKNOWLEDGEMENT

The authors would like to thank Dr. S. Marathe for supplying the hydroxamic acids used in this work. The excellent technical support of Ms. Janice Mayer is also gratefully acknowledged.

## REFERENCES

1 H. Kehl (Editor), *Chemistry and Biology of Hydroxamic Acids*, S. Karger, Farmington, CT, 1982.
2 S. Cramer, B. Nathanael and Cs. Horváth, *J. Chromatogr.*, 295 (1984) 405.
3 E. Lipczynska-Kochany, *J. Chromatogr.*, 260 (1983) 493.
4 P. C. Lyons, J. D. Hipskind, K. V. Wood and R. L. Nicholson, *J. Agric. Food Chem.*, 36 (1988) 57.
5 M. D. Corbett and B. R. Chipko, *Anal. Biochem.*, 98 (1979) 169.
6 J. D. Glennon, M. R. Woulfe, A. T. Senior and N. NiChoileain, *Anal. Chem.*, 61 (1989) 1474.
7 J. A. Hinson, L. R. Pohl and J. R. Gilette, *Anal. Biochem.*, 101 (1989) 462.
8 K. M. Tramposch, F. C. Zusi, S. Marathe, S. Stanley, S. Steiner, X. Nair and J. W. Quigley, *J. Invest. Dermatol.*, 92 (1989) 533.
9 K. M. Tramposch, F. C. Zusi, S. Marathe, S. Stanley, S. Steiner, X. Nair and J. W. Quigley, *Agents and Actions*, 30 (1990) 443.
10 The United States Pharmacopeia, United States Pharmacopeial Convention, Rockville, MD, 1990, p. 1567.
11 Y. Ohitsu, Y. Shiojima, T. Okumura, J. Koyama, K. Nakamura and O. Nakata, *J. Chromatogr.*, 481 (1989) 147.
12 J. Koyama, J. Nomura, Y. Ohtsu, O. Nakata and M. Takahashi, *Chem. Lett.*, 1990 (4) 687.
13 P. Sadek, C. Koester and L. Bowers, *J. Chromatogr. Sci.*, 352 (1987) 489.
14 M. Verzele, M. De Potter and J. Ghysels, *J. High Resolut. Chromatogr. Chromatogr. Commun.*, 2 (1979) 151.
15 Hamilton Company, Reno, NV, personal communication.
16 R. C. Weast, (Editor), *CRC Handbook of Chemistry and Physics*, CRC Press, Boca Raton, FL, 65th ed., 1984; p. D165.

*Journal of Chromatography*, 594 (1992) 217–223
Elsevier Science Publishers B.V., Amsterdam

CHROM. 23 822

# Determination of the mean ionic charge of the components of three $^{99m}$Tc bone scanning agents by gel chromatography with two eluents of different electrolyte composition

W. J. Gelsema, C. L. de Ligny*, Y. M. Huigen and J. Schuring

*Laboratory for Analytical Chemistry, P.O. Box 80083, 3508 TB Utrecht (Netherlands)*

(First received July 11th, 1991; revised manuscript received October 23rd, 1991)

ABSTRACT

A recently proposed method for the determination of ionic charge was evaluated by applying it to a problem in nuclear medicine, *viz.*, the determination of the mean ionic charge of the components of three $^{99m}$Tc bone scanning agents. The method is based on the partition coefficients of the investigated ions, observed in gel chromatography with two eluents containing different electrolytes, at a range of ionic strengths. The bone scanning agents are mixtures of complexes of $^{99m}$Tc(III) and $^{99m}$Tc(IV) with 1-hydroxyethylene-1,1-diphosphonic acid.

## INTRODUCTION

Recently, a method was described [1] for the determination of the charge of ions, based on their partition coefficients observed in gel chromatography with two eluents containing different electrolytes, at a range of ionic strengths. In this paper we report the application of this method to a relevant problem in the field of nuclear medicine, *viz.*, the determination of the (mean) anionic charge of the components of three bone scanning agents.

Briefly, the concept of this method is as follows. As the polarity of the gel is different from that of the eluent, the partition coefficient of any substance is not exactly unity. This is particularly true for (highly charged) ions. As only electroneutral combinations of ions can be transferred from the eluent to the gel and *vice versa*, the partition constant of a sample ion (*i.e.*, of an electroneutral combination with the ions of the electrolyte added to the eluent) depends on the charge $z$ of the sample ion and on the nature of the electrolyte in the eluent. From the combined results in the presence of two different electrolytes, the charge $z$ can be derived. When an ion $p^z$ with charge $z$ is chromatographed in two eluents containing, *e.g.*, $NaClO_4$ and $Na_2SO_4$, respectively, it holds that

$$\Delta\log K = Cz \qquad (1)$$

where $\Delta\log K$ is the difference in the values of $\log K$ in the two eluents ($K$ is the true or thermodynamic value of the partition coefficient) and $C$ is a constant. When $C$ is known and $\Delta\log K$ for an ion with unknown charge $z$ has been obtained, the value of $z$ can be calculated by eqn. 1.

The correction for activity coefficient effects in the experimental result $\Delta\log K'$ was performed as follows. The relationschip between $\Delta\log K$ and $\Delta\log K'$ is

$$\Delta\log K = \Delta\log K' + \log\left[\frac{y_s(NaClO_4)}{y_s(Na_2SO_4)}\right] \qquad (2)$$

where $y_s(NaClO_4)$ and $y_s(Na_2SO_4)$ are the activity coefficients of the ion $p^z$ in the $NaClO_4$ and $Na_2SO_4$

0021-9673/92/$05.00 

solutions in the interior of the gel beads, respectively. The extended Debye–Hückel equation yields the following result:

$$\Delta\log K = \Delta\log K' - z^2 A \sqrt{I} f(I,\mathring{a}_i) - f'(c) + C'I \quad (3)$$

where $A$ is a known constant, $I$ is the ionic strength, $c$ is the concentration, $\mathring{a}_i$ is the distance of closest approach of the electrolyte ions to the ion $p^z$, $f$ and $f'$ are known functional relationships and $C'$ is an unknown constant.

Tji *et al.* [1] measured $\Delta\log K'$ of nine species with $z$ ranging from $+2$ to $-4$ on Bio-Gel P-4 at ionic strengths of 0.03, 0.1 and 0.3 $M$. Making the (not very critical) assumption that $\mathring{a}_i$ is $5 \cdot 10^{-8}$ cm, they calculated the corresponding values of $\Delta\log K' - z^2 A \sqrt{I} f(I,\mathring{a}_i) - f'(c)$. These data were extrapolated to $I = 0$, which yielded the values of $\Delta\log K$. Linear regression of $\Delta\log K$ on $z$ (see eqn. 1) gave the final result:

$$\Delta\log K = (0.106 \pm 0.002)\, z - 0.010 \pm 0.006 \quad (4)$$

This equation can be used as a calibration line for the determination of unknown values of $z$. In doing so, the value of $\Delta\log K$ should be determined by the same method as used by Tji *et al.* for the determination of the values of $\Delta\log K$ for ions with known charge. A small complication is that the second term on the right-hand side of eqn. 3 depends on $z$, and that $z$ is unknown. Hence the determination of $z$ must be done by successive approximation.

The new method is based on the assumption that ion pairing between the investigated ion and the ions of the two different electrolytes in the eluents does not occur. This was probably true in the previous investigation [1], and also in the present case, with $NaClO_4$ and $Na_2SO_4$ as electrolytes and anionic complexes to be investigated.

The theory used in the new method is a bulk-distribution theory. It is not self-evident that it can be applied to gel chromatography, where surface effects may occur. In fact, the results of the previous investigation [1] demonstrated the presence of some carboxylate groups on the gel matrix. To suppress their influence on the distribution of the investigated ions, the ionic strength had to be at least 0.03 $M$.

A practical point is as follows. In the calculation of $K'$, the total liquid volume in the column must be estimated. The method that we adopted [1] is somewhat arbitrary: the total liquid volume is obtained as the difference between the bed volume and the volume of the gel matrix. The matrix volume is chosen so that $\Delta\log K$ for an uncharged solute (methanol) is equal to zero, as it should be. Other approaches to estimate the total liquid volume in the column are feasible.

Despite these theoretical and practical problems, the precision of the obtained calibration, eqn. 4, gives support for the correctness of the procedure.

The new method had distinct advantages over the classical method for determination of ionic charge, *viz.*, by ion-exchange chromatography. When the investigated ion has a high charge, in the latter method the electrolyte concentration in the eluent must be fairly high to avoid awkwardly long retention times. Corrections for activity coefficients are then virtually impossible, and electrolyte invasion into the ion exchanger cannot be neglected (as is usually done [2]). Further, because of the Donnan equilibrium, the pH in the ion exchanger is higher than that in the eluent, and ions with acidic properties may lose protons when they enter the ion exchanger [3].

The new method also has its limitations. It has been calibrated in the range $-4 \leqslant z \leqslant 2$, and it cannot be excluded that outside this range deviations from the proportionality of $\Delta\log K$ and $z$ occur (in fact, a plot of $\Delta\log K'$ of ribonuclease, obtained by gel chromatography on Sephadex G-75 in eluents containing NaSCN or $Na_2SO_4$, at ionic strength 0.5 $M$, *vs.* $z$ is linear in the range $-4 \leqslant z \leqslant 4$, but flattens outside this range [4]). Further, the resolution of mixtures of ions by gel chromatography is low, and it is a fairly slow method. The last point may be a drawback when a mixture of ions (*e.g.*, a mixture of metal complexes) that are interconvertible is investigated.

The performance of the new method in its application to single, stable ions within the calibration range has already been established [1]: unknown values of $z$ can be determined with a standard deviation of 0.18. Here, we give the method a very stringent test by applying it to a relevant problem in the field of nuclear medicine, *viz.*, the determination of the (mean) ionic charge of the components of three $^{99m}Tc$ bone scanning agents. The agents are mixtures of complexes of $^{99m}Tc(III)$ and $^{99m}Tc(IV)$ with 1-hydroxyethylene-1,1-diphosphonic acid

(HEDP). By high-performance anion-exchange chromatography seven components can be discerned [5]. In gel chromatography only four peaks are observed [6], so it is impossible to determine the charges of the individual complexes by the new method. At most, the mean charge of the complexes in the four gel chromatographic fractions can be determined. The low resolution obtained in gel chromatography may be partly caused by the slowness of the method, as the Tc–HEDP complexes are slowly interconvertible [6].

Even if it turns out that only the mean charge of all the complexes in the bone scanning agents can be determined, the result would be interesting in nuclear medicine. The agents are injected into the blood stream of patients and are taken up by normal bone, and in particular by bone tumours. Any tumours present can be detected by scintigraphy, owing to the $\gamma$-radiation that is emitted by $^{99m}$Tc. Several workers [7,8] believe that ionic charge is a major factor governing the uptake by the mineral constituent of bone. Hence, it is interesting to investigate whether the mean uptake of the components of the three bone scanning agents is correlated with their mean ionic charge. This might give a clue to further optimization of these agents.

The three $^{99m}$Tc–HEDP preparations that were the subject of this investigation have already been shown to have widely different compositions (by high-performance anion-exchange chromatography) and widely different adsorption on $Ca_3(PO_4)_2$ [9].

## EXPERIMENTAL

### *Apparatus and chemicals*

Materials were obtained from the following sources: $^{99m}$Tc generator (287 mCi Ultratechnekow FM, Mo-99/Tc-99m) from Byk-Mallinckrodt CIL (Petten, Netherlands); HEDP was a generous gift from Henkel (Düsseldorf, Germany); human serum albumin (HSA) from Bloedbank (Utrecht, Netherlands); Bio-Gel P-4 (200–400 mesh) from Bio-Rad Labs., Richmond, CA, USA); chromatography paper (Whatman No. 1) and DC-Alufolien cellulose from E. Merck (Darmstadt, Germany). Chromatographic columns (C10/40), laboratory valves (LV4), reservoir RC-10 and polyethylene capillary tubing were purchased from Pharmacia (Uppsala, Sweden). The Microperpex 2132 pump was obtained from LKB (Bromma, Sweden). The H.V. supply and ratemeter (PW 4620) and the well-type NaI crystal, for on-line detection of radiation, were purchased from Philips (Eindhoven, Netherlands). The two-channel, well-type NaI(Tl) detector counting system was Gamma 8000 system (Beckman Instruments, Irvine, CA, USA).

All other chemicals were of analytical-reagent grade.

### *Preparation of the reducing agents for the reduction of $^{99m}TcO_4^-$*

The following reducing agents were prepared: (1) 0.04 *M* $SnSO_4$ in 0.2 *M* nitrogen-saturated $H_2SO_4$; (2) 0.04 *M* $FeSO_4$ in 0.2 *M* nitrogen-saturated $H_2SO_4$; (3) 0.04 *M* $Sn(ClO_4)_2$ in 0.2 *M* nitrogen-saturated $HClO_4$, prepared by mixing 0.08 *M* solutions of $SnSO_4$ and $Ba(ClO_4)_2$ in 0.2 *M* nitrogen-saturated $HClO_4$; and (4) 0.04 *M* $Fe(ClO_4)_2$ in 0.2 *M* nitrogen-saturated $HClO_4$, prepared by mixing 0.08 *M* solutions of $FeSO_4$ and $Ba(ClO_4)_2$ in 0.2 *M* nitrogen-saturated $HClO_4$.

### *Preparation of bone scanning agents*

$^{99m}$Tc(Sn, pH 7.4)–HEDP and $^{99m}$Tc(Sn, pH 12)–HEDP were prepared by mixing 2 ml of 0.4 *M* HEDP (pH 7.4) and 2 ml of reducing agent 1 or 3. The pH was adjusted to 7.4 or 12, respectively, nitrogen was passed through the solution for 5 min and 1.5 ml of the eluate of the $^{99m}$Tc generator were added (the generator was eluted with 0.1 *M* $Na_2SO_4$ or 0.2 *M* $NaClO_4$, respectively). After passing nitrogen through the solution for 15 min, the pH was adjusted to 7.4 and the solution was diluted 400× with $Na_2SO_4$ or $NaClO_4$ of ionic strength 0.3 *M*.

Samples of this solution were chromatographed with eluents of ionic strength 0.3 *M*. For chromatography with eluents of ionic strength 0.1 and 0.03 *M*, the solutions were diluted 3× and 10×, respectively, with nitrogen-saturated doubly distilled water (the ratio of the concentrations of the HEDP ions in the sample solution and the $SO_4^{2-}$ or $ClO_4^-$ ions in the eluents should be constant at the three different ionic strengths of the eluents. In that case, this ratio will also stay constant, and very small, on extrapolation to zero ionic strength. This is a necessary prerequisite for the application of the calibration function [4]).

$^{99m}$Tc(Fe)–HEDP was prepared in the same way, but with the use of reducing agents 2 or 4 instead of 1 or 3.

The percentage of radioactivity, present as Tc-HEDP complexes, was determined by Zimmer and Pavel's method [10], slightly modified as described by Kroesbergen *et al.* [11].

*Gel chromatography*

The eluents of ionic strength 0.3 *M* had the following composition: 0.1 *M* $Na_2SO_4$ or 0.3 *M* $NaClO_4$, $10^{-3}$ *M* HEDP, $5 \cdot 10^{-4}$ *M* $SnSO_4$ or $Sn(ClO_4)_2$ (pH 7.4). The eluents of ionic strength 0.1 and 0.03 *M* were prepared by diluting the above eluent 3 × and 10 ×, respectively, with nitrogen-saturated doubly distilled water. All eluents were degassed and filtered before use and kept under nitrogen during chromatography.

The pretreatment of the Bio-Gel P-4 and the packing of the column were performed as recommended by the manufacturer (dimensions 35.5 × 1 cm I.D.).

Aliquots of the samples were applied to the column and eluted at a flow-rate of 10 ml $h^{-1}$. The flow-rates were accurately determined by weighing the column effluent. The radioactivity was detected on-line by passing the column effluent through a laboratory-made flow cell contained in the well of an NaI deector. The recovery of the applied radioactivity was determined by comparing the radioactivity of a chromatographed sample with that of a non-chromatographed sample.

The volume of the mobile phase was determined by measuring the elution volume of labelled HSA. The labelling was performed as follows. To 3.5 ml of 10% HSA and 0.5 ml of $TcO_4^-$, 100 $\mu$l of $4 \cdot 10^{-3}$ *M* $SnCl_2$ were added and the pH was adjusted to 3.0. The mixture was allowed to react for 10 min. After the pH had been adjusted to 7.4, an aliquot of the mixture was applied to the column. The total liquid volume of the column was obtained from $V_l = V_{bed} - W/\rho$, where $V_{bed}$ is the bed volume, $W$ is the weight of the gel used in the packing of the column and $\rho$ is its density. For $\rho$ an arbitrary value of 1.1 $g^{-1}$ was taken; this value results in a mean value $\Delta\log K_{CH_3OH} = 0$ [1].

Elution volumes were corrected for the extra-column dead space. Partition coefficients were calculated as follows:

$$K' = \frac{V_e - V_0}{V_l - V_0} \tag{5}$$

where $V_e$ is the corrected retention volume, $V_0$ is the corrected retention volume of HSA and $V_l$ is the total liquid volume in the column. Values of $\Delta\log K'$ were determined at $I = 0.30$, 0.10 and 0.03 *M*. After (partial) correction for the activity coefficients they were extrapolated to zero ionic strength. The charge $z$ was determined from eqn. 4 by successive approximation.

## RESULTS

The radioactivity in the complexed fraction was always more than 90%. With Tc(Sn, pH 7.4)–HEDP it was even more than 97%. The main side product was $TcO_2$; the $TcO_4^-$ concentration was never more than 0.03%. The recovery of radioactivity from the chromatographic column was about 95%.

Representative chromatograms of the three preparations obtained using eluents containing $Na_2SO_4$ and $NaClO_4$ are shown in Figs. 1 and 2, respectively.

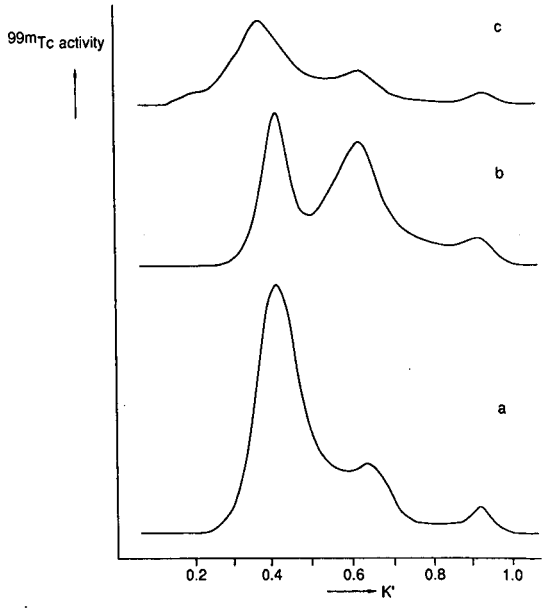


Fig. 1. Chromatograms of (a) $^{99m}$Tc(Sn, pH 7.4)–HEDP, (b) $^{99m}$Tc(Sn, pH 12)–HEDP and (c) $^{99m}$Tc(Fe)–HEDP on Bio-Gel P-4 with an eluent containing $Na_2SO_4$ of ionic strength 0.3 *M*.

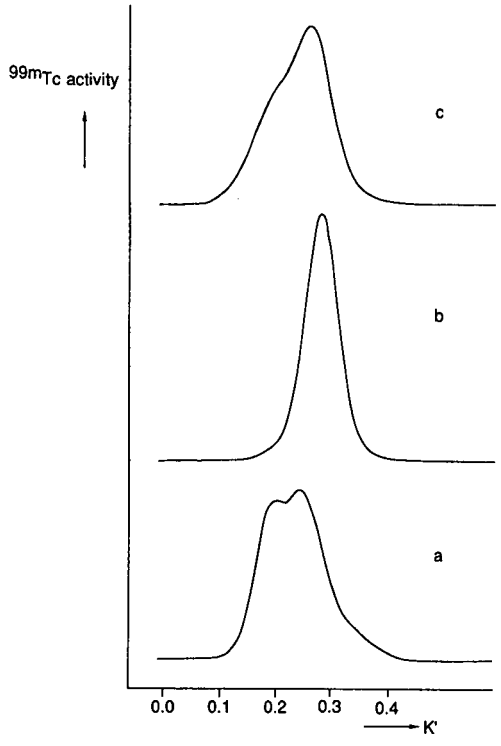


Fig. 2. Chromatograms of (a) $^{99m}$Tc(Sn, pH 7.4)–HEDP, (b) $^{99m}$Tc(Sn, pH 12)–HEDP and (c) $^{99m}$Tc(Fe)–HEDP on Bio-Gel P-4 with an eluent containing $NaClO_4$ of ionic strength 0.3 *M*.

With the eluents containing $Na_2SO_4$, three fractions can be discerned in all preparations. With the eluents containing $NaClO_4$, Tc(Sn, pH 12)–HEDP and Tc(Fe)–HEDP show only one broad peak. In the chromatograms of Tc(Sn, pH 7.4)–HEDP the early eluting main peak can be discerned. Hence we are able to determine the mean ionic charge of all the components of the three preparations, and in addition the mean ionic charge of the complexes present in the early eluting main peak of Tc(Sn, pH 7.4)–HEDP. The corresponding experimental values of the partition coefficients $K'$ are given in Table I.

Values of the correction terms $z^2A\sqrt{I}f(I,\mathring{a}_i = 5$ Å), for $z = 1, 2, 3$ or 4 (the calculation for other values of $z$ is straightforward), and $f'(c)$ were given by Tji *et al.* [1]. From the values of $\Delta\log K'$ and the above-mentioned correction terms, $z$ was calculated by successive approximation, as described in the Introduction. After 4–6 calculation cycles the differences between the input and output values of $z$ had become very small, ranging from 0.00 to 0.03. The final estimates of $z$, obtained after 4–6 calculation cycles, are given in Table II.

## DISCUSSION

It follows from Fig. 1 that the proportion of the first peak in the chromatograms decreases in the order $^{99m}$Tc(Sn, pH 7.4)–HEDP, $^{99m}$Tc(Fe)–HEDP, $^{99m}$Tc(Sn, pH 12)–HEDP. As a result in Fig. 2 the first peak can only be observed clearly in the chromatogram of $^{99m}$Tc(Sn, pH 7.4)–HEDP, and as a shoulder in the chromatogram of $^{99m}$Tc (Fe)–HEDP. Probably the poor resolution with the $NaClO_4$-containing eluent is partly caused by the low values of the partition coefficients of the anionic Tc complexes in this eluent. This phenomenon is caused by the high affinity of the gel for $ClO_4^-$. For the first peak in the chromatogram of $^{99m}$Tc(Sn, pH 7.4)–HEDP $K' = 0.20$ and 0.42 when the eluent contains $NaClO_4$ and $Na_2SO_4$ of ionic strength 0.3

TABLE I

PARTITION COEFFICIENTS, $K'$, OF THE EARLY-ELUTING MAIN PEAK OF $^{99m}$Tc(Sn, pH 7.4)–HEDP, AND MEAN VALUES OF $K'$ OF THE THREE BONE SCANNING AGENTS (OBTAINED BY DIVIDING THE CHROMATOGRAMS IN TWO PARTS OF EQUAL AREA), IN ELUENTS CONTAINING $NaClO_4$ OR $Na_2SO_4$ OF IONIC STRENGTH 0.03, 0.1 AND 0.3 *M*

| Species | | $NaClO_4$ | | | $Na_2SO_4$ | | |
|---|---|---|---|---|---|---|---|
| | | 0.03 *M* | 0.1 *M* | 0.3 *M* | 0.03 *M* | 0.1 *M* | 0.3 *M* |
| $^{99m}$Tc(Sn, pH 7.4)–HEDP | Main peak | 0.20 | 0.17 | 0.20 | 0.49 | 0.42 | 0.42 |
| | Mean | 0.22 | 0.19 | 0.23 | 0.54 | 0.45 | 0.45 |
| $^{99m}$Tc(Sn, pH 12)–HEDP | Mean | 0.26 | 0.24 | 0.28 | 0.63 | 0.57 | 0.57 |
| $^{99m}$Tc(Fe)–HEDP | Mean | 0.26 | 0.23 | 0.24 | 0.53 | 0.43 | 0.42 |

TABLE II

FINAL VALUES OF $\Delta$LOG $K$ AND $z$, OBTAINED BY SUCCESSIVE APPROXIMATION, AND THEIR STANDARD DEVIATIONS

The standard deviations of $\Delta\log K$ follow from regression analyses according to eqn. 3. The standard deviations of $z$ are obtained from error propagation using the standard deviations of $\Delta\log K$ along with regression parameters of eqn. 4.

| Species | | $I$ ($M$) | $\Delta\log K'$ | Corr.[a] | $\Delta\log K$ ($I$ = 0) | $z$ |
|---|---|---|---|---|---|---|
| $^{99m}$Tc(Sn, pH 7.4)–HEDP | Main peak | 0.03 | −0.39 | 0.16 | −0.51 ± 0.004 | −4.8 ± 0.1 |
| | | 0.1 | −0.39 | 0.22 | | |
| | | 0.3 | −0.47 | 0.32 | | |
| | Mean | 0.03 | −0.38 | 0.21 | −0.60 ± 0.03 | −5.6 ± 0.3 |
| | | 0.1 | −0.38 | 0.29 | | |
| | | 0.3 | −0.29 | 0.43 | | |
| $^{99m}$Tc(Sn, pH 12)–HEDP | Mean | 0.03 | −0.38 | 0.20 | −0.58 ± 0.02 | −5.4 ± 0.2 |
| | | 0.1 | −0.37 | 0.27 | | |
| | | 0.3 | −0.31 | 0.40 | | |
| $^{99m}$Tc(Fe)–HEDP | Mean | 0.03 | −0.31 | 0.09 | −0.39 ± 0.01 | −3.6 ± 0.1 |
| | | 0.1 | −0.27 | 0.13 | | |
| | | 0.3 | −0.25 | 0.19 | | |

[a] Corr. = $z^2A\sqrt{If}(I,\mathring{a}_i = 5\ \text{Å}) + f'(c)$

$M$, respectively. The equation for chromatographic resolution contains a factor $k'/(1 + k')$, where $k'$ is the capacity factor, which is equal to the product of $K'$ and the ratio of the volumes of stationary and mobile phase in the column. In the present instance, this ratio is 1.74, so for $K' = 0.20$ or 0.42, $k'/(1 + k') = 0.25$ or 0.42. The ratio of these values is 0.60. As the resolution is also proportional to the square root of the column length, the drawback of low $K'$ values with the $NaClO_4$-containing eluent might have been offset by increasing the column length by a factor of 3. However, in the present case of slowly interconvertible complexes, this would probably cause additional problems.

The standard deviation of the results for $z$ is small, but it must be noted that they are slightly out of the calibration range of the method [except the result for $^{99m}$Tc(Fe)–HEDP].

A comparison with literature data obtained by ion-exchange chromatography is only possible for the mean charge of all the components of $^{99m}$Tc(Sn, pH 7.4)–HEDP. Huigen *et al.* [12] used two ion exchangers, Aminex A-28 and DEAE-Trisacryl, and applied two methods, described by Wilson and Pinkerton [13] and by Russell and Bischoff [3] (the latter of which is probably more accurate). By Wilson and Pinkerton's method they obtained $z = -8$ and $-4$, respectively, and by Russell and Bischoff's method they obtained $z = -7$ and $-6$, respectively. Our, probably more accurate, value is $z = -5.6$.

The correlation between the values of $z$ for the three bone scanning agents and their adsorption on the mineral constituent of bone is discussed elsewhere [9].

## CONCLUSION

A recently proposed method for the determination of ionic charge has been demonstrated to be useful in a complicated case in the field of nuclear medicine: the determination of the mean ionic charge of the components of three $^{99m}$Tc bone scanning agents [these agents are mixtures of at least seven complexes of $^{99m}$Tc(III) and $^{99m}$Tc(IV) with 1-hydroxyethylene-1,1-diphosphonic acid, that are slowly interconvertible]. For $^{99m}$Tc(Fe)–HEDP the mean ionic charge is $-3.6 \pm 0.1$ at pH 7.4; for $^{99m}$Tc(Sn)–HEDP, prepared at two widely different pH values, 7.4 and 12, the mean ionic charges at pH 7.4 are $-5.6 \pm 0.3$ and $-5.4 \pm 0.2$, respectively. For the complexes eluting in the first peak of the gel chromatogram of $^{99m}$Tc(Sn, pH 7.4)–HEDP the mean ionic charge is $-4.8 \pm 0.1$.

REFERENCES


1 T. G. Tji, H. J. Krips, W. J. Gelsema and C. L. de Ligny, *J. Chromatogr.*, 504 (1990) 403.
2 Y. M. Huigen, T. G. Tji, W. J. Gelsema and C. L. de Ligny, *Appl. Radiat. Isot.*, 39 (1988) 25.
3 Ch. D. Russell and P. G. Bischoff, *Int. J. Appl. Radiat. Isot.*, 35 (1984) 859.
4 C. L. de Ligny, W. J. Gelsema and A. M. P. Roozen, *J. Chromatogr. Sci.*, 21 (1983) 174.
5 C. L. de Ligny, W. J. Gelsema and W. E. Meijs, *Nucl. Med. Biol.*, 18 (1991) 173.
6 G. J. de Groot, H. A. Das and C. L. de Ligny, *Appl. Radiat. Isot.*, 37 (1986) 23.
7 D. Gouaillardou and M. Conti, *Appl. Radiat. Isot.*, 38 (1987) 103.
8 M. E. Holland, W. R. Heineman and E. Deutsch, *Nucl. Med. Biol.*, 16 (1989) 301.
9 C. L. de Ligny, W. J. Gelsema, T. P. M. Hoevelaken and J. Schuring, *Nucl. Med. Biol.*, in press.
10 A. M. Zimmer and D. G. Pavel, *J. Nucl. Med.*, 18 (1977) 1230.
11 J. Kroesbergen, W. J. Gelsema and C. L. de Ligny, *Int. J. Nucl. Med. Biol.*, 12 (1985) 83.
12 Y. M. Huigen, M. Diender, W. J. Gelsema and C. L. de Ligny, *Appl. Radiat. Isot.*, 42 (1991) 71.
13 G. M. Wilson and T. C. Pinkerton, *Anal. Chem.*, 57 (1985) 246.

*Journal of Chromatography*, 594 (1992) 225–228
Elsevier Science Publishers B.V., Amsterdam

CHROM. 23 833

# Determination of major ions in snow and ice cores by ion chromatography

C. F. Buck*,☆, P. A. Mayewski, M. J. Spencer, S. Whitlow, M. S. Twickler and D. Barrett

*Glacier Research Group, Institute for the Study of Earth, Oceans, and Space, University of New Hampshire, Durham, NH 03824 (USA)*

(First received April 17th, 1991; revised manuscript received October 29th, 1991)

ABSTRACT

The determination of major anions ($Cl^-$, $NO_3^-$, $SO_4^{2-}$) and cations ($Na^+$, $NH_4^+$, $K^+$, $Mg^{2+}$, $Ca^{2+}$) in snow and ice cores by ion chromatography at trace level concentrations (ng/g) is presented. Total acidity ($H^+$) was determined using an acid titration method in order to complete the ionic balance. Unique sampling techniques and sample preparation methods were developed to avoid contamination of the snow and ice samples.

## INTRODUCTION

Recently, there has been a great amount of work and interest dedicated to the understanding of climatic changes in the paleoenvironment. Among the powerful tools which are available to scientists to examine global climatic records are the physical and chemical analyses of snow and ice cores collected at such locations as Antarctica and Greenland [1,2].

The deposition and subsequent burial of gases, aerosols, and particles onto the glacier surfaces provides a unique archive of paleoenvironmental data. The snow and ice may then be recovered and analyzed for a wide variety of physical properties (*i.e.*, density, texture, stratigraphy) and chemical species (*i.e.*, stable isotopes, radionuclides, major ions).

Since the introduction of ion chromatographic methods in 1975 by Small *et al.* [3], ion chromatography has found widespread applications. Early work by Legrand *et al.* [4] determined major ions ($Na^+$, $NH_4^+$, $K^+$, $Cl^-$, $NO_3^-$, $SO_4^{2-}$) at ng/g concentrations in Antarctic snow and ice cores by ion chromatography. Mayewski *et al.* [5] analyzed a South Greenland ice core for trace level anion ($Cl^-$, $NO_3^-$, $SO_4^{2-}$) concentrations by ion chromatographic methods. This paper describes an ion chromatographic method for determining major anions ($Cl^-$, $NO_3^-$, $SO_4^{2-}$) and cations ($Na^+$, $NH_4^+$, $K^+$, $Mg^{2+}$, $Ca^{2+}$) at trace level concentrations (ng/g) without the use of concentrator columns. The mono- and divalent cations were separated in a single isocratic run via column switching. Total acidity ($H^+$) was determined by using an acid titration method developed by Legrand *et al.* [6] in order to complete the ionic balance. Unique sampling techniques and sample preparation methods were developed to avoid contamination of the snow and ice samples.

## EXPERIMENTAL

### *Sampling techniques and sample preparation*

Depending on the sample density (snow, firn, ice), different sampling techniques and sample preparation methods were required to avoid contamination of the samples. Field sampling and processing personnel handling the snow and ice samples wore

☆ Present address: Warner-Lambert Co., 170 Tabor Road, Morris Plains, NJ 07950, USA.

0021-9673/92/$05.00 

non-particulating suits, face masks, and polyethylene gloves to minimize sample contamination. All sample containers, sampling tools, and processing equipment and clothing that came into contact with the samples were cleaned using Milli-Q ultrapure water (Millipore, Bedford, MA, USA). The cleaning procedure consisted of rinsing three times, followed by an extensive soaking period of 1–6 months, and rinsed for a final three times prior to use. All materials were tested for possible contamination using the ion chromatographic method. The samples were processed in a cold room (−20°C) and kept frozen prior to the laboratory sample preparation step.

Snow pit samples were collected using specially designed sampling tools and transferred to 125-ml polypropylene containers with polyethylene screw caps (Becton-Dickinson, Rutherford, NJ, USA). The snow samples were transferred directly to 250-ml polypropylene containers (Nalge, Rochester, NY, USA) in the laboratory. The samples were melted using a circulating hot water bath.

Firn and ice core samples were processed using commercially available Sears Craftsman bandsaws (Sears Roebuck, Chicago, IL, USA) after careful and thorough cleaning to remove all grease and dust. Tabletops, saw guides, and tools were modified or covered with either Teflon or Plexiglas. Lexan or flame-hardened steel blades (Sears Roebuck) were used. Firn and ice core samples were processed at measured intervals by removing the outside sections of the core to obtain a contamination-free center. Samples were then placed into polyethylene bags (Nasco-West, Modesto, CA, USA) and removed to a clean freezer for further porcessing, if necessary. At the time of laboratory analysis, samples were transferred to 250 or 500 ml polypropylene containers (Nalge) for melting. Ice samples were rinsed with Milli-Q ultrapure water (25–35%, w/w, sample weight loss) using a pair of surgical stainless steel tweezers prior to the melting of the sample to remove any possible contamination.

All melted laboratory samples were swirled at room temperature to obtain a homogenous solution, then 5.0-ml aliquots were placed into polypropylene sample tubes (Helena Plastics, San Rafael, CA, USA) for immediate analysis or refrozen. The laboratory sample preparation step was performed in rapid fashion on open laboratory benches without a clean hood.

*Acidity measurements*

Total acidity ($H^+$) was determined by using an acid titration method developed by Legrand *et al.* [6] with slight modifications to the original method.

*Ion chromatography*

A Dionex Series 4000i ion chromatograph (Dionex, Sunnyvale, CA, USA) was used for the determination of the major ions. The Dionex Series 4000i ion chromatograph was divided into two dedicated systems (anion and cation) and consisted of: two gradient pump modules, two conductivity detector modules (output range = 3 $\mu$s), and LCM-2 chromatography module. The samples for each system were introduced into 0.5-ml sample loops via two fixed-speed peristaltic pumps which initially draws approximately 1.0 ml of Milli-Q ultrapure water followed by approximately 2.0 ml of sample guaranteeing no cross contamination from the previous sample. The sampling system was automated using two AutoAnalyzer autosamplers. All time events and data collection were processed through the Dionex Autoion 450 Data software package and Advanced Computer Interface unit via personal computer. The analog output was recorded on two strip-chart recorders.

For the anion chromatographic system, the columns used for all experiments were a Dionex IonPac AS4A separator column with an Dionex IonPac AG4 guard column. A Dionex anion micromembrane suppressor was placed in line prior to the conductivity cell resulting in a background conductivity of approximately 11.0–15.0 $\mu$S. The mobile phase was 0.0018 *M* $Na_2CO_3$–0.0017 *M* $NaHCO_3$; 0.0125 *M* $H_2SO_4$ was used as the regenerant. The flow-rates for the mobile phase and regenerant were 2.0 and 4–5 ml/min, respectively.

For the cation chromatographic system, the columns used for all experiments were Dionex IonPac Fast Cation I and Cation II columns in conjunction with a high-pressure switching valve in order to separate the mono- and divalent cations in one isocratic run. A Dionex cation micromembrane suppressor was placed in line prior to the conductivity cell resulting in a background conductivity of approximately 450 nS–1.5 $\mu$S. The mobile phase was 19 m*M* HCl–0.3 m*M* DL-2,3-diaminopropionic acid monohydrochloride (DAP); 100 m*M* tetrabutylammonium hydroxide (TBAOH) was used as the regenerant. The flow-rates for the mobile phase and

TABLE I

LIMITS OF DETECTION ESTIMATED FOR THE ION CHROMATOGRAPHIC METHOD

| Ion | Concentration (ng/g) | Ion | Concentration (ng/g) |
|---|---|---|---|
| $Cl^-$ | 0.5 | $NH_4^+$ | 0.2 |
| $NO_3^-$ | 0.5 | $K^+$ | 0.1 |
| $SO_4^{2-}$ | 0.5 | $Mg^{2+}$ | 0.1 |
| $Na^+$ | 0.1 | $Ca^{2+}$ | 0.1 |

regenerant were 3.0 and 10–15 ml/min, respectively. The cation regenerant waste (TBACl) was collected and recycled off-line using a series of Dionex Auto-Regen cation cartridges.

## RESULTS AND DISCUSSION

Due to the large sample volumes available (10–25 ml), an injection volume of 0.5 ml was selected to avoid the use of concentrator columns. Larger injection volumes were not used because of the broad water peak resulting in poor resolution of the early eluting peaks. Excellent sensitivity was achieved for trace level concentrations (ng/g) for the ions. Limits of detection for the ion chromatographic method are shown in Table I. The limit of detection for the chromatographic method was defined as the amount of solute producing a signal-to-noise ratio of 2–3.

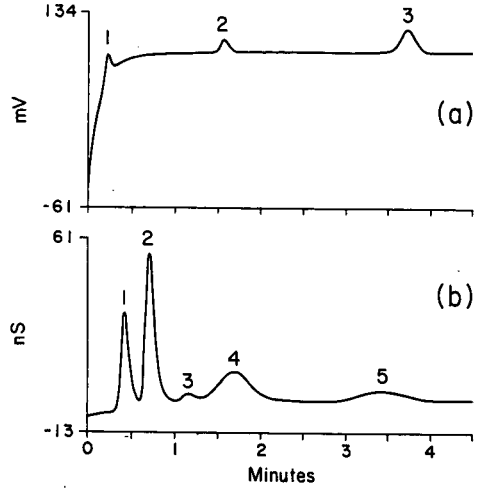


Fig. 1. (a) Anion standard solution: 1 = $Cl^-$ (3 ng/g), 2 = $NO_3^-$ (5 ng/g), 3 = $SO_4^{2-}$ (10 ng/g). (b) Cation standard solution: 1 = $Na^+$ (2 ng/g), 2 = $NH_4^+$ (2 ng/g), 3 = $K^+$ (0.5 ng/g), 4 = $Mg^{2+}$ (1 ng/g), 5 = $Ca^{2+}$ (1 ng/g).

Isocratic separations for anion and cation standard solutions are shown in Fig. 1. The anion system was significantly more stable than the cation system in terms of the daily background conductiv-

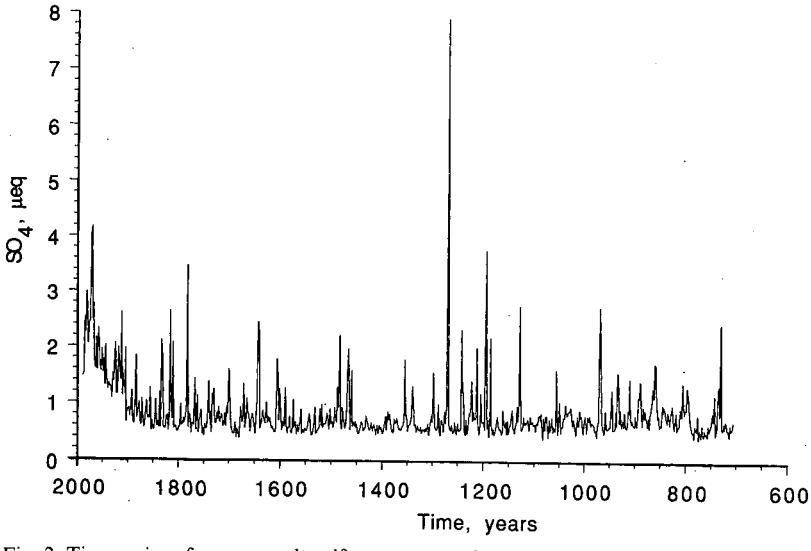


Fig. 2. Time-series of non-sea-salt sulfate concentration (in μequiv.) collected in Central Greenland.

ity. This problem was a result of the quality of recycled cation regenerant (TBAOH). The cation regenerant waste (TBACl) was collected and recycled off-line via a series of Dionex AutoRegen cation cartridges. The active sites in the cartridges are exhausted over time causing the cation regenerant waste (TBACl) not to be fully regenerated back to its original form (TBAOH). As a result, the daily background conductivity increased over time. The AutoRegen cation cartridges were regenerated with 1.0 *M* NaOH on a weekly basis to extend the life of the cartridges. It was found that the background conductivity of the cation system was influenced greatly by the flow-rate of the regenerant through the micromembrane suppressor.

The melting of all laboratory samples were conducted rapidly on open laboratory benches and not under a clean hood. A contamination control study conducted in our laboratories showed that the ammonium concentration in sample container blanks was approximately five times greater when sampled under a clean hood. This anomaly is due to the increased gas exchange caused by the continuous airflow of the clean hood. To further reduce the ammonium blank value to less than 0.5 ng/g, all sample tubes were kept tightly capped until approximately 1.0 min prior to the sample injection on the ion chromatograph. No chromatographic interferences were observed and filtering the samples was not necessary.

The ion chromatographic method described has been used for the investigation of various glaciochemical studies. An example is provided in Fig. 2 with the non-sea-salt sulfate time-series for the upper section of an ice core retrieved in Central Greenland as part of the Greenland Ice Sheet Project Two (GISP II). Detailed discussions concerning the glaciochemical data sets are presented in several of the references 7–12.

ACKNOWLEDGEMENTS

We thank C. Wake and K. Welch for their assistance in the laboratory. This research was supported by the Electric Power Research Institute, the US Environmental Protection Agency, le Centre de la Recherche Scientifique, and the National Science Foundation.

REFERENCES

1 R. Monastersky, *Sc. News (Washington, D.C.)* 140 (1991) 168.
2 M. R. Legrand, C. Lorius, N. I. Barkov and V. N. Petrov, *Atmos. Environ.*, 22 (1988) 317.
3 H. Small, T. S. Stevens and W. C. Bauman, *Anal. Chem.*, 47 (1975) 1801.
4 M. Legrand, M. De Angelis and R. J. Delmas, *Anal. Chim. Acta*, 156 (1984) 181.
5 P. A. Mayewski, W. B. Lyons, M. J. Spencer, M. Twickler, W. Dansgaard, B. Koci, L. I. Davidson and R. E. Honrath, *Science (Washington, D.C.)*, 232 (1986) 975.
6 M. R. Legrand, A. J. Aristarain and R. J. Delmas, *Anal. Chem.*, 54 (1982) 1336.
7 W. B. Lyons, P. A. Mayewski, M. J. Spencer and M. S. Twickler, *Ann. Glaciol.*, 14 (1990) 176.
8 P. A. Mayewski, M. J. Spencer, M. S. Twickler and S. Whitlow, *Ann. Glaciol.*, 14 (1990) 186.
9 C. P. Wake, P. A. Mayewski and M. J. Spencer, *Ann. Glaciol.*, 14 (1990) 310.
10 P. Laj, S. M. Drummey, M. J. Spencer, J. M. Palais and H. Sigurdsson, *Nature (London)*, 346 (1990) 45.
11 P. A. Mayewski and M. R. Legrand, *Nature (London)*, 346 (1990) 258.
12 P. A. Mayewski, W. B. Lyons, M. J. Spencer, M. S. Twickler, C. F. Buck and S. Whitlow, *Nature (London)*, 346 (1990) 554.

*Journal of Chromatography*, 594 (1992) 229–241
Elsevier Science Publishers B.V., Amsterdam

CHROM. 23 819

# Hydrogen bonding

# XXI. Solvation parameters for alkylaromatic hydrocarbons from gas–liquid chromatographic data

Michael H. Abraham* and Gary S. Whiting

*Department of Chemistry, University College London, 20 Gordon Street, London WC1H 0AJ (UK)*

(Received September 4th, 1991)

ABSTRACT

The truncated solvation equation

$$\log SP = c + rR_2 + l \log L^{16}$$

has been applied to numerous sets of gas–liquid chromatographic (GLC) data for alkylaromatic hydrocarbons on non-polar stationary phases. Here $SP$ can be $V_G$ or can be the relative retention time, and the retention index $I$ can in this context be used in place of log $SP$. $R_2$ is the solute excess molar refraction, easily obtained from refractive index. A set of solutes of known log $L^{16}$ is used to set up the equation and then values of log $L^{16}$ can be back-calculated for other solutes; $L^{16}$ is originally defined as the solute gas–liquid partition coefficient on hexadecane at 25°C. Through the above equation log $L^{16}$ values were calculated for 190 solutes. Once log $L^{16}$ is known, the reduced equation

$$\log SP = c + s\pi_2^H + l \log L^{16}$$

can be applied to GLC data on polar stationary phases, and the dipolarity/polarizability parameter $\pi_2^H$ obtained by back-calculation in a similar way. Values of $\pi_2^H$ for 120 solutes are listed. It is shown that *n*-alkyl substituents affect the $\pi_2^H$ value only slightly, but *ortho* substituents considerably increase $\pi_2^H$, *e.g.*, benzene (0.52), toluene (0.52), *o*-xylene (0.56), 1,2,3-trimethylbenzene (0.61), 1,2,3,4-tetramethylbenzene (0.65), pentamethylbenzene (0.66), hexamethylbenzene (0.72).

## INTRODUCTION

Previously, we have shown that the general solvation equation

$$\log SP = c + rR_2 + s\pi_2^H + a\alpha_2^H + b\beta_2^H + l \log L^{16} \quad (1)$$

can be used to characterize all types of gas–liquid chromatographic (GLC) stationary phases, ranging from non-polar hydrocarbons to liquid salts [1–3], and also polymers [4] and not too volatile, non-polymeric liquids [5]. In eqn. 1, log $SP$ is a retention property for a series of solutes on a given stationary phase, such as the retention volume as log $V_G$ or the gas–liquid partition coefficient as log $L$, but not the retention index $I$. The explanatory variables are solute properties as follows: $R_2$ is the solute excess molar refraction [6], $\pi_2^H$ is the solute dipolarity/polarizability [1], $\alpha_2^H$ and $\beta_2^H$ are the solute hydrogen-bond acidity and basicity [1] and $L^{16}$ is the solute gas–liquid partition coefficient on hexadecane at 25°C [7]. Note that in eqn. 1, $\pi_2^H$, $\alpha_2^H$ and $\beta_2^H$ are "effective" or "summation" values, appropriate to the situation in which a monomeric solute molecule is surrounded by a large excess of solvent molecules.

The constants in eqn. 1 are found by the method of multiple linear regression analysis, and serve to

0021-9673/92/$05.00 

characterize the particular stationary phase under investigation. Eqn. 1 can also be used to correlate a series of $I$ values, but the constants thus obtained are not characteristic constants for the particular stationary phase. As we shall see, however, the use of $I$ values can lead to equations that are useful in other ways.

The generality of eqn. 1 depends on the availability of the various solute parameters used as explanatory variables. We have set out an extensive table of these parameters, but the large majority of solutes therein were aliphatic rather than aromatic. In order to extend our data base of solutes, so as to make eqn. 1 more general, we now set out the determination of relevant parameters for aromatic hydrocarbons, especially the key parameter $\pi_2^H$.

As the solutes with which we shall deal are all non-hydrogen-bonded acids, the term $a\alpha_2^H$ in eqn. 1 will be redundant. Further, all the stationary phases we shall investigate will be either neutral or hydrogen-bonded bases. They will not be hydrogen-bonded acids and so the $b\beta_2^H$ term in eqn. 1 is also redundant, leaving

$$\log SP = c + rR_2 + s\pi_2^H + l\log L^{16} \qquad (2)$$

The excess molar refraction, $R_2$, can be obtained from the liquid refractive index, or can easily be estimated, so that there are only two unknown parameters, $\pi_2^H$ and $\log L^{16}$, for any solute in eqn. 2.

Our method is thus to set up equations for a series of known solutes on a non-polar phase, where the $s\pi_2^H$ term will either be zero or small, and then for any other solute knowing $\log SP$ and $R_2$ a value of $\log L^{16}$ can be obtained by back-calculation. Once $\log L^{16}$ is known, the only other required parameter is $\pi_2^H$. Now, if an equation can be constructed for known solutes on a polar phase, where the $s$-constant is very large, then for any other solute $\pi_2^H$ can be back-calculated, knowing $\log SP$, $R_2$ and $\log L^{16}$. Unlike the situation with characteristic constants, $\log SP$ in the above method can now be the retention index $I$. Indeed, many of the equations we shall use will be in terms of $I$, or of $I/10$, which for our purpose is slightly more convenient.

## RESULTS

There is a very large amount of literature data, mostly as retention index values, for aromatic hydrocarbons on non-polar phases such as squalane and other hydrocarbons [8–16] and poly(methylsiloxanes) such as OV-101 [14,17–20]. Most results are at temperatures around 100°C, where the $s\pi_2^H$ term in eqn. 2 is negligible. Then the correlation equation reduces to

$$\log SP = c + rR_2 + l\log L^{16} \qquad (3)$$

where $SP = V_G$ or the relative retention time $t$(rel), or to

$$I = c' + r'R_2 + l'\log L^{16} \qquad (4)$$

where $I$ is the retention index. The constants in eqn. 4 will not correspond to those in eqn. 3, but this does not matter as far as the back-calculation of $\log L^{16}$ is concerned.

Results of the back-calculations are summarized in Table I, where S.D. is the standard deviation in $\log L^{16}$ over the various determinations, and No. is the number of determinations. In a few instances, notably with benzene, there are slight differences between the squalane and the siloxane values, but we take the overall average as the obtained value. For a few solutes, it is possible to compare the overall average in Table I with our directly determined $\log L^{16}$ values on hexadecane [7] (see Table II). There is good agreement between the two sets of values, and if the new values were to replace the old set in any correlation equation, alterations in the equations would be insignificant. Typical equations used to back-calculate $\log L^{16}$ are for squalane at 96°C [11]

$$I/10 = 7.604 + 4.189R_2 + 19.747\log L^{16} \qquad (5)$$

$$n = 67, \quad R = 0.9996, \quad \text{S.D.} = 0.377$$

and for OV-101 at 100°C [18]

$$I/10 = 6.418 + 5.915R_2 + 19.979\log L^{16} \qquad (6)$$

$$n = 42, \quad R = 0.9992, \quad \text{S.D.} = 0.482$$

where $n$ is the number of solutes, $R$ is the overall correlation coefficient and S.D. is the standard deviation in $I/10$. As a rough indication of the error in the back-calculated $\log L^{16}$ values we can take the overall standard deviation divided by the particular constant, in this instance S.D./$l$. Expected errors in $\log L^{16}$ are thus estimated to be around 0.02 log units, in agreement with the various S.D. values given in Table I. Values of $R_2$ needed in the back-calculations are also given in Table I.

TABLE I

CALCULATED VALUES OF LOG $L^{16}$

| Solute | $R$ | Squalane average | S.D. | No. | Siloxane average | S.D. | No. | Overall average | S.D. | No. |
|---|---|---|---|---|---|---|---|---|---|---|
| Benzene | 0.610 | 2.778 | 0.003 | 8 | 2.803 | 0.002 | 4 | 2.786 | 0.013 | 12 |
| Toluene | 0.601 | 3.325 | 0.005 | 8 | 3.326 | 0.007 | 4 | 3.325 | 0.006 | 12 |
| Ethylbenzene | 0.613 | 3.774 | 0.003 | 8 | 3.785 | 0.004 | 5 | 3.778 | 0.006 | 13 |
| *o*-Xylene | 0.663 | 3.944 | 0.003 | 8 | 3.931 | 0.003 | 5 | 3.939 | 0.007 | 13 |
| *m*-Xylene | 0.623 | 3.850 | 0.003 | 8 | 3.821 | 0.005 | 5 | 3.839 | 0.016 | 13 |
| *p*-Xylene | 0.613 | 3.845 | 0.004 | 8 | 3.829 | 0.003 | 5 | 3.839 | 0.009 | 13 |
| *n*-Propylbenzene | 0.604 | 4.220 | 0.003 | 8 | 4.246 | 0.005 | 5 | 4.230 | 0.014 | 13 |
| Isopropylbenzene | 0.602 | 4.075 | 0.003 | 8 | 4.099 | 0.005 | 5 | 4.084 | 0.012 | 13 |
| 1,2,3-Trimethylbenzene | 0.728 | 4.571 | 0.005 | 8 | 4.554 | 0.010 | 5 | 4.565 | 0.011 | 13 |
| 1,2,4-Trimethylbenzene | 0.677 | 4.456 | 0.005 | 8 | 4.417 | 0.009 | 5 | 4.441 | 0.021 | 13 |
| 1,3,5-Trimethylbenzene | 0.649 | 4.371 | 0.005 | 8 | 4.301 | 0.006 | 5 | 4.344 | 0.036 | 13 |
| 2-Ethyltoluene | 0.680 | 4.346 | 0.004 | 8 | 4.348 | 0.005 | 5 | 4.346 | 0.004 | 13 |
| 3-Ethyltoluene | 0.630 | 4.276 | 0.006 | 8 | 4.273 | 0.003 | 5 | 4.275 | 0.005 | 13 |
| 4-Ethyltoluene | 0.630 | 4.292 | 0.004 | 8 | 4.283 | 0.002 | 5 | 4.289 | 0.005 | 13 |
| *n*-Butylbenzene | 0.600 | 4.722 | 0.005 | 8 | 4.746 | 0.007 | 4 | 4.730 | 0.013 | 12 |
| Isobutylbenzene | 0.580 | 4.493 | 0.005 | 8 | 4.525 | 0.004 | 2 | 4.500 | 0.014 | 10 |
| *sec.*-Butylbenzene | 0.603 | 4.489 | 0.005 | 8 | 4.533 | 0.008 | 5 | 4.506 | 0.023 | 13 |
| *tert.*-Butylbenzene | 0.619 | 4.400 | 0.009 | 8 | 4.439 | 0.008 | 4 | 4.413 | 0.021 | 12 |
| 1,2-Diethylbenzene | 0.688 | 4.721 | 0.005 | 6 | 4.749 | 0.006 | 4 | 4.732 | 0.015 | 10 |
| 1,3-Diethylbenzene | 0.637 | 4.676 | 0.009 | 8 | 4.701 | 0.010 | 5 | 4.686 | 0.016 | 13 |
| 1,4-Diethylbenzene | 0.645 | 4.732 | 0.007 | 8 | 4.732 | 0.006 | 5 | 4.732 | 0.006 | 13 |
| 1,2,4,5-Tetramethylbenzene | 0.739 | 5.048 | 0.009 | 7 | 5.008 | 0.009 | 6 | 5.029 | 0.022 | 13 |
| 1,2,3,5-Tetramethylbenzene | 0.748 | 5.074 | 0.009 | 7 | 5.027 | 0.017 | 6 | 5.052 | 0.027 | 13 |
| 1,2,3,4-Tetramethylbenzene | 0.794 | 5.179 | 0.009 | 7 | 5.171 | 0.019 | 4 | 5.176 | 0.013 | 11 |
| 2-*n*-Propyltoluene | 0.664 | 4.757 | 0.008 | 8 | 4.781 | 0.010 | 5 | 4.766 | 0.015 | 13 |
| 3-*n*-Propyltoluene | 0.624 | 4.707 | 0.006 | 6 | 4.713 | 0.004 | 5 | 4.710 | 0.006 | 11 |
| 4-*n*-Propyltoluene | 0.623 | 4.735 | 0.006 | 8 | 4.733 | 0.002 | 5 | 4.734 | 0.005 | 13 |
| 2-Isopropyltoluene | 0.669 | 4.611 | 0.006 | 6 | 4.635 | 0.015 | 5 | 4.622 | 0.016 | 11 |
| 3-Isopropyltoluene | 0.621 | 4.556 | 0.011 | 7 | 4.555 | 0.015 | 5 | 4.556 | 0.012 | 12 |
| 4-Isopropyltoluene | 0.607 | 4.593 | 0.008 | 7 | 4.584 | 0.011 | 5 | 4.590 | 0.010 | 12 |
| 1,2-Dimethyl-3-ethylbenzene | 0.742 | 4.951 | 0.005 | 4 | 4.936 | 0.003 | 2 | 4.946 | 0.009 | 6 |
| 1,2-Dimethyl-4-ethylbenzene | 0.685 | 4.880 | 0.003 | 6 | 4.860 | 0.007 | 3 | 4.873 | 0.011 | 9 |
| 1,3-Dimethyl-2-ethylbenzene | 0.757 | 4.866 | 0.006 | 4 | 4.865 | 0.011 | 2 | 4.866 | 0.007 | 6 |
| 1,3-Dimethyl-4-ethylbenzene | 0.690 | 4.852 | 0.007 | 6 | 4.834 | 0.008 | 3 | 4.846 | 0.011 | 9 |
| 1,3-Dimethyl-5-ethylbenzene | 0.653 | 4.774 | 0.006 | 4 | 4.741 | 0.008 | 3 | 4.760 | 0.018 | 7 |
| 1,4-Dimethyl-2-ethylbenzene | 0.693 | 4.824 | 0.005 | 6 | 4.826 | 0.013 | 3 | 4.824 | 0.007 | 9 |
| *n*-Pentylbenzene | 0.594 | 5.225 | 0.016 | 4 | 5.254 | | 1 | 5.230 | 0.019 | 5 |
| Isopentylbenzene | 0.574 | 5.053 | 0.004 | 2 | 5.097 | | 1 | 5.068 | 0.026 | 3 |
| *sec.*-Pentylbenzene | 0.600 | 4.937 | 0.009 | 4 | | | | 4.937 | 0.009 | 4 |
| *tert.*-Pentylbenzene | 0.620 | 4.890 | 0.011 | 3 | 4.965 | | 1 | 4.909 | 0.038 | 4 |
| Pentamethylbenzene | 0.850 | 5.795 | 0.013 | 4 | 5.805 | 0.019 | 2 | 5.798 | 0.014 | 6 |
| 2-*n*-Butyltoluene | 0.652 | 5.261 | | 1 | 5.292 | | 1 | 5.276 | 0.022 | 2 |
| 3-*n*-Butyltoluene | 0.617 | | | | 5.216 | | 1 | 5.216 | | 1 |
| 4-*n*-Butyltoluene | 0.621 | 5.234 | | 1 | 5.248 | | 1 | 5.241 | 0.010 | 2 |
| 3-*sec.*-Butyltoluene | 0.613 | | | | 4.963 | | 1 | 4.963 | | 1 |
| 4-*sec.*-Butyltoluene | 0.613 | 5.011 | 0.001 | 2 | 4.998 | | 1 | 5.006 | 0.007 | 3 |
| 2-*tert.*-Butyltoluene | 0.670 | 4.998 | 0.001 | 2 | | | | 4.998 | 0.001 | 2 |
| 3-*tert.*-Butyltoluene | 0.630 | 4.826 | 0.006 | 3 | | | | 4.826 | 0.006 | 3 |
| 4-*tert.*-Butyltoluene | 0.620 | 4.922 | 0.008 | 3 | 4.939 | | 1 | 4.926 | 0.011 | 4 |
| 1-Ethyl-2-*n*-propylbenzene | 0.660 | 5.144 | 0.001 | 2 | 5.176 | | 1 | 5.154 | 0.019 | 3 |
| 1-Ethyl-3-*n*-propylbenzene | 0.622 | 5.110 | 0.000 | 2 | 5.137 | | 1 | 5.119 | 0.016 | 3 |
| 1-Ethyl-4-*n*-propylbenzene | 0.625 | 5.174 | 0.007 | 3 | 5.205 | | 1 | 5.182 | 0.016 | 4 |

(*Continued on p. 232*)

TABLE I (*continued*)

| Solute | *R* | Squalane average | S.D. | No. | Siloxane average | S.D. | No. | Overall average | S.D. | No. |
|---|---|---|---|---|---|---|---|---|---|---|
| 1-Ethyl-2-isopropylbenzene | 0.658 | 4.943 | 0.001 | 2 | 5.012 | | 1 | 4.966 | 0.040 | 3 |
| 1-Ethyl-3-isopropylbenzene | 0.625 | 4.935 | 0.001 | 2 | 4.966 | 0.013 | 2 | 4.951 | 0.020 | 4 |
| 1-Ethyl-4-isopropylbenzene | 0.626 | 5.039 | 0.001 | 2 | 5.018 | 0.008 | 2 | 5.028 | 0.013 | 4 |
| 1,2-Dimethyl-3-*n*-propylbenzene | 0.750 | | | | 5.373 | | 1 | 5.373 | | 1 |
| 1,2-Dimethyl-4-*n*-propylbenzene | 0.690 | | | | 5.282 | | 1 | 5.282 | | 1 |
| 1,3-Dimethyl-2-*n*-propylbenzene | 0.757 | | | | 5.263 | | 1 | 5.263 | | 1 |
| 1,3-Dimethyl-4-*n*-propylbenzene | 0.690 | | | | 5.259 | 0.010 | 2 | 5.259 | 0.010 | 2 |
| 1,3-Dimethyl-5-*n*-propylbenzene | 0.653 | | | | 5.169 | 0.013 | 2 | 5.169 | 0.013 | 2 |
| 1,4-Dimethyl-2-*n*-propylbenzene | 0.693 | | | | 5.237 | 0.007 | 2 | 5.242 | | 1 |
| 1,2-Dimethyl-4-isopropylbenzene | 0.690 | | | | 5.150 | 0.011 | 2 | 5.150 | 0.010 | 2 |
| 1,3-Dimethyl-4-isopropylbenzene | 0.695 | | | | 5.102 | 0.008 | 2 | 5.102 | 0.008 | 2 |
| 1,3-Dimethyl-5-isopropylbenzene | 0.658 | | | | 5.007 | 0.003 | 2 | 5.007 | 0.003 | 2 |
| 1,4-Dimethyl-2-isopropylbenzene | 0.698 | | | | 5.079 | 0.011 | 2 | 5.079 | 0.011 | 2 |
| 1,2-Diethyl-3-methyltoluene | 0.740 | | | | 5.338 | | 1 | 5.338 | | 1 |
| 1,2-Diethyl-4-methylbenzene | 0.720 | | | | 5.190 | | 1 | 5.190 | | 1 |
| 1,3-Diethyl-4-methylbenzene | 0.708 | | | | 5.241 | 0.007 | 2 | 5.241 | 0.007 | 2 |
| 1,3-Diethyl-5-methylbenzene | 0.665 | | | | 5.075 | 0.062 | 3 | 5.075 | 0.062 | 3 |
| 1,4-Diethyl-2-methylbenzene | 0.708 | | | | 5.221 | | 1 | 5.221 | | 1 |
| 1,2,3-Trimethyl-4-ethylbenzene | 0.800 | | | | 5.594 | | 1 | 5.594 | | 1 |
| 1,2,3-Trimethyl-5-ethylbenzene | 0.760 | | | | 5.452 | | 1 | 5.452 | | 1 |
| 1,2,4-Trimethyl-3-ethylbenzene | 0.800 | | | | 5.559 | | 1 | 5.559 | | 1 |
| 1,2,5-Trimethyl-3-ethylbenzene | 0.760 | | | | 5.407 | | 1 | 5.407 | | 1 |
| 1,3,5-Trimethyl-2-ethylbenzene | 0.760 | | | | 5.402 | | 1 | 5.402 | | 1 |
| *n*-Hexylbenzene | 0.591 | 5.707 | 0.006 | 3 | 5.758 | | 1 | 5.720 | 0.026 | 4 |
| Hexamethylbenzene | 0.950 | 6.538 | | 1 | 6.576 | | 1 | 6.557 | 0.027 | 2 |
| 1,2-Di-*n*-propylbenzene | 0.665 | 5.492 | | 1 | | | | 5.492 | | 1 |
| 1,3-Di-*n*-propylbenzene | 0.625 | 5.514 | | 1 | 5.546 | | 1 | 5.530 | 0.023 | 2 |
| 1,4-Di-*n*-propylbenzene | 0.620 | 5.601 | | 1 | 5.605 | | 1 | 5.603 | 0.003 | 2 |
| 1,2-Diisopropylbenzene | 0.665 | 5.149 | 0.002 | 2 | 5.253 | | 1 | 5.183 | 0.060 | 3 |
| 1,3-Diisopropylbenzene | 0.605 | 5.148 | 0.006 | 4 | 5.213 | 0.006 | 2 | 5.170 | 0.034 | 6 |
| 1,4-Diisopropylbenzene | 0.616 | 5.319 | 0.010 | 4 | 5.309 | 0.011 | 2 | 5.315 | 0.010 | 6 |
| 1-*n*-Propyl-2-isopropylbenzene | 0.665 | | | | 5.394 | | 1 | 5.394 | | 1 |
| 1-*n*-Propyl-3-isopropylbenzene | 0.616 | | | | 5.408 | | 1 | 5.408 | | 1 |
| 1-*n*-Propyl-4-isopropylbenzene | 0.618 | 5.453 | | 1 | 5.447 | | 1 | 5.450 | 0.004 | 2 |
| 1,2-Dimethyl-3-*n*-butylbenzene | 0.750 | | | | 5.858 | | 1 | 5.858 | | 1 |
| 1,2-Dimethyl-4-*n*-butylbenzene | 0.690 | | | | 5.762 | | 1 | 5.762 | | 1 |
| 1,2-Dimethyl-4-*sec.*-butylbenzene | 0.690 | | | | 5.542 | | 1 | 5.542 | | 1 |
| 1,2-Dimethyl-4-*tert.*-butylbenzene | 0.690 | | | | 5.452 | | 1 | 5.452 | | 1 |
| 1,3-Dimethyl-4-*n*-butylbenzene | 0.695 | | | | 5.736 | | 1 | 5.736 | | 1 |
| 1,3-Dimethyl-4-*sec.*-butylbenzene | 0.695 | | | | 5.482 | | 1 | 5.482 | | 1 |
| 1,3-Dimethyl-5-*n*-butylbenzene | 0.640 | | | | 5.640 | | 1 | 5.640 | | 1 |
| 1,3-Dimethyl-5-*sec.*-butylbenzene | 0.640 | | | | 5.391 | | 1 | 5.391 | | 1 |
| 1,3-Dimethyl-5-*tert.*-butylbenzene | 0.640 | 5.292 | 0.010 | 2 | | | | 5.292 | 0.010 | 2 |
| 1,4-Dimethyl-2-*n*-butylbenzene | 0.690 | | | | 5.707 | | 1 | 5.707 | | 1 |
| 1,4-Dimethyl-2-*sec.*-butylbenzene | 0.695 | | | | 5.447 | | 1 | 5.447 | | 1 |
| 1-Methyl-2-*n*-pentylbenzene | 0.650 | 5.735 | | 1 | 5.740 | | 1 | 5.738 | 0.004 | 2 |
| 1-Methyl-3-*n*-pentyltoluene | 0.620 | | | | 5.672 | | 1 | 5.672 | | 1 |
| 1-Methyl-4-*n*-pentylbenzene | 0.620 | 5.727 | | 1 | 5.702 | | 1 | 5.715 | 0.018 | 2 |
| 1-Ethyl-2-*n*-butylbenzene | 0.650 | 5.598 | | 1 | | | | 5.598 | | 1 |
| 1-Ethyl-3-*n*-butyltoluene | 0.620 | | | | 5.602 | | 1 | 5.602 | | 1 |
| 1-Ethyl-4-*n*-butylbenzene | 0.620 | 5.681 | | 1 | 5.657 | | 1 | 5.669 | 0.017 | 2 |
| 1-Ethyl-2-*sec.*-butylbenzene | 0.650 | | | | 5.380 | | 1 | 5.380 | | 1 |

TABLE I (*continued*)

| Solute | *R* | Squalane average | S.D. | No. | Siloxane average | S.D. | No. | Overall average | S.D. | No. |
|---|---|---|---|---|---|---|---|---|---|---|
| 1-Ethyl-3-*sec.*-butyltoluene | 0.620 | | | | 5.347 | | 1 | 5.347 | | 1 |
| 1-Ethyl-4-*sec.*-butyltoluene | 0.620 | | | | 5.422 | | 1 | 5.422 | | 1 |
| 1-Ethyl-4-*tert.*-butylbenzene | 0.620 | 5.363 | 0.001 | 2 | | | | 5.363 | 0.001 | 2 |
| 1,2,3-Triethylbenzene | 0.780 | | | | 5.683 | | 1 | 5.683 | | 1 |
| 1,2,4-Triethylbenzene | 0.715 | 5.585 | 0.005 | 2 | 5.589 | | 1 | 5.586 | 0.004 | 3 |
| 1,3,5-Triethylbenzene | 0.672 | 5.504 | 0.004 | 3 | 5.520 | 0.001 | 2 | 5.510 | 0.009 | 5 |
| 1,2,3-Trimethyl-5-*n*-propylbenzene | 0.760 | | | | 5.882 | | 1 | 5.882 | | 1 |
| 1,2,3-Trimethyl-5-isopropylbenzene | 0.760 | | | | 5.717 | | 1 | 5.717 | | 1 |
| 1,2,4-Trimethyl-3-*n*-propylbenzene | 0.800 | | | | 5.969 | | 1 | 5.969 | | 1 |
| 1,2,4-Trimethyl-5-isopropylbenzene | 0.750 | | | | 5.653 | | 1 | 5.653 | | 1 |
| 1,2,5-Trimethyl-3-*n*-propylbenzene | 0.760 | | | | 5.872 | | 1 | 5.872 | | 1 |
| 1,3,5-Trimethyl-2-*n*-propylbenzene | 0.760 | | | | 5.802 | | 1 | 5.802 | | 1 |
| *n*-Heptylbenzene | 0.577 | 6.219 | | 1 | | | | 6.219 | | 1 |
| 1-Methyl-2-*n*-hexylbenzene | 0.647 | 6.218 | | 1 | | | | 6.218 | | 1 |
| 1-Methyl-4-*n*-hexylbenzene | 0.618 | 6.219 | | 1 | | | | 6.219 | | 1 |
| 1-Ethyl-2-*n*-pentylbenzene | 0.647 | 6.069 | | 1 | | | | 6.069 | | 1 |
| 1-Ethyl-4-*n*-pentylbenzene | 0.618 | 6.162 | | 1 | | | | 6.162 | | 1 |
| 1-*n*-Propyl-2-*n*-butylbenzene | 0.647 | 5.955 | | 1 | | | | 5.955 | | 1 |
| 1-*n*-Propyl-4-*n*-butylbenzene | 0.618 | 6.105 | | 1 | | | | 6.105 | | 1 |
| *n*-Octylbenzene | 0.579 | 6.714 | | 1 | | | | 6.714 | | 1 |
| 1,2-Di-*n*-butylbenzene | 0.642 | 6.409 | | 1 | | | | 6.409 | | 1 |
| 1,4-Di-*n*-butylbenzene | 0.611 | 6.612 | | 1 | | | | 6.612 | | 1 |
| 1,4-Diisobutylbenzene | 0.610 | 6.091 | | 1 | | | | 6.091 | | 1 |
| 1,4-Di-*sec.*-butylbenzene | 0.612 | 6.073 | | 1 | | | | 6.073 | | 1 |
| 1,4-Di-*tert.*-butylbenzene | 0.616 | 5.956 | | 1 | | | | 5.956 | | 1 |
| 1-*n*-Butyl-4-isobutylbenzene | 0.611 | 6.353 | | 1 | | | | 6.353 | | 1 |
| 1-*n*-Butyl-4-*sec.*-butylbenzene | 0.612 | 6.347 | | 1 | | | | 6.347 | | 1 |
| 1-*n*-Butyl-4-*tert.*-butylbenzene | 0.613 | 6.280 | | 1 | | | | 6.280 | | 1 |
| 1-Isobutyl-4-*sec.*-butylbenzene | 0.611 | 6.081 | | 1 | | | | 6.081 | | 1 |
| 1-Isobutyl-4-*tert.*-butylbenzene | 0.613 | 6.004 | | 1 | | | | 6.004 | | 1 |
| 1-*sec.*-Butyl-4-*tert.*-butylbenzene | 0.614 | 6.004 | | 1 | | | | 6.004 | | 1 |
| 1-Methyl-2-*n*-heptylbenzene | 0.642 | 6.714 | | 1 | | | | 6.714 | | 1 |
| 1-Methyl-4-*n*-heptylbenzene | 0.611 | 6.728 | | 1 | | | | 6.728 | | 1 |
| 1-Ethyl-2-*n*-hexylbenzene | 0.642 | 6.547 | | 1 | | | | 6.547 | | 1 |
| 1-Ethyl-4-*n*-hexylbenzene | 0.611 | 6.664 | | 1 | | | | 6.664 | | 1 |
| 1-*n*-Propyl-2-*n*-pentylbenzene | 0.642 | 6.418 | | 1 | | | | 6.418 | | 1 |
| 1-*n*-Propyl-4-*n*-pentylbenzene | 0.611 | 6.653 | | 1 | | | | 6.653 | | 1 |
| *n*-Nonylbenzene | 0.578 | 7.212 | | 1 | | | | 7.212 | | 1 |
| 1-Methyl-2-*n*-octylbenzene | 0.640 | 7.209 | | 1 | | | | 7.209 | | 1 |
| 1-Ethyl-2-*n*-heptylbenzene | 0.637 | 7.040 | | 1 | | | | 7.040 | | 1 |
| 1-*n*-Propyl-2-*n*-hexylbenzene | 0.637 | 6.892 | | 1 | | | | 6.892 | | 1 |
| 1-*n*-Butyl-2-*n*-pentylbenzene | 0.637 | 6.862 | | 1 | | | | 6.862 | | 1 |
| 1-Methyl-3,5-di-*tert.*-butylbenzene | 0.616 | 7.099 | | 1 | | | | 7.099 | | 1 |
| 1,3,5-Triisopropylbenzene | 0.627 | 5.999 | 0.011 | 3 | 6.104 | | 1 | 6.025 | 0.053 | 4 |
| *n*-Decylbenzene | 0.579 | 7.708 | | 1 | | | | 7.708 | | 1 |
| 1-Methyl-2-*n*-nonylbenzene | 0.636 | 7.705 | | 1 | | | | 7.705 | | 1 |
| 1-Ethyl-2-*n*-octylbenzene | 0.635 | 7.532 | | 1 | | | | 7.532 | | 1 |
| 1-*n*-Propyl-2-*n*-heptylbenzene | 0.635 | 7.379 | | 1 | | | | 7.379 | | 1 |
| 1-*n*-Butyl-2-*n*-hexylbenzene | 0.635 | 7.333 | | 1 | | | | 7.333 | | 1 |
| 1,2-Di-*n*-pentylbenzene | 0.635 | 7.317 | | 1 | | | | 7.317 | | 1 |
| 1,2,4,5-Tetraisopropylbenzene | 0.726 | 6.559 | | 1 | | | | 6.559 | | 1 |
| Styrene | 0.849 | 3.865 | 0.002 | 2 | 3.840 | | 1 | 3.856 | 0.014 | 3 |

(*Continued on p. 234*)

TABLE I (*continued*)

| Solute | *R* | Squalane average | S.D. | No. | Siloxane average | S.D. | No. | Overall average | S.D. | No. |
|---|---|---|---|---|---|---|---|---|---|---|
| α-Methylstyrene | 0.847 | 4.300 | 0.004 | 2 | 4.278 | | 1 | 4.292 | 0.013 | 3 |
| *trans*-β-Methylstyrene | 0.913 | 4.486 | 0.018 | 2 | | | | 4.486 | 0.018 | 2 |
| 2-Methylstyrene | 0.915 | 4.358 | 0.005 | 2 | 4.342 | | 1 | 4.352 | 0.010 | 3 |
| 3-Methylstyrene | 0.866 | 4.390 | 0.003 | 2 | 4.346 | | 1 | 4.375 | 0.025 | 3 |
| 4-Methylstyrene | 0.871 | 4.399 | 0.005 | 2 | | | | 4.399 | 0.005 | 2 |
| 2,4-Dimethylstyrene | 0.913 | 4.913 | 0.001 | 2 | | | | 4.913 | 0.001 | 2 |
| Phenylethyne | 0.679 | 3.692 | 0.005 | 2 | | | | 3.692 | 0.005 | 2 |
| Allylbenzene | 0.717 | 4.126 | 0.003 | 2 | 4.157 | | 1 | 4.136 | 0.018 | 3 |
| Naphthalene | 1.340 | 5.160 | 0.004 | 3 | 5.163 | 0.001 | 2 | 5.161 | 0.003 | 5 |
| 1-Methylnaphthalene | 1.344 | 5.756 | 0.007 | 2 | 5.821 | 0.082 | 2 | 5.789 | 0.061 | 4 |
| 2-Methylnaphthalene | 1.304 | 5.774 | 0.001 | 2 | 5.768 | 0.095 | 2 | 5.771 | 0.055 | 4 |
| 1,2-Dimethylnaphthalene | 1.431 | | | | 6.398 | | 1 | 6.398 | | 1 |
| 1,3-Dimethylnaphthalene | 1.387 | | | | 6.326 | | 1 | 6.326 | | 1 |
| 1,4-Dimethylnaphthalene | 1.400 | | | | 6.339 | | 1 | 6.339 | | 1 |
| 1,5-Dimethylnaphthalene | 1.369 | | | | 6.447 | | 1 | 6.447 | | 1 |
| 1,6-Dimethylnaphthalene | 1.369 | | | | 6.280 | | 1 | 6.280 | | 1 |
| 1,7-Dimethylnaphthalene | 1.369 | | | | 6.264 | | 1 | 6.264 | | 1 |
| 1,8-Dimethylnaphthalene | 1.400 | | | | 6.496 | | 1 | 6.529 | 0.047 | 2 |
| 2,3-Dimethylnaphthalene | 1.431 | | | | 6.291 | 0.062 | 2 | 6.291 | 0.062 | 2 |
| 2,6-Dimethylnaphthalene | 1.329 | | | | 6.226 | 0.024 | 2 | 6.226 | 0.024 | 2 |
| 2,7-Dimethylnaphthalene | 1.329 | | | | 6.228 | | 1 | 6.228 | | 1 |
| 2-Ethylnaphthalene | 1.371 | | | | 6.140 | | 1 | 6.140 | | 1 |
| 2,3,6-Trimethylnaphthalene | 1.429 | | | | 6.856 | | 1 | 6.856 | | 1 |
| 1-Allylnaphthalene | 1.474 | | | | 6.556 | | 1 | 6.556 | | 1 |
| Tetrahydronaphthalene | 0.891 | 5.183 | 0.005 | 3 | 5.234 | 0.037 | 2 | 5.203 | 0.034 | 5 |
| 1,2-Dihydronaphthalene | 1.093 | 5.119 | 0.004 | 2 | 5.151 | | 1 | 5.130 | 0.019 | 3 |
| Indene | 1.001 | 4.546 | 0.001 | 2 | 4.572 | 0.018 | 2 | 4.559 | 0.018 | 4 |
| 1-Methylindene | 0.980 | 4.737 | 0.018 | 2 | | | | 4.737 | 0.018 | 2 |
| 2-Methylindene | 1.123 | 4.735 | 0.002 | 2 | | | | 4.735 | 0.002 | 2 |
| 3-Methylindene | 1.123 | 5.041 | 0.004 | 2 | | | | 5.041 | 0.004 | 2 |
| 5-Ethylindene | 1.000 | 5.498 | | 1 | | | | 5.498 | | 1 |
| Indane | 0.829 | 4.574 | 0.003 | 3 | 4.614 | 0.013 | 2 | 4.590 | 0.023 | 5 |
| 1-Methylindane | 0.804 | 4.823 | | 1 | | | | 4.823 | | 1 |
| 2-Methylindane | 0.694 | 4.812 | | 1 | | | | 4.812 | | 1 |
| 4-Methylindane | 0.820 | 5.138 | | 1 | | | | 5.138 | | 1 |
| 5-Methylindane | 0.820 | 5.103 | | 1 | | | | 5.103 | | 1 |
| 1,2-Dimethylindane | 0.820 | 5.155 | 0.003 | 2 | | | | 5.155 | 0.003 | 2 |

Of the 190 log $L^{16}$ values in Table I, about 60 are averages of three or more values, and can be regarded as reasonably precise. The remaining values could be expected to alter slightly if further data were forthcoming, but we believe such alteration would be minimal.

In these back-calculations of log $L^{16}$, standard known values of log $L^{16}$ are available, either from previous determinations as shown in Table II or from the *n*-alkanes used to obtain the *I* values. However, if we wish to use eqn. 2 to back-calculate $\pi_2^H$ values, it is essential to have a reasonable number of values already available as standards. We therefore set up a number of regression equations using data that included aromatic hydrocarbons together with a variety of other solutes of known [1] $\pi_2^H$ values. We used the results of Langer and coworkers [21,22] on polyaromatic hydrocarbons [21] and dialkyl tetrachlorophthalate esters [22], and also several other series [19,23,24].

TABLE II

COMPARISON OF OVERALL AVERAGE LOG $L^{16}$ VALUES IN TABLE I WITH DIRECTLY DETERMINED VALUES

| Solute | Table I | Direct values[a] |
|---|---|---|
| Benzene | 2.786 | 2.803 |
| Toluene | 3.325 | 3.344 |
| *o*-Xylene | 3.939 | 3.937 |
| *m*-Xylene | 3.839 | 3.864 |
| *p*-Xylene | 3.839 | 3.858 |
| *n*-Propylbenzene | 4.230 | 4.221 |

[a] Ref. 7.

Results of these preliminary regressions are given in Table III. A typical equation, using Langer and Purnell's [21] results on 7,8-benzoquinoline at 110°C is given as

$$\log V_G^0 = -0.582 + 1.119\,\pi_2^H + 0.622 \log L^{16} \quad (7)$$

$$n = 30, \quad R = 0.9980, \quad \text{S.D.} = 0.029$$

We can estimate the expected error in back-calculated $\pi_2^H$ values as S.D./$s$, i.e. 0.029/1.119 = 0.026 units. For the seventeen solutes listed in Table III, the average of the S.D. ($\pi_2^H$) values is 0.012 units.

We can now use these seventeen aromatic solutes as standards to construct final equations for the back-calculation of $\pi_2^H$, using polar phases where the $s$ constant is large. As we have seen, the magnitude of $s$ is not the only factor that determines the expected error in $\pi_2^H$, and we have restricted our analysis to equations in which S.D./$s$ is $\leqslant 0.02$ units. Most of our final equations relate to Carbowaxes at various temperatures [14–16,25,26] or to a variety of dialkyltetrachloro- or -tetrabromophthalates [26–28], but a number of other phases [29–33] were also used. A typical equation is for the 35 aromatic solutes on di-*n*-propyl tetrachlorophthalate at 90°C [26], where, with no omissions, we find for log $t$ relative to *n*-propylbenzene

$$\log t(\text{rel}) = -3.433 + 1.640\,\pi_2^H + 0.618 \log L^{16} \quad (8)$$

$$n = 35, \quad R = 0.9986, \quad \text{S.D.} = 0.018$$

Although eqn. 8 is suitable for the calculation of $\pi_2^H$ values, with S.D./$s$ = 0.011 units, it is of course unsuitable as a general solvation equation because of the limited range of the explanatory variables.

TABLE III

PRELIMINARY CALCULATIONS OF $\pi_2^H$

| Solute | Overall average | S.D. | No. |
|---|---|---|---|
| Benzene | 0.515 | 0.011 | 16 |
| Toluene | 0.514 | 0.010 | 16 |
| Ethylbenzene | 0.511 | 0.012 | 16 |
| *o*-Xylene | 0.559 | 0.007 | 16 |
| *m*-Xylene | 0.519 | 0.010 | 16 |
| *p*-Xylene | 0.515 | 0.013 | 16 |
| *n*-Propylbenzene | 0.496 | 0.012 | 13 |
| Isopropylbenzene | 0.488 | 0.017 | 14 |
| 1,2,3-Trimethylbenzene | 0.610 | 0.019 | 15 |
| 1,2,4-Trimethylbenzene | 0.552 | 0.012 | 16 |
| 1,3,5-Trimethylbenzene | 0.505 | 0.027 | 13 |
| 2-Ethyltoluene | 0.546 | 0.007 | 12 |
| 3-Ethyltoluene | 0.500 | 0.016 | 12 |
| 4-Ethyltoluene | 0.499 | 0.005 | 12 |
| *n*-Butylbenzene | 0.493 | 0.009 | 12 |
| *tert.*-Butylbenzene | 0.475 | 0.016 | 12 |

Our final set of 123 calculated $\pi_2^H$ values is given in Table IV, together with the number of equations used, the standard deviation in $\pi_2^H$, and the maximum and minimum values of $\pi_2^H$ obtained as a result of the back-calculations. We also list the maximum deviation (Max − Min) and in the final column give the $\pi_2^H$ value we select. For a few cases, shown in parentheses, the selected value is not exactly the same as the calculated value. We shall deal with these later. These most recent values of $\pi_2^H$ in Table IV are in good agreement with those we have listed previously [1], although in a few instances, *e.g.*, *o*-xylene and 1,2,3-trimethylbenzene, our new values are higher than the old values. Where there are differences, the new values are to be preferred.

In general, the back-calculation method works very well. For the solutes where the number of equations used is two or more, the S.D. in $\pi_2^H$ averages out to 0.009, and the average value of Max − Min is 0.024 units. We can therefore claim that the final $\pi_2^H$ values are precise to *ca.* 0.01 unit. However, such precision disguises the fact that any individual determination may be subject to much larger errors. Thus, for the typical case of *n*-propylbenzene, the spread of results ranges from 0.511 to 0.483 units, and in the atypical case of benzene from 0.547 to 0.495 units. We therefore suggest that

TABLE IV

CALCULATED VALUES OF $\pi_2^H$

| Solute | No. | Average | S.D. | Max | Min | Max − Min | Taken value |
|---|---|---|---|---|---|---|---|
| Benzene | 26 | 0.520 | 0.014 | 0.547 | 0.495 | 0.052 | 0.52 |
| Toluene | 26 | 0.520 | 0.008 | 0.533 | 0.503 | 0.030 | 0.52 |
| Ethylbenzene | 26 | 0.511 | 0.007 | 0.527 | 0.501 | 0.026 | 0.51 |
| *o*-Xylene | 25 | 0.565 | 0.011 | 0.585 | 0.542 | 0.043 | 0.56 |
| *m*-Xylene | 25 | 0.523 | 0.006 | 0.535 | 0.515 | 0.020 | 0.52 |
| *p*-Xylene | 25 | 0.521 | 0.016 | 0.551 | 0.503 | 0.048 | 0.52 |
| *n*-Propylbenzene | 26 | 0.500 | 0.008 | 0.511 | 0.483 | 0.028 | 0.50 |
| Isopropylbenzene | 26 | 0.487 | 0.011 | 0.515 | 0.465 | 0.050 | 0.49 |
| 1,2,3-Trimethylbenzene | 21 | 0.613 | 0.011 | 0.633 | 0.591 | 0.042 | 0.61 |
| 1,2,4-Trimethylbenzene | 24 | 0.563 | 0.011 | 0.588 | 0.548 | 0.040 | 0.56 |
| 1,3,5-Trimethylbenzene | 25 | 0.520 | 0.012 | 0.536 | 0.489 | 0.047 | 0.52 |
| 2-Ethyltoluene | 22 | 0.553 | 0.007 | 0.563 | 0.536 | 0.027 | 0.55 |
| 3-Ethyltoluene | 22 | 0.510 | 0.012 | 0.527 | 0.490 | 0.037 | 0.51 |
| 4-Ethyltoluene | 21 | 0.509 | 0.006 | 0.518 | 0.499 | 0.019 | 0.51 |
| *n*-Butylbenzene | 26 | 0.505 | 0.011 | 0.521 | 0.484 | 0.037 | 0.51 |
| Isobutylbenzene | 15 | 0.471 | 0.010 | 0.495 | 0.456 | 0.039 | 0.47 |
| *sec.*-Butylbenzene | 17 | 0.480 | 0.004 | 0.488 | 0.471 | 0.017 | 0.48 |
| *tert.*-Butylbenzene | 16 | 0.489 | 0.007 | 0.500 | 0.473 | 0.027 | 0.49 |
| 1,2-Diethylbenzene | 15 | 0.540 | 0.009 | 0.549 | 0.527 | 0.022 | 0.54 |
| 1,3-Diethylbenzene | 16 | 0.506 | 0.009 | 0.522 | 0.487 | 0.035 | 0.50 |
| 1,4-Diethylbenzene | 16 | 0.505 | 0.009 | 0.516 | 0.488 | 0.028 | 0.50 |
| 1,2,4,5-Tetramethylbenzene | 17 | 0.604 | 0.013 | 0.625 | 0.584 | 0.041 | 0.60 |
| 1,2,3,5-Tetramethylbenzene | 17 | 0.610 | 0.010 | 0.629 | 0.592 | 0.037 | 0.61 |
| 1,2,3,4-Tetramethylbenzene | 17 | 0.656 | 0.018 | 0.685 | 0.623 | 0.062 | 0.65 |
| 2-*n*-Propyltoluene | 14 | 0.541 | 0.006 | 0.547 | 0.525 | 0.022 | 0.54 |
| 3-*n*-Propyltoluene | 10 | 0.505 | 0.003 | 0.509 | 0.499 | 0.010 | 0.50 |
| 4-*n*-Propyltoluene | 16 | 0.503 | 0.004 | 0.515 | 0.499 | 0.016 | 0.50 |
| 2-Isopropyltoluene | 10 | 0.529 | 0.012 | 0.536 | 0.498 | 0.038 | 0.53 |
| 3-Isopropyltoluene | 14 | 0.497 | 0.007 | 0.512 | 0.485 | 0.027 | 0.49 |
| 4-Isopropyltoluene | 12 | 0.490 | 0.009 | 0.509 | 0.474 | 0.035 | 0.49 |
| 1,2-Dimethyl-3-ethylbenzene | 10 | 0.607 | 0.008 | 0.615 | 0.594 | 0.021 | 0.61 |
| 1,2-Dimethyl-4-ethylbenzene | 16 | 0.558 | 0.010 | 0.579 | 0.542 | 0.037 | 0.56 |
| 1,3-Dimethyl-2-ethylbenzene | 8 | 0.596 | 0.006 | 0.606 | 0.587 | 0.019 | 0.60 |
| 1,3-Dimethyl-4-ethylbenzene | 16 | 0.554 | 0.006 | 0.563 | 0.543 | 0.020 | 0.55 |
| 1,3-Dimethyl-5-ethylbenzene | 12 | 0.517 | 0.013 | 0.530 | 0.490 | 0.040 | 0.52 |
| 1,4-Dimethyl-2-ethylbenzene | 16 | 0.553 | 0.008 | 0.572 | 0.537 | 0.035 | 0.55 |
| *n*-Pentylbenzene | 9 | 0.508 | 0.013 | 0.533 | 0.489 | 0.044 | 0.51 |
| Isopentylbenzene | 3 | 0.501 | 0.000 | 0.501 | 0.501 | 0.000 | 0.50 |
| *sec.*-Pentylbenzene | 1 | 0.467 | | | | | 0.48 |
| *tert.*-Pentylbenzene | 5 | 0.492 | 0.009 | 0.509 | 0.486 | 0.023 | 0.49 |
| Pentamethylbenzene | 6 | 0.662 | 0.013 | 0.681 | 0.650 | 0.031 | 0.66 |
| 2-*n*-Butyltoluene | 1 | 0.512 | | | | | (0.54) |
| 4-*n*-Butyltoluene | 3 | 0.498 | 0.002 | 0.500 | 0.496 | 0.004 | 0.50 |
| 3-*tert.*-Butyltoluene | 1 | 0.500 | | | | | 0.50 |
| 4-*tert.*-Butyltoluene | 2 | 0.495 | 0.001 | 0.496 | 0.494 | 0.002 | 0.50 |
| 1-Ethyl-2-*n*-propylbenzene | 1 | 0.546 | | | | | (0.53) |
| 1-Ethyl-4-*n*-propylbenzene | 3 | 0.491 | 0.003 | 0.494 | 0.488 | 0.006 | 0.49 |
| 1,3-Diethyl-5-methylbenzene | 1 | 0.542 | | | | | 0.52 |
| *n*-Hexylbenzene | 5 | 0.502 | 0.010 | 0.513 | 0.491 | 0.022 | 0.50 |
| 1-Methyl-2-*n*-pentylbenzene | 1 | 0.536 | | | | | 0.54 |
| 1-Methyl-4-*n*-pentylbenzene | 3 | 0.500 | 0.004 | 0.503 | 0.495 | 0.008 | 0.50 |
| 1-Ethyl-2-*n*-butylbenzene | 1 | 0.535 | | | | | 0.53 |

TABLE IV (*continued*)

| Solute | No. | Average | S.D. | Max | Min | Max − Min | Taken value |
|---|---|---|---|---|---|---|---|
| 1-Ethyl-4-*n*-butylbenzene | 3 | 0.489 | 0.004 | 0.492 | 0.485 | 0.007 | 0.49 |
| 1,2-Di-*n*-propylbenzene | 1 | 0.528 | | | | | 0.53 |
| 1,3-Diisopropylbenzene | 2 | 0.460 | 0.017 | 0.472 | 0.448 | 0.024 | (0.48) |
| 1,4-Diisopropylbenzene | 6 | 0.476 | 0.015 | 0.503 | 0.459 | 0.044 | 0.47 |
| 1-*n*-Propyl-4-isopropylbenzene | 3 | 0.470 | 0.007 | 0.474 | 0.462 | 0.012 | 0.47 |
| 1,3-Dimethyl-5-*tert*.-butylbenzene | 2 | 0.513 | 0.028 | 0.532 | 0.493 | 0.039 | 0.51 |
| 1,3,5-Triethylbenzene | 2 | 0.501 | 0.013 | 0.510 | 0.492 | 0.018 | 0.50 |
| Hexamethylbenzene | 4 | 0.719 | 0.009 | 0.726 | 0.707 | 0.019 | 0.72 |
| *n*-Heptylbenzene | 1 | 0.484 | | | | | 0.48 |
| 1-Methyl-2-*n*-hexylbenzene | 1 | 0.529 | | | | | 0.53 |
| 1-Methyl-4-*n*-hexylbenzene | 3 | 0.502 | 0.007 | 0.506 | 0.494 | 0.012 | 0.50 |
| 1-Ethyl-2-*n*-pentylbenzene | 1 | 0.529 | | | | | 0.53 |
| 1-Ethyl-4-*n*-pentylbenzene | 3 | 0.493 | 0.007 | 0.497 | 0.485 | 0.012 | 0.49 |
| 1-*n*-Propyl-2-*n*-butylbenzene | 1 | 0.510 | | | | | 0.51 |
| 1-*n*-Propyl-4-*n*-butylbenzene | 3 | 0.481 | 0.009 | 0.488 | 0.470 | 0.018 | 0.49 |
| *n*-Octylbenzene | 1 | 0.482 | | | | | 0.48 |
| 1-Methyl-2-*n*-heptylbenzene | 1 | 0.522 | | | | | 0.52 |
| 1-Methyl-4-*n*-heptylbenzene | 2 | 0.504 | 0.005 | 0.507 | 0.500 | 0.007 | 0.50 |
| 1-Ethyl-2-*n*-hexylbenzene | 1 | 0.520 | | | | | 0.52 |
| 1-Ethyl-4-*n*-hexylbenzene | 3 | 0.489 | 0.007 | 0.497 | 0.484 | 0.013 | 0.49 |
| 1-*n*-Propyl-2-*n*-pentylbenzene | 1 | 0.502 | | | | | 0.50 |
| 1-*n*-Propyl-4-*n*-pentylbenzene | 3 | 0.444 | 0.007 | 0.449 | 0.436 | 0.013 | (0.48) |
| 1,2-Di-*n*-butylbenzene | 1 | 0.518 | | | | | (0.50) |
| 1,4-Di-*n*-butylbenzene | 3 | 0.479 | 0.009 | 0.485 | 0.468 | 0.017 | 0.48 |
| 1,4-Diisobutylbenzene | 3 | 0.414 | 0.014 | 0.427 | 0.400 | 0.027 | 0.41 |
| 1,4-Di-*sec*.-butylbenzene | 3 | 0.432 | 0.010 | 0.440 | 0.421 | 0.019 | 0.43 |
| 1,4-Di-*tert*.-butylbenzene | 3 | 0.439 | 0.004 | 0.443 | 0.435 | 0.008 | 0.44 |
| 1-*n*-Butyl-4-isobutylbenzene | 3 | 0.444 | 0.011 | 0.452 | 0.431 | 0.021 | 0.44 |
| 1-*n*-Butyl-4-*sec*.-butylbenzene | 3 | 0.456 | 0.011 | 0.464 | 0.443 | 0.021 | 0.46 |
| 1-*n*-Butyl-4-*tert*.-butylbenzene | 3 | 0.456 | 0.006 | 0.462 | 0.450 | 0.012 | 0.46 |
| 1-Isobutyl-4-*sec*.-butylbenzene | 3 | 0.420 | 0.015 | 0.433 | 0.404 | 0.029 | 0.42 |
| 1-Isobutyl-4-*tert*.-butylbenzene | 3 | 0.424 | 0.010 | 0.433 | 0.413 | 0.020 | 0.42 |
| 1-*sec*.-Butyl-4-*tert*.-butylbenzene | 3 | 0.439 | 0.010 | 0.445 | 0.427 | 0.010 | 0.44 |
| *n*-Nonylbenzene | 1 | 0.477 | | | | | 0.48 |
| 1-Methyl-2-*n*-octylbenzene | 1 | 0.520 | | | | | 0.52 |
| 1-Ethyl-2-*n*-heptylbenzene | 1 | 0.520 | | | | | 0.52 |
| 1-*n*-Propyl-2-*n*-hexylbenzene | 1 | 0.498 | | | | | 0.50 |
| 1-*n*-Butyl-2-*n*-pentylbenzene | 1 | 0.501 | | | | | 0.50 |
| 1-Methyl-3,5-di-*sec*.-butylbenzene | 3 | 0.471 | 0.007 | 0.475 | 0.463 | 0.012 | 0.47 |
| 1,3,5-Triisopropylbenzene | 1 | 0.398 | | | | | 0.40 |
| *n*-Decylbenzene | 1 | 0.469 | | | | | 0.47 |
| 1-Methyl-2-*n*-nonylbenzene | 1 | 0.509 | | | | | 0.51 |
| 1-Ethyl-2-*n*-octylbenzene | 1 | 0.509 | | | | | 0.51 |
| 1-*n*-Propyl-2-*n*-heptylbenzene | 1 | 0.492 | | | | | 0.49 |
| 1-*n*-Butyl-2-*n*-hexylbenzene | 1 | 0.493 | | | | | 0.49 |
| 1,2-Di-*n*-pentylbenzene | 1 | 0.496 | | | | | 0.49 |
| 1,2,4,5-Tetraisopropylbenzene | 3 | 0.394 | 0.029 | 0.417 | 0.362 | 0.055 | 0.39 |
| Styrene | 7 | 0.649 | 0.011 | 0.674 | 0.642 | 0.032 | 0.65 |
| α-Methylstyrene | 2 | 0.643 | 0.014 | 0.653 | 0.633 | 0.020 | 0.64 |
| *trans*-β-Methylstyrene | 1 | 0.721 | | | | | 0.72 |
| Allylbenzene | 1 | 0.596 | | | | | 0.60 |
| Naphthalene | 6 | 0.917 | 0.018 | 0.937 | 0.885 | 0.052 | 0.92 |
| 1-Methylnaphthalene | 3 | 0.895 | 0.006 | 0.899 | 0.889 | 0.010 | 0.90 |

(*Continued on p. 238*)

TABLE IV (*continued*)

| Solute | No. | Average | S.D. | Max | Min | Max − Min | Taken value |
|---|---|---|---|---|---|---|---|
| 2-Methylnaphthalene | 3 | 0.881 | 0.001 | 0.882 | 0.880 | 0.002 | 0.88 |
| 1,2-Dimethylnaphthalene | 2 | 0.920 | 0.004 | 0.923 | 0.917 | 0.005 | 0.92 |
| 1,3-Dimethylnaphthalene | 2 | 0.921 | 0.001 | 0.922 | 0.920 | 0.002 | 0.92 |
| 1,4-Dimethylnaphthalene | 2 | 0.906 | 0.004 | 0.909 | 0.903 | 0.006 | 0.91 |
| 1,5-Dimethylnaphthalene | 2 | 0.871 | 0.003 | 0.873 | 0.869 | 0.004 | 0.87 |
| 1,6-Dimethylnaphthalene | 3 | 0.912 | 0.005 | 0.916 | 0.907 | 0.009 | 0.91 |
| 1,7-Dimethylnaphthalene | 2 | 0.894 | 0.004 | 0.896 | 0.891 | 0.005 | 0.89 |
| 1,8-Dimethylnaphthalene | 2 | 0.909 | 0.001 | 0.910 | 0.908 | 0.002 | 0.91 |
| 2,3-Dimethylnaphthalene | 3 | 0.945 | 0.009 | 0.953 | 0.935 | 0.018 | 0.94 |
| 2,6-Dimethylnaphthalene | 3 | 0.911 | 0.003 | 0.914 | 0.908 | 0.006 | 0.91 |
| 2,7-Dimethylnaphthalene | 2 | 0.911 | 0.001 | 0.911 | 0.910 | 0.001 | 0.91 |
| Tetrahydronaphthalene | 6 | 0.646 | 0.047 | 0.699 | 0.591 | 0.108 | 0.65 |
| Indene | 1 | 0.768 | | | | | 0.77 |
| Indane | 7 | 0.624 | 0.031 | 0.656 | 0.579 | 0.077 | 0.62 |
| 1-Methylindane | 3 | 0.621 | 0.004 | 0.625 | 0.618 | 0.007 | 0.62 |
| 2-Methylindane | 3 | 0.603 | 0.002 | 0.604 | 0.600 | 0.004 | 0.60 |
| 4-Methylindane | 3 | 0.671 | 0.009 | 0.680 | 0.663 | 0.017 | 0.67 |
| 5-Methylindane | 3 | 0.644 | 0.006 | 0.650 | 0.639 | 0.011 | 0.64 |

whenever possible, back-calculated solvation parameters are obtained from several equations and not just one.

We have just enough results in Table IV to reach a number of general conclusions as to structural effects on $\pi_2^H$. The effect of chain length of alkyl groups is very small. Thus, from benzene to *n*-hexylbenzene, $\pi_2^H$ decreases from 0.52 to 0.50 units. Beyond this, we have only one determination for each *n*-alkylbenzene and so we cannot make any definitive comment; even so, reduction of $\pi_2^H$ to 0.47 in the case of *n*-decylbenzene does show that after the first one or two members in any homologous series $\pi_2^H$ is approximately constant.

A much greater variation in $\pi_2^H$ is shown by positional isomers. In general, *o*-dialkyl groups have $\pi_2^H$ about 0.035 units larger than the corresponding *m*- or *p*-dialkyl groups. This seems to extend to any di-*n*-alkyl-substituted benzene, and probably also to di-*sec*.-alkylbenzenes, although unfortunately lack of data prevents any discussion of the *tert*.-alkyl substituents. The tri- and tetramethylbenzenes follow this trend almost exactly, and even pentamethylbenzene ($\pi_2^H$ = 0.66, calc. 0.66) and hexamethylbenzene ($\pi_2^H$ = 0.72, calc. 0.73) obey the rule when the number of *ortho* interactions is taken as four and six, respectively.

However, values of $\pi_2^H$ for tri- and tetrasubstituted benzenes involving *sec*.-alkyl or *tert*.-alkyl groups are appreciably less than calculated using the 0.035 unit rule for *ortho* groups. Thus, 1,2,4,5-tetramethylbenzene ($\pi_2^H$ = 0.60, calc. 0.59) shows the predicted elevation of $\pi_2^H$, but we find that 1,2,4,5-tetraisopropylbenzene has a lower $\pi_2^H$ value than benzene itself, *viz*., 0.39 units only. Clearly, more than one factor is at work with these complicated substituted benzenes.

For the simpler benzene derivatives, the very regular pattern of $\pi_2^H$ enables us to identify outliers to the general trend. These are solutes where our suggested value in Table IV is in parentheses and is significantly different to the determined value. Thus, in the series of 1-methyl-2-*n*-alkylbenzenes we have for the variation of the 2-*n*-alkyl group, methyl 0.56, ethyl 0.55, *n*-propyl 0.54, *n*-butyl 0.51, *n*-pentyl 0.54 and *n*-hexyl 0.53. Clearly, the value of 0.51 for 1-methyl-2-*n*-butylbenzene is too low, and we suggest in Table IV a value of 0.54 units. There are a few other cases shown in Table IV where similar reasoning leads to alternative suggested values.

We have listed in Table I the $R_2$ and $\log L^{16}$ values for alkyl aromatics and in Table IV the new $\pi_2^H$ values that we have calculated. As $\alpha_2^H$ is zero for the solutes that we are considering, the only remaining

TABLE V

VALUES OF $\beta_2^H$ FOR AROMATIC HYDROCARBONS

| Solute | A[a] | B[b] | C[c] | D[d] | Taken |
|---|---|---|---|---|---|
| Benzene | 0.15 | 0.15 | 0.13 | 0.15 | 0.14 |
| Toluene | 0.14 | 0.12 | 0.14 | 0.15 | 0.14 |
| Ethylbenzene | 0.15 | 0.14 | 0.15 | 0.17 | 0.15 |
| *n*-Propylbenzene | | 0.13 | 0.16 | 0.18 | 0.15 |
| *n*-Butylbenzene | | 0.11 | 0.16 | 0.18 | 0.15 |
| Isobutylbenzene | | | 0.10 | 0.16 | 0.15 |
| *n*-Pentylbenzene | | 0.07 | 0.17 | 0.18 | 0.15 |
| *n*-Hexylbenzene | | 0.04 | 0.17 | 0.18 | 0.15 |
| *n*-Octylbenzene | | 0.10 | | | 0.15 |
| *n*-Decylbenzene | | 0.09 | | | 0.15 |
| *n*-Dodecylbenzene | 0.17 | | | | 0.15 |
| Isopropylbenzene | 0.16 | 0.14 | 0.16 | 0.21 | 0.16 |
| *sec.*-Butylbenzene | | | 0.17 | 0.23 | 0.16 |
| *tert.*-Butylbenzene | 0.15 | 0.16 | 0.18 | 0.27 | 0.16 |
| *o*-Xylene | 0.16 | 0.15 | 0.16 | 0.16 | 0.16 |
| *m*-Xylene | 0.18 | 0.13 | 0.15 | 0.16 | 0.16 |
| *p*-Xylene | 0.18 | 0.14 | 0.16 | 0.16 | 0.16 |
| 2-Ethyltoluene | | 0.18 | 0.21 | 0.23 | 0.18 |
| 4-Ethyltoluene | | 0.15 | 0.22 | 0.24 | 0.18 |
| 4-Isopropyltoluene | | 0.16 | 0.22 | 0.30 | 0.19 |
| 1,2,3-Trimethylbenzene | | 0.16 | 0.20 | 0.20 | 0.19 |
| 1,2,4-Trimethylbenzene | | 0.15 | 0.18 | 0.18 | 0.19 |
| 1,3,5-Trimethylbenzene | 0.20 | 0.21 | 0.21 | 0.22 | 0.19 |
| 1,2,4,5-Tetramethylbenzene | 0.20 | 0.16 | | | 0.19 |
| 1,2,3,5-Tetramethylbenzene | 0.17 | 0.16 | | | 0.19 |
| 1,2,3,4-Tetramethylbenzene | | 0.18 | | | 0.19 |
| Pentamethylbenzene | 0.20 | 0.17 | | | 0.20 |
| Hexamethylbenzene | 0.22 | 0.26 | | | 0.21 |
| Indane | | 0.13 | 0.21 | 0.15 | 0.16 |
| Indene | | 0.20 | | | 0.18 |
| Styrene | 0.18 | 0.13 | 0.14 | 0.20 | 0.18 |
| α-Methylstyrene | 0.15 | 0.19 | 0.17 | 0.24 | 0.18 |
| Biphenyl | 0.20 | 0.24 | 0.18 | 0.24 | 0.20 |
| Naphthalene | 0.21 | 0.19 | 0.16 | 0.21 | 0.20 |
| 1-Methylnaphthalene | 0.22 | 0.19 | 0.20 | 0.22 | 0.20 |
| 2-Methylnaphthalene | 0.23 | 0.15 | | | 0.20 |
| 1,2-Dimethylnaphthalene | | 0.21 | | | 0.20 |
| 1,3-Dimethylnaphthalene | | 0.18 | | | 0.20 |
| 1,4-Dimethylnaphthalene | | 0.19 | | | 0.20 |
| 1,5-Dimethylnaphthalene | | 0.19 | | | 0.20 |
| 1,7-Dimethylnaphthalene | | 0.17 | | | 0.20 |
| 2,3-Dimethylnaphthalene | 0.22 | 0.19 | | | 0.20 |
| 2,6-Dimethylnaphthalene | 0.22 | 0.20 | | | 0.20 |
| 2-Ethylnaphthalene | | 0.19 | | | 0.20 |
| Allylbenzene | | 0.22 | | | 0.22 |
| Phenylethyne | | 0.25 | | | 0.24 |

[a] Values from 1:1 complexation constants in tetrachloromethane [35].
[b] From a regression of water–octanol partition coefficients for aromatics [34].
[c] From a regression of air–water partition coefficients, all solutes [34].
[d] From a regression of water–hexadecane partition coefficients, all solutes [34].

solvation parameter is $\beta_2^H$. We have listed already [1] a number of $\beta_2^H$ values for alkyl aromatics, either obtained by the back-calculation method [34] or deduced from the 1:1 complexation constants for hydrogen bonding in carbon tetrachloride as set out in detail before [35]. We can extend and update this list, as shown in Table V, where we have enough $\beta_2^H$ values to predict a number of outstanding values with some confidence. In Table V the solutes are ordered by the increasing number of alkyl substituents, to show the regular increase in $\beta_2^H$. Using values in Table V that have been determined, we can deduce that any *n*-dialkylbenzene will have a $\beta_2^H$ of 0.18 and any *n*-trialkylbenzene a value of 0.19 units: the only possible exceptions are compounds with di-*tert.*-butyl groups, for which we have no data. The results in Table V now complete the entire set of solvation parameters for about 120 alkyl aromatic solutes, and so greatly extend the scope of application of the general solvation eqn. 1.

Finally, we discuss briefly the effects of structure on the solvation parameters. As found before [1], branching in an alkyl chain always results in a decrease in log $L^{16}$. Oddly enough, polysubstituted isomers always have a larger log $L^{16}$ value than does the monosubstituted isomer, *e.g.*, the trimethylbenzenes all have larger log $L^{16}$ values than *n*-propylbenzene. However, there is little that is exceptional with the values of log $L^{16}$ in Table I. The $\beta_2^H$ values (or more correctly the $\Sigma\beta_2^H$ values) in Table V are also unexceptional; increasing alkyl substitution in the benzene ring slightly increases the hydrogen-bond basicity, as expected from the small negative Hammett $\sigma$ constants for alkyl groups. However, structural effects on the polarizability parameter $\pi_2^H$ are not easily interpreted, especially the marked increase in $\pi_2^H$ with *ortho*-alkyl groups. It is well known that *ortho*-methyl groups in the benzene ring suffer restricted rotation, as shown by thermodynamic [36] and spectroscopic evidence [37], including $^{13}C$ NMR studies [38], but why this should lead to an increase in polarizability is not clear. Baudour and Sanquer [39] have suggested that in 1,2,4,5-tetramethylbenzene the two sets of *ortho*-methyl groups are "wagging" above and below the plate of the benzene ring. This could possibly give rise to a local or instantaneous dipole moment that could lead to increased polarizability. What our results do show, however, is that it is very difficult to predict values of $\pi_2^H$ for new systems, and that for the time being they must be based on experimental results.

REFERENCES


1 M. H. Abraham, G. S. Whiting, R. M. Doherty and W. J. Shuely, *J. Chromatogr.*, 587 (1991) 213.
2 M. H. Abraham, G. S. Whiting, R. M. Doherty and W. J. Shuely, *J. Chromatogr.*, 587 (1991) 229.
3 M. H. Abraham, G. S. Whiting, J. Andonian-Haftvan, J. W. Steed and J. W. Grate, *J. Chromatogr.*, 588 (1991) 361.
4 M. H. Abraham, G. S. Whiting, R. M. Doherty, W. J. Shuely and P. Sakellariou, *Polymer*, in press.
5 M. H. Abraham, I. Hamerton, J. B. Rose and J. W. Grate, *J. Chem. Soc. Perkin Trans. 2*, (1991) 1417.
6 M. H. Abraham, G. S. Whiting, R. M. Doherty and W. J. Shuely, *J. Chem. Soc., Perkin Trans. 2*, (1990) 1451.
7 M. H. Abraham, P. L. Grellier and R. A. McGill, *J. Chem. Soc., Perkin Trans. 2*, (1987) 797.
8 T.-C. L. Chang and C. Karr, *Anal. Chim. Acta*, 21 (1959) 474.
9 J.-C. Dutoit, *J. Chromatogr.*, 555 (1991) 191.
10 D. Papazova and N. Dimov, *J. Chromatogr.*, 356 (1986) 320.
11 J. Macák, V. Nabivach, P. Buryan and S. Šindler, *J. Chromatogr.*, 234 (1982) 285.
12 L. Soják and J. A. Rijks, *J. Chromatogr.*, 119 (1976) 505.
13 L. Soják, J. Janák and J. A. Rijks, *J. Chromatogr.*, 135 (1977) 71.
14 E. Matisová, *J. Chromatogr.*, 438 (1988) 131.
15 W. Engewald and L. Wennrich, *Chromatographia*, 9 (1976) 540.
16 L. Soják and J. Hrivnak, *Ropa Uhlie*, 11 (1969) 364.
17 V. A. Gerasimento, A. V. Kirelenko and V. M. Nabivach, *J. Chromatogr.*, 208 (1981) 9.
18 E. Matisová, M. Rukríglová, J. Krupčík, E. Kovačičová and Š. Holotík, *J. Chromatogr.*, 455 (1988) 301.
19 A. R. Couper, C. W. P. Crowne and P. G. Farrell, *J. Chromatogr.*, 29 (1967) 1.
20 N. Dimov and E. Matisová, *J. Chromatogr.*, 549 (1991) 325.
21 S. H. Langer and J. H. Purnell, *J. Phys. Chem.*, 67 (1963) 263.
22 S. H. Langer, B. M. Johnson and J. R. Conder, *J. Phys. Chem.*, 72 (1968) 4020.
23 R. Uehori, T. Nagata, K. Kimura, K. Kudo and M. Noda, *J. Chromatogr.*, 411 (1987) 251.
24 O. E. Schupp and J. S. Lewis (Editors), *Compilation of Gas Chromatographic Data* (ASTM Series DS 25A), American Society for Testing and Materials, Philadelphia, 1967.
25 B. Wallaert, *Bull. Soc. Chim. Fr.*, (1971) 1107.
26 H. Miyake, M. Mitooka and T. Matsumoto, *Bull. Chem. Soc. Jpn.*, 38 (1965) 1062.
27 S. H. Langer, C. Zahn and C. Pantazoplos, *J. Chromatogr.*, 3 (1960) 154.
28 M. Ryba, *J. Chromatogr.*, 123 (1976) 327.
29 C. L. Stuckey, *J. Chromatogr. Sci.*, 7 (1969) 179.
30 M. S. Vigdergauz and R. V. Vigalot, *Neftekhimiya*, 11 (1971) 144.
31 L. Soják and M. S. Vigdergauz, *J. Chromatogr.*, 148 (1978) 159.

32 W. Engewald, I. Topolova, N. Petsov and C. Dmitrov, *Chromatographia*, 23 (1987) 561.
33 V. Svob and D. Deur-Siftar, *J. Chromatogr.*, 91 (1974) 677.
34 M. H. Abraham and G. S. Whiting, unpublished results.
35 M. H. Abraham, P. L. Grellier, D. V. Prior, J. J. Morris and P. J. Taylor, *J. Chem. Soc., Perkin Trans. 2*, (1990) 521.
36 K. S. Pitzer and D. W. Scott, *J. Am. Chem. Soc.*, 65 (1943) 803.
37 R. C. Livingstone, D. M. Grant, R. J. Pugmire, K. A. Strong and R. M. Brugger, *J. Chem. Phys.*, 58 (1973) 1438.
38 D. K. Dalling, K. H. Ladner, D. M. Grant and W. R. Woolfenden, *J. Am. Chem. Soc.*, 99 (1977) 7142.
39 J. L. Baudour and M. Sanquer, *Acta Crystallogr., Sect. B*, 30 (1974) 2371.

*Journal of Chromatography*, 594 (1992) 243–251
Elsevier Science Publishers B.V., Amsterdam

CHROM. 23 821

# Preparation and capillary column gas chromatographic characterization of aza-crown ether polysiloxane stationary phases

Caiying Wu*, Jinshong Cheng, Wenhui Gao☆, Zaorui Zeng, Xueran Lu and Shulin Gong

*Chemistry Department, Wuhan University, Wuhan 430072, Hubei Province (China)*

(First received July 18th, 1991; revised manuscript received October 18th, 1991)

ABSTRACT

Two new kinds of aza-crown ethers, ω-undecylene aza-18-crown-6 polysiloxane (PUAC-18-C-6) and ω-undecylene aza-15-crown-5 polysiloxane (PUAC-15-C-5), were synthesized for use as stationary phases in capillary column gas chromatography. These two stationary phases demonstrate high column efficiency, a wide operating temperature range, good thermal stability, medium polarity and excellent selectivity for *n*-alcohols, esters and aromatic compounds, similarly to ω-undecyloxymethyl-18-crown-6 polysiloxane phase (PSO-11-18-C-6), and they have unique characteristics which are responsible for the success of separating aniline and other basic compounds without derivatization. The factors which affect the separation mechanism, including dipole–dipole interactions, hydrogen-bonding forces and fitting of solute molecules in the crown ether cavity, are discussed.

## INTRODUCTION

Crown ethers are becoming increasingly important as stationary phases in gas chromatography (GC) owing to the cavity structure and the strong electronegative effect of heteroatoms on the crown ether ring [1–4]; especially polymeric crown ethers are suitable for this purpose because of their ease of coating on capillary columns and their high column efficiency, wide operating temperature and good thermal stability [5–8], and they can also be used in temperature-programmed work.

In 1988, Rouse *et al.* [5] first synthesized a crown ether-substituted polysiloane with a polymer spacing of three methylene groups, which showed unique selectivity for nitrogen-containing polycyclic aromatic compounds. In recent work [6–8], we developed PSO-11-18-C-6 substituted polysiloxane with a polymer spacing of 11 methylene groups, which is convenient for cross-linking on fused-silica capillary columns with aza-*tert.*-butane (ATB) and dicumyl peroxide (DCUP) [6,7]. We also introduced another new method for preparing crown ether polysiloxane stationary phases by direct cross-linking a crown ether with SE-54 in different proportions inside a column [8]. We succeeded in separating aromatic compounds and their derivatives, phenols and their isomers, ethyl-substituted diphenyl ketone isomeric mixtures, etc.

In this work, two new kinds of aza-crown ether, ω-undecylene aza-18-crown-6 and ω-undecylene aza-15-C-5, were substituted on a polysiloxane backbone to yield two stationary phases for capillary GC (Fig. 1). The tertiary nitrogen atom in the crown ether ring makes these two polymeric stationary phases basic, and they were expected to have strong abilities for separating anilines and other basic compounds without derivatization; these compounds are difficult to separate by GC.

☆ Present address: Hebei Chemical and Light Engineering Institute, Hebai, China.

0021-9673/92/$05.00 

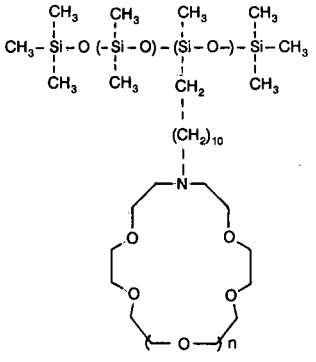

Fig. 1. Structure of the aza-crown ethers: $n = 0$, PUAC-15-C-5; $n = 1$, PUAC-18-C-6.

## EXPERIMENTAL

### *Syntheses*

The two aza-crown ether polymers were synthesized with a hydrosilylation technique [9]. ω-Undecylene aza-18-C-6 and ω-undecylene aza-15-C-5 were obtained from the Department of Chemistry, Polymeric Major, Wuhan University, China. These starting materials were both purified by passing them through a silica gel G column, using in order pure chloroform, ethyl acetate, acetone and ethanol as eluents. Polymethylhydrosiloxane (40%) was obtained from Xing Huo Chemical Plant, Jiang Xi Province, China.

*Synthesis of ω-undecylamine aza-18-crown-6 polysiloxane (PUAC-18-C-6).* Purified ω-undecylene aza-18-C-6 (0.35 g) and 0.06 g of 40% polymethylhydrosiloxane were mixed in 5 ml of pure benzene and the mixture was heated at 90°C for 1 h in a three-necked flask under an argon atmosphere. A 10-μl volume of chloroplatinic acid solution (1% $H_2PtCl_6 \cdot 6H_1O$, 1% ethanol and 98% tetrahydrofuran) was then added to the mixture, and the reaction was nearly completed after 16 h, when the products became viscous, as measured by the remaining Si–H band in the IR spectrum. A 1-ml volume of *n*-decylene was then added to the mixture to react with all of the residual Si–H units under the same conditions as above, and after 1 h the mixture was allowed to cool, the gummy product was dissolved in 2 ml of dichloromethane and precipitated with 10 ml of methanol–water (1:1). The precipitate was centrifuged and the solvents were decanted. The process of precipitation with aqueous methanol was repeated seven more times to remove the catalyst. The product (0.4 g), a yellow gum, was dried overnight under reduced pressure.

*Synthesis of ω-undecylamine aza-15-crown-5 polysiloxane (PUAC-15-C-5).* The synthesis of PUAC-15-C-5 was similar to that for PUAC-18-C-6, except that the weight of polymethylhydrosiloxane was 0.12 g and that of purified ω-undecylene aza-15-C-5 was 0.59.

### *Column preparation*

Fused-silica capillary columns (Yong Nian Optical Fibre Factory, Hebei Province, China) were rinsed with 10 ml of methanol and purged with nitrogen at 250°C for 2 h to remove acidic impurities. The columns were then statically coated with a solution of 0.4–0.6% (w/v) PUAC-15-C-5 or PUAC-18-C-6 in dichloromethane at 30°C. Following the coating procedure and flushing with nitrogen for 3 h, the columns were conditioned at 280°C for 10 h under a slow flow of nitrogen before use.

### *Column evaluation*

An Sc-7 gas chromatograph (Sichuan Analytical Apparatus Plant, Sichuan, China) equipped with a capillary split injection system and flame ionization detector was used throughout. Nitrogen was the carrier gas at a linear velocity of 12–15 cm/s. Solutes (0.5 μl) were injected using the split mode (80:1) and the injector and detector temperatures were maintained at 250 and 280°C, respectively.

The efficiency of the columns was determined as the number of plates per metre for naphthalene at 120°C. The polarity of the stationary phases was characterized by the McReynold's constants and *A* values (the slope of the graph obtained when the logarithm of the adjusted retention times of *n*-alkanes is plotted as a function of the number of carbon atoms at 170°C). The *A* value represents only dispersion forces, but the McReynold's constants include dispersion forces, dipole–dipole forces, hydrogen-bonding forces, etc. The glass transition temperature was determined by the change in slope of the plot of the logarithm of capacity factor *versus* reciprocal absolute temperature for naphthalene. Some standard mixtures of alcohols, normal fatty acid methyl esters and aromatic hydrocarbons and also some polar positional isomers were used to

demonstrate the unique selectivity of these two stationary phases. The thermal stabilities of these two stationary phases were tested by measuring column bleeding; after measuring column bleeding, the column efficiency remain unchanged and the column capacity factors had decreased by 3–5%.

## RESULTS AND DISCUSSION

PUAC-15-C-5 and PUAC-18-C-6 have a non-polar polysiloxane chain, a long aliphatic spacer arm and a polar crown ether ring, with a tertiary nitrogen atom in the polar crown ether ring. They are predicted to have good film-forming ability and high thermal stability [10] and a unique selectivity for aniline compounds.

Table I shows the characteristics of these two crown ether capillary columns. The data indicate that the columns have an efficiency above 3850 plates/m, decreasing slightly with increase in film thickness. The coating efficiencies are more than 81% and the reproducibility is good. The peak-area ratio of acidic 2,6-dimethylphenol and basic 2,4-dimethylaniline between 0.32 and 0.43 indicates that these two stationary phases exhibit basic properties. The peak asymmetry factors for octanol on the fused-silica columns are close to 1.0, indicating that the aza-crown ether polysiloxanes possess the good film-forming ability.

Fig. 2 shows chromatograms for the Grob test mixture obtained on the PUAC-18-C-6 and PUAC-15-C-5 columns. They show that the mixtures were well separated and each peak is symmetrical. It is notable that 1-octanol and 1,3-butanediol both eluted behind *n*-dodecane, which has the highest molecular weight of the three. It is obvious that these two stationary have strong hydrogen-bonding forces to alcohols.

The selectivities and average polarities of the two aza-crown ether polysiloxane stationary phases, represented by the McReynold's constants and *A* values, are shown in Table II. It can be seen that they both have an average polarity similar to that of PSO-11-18-C-6 which was cross-linked by ATB [6], and lower than that of Carbowax 20M owing to their long non-polar alkyl groups and polysiloxane chain. The *A* values decrease with increasing polarity of the phases, indicating that these crown ether stationry phases are more suitable than Carbowax 20M for separating non-polar compounds.

The operating temperature range is determined by the glass transition temperature and column bleeding. These transitions occur at temperatures which may correspond to the glass transition temperature

TABLE I

CHROMATOGRAPHIC PROPERTIES OF PUAC-15-C-5 AND PUAC-18-C-6 COLUMNS

| Parameter | PUAC-15-C-5 | | | | PUAC-18-C-6 | | |
|---|---|---|---|---|---|---|---|
| Column No. | 1 | 2 | 3 | 4 | 5 | 6 | 7 |
| Synthesis No. | 1 | 2 | 3 | 3 | 4 | 5 | 5 |
| Column dimensions, length × I.D. (m × mm) | 13 × 0.25 | 14 × 0.25 | 11.5 × 0.25 | 22.5 × 0.25 | 12 × 0.25 | 15 × 0.25 | 15 × 0.25 |
| Coating efficiency (%) | 89.8 | 98.3 | 93.3 | 81 | 102 | 101.8 | 102.7 |
| Film thickness ($\mu$m) | 0.4 | 0.4 | 0.4 | 0.4 | 0.44 | 0.44 | 0.3 |
| Column efficiency (plates/m) | 4489 | 4715 | 4428 | 3850 | 4621 | 4627 | 4839 |
| Naphthalene capacity factor ($k'$) | 2.44 | 3.63 | 4.04 | 3.93 | 7.45 | 7.03 | 4.4 |
| Peak asymmetry | 1.05 | 1.04 | 1.05 | 1.06 | 1.0 | 1.0 | 1.0 |
| Peak-area ratio[a] | 0.39 | 0.36 | 0.40 | 0.41 | 0.4 | 0.32 | 0.43 |

[a] 2,6-Dimethylphenol to 2,4-dimethylaniline.

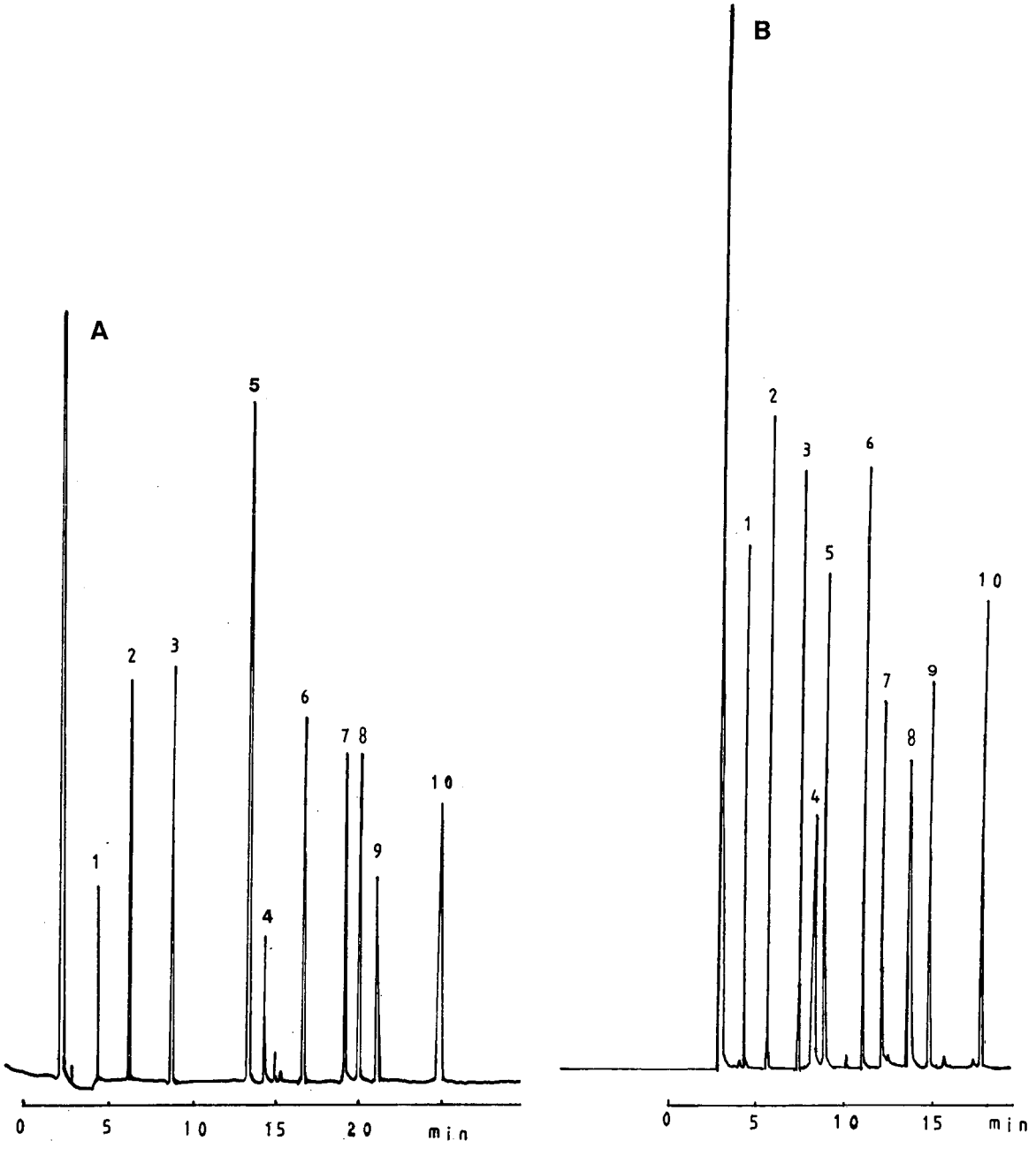


Fig. 2. Chromatogram of Grob test mixture on (A) the PUEC-18-C-6 and (B) the PUAC-15-C-5 columns. Temperature programmed from 80 to 150°C at 4°C/min. Peaks: 1 = *n*-decane; 2 = *n*-undecane; 3 = *n*-dodecane; 4 = 1,3-butanediol; 5 = 1-octanol; 6 = naphthalene; 7 = 2,4-dimethylaniline; 8 = 2,6-dimethylphenol; 9 = methyl undecanoate; 10 = methyl dodecanoate. The unlabelled peak represents the solvent.

TABLE II

McREYNOLD'S CONSTANTS AND *A* OF VALUES FOR THE VARIOUS STATIONARY PHASES

| Stationary phase | Benzene | Butanol | 2-Pentanone | Nitropropane | Pyridine | Mean | *A* |
|---|---|---|---|---|---|---|---|
| PUAC-15-C-5 | 147.5 | 258 | 263 | 261 | 224 | 231 | 0.1962 |
| PUAC-18-C-6 | 150 | 300.5 | 283 | 254 | 211 | 239 | 0.1965 |
| PSO-11-18-C-6 | 304 | 229 | 141 | 252 | 218 | 229 | 0.1975 |
| Carbowax 20M | 332 | 536 | 368 | 572 | 510 | 464 | 0.1905 |

and a liquid–liquid transition [3]. Fig. 3 shows the plot of the logarithm of the capacity factor for naphthalene on the PUAC-18-C-6 and PUAC-15-C-5 columns. The changes in slope at 119°C for PUAC-15-C-5 and 121°C for PUAC-18-C-6 correspond to the changes. These results also corresponded to the glass transition temperature determined by differential scanning calorimetry (DSC) of these two polymers. Such a change in slope was not observed with PSO-11-18-C-6, which is not cross-linked, and the transition points are lower than that of PSO-11-18-C-6, because the aza-crown ether molecules are regular and the interaction forces of the molecules are lower than those with PSO-11-18-C-6. This indicates that aza-crown ethers have lower minimum operating temperature than PSO-11-18-C-6. Xylene mixtures can be separated very well on the PUAC-18-C-6 column at 55°C (Fig. 4). Also, the efficiencies of both columns are more than 3300 plates/m at 70°C.

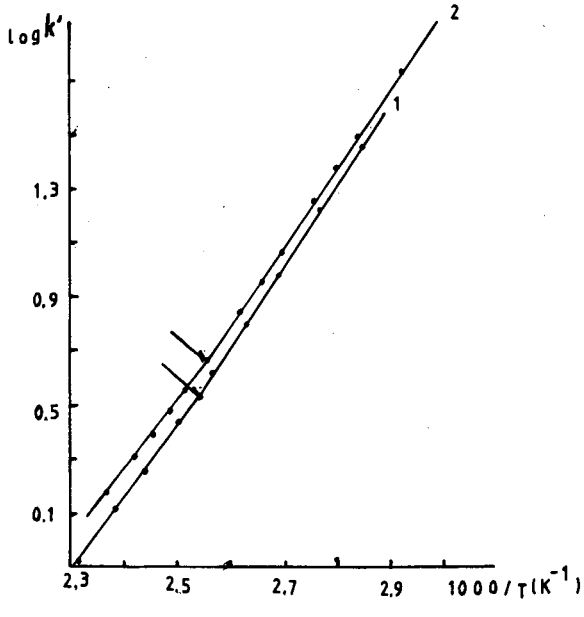


Fig. 3. Logarithm of capacity factor (*k'*) *vs.* reciprocal absolute temperature for naphthalene on (1) PUAC-18-C-6 and (2) PUAC-15-C-5 columns.

The column bleeding was measured by heating the columns from 120 to 300°C. The baseline did not increase when the column temperature was below 250°C and the shift of the baseline was $4.5 \cdot 10^{-13}$ A for PUAC-15-C-5 and $6.5 \cdot 10^{-13}$ A for PUAC-18-C-6 at 300°C. It can be seen that aza-crown ether stationary phases have a wider operating temperature range than PSO-11-18-C-6, which represents an appreciable improvement over the crown ether polysiloxane stationary phase reported by Rouse *et al.* [5]. These capillary columns were used at about 200°C for 3 months without a decrease in column efficiency and capacity factor.

Fig. 5 shows the relationship between the logarithm of the adjusted retention times and the number of carbon atoms in alcohol and normal fatty acid methyl ester homologues. The slopes of the straight lines for PUAC-15-C-5 and PUAC-18-C-6 are higher than that for Carbowax 20M and similar to that for PSO-11-18-C-6. These results indicate that the crown ether polysiloxane phases have a strong directional force and a higher selectivity for alcohols and esters than Carbowax 20M. The slopes are given in Table III.

Crown ethers show special selectivity, especially for aromatic compounds and their derivatives, amines, anilines, etc. [11]. These two aza-crown ether stationary phases give good separations of aniline compounds without derivatization (Fig. 6). It is interesting that the solutes did not elute only

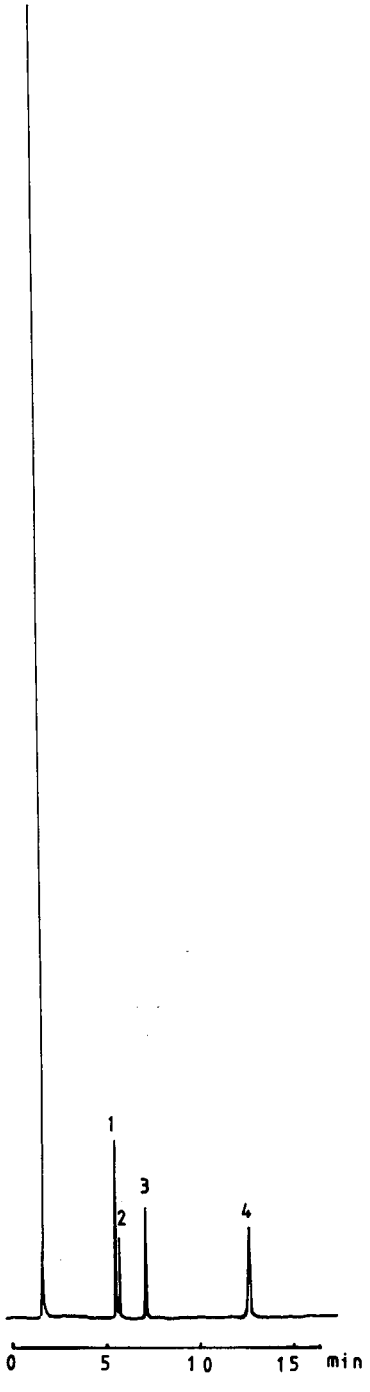


Fig. 4. Chromatogram of methyl-substituted benzene compounds on the PUAC-18-C-6 column (15 m × 0.25 mm I.D.). Temperature, 55°C (isothermal). Peaks: 1 = *p*-xylene; 2 = *m*-xylene; 3 = *o*-xylene; 4 = 1,3,5-trimethylbenzene.

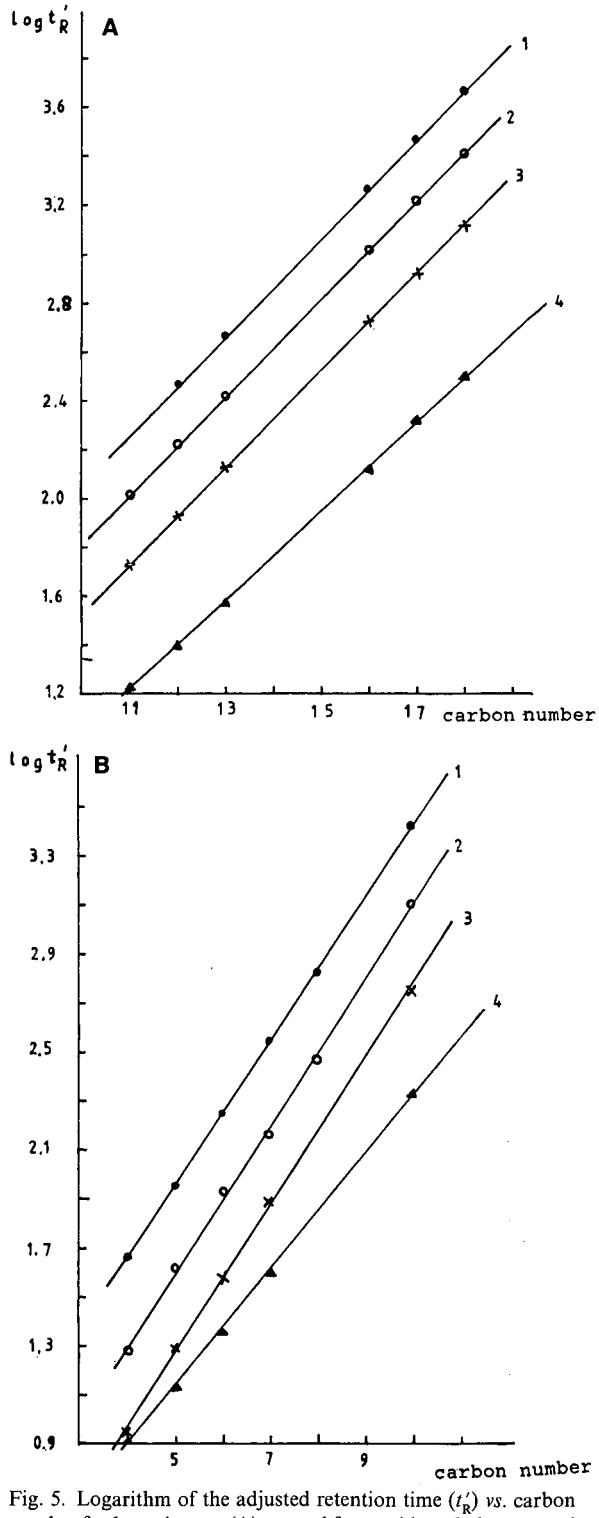


Fig. 5. Logarithm of the adjusted retention time ($t_R'$) *vs.* carbon number for homologous (A) normal fatty acid methyl esters and (B) alcohols. Column: (1) PUAC-18-C-6; (2) PUAC-15-C-5; (3) PSO-11-18-C-6; (4) Carbowax 20M.

TABLE III

SLOPES OF THE STRAIGHT LINE OF LOGARITHM OF ADJUSTED TIMES *VERSUS* CARBON NUMBER OF HOMOLOGOUS ALCOHOLS (110°C) AND NORMAL FATTY ACID METHYL ESTERS (170°C)

| Stationary phase | Alcohols | Esters |
|---|---|---|
| PUAC-18-C-6 | 0.2943 | 0.1997 |
| PUAC-15-C-5 | 0.298 | 0.1988 |
| PSO-11-18-C-6 | 0.2983 | 0.1979 |
| Carbowax 20M | 0.2368 | 0.1827 |

according to the dipole–dipole interactions; the decreasing order of dipole–dipole force of methylaniline (MA) isomers is *o*-MA, *m*-MA and *p*-MA, but the sequence of elution of MA isomers on the PUAC-18-C-6 column is *o*-MA, *p*-MA and *m*-MA. This may be caused by the co-action of dipole–dipole and hydrogen-bonding forces. The retention times of N-ethyl-substituted *m*-MA isomers increase in the order *m*-MA, N,N-diethyl-*m*-MA and N-ethyl *m*-MA. These differences in elution may be due to the fact that the N,N-diethyl-*m*-MA molecule does not fit well in the cavity of the crown ether ring and does not have hydrogen atoms to form hydrogen bonds with the crown ether ring.

Aza-crown ethers also provide selectivity for strongly polar organic compounds such as nitrobenzene positional isomers (Fig. 7). Relatively small molecules which have few substituent groups and cannot form hydrogen bonds elute in the order of dipole–dipole interactions. For example, xylene isomers elute from the PUAC-18-C-6 columns in the order *p*-xylene, *m*-xylene and *o*-xylene, which is the sequence of the dipole–dipole interactions (Fig. 4). Mononitrotoluene (MNT) isomers elute from the PUAC-18-C-6 column in the order *o*-MNT, *m*-MNT and *p*-MNT, which is also the sequence of dipole–dipole interactions (Fig. 7). However, dinitrotoluene (DNT) isomers eluted from the PUAC-18-C-6 column in the order 2,6-DNT, 2,5-DNT, 2,4-DNT, 3,5-DNT and 3,4-DNT (Fig. 7), whereas the increasing sequence of dipole–dipole forces is 2,5-DNT, 2,4-DNT, 2,6-DNT, 3,5-DNT and 3,4-DNT. This different elution is also possibly caused by the 2,6-DNT molecule not fitting well in the cavity of the aza crown ether ring.

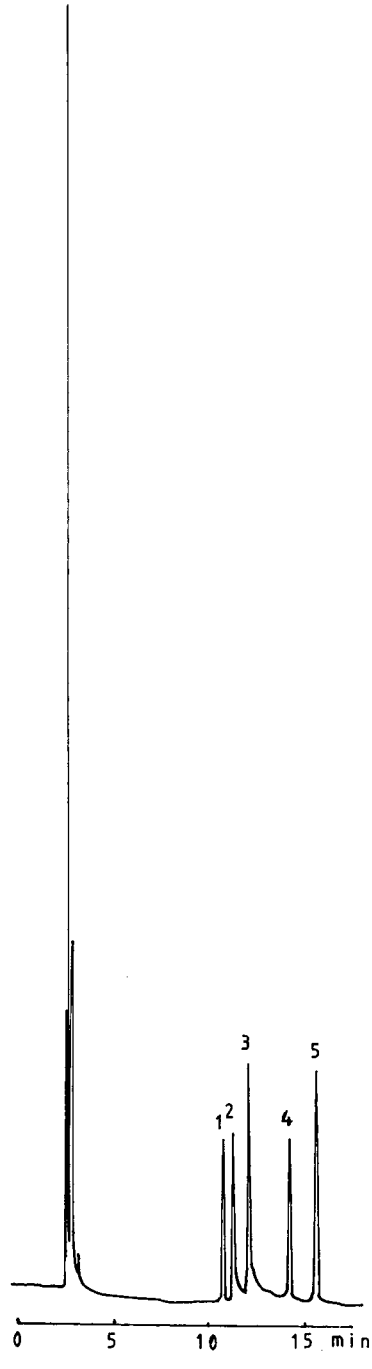


Fig. 6. Chromatogram of aniline compounds on the PUAC-18-C-6 column (15 m × 0.25 mm I.D.). Temperature, 120°C (isothermal). Peaks: 1 = *o*-methylaniline; 2 = *p*-methylaniline; 3 = *m*-methylaniline; 4 = N,N-diethyl-*m*-methylaniline; 5 = N-ethyl-*m*-methylaniline.

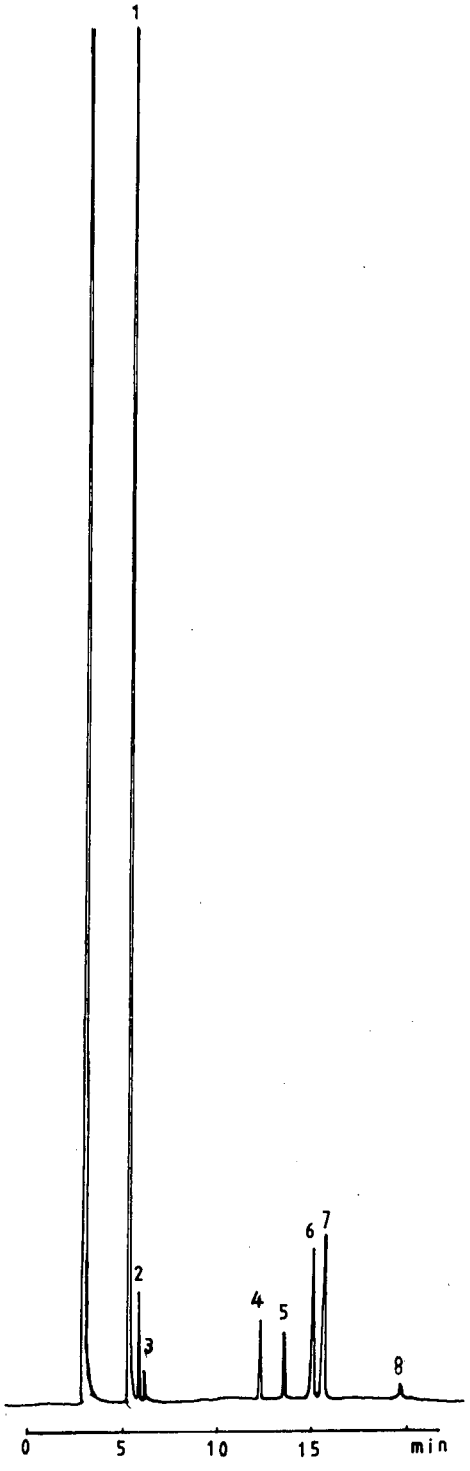


Fig. 7. Chromatogram of nitro compounds on the PUAC-18-C-6 column (15 m × 0.25 mm I.D.). Temperature programmed from 160 to 200°C at 4°C/min. Peaks: 1 = *o*-MNT; 2 = *m*-MNT; 3 = *p*-MNT; 4 = 2,6-DNT; 5 = 2,5-DNT; 6 = 2,4-DNT; 7 = 3,5-DNT; 8 = 3,4-DNT.

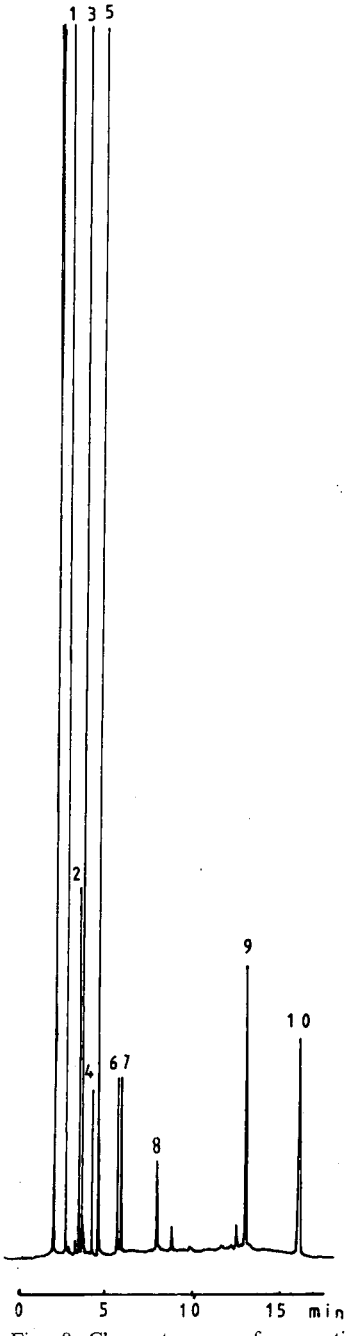


Fig. 8. Chromatogram of aromatic hydrocarbons on the PUAC-15-C-5 column (14 m × 0.25 mm I.D.). Temperature programmed from 150 to 200°C at 4°C/min. Peaks: 1 = naphthalene; 2 = 2-methylnaphthalene; 3 = 1-methylnaphthalene; 4 = biphenyl; 5 = diphenylmethane; 6 = bibenzil; 7 = acenaphthalene; 8 = fluorene; 9 = phenanthrene; 10 = triphenylmethane.

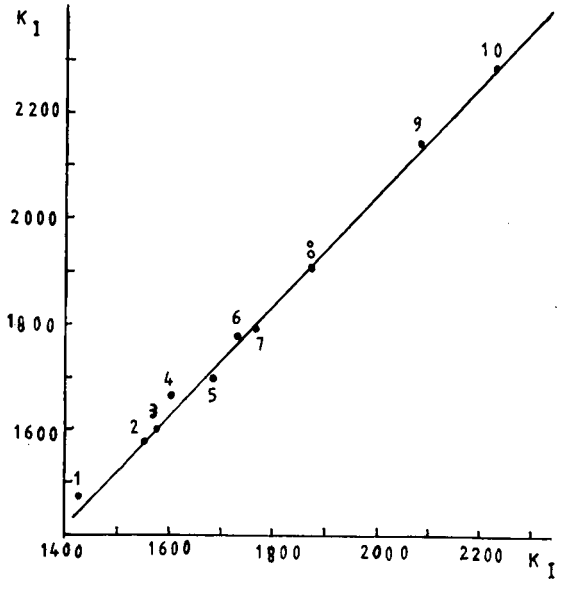


Fig. 9. Kováts retention indices of a series of aromatic hydrocarbons on PUAC-18-C-6 (ordinate) plotted against those on PSO-11-18-C-6 (abscissa). Column temperature, 170°C (isothermal). Compound numbers as in Fig. 8.

Fig. 8 shows that aza-crown ethers also provide good selectivity for easily polarizable aromatic hydrocarbons. Fig. 9 shows a plot of the Kováts retention indices of these aromatic compounds on PUAC-18-C-6 against those on PSO-11-18-C-6. There is a good linear relationship for most aromatic hydrocarbons, indicating that aza-crown ethers have the same mechanism as PSO-11-18-C-6 in separating easily polarizable aromatic compounds.

## CONCLUSIONS

Aza-crown ether stationary phases are medium-polarity stationary phases that possess good film-forming ability and a wide operating temperature range of 55–300°C. These stationary phases present excellent selectivity for non-polar compounds, easily polarizable aromatic compounds and polar compounds such as alcohols, esters, nitrobenzene compounds and anilines.

## ACKNOWLEDGEMENT

This work was supported by the National Science and Hubei Province Foundation.

## REFERENCES

1 R.-S. Li, *SEPU*, 4 (1986) 304.
2 Y.-H. Jin, R.-N. Fu and Z.-F. Huang, *J. Chromatogr.*, 469 (1989) 153.
3 D. D. Fine, H. L. Geargart, II and H. A. Mottola, *Talanta*, 32 (1985) 751.
4 Y.-H. Jin and R.-N. Fu, *Huaxue Shiji*, 11 (1989) 339.
5 C. A. Rouse, A. C. Fintinson, B. J. Tarbet, J. C. Pixton, N. M. Djordjevic, K. Z. Markides, J. S. Bradshaw and M. L. Lee, *Anal. Chem.*, 60 (1988) 901.
6 C.-Y. Wu, C.-M. Wang, Z.-R. Zeng and X.-R. Lu, *Anal. Chem.*, 62 (1990) 968.
7 C.-Y. Wu, H.-Y. Li, Y.-Y. Chen and X.-R. Lu, *J. Chromatogr.*, 504 (1990) 279.
8 C.-Y. Wu, C.-M. Wang, J.-S. Cheng and X.-R. Lu, *SEPU*, 8 (1990) 355.
9 B. A. Jones, J. S. Bradshaw, M. Nishioka and M. L. Lee, *J. Org. Chem.*, 49 (1984) 4947.
10 L. Blomberg, *J. High Resolut. Chromatogr. Chromatogr. Commun.*, 5 (1982) 520.
11 E. V. Zagorevskaya and N. Y. Kovaleva, *J. Chromatogr.*, 365 (1986) 7.

*Journal of Chromatography*, 594 (1992) 253–257
Elsevier Science Publishers B.V., Amsterdam

CHROM. 23 863

# Simultaneous determination of sorbic acid, dehydroacetic acid and benzoic acid by gas chromatography–mass spectrometry

Michiko Kakemoto

*Department of Applied Chemistry, Faculty of Science and Engineering, Chuo University, 1-13-17 Kasuga, Bunkyo-ku, Tokyo 112 (Japan)*

(First received July 5th, 1991; revised manuscript received October 30th, 1991)

ABSTRACT

A method for the simultaneous determination of sorbic acid, dehydroacetic acid and benzoic acid using gas chromatography–chemical ionization mass spectrometry is described. The three components were separated on diethylene glycol succinate and eluted in the order of sorbic acid, dehydroacetic acid and then benzoic acid. In chemical ionization, the multiple-ion monitor is set to the quasi-molecular ion, that is *m/z* 113 for sorbic acid, *m/z* 169 for dehydroacetic acid and *m/z* 123 for benzoic acid. The linear dynamic detection range was approximately $1 \cdot 10^3$ ($5 \cdot 10^{-10}$ to $5 \cdot 10^{-7}$ g). The minimum detectable amounts of the three components were found to be 200–500 pg. The chemical ionization mass fragmentographic method was about ten-fold more sensitive than the electron impact method. This method was sensitive and selective without any influence of solvent peak and other contaminants. The method has been applied to the determination of preservatives in foods.

## INTRODUCTION

Recently many kinds of preservatives have been used to protect food, pharmaceutical and cosmetic products from damage by oxidation as well as microbial and fungal attack. Sorbic acid, dehydroacetic acid and benzoic acid are used extensively as preservatives in foods. They are added to food individually or as mixtures, and hence simultaneous determination is required.

In general, extraction or clean-up of three components from a sample is accomplished by homogenization followed by steam distillation [1,2] or liquid–liquid partition [3,4]. In other cases, *e.g.*, liquid samples such as soft drinks, only dilution with solvent is necessary [5,6].

The determination of three components individually or collectively has been reported using titration [7,8], visible or UV spectrometry [4,9,10], high-performance liquid chromatography (HPLC) [1,11–13] and gas chromatography (GC) [2,14–16]. In the case of GC, they are determined after derivatization of the acid. In any case, detection is accomplished by flame ionization detection (FID).

The author regards multiple-ion monitoring in GC–mass spectrometry (MS) as a sensitive and selective detection method in comparison with FID. This is because multiple-ion monitoring is not susceptible to interference by contaminants in the sample.

In this paper, the simultaneous determination of sorbic, dehydroacetic and benzoic acids by GC–MS utilizing chemical ionization is reported.

## EXPERIMENTAL

### *Chemicals and reagents*

Sorbic acid, dehydroacetic acid and benzoic acid were guaranteed reagents from Tokyo Kasei Kogyo (Tokyo, Japan). Diethyl ether, acetone and other solvents and chemicals were of analytical-reagent grade and obtained from Wako (Tokyo, Japan).

0021-9673/92/$05.00 

*Instrumentation*

GC–MS was performed on a NEVA GC–MS TE 600 S System (Nichiden Varian, Japan). The GC column used was 200 cm × 2 mm I.D. Pyrex glass tubing packed with 5% diethylene glycol succinate (DEGS) on Neosorb NS (pretreated with phosphoric acid, 80–100 mesh). The column temperature was 160 or 170°C and the carrier gas flow-rate was 10 m/min. MS conditions were as follows: total ion current (TIC), 180 $\mu$A; electron accelerated voltage, 70 V; ion accelerated voltage, 10.6 V; secondary electron multiplier voltage, −2.5 kV; reagent gas, methane.

*Sample*

The samples were commercially available foodstuffs consisting of cheese, jam, marmalade, juice and cuttlefish.

*Procedures*

The samples (2 g) were weighed, and 2 ml of saturated sodium chloride solution and 2 ml of 10% sulphuric acid were added to the samples, which were then homogenized. The homogenized samples were extracted twice with 20 and 10 ml of diethyl ether. The extracts were combined and washed with 4 ml of saturated sodium chloride solution and then dried with anhydrous sodium sulphate and evaporated. The residue was dissolved in 1 ml of acetone, and 2 $\mu$l of this solution were injected into the GC–MS system.

## RESULTS AND DISCUSSION

*Gas chromatographic separation*

Sorbic, dehydroacetic and sorbic acids were well separated using DEGS on Neosorb NS (80–100 mesh pretreated phosphoric acid) in a glass column. Under these conditions, tailing of the chromatographic peaks was absent. Typical TIC chromatograms are shown in Fig. 1. Sorbic, dehydroacetic and benzoic acids are eluted within 4 min.

*Mass spectra*

The electron impact (EI) and chemical ionization (CI) mass spectra of sorbic, dehydroacetic and benzoic acids are shown in Figs. 2, 3 and 4, respectively.

The EI mass spectrum of sorbic acid in Fig. 2 is characterized by molecular ion peaks at *m/z* 112 and *m/z* 97, corresponding to elimination of $CH_3$, (M − 15) and at *m/z* 67 caused by elimination of COOH (M − 45). The CI ($CH_4$) mass spectrum of sorbic acid (Fig. 2, bottom) is characterized by a quasi-molecular peak, M + 1 (*m/z* 113), and weak fragment peaks for M + 29 (*m/z* 141) and M + 41 (*m/z* 153) arising from $C_2H_5^+$ and $C_3H_5^+$ ions as a result of methane ionization. Additionally, the *m/z* 97 peak appeared to be due to (M − 15 + 1).

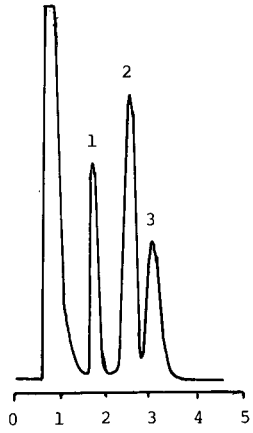


Fig. 1. Typical chromatogram of sorbic acid (1), dehydroacetic acid (2) and benzoic acid (3) on DEGS at 160°C.

The EI mass spectrum of dehydroacetic acid in Fig. 3 shows a peak at *m/z* 168, a molecular peak of

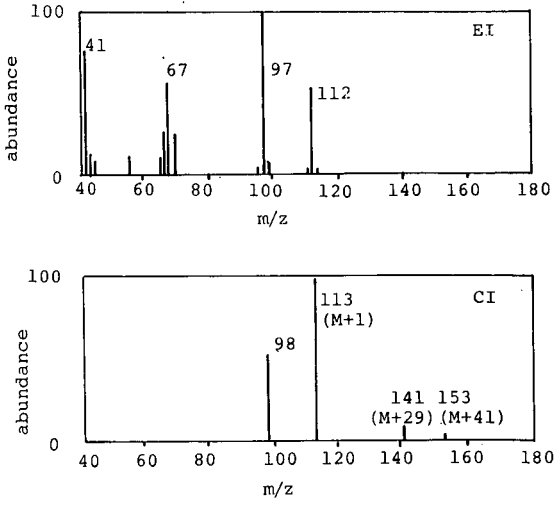


Fig. 2. EI and CI mass spectra of sorbic acid.

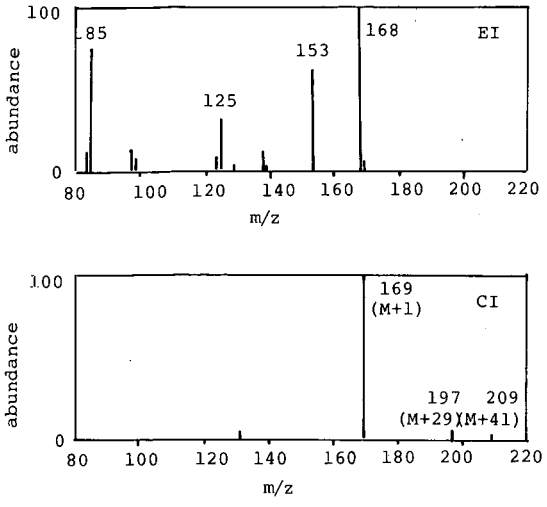


Fig. 3. EI and CI mass spectra of dehydroacetic acid.

medium intensity at $m/z$ 153 due to loss of $CH_3$ (M − 15) and a peak at $m/z$ 125 caused by loss of CO (M − 43). The CI mass spectrum of dehydroacetic acid (Fig. 3, bottom) consists of peaks at $m/z$ 169 (M + 1), $m/z$ 197 (M + 29) and $m/z$ 209 (M + 41).

The EI mass spectrum of benzoic acid (Fig. 4) consists of the molecular ion peak at $m/z$ 122; other prominent peaks are those at $m/z$ 105 caused by loss of OH (M − 17) and at $m/z$ 77 due to loss of COOH (M − 45). The CI mass spectrum reveals quasi-molecular ion peaks at $m/z$ 123 (M + 1) and $m/z$ 106 (105 + 1). The principal advantages of CI over EI

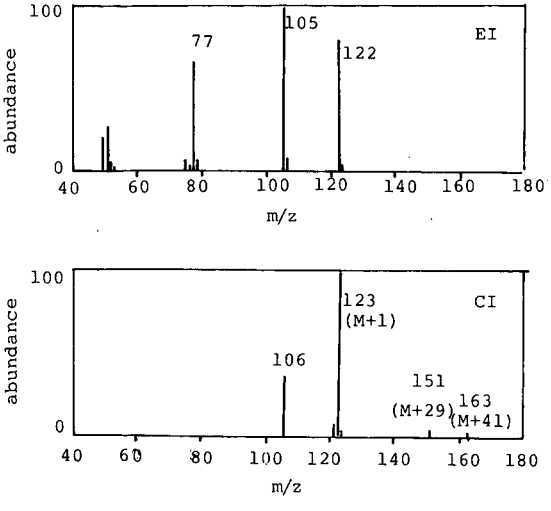


Fig. 4. EI and CI mass spectra of benzoic acid.

are simple fragmentation patterns and strong peaks related to the molecular ion.

*Mass fragmentography*

CI mass fragmentography is appropriate for the simultaneous determination of a small number of different structural components. Accordingly, the multiple-ion monitor was set to the quasi-molecular ion (M + 1) of each compound, that is $m/z$ 113 for sorbic acid, $m/z$ 169 for dehydroacetic acid and $m/z$ 123 for benzoic acid. Fig. 5 shows the fragmento-

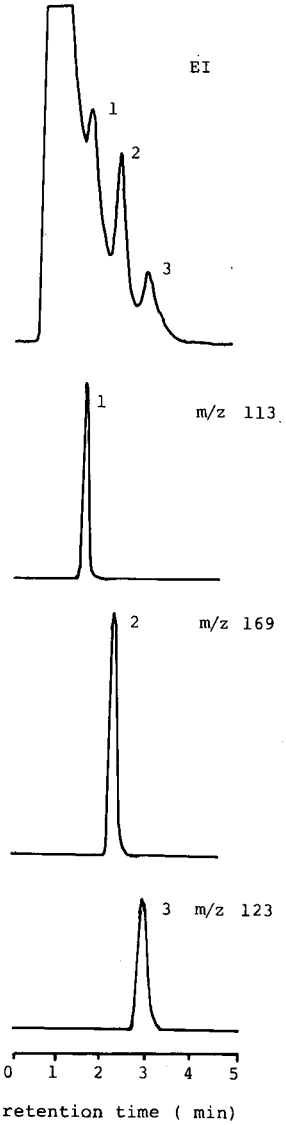


Fig. 5. CI mass fragmentograms of sorbic acid (1), dehydroacetic acid (2) and benzoic acid (3), 30 ng each, on DEGS at 170°C.

TABLE I

RECOVERIES OF SORBIC ACID, DEHYDROACETIC ACID AND BENZOIC ACID FROM FOODS

| Compound | Average (%) | R.S.D. ($n$ = 3) (%) |
|---|---|---|
| *Strawberry jam* | | |
| Sorbic acid | 98 ± 3 | 2.2 |
| Dehydroacetic acid | 101 ± 2 | 1.8 |
| Benzoic acid | 102 ± 2 | 1.9 |
| *Cheese* | | |
| Sorbic acid | 97 ± 5 | 3.7 |
| Dehydroacetic acid | 99 ± 4 | 3.0 |
| Benzoic acid | 95 ± 6 | 4.5 |

gram of settings $m/z$ 113, 169 and 123. The large solvent peak interfered with the sorbic, dehydroacetic and benzoic acids peaks in the TIC chromatogram, whereas in the CI mass fragmentogram every peak was detected sensitively and selectively without any interference.

*Linearity and minimum detectable amounts*

A linear correlation was observed between $5 \cdot 10^{-10}$ and $5 \cdot 10^{-7}$ g. The minimum detectable amounts were determined until a signal-to-noise ratio of 3 was reached. In this way, the minimum detectable amounts obtained were 200 pg for dehydroacetic acid, 300 pg for sorbic acid and 500 pg for benzoic acid. The sensitivity of the CI mass fragmentography method was about ten-fold greater than that of the EI method.

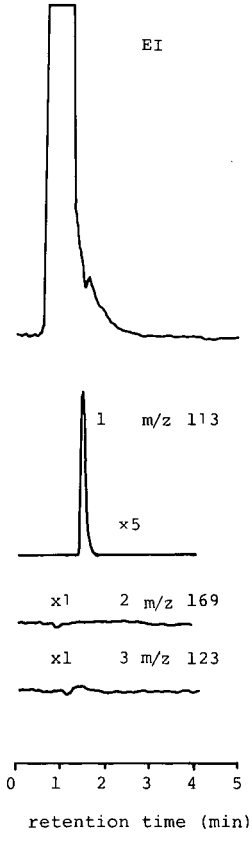


Fig. 6. Chromatograms of commercial orange marmalade.

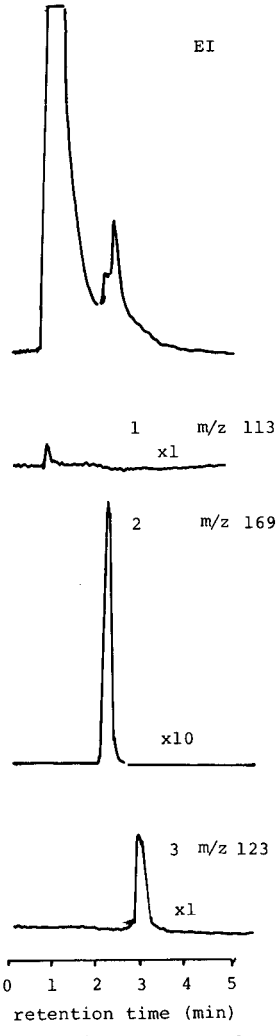


Fig. 7. Chromatograms of commercial cheese.

TABLE II

DETERMINATION OF SORBIC ACID, DEHYDROACETIC ACID AND BENZOIC ACID IN FOODS

| | Contents (ppm) | | |
|---|---|---|---|
| | Sorbic acid | Dehydroacetic acid | Benzoic acid |
| Strawberry jam | 200 | – | – |
| Orange marmalade | 224 | – | – |
| Smoked cuttlefish | 560 | – | – |
| Concentrated orange juice | – | – | 570 |
| Cheese | – | 280 | 10 |
| Cheese (slice) | 1000 | – | 8 |

*Determination of sorbic, dehydroacetic and benzoic acids in foods*

Recoveries were determined by adding 100 ppm sorbic, dehydroacetic and benzoic acids to blank homogenized strawberry jam and cheese from which it had been previously confirmed that the three components were absent. The results are given in Table I. The recoveries ranged from 95 to 102% with a relative standard deviation (R.S.D.) of 1.7–4.5%.

This method was applied to the determination of sorbic, dehydroacetic and benzoic acids in jam, juice and cheese, etc. The results are shown in Table II. Typical chromatograms of orange marmalade and cheese are shown in Figs. 6 and 7, respectively. The preservatives contained in each food were described on the labels, but not the types or quantities.

Using this method, sorbic acid, dehydroacetic acid and benzoic acid were simultaneously determined using the multiple-ion monitor set to the quasi-molecular peak of $m/z$ 113, 169 and 123 in the CI mass fragmentograph. This method was selective without interference from other contaminants or the solvent peak. The sensitivity of the method was such that 200–500 pg amounts of each component could be detected.

ACKNOWLEDGEMENT

The author thanks Professor Eigo Kobayashi of Tokyo Metropolitan University for CI-MS measurements.

REFERENCES

1 H. Terada and Y. Sakabe, *J. Chromatogr.*, 346 (1985) 333.
2 I. Saito, H. Oshima, N. Kawamura, K. Uno and M. Yamada, *J. Assoc. Off. Anal. Chem.*, 70 (1987) 507.
3 F. Ureta, *Connaiss. Vigne Vin.*, 18 (1984) 287.
4 O. W. Law, S. F. Luk and R. K. M. Lam, *Analyst (London)*, 114 (1989) 217.
5 T. Mine and M. Horiuchi, *Shokuhin Eiseigaku Zasshi*, 26 (1985) 61.
6 J. T. Hann and S. I. Gilkison, *J. Chromatogr.*, 395 (1987) 317.
7 F. X. Demers and R. L. Yates, *J. Assoc. Off. Anal. Chem.*, 65 (1982) 82.
8 O. W. Law and S. F. Luk, *Analyst (London)*, 112 (1987) 1269.
9 J. Dumain, A. Parmentier, C. Banner and F. M. Pailler, *Ann. Falsif. Expert. Chim. Toxicol.*, 80 (1987) 85.
10 G. Schwedt and K. Schwardorf, *Inst. Lebensmittelchem.*, 82 (1986) 209.
11 H. S. Lee, R. L. Rouseff and J. F. Fisher, *J. Food Sci.*, 51 (1986) 568.
12 K. Fujimura and M. Tsuchiya, *Bunseki Kagaku*, 37 (1988) 56.
13 F. J. E. M. Kueppers and J. A. Jans, *J. Assoc. Off. Anal. Chem.*, 71 (1988) 1068.
14 Y. Chen, Q. Li, L. He and L. Zheng, *Sepu*, 5 (1987) 238.
15 D. H. Daniels, C. R. Warner, S. Selim and F. L. Joe, *J. Assoc. Off. Anal. Chem.*, 66 (1983) 893.
16 I. M. Perl, M. P. Szakacs and M. Morvai, *Magy. Kem. Foly.*, 93 (1987) 71.

*Journal of Chromatography*, 594 (1992) 259–267
Elsevier Science Publishers B.V., Amsterdam

CHROM. 23 852

# Analysis of zapatera olives by gas and high-performance liquid chromatography

Alfredo Montaño*, Antonio de Castro, Luís Rejano and Antonio-Higinio Sánchez

*Unidad E.I. Biotecnología de Alimentos, Instituto de la Grasa y sus Derivados (CSIC), Apartado 1078, 41012 Seville (Spain)*

(First received July 19th, 1991; revised manuscript received October 29th, 1991)

ABSTRACT

Gas chromatography and high-performance liquid chromatography were applied to normal and "zapatera" olive brines obtained from typical fermentation brines of green table olives after different treatments. The zapatera samples were obtained by pH adjustment to 5.1 followed by inoculation with a suspension of sediment from a zapatera brine and incubation at 30°C for 40 days. The compounds determined were lactic acid, $C_2$–$C_6$ fatty acids, acetaldehyde, methanol, ethanol, 2-butanol and *n*-propanol. Normal and zapatera brines were compared to identify components that indicated spoilage. One of these components was found in the gas chromatogram of the volatile fatty acids from the zapatera samples and identified as cyclohexanecarboxylic acid by gas chromatography–mass spectrometry. A comparison of the corresponding aromagrams revealed quantitative differences in aroma composition. Various relationships calculated from the peak areas of selected unknown components in these aromagrams were so distinct as to provide a basis for characterizing zapatera spoilage.

## INTRODUCTION

The table olive is an important product for Spain, during 1989 128 000 tonnes valued at $3 \cdot 10^{10}$ pesetas being exported [1]. The most important of the different commercial preparations is the Spanish-style green olive, characterized by a lactic acid fermentation. At present, owing to the lack of a pure culture fermentation that guarantees the uniformity and safety of the product, these olives are still prepared by natural, spontaneous fermentation. One risk of such a practice is that there will be an increased likelihood of microbial spoilage, including the clearly differentiated and defined "gas pocket", putrid fermentation, butyric fermentation and "zapatera" spoilage [2]. The last type of spoilage is frequent in Spanish-style green olives and causes large losses to the industry. It is characterized by the development of a very penetrating, unpleasant odour in olives undergoing fermentation. It seems that the spoilage results from decomposition of organic acids at a time when little or no sugar is present and the lactic acid fermentation stops before the pH has decreased below 4.5 [2]. Zapatera spoilage seems to be caused by the participation of species of at least two genera of bacteria, *Clostridium* and *Propionibacterium* [3]. Although the characteristic odour of zapatera samples is different to that of other malodorous fermentations (*e.g.*, butyric fermentation), there is sometimes confusion over the term "zapatera", with a tendency to classify as such most olives with abnormal flavour [2].

Detection of zapatera samples by sensory methods depends on both the olfactory detection threshold of the taster and the stage of development of the spoilage. Detection is almost impossible in zapatera olives corrected by dilution and/or masked by addition of aroma-giving substances, a frequent type of fraud in the olive industry.

Traditional microbiological methods for detection spoilage in food present two main problems: (a) they take days, or even weeks, to carry out and (b) the microorganisms responsible may not be detected on analysis. However, the chemical changes

0021-9673/92/$05.00 

originating from microbial activity remain detectable independently of whether the microorganisms are viable or not [4].

The foregoing more than justifies the proposed aims of this work, namely to separate by chromatographic methods the volatile component or components contributing significantly to the typical unpleasant smell of zapatera olives, and to establish an analytical method to detect the spoilage.

## EXPERIMENTAL

### *Samples*

A typical fermentation brine of green olives from our laboratory was used. It had the following physico-chemical characteristics: pH 4.50, titratable acidity (expressed as lactic acid) 0.60%, sodium chloride content 5.8% and volatile acidity (expressed as lactic acid) 0.62%. Aliquots of this brine (200 ml) were placed in ten flasks each of 300-ml capacity, and were treated as shown in Table I. A 1-l volume of a zapatera brine supplied by the industry was centrifuged at 16 300 *g* for 10 min and the sediment obtained was washed with saline solution (1% NaCl) and finally resuspended in 25 ml of the same solution. A 3-ml portion of this suspension was used as inoculum.

In addition, 24 zapatera brines and 20 normal brines from different olive-processing plants were analysed.

### *Apparatus*

The following instruments were used: a gas chromatograph (Perkin-Elmer Model 3920B) fitted with a flame ionization detector coupled to a recording integrator (Hewlett-Packard Model 3394A), a liquid chromatograph (Perkin-Elmer Series 4) with a manual injector (Rheodyne Model 7125), in combination with a spectrophotometric detector (Perkin-Elmer Model LC-85B) coupled to a recording integrator (Hewlett-Packard Model 3390A), and a mass spectrometer (AEI MS-30/VG-70) with a VG11-250 data system connected to a gas chromatograph (Hewlett-Packard Model 5890).

### *Analytical methods*

*Chemical characteristics.* Titratable acidity, pH, volatile acidity and sodium chloride content of the brines were determined by the usual methods used in our laboratory [2].

*Volatile acids by gas chromatography (GC).* The following procedure was used to determine the volatile acids by GC: 20 ml of the sample were placed in a Kjeldhal apparatus used for the determination of volatile acidity, collecting *ca.* 250 ml of distillate. After neutralization with 0.2 *M* NaOH, it was transferred to a porcelain capsule and evaporated to dryness in a water-bath at 100°C. Immediately, 2 ml of 2 *M* $H_2SO_4$ were added to the residue and extracted twice with 25-ml portions of diethyl ether. After adding 0.5 ml of isocaproic acid solution (105 ppm in diethyl ether) as internal standard, the extract was dried over anhydrous sodium sulphate and concentrated *in vacuo* at 30°C to a volume of 0.5 ml or less. An aliquot (0.2–0.3 $\mu$l) of this concentrate was taken for GC analysis. A Supelcowax 10 fused-silica capillary column (30 m × 0.53 mm I.D., 1.0-$\mu$m film thickness) (Supelco) was used for

TABLE I

TREATMENTS CARRIED OUT WITH THE AIM OF REPRODUCING ZAPATERA SPOILAGE

| Treatment | Sample | | | | |
|---|---|---|---|---|---|
| | S1–S2 | S3–S4 | S5–S6 | S7–S8 | S9–S10 |
| pH adjustment[a] | No | Yes | Yes | Yes | Yes |
| Inoculation[b] | No | No | Yes | Yes | No |
| Addition of glucose and pasteurisation[c] | No | No | No | Yes | Yes |
| Storage at 30°C[d] | Yes | Yes | Yes | Yes | Yes |

[a] Concentrated NaOH was added to pH 5.1.
[b] 3 ml of inoculum, prepared as described in the text, were added.
[c] 3 g of glucose were added before pasteurization in a water-bath at 80°C for 10 min.
[d] Paraffin oil was added previously to form a surface layer *ca.* 1 cm thick.

the analysis of the volatile acids. The oven temperature was maintained at 150°C, the injector at 200°C and the detector at 230°C. Nitrogen was used as the carrier gas and auxiliary gas at flow-rates of 9 and 60 ml/min, respectively. Identification of $C_2$–$C_6$ volatile acids was made by comparing their retention times with authentic standards on different chromatographic columns. These columns and the conditions were as follows: (1) Supelcowax 10, as described above; (2) 2 m x 1/4 in.- O.D. glass column packed with 0.3% Carbowax 20M + 0.1% $H_3PO_4$ on 60–80-mesh Carbopack C at 140°C with nitrogen as carrier gas at 50 ml/min; and (3) 1.5 m × 1/8 in. O.D. stainless-steel column, packed with 20% sebacic acid on 80–100-mesh Chromosorb W AW at 135°C with nitrogen (saturated with formic acid) as carrier gas at 30 ml/min. The GC results were calculated from the peak areas obtained from the integrator, using the internal standard method. Identification of the "key compound" in the chromatograms of volatile acids from the zapatera brines was carried out by GC on a Supelcowax 10 column (30 m × 0.25 mm I.D.) (Supelco) with helium as carrier gas at 150°C for 5 min, then programmed to 180°C at 6°C/min, in conjunction with mass spectrometric analysis (GC–MS). Peak identification was confirmed by comparing the GC retention time and mass spectrum with that of an authentic standard.

*Headspace components.* Analysis of the major volatile components of the brines was carried out by the headspace method of Montaño *et al.* [5]. Quantification was effected using the peak areas using the internal standard method with dioxane as internal standard.

*Volatile compounds by GC.* The volatile compounds (excluding the organic acids) responsible for the flavour were separated from the brines by extraction with diethyl ether and analysed by GC. A determined volume of brine (> 50 ml) was neutralized to pH 7–8 with solid magnesium oxide and the aid of a pH meter and magnetic stirrer. The precipitate was separated by filtration and the filtrate (50 ml) extracted three times with 25-ml portions of diethyl ether, stirring slowly to prevent emulsion formation. An internal standard, 0.5 ml of a dodecane solution in diethyl ether (0.054%), was added to the extract, which was immediately dried over anhydrous sodium sulphate. Most of the solvent was removed *in vacuo* at 30°C and an aliquot (0.2–0.3 μl) of the concentrate injected into the gas chromatograph. The same analytical column was used as in the analysis of volatile acids, under the following operating conditions: carrier gas (nitrogen) flow-rate, 8 ml/min; auxiliary gas flow-rate, 60 ml/min; injector temperature, 120°C; detector temperature, 270°C; oven temperature, 60°C for 4 min, then programmed to 230°C at 4°C/min.

*Volatile and non-volatile acids by high-performance liquid chromatography (HPLC).* The organic acids, both volatile and non-volatile, were monitored together by HPLC using a cation-exchange column (Aminex HPX-87H, 300 × 7.8 mm I.D.) (Bio-Rad Labs.), with a cation-exchange guard column and UV detection at 220 nm. In this instance, sample preparation included only a dilution stage (1:10 with deionized water) followed by passage through a minicolumn containing a cation-exchange resin (2-ml bed of Amberlite IR-120H) to remove $Na^+$. To avoid dilution on being passed through the resin, 6 ml of sample were added and discarded before collecting 2 ml for chromatographic analysis. An aliquot (50 μl) of this fraction was injected into the chromatograph after filtration through a 0.45-μm membrane filter. The analytical column was kept at 65°C during analysis, in which 0.005 *M* $H_2SO_4$ was used as mobile phase at a flow-rate of 0.8 ml/min.

## RESULTS AND DISCUSSION

For the satisfactory use of GC or HPLC in the investigation of food spoilage, it is necessary to compare the compositions of spoiled samples with those of normal samples of the same product lot in order to characterize the spoiled samples [4]. Owing to the difficulty of obtaining brines of zapatera olives with their corresponding unchanged controls, we tried to reproduce spoilage in the laboratory by applying the treatments shown in Table I. An initial exploratory examination of the odd-numbered samples, carried out after 20 days of storage, revealed the presence of the typical zapatera smell in one of them (S5). Moreover, a considerable increase (0.8%) was obtained in the volatile acidity of this sample compared with the remainder, which did not show any apparent signs of spoilage.

TABLE II

PHYSICO-CHEMICAL ANALYSIS AND OTHER OBSERVATIONS OF THE SAMPLES AFTER 40 DAYS OF STORAGE

| Sample | pH | Volatile acid[a] | Colour[b] | "Zapatera" smell[c] |
|---|---|---|---|---|
| S1 | 4.67 | 0.66 | NY | – |
| S2 | 4.67 | 0.66 | NY | – |
| S3 | 5.24 | 0.88 | NY | – |
| S4 | 5.26 | 0.80 | NY | + |
| S5 | 5.39 | 1.58 | NY | ++ |
| S6 | 5.39 | 1.52 | NY | ++ |
| S7 | 4.06 | 0.64 | DY | – |
| S8 | 4.06 | 0.62 | DY | – |
| S9 | 4.24 | 0.66 | DY | – |
| S10 | 4.37 | 0.70 | DY | – |

[a] Expressed as % lactic acid.
[b] NY = Normal Yellow; DY = dark yellow.
[c] – = Not detected; + = intense; ++ = very intense.

*Determination of organic acids and headspace components*

Chemical and chromatographic analyses of the samples were performed after 40 days of storage. Sample S5 and its replicate S6 were detected by smell as clearly spoiled, and brine S4 (but not its replicate) was weakly so. Apart from smell, S5 and S6 were appreciably different from the others in the values of their physico-chemical characteristics pH and volatile acidity, and also in the concentration of some of the compounds determined in this study (Tables II and III). Thus, lactic acid was not detected in the zapatera samples (S5 and S6), which on the other hand showed a large increase in the concentration of the $C_2$–$C_6$ volatile acids. Similar results were obtained by Fleming *et al.* [6] in studies of butyric acid spoilage of fermented cucumber, although the concentrations of the major volatile acids (propionic and butyric acids) were clearly different to those in the zapatera olive brines. Cucumber brine after butyric acid spoilage contained a concentration of butyric acid of about 3500 ppm [6], more then fifteen times as much as in the zapatera samples S5 and S6. The concentration of this acid in the latter samples was similar to that obtained in an abnormal fermentation of sauerkraut, characterized by a "cheese-like" off-odour [7]. In contrast, the concentration of propionic acid in the zapatera samples (*ca.* 10 000 ppm) was much higher than those of both the butyric cucumber brine and off-odour sauerkraut (600 and 7 ppm, respectively). Degradation of lactic acid and concomitant formation of volatile acids in the zapatera samples S5 and S6 caused a rise in pH (Table II) owing to the lower dissociation constants of these acids compared with that of lactic acid, as observed by Borbolla and Re-

TABLE III

DETERMINATION OF LACTIC ACID AND THE VOLATILE $C_2$–$C_6$ FATTY ACIDS AFTER 40 DAYS OF STORAGE

| Sample | Acid (ppm) | | | | | | |
|---|---|---|---|---|---|---|---|
| | Lactic[a] | Acetic[a] | Propionic[b] | *n*-Butyric[b] | Isovaleric[b] | *n*-Valeric[b] | *n*-Caproic[b] |
| S1 | 8750 | 4962 | 1628 | 2.0 | 0.6 | ND[c] | 0.4 |
| S2 | 10882 | 3601 | 1080 | 2.2 | 0.5 | Tr[d] | 0.1 |
| S3 | 5622 | 3920 | 4280 | 1.1 | 0.7 | Tr | 0.2 |
| S4 | 6331 | 3902 | 3896 | 1.2 | 0.8 | Tr | 0.2 |
| S5 | ND | 5550 | 11023 | 225.2 | 2.3 | 292.1 | 8.0 |
| S6 | ND | 5291 | 9462 | 189.0 | 2.1 | 240.3 | 6.4 |
| S7 | 19771 | 3340 | 321 | 0.7 | 0.2 | Tr | 0.1 |
| S8 | 17790 | 3031 | 339 | 1.0 | 0.3 | ND | 0.2 |
| S9 | 17971 | 6162 | 597 | 0.9 | 0.6 | ND | 0.2 |
| S10 | 14972 | 3910 | 443 | 1.4 | 0.7 | ND | ND |

[a] Determined by the HPLC procedure described in the text, using the external standard method.
[b] Determined by the GC procedure described in the text, using the internal standard method.
[c] ND = Not detected.
[d] Tr = Trace amounts (<0.1 ppm).

TABLE IV

DETERMINATION OF THE MAJOR HEADSPACE COMPONENTS OF THE BRINES

| Sample | Compound (ppm) | | | | |
|---|---|---|---|---|---|
| | Acetaldehyde | Methanol | Ethanol | 2-Butanol | *n*-Propanol |
| S1 | 4.2 | 647.7 | 546.6 | 17.0 | 452.9 |
| S2 | 5.1 | 685.2 | 569.1 | 15.3 | 430.5 |
| S3 | 4.7 | 690.1 | 470.5 | 19.0 | 144.8 |
| S4 | 10.9 | 633.5 | 513.9 | 23.8 | 201.5 |
| S5 | 9.3 | 938.9 | ND[a] | 17.9 | ND |
| S6 | 11.8 | 954.3 | ND | 18.9 | ND |
| S7 | 4.5 | 646.2 | 532.4 | 15.3 | 157.1 |
| S8 | 4.8 | 628.1 | 518.0 | 14.7 | 146.1 |
| S9 | 3.3 | 594.3 | 2968.1 | 15.4 | 153.4 |
| S10 | 4.2 | 572.7 | 1962.1 | 14.7 | 149.8 |

[a] ND = Not detected.

jano [8]. $C_4$–$C_6$ fatty acids were also detected in the normal samples, although in small amounts. These were not detected by Delmouzos *et al.* [9], undoubtedly owing to the lower sensitivity of the chromatographic techniques that they used.

Another important difference was observed in the concentration of the major headspace components of the brines (Table IV). The absence of ethanol and *n*-propanol and the larger amounts of methanol and acetaldehyde in the zapatera brines S5 and S6 are noteworthy. In turn, the other (weakly) zapatera sample, S4, did not differ significantly from its replicate S3 with respect to the organic acids and volatile components, except perhaps in the higher concentrations of acetaldehyde and *n*-propanol.

*Comparison of the profiles of organic acids and volatile components.*

In order to find any differences between the normal and the zapatera samples, an examination of the chromatograms of organic acids and headspace components was carried out. In addition, the chromatograms of volatile compounds responsible for flavour (aromagrams) were compared.

*Organic acids (HPLC).* HPLC, using a cation exchange column (Aminex HPX-87H), has been used previously in a qualitative way to obtain profiles of microbial metabolites [10]. The chromatograms obtained as "fingerprints" for the brines S3 and S5 are shown in Fig. 1. The zapatera samples S5 and S6 show distinct characteristics, mainly because of the different concentrations of organic acids. However, the zapatera brine S4 hardly differed from its replicate in this type of analysis, limiting the application of this method for the detection of zapatera spoilage.

*Volatile fatty acids (GC).* The profile of volatile fatty acids obtained by GC presented a peculiarity common to the three zapatera samples that differentiated them clearly from the others, namely an intense peak at a retention time of 35 min (Fig. 2). Apparently the concentration of the compound responsible was directly related to the intensity of the typical smell of the spoilage, with an appreciably smaller area of the peak in sample S4 corresponding to a less intense smell. This "key compound" was identified as cyclohexanecarboxylic acid by GC–MS. When added to normal olive brines, taste panelists at our laboratory remarked that this compound imparted a "zapatera-like" odour to the brine. In addition, a large peak (retention time 35 min) was also detected in all the zapatera brines supplied by industry, but not detected (or detected as a small peak) in the normal samples analysed. This peak can also be attributed to cyclohexanecarboxylic acid, although a mass spectrometric analysis to confirm this point was not carried out.

This is the first report of cyclohexanecarboxylic acid as a constituent of zapatera olives. Additional work is necessary to establish both its detection threshold and its limit of detection by the GC method used. However, it is possible to speculate on the

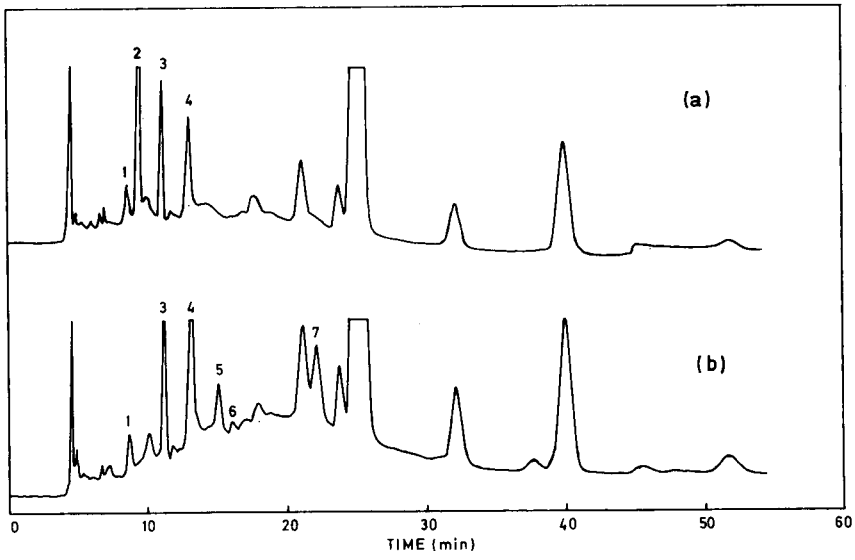


Fig. 1. HPLC of organic acids (Aminex HPX-87H column) from (a) normal brine S3 and (b) zapatera brine S5. Peaks: 1 = succinic acid; 2 = lactic acid; 3 = acetic acid; 4 = propionic acid; 5 = isobutyric acid; 6 = *n*-butyric acid; 7 = *n*-valeric acid.

origin of this compound in zapatera brines. Phenolic compounds from olives appear as constituents in olive brines (0.20–0.35% expressed as caffeic acid) and their concentrations remain almost unchanged during the fermentation process [11]. Anaerobic biodegradation of phenols, using a sewage sludge inoculum, has been reported to produce cyclohexanecarboxylic acid, and several pathways have been proposed to explain this finding [12]. Therefore, it could be that the presence of this acid in zapatera brines is due to biodegradation of phenolic compounds by the anaerobic bacteria involved in this spoilage (*Clostridia* and *Propionibacteria*).

*Headspace components (GC).* Although the profiles of the volatile components of the headspace (Fig. 3) of the zapatera samples S5 and S6 differed appreciably from the rest, mainly owing to the absence of ethanol and *n*-propanol, the fact that no important differences were observed between S3 and S4 limits the application of the method, as in the HPLC method described above. It is necessary to bear in mind that direct injections of a very dilute vapour sample (headspace gas) produce peaks only for those major components which possess relatively high vapour pressures and are present in sufficient amounts to activate the detector [13]. The minor components may also be extremely important in the flavour of a food, and in some instances more important than the major components owing to their lower detection threshold [14]. Therefore, the use of a dynamic method (purge and trap) may be advisable for the analysis of the headspace components, including the minor ones.

*Volatile components (GC).* The high proportions of acetic and propionic acids relative to the amounts of other volatile compounds in olive brine interfere with the separation of the latter components, present only in trace amounts. Consequently, volatile acids were eliminated by neutralization prior to extraction. Magnesium oxide was used as a neutralizing agent, following the procedure of Kahn *et al.* [15]. Fig. 4 shows the gas chromatograms of volatile components extracted with diethyl ether from samples S3 and S6. Addition of an internal standard (*n*-dodecane, as used by Lafuente *et al.* [16] in juices) helped to assign the peaks and allowed checking of the good reproducibility of the method for a future determination of the principal components. No significant ($p<0.05$) differences were found between the ratios of the areas $A$ (peak)/$A$ (dodecane) in three consecutive analyses using the same brine.

Comparison of the chromatograms revealed clear, mainly quantitative, differences in the compo-

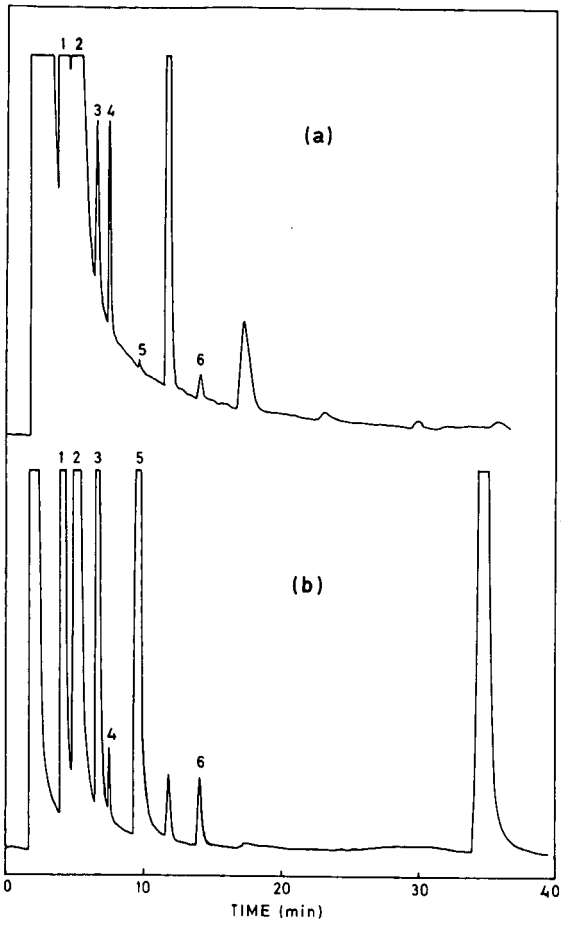


Fig. 2. GC of volatile acids from (a) normal brine S3 and (b) zapatera brine S6. Peaks: 1 = acetic acid; 2 = propionic acid; 3 = *n*-butyric acid; 4 = isovaleric acid; 5 = *n*-valeric acid; 6 = *n*-caproic acid. The last peak in the zapatera sample was identified as cyclohexanecarboxylic acid.

sition of aroma, but at the same time it raised the problem of recognizing, among the many components, that or those specifically associated with the spoilage. To simplify this task, the chromatograms were divided into three well differentiated sections: (A) from the start until 20 min; (B) from 20 until 40 min; (C) from 40 min until the end. The main differences are apparently in section B, and the key substances within it are indicated by numbers (Fig. 4). Comparison of the peak areas of these substances in each of the samples gave the ratios shown in Table V. It can be observed that there are marked differences between the ratios calculated for the zapatera samples (S4, S5 and S6) and those for the unspoiled samples (S2, S3, S7 and S9). The same was seen with brines supplied by different companies (data not shown). Thus, of the zapatera brines analysed, the ratio of components *A* (peak 5)/*A*(peak 2) was never lower than 200, whereas for the normal samples it never exceeded 20. Consequently, this type of study could be of great use for the detection of spoilage, in the same way that it has been applied successfully to the characterization by GC of different varieties of grape [17].

In summary, it is deduced that it is possible to differentiate clearly between as zapatera and a normal olive brine, either from the gas chromatograms of volatile acids or from the gas chromatograms of the volatile components responsible for flavour (aromagrams). Cyclohexanecarboxylic acid, in combination with other volatile acids, seems to be

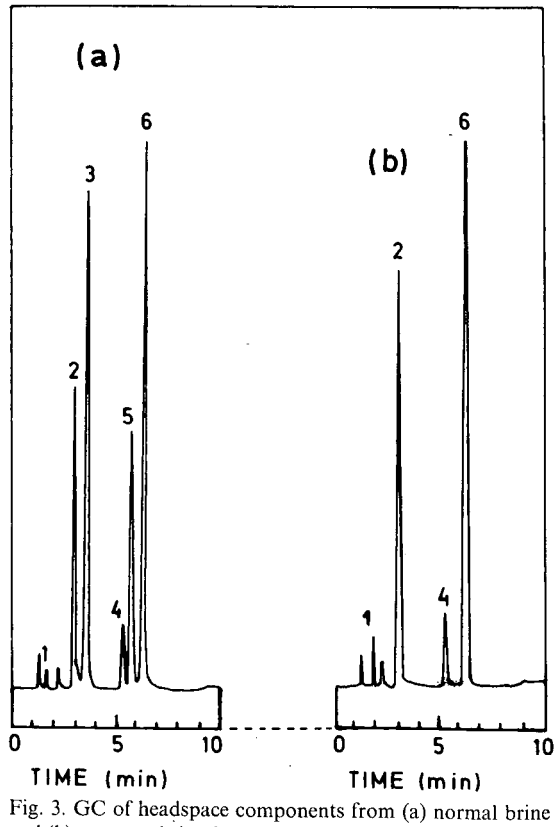


Fig. 3. GC of headspace components from (a) normal brine S3 and (b) zapatera brine S5. Peaks: 1 = acetaldehyde; 2 = methanol; 3 = ethanol; 4 = 2-butanol; 5 = *n*-propanol; 6 = dioxane (internal standard).

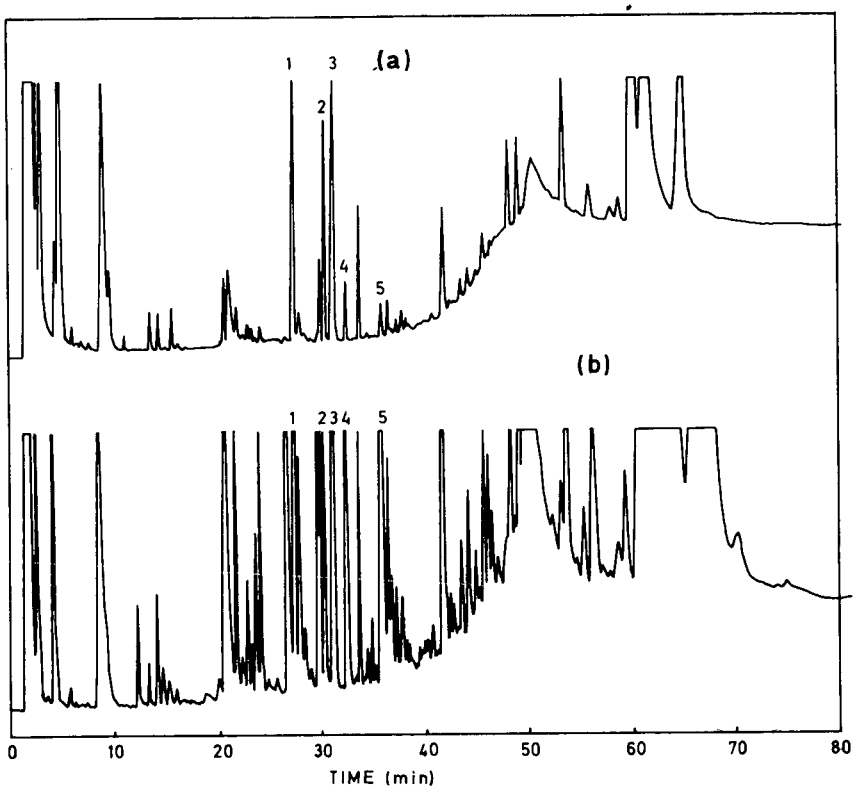


Fig. 4. GC of volatile components extracted with diethyl ether from (a) normal brine S3 and (b) zapatera brine S6. The numbered peaks correspond to the selected key compounds.

responsible for the unpleasant, typical smell of zapatera olives. This suggests that the determination of this compound by GC could be used to check the quality of suspect samples at the point of purchase. This would undoubtedly help to detect possible commercial fraud in which there is an attempt to mask spoilage either by dilution or by addition of aroma-giving substances.

ACKNOWLEDGEMENTS

The authors thank J. L. Rios for the mass spectrometric analysis and interpretations. A. M. is grateful to the Ministerio de Educación y Ciencia of the Spanish Government for a grant (Beca de Perfeccionamiento para Doctores y Tecnólogos). This work is part of the research project ALI88-01151-

TABLE V

RATIOS CALCULATED FROM THE PEAK AREAS OF SELECTED KEY COMPONENTS

Ratio of area × 100.

| Ratio of components[a] | Sample | | | | | | |
|---|---|---|---|---|---|---|---|
| | S2 | S3 | S4 | S5 | S6 | S7 | S9 |
| 5:1 | 20 | 10 | 270 | 1960 | 690 | 4 | 1 |
| 5:2 | 50 | 20 | 480 | 2320 | 3780 | 15 | 17 |
| 5:3 | 30 | 10 | 350 | 1160 | 2100 | 6 | 7 |
| 5:4 | 180 | 70 | 2220 | 390 | 790 | 60 | 60 |

[a] Peak numbers shown in Fig. 4.

CO2-01 supported by the Spanish Government through CICYT.

REFERENCES

1 ACEMESA, XXIV Asamblea de Miembros del Instituto de la Grasa y sus Derivados, Seville, May 1990.
2 M. J. Fernández Díez, Biotecnología de la Aceituna de Mesa, CSIC Seville, 1985.
3 R. H. Vaughn, in J. G. Carr, C. V. Cutting and G. C. Whiting (Editors), *Lactic Acid Bacteria in Beverages and Food*, Academic Press, New York, 1975, Ch. V. 3, P. 307.
4 M. J. Eyles and R. F. Adams, *Int. J. Food Microbiol.*, 3 (1986) 321.
5 A. Montaño, A. H. Sánchez and L. Rejano, *J. Chromatogr.* 521 (1990) 153.
6 H. P. Fleming, M. A. Daeschel. R. F. McFeeters and M. D. Pierson, *J. Food Sci.*, 54 (1989) 636.
7 M. L. Vorbeck, L. R. Mattick, F. A. Lee and C. S. Pederson, *J. Food Sci.*, 26 (1961) 569.
8 J. M. R. Borbolla and L. Rejano, *Grasas Aceites*, 32 (1981) 103.
9 J. G. Delmouzos, F. H. Stadtman and R. H. Vaughn, *J. Agric. Food Chem.*, 1 (1953) 333.
10 R. F. Adams, R. L. Jones and P. L. Conway, *J. Chromatogr.*, 336 (1984) 125.
11 A. Vazquez Roncero and M. L. Janer del Valle, *Grasas Aceites*, 29 (1978) 23.
12 A. W. Obayashi and J. M. Gorgan, *Management of Industrial Pollutants by Anaerobic Processes*, Lewis, Chelsea, MI, 1985.
13 W. G. Jennings and M. Filsoof, *J. Agric. Food Chem.*, 25 (1977) 440.
14 D. A. Cronin, in I.D. Morton and A. J. MacLeod (Editors), *Techniques of Analysis of Flavours –Food Flavours, Part A Introduction*, Elsevier, Amsterdam, 1982, Ch. IIa.
15 J. H. Kahn, G. B. Nickol and H. A. Conner, *J. Agric. Food Chem.* 20 (1972) 214.
16 B. Lafuente, J. Benedito, A. Mansanet and M. I. Nadal, *Rev. Agroquim. Tecnol. Aliment.*, 16 (1976) 89.
17 A. Rapp, H. Hastrich, L. Engel and W. Knipser, in G. Charalambous and G. E. Inglett (Editors), *Flavor of Foods and Beverages –Chemistry and Technology*, Academic Press, New York, 1978, Ch. 25, p. 391.

*Journal of Chromatography*, 594 (1992) 269–273
Elsevier Science Publishers B.V., Amsterdam

CHROM. 23 923

# Gas chromatographic elution patterns of chlorinated dioxins *versus* column polarity

Joseph R. Donnelly*

*Lockheed Engineering & Sciences Co., 1050 E. Flamingo Road, Las Vegas, NV 89119 (USA)*

G. Wayne Sovocool

*US Environmental Protection Agency, P.O. Box 93478, Las Vegas, NV 89193-3478 (USA)*

(Received September 20th, 1991)

ABSTRACT

A model has been developed which successfully predicts the order of elution and relative retentions of tetra-, penta- and hexachlorodibenzo-*p*-dioxins for gas chromatography (GC) columns of different polarity. These congeners include the most toxic 2,3,7,8-substituted isomers, and contain numerous difficult-to-separate isomers. This model allows the correlation of GC retention time to dioxin substitution pattern. The model also allows the prediction of dioxin elution order and relative retention time spacing for GC columns of different polarity.

## INTRODUCTION

Environmental monitoring for chlorinated dibenzo-*p*-dioxins (PCDDs) is considered important, since many toxicological studies have demonstrated their potential toxicity, especially that of 2,3,7,8-tetrachlorodibenzo-*p*-dioxin (2,3,7,8-TCDD) [1,2]. Isomer-specific analyses of the 75 PCDDs by gas chromatography–mass spectrometry (GC–MS) have traditionally employed both very slightly polar GC columns (J&W DB-5, Restek $RT_x$-5, etc.) and highly polar columns (Supelco SP-2330, SP-2340, Restek $RT_x$-2330, etc.) [3–6]. The choice of GC column is important because the electron impact mass spectra of PCDDs are specific for level of halogenation but are not isomer specific. Therefore, isomer specificity results from the use of a GC column which maximizes the separation of the PCDD isomers within each congener group. The slightly polar GC column type allows elution of all congeners within a short analysis time while giving good separation of most isomers from each other. Highly polar GC columns are applied primarily to maximize the separation of 2,3,7,8-TCDD from the other 21 TCDDs, at the expense of longer analysis times and less column durability. It has been known for some time that the elution order of the PCDDs vary between the two column types, but these elution order changes were not quantified, so that a column having optimum polarity for separating other isomers could be developed efficiently. Recently it has been agreed internationally that those congeners having 2,3,7,8-substitution should be separately quantified for risk assessment [1]. These individual congeners [1 of 22 TCDDs; 1 of 14 pentachlorodibenzo-*p*-dioxins (PeCDDs); 3 of 10 hexachlorodibenzo-*p*-dioxins (HxCDDs); 1 of 2 heptachlorodibenzo-*p*-dioxins (HpCDDs), and octachlorodibenzo-*p*-dioxin (OCDD)] were assigned Toxicity Equivalency Factors (TEF) of 1, 0.5, 0.1, 0.01 and 0.001 for the TCDD, PeCDD, HxCDDs, HpCDD and OCDD, respectively [2]. Because of this development, it is worthwhile to develop a model for predicting elution profiles on new GC

0021-9673/92/$05.00 

TABLE I

SCALED RELATIVE RETENTION INDICES (SRRI) FOR PCDDs AND MOLECULAR SHIFT INDICES (SI) FOR CHANGES IN GC COLUMN POLARITY

M = Compound selected to develop the SI model.

| Congener | SRRI | | SI | | ΔSI exptl. − calcd. |
|---|---|---|---|---|---|
| | DB-5 | SP-2330/ SP-2340 | exptl. | calcd. | |
| 1,3,6,8 | 0 | 0 | 0 | M (1,3) | |
| 1,3,7,9 | 10 | 12 | 2 | 6 | −4 |
| 1,3,6,9 | 18 | 31 | 13 | 14 | −1 |
| 1,2,4,7 | 36 | 31 | −5 | M (2) | |
| 1,2,4,8 | 36 | 31 | −5 | −5 | 0 |
| 1,3,7,8 | 36 | 23 | −13 | −12 | −1 |
| 1,4,6,9 | 37 | 66 | 29 | M (1,4) | |
| 1,2,4,6 | 41 | 48 | 7 | 5 | 2 |
| 1,2,4,9 | 41 | 48 | 7 | 5 | 2 |
| 1,2,6,8 | 43 | 37 | −6 | −2 | −4 |
| 1,4,7,8 | 46 | 43 | −3 | −4 | 1 |
| 1,2,7,9 | 54 | 52 | −2 | 4 | −6 |
| 1,2,3,4 | 65 | 47 | −18 | M (unsub.) | |
| 1,2,3,6 | 64 | 52 | −12 | M (1) | |
| 1,2,6,9 | 64 | 73 | 9 | 12 | −3 |
| 1,2,3,7 | 67 | 48 | −19 | −16 | −3 |
| 1,2,3,8 | 67 | 48 | −19 | −16 | −3 |
| 2,3,7,8 | 70 | 45 | −25 | M (2,3) | |
| 1,2,3,9 | 74 | 68 | −6 | M (1,9) | |
| 1,2,7,8 | 79 | 65 | −14 | −14 | 0 |
| 1,2,6,7 | 82 | 78 | −4 | M (1,2) | |
| 1,2,8,9 | 100 | 100 | 0 | | |
| 1,2,4,6,8 | 0 | 0 | 0 | | |
| 1,2,4,7,9 | 0 | 0 | 0 | | |
| 1,2,4,6,9 | 19 | 47 | 28 | 21 | 7 |
| 1,2,3,6,8 | 31 | 12 | −19 | −10 | −9 |
| 1,2,4,7,8 | 36 | 25 | −11 | M (1,2,4) | |
| 1,2,3,7,9 | 44 | 33 | −11 | −4 | −7 |
| 1,2,3,6,9 | 51 | 60 | 9 | 4 | 5 |
| 1,2,4,6,7 | 56 | 63 | 7 | 5 | 2 |
| 1,2,4,8,9 | 56 | 63 | 7 | 5 | 2 |
| 1,2,3,4,7 | 64 | 48 | −16 | −21 | 5 |
| 1,2,3,4,6 | 70 | 72 | 2 | −11 | 13 |
| 1,2,3,7,8 | 78 | 56 | −22 | M (1,2,3) | |
| 1,2,3,6,7 | 85 | 75 | −10 | −12 | 2 |
| 1,2,3,8,9 | 100 | 100 | 0 | | |
| 1,2,4,6,7,9 | 0 | 0 | 0 | | |
| 1,2,4,6,8,9 | 0 | 0 | 0 | | |
| 1,2,3,4,6,8 | 29 | 0 | −29 | −9 | −20 |
| 1,2,3,6,7,9 | 43 | 23 | −20 | −3 | −17 |
| 1,2,3,6,8,9 | 43 | 23 | −20 | −3 | −17 |
| 1,2,3,4,6,9 | 52 | 66 | 14 | 5 | 9 |
| 1,2,3,4,7,8 | 69 | 42 | −27 | M (1,2,3,4) | |
| 1,2,3,6,7,8 | 76 | 46 | −30 | −20 | −10 |
| 1,2,3,7,8,9 | 82 | 81 | −1 | −14 | 13 |
| 1,2,3,4,6,7 | 100 | 100 | 0 | | |

column types, so that optimum separations of those congeners having assigned TEF values could be achieved with minimum column development and testing. Additionally, for quality assurance, data obtained on one type of column could be more readily compared with data from another type, even if a limited number of standards were employed in the analyses.

## EXPERIMENTAL

Data were selected from available literature [3–7] for the $Cl_4$, $Cl_5$ and $Cl_6$ congener groups and the reported chromatograms were labelled so that retention times were expressed on a 0–100 scale, with the first eluting isomer set at 0 and the last eluting isomer of that congener group set at 100. DB-5 is a relatively non-polar GC column phase. SP-2330 and the very similar SP-2331, SP-2340 are highly polar phases. Compounds chosen for the shift index (SI) model are indicated in Table I. Where appropriate, 2,3,7,8-substituted congeners were selected; these congeners are those of greatest interest, and for which the most reliable standards are available. Elution of TCDDs from DB-1701 and DB-225 columns were also modelled in the same way. TCDD isomer assignments (1,2,6,8-, 1,2,7,8- and 1,2,7,9-TCDD) were corrected where necessary [7,8].

## DISCUSSION

The DB-5 and SP-2330 types of phases are frequently employed for dioxin analysis, and data are readily available in the literature. However, a model correlating dioxin substitution pattern to GC retention index ($I$) has been reported only for non-polar columns [7–9]. Because such a model is useful for isomer identifications, it was deemed worthwhile to extend this structure–$I$ modelling concept to the popular SP-2330 polar types of GC columns. Both non-polar and polar phases were chosen in this study to model the relative retention time (RRT) shifts with change in column polarity. Susceptibility to RRT shifts was modelled for the TCDDs, PeCDDs and HxCDDs. These congener groups include the congeners having the highest assigned TEFs, and these congener groups have sufficiently large numbers of isomers to make modelling valuable. Because the normally employed GC column temperature programs have varied widely among column types and individual analyses, the RRTs were normalized, for each congener group addressed in this study, to a range of 0–100. In this way, a standardized scale for the isomers' RRTs was achieved for the various temperature programs utilized, and isomer shifts relative to each other could be quantified, independent of the GC temperature program. Since the first and last eluting isomers were found to remain the same regardless of GC column polarity, this strategy provided a means of determining the magnitudes of isomer RRT shifts within the congener elution profile, as column polarity was varied.

Shifts in scaled relative retention indices (SRRIs)

TABLE II

SINGLE RING SHIFT INDEX (SRSI) VALUES TO CONVERT SRRI FOR DB-5 TO SRRI FOR SP-2330 COLUMN PHASES

| Single ring substitution pattern | Calculation process: [SRRI]/2 or [SRRI] − [SRSI] | SRSI |
|---|---|---|
| 1− | [1,2,3,6] − [1,2,3−] = −12 − (−10) | −2 |
| 2− | [1,2,4,7] − [1,2,4−] = −5 − 1 | −6 |
| 1,2− | [1,2,6,7]/2 = −4/2 | −2 |
| 1,3− | [1,3,6,8]/2 = 0/2 | 0 |
| 1,4− | ([1,4,6,9]-2RRI)/2 = (29 − 12)/2 | +8 |
| 2,3− | [2,3,7,8]/2 = −25/2 | −12 |
| 1,2,4− | [1,2,4,7,8] − [2,3−] = −1 − (−12) | +1 |
| 1,2,3− | [1,2,3,7,8] − [2,3−] = −22 − (−12) | −10 |
| 1,2,3,4− | [1,2,3,4,7,8] − [2,3−] = −27 − (−12) | −15 |
| Unsubstituted | [1,2,3,4] − [1,2,3,4−] = −18 − (−15) | −3 |
| 1,9-Ring–ring interaction (RRI) | [1,2,3,9] − [1,2,3,6] = −6 − (−12) | +6 |

TABLE III

SCALED RELATIVE RETENTION INDICES FOR DIFFERENT POLARITY COLUMN PHASES

| PCDD Isomer | SRRI | | | |
|---|---|---|---|---|
| | DB-5 | DB-1701 | DB-225 | SP-2330/SP-2331/ SP-2340 |
| 1,3,6,8 | 0 | 0 | 0 | 0 |
| 1,3,7,9 | 10 | 10 | 10 | 12 |
| 1,3,6,9 | 18 | 23 | 28 | 31 |
| 1,2,4,7 | 36 | 34 | 32 | 31 |
| 1,2,4,8 | 36 | 34 | 32 | 31 |
| 1,3,7,8 | 36 | 30 | 23 | 23 |
| 1,4,6,9 | 37 | 49 | 59 | 66 |
| 1,2,4,6 | 41 | 44 | 48 | 48 |
| 1,2,4,9 | 41 | 44 | 48 | 48 |
| 1,2,6,8 | 43 | 41 | 39 | 37 |
| 1,4,7,8 | 46 | 44 | 43 | 43 |
| 1,2,7,9 | 54 | 53 | 52 | 52 |
| 1,2,3,4 | 65 | 57 | 51 | 47 |
| 1,2,3,6 | 64 | 59 | 54 | 52 |
| 1,2,6,9 | 64 | 67 | 71 | 73 |
| 1,2,3,7 | 67 | 57 | 49 | 48 |
| 1,2,3,8 | 67 | 59 | 51 | 48 |
| 2,3,7,8 | 70 | 57 | 45 | 45 |
| 1,2,3,9 | 74 | 72 | 68 | 68 |
| 1,2,7,8 | 79 | 72 | 66 | 65 |
| 1,2,6,7 | 82 | 82 | 81 | 78 |
| 1,2,8,9 | 100 | 100 | 100 | 100 |
| 1,2,4,6,8 | 0 | | 0 | 0 |
| 1,2,4,7,9 | 0 | | 0 | 0 |
| 1,2,4,6,9 | 19 | | 41 | 47 |
| 1,2,3,6,8 | 31 | | 15 | 11 |
| 1,2,4,7,8 | 38 | | 26 | 23 |
| 1,2,3,7,9 | 44 | | 32 | 30 |
| 1,2,3,6,9 | 52 | | 56 | 59 |
| 1,2,4,6,7 | 56 | | 62 | 62 |
| 1,2,4,8,9 | 56 | | 62 | 64 |
| 1,2,3,4,7 | 65 | | 50 | 47 |
| 1,2,3,4,6 | 69 | | 71 | 71 |
| 1,2,3,7,8 | 78 | | 56 | 53 |
| 1,2,3,6,7 | 86 | | 77 | 74 |
| 1,2,3,8,9 | 100 | | 100 | 100 |
| 1,2,4,6,7,9 | 0 | | 0 | 0 |
| 1,2,4,6,8,9 | 0 | | 0 | 0 |
| 1,2,3,4,6,8 | 29 | | 6 | 0 |
| 1,2,3,6,7,9 | 43 | | 26 | 24 |
| 1,2,3,6,8,9 | 43 | | 26 | 25 |
| 1,2,3,4,6,9 | 50 | | 60 | 68 |
| 1,2,3,4,7,8 | 78 | | 47 | 43 |
| 1,2,3,6,7,8 | 83 | | 53 | 47 |
| 1,2,3,7,8,9 | 100 | | 81 | 80 |
| 1,2,3,4,6,7 | 100 | | 100 | 100 |

for the TCDDs, PeCDDs and HxCDDs were described with reference to the substitution patterns of the single rings, as has been reported for calculating retention indices on non-polar and very slightly polar GC columns for the PCDDs [7]. As shown in Tables I and II, shifts to higher RRTs occurred, as column polarity increased, with the 1,4 and 1,2,4 single rings, and with the presence of 1,9-dichloro ring–ring interactions (RRI). The unsubstituted and the 1-, 2-, 1,2-, 2,3-, 1,2,3- and 1,2,3,4-chlorine-substituted single rings shortened RRTs as column polarity increased. For the compounds not used in developing this model, RRT shifts were calculated using the model; in general, very good agreements were obtained between predicted and observed values, with variations of the same magnitude as that observed between different data sets using these GC column phases. The fits of calculated to experimental SRRI were best for the TCDDs; RRT predictions for the TCDDs are perhaps the most useful, because the number of isomers is greatest. Fewer HxCDD data were available for comparison and validation of published isomer assignments *vs.* GC retention times. Additionally, some temperature programs used for measuring those data terminated before elution of all HxCDDs; retention time–index modelling is more accurate for isomers eluting during the linear temperature program ramp. These situations may have caused the fits of predicted to observed SI values to be somewhat poorer for the HxCDDs. Quantitative single ring shift index (SRSI) values for the single rings and for the 1,9-dichloro ring–ring interaction are shown in Table II. The SI value for a dioxin molecule in SRRI units which is observed for a PCDD upon changing GC column phase may thus be expressed as the sum of contributions from the SRSI of the single rings plus that of the 1,9-ring–ring intereaction effect, if applicable.

Values of SRRI were calculated for the TCDD isomers on intermediate polarity columns, DB-1701 and DB-225 (see Table III), using reported retention time data [6]. These columns have intermediate levels (14% and 50%, respectively) of cyanopropylphenyl substituents in their liquid phases to increase column polarity, as compared to 0% and 68% for DB-5 and SP-2330, respectively. Elution profiles of the TCDDs on DB-1701 and DB-225 were also intermediate, as would be expected, between the

DB-5 and SP-2330 elution profiles. The SRRI shifts from one column type to another agreed well with these increases in phase polarity. The results obtained with these two columns will facilitate the estimation of SI values for other GC columns. The SRRI values were also calculated for DB-5, SP-2331, and DB-225 phases for PeCDDs and HxCDDs (see Table III) from recently reported data [8]. These data for SP-2331 agreed well with the data for the very similar SP-2330 and SP-2340 columns. One retention data were scaled into SRRI units, the various data sets were found to be in close agreement for a given column type (entries generally + 2 SRRI units).

## CONCLUSIONS

The 1,4 and 1,2,4 single rings and 1,9 ring/ring interactions tended to shift the relative retention times to higher normalized values with increasing GC column polarity. The 1-, 2-, 1,2-, 2,3-, 1,2,3- and 1,2,3,4-substituted (chlorinated) single rings tended to shift the isomers to lower normalized relative retention times with increased GC column polarity. These effects were quantifiable with good precision across the different analyses, temperature programs, and GC columns utilized and reported by various investigators, and applied to this study. This SI model allows the extension of a structure–*I* model for chlorinated dioxins from the DB-5 type GC column to other types of GC columns. With this SI model, retention indices of the 2,3,7,8-substituted congeners can be calculated. Knowledge of these retention indices facilitates environmental monitoring by GC–MS for the congeners having assigned TEF values. Elution order and spacing of dioxin isomers within a congener series (TCDDs, PeCDDs or HxCDDs) can be predicted for GC columns of different polarity by the application of this modelling technique.

## NOTICE

Although the research described in this article has been funded wholly or in part by the Environmental Protection Agency under contract 68-CO-0049 to Lockheed Engineering & Sciences Co., it has not been subject to the Agency's review and therefore does not necessarily reflect the views of the Agency, and no official endorsement should be inferred. Mention of trade names or commercial products does not constitute an endorsement for use.

## REFERENCES

1 *International Toxicity Equivalency Factor (I-TEF) Method of Risk Assessment for Complex Mixtures of Dioxins and Related Compounds, Report No. 176*, North Atlantic Treaty Organization, Committee on the Challenges of Modern Society (NATO/CCMS), Brussels, 1988.
2 J. S. Bellin, D. G. Barnes, F. W. Kutz and D. P. Bottimore, *Interim Procedures for Estimating Risks Associated with Exposures to Mixtures of Chlorinated Dibenzo-p-Dioxins and -Dibenzofurans (CDDs and CDFs) and 1989 Update, Document No. EPA/625/3-89/016*, U. S. Environmental Protection Agency, Risk Assessment Forum, Washington, DC, March 1989.
3 G. Choudhary, L. H. Keith and C. Rappe (Editors), *Chlorinated Dioxins and Dibenzofurans in the Total Environment*, Butterworth, Boston, MA, 1983.
4 L. H. Keith, C. Rappe and G. Choudhary (Editors), *Chlorinated Dioxins and Dibenzofurans in the Total Environment II*, Butterworth, Boston, MA, 1985.
5 H. Y. Tong, S. Arghestani, M. L. Gross and F. W. Karasek, *Chemosphere*, 18 (1989) 577.
6 L. A. Harden, J. H. Garrett, J. G. Solch, T. O. Tiernan, D. J. Wagel and M. L. Taylor, *Chemosphere*, 18 (1989) 85.
7 J. R. Donnelly, W. D. Munslow, R. K. Mitchum and G. W. Sovocool, *J. Chromatogr.*, 392 (1987) 51.
8 J. J. Ryan, H. B. S. Conacher, L. G. Panopio, B. P.-Y. Lau, J. A. Hardy and Y. Masuda, *J. Chromatogr.*, 541 (1991) 131.
9 J. R. Donnelly, W. D. Munslow, A. H. Grange, T. L. Pettit, R. D. Simmons and G. W. Sovocool, *J. Chromatogr.*, 540 (1991) 293.

*Journal of Chromatography*, 594 (1992) 275–282
Elsevier Science Publishers B.V., Amsterdam

CHROM. 23 781

# Determination of $Pb^{2+}$ in water by isotope dilution gas chromatography–mass spectrometry of tetraethyllead formed by reaction with sodium tetraethylborate

B. J. Feldman, H. Mogadeddi and J. D. Osterloh*

*Department of Laboratory Medicine, Center for Occupational and Environmental Health, University of California/San Francisco, San Francisco General Hospital Toxicology Laboratory, Ward 35, 1001 Potrero Ave., San Francisco, CA 94110 (USA)*

(First received July 12th, 1991; revised manuscript received September 30th, 1991)

ABSTRACT

Aqueous $Pb^{2+}$ samples in the low ng/g concentration range were spiked with stable isotope $^{206}Pb$ standards and subsequently ethylated by a simple room-temperature reaction with sodium tetraethylborate. After extraction into heptane, samples were analyzed by gas chromatography–mass spectrometry on a bench-top quadrupole instrument. Detection was performed by single ion monitoring at *m/z* 293 (triethyl-$^{206}Pb$ ion) and 295 (triethyl-$^{208}Pb$ ion). The technique is rapid, convenient and has good linearity over the tested concentration range of 0.5–100 ng/g. Internal standardization by stable isotope dilution improves the relative standard deviation (for 20–50 ng/g samples) from 24.9% (for externally calibrated determinations) to 4.2% for intra-assay precision and from 35.0% to 8.7% for inter-assay precision. The $^{206}Pb$ internal standard also discriminates against interference by other metals. The detection limit ($3\sigma$) of 0.3 ng/g (for a 2-ml sample) is due primarily to the large relative standard deviation of the blank. Applications to biological matrices are discussed.

## INTRODUCTION

Lead in drinking water is a priority pollutant and the EPA standard is 50 ng/g. Epidemiological evidence has suggested that low levels of blood lead due to environmental exposure (air, water, diet) may be associated with health risks [1–3]. Reassessment of the water standard is being considered [4].

The standard methods for determination of aqueous lead are atomic absorption spectrometry (AAS) and anodic stripping voltammetry (ASV). Although fairly sensitive, these methods can require extensive calibration procedures and, depending on the amount of sample workup required, can be prone to contamination.

Recently, the determination of lead and its ionic alkylated derivatives was performed following ethylation with sodium tetraethylborate (STEB) [5–8]. For $Pb^{2+}$ ion, the derivatization reaction stoichiometry is as follows [9]:

$$2Pb^{2+} + 4B(C_2H_5)_4^- \rightarrow Pb + Pb(C_2H_5)_4 + 4B(C_2H_5)_3 \quad (1)$$

The tetraethyllead (TEL) thus formed was subsequently volatilized and measured by AAS. Rapsomanikis *et al.* [5] pioneered this method for alkyllead ions. Using *in situ*, aqueous STEB ethylation followed by purging, trapping, thermal desorption and subsequent AAS analysis, they were able to obtain an absolute detection limit of 8.7 pg for $(CH_3)_3Pb^+$. Inorganic and organic lead ions have also been determined by liquid chromatography as their tetramethylenedithiocarbamate complexes, followed by postcolumn STEB ethylation [6]. Sturgeon *et al.* [7] were able to determine $Pb^{2+}$ at pg/g levels (in a 10-ml sample) by ethylation and *in situ* concentration in a graphite furnace [7]. Other workers have reported the determination of Sn, Hg, Se, Ge [8] and Cd [10] by ethylation with STEB, although the

0021-9673/92/$05.00 

molecular structure of the derivative formed is not clear in all instances.

Ethylation of $Pb^{2+}$ by STEB to form TEL for subsequent analysis is an analytically useful reaction for a number of reasons. Ethylation can be conveniently performed in aqueous solutions, as opposed to alkylation by Grignard reagents, which cannot be performed in water. TEL is volatile, and amenable to gas chromatography, which can be used to remove interfering metals and organics. Also, TEL is virtually absent as a laboratory contaminant, and therefore once the analyte solutions have been ethylated, the chances for subsequent $Pb^{2+}$ contamination are greatly reduced.

To date, lead determinations using STEB ethylation have relied on AAS detection. The mass spectrometer is an attractive, alternative detector. Single ion monitoring (SIM) provides excellent sensitivity, and the isotope dilution method [11–13] is unique in providing an internal standard with chemical reactivity identical with that of the species of interest. In addition, the proliferation of inexpensive bench-top gas chromatographic–mass spectrometric (GC–MS) instruments makes this method of detection attactive for many laboratories.

We present here a method for the determination of $Pb^{2+}$, without preconcentration, in the low ng/g range, based on isotope-dilution GC–MS detection of TEL produced by ethylation with an aqueous STEB solution. The method is rapid, accurate and precise, requires less than 1 ml of sample and utilizes commonly available equipment and materials. In addition, the relatively simple sample workup and the nature of the ethylation process render this method less vulnerable to $Pb^{2+}$ contamination, an omnipresent consideration with this ubiquitous metal. Common sources of contamination were studied and are discussed. It is demonstrated that, under our reaction conditions, the isotope dilution technique discriminates against fluctuations in absolute recovery, as the $^{206}Pb$ internal standard behaves in a chemically identical manner to analyte $Pb^{2+}$. The result is enhanced precision and accuracy.

## EXPERIMENTAL

### *Materials*

Reverse osmosis/deionized (RO/DI) water with a resistivity of 18 MΩ/cm was prepared using a Millipore (Bedford, MA, USA) Milli-Q system. A 1% (w/w) solution of STEB (Alfa, Dandridge, MA, USA) was prepared fresh daily. Special care was taken to protect the integrity of this reagent. Factory-sealed (under argon), the STEB was opened in an argon-filled glove-bag and decanted into preweighed, acid-cleaned, darkened glass vials. The vials were sealed with crimp-tops and septa before being retrieved from the glove-bag, then re-weighed and refrigerated. Aqueous 1% STEB reagent was prepared by adding the appropriate amount of water to a preweighed STEB-containing vial. Considerable variability was observed in the reactivity of factory-fresh STEB.

A lead standard solution of mixed isotopic composition (1015 ng/g) was prepared by dilution of a 1015 μg/g spectroscopic standard (Aldrich, Milwaukee, WI, USA). A $^{206}Pb$ standard solution (1000 ng/g) was prepared by dissolution of isotopically enriched $PbCO_3$ (99.66% $^{206}Pb$) (ORNL, Oak Ridge, TN, USA) in 1% conc. nitric acid (Seastar Chemical, Vancouver, Canada; lead concentration = 12 pg/g). The level of $^{208}Pb$ contamination in the $^{206}Pb$ was 0.05%. Heptane (Mallinckrodt, St. Louis, MO, USA) was of analytical-reagent grade. A 0.68 *M* acetate buffer (pH 4.38) was prepared from ultra-clean 2 *M* ammonium acetate solution (Dionex, Sunnyvale, CA, USA; Pb < 0.5 ng/g), concentrated-nitric acid and RO/DI water. Tetraethyllead (TEL) standard was from NIST (Gaithersburg, MD, USA) Standard Reference Material (SRM) 2712 (11.4 ± 0.4 μg/g Pb).

Isotopic abundances for the mixed isotopic lead sample were measured by STEB ethylation of a 92.3 ng/g sample, followed by gas chromatography and SIM detection of *m/z* values 291, 293, 294 and 295, corresponding to the triethyl derivatives (see below) of $^{204}Pb$, $^{206}Pb$, $^{207}Pb$ and $^{208}Pb$, respectively. The measured abundances of triethyllead isotopes were corrected for mass contributions due to $^{13}C$ in order to yield true isotopic abundances of 0.514 for $^{208}Pb$ and 0.256 for $^{206}Pb$.

### *Sample handling*

Polyethylene tubes (5 ml) and pipette tips were washed with 10% conc. nitric acid (overnight or longer), then rinsed at least three times with RO/DI water. GC syringes were rinsed with analytical-reagent grade methanol (Mallinckrodt), then at least

three times with sample, prior to sample injection. All samples and reagents were dispensed inside a Sterigard (Baker, Sanford, Me) positive-flow hood with HEPA filter.

*Gas chromatography–mass spectrometry*

GC of TEL in heptane was performed on a Hewlett-Packard Model 5890 gas chromatograph equipped with a 25 m × 0.2 mm I.D. HP-5 (0.11-μm film thickness) capillary column. The carrier gas (helium) flow-rate was 0.6 ml/min and the injector temperature was 150°C. The initial column temperature was 50°C, which was maintained for 5 min then increased at 20°C/min to a final temperature of 120°C. Under these conditions, TEL eluted at 8.3 minutes (106°C).

TEL detection was performed with an HP 5971A mass-selective detector in the electron impact ionization mode. The transfer line and mass spectrometer ionization source were maintained at 280°C. Single ion monitoring was performed simultaneously at $m/z$ ratios of 293 (triethyl-$^{206}Pb^+$) and 295 (triethyl-$^{208}Pb^+$) at dwell times of 250 ms for each ion. The instrument was calibrated for masses of 69, 219 and 502 with perfluorotributylamine. This detector is capable of a resolution of 1 u. The ionization voltage was 70 eV.

*Standard procedure*

A lead-containing aqueous sample (0.5–2 ml) was placed in a clean polyethylene tube, 10 μl of 0.68 *M* acetate buffer (pH 4.38) and 10 μl of 1000 ng/g $^{206}Pb$ standard were added and the tube was vortex-mixed. A 300-μl volume of heptane and 10 μl of a 1% STEB solution were added and the tube was capped and shaken for 30 min at room temperature. A 100-μl volume of the (TEL-containing) heptane phase was withdrawn and placed in a 2-ml glass vial, which was then septa-sealed. The heptane extracts TEL, but not STEB. Therefore, after reaction with STEB, the TEL-containing heptane phase is relatively invulnerable to contamination as background environmental levels of TEL are low. A 1-μl volume of the heptane phase was injected onto the GC–MS column for analysis.

Sample lead concentrations were calculated as follows (all lead concentrations are in ng/g):

$$\text{total Pb} = \frac{C_{208}}{0.514} = \frac{P_{208}\,C_{206}\,MR}{0.514(P_{206} - P_{208}\cdot 0.256/0.514)} \quad (2)$$

where $C_{208}$ is the concentration of $^{208}Pb$ in the unspiked sample, $C_{206}$ is the concentration of $^{206}Pb$ added to the sample (after correction for volume change), $P_{206}$ and $P_{208}$ are the natural isotopic peak areas (corrected for effects due to the presence of $^{13}C$) from SIM–GC–MS, 0.514 and 0.256 are the measured abundances of $^{208}Pb$ and $^{206}Pb$ in the sample, respectively, and $MR$ is the mass ratio of $^{208}Pb/^{206}Pb$ (1.0097). The contribution of $^{208}Pb$ as an impurity (0.05%) in the $^{206}Pb$ standard was ignored.

*Methods validation*

The accuracy was assessed by addition of premeasured amounts of 1015 or 101.5 ng/g lead standard solution (prepared by dilution of the 1015 μg/g standard) to RO/DI water to give solutions of known lead concentrations. The standard procedure (see above) as applied to these solutions gave a measured lead concentration ($Pb_{meas}$) which was compared with the calculated amount of Pb ($Pb_{added}$) added to the solution. Each concentration was determined in triplicate.

Single-sample (instrumental) precision was determined by repeated injection ($n = 10$) of a single preparation from a 40.6 ng/g sample. Intra-assay precision was determined by replicate preparations ($n = 10$), of a single concentration, performed on a single day, of samples containing either 5.0 or 49.8 ng/g of lead. Interassay precision was evaluated by analyzing a 19.9 ng/g sample in triplicate on five successive days.

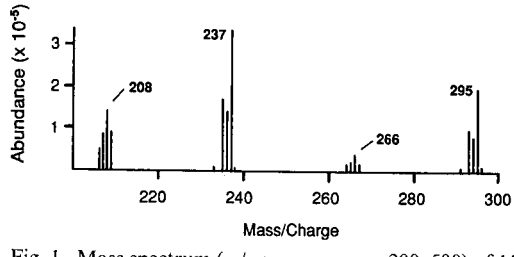


Fig. 1. Mass spectrum ($m/z$ scan range = 200–500) of 11.4 μg/g TEL in fuel (NIST SRM 2712). Injection volume, 1.5 μl. TEL eluted at 8.276 min.

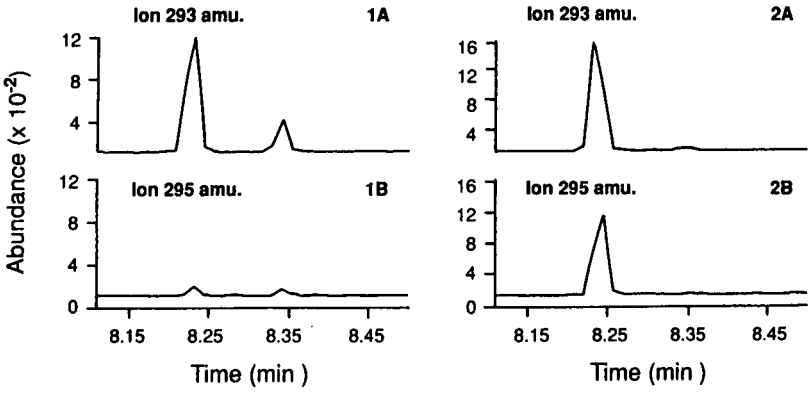


Fig. 2. SIM ion chromatograms for $m/z$ = 293 (triethyl-$^{206}$Pb ion, A) and 295 (triethyl-$^{208}$Pb ion, B). Nominal Pb concentrations: sample 1, $^{206}$Pb = 19.6 ng/g; sample 2, $^{206}$Pb = 28.6 ng/g, $^{208}$Pb = 20.8 ng/g.

## RESULTS

Fig. 1 shows a mass spectrum of TEL. Peaks clustered about $m/z$ 208, 237, 266 and 295 are due to the fragmentation products $Pb^+$, ethyl-$Pb^+$, di-ethyl-$Pb^+$ and tri-ethyl $Pb^+$, respectively. Isotopic abundances of ethylated fragments are those expected for Pb-containing ions. Peaks at $m/z$ 293 (triethyl-$^{206}Pb^+$) and 295 (triethyl-$^{208}Pb^+$) were chosen for quantification of lead. Although these peaks had a lower total abundance than peaks at $m/z$ 235 and 237 (ethyllead isotopes), the smaller background counts at the higher mass were judged to yield a greater signal-to-noise ratio.

Fig. 2 shows typical ion chromatograms at $m/z$ 293 and 295 of two lead-containing samples. Nominal lead concentrations were as follows: sample 1 contained a 19.6 ng/g spike of $^{206}$Pb, while sample 2 contained 28.6 ng/g of $^{206}$Pb and 20.9 ng/g of $^{208}$Pb (the latter added as a 40.6 ng/g spike of mixed-isotope lead). The peak at $m/z$ 295 in sample 1 is due to lead contamination, from atmospheric dust, sample containers or reagents (see below). Comparison of the two sample 1 peak areas gives a value for lead contamination of 0.5 ng/g (0.26 ng) in this particular sample (0.51 ml). In sample 2, a ratio of the two peak areas gives a measured total lead concentration (exclusive of added $^{206}$Pb spike) of 41.6 ng/g, close to the nominal value of 40.6 ng/g. Note that there are no interfering peaks which co-elute with the analytes, facilitating quantification.

In order to determine the accuracy and linearity of this technique, ion chromatograms such as those shown in Fig. 2 were obtained for a range of nominal lead concentrations (exclusive of added $^{206}$Pb spikes) varying from 0 to 91.5 ng/g. Fig. 3 shows a comparison of the measured lead concentration ($Pb_{meas}$) plotted against the nominal, added lead concentration ($Pb_{added}$), which varies from 0 to 91.5 ng/g. The regression line calculated through the data

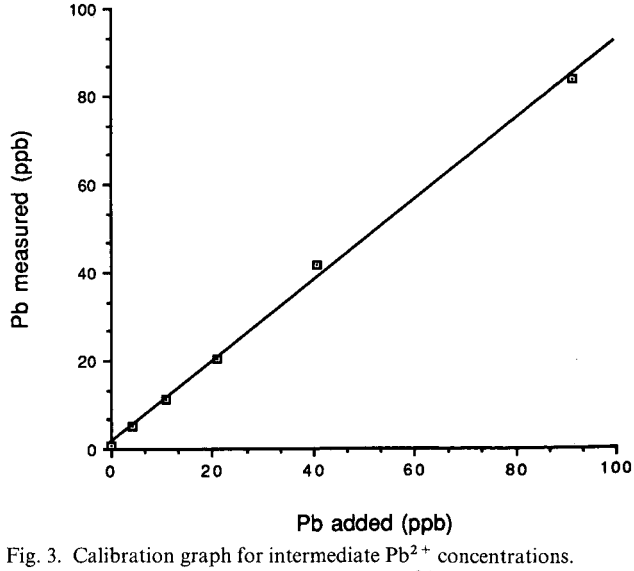


Fig. 3. Calibration graph for intermediate $Pb^{2+}$ concentrations. "Pb added" is the calculated amount of $Pb^{2+}$ in the analyte sample; "Pb measured" is the $Pb^{2+}$ concentration determined by isotope dilution mass spectral analysis (ppb = ng/g). See Experimental for other details.

TABLE I

RELATIVE STANDARD DEVIATIONS FOR EXPERIMENTAL PRECISION

| Precision | $n$ | R.S.D. (%)[a] | R.S.D. (%) ($A_{295}$)[b] |
|---|---|---|---|
| Instrumental (40.6 ng/g Pb) | 10 | 2.8 | 6.7 |
| Intra-assay (49.8 ng/g Pb) | 10 | 4.2 | 24.9 |
| Intra-assay (5.0 ng/g Pb) | 10 | 9.3 | 10.0 |
| Inter-assay (19.9 ng/g Pb) | 5 | 8.7 | 35.0 |

[a] R.S.D. of the standard procedure (see Experimental).
[b] R.S.D. for area of peak at $m/z$ 295 (triethyl-$^{208}Pb^+$), assuming a constant injection volume of 1 μl.

points has an intercept of 1.66 ng/g and a slope of 0.91 (the theoretical value is 1). The correlation coefficient was 0.9988.

Fig. 4 shows a graph similar to that in Fig. 3, but which encompasses a lower range of concentrations, with nominal lead values varying from 0 to 2.5 ng/g. This graph also shows excellent linearity and precision (correlation coefficient = 0.9955), with an intercept of 0.45 ng/g and a slope of 0.70. The reasons for this low slope are not clear; however, it is possible that the polyethylene tubes absorb small amounts of $Pb^{2+}$ and make it unavailable for ethylation. As the samples are exposed to the

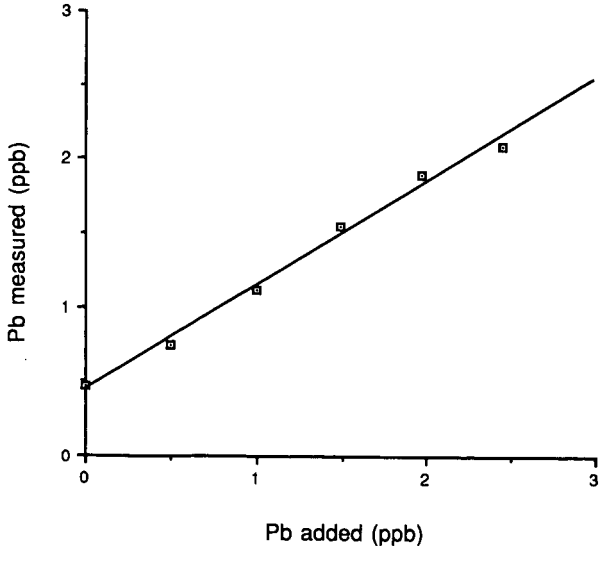


Fig. 4. Calibration graph for low $Pb^{2+}$ concentrations. Axis labels as in Fig. 3. See Experimental for other details.

polyethylene tubes for longer than the $^{206}Pb$ spikes, a disproportionate amount of the sample lead may gave been absorbed. This phenomenon is important only at low concentrations.

Relative standard deviations (R.S.D.s) for instrumental, intra-assay (at two concentrations, 5.0 and 49.8 ng/g) and inter-assay precision are given in Table I. For purposes of comparison, the R.S.D.s for the areas of the analytical peaks ($m/z$ = 295), *not* ratioed to the internal standard, at a constant 1-μl injection volume, were also calculated.

As the yield of TEL is believed to be dependent on reaction stoichiometry [9], and as STEB may be an important source of contaminating lead, the effect of varying reagent (1% STEB) volumes on this procedure was investigated. $^{206}Pb$ (due to a standard spike of 10 μl of 1 μg/g $^{206}Pb$ solution) peak area and contaminating lead were determined for volumes of 1% STEB ranging from 10 to 500 μl (all solutions contained 200 μl of 0.68 *M* acetate buffer to insure pH control when using larger volumes of 1% STEB reagent). Fig. 5 shows a plot of nanograms of contaminating lead *vs.* amount of STEB reagent. For STEB volumes of 10–50 μl, the amounts of contaminating lead appear constant and within experimental error. At these volumes, STEB is apparently not the major source of lead contamination. At higher volumes (100–500 μl), lead contamination varies linearly with STEB volume. The slope of the line drawn through the data points in Fig. 5 allows a calculation of lead contamination within our 1% STEB reagent of ca. 10.5 ng/ml. This is an important consideration as previously published methods utilizing STEB reported reagent volumes as high as 2 ml of 0.5% reagent [7] and 3 ml of 0.43% reagent [5].

We also studied the effect of different sample tube types on residual lead contamination and the results are given in Table II (measurements are averages of three determinations.) Little difference was observed between the various tube types, suggesting that the tubes are not the source of the observed lead blank contamination, which is typically 0.2–0.6 ng.

Other workers have reported some interference by non-lead metal ions (*e.g.*, a 15% signal suppression by a 1000-fold excess of $Cu^{2+}$ [7]). Table III shows the effect on the standard procedure of one- and tenfold excesses of $Fe^{2+}$, $Zn^{2+}$ and $Cu^{2+}$ ions. A tenfold excess of $Fe^{2+}$ results in some suppression of

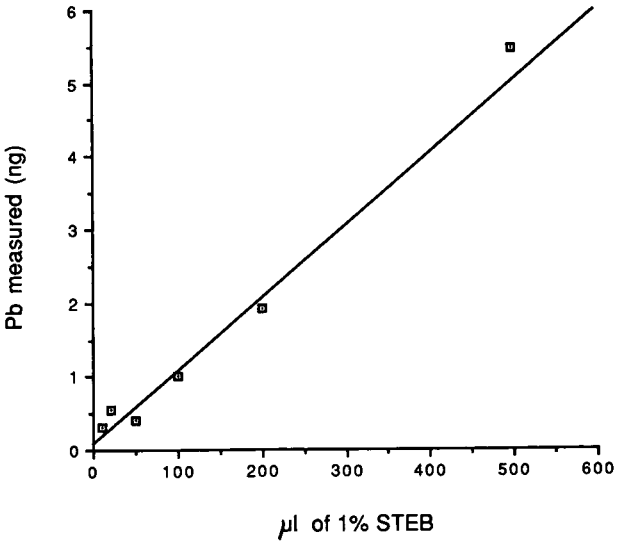


Fig. 5. $Pb^{2+}$ contamination resulting in solutions containing no added $^{208}Pb$ and derivatized with the indicated amount of 1% STEB solution. Solutions were buffered with 200 µl of 0.68 *M* acetate buffer and spiked with 10 µl of 1 µg/g $^{206}Pb$ solution.

TEL formation ($A_{295}$), $Zn^{2+}$ has little effect on the signal and both one- and tenfold excesses of $Cu^{2+}$ result in a *ca.* tenfold decrease in TEL formation. Whereas $Fe^{2+}$ and $Cu^{2+}$ reduce TEL formation, internal standardization with $^{206}Pb$ reduces the error due to decreased TEL formation. This compensation is only partial in cases of severe interference ($Cu^{2+}$), where $Pb_{meas}$ values vary more substantially (10–30%) from the nominal values.

Finally, the amount of lead present was measured in delayed- and first-draw San Francisco city water. Compared with our blank solution, which contained 0.1 ng/g contamination, first- and delayed-draw San Francisco city water contained 3.9 and 1.4 ng/g of lead, respectively. This finding confirms the relatively low concentration of lead attributed to San Francisco city water [14], and reaffirms the expected result that water stagnation in pipes is a source of lead contamination.

TABLE II

EFFECT OF TUBE TYPE ON LEAD CONTAMINATION

| Tube type | Pb contamination (ng) |
|---|---|
| Polyethylene[a] | 0.28 |
| Polyethylene[b] | 0.25 |
| Polyethylene[c] | 0.44 |
| Glass, Pyrex[a] | 0.24 |
| Glass, borosilicate[a] | 0.37 |

[a] Tube freshly acid cleaned.
[b] Tube kept open in clean hood for 5 days.
[c] Tube kept open in room air for 5 days.

TABLE III

EFFECT OF CONTAMINATING METALS ON TEL PRODUCTION

| Contaminant | Concentration (ng/g) | *n* | $A_{295}$[a] | $Pb_{added}$ (ng/g)[b] | $Pb_{meas}$ (ng/g)[c] |
|---|---|---|---|---|---|
| None | – | 2 | 19 345 | 19.5 | 21.2 |
| Fe | 18.9 | 3 | 22 206 | 19.5 | 20.5 |
| | 161.0 | 3 | 9976 | 16.6 | 17.9 |
| Zn | 18.9 | 3 | 22 813 | 19.5 | 21.0 |
| | 161.0 | 3 | 20 775 | 16.6 | 17.8 |
| Cu | 18.9 | 3 | 2220 | 19.5 | 23.2 |
| | 161.0 | 3 | 1808 | 16.6 | 22.1 |

[a] Average area (arbitrary units) of peak at *m/z* 295 (triethyl-$^{208}Pb^{+}$).
[b] Nominal Pb concentration calculated from amount of added standard.
[c] Pb concentration determined by standard procedure (see Experimental).

## DISCUSSION

This procedure for the determination of lead in aqueous samples at low-ng/g concentrations is based on aqueous ethylation of a $^{206}Pb$-spiked sample by STEB. The TEL thus formed is extracted into heptane and determined by GC–MS. It is an extension of the work of Rapsomanikis *et al.* [5], who first applied the STEB derivatization procedure to the determination of alkyllead cations, and of Sturgeon *et al.* [7], who first applied STEB ethylation for the determination of $Pb^{2+}$. We have added the use of a $^{206}Pb$ internal standard and have detected the product TEL by SIM–GC–MS. The technique is rapid and convenient; all the required reagents are inexpensive and the equipment is commercially available. In particular, the reaction vessel is a simple polyethylene tube, as opposed to the complicated reaction vessels [6,7] and cold traps [5] required in previous procedures.

The use of a $^{206}Pb$ internal standard improves

both precision and accuracy. Although Sturgeon *et al.* [3] reported an excellent R.S.D. of 4% with their method, we observed up to an eight-fold larger variation in the absolute amounts of TEL formed (see Table I). Variability in the extent of ethylation may result, as the $B(C_2H_5)_3$ produced in eqn. 1 is itself capable of ethylating $Pb^{2+}$ [6]; therefore, the recovery of $Pb^{2+}$ (theoretically 50%) may vary with the relative ratios of STEB and $Pb^{2+}$ in solution. Sturgeon *et al.* [7] found a recovery of 58%. We observed that $^{206}Pb$-derived peak areas actually decreased with increasing volumes of STEB reagent. Variability in the extent of ethylation is compensated for by the stable isotope internal standard, as both $^{206}Pb$ and $^{208}Pb$ can be expected to undergo ethylation to the same extent. Also, the extent of the ethylation reaction is dependent on the freshness of the reagent (1-week-old STEB solution was observed to produce 75% of the response given by freshly prepared STEB) [7]. Second, other metals (especially $Cu^{2+}$, which may be expected to be relatively common in aqueous samples) may attack TEL [15], or interfere with the ethylation reaction. The results in Table III show that, whereas other metals can decrease the yield of TEL, the isotope dilution procedure still yields accurate $Pb^{2+}$ concentration values. Lastly, the use of a $^{206}Pb$ internal standard corrects for variabilities in injection volume, injection port volatility and ionization or collection efficiency, in addition to recovery losses due to evaporation of TEL or heptane.

Note that for intermediate concentrations (40–50 ng/g), the instrumental (2.8%) and intra-assay precision (4.2%) are very similar, suggesting that at these concentrations, preparative imprecision contributes little to the total procedural imprecision, *i.e.*, errors are dominated by noise in the mass-sensing detector.

The blank ($n = 9$) for the standard procedure is calculated to be $0.40 \pm 0.20$ ng of lead. The blank due to a 10-$\mu$l aliquot of 1% STEB is calculated (from the slope of Fig. 5) as 0.10 ng of lead. Hence the STEB contributes substantially, but does not dominate the blank. The relatively constant blank from different tube types suggests that our RO/DI water may be the source of much of the $Pb^{2+}$ blank.

The detection limit ($3\sigma$) is calculated to be 0.6 ng, or 0.3 ng/g for a 2-ml sample (note that the concentration detection limit could be improved by using a larger sample volume). Sturgeon *et al.* (7) achieved a detection limit of 14 pg (1 pg/g for a 10-ml sample). Our relatively higher detection limit is caused by a higher level of background lead contamination and a greater R.S.D. in the blank. The former problem could probably be obviated by obtaining cleaner water and by invoking more stringent clean room procedures, and the latter is probably due to the mass spectrometer instrumental noise. In any event, this procedure retains advantages of convenience for the analysis of low ng/g lead-containing aqueous samples.

This method is applicable to more complicated matrices (*e.g.*, blood, urine, soft drinks), but will require some modification. For example, the standard procedure utilizes a fairly low buffering capacity (about 10 m*M*), and hence might be overwhelmed by a concentrated biological fluid. Although published data [7] show that a wide pH range can support ethylation by STEB, pH values $<2$ or $>9$ should be avoided. We used a modified procedure (with an acid digestion and increased buffering capacity) to analyze 100-$\mu$l aliquots ($n = 6$) of human blood with a nominal lead level of 620 ng/g (from atomic absorption spectrometry). The modified isotope dilution procedure gave $798 \pm 146$ ng/g. Relatively low peak areas (reduced by nearly a factor of 100 compared with aqueous samples with comparable concentrations) were observed for $m/z = 295$; this resulted in a fairly large R.S.D. (18.3%), which may have been increased by the interference of $Cu^{2+}$ and/or $Fe^{2+}$ ions. Extension of this method to more complicated media will require strategies (*e.g.*, complexation of non-lead metal ions) for discriminating against interferents which can greatly reduce the yield of TEL.

## REFERENCES

1 J. L. Pirkle, J. Schwarz, J. R. Landis and W. R. Harlan, *Am. J. Epidemiol.*, 121 (1985) 246.
2 D. S. Sharp, J. Osterloh, C. E. Becker, B. L. Holman, A. H. Smith and J. M. Fisher, *Arch. Environ. Health*, 44 (1989) 18.
3 A. J. McMichael, P. A. Baghurst, N. R. Wigg, G. V. Vimpani, E. F. Robertson and R. J. Roberts, *N. Engl. J. Med.*, 319 (1988) 468.
4 *The Nature and Extent of Lead Poisoning in Children in the United States: a Report to Congress*, Agency for Toxic Substances and Disease Control Registry, U.S. Department of Health and Human Services, Atlanta, GA, 1988, pp. 3–4.
5 S. Rapsomanikis, O. F. X. Donard and J. H. Weber, *Anal. Chem.*, 58 (1986) 35.

6 J. S. Blais and W. D. Marshall, *J. Anal. At. Spectrom.*, 4 (1989) 641.
7 R. E. Sturgeon, S. N. Willie and S. S. Berman, *Anal. Chem.*, 61 (1989) 1867.
8 J. Ashby, S. Clark and P. J. Craig, *J. Anal. At. Spectrom.*, 3 (1988) 735.
9 J. B. Honeycutt and J. M. Riddle, *J. Am. Chem. Soc.*, 82 (1961) 369.
10 A. D'Ulivo and Y. Chen, *J. Anal. At. Spectrom.*, 4 (1989) 319.
11 J. W. McLaren, D. Beauchemin and S. S. Berman, *Anal. Chem.*, 59 (1987) 610.
12 J. R. Dean, L. Ebdon and R. C. Massey, *Food Additives Contam.*, 7 (1990) 109.
13 A. R. Flegal and V. J. Stukas, *Mar. Chem.*, 22 (1987) 163.
14 *1990 Annual Water Quality Report*, San Francisco Water Department, San Francisco, 1990.
15 A. W. P. Jarvie, R. N. Markall and H. R. Potter, *Environ. Res.*, 25 (1981) 241.

*Journal of Chromatography*, 594 (1992) 283–290
Elsevier Science Publishers B.V., Amsterdam

CHROM. 23 886

# Synthesis of (1*R-trans*)-N,N′-1,2-cyclohexylenebisbenzamideoligodimethylsiloxane copolymers for use as chiral stationary phases for capillary supercritical fluid chromatography

Deborah F. Johnson, Jerald S. Bradshaw*, Masakatsu Eguchi, Bryant E. Rossiter and Milton L. Lee

*Department of Chemistry, Brigham Young University, Provo, UT 84602 (USA)*

Patrick Petersson and Karin E. Markides

*Department of Analytical Chemistry, Uppsala University, Box 531, S-751 21 Uppsala (Sweden)*

(First received October 2nd, 1991; revised manuscript received November 18th, 1991)

ABSTRACT

Eight new copolymers have been prepared as chiral stationary phases for capillary supercritical fluid chromatography (SFC) by the copolymerization hydrosilylation of α,ω-dihydromethyloligosiloxanes with four dialkene derivatives of (1*R-trans*)-N,N′-1,2-cyclohexylenebisbenzamide. This represents a novel approach to the synthesis of chiral stationary phases in that copolymers are formed from achiral α,ω-dihydrosiloxane and chiral diolefinic diamide monomers. The siloxane units ensure good general chromatographic performance (*e.g.*, high efficiency and thermal stability), while the chiral units facilitate enantioselectivity by providing specific interaction sites and selective chiral grooves or cavities. Several of these polymers are useful for the separation of enantiomeric diols.

## INTRODUCTION

Recent advances in the analytical chromatographic separation of enantiomers can be attributed in part to the increasing interest in the resolution and enantiomeric purity of drugs [1]. It is well known that enantiomers can produce different biological activities according to their absolute configurations [1]. Approximately 40% of the pharmaceuticals obtained synthetically are chiral, however, only 10% of them are utilized as pure enantiomers, 90% being used in the racemic form [2]. This situation is expected to change as governmental drug regulatory agencies adopt more stringent standards relative to the enantiomeric purity of drugs. The development of accurate analytical tools is necessary for monitoring asymmetric syntheses and for assessing the enantiomeric purities of chiral drug substances. Chromatography using indirect methods (separations of diastereomers on achiral stationary phases) or direct methods using a chiral selecting agent in the mobile phase or on a chiral stationary phase (CSP) has proven to be the best technique for chiral separations [3].

Much effort has been expended in the development of CSPs for liquid chromatography (LC) and gas chromatography (GC) [3–5]. Since supercritical fluid chromatography (SFC) can be performed at lower temperatures than GC and it can produce higher practical efficiencies than LC, SFC is a potentially important technique for the resolution of enantiomers [6]. We have therefore initiated studies to develop CSPs capable of resolving enantiomers by SFC. CSPs for capillary SFC must have certain

0021-9673/92/$05.00 

characteristics: (a) these materials must be suitable for efficient coating and immobilization inside the fused-silica columns; (b) they must be resistant to thermal and chemical stress; (c) they must allow efficient diffusion of analytes and mobile phases; and (d) they must interact differentially with the two enantiomers of the chiral analyte. The first three characteristics are desirable properties of any good stationary phase. The fourth characteristic relates to their chiral recognition properties.

## EXPERIMENTAL

### *Preparation of chiral starting materials*

*Preparation of (1R-trans)-N,N'-1,2-cyclohexylenebis(4-allyloxybenzamide)* (**9**). Oxalyl chloride (4.3 g, 33.9 mmol) was added to a suspension of 5.09 g (28.1 mmol) of 4-allyloxybenzoic acid (prepared from allyl bromide and 4-hydroxybenzoic acid) in 70 ml of benzene at room temperature. The reaction mixture was stirred for 10 min at room temperature followed by refluxing until the acid dissolved (10–15 min). The solvent was removed under reduced pressure to give an oily residue which was dissolved in 60 ml of tetrahydrofuran (THF). 4-Methylmorpholine (3.4 g, 33.7 mmol) was added to the reaction mixture at 0°C under an argon atmosphere. A solution of 1.15 g (10.1 mmol) of (1*R*,2*R*)-*trans*-1,2-diaminocyclohexane (Fluka, Ronkonkoma, NY, USA) in 15 ml of THF was added to the reaction mixture at room temperature. The reaction mixture was stirred for 10 min at room temperature followed by refluxing for 2 h. The reaction mixture was evaporated under reduced pressure to give a solid residue which was then dissolved in 200 ml of chloroform. The chloroform solution was extracted with 100 ml of water, 100 ml of 1 *M* aqueous HCl, twice with 150-ml portions of 5% aqueous $Na_2CO_3$, and again with 100 ml of water to remove impurities. The chloroform layer was dried over anhydrous $Na_2SO_4$ and evaporated under reduced pressure to give a crude product, which was purified by preparative high-performance liquid chromatography (HPLC) (silica gel, chloroform–ethyl acetate = 3:1). The resulting white solid was recrystallized from ethyl acetate–hexane to give 2.47 g (56%) of product; m.p. 159–161°C; $[\alpha]_D = -125.88°$ ($c$ = 3.98, $CH_2Cl_2$); NMR ($C^2HCl_3$) $\delta$ 1.45 (m, 4 H), 1.82 (m, 2 H), 2.20 (m, 2 H), 4.0 (m, 2 H), 4.45 (dd, 4 H), 5.20–5.50 (dd, 4 H), 5.9–6.1 (m, 2 H), 6.75 (d, 4 H), 6.9 (m, 2 H), 7.65 (d, 4 H); IR (KBr) 3297, 3083, 1685, 841, 767 $cm^{-1}$.

*Preparation of (1R-trans)-N,N'-1,2-cyclohexylenebis(2-allyloxybenzamide)* (**10**). Sodium metal (4.0 g, 0.17 mol) was dissolved in 100 ml of methanol under nitrogen, and 25.0 g (0.17 mol) of methyl 2-hydroxybenzoate were added. After addition of the ester, 39.7 g (0.33 mol) of allyl bromide was slowly dripped into the reaction mixture. The mixture was refluxed overnight, cooled and acidified with 6 *M* acetic acid. The methanol and excess allyl bromide were evaporated. The material was dissolved in 150 ml of diethyl ether and the ether solution was washed with 100 ml of water. The ether was dried over anhydrous $MgSO_4$ and distilled to give 21.1 g (67%) of the methyl 2-allyloxybenzoate; b.p. 71–83°C/0.12 mmHg. This ester was hydrolyzed to give 14.1 g (72%) of 2-allyloxybenzoic acid; m.p. 70–71°C.

2-Allyloxybenzoic acid (1.94 g, 0.011 mol) was treated as above with oxalyl chloride (1.66 g, 0.13 mol) to give 2-allyloxybenzoyl chloride; b.p. 71–71°C/0.065 mmHg. The acid chloride (1.85 g, 9.4 mmol) was reacted with (1*R*,2*R*)-*trans*-1,2-diaminocyclohexane (1.01 g, 8.8 mmol) as above for the preparation of **9** to give 1.29 g (63%) of **10** after recrystallization from ether–hexane; m.p. 90–91°C; $[\alpha]_D = -78.4°$ ($c$ = 0.324, $CHCl_3$); NMR $\delta$ 1.15–1.5 (4 H, bm), 2.7–2.85 (2 H, bm), 2.15–2.3 (2 H, bm), 3.95–4.15 (2 H, bm), 4.6 (4 H, m), 5.2–5.4 (4 H, dd), 5.9–6.1 (2 H, m), 6.8–7.0 (4 H, m), 7.25–7.4 (2 H, m), 8.0–8.2 (4 H, m). Analysis for $C_{26}H_{30}O_4N_2$; calculated: C, 71.87; H, 6.96; found: C, 71.10; H, 7.17.

*Preparation of (1R-trans)-N,N'-1,2-cyclohexylenebis(3-allyloxybenzamide)* (**11**). 3-Hydroxybenzoic acid (3.90 g, 0.028 mol) was treated as above for the formation of 2-alkyloxybenzoic acid to give 1.60 g (32%) of 3-allyloxybenzoic acid after recrystallization from dichloromethane–hexane; m.p. 77–79°C.

3-Allyloxybenzoic acid (1.60 g, 9.0 mmol) was reacted with 1.37 g (0.011 mol) of oxalyl chloride as above for the formation of **9** to give 0.78 g (44%) of 3-allyloxybenzoyl chloride. As the acid chloride distilled, it began to decompose so that the vacuum fluctuated widely and no b.p. was obtained. The acid chloride (0.78 g, 4.0 mmol) was reacted with

0.22 g (1.9 mmol) of (1*R*,2*R*)-*trans*-1,2-diaminocyclohexane as above for the preparation of **9** to give 0.48 g (57%) of **11** after recrystallization from dichloromethane–hexane; m.p. 178–181°C; $[\alpha]_D = -42.2°$ ($c$ = 0.694, $CHCl_3$); NMR $\delta$ 1.35–1.5 (4 H, m), 2.7–2.9 (2 H, m), 2.1–2.3 (2 H, m), 3.9–4.0 (2 H, m), 4.5 (4 H, d), 5.2–5.45 (4 H, dd), 5.9–6.1 (2 H, m), 6.6–6.8 (2 H, d), 6.9–7.0 (2 H, m), 7.2–7.3 (6 H, m). Analysis for $C_{26}H_{30}O_4N_2$; calculated: C, 71.87; H, 6.96; found: C, 72.00; H, 6.93.

*Preparation of (1R-trans)-N,N'-1,2-cyclohexylenebis[4-(3-butenyl)benzamide]* (**12**). 4-Allylbromobenzene (3.00 g, 0.015 mol) (Aldrich) dissolved in HPLC-grade THF was slowly added to 0.38 g (0.16 mol) of magnesium in 100 ml of HPLC-grade THF. The Grignard was allowed to form and then a gas dispersion tube was placed in the Grignard mixture. Carbon dioxide was passed through a drying tube filled with Drierite before it entered the reaction. The mixture was stirred at −10°C for 1 h and for 1 h at room temperature while carbon dioxide was bubbled into the reaction mixture. The THF was evaporated and 50 ml of water were added. The reaction was acidified with glacial acetic acid. The aqueous solution was extracted twice with 50-ml portions of chloroform and with 50 ml of diethyl ether. The chloroform and ether layers were each washed with water until neutral and then combined and dried over anhydrous $MgSO_4$. The solvents were evaporated and the product was chromatographed on 20 g of silica gel with 100 ml of hexane and then hexane–acetic acid (10:0.1) as eluents. The 4-allylbenzoic acid (0.5 g, 20%) was isolated by recrystallization from ether–hexane. Even after column chromatography, there was some type of aromatic impurity. This material was used in the next step without further purification.

4-Allylbenzoic acid (0.50 g, 3.1 mmol) was treated as above with 0.51 g (4.0 mmol) of oxalyl chloride to give 4-allylbenzoyl chloride which was not purified but used directly with 0.17 g (1.5 mmol) of (1*R*,2*R*)-*trans*-1,2-diaminocyclohexane as above for the preparation of **9** to give 0.22 g (37%) of **12**. Compound **12** was purified by column chromatography on 5 g of silica gel with toluene–acetic acid (10:0.2) as eluent and then on 5 g of silica gel with hexane–acetic acid (10:0.2) as eluent. The product was recrystallized from dichloromethane–hexane; m.p. 207.5–209°C; $[\alpha]_D = -136°$ ($c$ = 0.184, $CHCl_3$); NMR $\delta$ 1.2–1.65 (4 H, bm), 2.7–2.9 (2 H, bm), 2.1–2.35 (2 H, bm), 3.3–3.5 (4 H, m), 3.85–4.1 (2 H, m), 5.0–5.2 (3 H, m), 5.8–6.0 (2 H, m), 7.7–7.9 (2 H, m), 7.1–7.3 (4 H, m), 7.4–7.8 (4 H, bm). Analysis for $C_{26}H_{30}O_2N_2 \cdot 1.5\ H_2O$; calculated: C, 72.71; H, 7.04; found: C, 72.63; H, 6.93.

*Preparation of (1R-trans)-N,N'-1,2-cyclohexylenebisbenzamideoligodimethylsiloxane copolymer phases*

The chiral stationary phases were prepared according to Fig. 1. Specific details for these syntheses are outlined as follows.

*Preparation of (1R-trans)-α-(dimethyloctylsilyl)-ω-[(dimethyloctylsiloxanyl)oxy]poly[oxy(dimethylsilanediyl)-1,3-propanediyloxy-1,4-phenylenecarbonylimino-1,2-cyclohexyleneiminocarbonyl-1,4-phenyleneoxy-1,3-propanediyl(dimethylsilylene)]* (**1**) (Fig. 1). Chiral monomer **9** (0.34 g, 7.8 mmol), 11.0 μl of 1-octene (for endcapping) and tetramethyldisiloxane (**13**) (Aldrich, Milwaukee, WI, USA) (0.11 g, 8.5 mmol) were placed in a 50-ml PTFE centrifuge tube and dissolved in 20 ml of toluene. Chloroplatinic acid (15 μl, 1%) was added, and the vial was capped and placed in a sonic bath at 50°C for *ca.* 36 h. The polymer was dissolved in 10 ml of dichloromethane and precipitated by a mixture of 5 ml of methanol and 5 ml of water. The solvents were decanted and the polymer was again dissolved and precipitated three more times. This process separated the polymer from low-molecular-weight impurities. The polymer was again dissolved in 10 ml of dichloromethane and filtered through a 0.2-μm filter to remove high-molecular-weight material. The dichloromethane was evaporated and the polymer was dried under vacuum at 60°C for 15 h to give 0.38 g (86%) of a brown crystalline polymer (**1**). The NMR spectrum showed that there was still alkene present in the polymer. This polymer was crystalline and was not studied further.

*Preparation of (1R-trans)-α-(dimethyloctylsilyl)-ω-[(1,1,3,3,5,5-hexamethyl-5-octyltrisiloxanyl)oxy]poly[oxy(1,1,3,3,5,5-hexamethyltrisiloxane-1,5-diyl)-1,3-propanediyloxy-1,4-phenylenecarbonylimino-1,2-cyclohexyleneiminocarbonyl-1,4-phenyleneoxy-1,3-propanediyl(dimethylsilylene)]* (**2**) (Fig. 1). Compound **9** (0.34 g, 7.8 mmol), 7 μl of 1-octene (for endcapping) and 0.23 g (8.3 mmol) of octamethyltetrasiloxane (**14**) (Aldrich) were placed

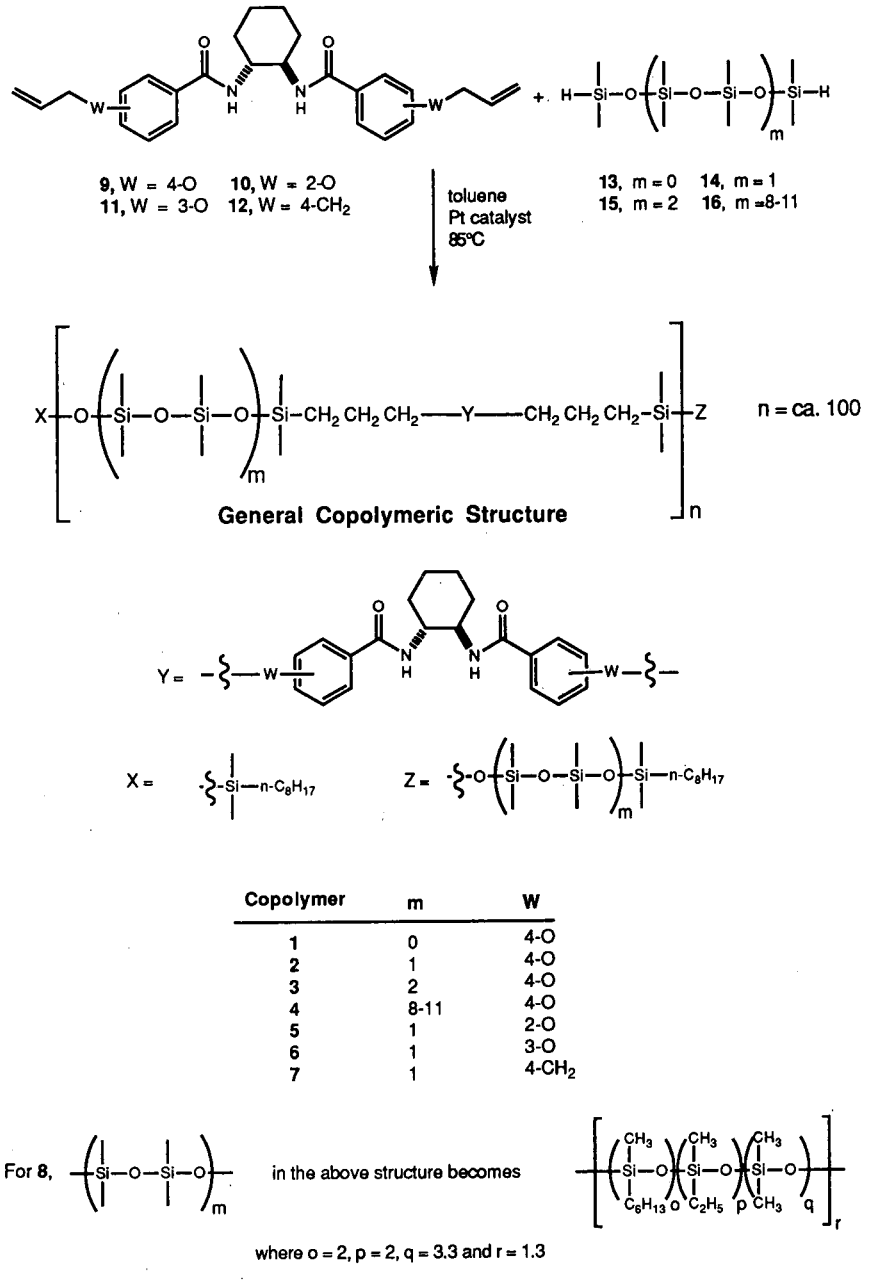


| Copolymer | m | W |
|---|---|---|
| 1 | 0 | 4-O |
| 2 | 1 | 4-O |
| 3 | 2 | 4-O |
| 4 | 8-11 | 4-O |
| 5 | 1 | 2-O |
| 6 | 1 | 3-O |
| 7 | 1 | 4-$CH_2$ |

Fig. 1. Preparation of copolymer phases **1–8**.

in a 50-ml PTFE centrifuge tube and dissolved in 7 ml of toluene. A few small crystals of dicyclopentadienyl platinum were added to the reaction mixture which was then capped and placed in the sonic bath at 50°C and allowed to react until all the alkene was gone. The toluene was evaporated and then the polymer was treated as above for **1** with dichloromethane, methanol and water to give 0.53 g (64%)

of **2**. The polymer was a brown crystalline material; $[\alpha]_D = -63.1°$ ($c$ = 4.52, $CH_2Cl_2$).

*Preparation of (1R-trans)-α-(dimethyloctylsilyl)-ω-[(1,1,3,3,5,5,7,7,9,9-decamethyl-9-octylpentasiloxanyl)oxy]poly[oxy(1,1,3,3,5,5,7,7,9,9-decamethylpentasiloxane-1,9-diyl)-1,3-propanediyloxy-1,4-phenylenecarbonylimino-1,2-cyclohexyleneiminocarbonyl-1,4-phenyleneoxy-1,3-propanediyl(dimethylsilylene)]* (**3**) (Fig. 1). Dodecamethylhexasiloxane (**15**) was first prepared by placing 3.00 g (0.010 mol) of **14** and 1.41 g (0.011 mol) of **13** in a 50-ml PTFE centrifuge tube with a magnetic stir bar. The silanes were stirred for 5 min to give a homogenous mixture and then one drop of triflic acid was added. The reaction was stirred at room temperature for 2 min and then 10 drops of hexamethyldisilazane (HMDS) were added. An aliquot of 10 ml of dichloromethane was added and the polymer was washed 4 times with 10 ml of water. The dichloromethane was evaporated and the product was distilled to give 1.43 g (33%) of **15**; b.p. 45–51°C/0.70 mmHg. A GC–mass spectrometric (MS) analysis of **15** showed one peak with a parent mass of 431.

Siloxane **15** (0.40 g, 0.9 mmol), 0.40 g (0.9 mmol) of **9** and 8 μl of 1% chloroplatinic acid were placed in a 50-ml PTFE centrifuge tube and dissolved in 10 ml of toluene. The vial was capped and placed in the sonic bath at 50°C for 16 h, and then 10 μl of 1-octene were added for endcapping purposes. The reaction was carried out until the Si–H band in the IR spectrum was gone. The toluene was evaporated and the polymer was treated as above for **1** with dichloromethane, methanol and water to give 0.62 g (78%) of **3** as a viscous light tan liquid.

*Preparation of copolymer* **4** (Fig 1). Polysiloxane **16** was first prepared by placing 1.50 g (5.1 mmol) of **14** and 0.21 g (1.6 mmol) of **13** in a 50-ml PTFE centrifuge tube with a magnetic stir bar. The mixture was stirred for 3 min at room temperature and then 10 mg of triflic acid were added. The vial was capped and the reaction was stirred overnight at room temperature. The reaction was neutralized with 15 drops of HMDS, and then 10 ml of dichloromethane were added. The polymer solution was washed 3 times with 10-ml portions of water and then filtered through a 0.2-μm filter. The solvent was evaporated and the polymer was dried under vacuum at 80°C for 24 h. The NMR spectrum of **16** indicated the structure shown in Fig. 1.

Siloxane **16** (0.66 g, 0.51 mmol) and 0.20 g (0.46 mmol) of **9** were placed in a 50-ml PTFE centrifuge tube and dissolved in 15 ml of toluene. Chloroplatinic acid (15 μl, 1%) was added to the reaction, and a condenser was fitted into the top of the vial. The toluene level eventually dropped to about 3 ml. At this point hydrosilylation began. When all of the alkene had reacted, 10 ml of dichloromethane were added and the polymer was treated as **1** above except the dichloromethane solution was also filtered through a 2-inch column of Superlig VIII (IBC Advanced Technologies, Provo, UT, USA) to remove residual platinum. The solvent was evaporated to give 0.60 g (75%) of **4** as a cream colored viscous liquid; $[\alpha]_D = -31.1°$ ($c$ = 0.238, $CHCl_3$).

*Preparation of (1R-trans)-α-(dimethyloctylsilyl)-ω-[(1,1;3,3,5,5-hexamethyl-5-octyltrisiloxanyl)oxy]poly[oxy(1,1,3,3,5,5-hexamethyltrisiloxane-1,5-diyl)-1,3-propanediyloxy-1,2-phenylenecarbonylimino-1,2-cyclohexyleneiminocarbonyl-1,2-phenyleneoxy-1,3-propanediyl(dimethylsilylene)]* (**5**) (Fig. 1). Alkene **10** (0.41 g, 0.94 mmol) and 0.28 g (1.0 mmol) of siloxane **14** were placed in a 50-ml PTFE centrifuge tube with a magnetic stir bar and dissolved in a mixture of 3 ml of toluene and 2 ml of dichloromethane. 1% Chloroplatinic acid (15 μl) was added and a reflux condenser was fitted into the top of the vial. The reaction was heated at 85°C until the alkene was gone. The toluene was evaporated and the polymer was treated as above for **1** to give 0.59 g (88%) of **7** as a light brown viscous liquid; $[\alpha]_D = -73.8°$ ($c$ = 0.496, $CHCl_3$).

*Preparation of (1R-trans)-α-(dimethyloctylsilyl)-ω-[(1,1,3,3,5,5-hexamethyl-5-octyltrisiloxanyl)oxy]poly[oxy(1,1,3,3,5,5-hexamethyltrisiloxane-1,5-diyl)-1,3-propanediyloxy-1,3-phenylenecarbonylimino-1,2-cyclohexyleneiminocarbonyl-1,3-phenyleneoxy-1,3-propanediyl(dimethylsilylene)]* (**6**) (Fig. 1). Copolymer **6** was prepared in the same manner as **5** using 0.14 g (0.32 mmol) of **11** and 0.10 g (0.35 mmol) of siloxane **14** in 3 ml of toluene and 2 ml of dichloromethane. The polymer was purified as described for **5** above to give 0.14 g (58%) of **6** as a white glassy polymer; $[\alpha]_D = -18.7°$ ($c$ = 0.230, $CHCl_3$).

*Preparation of copolymer (1R-trans)-α-(dimethyloctylsilyl)-ω-[(1,1,3,3,5,5-hexamethyl-5-octyltrisiloxanyl)oxy]poly[oxy(1,1,3,3,5,5-hexa-*

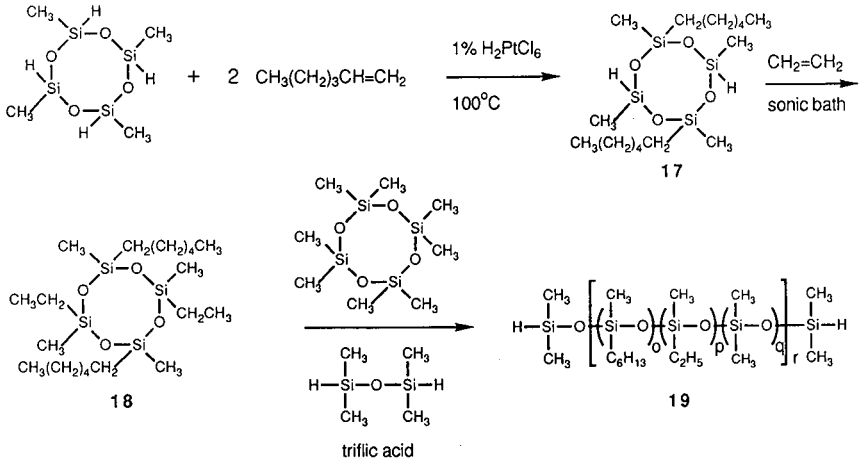


Fig. 2. Preparation of cross-linkable oligosiloxane **19**.

*methyltrisiloxane-1,5-diyl)-1,4-butanediyl-1,4-phenylenecarbonylimino-1,2-cyclohexyleneiminocarbonyl-1,4-phenylene-1,4-butanediyl(dimethylsilylene)]*(**7**) (Fig. 1). This copolymer was synthesized following the procedure described for **5** above using 0.22 g (0.55 mmol) of dialkene **12** and 0.16 g (0.58 mmol) of siloxane **14** to give 0.34 g (92%) of **7**; $[\alpha]_D = -61.0°$ ($c$ = 0.184, $CHCl_3$).

*Preparation of copolymer* **8** (Fig. 1). Oligosiloxane **19** was first prepared (Fig. 2) by placing 2,4,6,8-tetramethylcyclotetrasiloxane (7.0 g, 0.12 mol) and 4.90 g (0.058 mol) of 1-hexene in a flask along with 15 μl of 1% chloroplatinic acid. The reaction mixture was heated overnight at 100°C to give **17** which was then transferred to a 50-ml PTFE centrifuge tube. Ethylene was bubbled into the mixture for 2 h and then the vial was capped and placed in a sonic bath. The reaction was continued until there was no Si–H band in the IR spectrum. The products were vacuum distilled to give 2.19 g of tetramethyldihexyldiethylcyclotetrasiloxane (**18**) (b.p. 105–125°C/0.055 mmHg) and 1.52 g of by-product tetramethyltrihexylethylcyclotetrasiloxane (b.p. 125–140°C/0.055–0.1 mmHg).

Compound **18** (0.39 g, 0.84 mmol) was combined with 0.25 g (0.84 mmol) of octamethylcyclotetrasiloxane **14** and 0.17 g (1.27 mmol) of siloxane **13** (for endcapping) in a 50-ml PTFE centrifuge tube. The siloxanes were stirred together with a magnetic stir bar for 5 min and one drop of triflic acid was added. The reaction was continued for 2 min and 1.5 ml of hexane were added and the mixture was stirred for an additional 10 min. HMDS (15 drops) was used to stop the reaction. The polymer was dissolved in 10 ml of dichloromethane and washed four times with 10-ml portions of water. The dichloromethane was evaporated and the polymer was dissolved in 10 ml of diethyl ether and filtered through a 0.2-μm filter to remove a white precipitate. The ether was evaporated to give 0.39 g (52%) of **19**. An NMR spectrum indicated the structure shown in Fig. 2.

Siloxane **19** (0.39 g, 0.45 mmol) and 0.18 g (0.41 mmol) of **9** were dissolved in 3 ml of toluene. Chloroplatinic acid (10 μl, 1%) was added and a condenser was placed in the top of the vial. The reaction was heated and stirred at 85°C under nitrogen until all of the alkene reacted. The polymer was treated as above for **4** to give 0.45 g (83%) of **8**; $[\alpha]_D = -31.3°$ ($c$ = 0.418, $CHCl_3$).

## RESULTS AND DISCUSSION

The typical chiral polysiloxane stationary phases for GC contain chiral moieties attached to a polymethylsiloxane backbone [4]. The chiral phases prepared in this study are different in that the polymers are composed of alternating chiral hydrocarbon and achiral polysiloxane units (Fig. 1). They were synthesized by a polymeric hydrosilylation of a bis (hydrosiloxane) and a dialkene-containing bisbenzamide as shown.

The (1*R*,2*R*)-*trans*-1,2-diaminocyclohexane was

chosen as the chiral organic moiety because it is commercially available, has $C_2$ symmetry, and the amine groups are held in a semi-rigid position. The allyloxybenzoic acid portion of monomers **9–12** were used as the dialkene source (see Fig. 1) because they hydrosilylate well onto hydrosiloxanes and they are chemically and thermally stable under chromatographic conditions [7].

Once the chiral portion of the copolymer had been selected, the achiral bis(hydrosiloxane) monomers were chosen to study the effect of the length of the siloxane oligomer on the selectivity and efficiency of the chiral stationary phase. The original tetramethyldisiloxane spacer (**13**) reacted with **9** to give a highly crystalline material (**1**). Because of its high crystallinity, this copolymer was difficult to coat inside the fused-silica capillary column and manifested poor overall chromatographic properties. We felt that we could remedy this by increasing the number of siloxane units in the achiral spacer. Octamethyltetrasiloxane (**14**) was used to give polymer (**2**) which was still crystalline, but gave much better solute diffusion in the phase. Phase **2** proved to be an efficient stationary phase for the enantiomeric separation of a number of chiral diols [8,9].

Because phase **2** was still crystalline, a phase containing a dodecamethylhexasiloxane spacer (**3**) was synthesized as shown in Fig. 1. Dodecamethylhexasiloxane (**15**) needed for the preparation of phase **3** was prepared by equilibrating octamethylcyclotetrasiloxane (**14**) with tetramethyldisiloxane (**13**) using triflic acid. Equilibrium favoring higher-molecular-weight polysiloxanes occurs very rapidly in this reaction. In the first reaction to form **15**, very little of the desired product was formed when the siloxanes and triflic acid were stirred overnight. The desired material could be isolated after allowing the reaction to run for only 4.5 min. GC, MS and NMR spectroscopy were used to characterize siloxane **15**. We have since found the procedure of Uchida *et al.* [10] to be a convenient source of this dihydrosiloxane. The dodecamethylhexasiloxane (**15**) was distilled and reacted with alkene **9** to form phase **3** as a viscous liquid.

Phases **5** and **6** were prepared to determine the effect on enantiomeric selection of altering the position of the allyloxy group on the benzamide portion of the chiral monomer. Phase **5** has the *ortho* orientation of the alkoxy and carboxamide moieties on the benzene rings and **6** has the *meta* orientation. Fig. 3 illustrates the excellent efficiency and selectivity obtained using a column coated with phase **6** for the separation of the *cis*-1,2-dihydroxycyclohexyl methyl ketone enantiomers.

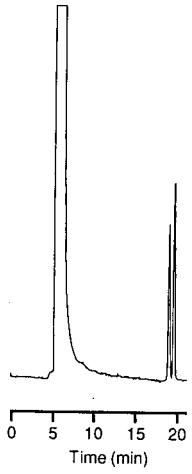


Fig. 3. SFC separation of the enantiomers of *cis*-1,2-dihydroxycyclohexyl methyl ketone using a column coated with copolymer **6**. Conditions: $CO_2$ at 60°C, 5 m × 50 μm I.D. fused-silica column (film thickness ≈ 0.20 μm), density programmed from 0.30 to 0.55 g $ml^{-1}$ at 0.01 g $ml^{-1}$ $min^{-1}$ after an initial 5-min isopycnic period.

An NMR–molecular modelling study involving alkene **9** and (+)- and (−)-diethyl tartrate indicated that the tartrate might be hydrogen bonding with the ether oxygen of the *p*-allyloxy group [11]. (1*R*-*trans*)-1,2-Cyclohexylenebis(4-butyl)benzamide was prepared for molecular modelling studies with (+)- and (−)-diethyl tartrate. It was predicted from these studies [11] that a phase containing a chiral monomer with no ether oxygen atoms could provide even better resolution of chiral diol enantiomers. To test this prediction we synthesized copolymer **7**.

One of the requirement of a stationary phase for SFC is that it must be insoluble in the supercritical fluid over the density programming range. This can be accomplished by cross-linking the phase using azo-*tert.*-butane (ATB) or dicumyl peroxide (DCP) [12]. Phase **2** does not contain any vinyl or octyl groups which are normally added to aid cross-linking. When this phase was tested before and after free radical cross-linking, it showed a marked de-

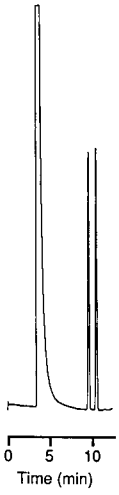


Fig. 4. SFC separation of an anticonvulsant drug (±-mephenytoin) using a column coated with copolymer **8**. Conditions: $CO_2$ at 80°C, 5 m × 50 μm I.D. fused-silica column, density programmed from 0.50 to 0.80 g $ml^{-1}$ $min^{-1}$ after an initial 5-min isopycnic period.

crease in efficiency and selectivity. To overcome this problem, the cross-linkable phase **8** was prepared as shown in Fig. 1. The α,ω-dihydrosiloxane **19** containing hexyl and ethyl substituents was prepared as shown in Fig. 2. Preliminary work showed that phase **8** bled heavily from the column before cross-linking at 0.50 g $ml^{-1}$ at 60°C, but after cross-linking, the phase did not bleed until 0.85 g $ml^{-1}$ at 60°C. The ATB initiated cross-linking of **8** resulted in a phase with poor selectivity and efficiency while the phase cross-linked with DCP gave good chromatographic performance. Fig. 4 is a chromatogram showing the enantiomeric separation of the anticonvulsant drug (±)-mephenytoin on a DCP cross-linked phase (**8**).

Details of the preparation and chromatographic characterization of columns coated with these polymers are reported elsewhere [9]. Development of similar copolymers containing other chiral organic moieties is presently underway.

ACKNOWLEDGEMENT

This work was supported by a grant from Supelco. We would like to thank Dr. J. Curtis (Brigham Young University) for performing the NMR and molecular modelling experiments, for data interpretation, and for helpful discussions.

REFERENCES

1 *Chem. Eng. News*, 68 (March 19, 1990) 38.
2 W. A. König, S. Lutz, P. Evers and J. Knabe, *J. Chromatogr.*, 503 (1990) 256.
3 D. Stevenson and I. D. Wilson (Editors), *Chiral Separations*, Plenum Press, New York, 1988.
4 W. A. König, *The Practice of Enantiomer Separation by Capillary Gas Chromatography*, Huethig, Heidelberg, 1987.
5 A. M. Krstulovic (Editor), *Chiral Separations by HPLC, Applications to Pharmaceutical Compounds*, Ellis Horwood, Chichester, 1989.
6 M. L. Lee and K. E. Markides (Editors), *Analytical Supercritical Fluid Chromatography and Extraction*, Chromatography Conferences, Provo, UT, 1990.
7 B. A. Jones, J. S. Bradshaw, M. Nishioka and M. L. Lee, *J. Org. Chem.*, 49 (1984) 4947.
8 B. E. Rossiter, P. Petersson, D. F. Johnson, M. Eguchi, J. S. Bradshaw, K. E. Markides and M. L. Lee, *Tetrahedron Lett.*, 32 (1991) 3609.
9 P. Petersson, K. E. Markides, D. F. Johnson, J. Curtis, B. E. Rossiter, J. S. Bradshaw and M. L. Lee, *J. Microcol. Sep.*, in press.
10 H. Uchida, Y. Kabe, K. Yoshino, A. Kawamata, T. Tsumuraya and S. Masamune, *J. Am. Chem. Soc.*, 112 (1990) 7077.
11 J. Curtis, D. F. Johnson, J. S. Bradshaw, B. E. Rossiter and M. L. Lee, in preparation.
12 R. C. Kong, S. M. Fields, W. P. Jackson and M. L. Lee, *J. Chromatogr.*, 289 (1984) 105.

*Journal of Chromatography*, 594 (1992) 291–295
Elsevier Science Publishers B.V., Amsterdam

CHROM. 23 838

# Correlation between column surface area and retention of polar solutes in packed-column supercritical fluid chromatography

Terry A. Berger* and Jerome F. Deye

*Hewlett-Packard Co., P.O. Box 900, Avondale, PA 19311-0900 (USA)*

(First received May 14th, 1991; revised manuscript received October 30th, 1991)

ABSTRACT

The retention of organic acids, amines, aminophenols, and amides was directly proportional to the surface area of Diol coated silica particles. Surface area was measured *in situ* using the method of Hong and Parcher [*Anal. Chem.*, 62 (1990) 2313–2317]. Linear regression analysis was performed on the results from four pore diameters (100, 300, 500 and 4000), plus the origin. Correlation coefficients between retention and surface area were as high as 0.9991. Both the surface area of the chromatographic support and solute retention changed by more than 14 times. All the solutes tested behaved similarly, indicating that changing the surface area is a viable means of retention control.

The smallest pore diameter tested (100 Å) produced the same efficiency as some of the larger pore sizes (*i.e.*, 300 and 500 Å) suggesting that still smaller sizes, like 60 Å, might be useful for supercritical fluid chromatography. Particles with 4000 Å pores produced poor efficiency, due to peak tailing, which suggests that deactivation was inadequate.

## INTRODUCTION

In adsorption chromatography (liquid–solid chromatography, LSC), retention is a linear function of surface area [1]. However, in bonded-phase chromatography, multiple retention mechanisms are more likely (solute interactions with both bonded phase and silanols), leading to poor peak shapes. Little attention is, subsequently, paid to the effects of surface area on retention. Studies on the physical, chemical and retention characteristics of the silica particles [*i.e.* ref. 11] used in liquid chromatography (LC) are preoccupied with the effects of silanols and other active sites. Little attention is paid to the effects of surface area. Further, it is widely accepted that bonded phases, particularly long alkyl phases like ($C_{18}$), tend to block access of solutes to the full surface area inside smaller pores.

In supercritical fluid chromatography (SFC), only one report has examined the relationship between the pore structure of silica gel and retention [2]. The retention of low-molecular-weight polymer oligomers appeared to be unrelated to the $C_{18}$ phase loading, but was related to pore diameter (but not surface area). Polar molecules produced substantially different behavior [2]. Phenol was nearly unretained and retention was independent of the pore diameter (or surface area). However, the retention of pyridine changed as much as 20 times when the nominal surface area was changed by 6.2 times. The difference was attributed to interactions between the basic pyridine and acidic residual silanols on the packing surface. Since both phenol and silanols are acidic, it was reasoned that there should be little interaction between the two. However, if the retention of acidic solutes was unrelated to the characteristics of either the bonded stationary phase, or the silanols, then there was no controlled interaction. Similarly, the retention of the basic solute appeared to depend on characteristics of the uncontrolled silanols, not on the bonded stationary phase. In either case, octadecyl phases must be considered inappropriate

0021-9673/92/$05.00 

for the separation of these polar solutes and only marginally appropriate for the separation of the polymers investigated.

The separation of polar solutes is best accomplished on polar stationary phases. Phenols [3], hydroxybenzoic acids [4] polycarboxylic acids [5] and benzylamines [6] all yield the best peak shapes on polar phases like Diol when separated with modified fluids. Low-polarity phases, like $C_{18}$, tend to produce little retained but tailed or asymmetric peaks. Pure carbon dioxide failed to elute most of these solutes from either standard or deactivated low polarity stationary phases.

The effect of the packing surface area on retention in polar systems has not been studied. In this work, retention of polar solutes on Diol packings with methanol-modified carbon dioxide is reported as a function of measured surface area. The relative efficiencies of packings with different pore diameters is also briefly examined.

## EXPERIMENTAL

The chromatographic system was described previously [3–6] and included two Hewlett-Packard (HP) Model 1050 high pressure pumps. One pump was modified with a passive inlet check valve and the head was chilled to 4.0°C to pump liquified carbon dioxide. The other pump was an unmodified isocratic unit for delivering liquid modifiers. Both pumps were operated in the flow control mode. A "tee" and a 200 × 2 mm column packed with stainless-steel balls were used to dynamically mix the two fluids. A Rheodyne Model 7520 valve with a 0.2-μl loop was used as the injector. An HP Model 5890 GC acted as the column oven. Detection was via an HP photodiode array UV–VIS detector with a high-pressure 8-μl flow cell. The signal wavelength was 210 nm with a 4-nm bandwidth. The reference wavelength was 450 nm with an 80-nm bandwidth. Pressure was monitored both upstream and downstream of the column and controlled at the detector outlet with an electronic backpressure regulator built in-house.

*In situ* surface areas were measured using the technique of Hong and Parcher [7] and the results are presented in Table I. The columns were 100 × 2 mm, containing 7 μm diameter Nucleosil Diol packings, purchased from Keystone Scientific, Bellefonte, PA, USA. The pore diameters were 100, 300, 500 and 4000 Å, corresponding to nominal surface areas of 350, 100, 35 and 10 $m^2/g$, respectively. The Diol coating was applied by the silica manufacturer. No information on phase loading was available.

The carbon dioxide was supercritical grade purchased from Scott Specialty Gases, Plumsteadville, PA, USA. Methanol was high-purity grade, purchased from Burdick & Jackson, Muskegon, MI, USA. The methanol concentration is presented as mol%. The methanol contained 0.1 *M* citric acid or 0.6% v/v isopropylamine (IPAm) as a very polar additive [8]. The IPAm was 99% pure, purchased from Aldrich Chemicals, Milwaukee, WI, USA.

TABLE I

MEASURED AND CALCULATED VALUES FOR THE SURFACE AREA ON FOUR DIOL PACKINGS, ALONG WITH CALCULATED PACKING WEIGHT, AND TRANSIT TIMES

| Pore diameter[a] (Å) | Nominal area[a] ($m^2/g$) | Measured area[b] ($m^2$) | Calculated packing weight[b] (g) | Transit time, $t_0$ (min) |
|---|---|---|---|---|
| 100 | 350 | 43 | 0.120 | 0.103 |
| 300 | 100 | 15 | 0.150 | 0.122 |
| 500 | 35 | 8.6 | 0.250 | 0.192 |
| 4000 | 10 | 3.0 | 0.300 | 0.179 |

[a] Manufacturer's value.
[b] From ref. 7.

## RESULTS AND DISCUSSION

The retention times of a wide range of solutes were measured on columns containing each of the four different pore size silica based Diol particles. Although each of the column packing materials is characterized by the manufacturer with a bulk measurement of the surface area per unit weight, the density of silica particles varies greatly with the pore diameter making such nominal comparisons relatively meaningless. Retention times of 4-hydroxybenzoic acid using five methanol concentrations in carbon dioxide were plotted against nominal surface areas as shown in Fig. 1. The results are nonlinear due to the difference in densities of the particles and, thus, the weight of packing in the different columns. The modifier contained 0.1 *M* citric acid.

The polar additive was included in the mobile phase to improve peak shapes and suppress unwanted interactions [3–8]. Temperature was fixed at 40°C. Pressure was varied slightly to maintain [9] a constant inlet density of 0.84 g/cm$^3$ and an outlet density of 0.75 g/cm$^3$.

For a more realistic correlation, the solute partition ratio ($k'$) should be plotted against the actual column surface area. To convert raw retention times ($t_R$) into partition ratios [$k' = (t_R - t_0)/t_0$], a value for the column transit time of an unretained peak ($t_0$) is required. In packed column SFC, the transit time can almost never be directly measured when modified fluids are used, because the modifier is usually significantly retained and solutes seldom elute before the modifier.

Column transit times were estimated based on the volume of the empty columns minus both the calculated interstitial and pore volumes of the particles together with the likely average mobile phase density in the column [9]. It was recently verified that both the interstitial and pore volumes contribute to the column void volume [10]. The pore volumes were obtained from the manufacturers measured values expressed in ml/g together with the weight of packing in each column. The weight was obtained by dividing the nominal surface area of the packings (in m$^2$/g) by the measured surface area (in m$^2$) for each column.

Partition ratios using the calculated transit times and measured retention times of 4-hydroxybenzoic acid are plotted against measured surface area in Fig. 2. All the plots suggest a linear relationship between area and retention.

The retention of other solutes was also studied as a function of column surface area. Plots of partition ratios *vs.* measured surface area for representative solutes is presented in Fig. 3. Solutes presented include acids, bases, and amides. In addition several amphoteric solutes containing both weakly acidic and weakly basic functional groups were included. As with 4-hydroxbenzoic acid, the plots were linear. The retention data for these and other solutes was subjected to a linear regression analysis with the origin included in the data sets. The results are summarized in Table II.

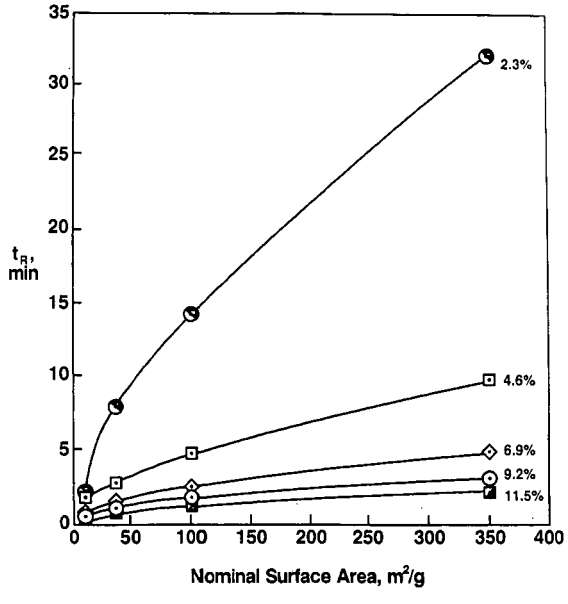


Fig. 1. Retention times of 4-hydroxybenzoic acid plotted against surface area at 5 different concentrations of methanol (containing 0.1 *M* citric acid) in carbon dioxide all at constant density. Areas are nominal values from manufacturer. Columns: 100 × 2 mm, particle diameter 7 μm, Nucleosil Diol; flow, 1.0 ml/min; average column density, 0.76 g/cm$^3$; column temperature, 40°C.

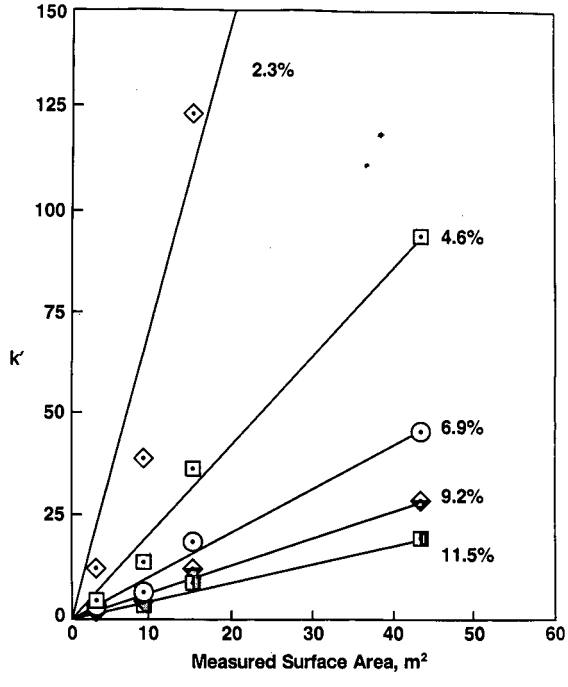


Fig. 2. Retention data for 4-hydroxybenzoic acid from Fig. 1 reduced to partition ratios plotted against *in situ* measured surface areas. Other conditions as in Fig. 1.

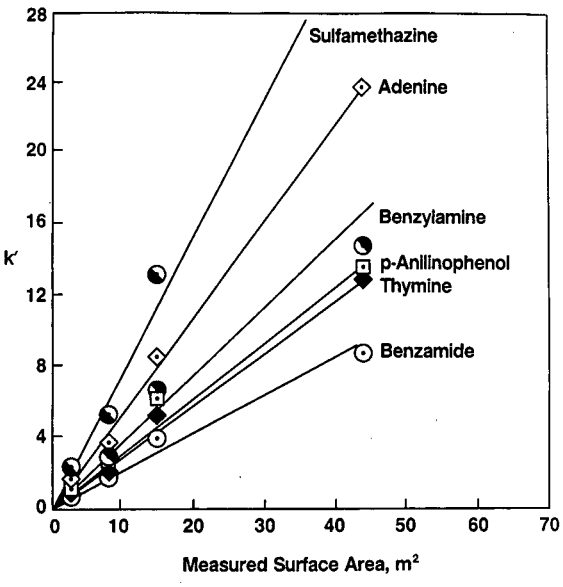


Fig. 3. Plots of the partition ratio of various solutes against the *in situ* measured surface area of the Nucleosil Diol columns used in Fig. 1. Conditions: 1.0 ml/min of 10% (v/v) methanol (containing 0.6% isopropylamine) in carbon dioxide at 40°C, 182 bar outlet pressure.

All solutes (except N,N-diethylaminophenol, $r$ = 0.9831) produced correlation coefficients greater than 0.99. Such high correlation coefficients indicate that, despite some scatter in the data, the relationship between retention and surface area is, indeed, linear. The scatter in the data is largely due to the uncertainty in both the surface area measurements and in the accuracy of the mobile phase composition, particularly at low modifier concentration.

The slopes from the linear regressions were further used to calculate the idealized ratio of retention times of each solute at the highest and lowest surface areas. The mean and standard deviation of these ratios for twelve different solutes were then determined. For a measured surface area change of 14.3 times, retention of the solutes changed 14.4 ± 6 times. Thus, surface area and retention were directly proportional.

Since the retention of both acidic and basic solutes is linearly related to the surface area of the packing, one can conclude that the separation process is under control. The same mechanism appears to operate on all pore sizes. In addition, the

TABLE II

PARTITION RATIOS OF SOLUTES ON FOUR DIFFERENT SURFACE AREA COLUMNS AND THE CORRELATION COEFFICIENT, $r$, FROM LINEAR REGRESSION INDICATING THE DEGREE OF FIT TO A STRAIGHT LINE

The origin was included in the calculation of the correlation coefficient. Columns: 100 × 2 mm, 7 μm Nucleosil Diol, 1 ml/min, 10% methanol (containing 0.6% isopropylamine), 40°C, 182 bar outlet pressure.

| Solute | Partition ratios, $k'$ | | | | Correlation coefficient, $r$ |
|---|---|---|---|---|---|
| | Pore diameter (Å)/measured surface area (m²) | | | | |
| | 4000/3 | 500/8.6 | 300/15 | 100/43 | |
| Thymine | 1.17 | 2.08 | 5.09 | 12.66 | 0.9967 |
| Adenine | 1.41 | 3.39 | 8.64 | 24.07 | 0.9979 |
| Cytosine | 4.66 | 10.90 | 23.27 | 68.77 | 0.9991 |
| Benzylamine | 1.65 | 2.64 | 6.62 | 14.97 | 0.9934 |
| Benzamide | 0.95 | 1.46 | 3.79 | 8.78 | 0.9938 |
| Nicotinic acid | 3.62 | 10.58 | 18.47 | 41.91 | 0.9957 |
| *p*-Anilinophenol | 1.41 | 2.57 | 6.22 | 13.77 | 0.9931 |
| N,N-Diethylaminophenol | 0.90 | 1.27 | 3.20 | 6.19 | 0.9831 |
| Sulfamethazine | 2.11 | 4.97 | 12.90 | 34.92 | 0.9976 |
| Sulfanilamide | 3.70 | 8.48 | 18.24 | 51.97 | 0.9991 |
| Sulfisomidine | 2.96 | 14.75 | 18.78 | 46.49 | 0.9912 |
| Sulfapyridine | 2.77 | 6.35 | 15.75 | 43.17 | 0.9980 |

chemistry employed to produce the bonded stationary phase appears to be equally effective on all the pore sizes producing the same loading per unit area.

None of the separation problems associated with acids and bases in a previous report [2] were encountered.

*Efficiency*

Efficiency measurements were not the primary objective of this study. However, changing retention by varying surface area is useful only if efficiency is similar on all the columns.

Extracolumn effects tended to limit the measured efficiencies, particularly at short retention times. The columns were all 100 × 2 mm I.D., operated with a flow of 1 ml/min (approximately 2 times optimum). Components contributing to post-column band broadening included: approximately 1 m of 125 μm I.D. connector tubing, several zero dead volume (ZDV) fittings, and an 8-μl detector flow cell. Despite these limitations, a few general comments can be made. At very long retention times the columns produced up to 6720 theoretical plates [$N = 6.28\ (t_R/W_e)^2$] on 7-μm particles, corresponding to 94% of the theoretical maximum (assuming $h_{min} = 2d_p$). Peaks were symmetrical even at partition ratios approaching 200 ($k' = 188$). Since the flow rate is up to twice the optimum value, these results are quite satisfactory. There was no significant difference in efficiency between the 100 and 300 Å pore diameter packings. The 500 Å column produced 83% of theoretical efficiency. The 4000 Å columns produced no more than 32% of theoretical efficiency, due to significantly tailed peaks. However, retention on both the 500 and 4000 Å packings was much lower than on the smaller pore sizes, making extracolumn effects more important on the former.

## CONCLUSIONS

Unlike previous results with $C_{18}$ packings [2], the retention of polar acids and bases was linearly proportional to the packing surface area. No difference in behavior was noted between acids or bases. Linear regressions of better than 0.99 were typical. Statistical analysis showed that retention changed 14.4 ± 6 times for a surface area change of 14.3 times. The linear, proportional relationship between surface area and retention indicates that the Diol phase was equally applied (the same loading) to a wide range of pore sizes. These results also suggest that the inside of all the pore sizes were equally accessible to the solutes. These observations are in contrast to reversed-phase LC, where long-chain (*i.e.*, $C_{18}$) bonded phases appear to be more difficult to apply to smaller pores (more residual activity) and decrease accessibility of solutes to the interior of pores.

Changing pore diameter appears to be an effective, and predictable means of adjusting the retention of a wide range of solutes. The high efficiency on the smaller pore diameters suggest that even smaller diameters might be useful in packed-column SFC.

## ACKNOWLEDGEMENTS

The authors wish to thank Jon Parcher and his graduate students at the University of Mississippi for making the surface area measurements on the columns used in this study. They also thank Bill Wilson of this laboratory for helpful discussions and review of the manuscript.

## REFERENCES

1 L. R. Snyder, *Principles of Adsorption Chromatography*, Marcel Dekker, New York, 1968, Ch. 6.
2 A. Nomura, J. Yamada and K.-I. Tsunoda, *J. Chromatogr.*, 448 (1988) 87–93.
3 T. A. Berger and J. F. Deye, *J. Chromatogr. Sci.*, 29 (1991) 54–59.
4 T. A. Berger and J. F. Deye, *J. Chromatogr. Sci.*, 29 (1991) 26–30.
5 T. A. Berger and J. F. Deye, *J. Chromatogr. Sci.*, 29 (1991) 141–146.
6 T. A. Berger and J. F. Deye, *J. Chromatogr. Sci.*, 29 (1991) 310–317.
7 H. Song and J. F. Parcher, *Anal. Chem.*, 62 (1990) 2313–2317.
8 T. A. Berger and J. F. Deye, *J. Chromatogr.*, 547 (1991) 377–392.
9 T. A. Berger and J. F. Deye, *Anal.Chem.*, 62 (1990) 1181–1185.
10 H. G. Janssen, H. M. J. Snijders, J. A. Rijks, C. A. Cramers and P. J. Schoenmakers, *J. High Resolut. Chromatogr.*, 14 (1991) 438–445.
11 J. Nawrocki and B. Buszewski, *J. Chromatogr.*, 449 (1988) 1–24.

*Journal of Chromatography*, 594 (1992) 297–307
Elsevier Science Publishers B.V., Amsterdam

CHROM. 23 812

# Effects of collection solvent parameters and extraction cell geometry on supercritical fluid extraction efficiencies

John J. Langenfeld, Mark D. Burford, Steven B. Hawthorne* and David J. Miller

*University of North Dakota, Energy and Environmental Research Center, Grand Forks, ND 58202 (USA)*

(First received August 6th, 1991; revised manuscript received October 18th, 1991)

## ABSTRACT

Supercritical fluid extraction (SFE) collection efficiencies of 66 compounds with a wide range of volatility and polarity were examined. Good collection efficiencies required efficient partitioning of the analyte into the collection solvent after depressurization, and factors including collection solvent polarity and temperature were found to be more important than collection solvent volume and height. Heating the collection solvent with a heat gun to avoid plugging of the outlet restrictor resulted in 20–50% losses of the more volatile analytes, while >90% trapping of all test analytes could be attained by controlling the solvent temperature at 5°C. Extraction cell geometry ("long, narrow" *versus* "short, broad" vessel) at constant internal volume and the orientation of the extraction cell were found to have negligible effects on the extraction rates of polycyclic aromatic hydrocarbons (PAHs) from railroad bed soil and flavor and fragrance compounds from lemon peels. The supercritical fluid flow-rate also had little effect on the extraction rate of native PAHs provided that it was sufficient to sweep the cell dead volume every *ca.* 3 min.

## INTRODUCTION

The use of supercritical fluids for the extraction of organic compounds from a wide variety of matrices is rapidly increasing because of the attractive properties that supercritical fluids exhibit and their potentially wide applicability for sample extractions. Supercritical fluids have lower viscosities and higher solute diffusivities than liquid solvents, which improves mass transfer and reduces the extraction time needed, and the solvent strength of a supercritical fluid is a function of density and can be controlled by simply changing the pressure or temperature. Supercritical fluids such as carbon dioxide can be inexpensive, available in high purity and chemically inert, and as they are gases under ambient conditions the need for liquid solvents and concentration steps is nearly eliminated.

There have been several reports of different methods for trapping analytes after the SFE depressurization step, including collection in an open vessel [1–3], collection on sorbent resins such as Tenax, $C_{18}$, silica gel and XAD traps [4–6], collection on cryogenically cooled surfaces [7] and on-line methods coupled to various chromatographic instrumentation [8–11]. In this investigation, a simple off-line analyte trapping technique was investigated which consisted of depressurizing the supercritical fluid into an organic collection solvent [12–14]. This method was chosen because it has been the most commonly used method in supercritical fluid extraction (SFE) studies, is relatively simple and inexpensive to perform and because the extracts are immediately ready for chromatographic analysis using conventional injection techniques.

There have been numerous reports of quantitative extractions using supercritical fluids [15], but most have dealt with fairly non-volatile species that are more easily trapped using the collection methods mentioned above. However, many analytes of interest for SFE exhibit a high vapor pressure, which may make collection after SFE difficult. For such analytes, low recoveries may be wrongly attributed to poor extraction efficiency when the real problem is poor collection of extracted analytes on depressurization of the supercritical fluid. In addition,

0021-9673/92/$05.00 

many real environmental and natural matrices contain high concentrations of water that can freeze and cause restrictor plugging owing to the rapid cooling from the carbon dioxide depressurization. Heating the collection solvent is an effective method to prevent the restrictor from becoming blocked, but may further reduce the collection efficiencies of volatile analytes.

This paper describes the collection efficiencies of 60 environmentally hazardous pollutants from the US Environmental Protection Agency (EPA)'s semivolatile target compound list and six flavor and fragrance compounds. It must be emphasized that the investigations reported here were focused on determining the collection efficiencies under SFE conditions, not SFE extraction efficiencies, and thus are based on the extraction of test analytes that were added to relatively inert matrices. Even though the use of such spikes is not always a valid approach to determining extraction efficiencies (as spikes do not necessarily interact with the same matrix active sites as native analytes), spiking is an effective and reliable method for determining trapping efficiencies as the spiked analytes are introduced into the collection system under the identical SFE conditions experienced by native analytes. The effect of different solvent trapping conditions on SFE collection efficiencies, including collection solvent polarity, solvent volume and height, solvent temperature and supercritical fluid flow-rate, were investigated. In addition, the effects of SFE flow-rate, cell geometry and cell orientation on the extraction rates of native (not spiked) polycyclic aromatic hydrocarbons (PAHs) from railroad bed soil and native flavor and fragrance compounds from lemon peel are discussed.

## EXPERIMENTAL

### *Samples and standards*

Standards (0.6 mg/ml each) of 60 compounds from the semivolatile target compound list were prepared in methylene chloride and stored at 0°C until used. An additional standard of six flavor and fragrance compounds in methylene chloride (100 mg/ml each) was prepared and stored in the same manner. Spiking levels for the semivolatile pollutants and the flavor and fragrance compounds were 18 μg and 600 μg of each compound, respectively. Internal standards added to each extract for gas chromatographic (GC) analysis after SFE were 10 μg of 1,4-dichlorobenzene-$d_4$ for the semivolatile pollutants and 500 μg of *n*-heptadecane for the flavor and fragrance compounds.

Two real samples with different physical and chemical characteristics were chosen to investigate the effect of cell geometry and orientation on SFE extraction rates of native analytes. Railroad bed soil was chosen because it contained native PAHs of environmental interest. Lemon peel was selected to represent a non-homogeneous, odd-shaped (not conforming to the extraction vessel shape and therefore increasing the cell dead volume) matrix that contained a wide range of volatile components such as monoterpenes and sesquiterpenes, and because it also had a high water content (85% as determined by oven drying overnight at 100°C) which consistently led to restrictor plugging from frozen water unless the collection solvent was heated during SFE. Prior to extraction, the railroad bed soil was sieved to < 2 mm to remove any debris and fresh lemon peel was cut into strips of *ca.* 10 mm × 2 mm × 1 mm.

### *Supercritical fluid extractions*

All supercritical fluid extractions were performed using SFC-grade carbon dioxide (Scott Specialty Gases, Plumsteadville, PA, USA) and an ISCO (Lincoln, NE, USA) Model 260D syringe pump operated at 400 atm. The extraction cell temperature was maintained at 50°C using a thermostatically controlled tube heater. Extractions were performed using 2.5-ml "long, narrow" (132 mm × 5 mm I.D.) or 2.5-ml "short, broad" (33 mm × 10 mm I.D.) extraction cells from Keystone Scientific (Bellefonte, PA, USA). The flow-rate of supercritical fluid through the extraction cells was controlled by a 10-cm outlet restrictor (26 μm I.D. unless noted otherwise, resulting in a flow-rate of *ca.* 0.6 ml/min measured as a liquid at the pump and a gaseous carbon dioxide flow-rate of *ca.* 300 ml/min) made from fused-silica tubing (Polymicro Technologies, Phoenix, AZ, USA). All organic solvents used were of pesticide grade.

Collection efficiencies were determined by filling the 2.5-ml "long, narrow" extraction cell with 3.5 g of 70–80-mesh glass beads for the flavor and fragrance compounds or 3.5 g of clean sea sand for the

semivolatile pollutants, and spiking the standard solutions into the center of the glass beads or sea sand. The cell was immediately sealed to prevent any loss of the volatile spike components, placed inside the tube heater and the samples were extracted for 5–30 min. Extracted analytes were collected into 3.7-ml (33 mm × 12 mm I.D.), 7.4-ml (48 mm × 14 mm I.D.) or 15.0-ml (59 mm × 18 mm I.D.) vials containing 2.5–10.0 ml of collection solvent. Solvent volume was maintained by small additions of solvent during SFE. Heat was applied to the collection solvent using a heat gun or a temperature-controlled block made from aluminum (75 mm × 50 mm × 38 mm) with four holes (26 mm × 23 mm I.D.) bored into it for the sample vials. Water was placed between the vial and the heating block to ensure proper thermal transfer was achieved.

The effect of cell geometry and orientation was investigated using 3 g of railroad bed soil or 1 g of lemon peel placed inside one of the 2.5-ml extraction cells ("long, narrow" or "short, broad"). The extraction vessel was sealed and placed inside the thermostated tube heater, and the native analytes were extracted from the sample into a 7.4-ml vial containing 5 ml of methylene chloride. The collection solvent was maintained at 5°C using the temperature-controlled block (no provision was made to cool the block to 5°C; however, as discussed later, the solvent temperature rapidly drops to 5°C on beginning SFE). The flow-rate of the supercritical fluid was varied from 0.15 to 1.2 ml/min using 10-cm lengths of 15, 24, 26, 29 or 32 μm I.D. restrictors. Fractions of the extracts were collected at timed intervals over a period of 100 min to compare extraction rates for different extraction cell geometries, cell orientations and flow-rates. Each fraction was immediately spiked with the appropriate internal standard and analyzed.

*Gas chromatographic analysis*

All GC analyses were done with a Hewlett-Packard Model 5890 gas chromatograph with flame ionization detection and hydrogen as the carrier gas. The injections were performed in the split mode with a 20:1 splitting ratio into a wide-bore (25 m × 0.32 mm I.D., 0.17 μm film thickness) HP-1 (Hewlett-Packard, Avondale, PA, USA) or a wide-bore (25 m × 0.32 mm I.D., 0.17 μm film thickness) HP-5 fused-silica capillary column. The injector and detector temperatures were maintained at 300°C. Compound identifications were confirmed using a Hewlett-Packard Model 5985 gas chromatograph–mass spectrometer and by the injection of standards.

## RESULTS AND DISCUSSION

*Collection efficiencies during supercritical fluid extraction*

As previously discussed, SFE of wet (*e.g.*, containing more than *ca.* 1% water) real samples often requires heating to prevent restrictor plugging from ice formation. To mimic an extraction scheme when the sample contains significant amounts of water, mild heating (heated every 30 s for 5 s during the first 5 min and thereafter heated every 2 min for 5 s) with a heat gun was applied to the collection solvent, and the collection efficiencies were determined for several different collection solvents of differing polarity and boiling point (GC calibration standards were prepared in each solvent tested to ensure that any differences in SFE collection efficiencies that were observed between solvents were not a result of differences in the GC analysis that might be caused by the solvent). The effect of mild heating on collection solvent temperature is shown in Fig. 1. As shown in Table I for 40-min extractions, analyte losses of up to 60% occurred, with a general trend in

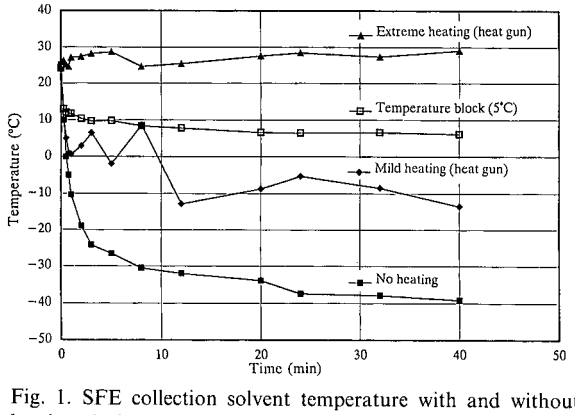


Fig. 1. SFE collection solvent temperature with and without heating during SFE. Supercritical $CO_2$ flow-rate was *ca.* 0.6 ml/min (*ca.* 300 ml/min gaseous $CO_2$) into 5 ml of methylene chloride. Mild heating (heated every 30 s for 5 s during the first 5 min and thereafter heated every 2 min for 5 s) and extreme heating (heated every 30 s for 15 s during the first 5 min and thereafter heated every 2 min for 15 s) were performed for 40 min using a heat gun. The temperature-controlled block was set at 5°C as described in the text.

TABLE I

COLLECTION EFFICIENCIES OF SEMIVOLATILE POLLUTANTS INTO VARIOUS TRAPPING SOLVENTS WHILE USING MILD HEATING

| Compound | Recovery (%)[a] | | | | |
|---|---|---|---|---|---|
| | Methylene chloride | Chloroform | Acetone | Methanol | Hexane |
| Phenol | 77.4 (2.4) | 72.3 (3.1) | 67.6 (1.6) | 54.9 (11.6) | 42.5 (1.6) |
| Di(2-chloroethyl) ether | 73.1 (5.6) | 68.7 (2.6) | 72.5 (1.1) | 56.4 (13.8) | 60.5 (5.6) |
| 1,3-Dichlorobenzene | 70.4 (5.5) | 66.5 (3.1) | 57.4 (0.9) | 53.4 (19.2) | 54.5 (2.7) |
| 1,4-Dichlorobenzene | 76.8 (3.0) | 72.5 (3.4) | 69.9 (1.4) | 53.4 (13.0) | 44.2 (4.7) |
| 1,2-Dichlorobenzene | 77.6 (4.9) | 74.3 (3.5) | 74.9 (0.8) | 57.8 (13.3) | 45.6 (4.6) |
| N-Nitrosodipropylamine | 77.6 (7.3) | 77.3 (2.8) | 75.9 (1.4) | 55.8 (10.7) | 48.8 (6.2) |
| 4-Methylphenol | 78.5 (3.6) | 74.8 (3.7) | 70.4 (1.1) | 54.7 (16.0) | 46.4 (5.8) |
| Nitrobenzene | 82.2 (3.6) | 82.3 (4.6) | 73.7 (1.3) | 57.7 (10.2) | 60.4 (1.6) |
| Isophorone | 79.7 (3.9) | 74.9 (3.0) | 73.2 (1.4) | 55.9 (15.6) | 50.5 (2.7) |
| 2-Nitrophenol | 80.0 (5.0) | 79.6 (5.3) | 82.0 (0.2) | 60.8 (8.3) | 56.8 (5.1) |
| 2,4-Dichlorophenol | 77.7 (4.5) | 75.4 (5.2) | 67.6 (1.3) | 63.8 (18.6) | 55.5 (5.9) |
| 1,2,4-Trichlorobenzene | 78.7 (5.5) | 76.2 (3.4) | 70.4 (1.3) | 59.4 (17.9) | 55.9 (4.9) |
| 4-Chloro-3-methylphenol | 83.6 (6.1) | 86.8 (5.9) | 81.4 (3.9) | 49.7 (15.4) | 72.0 (0.9) |
| Hexachlorocyclopentadiene | 78.2 (1.4) | 77.1 (4.4) | 70.1 (1.6) | 58.6 (16.3) | 60.9 (1.9) |
| 2,4,5-Trichlorophenol | 83.9 (2.9) | 83.6 (3.8) | 85.5 (1.8) | 59.4 (3.4) | 71.1 (1.8) |
| 2,4,6-Trichlorophenol | 85.3 (3.9) | 85.4 (4.8) | 87.4 (2.4) | 57.9 (4.9) | 73.4 (1.9) |
| 2-Chloronaphthalene | 82.5 (4.0) | 81.9 (2.6) | 79.8 (1.7) | 60.2 (11.2) | 67.1 (2.9) |
| 2-Nitroaniline | 86.4 (1.4) | 86.4 (2.5) | 88.4 (1.3) | 57.3 (4.7) | 72.4 (3.1) |
| Acenaphthylene | 83.7 (3.8) | 85.4 (1.7) | 82.7 (1.4) | 60.0 (8.3) | 66.3 (9.9) |
| Dimethyl phthalate | 85.5 (3.1) | 91.6 (2.0) | 87.1 (0.9) | 59.9 (2.8) | 76.7 (2.8) |
| 2,6-Dinitrotoluene | 85.9 (3.3) | 90.1 (1.1) | 88.1 (0.8) | 60.9 (3.0) | 76.7 (3.3) |
| Acenaphthene | 84.1 (3.5) | 85.1 (3.6) | 82.9 (1.4) | 60.6 (7.3) | 72.2 (2.0) |
| 3-Nitroaniline | 85.8 (3.9) | 87.1 (2.8) | 88.3 (2.2) | 54.5 (5.6) | 74.1 (6.5) |
| Dibenzofuran | 84.2 (4.3) | 85.8 (3.1) | 86.1 (0.9) | 63.1 (5.8) | 73.9 (5.1) |
| 2,4-Dinitrotoluene | 92.3 (4.4) | 86.9 (4.5) | 96.4 (3.0) | 60.1 (11.0) | 67.8 (1.8) |
| Fluorene | 85.5 (3.9) | 88.1 (3.7) | 87.4 (1.2) | 61.8 (3.4) | 76.1 (2.6) |
| 4-Chlorophenyl phenyl ether | 85.5 (2.8) | 88.4 (4.3) | 86.6 (1.2) | 62.1 (3.9) | 75.5 (2.3) |
| Diethyl phthalate | 87.3 (1.7) | 90.7 (4.4) | 88.9 (0.8) | 59.9 (2.7) | 79.3 (3.3) |
| 4-Nitroaniline | 87.0 (8.3) | 89.1 (3.5) | 89.6 (3.6) | 48.2 (13.3) | 53.2 (20.6) |
| N-Nitrosodiphenylamine | 86.5 (8.3) | 90.2 (6.2) | 91.8 (2.4) | 64.6 (2.9) | 74.0 (11.3) |
| 4-Bromophenyl phenyl ether | 86.4 (2.3) | 94.3 (9.8) | 89.3 (1.2) | 60.2 (3.6) | 81.7 (6.4) |
| Hexachlorobenzene | 86.0 (2.1) | 90.6 (8.7) | 88.7 (0.8) | 61.7 (3.2) | 79.4 (1.2) |
| Phenanthrene | 86.9 (2.9) | 89.0 (3.9) | 90.9 (1.7) | 59.7 (3.5) | 79.1 (4.0) |
| Anthracene | 87.5 (2.6) | 88.0 (3.7) | 89.6 (1.6) | 58.9 (3.8) | 78.7 (3.5) |
| Dibutyl phthalate | 90.4 (1.8) | 89.4 (1.7) | 96.6 (3.5) | 57.5 (10.2) | 81.8 (2.5) |
| Fluoranthene | 89.1 (2.9) | 89.9 (4.9) | 91.5 (3.0) | 56.2 (7.1) | 78.3 (2.3) |
| Pyrene | 89.5 (3.1) | 90.8 (1.7) | 92.8 (1.8) | 57.7 (6.7) | 79.6 (4.5) |
| Butylbenzyl phthalate | 89.4 (2.4) | 89.4 (3.6) | 92.1 (2.7) | 54.7 (9.8) | 77.3 (3.8) |
| Chrysene | 90.4 (3.5) | 91.9 (4.5) | 92.1 (2.0) | 56.7 (9.2) | 80.3 (3.5) |
| 3,3′-Dichlorobenzidine | 88.8 (2.4) | 88.9 (4.4) | 91.6 (4.4) | 49.6 (17.8) | 76.8 (3.2) |
| 2-Ethylhexyl phthalate | 92.2 (2.4) | 90.5 (2.5) | 98.6 (7.0) | 56.1 (10.0) | 90.7 (1.3) |
| Dioctyl phthalate | 91.1 (1.5) | 88.9 (3.5) | 90.9 (1.6) | 53.9 (13.6) | 77.8 (4.5) |
| Benzo[*b*]fluoranthene | 91.6 (2.3) | 88.1 (3.0) | 91.5 (2.9) | 54.9 (15.8) | 77.3 (2.5) |
| Benzo[*k*]fluoranthene | 91.5 (2.3) | 88.5 (3.5) | 91.5 (2.8) | 55.7 (14.6) | 77.9 (2.9) |
| Benzo[*a*]pyrene | 92.2 (2.1) | 86.9 (4.5) | 91.4 (3.7) | 56.9 (17.9) | 76.3 (1.8) |
| Dibenzo[*a,h*]anthracene | 93.7 (4.7) | 82.3 (2.4) | 90.0 (7.6) | 63.2 (12.2) | 72.6 (2.8) |
| Benzo[*ghi*]perylene | 93.2 (2.2) | 81.1 (2.3) | 87.6 (6.5) | 66.5 (11.2) | 71.4 (1.7) |

[a] Values in parentheses are relative standard deviations (%) for triplicate 40-min extractions.

recoveries based on the volatility of the analyte (the compounds in Table I are listed in order of GC retention indices) and analyte solubility in the collection solvent. Based on a comparison of chloroform (b.p. = 60.9°C) and methylene chloride (b.p. = 40°C), the boiling point of the collection solvent did not affect the collection efficiencies as both of these solvents showed similar losses of 10–25% of the tested compounds. Acetone yielded trapping efficiencies similar to methylene chloride and chloroform, but methanol failed to collect *ca.* 35–50% of each of the species. Hexane was the poorest collection solvent for several of the most volatile test species, but was better than methanol for the less volatile components. As methylene chloride was the best overall collection solvent (and a good solvent for GC), it was used to test the collection efficiencies for the test species in subsequent studies.

The cooling effect on the collection solvent (methylene chloride) that results from carbon dioxide depressurization with and without solvent heating for 40 min is shown in Fig. 1. Without any heating the temperature of the collection solvent rapidly drops to −25°C, then slowly approaches −40°C. All of the semivolatile pollutants were quantitatively collected (>95%) into methylene chloride with no heating, but this is an unrealistic experimental approach because the collection solvent becomes so cold that real samples containing significant amounts of water can cause restrictor plugging from freezing water (such plugging has been observed for nearly all samples that we have encountered which contain more than *ca.* 1% water). As previously discussed, this problem is easily solved by using a heat gun to warm the restrictor and collection solvent but, as shown in Fig. 1, this results in temperature fluctuations that depend on the degree of heating and that can approach the boiling point of methylene chloride. As shown in Table I, even mild heating with the heat gun resulted in significant losses of the more volatile analytes. To avoid the solvent temperature fluctuations resulting from the heat gun, an alternative method of heating the collection solvent, the temperature-controlled block, was designed and tested. Fig. 1 shows that when the temperature-controlled block was set at 5°C, the collection solvent rapidly cooled to *ca.* 6°C and the block was able to maintain a relatively constant solvent temperature. (Note that the block contains no cooling device and was at room temperature at the beginning of the SFE step. The temperature profile results from the cooling effect of the expanding carbon dioxide combined with the block heater set to turn on at 5°C.) The temperature-controlled block set at 5°C also eliminated restrictor plugging from freezing water during SFE of wet samples.

Collection efficiencies of the semivolatile pollutants from the target compound list were again determined (40-min extractions and methylene chloride as the collection solvent) using the temperature-controlled block set at 5°C. As shown in Table II, the collection efficiencies of all of the compounds on the list were good, with a range of 92–104%. The collection efficiencies also showed excellent reproducibility, with the relative standard deviations for all of the test species being <6% for triplicate spike extractions.

As the temperature-controlled block was effective in eliminating restrictor plugging from ice formation during SFE of wet samples, such as lemon peel, and yielded quantitative collection of the semivolatile pollutants, this method of collection was used to test the collection efficiencies of several additional flavor and fragrance compounds including α-pinene, carvone, eugenol, cedrene, cedrol and santonin. The collection efficiencies achieved during the 10-min SFE using different trapping solvents (5 ml, resulting in a 33-mm solvent height) were again found to depend on the solubility and volatility of the test analytes. Acetone and toluene behaved similarly and recovered *ca.* 90% of all the compounds except α-pinene, which was only 76% and 78% recovered, respectively. Methanol was able to trap 100% of the santonin and *ca.* 90% of the remaining compounds, but only trapped 79% of the α-pinene. Hexane was an excellent trapping solvent for all of the compounds (>95%) except santonin, which was only 69% recovered. Methylene chloride was able to trap >90% of all of the components that were tested. Since methylene chloride was also the best collection solvent for the semivolatile pollutants, it was again chosen as the collection solvent in the remainder of the collection experiments.

It should be noted that some losses of the flavor and fragrance compounds can occur when concentrating the extracts under a gentle stream of nitrogen. For example, when extracts collected in

TABLE II

COLLECTION EFFICIENCIES OF SEMIVOLATILE POLLUTANTS IN METHYLENE CHLORIDE HELD AT 5°C

| Compound | Recovery (%)[a] | Compound | Recovery (%)[a] |
|---|---|---|---|
| 2-Chlorophenol | 96.8 (1.1) | Dimethyl phthalate | 100.1 (1.9) |
| Phenol | 97.8 (0.3) | 2,6-Dinitrotoluene | 99.0 (2.0) |
| Di(2-chloroethyl) ether | 100.3 (1.9) | Acenaphthene | 98.3 (1.4) |
| 1,3-Dichlorobenzene | 99.8 (2.5) | 3-Nitroaniline | 93.2 (6.4) |
| 1,4-Dichlorobenzene | 101.4 (2.7) | Pentachlorophenol | 97.8 (1.4) |
| 1,2-Dichlorobenzene | 99.8 (2.2) | Dibenzofuran | 98.1 (5.0) |
| Benzyl alcohol | 95.4 (1.2) | 2,4-Dinitrotoluene | 99.6 (1.8) |
| Di(2-chloroisopropyl) ether | 95.5 (0.6) | Fluorene | 99.7 (2.1) |
| 2-Methylphenol | 95.1 (1.5) | 4-Chlorophenyl phenyl ether | 100.4 (1.0) |
| Hexachloroethane | 95.6 (1.8) | Diethyl phthalate | 97.1 (4.0) |
| N-Nitrosodipropylamine | 97.9 (1.6) | 4-Nitroaniline | 102.9 (5.2) |
| 4-Methylphenol | 98.9 (2.0) | N-Nitrosodiphenylamine | 101.1 (4.6) |
| Nitrobenzene | 100.0 (2.2) | 4-Bromophenyl phenyl ether | 99.7 (1.7) |
| Isophorone | 98.6 (2.5) | Hexachlorobenzene | 99.9 (3.5) |
| 2-Nitrophenol | 99.0 (0.6) | Phenanthrene | 100.3 (2.8) |
| 2,4-Dimethylphenol | 95.4 (0.9) | Anthracene | 97.0 (5.1) |
| 2-Chloroethoxymethane | 103.9 (1.9) | Dibutyl phthalate | 99.1 (2.6) |
| 2,4-Dichlorophenol | 98.5 (1.4) | Fluoranthene | 96.1 (4.5) |
| 1,2,4-Trichlorobenzene | 99.7 (1.0) | Pyrene | 99.1 (4.6) |
| Naphthalene | 98.6 (1.3) | Butylbenzyl phthalate | 98.4 (2.1) |
| 4-Chloroaniline | 97.6 (2.5) | Benz[*a*]anthracene | 98.6 (1.2) |
| Hexachlorobutadiene | 97.8 (1.6) | Chrysene | 100.9 (1.4) |
| 2-Methylnaphthalene | 97.5 (2.6) | 3,3′-Dichlorobenzidine | 92.4 (4.1) |
| 4-Chloro-3-methylphenol | 100.5 (1.3) | 2-Ethylhexyl phthalate | 99.5 (2.9) |
| Hexachlorocyclopentadiene | 103.5 (1.7) | Dioctyl phthalate | 96.7 (2.3) |
| 2,4,5-Trichlorophenol | 97.7 (1.7) | Benzo[*b*]fluoranthene | 97.0 (3.6) |
| 2,4,6-Trichlorophenol | 99.0 (2.3) | Benzo[*k*]fluoranthene | 98.6 (3.2) |
| 2-Chloronaphthalene | 99.5 (1.4) | Benzo[*a*]pyrene | 96.8 (2.2) |
| 2-Nitroaniline | 98.3 (2.4) | Dibenzo[*a,h*]anthracene | 92.7 (5.3) |
| Acenaphthylene | 99.4 (1.7) | Benzo[*ghi*]perylene | 98.8 (3.8) |

[a] Values in parentheses are relative standard deviations (%) for triplicate 40-min extractions.

methylene chloride were evaporated from 5 to 1 ml under a gentle stream of nitrogen, 7% of the α-pinene was lost and *ca.* 4% of the other compounds were lost. To avoid these losses, no concentration of the extracts was performed for the flavor and fragrance recovery studies.

To investigate whether losses of analytes occur during SFE because they are purged out of the collection solvent by the high flow-rate of gaseous carbon dioxide or because they fail to partition into the collection solvent, the flavor and fragrance standard was spiked into a 7.4-ml vial containing 5.0 ml (33-mm height) of methylene chloride, and carbon dioxide was allowed to bubble through the spiked solvent for 5–30 min under normal SFE conditions. Table III shows the effect of purging under different supercritical fluid flow-rates and purging times. At 0.3 and 0.6 ml/min, there are no significant losses ($< 5\%$) except for α-pinene, which showed a 6% loss at 0.3 ml/min and a 13% loss at 0.6 ml/min after 30 min. At 1.2 ml/min, α-pinene showed a 24% loss and the losses of the other flavor and fragrance compounds ranged from 4 to 7% after 30 min. As none of the test species showed significant losses after 5 min, these results demonstrate that excessively high flow-rates coupled with long extraction times may result in lower overall recoveries of volatile analytes because of purging losses.

To determine the effect of collection solvent volume on the trapping efficiencies of the flavor and

TABLE III

$CO_2$ PURGING EFFECT ON FLAVOR AND FRAGRANCE COMPOUND LOSSES

| Compound | Flow-rate (ml/min)[a] | Amount remaining (%)[b] | |
|---|---|---|---|
| | | 5 min | 30 min |
| α-Pinene | 0.3 | 98.8 (0.8) | 94.5 (3.3) |
| Carvone | | 100.1 (0.6) | 101.7 (1.9) |
| Eugenol | | 100.2 (0.8) | 101.7 (2.4) |
| Cedrene | | 100.5 (1.1) | 101.1 (2.1) |
| Cedrol | | 100.4 (1.9) | 101.2 (3.0) |
| Santonin | | 100.3 (1.3) | 100.8 (3.1) |
| α-Pinene | 0.6 | 96.9 (3.4) | 86.8 (0.9) |
| Carvone | | 99.4 (2.9) | 100.4 (1.2) |
| Eugenol | | 99.4 (2.3) | 100.5 (1.5) |
| Cedrene | | 99.1 (2.6) | 99.7 (1.8) |
| Cedrol | | 99.9 (2.3) | 100.6 (1.1) |
| Santonin | | 98.7 (1.2) | 98.1 (1.5) |
| α-Pinene | 1.2 | 98.3 (0.6) | 76.6 (3.1) |
| Carvone | | 100.6 (1.8) | 93.4 (3.1) |
| Eugenol | | 100.9 (0.5) | 94.9 (3.7) |
| Cedrene | | 100.6 (0.6) | 92.7 (3.2) |
| Cedrol | | 99.8 (0.6) | 95.7 (3.0) |
| Santonin | | 99.3 (0.3) | 95.8 (3.3) |

[a] Flow-rate of $CO_2$ measured as a liquid at the pump.
[b] Values in parentheses are relative standard deviations (%) for triplicate extractions.

fragrance compounds, collection for 10 min into different solvent volumes (2.5, 5.0 and 10.0 ml) with a supercritical fluid flow-rate of 0.6 ml/min was tested. The results in Table IV show that the collection solvent volume was less important for efficient trapping than was originally expected. When only 2.5 ml of collection solvent (22-mm solvent height) were used, the losses of analytes ranged from 6 to 13% and when 5.0 or 10.0 ml of collection solvent were used the losses were similar, ranging from 7 to 10%. It should also be noted that the solvent height can possibly affect the collection efficiencies because the analytes need a certain amount of time after the depressurization step to diffuse into the collection solvent. At a constant bubble rise rate, a greater solvent height should permit longer solvent–analyte contact and thus increase the chances that the analyte will be trapped in the collection solvent. This was investigated by using two collection vials of differing dimensions (48

TABLE IV

COLLECTION EFFICIENCIES OF FLAVOR AND FRAGRANCE COMPOUNDS INTO VARIOUS TRAPPING SOLVENT VOLUMES AND HEIGHTS

| Compound | Trapping efficiency (%)[a] | | | |
|---|---|---|---|---|
| | 2.5 ml | | 5.0 ml | |
| | 8 mm[b] | 22 mm[b] | 33 mm[b] | 41 mm[b] |
| α-Pinene | 87.8 (1.5) | 86.6 (1.4) | 90.0 (4.1) | 90.4 (1.6) |
| Carvone | 82.6 (1.3) | 93.3 (2.0) | 91.1 (1.1) | 92.3 (1.7) |
| Eugenol | 84.3 (0.6) | 92.6 (1.6) | 89.6 (1.0) | 91.1 (1.9) |
| Cedrene | 86.7 (0.5) | 92.6 (1.7) | 92.3 (2.7) | 92.2 (1.6) |
| Cedrol | 90.9 (1.2) | 92.4 (1.4) | 90.4 (2.6) | 92.3 (2.1) |
| Santonin | 90.2 (1.5) | 93.8 (0.3) | 92.5 (2.5) | 91.9 (0.7) |

[a] Values in parentheses are the relative standard deviations (%) for triplicate 10-min extractions.
[b] Solvent height in the collection vial using 48 mm × 24 mm I.D., 33 mm × 12 mm I.D., 48 mm × 14 mm I.D., and 59 mm × 18 mm I.D. vials.

mm × 24 mm I.D. and 33 mm × 12 mm I.D.), each containing 2.5 ml of collection solvent (resulting in solvent heights of 8 and 22 mm, respectively). The results in Table IV show that, with the exception of α-pinene, the 8-mm collection solvent height trapped up to 11% less of the flavor and fragrance compounds than the 22-mm solvent height. Even though the collection solvent height did affect the recoveries of the flavor and fragrance compounds, the differences in the recoveries were still small, which indicates that the mass transfer of the analyte from the gaseous carbon dioxide into the collection solvent is very fast, and the collection solvent height is not as important as might be expected. As the results for collection into 2.5, 5.0 and 10.0 ml were nearly identical, a 5.0-ml collection solvent volume (33-mm solvent height) was arbitrarily selected for convenience to be used throughout the remainder of the collection experiments.

The effect of supercritical fluid flow-rate on the trapping efficiencies of the flavor and fragrance compounds was also determined using 5.0 ml of collection solvent over a range of flow-rates from 0.3 to 1.2 ml/min for 10 min. There was little effect on the recoveries of these analytes based on supercritical fluid flow-rate. For example, at 0.3 ml/min

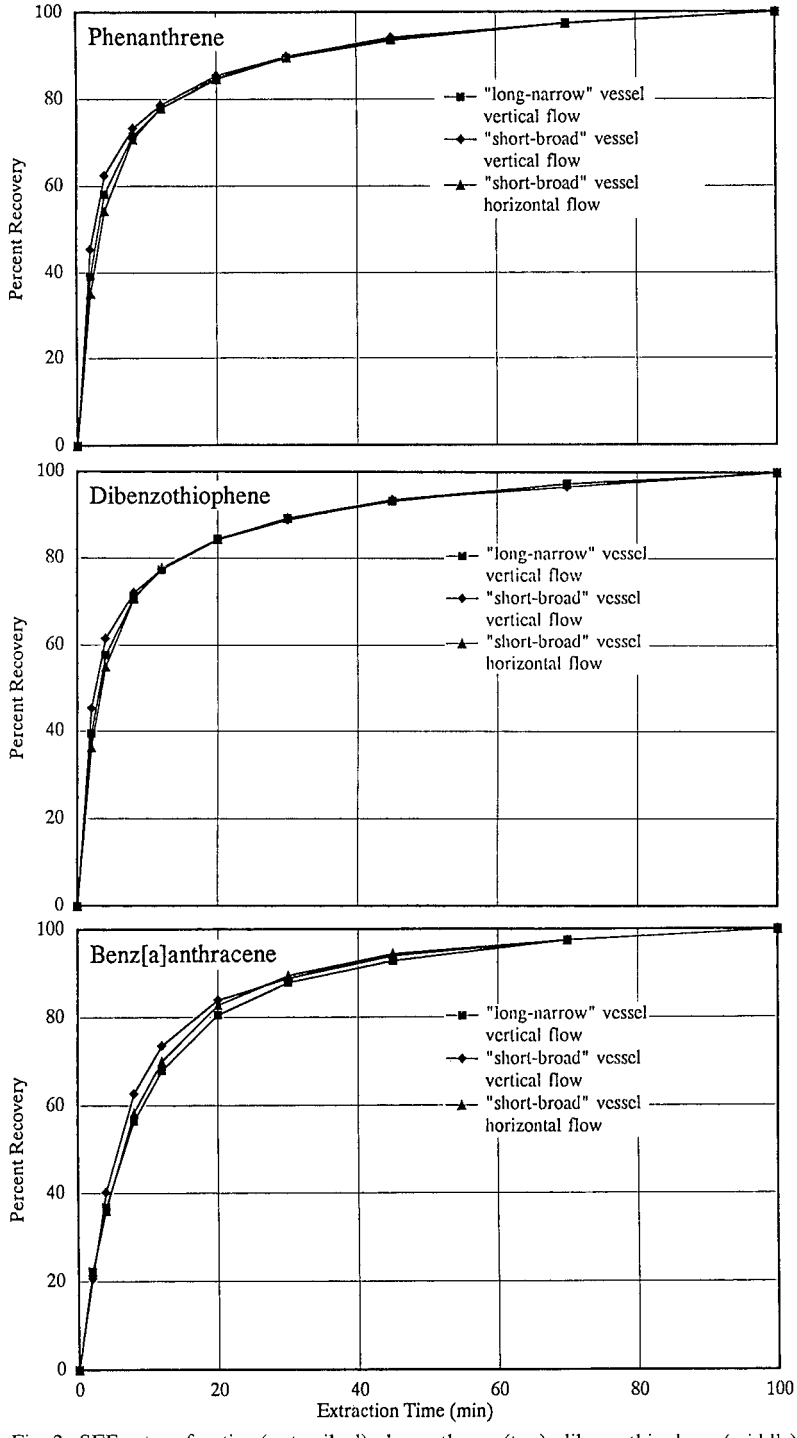


Fig. 2. SFE rates of native (not spiked) phenanthrene (top), dibenzothiophene (middle) and benz[*a*]anthracene (bottom) from 3 g of railroad bed soil using a "long, narrow" extraction vessel (132 mm × 5 mm I.D.) with vertical flow, a "short, broad" extraction vessel (33 mm × 10 mm I.D.) with vertical flow and a "short, broad" extraction vessel with horizontal flow. A 100% recovery was based on 100 min of SFE with carbon dioxide.

α-pinene showed losses of only 10% whereas at 1.2 ml/min the losses were 15%. Similarly, the least volatile compound, santonin, had losses of 5% at 0.3 ml/min and 7% at 1.2 ml/min. Whereas, as discussed earlier, high flow-rates coupled with long extraction times were responsible for volatile analyte losses due to purging (*i.e.*, the losses occurred after the analytes were dissolved in the collection solvent as shown in Table III), these results demonstrate that trapping efficiencies were relatively independent of flow-rate.

*Effect of extraction cell geometry, flow-rate and cell orientation on supercritical fluid extraction rates from real samples*

The effect of extraction cell geometry and orientation on SFE rates (extraction efficiency *versus* extraction time) was investigated using two extraction cells with different dimensions (132 mm × 5 mm I.D. and 33 mm × 10 mm I.D.) but the same internal volume (2.5 ml). The extraction rate curves (400 atm, 50°C) for native PAHs ranging from 2-methylnaphthalene to benzo[*a*]pyrene and heteroatom-containing PAHs such as dibenzofuran and dibenzothiophene from 3 g of railroad bed soil, and for monoterpenes, oxygenated monoterpenes and sesquiterpenes (α-pinene, nerol, limonene and $C_{15}H_{24}$) from 1-g samples of lemon peel were determined for a 100-min extraction period. Although a previous study reported that chromatographic retention of PAHs spiked on a sorbent was increased when using a "long, narrow" vessel instead of a "short, broad" vessel [16], we observed no significant differences in extraction rates from real samples. As shown in Fig. 2 for phenanthrene, dibenzothiophene and benz[*a*]anthracene and in Fig. 3 for limonene and nerol, extraction cell geometry and orientation (horizontal *versus* vertical) had virtually no effect on SFE rates of native PAHs and flavor and fragrance compounds from the railroad bed soil and the lemon peel.

The effect of supercritical fluid flow-rate on the extraction rates of native (not spiked) PAHs and heteroatom-containing PAHs from 3-g samples of railroad bed soil was also investigated at supercritical fluid flow-rates ranging from 0.15 to 1.2 ml/min using the 2.5-ml "long, narrow" extraction cell. As shown in Fig. 4 for phenanthrene and dibenzothiophene, flow-rates from 0.3 to 1.2 ml/min did not have an appreciable effect on the extraction rates of

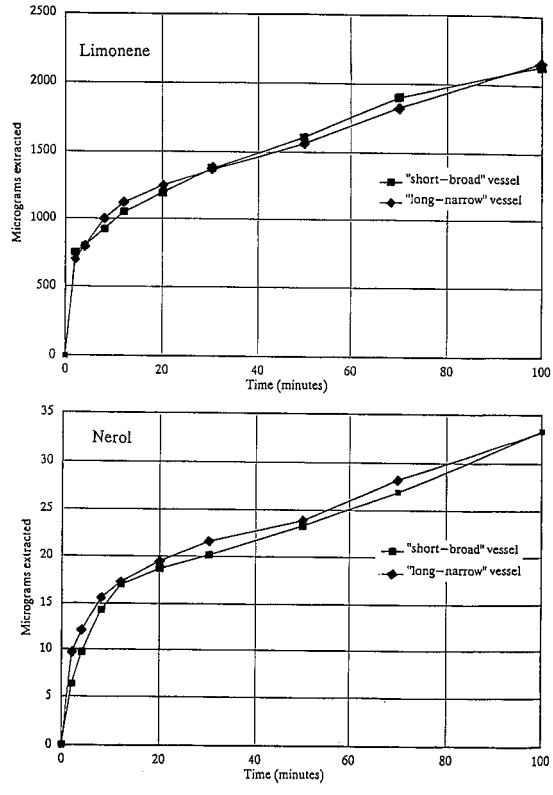


Fig. 3. SFE rates of limonene (top) and nerol (bottom) from 1 g of lemon peel using a "short, broad" extraction vessel (33 mm × 10 mm I.D.) and a "long, narrow" extraction vessel (132 mm × 5 mm I.D.).

these PAHs from the 3-g samples. When the flow-rate was reduced to 0.15 ml/min, the recovery rates were significantly slower, as would be expected by dead volume considerations since *ca.* 6–7 min would be required to sweep 1 void volume (estimated to be *ca.* 50% of the total internal volume of the extraction vessel) of the extraction cell. As reported by Bartle *et al.* [17], extraction rates of PAHs from soil show kinetic limitations that can mimic a diffusion-controlled process of the analytes in the sample matrix. As the SFE rate for this sample is probably limited by another rate-controlling mechanism (*e.g.*, analyte–matrix–supercritical fluid interactions), increasing the supercritical fluid flow-rate might not be expected to have a large effect on the extraction kinetics unless the supercritical fluid becomes saturated with analytes (*e.g.*, SFE of fats from meats [3]). For the railroad bed soil sample (and many environ-

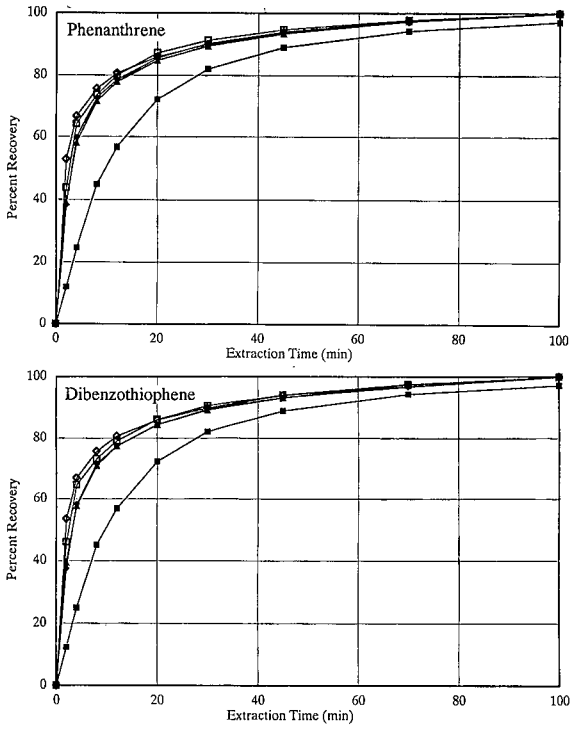


Fig. 4. Effect of supercritical fluid flow-rate on the extraction rates of phenanthrene (top) and dibenzothiophene (bottom) from 3 g of railroad bed soil. A 100% recovery was based on 100 min of SFE with carbon dioxide. Flow-rates (ml/min): ■ = 0.15; ◆ = 0.3; ▲ = 0.6; □ = 0.9; ◇ = 1.2.

mental samples) the concentration of the analytes present on the sample matrix is well below their saturation solubility limit in supercritical carbon dioxide. For example, the saturation concentration of phenanthrene in carbon dioxide is *ca.* 13 mg/ml (400 atm, 50°C [18], but the total amount of phenanthrene present on the railroad bed soil (3 g) was only *ca.* 100 μg (based on 100 min of SFE with carbon dioxide at 400 atm and 50°C).

## CONCLUSIONS

Improper solvent trapping conditions for analytes that have been extracted using SFE can result in losses which may be wrongly attributed to poor SFE extraction efficiencies. Proper choice of collection solvent and temperature were most important for obtaining good collection efficiencies of semivolatile pollutants and flavor and fragrance compounds, whereas solvent volume and height had minimal effect. Quantitative (90–104%) collection efficiencies of all 66 test compounds were achieved when methylene chloride collection solvent was placed in a temperature-controlled block set at 5°C, a procedure that also prevented restrictor plugging while extracting wet samples. Excessively long extraction times and high supercritical fluid flow-rates can cause losses of highly volatile analytes from the collection solvent because of purging. Extraction cell geometry and orientation had negligible effects on the extraction rates of native analytes, as demonstrated by the extraction of PAHs from railroad bed soil and flavor and fragrance compounds from lemon peel. The flow-rate of the supercritical fluid was also found to have negligible effects on the extraction rates of PAHs from railroad bed soil as long as it was sufficient to sweep the void volume of the extraction vessel in a reasonable time period.

## ACKNOWLEDGEMENTS

The partial financial support of the New Jersey Department of Environmental Protection (Division of Science and Research) is gratefully acknowledged. The authors also thank ISCO (Lincoln, NE, USA) for instrument loans.

## REFERENCES

1 R. D. Smith, J. L. Fulton, R. C. Petersen, A. J. Kopriva and B. W. Wright, *Anal. Chem.*, 58 (1986) 2057.
2 M. E. P. McNally and J. R. Wheeler, *J. Chromatogr.*, 447 (1988) 53.
3 J. W. King, J. H. Johnson and J. P. Friedrich, *J. Agric. Food Chem.*, 37 (1989) 951.
4 M. Miller Schantz and S. N. Chesler, *J. Chromatogr.*, 363 (1986) 397.
5 J. L. Hedrick and L. T. Taylor, *J. High. Resolut. Chromatogr.*, 13 (1990) 312.
6 M. A. Schneiderman, A. K. Sharma and D. C. Locke, *J. Chromatogr.*, 409 (1987) 343.
7 B. W. Wright, C. W. Wright, R. W. Gale and R. D. Smith, *Anal. Chem.*, 59 (1987) 38.
8 S. B. Hawthorne, D. J. Miller and J. J. Langenfeld, *J. Chromatogr. Sci.*, 28 (1990) 2.
9 J. M. Levy, R. A. Cavalier, T. N. Bosch, A. M. Rynaski and W. E. Huhak, *J. Chromatogr. Sci.*, 27 (1989) 341.
10 S. B. Hawthorne, M. S. Krieger and D. J. Miller, *Anal. Chem.*, 60 (1988) 472.
11 Q. L. Xie, K. E. Markides and M. L. Lee, *J. Chromatogr. Sci.*, 27 (1989) 365.
12 R. M. Campbell and M. L. Lee, *Anal. Chem.*, 58 (1986) 2247.

13 N. Alexandrou and J. Pawliszyn, *Anal. Chem.*, 61 (1989) 2770.
14 V. Lopez-Avila, N. S. Dodhiwala and W. F. Beckert, *J. Chromatogr. Sci.*, 28 (1990) 468.
15 S. B. Hawthorne, *Anal. Chem.*, 62 (1990) 633A.
16 J. Rein, C. M. Cork and K. G. Furton, *J. Chromatogr.*, 545 (1991) 149.
17 K. D. Bartle, A. A. Clifford, S. B. Hawthorne, J. J. Langenfeld, D. J. Miller and R. Robinson, *J. Supercrit. Fluids*, 3 (1990) 143.
18 K. D. Bartle, A. A. Clifford, S. A. Jafar and G. F. Shilstone, *J. Phys. Chem. Ref. Data*, 20 (1991) 713.

*Journal of Chromatography*, 594 (1992) 309–315
Elsevier Science Publishers B.V., Amsterdam

CHROM. 23 850

# Supercritical carbon dioxide extraction of resin and fatty acids from sediments at pulp mill sites

Hing-Biu Lee* and Thomas E. Peart

*Research and Applications Branch, National Water Research Institute, Environment Canada, P.O. Box 5050, Burlington, Ontario L7R 4A6 (Canada)*

(First received August 20th, 1991; revised manuscript received November 5th, 1991)

ABSTRACT

A rapid and efficient method for the extraction of resin and fatty acids commonly found in sediments collected from pulp mill locations was developed by using modified supercritical carbon dioxide. In the presence of a 1:1 mixture of methanol and formic acid, quantitative recovery of all acids except for palustric and neoabietic acids was achieved with a 5 min static and 10 min dynamic extraction with carbon dioxide at 365 bar and 80°C. Although the above two resin acids were only 40% recovered from spiked samples, these values were at least 250% better than those obtained by the classical Soxhlet technique. The cleaner supercritical fluid extract permitted a less stringent cleanup after the off-line derivatization of the acids, thus it further reduced analytical time and the use of solvent. An *in situ* extraction and on-line derivatization of the resin and fatty acids also proved feasible for the semi-quantitative screening of the toxic acids in sediments near pulp mill locations.

## INTRODUCTION

A large number of environmental pollutants have been identified in the discharges from the pulp and paper industry. Chlorinated phenols, guaiacols, catechols, aliphatic neutrals and acids, as well as furans and dioxins have been identified from chloro-bleaching mills [1,2]. Resin acids, natural products derived from wood and pulp, occur in effluent samples from every paper mill [3,4]. Many of the above chemicals are toxic to fish and have a life time long enough for bioaccumulation in aquatic organisms. Among them, resin acids and a few unsaturated fatty acids have been identified as the major components of effluents which contribute to the toxicity to fish [5–7]. The pulp and paper industry in Canada and elsewhere has implemented various techniques to detoxicate the effluents before they are discharged into the receiving waters. However, effluent levels of resin and fatty acids (RFAs) from those mills without an effective secondary (microbiological) waste treatment are so high that they can be acutely toxic to fish. Owing to their low solubilities, resin acids are readily adsorbed by sediments and are easily detected in samples downstream of the paper mills.

RFAs in sediments are extracted by using the classical Soxhlet technique with polar organic solvents [8,9]. In a recent study, we have found that, by addition of a trace amount of concentrated hydrochloric acid to the polar solvents, the recoveries of RFAs in sediments were improved by 200 to 300% [9]. However, the presence of a strong acid caused degradation of palustric and neoabietic acids into abietic acid. Therefore this techniques would produce biased low results for the above two unstable resin acids and biased high results for abietic acids in sediment samples.

Supercritical fluid extraction (SFE) has been applied to many organic pollutants in various environmental matrices [10–13]. In general, supercritical carbon dioxide produces good recoveries for non-polar compounds such as polychlorinated biphenyls [10]. However, for the extraction of more polar compounds, carbon dioxide modified by methanol or other polar solvent or supercritical

0021-9673/92/$05.00 

nitrous oxide is required to improve the recoveries to a level comparable to Soxhlet extraction. Until recently, there were few reports on the supercritical fluid extraction of organic acid from sediments. This work describes the optimization of the extraction of resin and fatty acids from sediments using modified supercritical carbon dioxide.

## EXPERIMENTAL

All resin acids (Table I) were obtained from Helix-Biotech Scientific (Vancouver, Canada) and used without further purification. Fatty acids and α-bromo-2,3,4,5,6-pentafluorotoluene (pentafluorobenzyl bromide, PFBBr) were purchased from Aldrich (Milwaukee, WI, USA). Stock solutions of individual resin and fatty acids were prepared in acetone at 1000 μg/ml and kept at −20°C in the dark. Spiking solutions of mixed RFAs also in acetone were stored at 4°C in the dark. A PFBBr solution was prepared by dissolving 1 g of the reagent in 20 ml of acetone and kept at −20°C until use.

All solvents used were distilled-in-glass grade supplied by Burdick & Jackson. SFC-grade carbon dioxide with a helium head pressure of 10500 kPa was purchased from Scott Specialty Gases (Troy, MI, USA).

Several river sediment samples were collected from different locations near an Ontario paper mill in September 1990. Among them, a sample obtained from a site approximately 2 km downstream of the mill was, as shown by previous analysis using Soxhlet extraction, contaminated with RFAs at levels typically found in paper mill sediments. This sediment was air-dried, crushed, homogenized and used for the development of the extraction method.

Supercritical carbon dioxide extraction of the sediment was performed with the Hewlett-Packard 7680A extraction module and the available 7.0-ml stainless-steel thimbles and caps. Instead of using a restrictor to depressurize the supercritical fluid and deposit the extract into a test tube containing an organic solvent, the HP 7680A extractor employs an unique nozzle/trap assembly [14]. The nozzle allows instant depressurization of the carbon dioxide, and at the same time permits the decoupling of flow and pressure; thus, the density can be set independent of the flow of the fluid. During the dynamic extraction stage, the SFE extract is deposited onto a packed trap made of octadecylsilane (ODS) material. At the end of the extraction, the analytes are then rinsed off the trap with a predetermined amount of solvent into a glass vial and the extract is ready for analysis, cleanup, or further workup. The operation is fully automated from the point where the thimble is placed into the extraction chamber and on.

To minimize contamination and plugging of the bottom cap by the sample, two circles of Whatman GF/C filter paper of the same diameter as the thimble were cut by pressing the edge of the thimble against the paper and placed above the bottom cap after it was screwed in. A sediment sample typically of 500 mg was weighed and 25 μl of water and 300 μl of modifier added directly to the sample. In some cases, the sample was placed in between two layers of

TABLE I

IUPAC NAMES FOR SELECTED RESIN ACIDS

Structures of these resin acids are given in ref. 9.

| Common name | IUPAC name |
|---|---|
| Pimaric acid | 8(14),15-Pimaradien-18-oic acid |
| Sandaracopimaric acid | 8(14),15-Isopimaradien-18-oic acid |
| Isopimaric acid | 7,15-Isopimaradien-18-oic acid |
| Palustric acid | 8,13-Abietadien-18-oic acid |
| Dehydroabietic acid | 8,11,13-Abietatrien-18-oic acid |
| Abietic acid | 7,13-Abietadien-18-oic acid |
| Neoabietic acid | 8(14),13(15)-Abietadien-18-oic acid |
| 14-Chlorodehydroabietic acid | 14-Chloro-8,11,13-abietatrien-18-oic acid |
| 12,14-Dichlorodehydroabietic acid | 12,14-Dichloro-8,11,13-abietatrien-18-oic acid |

Celite of 200 mg each (see later discussion). A 5 min static and a 10 min dynamic extraction was carried out at a chamber temperature of 80°C using supercritical carbon dioxide of 0.80 g/ml density (approximate pressure 365 bar) at a flow-rate of 2.0 ml/min. The ODS trap was maintained at 15°C with cryogenic carbon dioxide during the extraction stages. Following the extraction, the RFAs were collected in glass vials by eluting the trap, which was then warmed up to 40°C, with two 1-ml aliquots of acetone. The entire extraction cycle completed in *ca.* 35 min.

The acetone extract containing the RFAs were combined and reduced to 1 ml before the acids were converted into their pentafluorobenzyl (PFB) esters as described before [9]. After solvent exchange into light petroleum (b.p. 30–60°C), the derivatized products were cleaned up on a 5 cm 5% deactivated silica gel column prepared in a 20 cm × 0.7 cm I.D. disposable Pasteur pipet. Following the application of the derivatized extract to the column prewashed with 2 ml of light petroleum, the column was eluted with 5 ml of dichloromethane–light petroleum (5:95, v/v) and then with 7 ml of dichloromethane–light petroleum (1:1). The last fraction was saved and the solvent exchanged into 5 ml of isooctane for analysis by gas chromatography–electron-capture detection using a 30 m × 0.25 mm I.D. DB-17 column [15].

Gas chromatographic conditions: oven temperature was held initially at 70°C for 0.75 min and programmed to 160°C at 30°C/min, then to 290°C/min at 2°C/min. Injector and detector temperatures were 250 and 300°C, respectively. Helium was used as the carrier gas and the column head pressure was 105 kPa. Samples of 2 μl were injected in the splitless mode with a valve time of 0.75 min.

## RESULTS AND DISCUSSION

### *Supercritical carbon dioxide extraction of RFAs from sediments*

RFAs in sediment were poorly extracted by supercritical carbon dioxide. Even at the maximum extraction chamber temperature of 80°C and a fluid density of 0.80 g/ml, only a small amount of palmitic acid yet no resin acids were recovered from the reference sample after a 5 min static and another 10 min dynamic extraction at a flow-rate of 2 ml/

TABLE II

EFFECT OF MODIFIER ON THE RECOVERY OF RFAs IN SEDIMENT

| | Recovery (%)[a] with modifier | | | | | Soxhlet (μg/g) |
|---|---|---|---|---|---|---|
| | None | Methanol | Acetic acid | Formic acid | Methanol–formic acid | |
| Palmitic | 3 | 63 | 71 | 74 | 94 | 18.0 |
| Stearic | <1 | 64 | 69 | 73 | 94 | 6.4 |
| Oleic | <1 | 65 | 78 | 82 | 94 | 6.8 |
| Linoleic | <1 | 73 | 68 | 88 | 90 | 13.9 |
| Pimaric | <1 | 44 | 90 | 87 | 102 | 12.7 |
| Isopimaric | <1 | 33 | 67 | 84 | 88 | 40.2 |
| Palustric | <1 | 117 | 204 | 141 | 267 | 4.6 |
| Abietic | <1 | 37 | 64 | 73 | 89 | 52.7 |
| Dehydroabietic | <1 | 44 | 76 | 84 | 102 | 65.8 |
| Neoabietic[b] | <1 | (1.9 μg/g) | (3.8 μg/g) | (0.7 μg/g) | (4.4 μg/g) | <0.1 |
| Chlorodehydroabietic[c] | <1 | 23 | 71 | 81 | 89 | 48.9 |
| Total fatty acids[d] | 3 | 65 | 70 | 80 | 92 | 55.3 |
| Total resin acids[e] | <1 | 34 | 66 | 79 | 94 | 232 |

[a] All SFE recoveries were relative to Soxhlet results.

[b] The recoveries of neoabietic acid under various SFE conditions were given in μg/g since this acid was not recovered by the Soxhlet method.

[c] Sum of 12- and 14-chlorodehydroabietic acids.

[d] Sum of the fatty acids listed together with lauric, myristic, linolenic and eicosanoic acids.

[e] Sum of the resin acids listed together with sandaracopimaric and dichlorodehydroabietic acids.

min. Addition of 300 μl of methanol improved the recoveries of the total fatty and resin acids to 65 and 34%, respectively, of the Soxhlet values (Table II). Analogous to the fact that the presence of an acid substantially improved the recovery of RFAs in the Soxhlet extractions, the SFE recovery of RFAs was also greatly improved by the presence of 300 μl of acetic acid in the sample. Using a stronger acid such as formic acid further enhanced the recovery of total RFA to *ca.* 80%, however, it was noted that the recoveries of palustric and neoabietic acids were lower when the stronger acid was used. The use of dichloroacetic acid, 10% hydrochloric acid in methanol and a 1:1 mixture of acetic acid and methanol as modifiers all proved to be less effective than formic acid for the extraction of all RFAs, although a mixture of methanol–formic acid (1:1) provided the best recovery of RFAs in sediment. The effect of each modifier on the recovery of the major RFAs in sediments is shown in Table II.

The effect of the amount of modifier used on the recovery was also studied. Based on a 500 mg sample size, 300 μl of methanol–formic acid (1:1) was found to produce the optimal recovery of RFAs. Smaller amounts such as 100 or 200 μl of the modifier were insufficient and a larger volume such as 500 μl did not further improve the recovery.

*Other factors affecting the recovery of RFAs in sediments*

At the early stage of our work, extraction of sediments was carried out at either 50 or 60°C. Within the working temperature range of 40 to 80°C for the HP 7680A, recovery of RFAs from the reference sediment was found to increase with increasing chamber temperature. Therefore all subsequent extraction were done at a temperature of 80°C. Note that supercritical carbon dioxide of the maximum density attainable by the HP 7680A at each temperature was used in each case so that highest extraction efficiency could be achieved.

The moisture content of a sample also plays an important role in the extraction of RFAs from sediments. Our results indicated that the best recovery of RFAs was obtained from samples containing 5 to 10% moisture content. If freeze-dried sediments were used, a reduction of 25 to 40% in the recovery of the RFAs was observed. However, an addition of 5% (w/w) of water to the dry sediment prior to the extraction would bring the recovery back to quantitative. The enhancement in RFA extractability in this case could be attributed to the increase in acidity due to the presence of water in supercritical carbon dioxide.

It was also observed that, an improvement of *ca.* 10% in the recovery of RFAs was achieved by sandwiching the sediment with 200 mg layers of Celite and spiking each layer with half the amount of modifier. Presumably the slightly better recovery was attributed to the longer retainment of the modifier with solids during the dynamic extraction stage. While longer extraction times (both static and dynamic) did not further improve the recovery, shorter extraction times resulted in incomplete recovery of RFAs.

Under the optimized conditions, a second extraction of the sediment with fresh modifier recovered less than 5% of additional RFAs, indicating that the first extraction was essentially complete.

*Cleanup of derivatized extracts*

In comparison to the exhaustive but often nonselective Soxhlet extraction, supercritical carbon dioxide extraction of RFAs from sediment produced a much smaller amount of coextractives in the extract. The cleaner extract enabled us to employ a

TABLE III

RECOVERY OF RESIN AND FATTY ACIDS FROM FORTIFIED SEDIMENT SAMPLES BY SUPERCRITICAL FLUID EXTRACTION

Recoveries and standard deviations were calculated from replicate determinations of six identical samples.

| RFA | Recovery (%) | |
|---|---|---|
| | Fortification 10 μg/g | Fortification 1 μg/g |
| Palmitic | 99 ± 7 | 94 ± 10 |
| Stearic | 97 ± 7 | 85 ± 7 |
| Oleic | 94 ± 7 | 105 ± 5 |
| Linoleic | 88 ± 8 | 107 ± 7 |
| Pimaric | 91 ± 6 | 98 ± 6 |
| Isopimaric | 90 ± 7 | 95 ± 3 |
| Palustric | 38 ± 8 | 35 ± 4 |
| Abietic | 90 ± 10 | 98 ± 10 |
| Dehydroabietic | 108 ± 5 | 104 ± 8 |
| Neoabietic | 36 ± 7 | 40 ± 5 |
| Chlorodehydroabietic | 89 ± 6 | 96 ± 9 |

smaller (0.8 g *vs.* 5.0 g) column for sample cleanup after the derivatization [9], and thus it further improves the saving in time and the amount of solvent used. This cleanup step effectively removed interferences deriving from sediment coextractives as well as the blank of the SFE-grade carbon dioxide which was found to contain various amounts of impurities from all samples provided by three different suppliers. The purity problem of supercritical carbon dioxide for electron-capture detection has also been reported lately [16].

*Method performance*

With the exception of palustric and neoabietic acids, the recoveries of other major fatty and resin acids found in pulp mill sediments from spiked samples were better than 85% at fortification levels of 10 and 1 μg/g (Table III). Recoveries for palustric and neoabietic acids were between 35 and 40% at the same levels, presumably due to degradation of these two acids under acidic extraction conditions. It should be noted that, with Soxhlet extraction, the recoveries were even poorer for palustric (5 to 15%) and neoabietic (<5%) acids [9]. This extraction procedure has been successfully applied to sample sizes from 25 mg to 1 g. Larger sample sizes were not tried since with a 1 g sample, a detection limit of 0.05 μg/g [9] can easily be achieved for most monitoring purposes.

*In situ extraction and derivatization of RFAs in sediments*

Although derivatization analysis of polar organics enjoys many advantages such as improved chromatographic properties and enhanced detector response of the derivatives, this approach is more cumbersome because of the extra step. Therefore, an ideal method would be one which combines the extraction and derivatization steps into one. In our case, experimental conditions had to be modified since the SFE conditions and the esterification reaction with the PFBBr reagent were incompatible with each other. The esterifying agent reacts with acids and methanol and the reaction requires a base to catalyze the formation of esters. This problem was solved by replacing the methanol–formic acid modifier with 250 μl of 5% solution of the PFBBr reagent in acetone and 50 μl of triethylamine. An initial extraction was attempted by using a 10 min static and 5 min dynamic extraction time. The

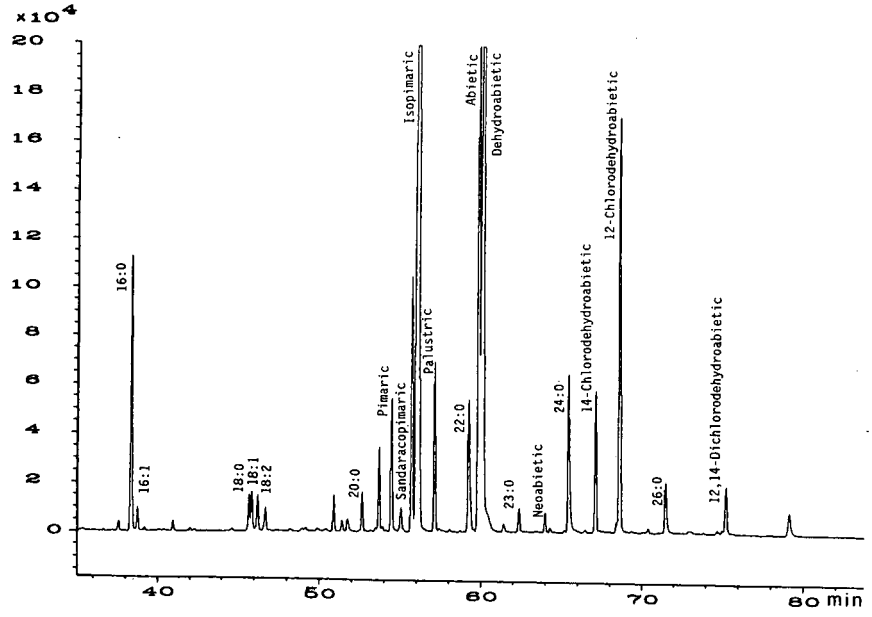


Fig. 1. Gas chromatography–electron-capture detection of the RFA PFB esters in the reference sediment sample as recovered by the *in situ* extraction/derivatization route. Splitless injection (2 μl) onto a 30 m × 0.25 mm I.D. DB-17 column. See Experimental section for conditions.

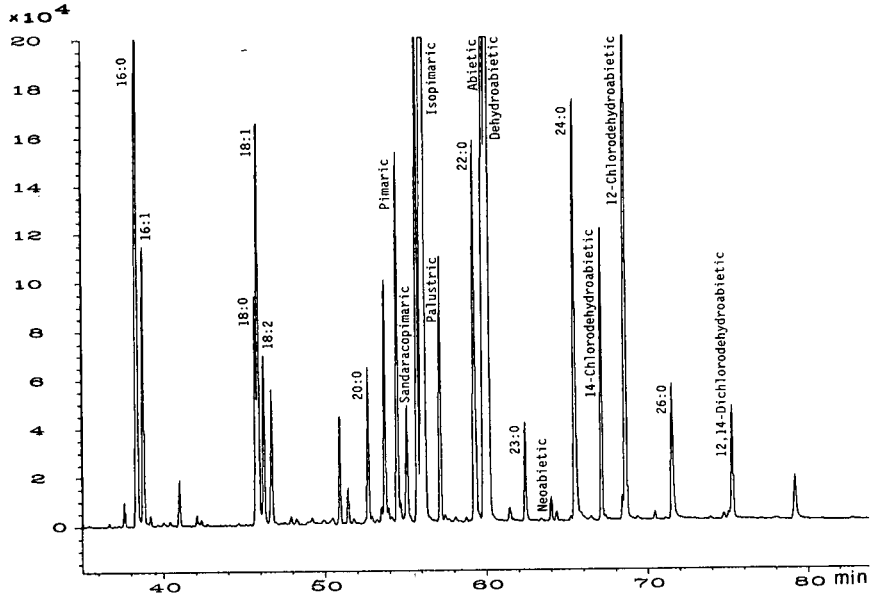


Fig. 2. Gas chromatography–electron-capture detection of the RFA PFB esters in the reference sediment sample as recovered by the off-line derivatization route. Conditions as in Fig. 1.

derivatized RFA extract was then eluted from the ODS trap by isooctane, cleaned up on a silica gel column and solvent exchanged as described previously before gas chromatography–electron-capture detection. Although the recoveries of RFAs by this *in situ* method (Fig. 1) were only 35–45% of the off-line derivatization technique (Fig. 2), the results nevertheless indicated that the *in situ* derivatization was feasible for the determination of RFAs in sediments. The lower recoveries were not unexpected since acetone was a less effective modifier than the methanol–formic acid (1:1) mixture for the extraction of RFAs and also the complete conversion of the acids into their PFB esters required 1 to 2 h at 60°C. Indeed, by extending the static extraction time from 10 to 60 min, the recoveries were improved to *ca.* 60% for the RFAs by comparison to the best off-line SFE extraction and derivatization results. However, the amounts of palustric and neoabietic acids extracted by the *in situ* method were proportionally higher, since these two acids are less stable under acidic conditions. Doubling the amounts of PFBBr and triethylamine only improved the recovery of RFA by another 5 to 10%. Further extension of the static extraction time is impractical since the sample throughput would be severely reduced.

## CONCLUSIONS

Most RFAs commonly found in sediments downstream of pulp and paper mill locations are quantitatively extracted by supercritical carbon dioxide in the presence of methanol and formic acid as modifiers. Although the recoveries of the unstable palustric and neoabietic acids are *ca.* 40% as indicated by the recovery experiments for the spiked sediments, the SFE results of the above two acids are at least 250% better thant he Soxhlet values on both spiked and naturally contaminated samples. Because of the feasibility of a rapid, one-step *in situ* extraction and derivatization of RFAs, this technique is most suitable for the semi-quantitative screening of the toxic RFAs in sediments for quick sample turn around time.

## ACKNOWLEDGEMENTS

The authors are grateful to Hewlett-Packard (Canada) Ltd. for the generous loan of the HP 7680A

supercritical fluid extractor module. We also thank W. Pipkin of Hewlett-Packard, Avondale, PA, USA, for helpful discussions.

REFERENCES

1 R. H. Voss, J. T. Wearing, R. D. Mortimer, T. Kovacs and A. Wong, *Pap. Puu.*, 62 (1980) 809.
2 K. Lindström and F. Österberg, *Environ. Sci. Technol.*, 20 (1986) 133.
3 A. B. McKague, J. M. Leach, R. N. Soniassy and A. N. Thakore, *Pulp Pap. Can. Trans. Tech. Sect.*, 3 (1977) TR75.
4 I. Rogers, H. Mahood, J. Servizi and R. Gordon, *Pulp Pap. Can.*, 80 (1979) T286.
5 C. C. Walden and T. E. Howard, *Tappi*, 60 (1977) 122.
6 C. C. Walden and T. E. Howard, *Pulp Pap. Can.*, 82 (1981) T143.
7 M. H. Priha and E. T. Talka, *Pulp Pap. Can.*, 87 (1986) T447.
8 B. Brownlee, M. E. Fox, W. M. J. Strachan and S. R. Joshi, *J. Fish. Res. Board Can.*, 34 (1977) 838.
9 H. B. Lee and T. E. Peart, *J. Chromatogr.*, 547 (1991) 315.
10 M. M. Schantz and S. N. Chesler, *J. Chromatogr.*, 363 (1986) 397.
11 S. B. Hawthorne and D. J. Miller, *Anal. Chem.*, 59 (1987) 1705.
12 N. Alexandrou and J. Pawliszyn, *Anal. Chem.*, 61 (1989) 2770.
13 S. B. Hawthorne, *Anal. Chem.*, 62 (1990) 633A.
14 W. Pipkin, *Am. Lab.*, Nov. (1990) 40D.
15 H. B. Lee, T. E. Peart and J. M. Carron, *J. Chromatogr.*, 498 (1990) 367.
16 W. Beckert, V. Lopez-Avila and S. Cram. *Am. Environ. Lab.*, Oct. (1991) 21.

*Journal of Chromatography*, 594 (1992) 317–324
Elsevier Science Publishers B.V., Amsterdam

CHROM. 23 878

# Charge-reversed, polymer-coated capillary column for the analysis of a recombinant chimeric glycoprotein

Kiyoshi Tsuji* and Richard J. Little

*Control Biotechnology, Pharmaceutical Product Control Division, The Upjohn Company, Kalamazoo, MI 49001 (USA)*

(First received September 6th, 1991; revised manuscript received November 12th, 1991)

ABSTRACT

Fused-silica capillary columns coated with an amphiphatic polymer were used to characterize a recombinant, basic, chimeric glycoprotein. Composition, ionic strength, and pH of the electrophoretic buffers were found to affect significantly the selectivity, resolution, and rate of migration of the basic glycoprotein peaks. Out of seven buffers evaluated, sodium citrate–acetic acid buffer gave the best peak resolution while maintaining peak migration at less than 20 min. The peak resolution ($R_s$) was greater than 1.0 above a pH of 5.0; however, the $R_s$ was near zero below a pH of 4.5. Peak migration time increased exponentially with increase in pH of the running buffer. The $R_s$ increases linearly with increase in the concentration of the running buffer from 20 to 60 m*M*; the number of theoretical plates peaked at about 50 m*M* buffer concentrations. The condition selected for electrophoretic analysis of the glycoprotein uses a 50 m*M* concentration of sodium citrate-acetic acid buffer at pH of about 5.2. The standard curve for the analysis of the glycoproteins is linear over the range from 50 to 200 μg/ml glycoprotein with the number of theoretical plates over 60 000 per meter. The relative standard deviation of the assay method is approximately 4.6% and that of the peak migration time is about 3%. The polymer-coated capillary column electrophoretic analysis method has been demonstrated to be capable of monitoring degradation of the chimeric, basic FG glycoprotein.

## INTRODUCTION

Analysis of recombinant proteins, especially of basic glycoproteins, by fused-silica capillary column electrophoresis presents a unique challenge due to non-specific adsorption of the proteins on the capillary wall. Unless the active binding sites on the surface of the capillary wall are masked, the proteins strongly interact with the wall resulting in severely skewed peaks or no migration of the protein. Conventionally, electrophoretic separation of proteins by the capillary column uses buffers of very low ($<2.5$) or very high pH ($>10$) to minimize the protein-to-wall interaction. However, this strategy limits the selection of an electrophoretic buffer and severely compromises peak resolution and selectivity.

Recent advancements in capillary wall modification technologies to decrease the protein–wall interactions have resulted in the commercialization of columns and column coating reagents. These technologies include coating of the capillary wall by amphipathic polymers [1], inclusion of zwitterions in the running buffer [2], and partially deactivating columns by derivatization with hydrocarbons and neutral hydrophilic compounds [3].

Samples of a recombinant glycoprotein used in this experiment were manufactured by The Upjohn Company (Kalamazoo, MI, USA). The glycoprotein, FG, is a chimeric protein composed of the fusion protein (F) and the receptor protein (G) of respiratory syncytial virus (RSV) [4]. The terms F and G are the designation of peptide segments in the RSV glycoprotein. The portion of the genes coding for the anchor region of the F and G gene were truncated and the remaining portions of the genes fused. The FG glycoprotein contains amino acids 1 to 489 of F and 97 to 279 of G and the amino acid sequence translated from the DNA sequence is presented in Table I. The F portion of FG consists of

TABLE I

PRIMARY AMINO ACID SEQUENCE OF THE CHIMERIC FG GLYCOPROTEIN OF THE RESPIRATORY SYNCYTIAL VIRUS

| | |
|---|---|
| 1 | MELLILKANA ITTILTAVTF CFASGQNITE EFYQSTCTAV SKGYLSALRT |
| 51 | GWYISVITIE LSNIKENKCN GTDAKVKLIK QELDKYKNAV TELQLLMQST |
| 101 | PATNNRARRE LPRFMNYTLN NAKKTNVTLS KKRKRRFLGF LLGVGSAIAS |
| 151 | GVAVSKVLHL EGEVNKIKSA LLSTNKAVVS LSNGVSVLTS KELDLKNYID |
| 201 | KQLLPIVNKQ SCSISNIETV IEFQQKNTRL LEITREFSVI AGVTTPVSTY |
| 251 | MLTNSELLSL INDMPITNDQ KKLMSNNVQI VRQQSYSIMS IIKEEVLAYV |
| 301 | VQLPLYGVID TPCWKLHTSP LCTTNTKEGS NICLTRTDRG WYCDNAGSVS |
| 351 | FFPQAETCKV QSNRVFCDTM NSLTLPSEVN LCNVDIFNPK YDCKIMTSKT |
| 401 | DVSSSVITSL GAIVSCYGKT KCTASNKNRG IIKTFSNGCD YVSNKGVDTV |
| 451 | SVGNTLYYVN KQEGKSLYVK GEPIINFYDP LVFPSDEFDQ LGISPSNPSE |
| 501 | ITSQITTILA STTPGVKSTL QSTTVKTKNT TTTQTQPSKP TTKQRQNKPP |
| 551 | SKPNNDFHFE VFTFVPCSIC SNNPTCWAIC KRIPNKKPGK KTTTKPTKKP |
| 601 | TLKTTKKDPK PQTTKSKEVP TTKPTEEPTI NTTKTNIITT LLTSNTTGNP |
| 651 | ELTSQMETFH STSSEGNPSP SQVNISSQRE D |

a F1 (48 000 dalton) and a F2 (20 000 dalton) subunit which are connected by a disulphide bridge. The FG is heavily glycosylated and appears on a sodium dodecyl sulphate–polyacrylamide gel electrophoresis (SDS-PAGE) slab-gel to migrate at about 100 000 daltons. The FG glycoprotein is produced by infecting an insect cell, SF-9 (DT), with a recombinant baculovirus vector containing the FG gene [4]. The FG protein is excreted into the cell supernate. The G glycoprotein is associated with human immunoresponse [5]. The p*I* of the FG glycoprotein is *ca.* 9.4.

The chimeric FG glycoprotein is being developed at Upjohn as a vaccine for RSV. RSV is the primary etiological agent for lower respiratory disease in children under two years of age. Most children by the age of five will have experienced three episodes of RSV related disease. The disease occurs worldwide and mortality rates can be higher in those countries with poor health care. RSV also has been associated with respiratory disease in the elderly especially those residing in nursing homes.

The purpose of this paper is to develop a stability indicating method for the assay of a basic glycoprotein in its native form by use of surface modified capillary columns. Surface-modified columns have potential of greater peak selectivity and resolution of basic proteins unattainable by the conventional bare fused-silica capillary column.

## EXPERIMENTAL

### *HPCE instrumentation*

A P/ACE System 2100 high-performance capillary electrophoretic (HPCE) instrument (Beckman, Palo Alto, CA, USA) was used throughout the study. Each HPCE run involves a 5-s nitrogen pressure (0.5 p.s.i.) injection of a sample into a coated capillary column. The compounds migrating in the column were monitored at 214 nm. The temperature in a column cartridge was maintained at 25°C with a circulating coolant and an electrophoretic run was conducted at a constant voltage of −20 kV (−350 V/cm). The area under the protein peak was integrated by means of a program residing in a VAX mainframe computer.

### *Reagents*

Buffers used for the electrophoretic analysis were made of analytical reagent-grade chemicals obtained from Baker (Phillipsburg, NJ, USA), Mallinckrodt (Paris, KY, USA), and Aldrich (Milwaukee, WI, USA). Buffer solution was prepared by mixing two 100 m*M* solutions, *e.g.*, sodium citrate and acetic acid, to a desired pH. The amphipathic polymer column coating reagent (Micro-Coat protein analysis reagent) [1] was obtained from Applied Biosystems (ABI, Foster City, CA, USA). Following the direction of ABI, the polymeric column coating reagent was reconstituted in an aqueous solution containing 2% ethylene glycol.

### *Preparation of a polymer-coated column*

A roll of fused-silica capillary tubing (75 μm I.D. × 375 μm O.D.) was obtained from Polymicro Technologies (Phoenix, AZ, USA). Capillaries were cut to few centimeters longer than the final column length of 57 cm and a window was created at just over 7 cm from one end by removing the polyimid coating with a polyimid stripper (Model S200, Polymicro). The tubing was mounted in the column cartridge (Beckman) and cut to an effective column length of 50 cm. The capillary column was treated with a 0.1 *M* NaOH for 5 min. After rinsing with water for 3 min, the column was coated with the polymeric reagent by filling the capillary for 1 min

under high nitrogen pressure (20 p.s.i.) followed by 5 min under low pressure (0.5 p.s.i.). The polymeric reagent was allowed to contact statically with the column for 15 min prior to sample analysis. Just before each sample analysis, the column was briefly coated with the polymeric reagent for 0.5 min and rinsed for 2 min with the running buffer.

Capillary columns bonded with $C_{18}$ and $C_8$ were purchased from Supelco (Bellefonte, PA, USA). A window was created by treating the capillary with hot nitric acid and the column was mounted in a column cartridge (Beckman) prior to an electrophoretic run.

*Separation of glycoproteins*

The chimeric FG glycoprotein used in this study (Upjohn) was analyzed at a concentration of about 80 $\mu$g/ml in the native form by dilution in water or as denatured by dilution in 0.1% trifluoroacetic acid (TFA). After a brief coating with the polymeric agent (0.5 min), the column was rinsed for 2 min with a 50 m*M* sodium citrate–acetic acid buffer (pH 5.2). The sample was injected into the column by nitrogen pressure (0.5 p.s.i.) for 5 s and analyzed for 15 min under a constant voltage of $-20$ kV (130 $\mu$A).

## RESULTS AND DISCUSSION

*Polymeric, amphipathic column coating reagent*

The polymeric, amphipathic column coating reagent used is a neutral lipophilic polymer molecule containing a hydrophilic group on a side chain [1]. The polymer coats the wall of the capillary column through an ionic interaction with the silanol group. The polymeric molecule immobilizes the hydrophilic group forming a stable, net positively charged amine layer on the capillary wall surface. The positively charged column reverses the electroosmotic flow to the anode.

Positive charge on the capillary surface minimizes non-specific binding of positively charged proteins to the wall. Thus, the amphipathic polymer-coated, positively charged column allows manipulation of net charges of proteins by selection of a wide variety of buffers to fine-tune electrophoretic conditions for the separation of proteins. Unlike when using zwitterions [2], the buffer contains no column coating reagent. In our experience, the amphipathic polymer-coated column is stable for one electrophoretic run and the column must be briefly recoated with the reagent just before each analysis in order to attain a reasonable precision of peak migration time.

*Selection of buffer*

Variety of buffers, all at 20 m*M* concentration and pH of approximately 5.2, were prepared: sodium acetate–acetic acid, sodium citrate–acetic acid, sodium citrate–citric acid, sodium acetate–phosphoric acid, sodium citrate–phosphoric acid, sodium phosphate–phosphoric acid, and sodium citrate–formic acid. These buffers were used to examine peak resolution and selectivity for the analysis of the chimeric FG glycoproteins.

Migration of a single FG glycoprotein peak was noted when sodium acetate–acetic acid, sodium citrate–citric acid, sodium acetate–phosphoric acid, and sodium citrate–phosphoric acid were used as the running buffers. No FG glycoprotein peak was detected when a sodium phosphate–phosphoric acid buffer was used. Presence of 2 peaks was observed in a crude preparation of the FG glycoprotein when sodium citrate–acetic acid and sodium citrate–formic acid buffers were used. The sodium citrate–acetic acid buffer was chosen for further study since the peak migration time was less than 20 min. The peak migration time of the FG glycoprotein was twice as long with inferior peak resolution when the sodium citrate–formic acid buffer was used.

When the phosphate buffer at pH 2.5 was used with an untreated column, no migration of the FG glycoprotein was noted. A single FG peak was detected by use of a borate buffer at pH 11.

*Effect of pH on peak resolution*

To study the effect of pH on peak resolution ($R_s$), a 100 m*M* concentration of sodium citrate and acetic acid was prepared and mixed to obtain pH values of 4.0, 4.5, 5.0, 5.5, 6.0 and 7.0. These buffer solutions were diluted to 50 m*M* just before use.

As shown in Fig. 1, the $R_s$ improved dramatically from near zero to over 1.0 between the pH of 4.5 and 5.0. Only a gradual increase in $R_s$ was noted above the pH of 5.0. The $R_s$ remained near zero below the pH of 4.5. Increase of the $R_s$ follows the equation $y = 0.0199x^{4.26}$, where $y$ represents the $R_s$ and $x$ represents the pH values.

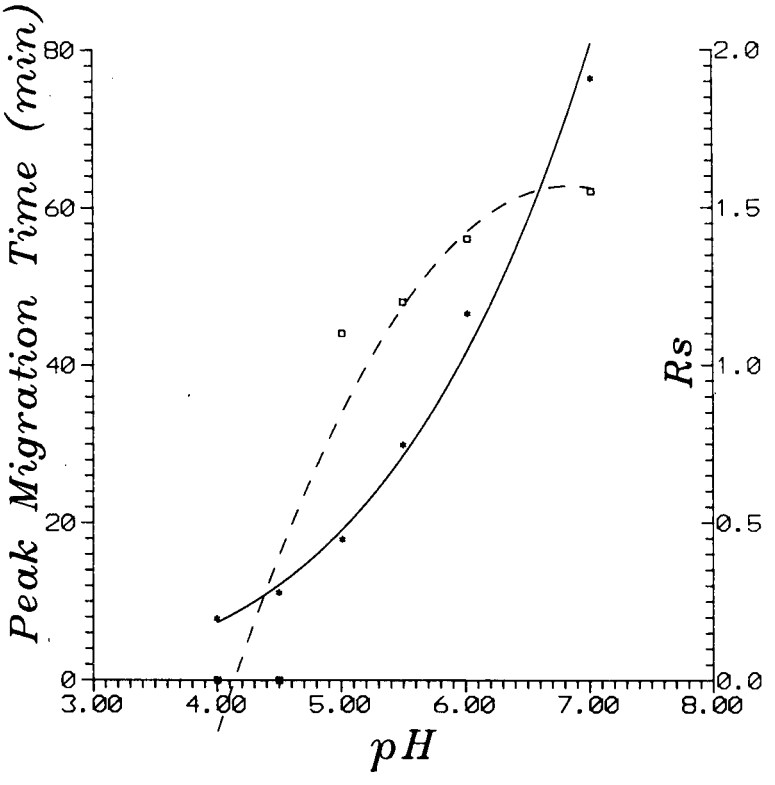


Fig. 1. Effects of pH of the running buffer on resolution ($R_s$) (□) and migration (∗) of the chimeric FG glycoprotein peaks. Conditions: −350 V/cm; column temperature, 25°C; migration distance, 50 cm; polymer-coated fused-silica capillary column, 75 μm I.D.; running buffer, 20 m*M* sodium citrate–acetic acid.

Unlike in conventional capillary electrophoresis, the direction of eletroosmotic flow in a polymer-coated, positively charged column is toward the anode. The rate of the reversed electroosmotic flow increases by lowering the pH of the buffer. Since the electroosmotic flow is inversely proportional to the pH of the running buffer, it was not surprising that the peak migration time increased exponentially with increase in pH. A running buffer with a pH of between 5.0 and 5.5 was selected for further study in order to consistently attain an $R_s$ value of over 1.0 while maintaining the peak migration time at less than 20 min.

*Effect of buffer concentration on peak resolution and theoretical plates*

A 100 m*M* concentration of sodium citrate–acetic acid buffer at pH 5.2 was diluted to 20, 30, 40, 50, 60, 70 and 80 m*M* to examine effects of the buffer concentration on the $R_s$ and the number of theoretical plates ($N$). The results are presented in Fig. 2.

The $R_s$ increased linearly with an increase of the buffer concentration from 20 to 60 m*M*. The increase followed the linear equation $y = 0.031x - 0.41$, where $y$ represents the $R_s$ value and $x$ represents the buffer concentration in m*M*. The $R_s$, however, suddenly dropped to near zero when the buffer concentration increased beyond the concentration of 70 m*M*. Increase of the buffer concentration proportionally increased the flow of the electric current. The increase of the electric current followed the linear equation $y = 1.26x + 0.174$ ($r > 0.999$), where $y$ represents current in mA and $x$ represents the buffer concentration in m*M*.

Increase in the apparent $N$ value peaked at about 60 000/m with a buffer concentration of approximately 40 to 50 m*M*. This phenomenon, a sharp decrease of $N$ above a buffer concentration of

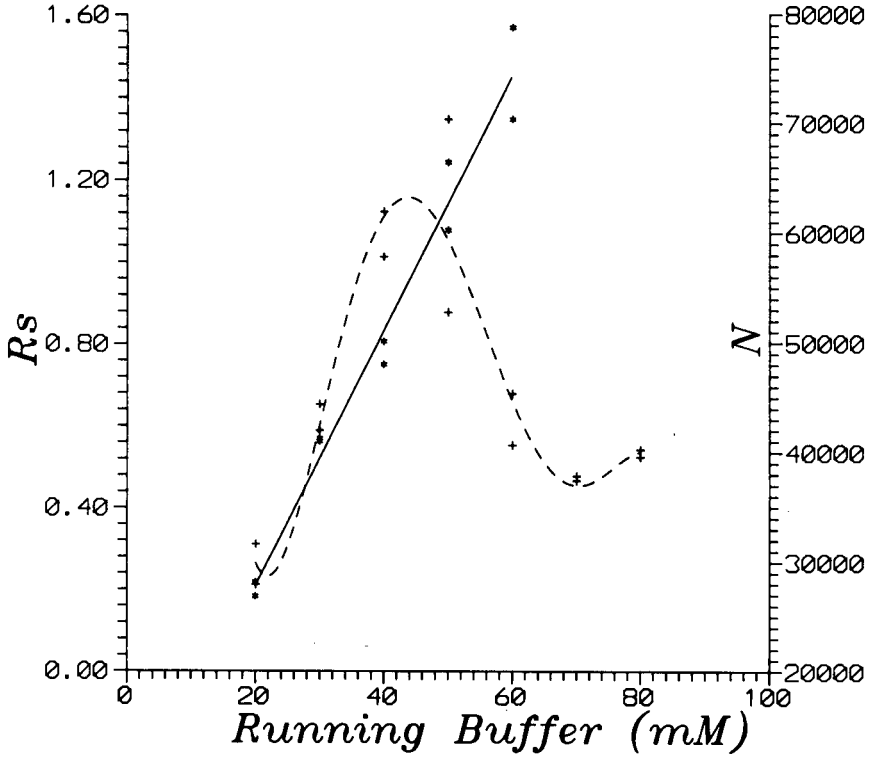


Fig. 2. Effects of concentration of the running buffer on resolution ($R_s$) (*) and number of theoretical plates ($N$) (+) of the chimeric FG glycoprotein peaks. Running buffer, pH 5.2 sodium citrate–acetic acid; conditions as in Fig. 1.

50 m$M$, was not observed when another basic protein, sCD4, was tested. Thus, in addition to the high salt concentration and the Joule heating, the microheterogeneities of carbohydrate moieties in the FG glycoprotein may also be contributing to the phenomenon. Since the FG glycoprotein is indicated to be extensively glycosylated and contains both N- and O-glycosylation sites (data not shown), increase in $N$ of a mere 10 000 to 20 000/m would not be sufficient to separate each and every FG glycoprotein form. Although the observed $N$ value decreased, it may be theorized that it actually increased above the buffer concentration of 50 m$M$. The polymer coated column, in reality, tried to separate the glycoproteins containing minor differences in the carbohydrates. The net effects, therefore, were broadening of the FG glycoprotein peaks. Indeed, the FG protein appeared as a diffused peak by the SDS-polyacrylamide gel-filled capillary electrophoresis column [6] and as a smeared band on a SDS-PAGE slab gel. Thus, increase in the true $N$ value caused an apparent broadening of the FG peak which in turn resulted in a sharp drop in the observed $N$ value and loss of the $R_s$ value. Tran *et al.* [7] successfully split a glycoprotein, erythropoietin, into four peaks by use of a very short column with an exact capillary zone electrophoresis condition.

Since the buffer concentration showed minimum effect on the electroosmotic flow of the polymer-coated capillary column, effect of the buffer concentration on peak migration time was minimal.

The following conditions for the polymer-coated capillary column electrophoretic separation were considered optimum for the analysis of the chimeric FG glycoproteins: running buffer, 50 m$M$ sodium citrate–acetic acid at a pH of *ca.* 5.2; polymer-coated fused-silica capillary column, 75 $\mu$m I.D.; effective column length, 50 cm; column temperature, 25°C; constant voltage at −350 V/cm.

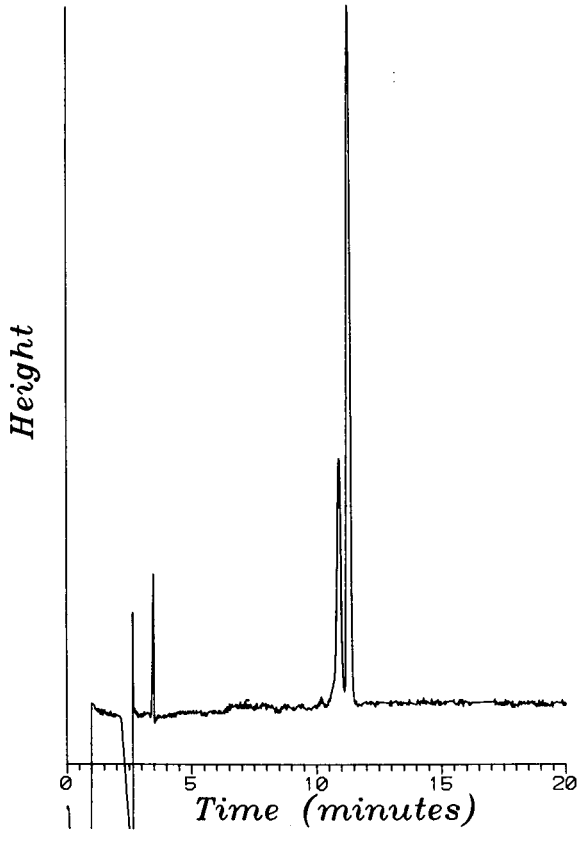


Fig. 3. Capillary electrophoretic separation of the chimeric FG glycoproteins of the respiratory syncytial virus using a polymer-coated fused-silica capillary column as monitored at 214 nm. Running buffer, 50 m*M* sodium citrate–acetic acid at pH 5.2; conditions as in Fig. 1.

*Capillary electrophoretic analysis of the chimeric FG glycoproteins*

A typical electropherogram indicating separation of peaks in the chimeric FG glycoprotein is presented in Fig. 3. The standard curve for the analysis of the FG glycoprotein is linear ($r > 0.996$) between the glycoprotein concentration of 50 and 200 $\mu$g/ml (Fig. 4). A linear regression equation follows $y = 15\,300x - 546\,000$, where $y$ represents the peak area and $x$ represents the glycoprotein concentration in $\mu$g/ml. The curve intersects the $x$ axis at about 35 $\mu$g/ml glycoprotein indicating adsorption of the glycoprotein on the capillary wall. The adsorption of the glycoprotein may be due to incomplete coating of the capillary wall with the polymeric agent.

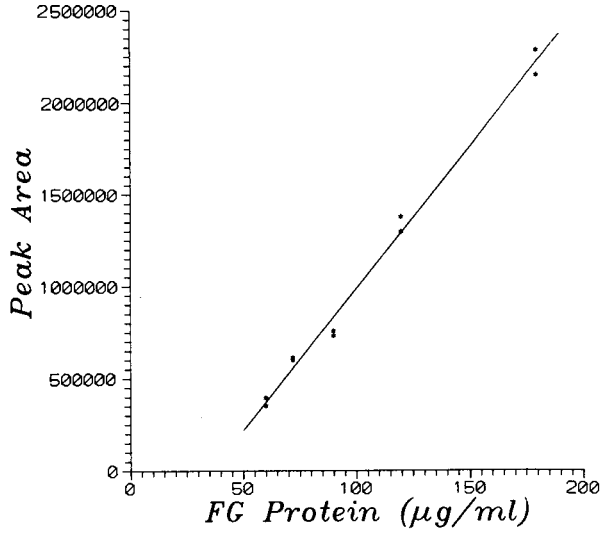


Fig. 4. Standard curve for the electrophoretic analysis of the chimeric FG glycoprotein using a polymer-coated fused-silica capillary column. Peaks migrated were monitored at 214 nm. The curve indicates existence of a linear relationship ($r > 0.996$) between the weight of the FG glycoprotein and the peak area. Running buffer, 50 m*M* sodium citrate–acetic acid at pH 5.2; conditions as in Fig. 1.

The precision for the assay of the biotechnology-derived chimeric FG glycoprotein of RSV was evaluated by repeated injection of the glycoprotein sample at *ca.* 80 $\mu$g/ml concentration. The relative standard deviation (R.S.D.) for the assay of the glycoprotein was about 4.6% and that of the peak migration time was approximately 3.0% (Table II). The R.S.D. of the peak migration time obtained in this study was approximately twice that of a capillary zone electrophoretic assay method [8]. This high R.S.D. may be caused by difficulties in obtaining a consistent/homogeneous coating of the column allowing a minor, inconsistent binding of the glycoprotein on the column surface.

A crude FG glycoprotein preparation contaminated with a trace amount of a proteolytic enzyme was diluted with water and incubated in the native form at about 30°C. The sample was assayed at 60-min intervals. Fig. 5 depicts the electropherograms when the sample was analyzed after 0, 3 and 6 h of incubation. Appearance of a peak with corresponding decrease of the peak, numbered as 2, was noted. The peak, numbered as 1, was unaffected by the treatment. Thus, the polymer-coated capillary

column electrophoretic method may be of value to assess stability characteristics of the chimeric FG glycoprotein. Identification of the peaks which appeared in the electropherogram awaits the successful interfacing of a capillary electrophoretic instrument with a mass spectrometer.

An FG glycoprotein sample was denatured by diluting the sample with a 0.1% TFA solution. A 40-$\mu$l quantity of the denatured sample was pipetted onto a polyolefin microvial (Beckman). The microvial was then placed with a vial spring in a glass vial (4 ml capacity) containing 2 ml water and capped with a silicon vial cap (Beckman). Water was added to the vial to minimize evaporation. When the sample was analyzed at 60-min intervals, a progressive increase in the peak area was noted (Fig. 6). The peak area nearly doubled within 250 min while the sample was waiting in a sample tray for analysis. The sample vial was sealed with a silicone rubber vial cap, but the cap has a crosswise cut on its top for easy insertion of the capillary column for injection of a sample. The instrument has no provision for cooling samples and the sample vials easily reach 30°C. Thus, increase in the peak area during the prolonged assay period may be caused by evaporation of the sample solution through the cut made in the vial cap. Inclusion of an internal standard is essential to correct for sample evaporation.

TABLE II

PRECISION OF THE HIGH-PERFORMANCE CAPILLARY ELECTROPHORETIC ANALYSIS OF A CHIMERIC FG GLYCOPROTEIN USING A POLYMER-COATED FUSED-SILICA CAPILLARY COLUMN

Peaks migrating were monitored at 214 nm. Conditions: −350 V/cm (85 $\mu$A); column temperature, 25°C; migration distance, 50 cm; column 75 $\mu$m I.D.; running buffer, 50 m*M* sodium acetate–citric acid at pH 5.2.

| Run No. | Peak migration (min) | FG glycoprotein peak area |
|---|---|---|
| 1 | 10.24 | 1 226 000 |
| 2 | 9.74 | 1 168 000 |
| 3 | 9.78 | 1 259 000 |
| 4 | 9.79 | 1 343 000 |
| 5 | 9.86 | 1 311 000 |
| 6 | 9.87 | 1 247 000 |
| 7 | 9.29 | 1 247 000 |
| 8 | 9.33 | 1 351 000 |
| 9 | 9.39 | 1 285 000 |
| Average | 9.70 | 1 271 000 |
| R.S.D. (%) | 3.18 | 4.60 |

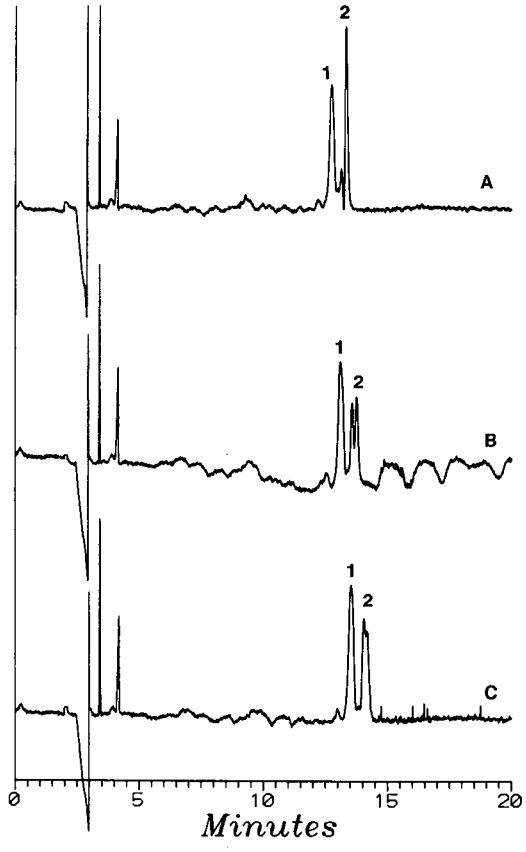


Fig. 5. Composite electropherograms of a crude chimeric FG glycoprotein sample indicating formation of a degradation compound when held at 30°C. Electropherograms: A, 0 h; B, 3 h; C, 6 h at 30°C. Sample diluted to 60 $\mu$g glycoprotein per ml water. Running buffer, 50 m*M* sodium citrate–acetic acid at pH 5.2; conditions as in Fig. 1.

Appearance of a new peak, as observed in the FG sample without TFA (Fig. 5), was not noted. This was expected as TFA solution inactivates proteolytic enzymes.

*$C_8$ and $C_{18}$ derivatized column*

Capillary columns derivatized with $C_8$ and $C_{18}$ were examined for the analysis of the chimeric FG glycoprotein. A single, highly skewed FG glycoprotein eluted from the columns. Variety of buffers with differing pH values were used in an attempt to

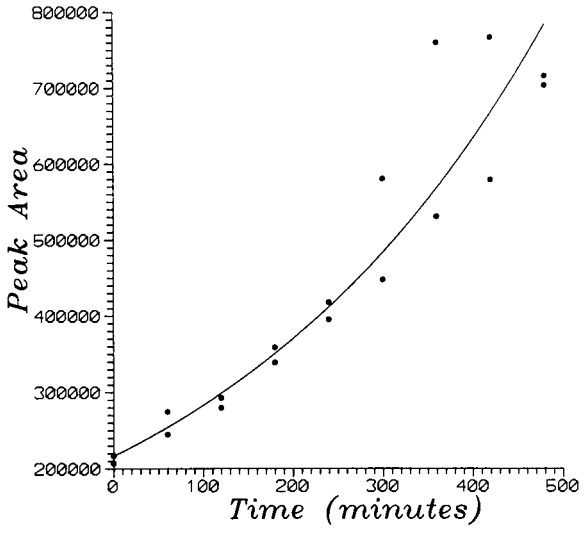


Fig. 6. Peak area of a chimeric FG glycoprotein analyzed at 60-min intervals indicating evaporation of the sample solution.

improve selectivity of the column. No improvement was attained.

REFERENCES

1 J. E. Wiktorowiez and J. C. Colburn, *Electrophoresis*, 11 (1990) 769–773.
2 M. Merion, B. Bell-Alden, E. Grover, U. Neue and J. Petersen, presented at the *3rd International Symposium on High-Performance Capillary Electrophoresis, San Diego, CA, February 3–6, 1991*, Poster 69.
3 A. M. Dougherty, C. L. Wooley, D. L. Williams, D. F. Swaile, R. O. Cole and M. J. Sepaniak, *J. Liq. Chromatogr.*, 14 (1991) 907–921.
4 M. W. Wathen, R. J. Brideau, D. R. Thomsen and B. R. Murphy, *J. Gen Virol.*, 70 (1989) 2625–2635.
5 D. K. Wagner, P. Muelenaer, F. W. Henderson, M. H. Snyder, C. B. Reimer, E. E. Walsh, L. J. Anderson, D. L. Nelson and B. R. Murphy, *J. Clin. Microbiol.*, 27 (1989) 589–592.
6 K. Tsuji, *J. Chromatogr.*, 550 (1991) 823–830.
7 A. D. Tran, S. Park, P. J. Lisi, Q. T. Huynh, R. R. Ryall and P. A. Lane, *J. Chromatogr.*, 542 (1991) 459–471.
8 K. Tsuji, L. Baczynskyj and G. E. Bronson, *Anal. Chem.*, submitted for publication.

*Journal of Chromatography*, 594 (1992) 325–334
Elsevier Science Publishers B.V., Amsterdam

CHROM. 23 859

# Capillary modification and evaluation using streaming potential and frontal chromatography for protein analysis in capillary electrophoresis

Tiansong Wang and Richard A. Hartwick*

*Department of Chemistry, State University of New York, Binghamton, NY 13902 (USA)*

(First received August 26th, 1991; revised manuscript received November 1st, 1991)

ABSTRACT

The modification of capillary surfaces in capillary electrophoresis requires accurate chemical characterization of the synthesized materials. A three-step procedure was developed for the evaluation of capillaries used for protein separations in capillary electrophoresis. These measurements include $\zeta$ potential determination via streaming potential measurements, adsorption characteristics using frontal chromatography measurements of test solutes, and overall performance under running conditions using selected test solutes. The $\zeta$ potential determined from the streaming potential reflects the degree to which the capillary wall can undergo electrostatic interactions with proteins as well as the magnitude of the electroosmotic flow. Frontal chromatography measurements with selected probe proteins can indicate both the amount of adsorption as well as the probable types of interactions involved in the adsorption. Kinetic information can also be obtained in some instances. Electrophoresis with test solutes reflects the overall effect of adsorption.

For this study, three types of capillaries were evaluated: (1) bare fused-silica capillaries, (2) capillaries coated with several thickness of cross-linked polyethylene glycol and (3) cross-linked polyethyleneimine. The polyethylene glycol column displayed much weaker electrostatic and similar hydrophobic and/or hydrogen bonding interactions as compared with underivatized fused-silica columns. The polyethyleneimine column exhibited poor performance for the test proteins used. Good electrophoretic performance seems to be possible only if adsorption measurements were below 0.2 ng/cm$^2$ (corresponding to 0.1% of available surface area) for all of the test proteins.

## INTRODUCTION

Electrophoresis has long been an important separation technique for proteins. When high-performance capillary electrophoresis (HPCE) was developed in early 1980s, it was anticipated that HPCE would result in dramatically improved protein separations [1], and many successful separations have been reported. In the past several years, capillary zone electrophoresis [2–6], capillary gel electrophoresis [7] and capillary isoelectric focusing [8–10] have been applied to protein separations with good results. However, despite these successes, the routine application of HPCE to proteins and other macromolecules remains hindered by solute adsorption to the capillary walls.

In order to overcome the problems of protein adsorption, various methods have been applied, such as pH selection [2,3], high salt concentration [4] and surface modification [5,6]. The degree of adsorption is usually measured indirectly by the evaluation of column efficiency. However, separation efficiency alone can be an inaccurate indicator of adsorption problems, since column efficiency is affected not only by adsorption, but also by sample concentration [1,11], injection conditions [12,13] and applied voltage [3]. Second, even when efficiency problems are due to adsorption effects, little or no insight is gained as to the mechanisms of adsorption. To measure protein adsorption on capillaries, Green and Jorgenson [4] employed an elution chromatographic method and monitored the peak capacity factors ($k'$) of proteins. This method was more reliable than column efficiency, but the

0021-9673/92/$05.00 

accuracy of the method was limited, and it was difficult to measure weakly adsorbed solutes with $k' < 0.02$. Zhu *et al.* [14] reported a flow injection procedure to measure the residual adsorption of protein. This procedure was convenient but suffered from the low sensitivity inherent to on-column detection. Recently, Towns and Regnier [15] described a dual-detector method to monitor the peak area change of proteins in a capillary.

An important property of a capillary is its $\zeta$ potential. The $\zeta$ potential is generated by surface charges of the capillary. Therefore, the $\zeta$ potential reflects the potential for electrostatic interactions, as well as the expected capillary electroosmotic flow. The $\zeta$ potential can be estimated from the resulting electroosmotic flow, but more reliably by direct measurements of the streaming potential [16–18]. The streaming potential is a well-known electrokinetic property of a charged surface, and can be considered as the inverse property of electroosmotic flow. When a solution of ions flows through a charged tube, an electric potential, *i.e.*, the streaming potential, will arise. The relationship of the $\zeta$ potential to the streaming potential is [16]

$$\zeta = (4\pi\eta E_s/\varepsilon p)(K_b + 2K_s/R) \quad (1)$$

where $\eta$ and $\varepsilon$ are the viscosity and dielectric constant in the diffuse double layer, respectively, $E_s$ is the streaming potential, $p$ is the pressure difference across the tube, $K_b$ and $K_s$ are the specific bulk and surface conductance, respectively, and $R$ is the radius of the tube. For large inner diameter capillaries operated under moderate electrolyte concentrations, $K_s/R \ll K_b$, and grouping the $4\pi$ constant and the units into a single constant, eqn. 1 can be simplified as follows:

$$\zeta = 4\pi\eta E_s K_b/\varepsilon p = 84.9 \cdot 10^7 \eta K_b E_s/\varepsilon p \quad (2)$$

In practice, $\eta$ and $\varepsilon$ are assumed to be equal to bulk values. $\eta$ is in poises, $K_b$ in $cm^{-1}\ \Omega^{-1}$, $E_s$ in mV, $p$ in cmHg and $\zeta$ in mV. Although the streaming potential measurements have been applied to evaluate capillaries used for HPCE [17,18], the precision (about 5 mV) was unsatisfactory, and no report on capillaries below 100 $\mu$m inner diameters was found.

During the course of research in our laboratory in the synthesis of new capillary bonding materials, it became necessary to evaluate surfaces for their adsorption characteristics and overall performance potential in HPCE. The evaluation procedures must be sensitive to adsorption, but insensitive to operating conditions. The procedures should also present information to distinguish among different interactions in the protein adsorption (hydrophobic, electrostatics, hydrogen bonding, etc.). In this paper, a three-step evaluation procedure was developed using streaming potential measurements, frontal chromatography of selected test solutes and overall column performance measurements under capillary zone electrophoresis (CZE) operating conditions. The capillaries bonded with polyethylene glycol (PEG) and polyethyleneimine (PEI) as well as bare fused silica were evaluated by the procedure.

## EXPERIMENTAL

### *Streaming potential*

The experimental setup is shown in Fig. 1. The nitrogen pressure was controlled by a Varian 3700 gas chromatograph (Sunnyvale, CA, USA), and was read out from a laboratory constructed mercury manometer. The nitrogen pressure could be applied to either reservoir by switching the six-port valve (Rheodyne 7000, Cotati, CA, USA) in order to alternate the flow direction. The volume of the reservoir was about 18 ml. The electrode was 0.5 mm O.D. Ag wire treated in 5 *M* HCl (+1.5 V for 10 min) [19]. The reservoirs and the capillary (typically length of 6–7 cm) were put into a metal thermostatic jacket which also functioned as a Faraday cage. The streaming potential was measured with a Keithley

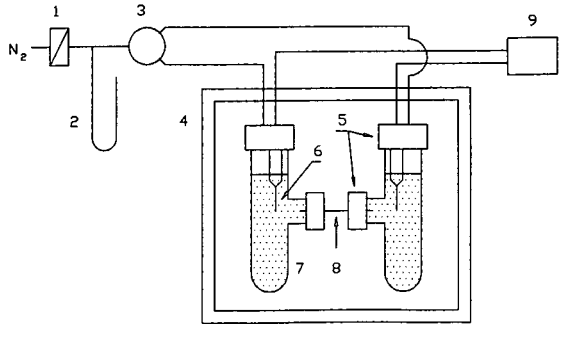


Fig. 1. Apparatus for streaming potential measurements. 1 = Pressure control valve; 2 = mercury manometer; 3 = 6-port valve; 4 = metal thermostatic jacket (Faraday cage); 5 = cap; 6 = Ag/AgCl electrode; 7 = glass reservoir with electrolyte solution; 8 = capillary; 9 = electrometer.

616 digital electrometer (Cleveland, OH, USA) with 0.01 mV resolution.

A typical electrolyte solution was 18 m*M* KCl + 0.5 m*M* $KH_2PO_4$ + 0.5 m*M* $K_2HPO_4$, using NaOH solution to adjust the pH to 7.2 and applying one drop of 0.5% $AgNO_3$ solution into 100 ml solution. Before measuring, capillaries were equilibrated overnight with the electrolyte solution, then the solution was pumped back and forth (about 10 min each time) until the difference of potential readings was below 0.1 mV. The streaming potential was measured at 4–5 different pressure values (typically, from 15 to 40 cmHg), and at each pressure, two readings with different flow directions were taken. From these data, the $E_s/p$ ratio was determined from the regression equation of $E_s$–$p$ plot.

*Frontal chromatography*

Fig. 2 shows a schematic graph of the frontal chromatograph used in this research. The nitrogen pressure was controlled by the Varian 3700 gas chromatograph, the split needle valve functioned as low pressure (below 10 cmHg) controller. The reservoir was a 4-ml glass vial and could be quickly changed. On-column detection was accomplished using a modified Spectroflow 757 absorbance detector (Kratos Analytical, Ramsey, NJ, USA) at 200 nm. The signal was recorded with an OmniScribe A5111-5 recorder (Houston Instrument, Austin, TX, USA). The typical effective length of capillary was 40 cm, the total length was 50 cm.

Three buffers were used, *i.e.*, 5 m*M* $KH_2PO_4$ + 5 m*M* $K_2HPO_4$–NaOH(pH 7.2), 20 m*M* acetic acid–NaOH(pH 4.7) and 20 m*M* $H_3PO_4$(pH 2.1). The

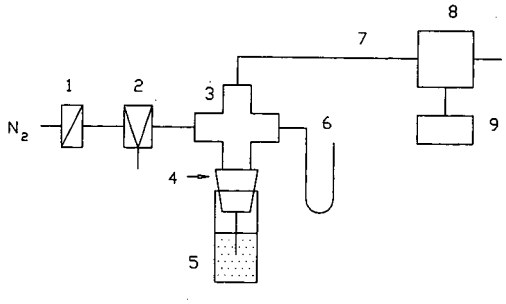


Fig. 2. Frontal chromatograph. 1 = Pressure control valve; 2 = split needle valve; 3 = four-way connector; 4 = rubber stopper; 5 = glass reservoir; 6 = mercury manometer; 7 = capillary; 8 = detector; 9 = chart recorder.

dead time was determined by injection of water (for pH 7.2 and 4.7 buffers) or acetone solution (for pH 2.1 buffer), and the linear flow-rate was controlled within 0.9–1.1 mm/s.

Three proteins (albumin, lysozyme and hemoglobin) were used as probes, and were dissolved separately in the measuring buffer at *ca.* 0.01 or 0.1 mg/ml. Two measuring procedures were performed: procedure A used the same capillary for all proteins, procedure B employed one capillary for just one protein. Both procedures start with fresh capillaries.

*Procedure A.* After a stable baseline was obtained with the buffer, a protein solution was flowed through the column until saturation was achieved and the breakthrough volume measured. Then, the column was cleaned as follows: 2–3 $V_0$ (column volume) of distilled water followed by about 15 $V_0$ 1% sodium dodecyl sulfate (SDS, for negatively charged columns) or 1% cetyltrimethylammonium bromide (CTAB, for positively charged columns) followed by 2–3 $V_0$ distilled water then followed by about 15 $V_0$ buffer. Following this cleaning procedure, the next protein would be measured on the same column.

*Procedure B.* A single fresh column would be dedicated to one type of protein, with three identical columns from a single bonding being studied. For these studies, after breakthrough, the flow of protein solution was continued for about 1 $V_0$, then the flow was switched back to the buffer solution and keep running for at least 1.5 $V_0$. Then the columns were washed as follows: applying 7 p.s.i. nitrogen pressure for a 50 cm long column, wash cycles were 2–3 min with distilled water, 5 min with methanol, 15 min with methylene chloride, 5 min with methanol and 2–3 min with distilled water. Prior to any measurements, columns were equilibrated overnight with the appropriate buffers.

*CZE performance evaluations*

A Spectra Phoresis 1000 with a SP4400 integrator (Spectra-Physics, Reno, NV, USA) was used during capillary performance evaluations. All columns were 75 μm I.D. × 360 μm O.D., 35 cm effective length and 42.5 cm total length. The column temperature was 25°C. Running voltage was 12 kV. Injection conditions were 1 s for hydrodynamic or 5 s × 5 kV for electrokinetic injection. Detector wavelength was 200 nm with 0.5 s rise time.

*Capillary modification*

The capillary modifications using PEG 8M-10 and PEI-3M were produced by thermally cross-linking according to the temperature protocols recommended by the manufacturer. Prior to bonding, fused-silica capillaries (75 $\mu$m I.D. × 360 $\mu$m O.D., Polymicro Technologies, Phoenix, AZ, USA) of about 2 m in length were washed with a 0.1 *M* NaOH solution at 80°C for 1–1.5 h. After cooling, they were washed with distilled water followed by methanol. They were dried with nitrogen at 130°C for at least 4 h. The capillary was then filled to a length 12–15 cm with PEG 8M-10 or PEI-3M–methylene chloride solution (5–20%, w/v) and the solution was slowly pushed through the capillary with nitrogen. The capillary was then placed in the column oven of a Varian 3700 gas chromatograph under high-purity nitrogen flow. For PEG bonding, the temperature program was 30°C → 225°C at 5°C/min, holding at the upper temperature overnight (> 12h). For PEI bonding, the same procedure was used, but with a final temperature of 175°C. Following this cross-linking, each column was washed for half hour with methylene chloride, followed by methanol. The window on the modified capillary was created with hot sulfuric acid.

*Reagents and supplies*

PEG 8M-10 and PEI-3M polymer solutions were obtained from Innophase Corporation (Portland, CT, USA), bovine serum albumin (A-7030), chicken egg lysozyme (L-6876) and human hemoglobin (H-7379) from Sigma (St. Louis, MO, USA). A protein test mixture normally used for high-performance liquid chromatography was obtained from Applied Biosystems (Foster City, CA, USA), SDS from Bio-Rad Labs. (Richmond, CA, USA), acetic acid, phosphoric acid and sulfuric acid from J. T. Baker (Phillipsburg, NJ, USA), and all other chemicals from Fisher (Fair lawn, NJ, USA).

## RESULTS AND DISCUSSION

*Streaming potential*

There are two requirements for the application of eqn. 2: a laminar flow and $K_s/R \ll K_b$. The flow situation in a capillary can easily be established by measuring the flow-rate and calculating the Reynolds number ($R_e$) as follows:

$$R_e = \rho u d/\eta \quad (3)$$

where $\rho$ is the density of the solution in g/cm$^3$, $u$ is the linear flow velocity in cm/s, $d$ is the inner diameter of the capillary in cm, and $\eta$ is the viscosity of the solution in poises. For example, applying 30 cmHg pressure, the flow-rate in a 6 cm long × 75 $\mu$m I.D. capillary is 33 $\mu$l/min or 12.4 cm/s, thus, $R_e = 9.3$. Since a turbulent flow corresponds to a Reynolds number > 2000 in a straight open tube, all measurements could safely be assumed to in the laminar region.

When the inner diameter of a capillary is larger than 100 $\mu$m, it is usually believed that $K_s/R \ll K_b$. However, when the inner diameter is reduced to 50 or 25 $\mu$m, $K_s/R$ term may no longer be negligible. To establish the magnitude of the $K_s/R$ term, two capillaries (A and B) with different inner diameters must be used. Assuming both capillaries have the same $\zeta$ potential, from eqn. 1, we have

$$(E_s/p)_A(K_b + 2K_s/R_A) = (E_s/p)_B(K_b + 2K_s/R_B) \quad (4)$$

after rearrangement and for convenience letting $S_A = (E_s/p)_A$, $S_B = (E_s/p)_B$,

$$K_s = (1 - S_A/S_B)K_b/2(S_A/(S_B R_A) - 1/R_B) \quad (5)$$

In this research, a 100 $\mu$m and a 25 $\mu$m I.D. capillary were used to estimate the surface conductance, and in the pH 7.2 buffer (ionic strength, 20 m*M*), $K_s$ is $1.5 \cdot 10^{-7}\ \Omega^{-1}$ according to eqn. 5. For a 25 $\mu$m I.D. capillary, $K_s/R$ is $1.2 \cdot 10^{-4}\ (\Omega\ \text{cm})^{-1}$ and corresponds to 4.7% of the bulk conductance [$K_b = 2.53 \cdot 10^{-3}\ (\Omega\ \text{cm})^{-1}$]; 50 $\mu$m, 2.4%, and 100 $\mu$m, 1.2%. These results represent the most severe possible error from this source in regards to eqn. 2. There is also possible error in the $K_s$ value due to differences in the $\zeta$ potential of the two capillaries, despite their being made of the same material, and being pre-treated equally. Nevertheless, the magnitude of these possible errors are still relatively small, and for capillaries with diameters on the order of 50–100 $\mu$m I.D., the surface conductance is negligible in the streaming potential measurement, although for 25 $\mu$m I.D. capillaries it can start to become significant.

The quality of the electrode has a great effect on the streaming potential measurement. Poor electrodes show potential differences and drift. It was found that an acceptable electrode could be made with freshly sanded silver wire, and that the potenti-

al difference between two electrodes could be kept below 0.02 mV. The flow direction has been reported to affect the streaming potential [16]. In this research, differences in potentials measured in different flow directions were also observed. However, the magnitude of the effect was only about 2%, and by taking average measurements, the effect of this difference on the $E_s/p$ value is negligible. Moreover, the direction reversal operation is still necessary in order to keep the liquid level even in the reservoirs, and thus prevent syphon-induced flow.

Using the streaming potential to calculate the $\zeta$ potential was found to be convenient and reliable, especially for the modified capillaries with very low $\zeta$ potential, which would result in low electroosmotic flows. Measurements required only about 1 h (excluding capillary equilibration time). The only limitation of the method is the need for a precision electrometer, and reduction of extraneous noise through the use of a Faraday cage. The evaluation results of some modified capillaries are summarized in Table I.

*Frontal chromatography*

Potential interactions between proteins and the capillary wall are very complex, with various mechanisms such as electrostatic attraction, hydrophobic interaction and hydrogen bonding, as well as protein-specific geometries, all contributing to the magnitude of adsorption. No single measurement could ever reliably predict capillary performance under all conditions. The $\zeta$ potential is only an indicator for the possibility of electrostatic interactions, and more information can be obtained from the direct measurement of adsorption.

An accurate and convenient method to measure adsorption is that of frontal chromatography, which has long been applied to both gas–solid and liquid–solid adsorption measurements [20,21]. Frontal chromatography involves the transportation of a continuous flow of adsorbate solution through a column containing the adsorbent by a inert carrier. Upon saturation of the column, the adsorbed material is eluted by the carrier alone, and the concentration rises to the bulk adsorbate concentration. A typical signal profile of the frontal chromatography is shown in Fig. 3. From frontal elution measurements, four kinds of information can be obtained:

(1) The quantity of solute adsorbed. It is obvious that the sample loss between $t_0$ and $t_R$ is caused by adsorption in the column, and the amount of adsorption ($Q_{ad}$) is [21]

$$Q_{ad} = (t_R - t_0)FC_0 \quad (6)$$

where $t_R$ and $t_0$ are the retention and dead time, respectively, $F$ is the flow-rate, and $C_0$ is the sample concentration. For capillaries, $Q_{ad}$ is easily converted into adsorption per unit surface area, since the surface area of the adsorbent is equal to the inner surface of the capillary.

(2) The residual adsorption. This parameter is measured from the concentration difference between the b and c lines (Fig. 3), and can be expressed in percentage relative to the sample concentration. Irreversible adsorption will lead to a high residual percentage.

TABLE I

STREAMING POTENTIAL ($E_s$) AND $\zeta$ POTENTIAL OF COLUMN

| Column | pH[a] | $E_s$ (mV) | $\zeta$ (mV) |
|---|---|---|---|
| Bare | 7.2 | 2.97–12.42 | −73.1 |
| 5% PEG | 7.2 | 1.14–2.78 | −24.4 |
| 10% PEG | 7.2 | – | −16.0 |
| 20% PEG | 7.2 | 0.06–0.14 | −0.6 |
| 20% PEI | 7.2 | 1.56–3.83 | −22.7 |
| 20% PEI | 4.7 | 2.18–5.72 | +47.0 |

[a] Ionic strength = 20 m*M*.

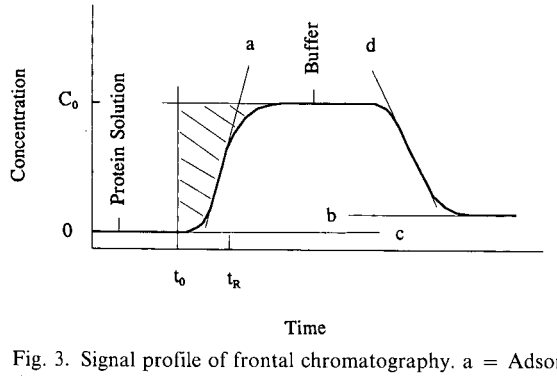


Fig. 3. Signal profile of frontal chromatography. a = Adsorption slope; b = ending baseline; c = beginning baseline; d = desorption slope. $t_R$ is determined from the shaded area. $C_0$ = sample concentration.

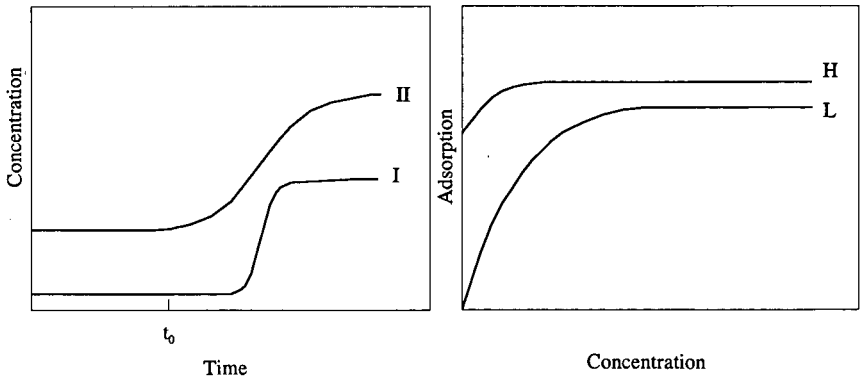


Fig. 4. Frontal chromatographic curves and adsorption isotherm types. Curve I corresponds to H-type isotherm, curve II to L-type isotherm.

(3) The ratio of desorption slope over adsorption slope, which is related to the adsorption isotherm and/or kinetic rate [22,23]. The slope is determined at the inflection point.

(4) Estimation of the shapes of adsorption isotherms and the overall adsorption rates [22,24], especially for the recognition of strong interaction. For example, in Fig. 4, a delayed and steep frontal chromatographic curve (curve I) corresponds to a H-type isotherm, which indicates a very strong adsorption onto part of the surface [22].

In adsorption measurements, the selection of probe proteins are critical. Ideally, each protein should be most sensitive to one type of interactions. Some properties of the probe proteins used in this research are summarized in Table II. As a probe, albumin tends to indicate the hydrophobic interaction as well as hydrogen bonding, provided that the capillary is of either same sign charge or neutral. Lysozyme is positively charged at pH values less than *ca.* 11, and thus will be sensitive to the electrostatic interactions with anionic sites. Hemoglobin was chosen because of its high surface activity [28].

The preliminary results of adsorption evaluations using these test proteins are listed in Table III. In neutral buffer, the adsorption of albumin on the bare capillary is quite weak, while lysozyme and hemoglobin demonstrate very strong adsorption. When the capillary is modified with PEG, the adsorption of albumin remained approximately constant, while the adsorption of lysozyme and hemoglobin were substantially reduced. Further more, the thicker the PEG coating, the weaker the adsorption. This change indicates that the dominant interaction under these conditions is probably elec-

TABLE II

PROPERTIES OF PROBE PROTEINS

| Protein | Mol.wt.[a] | p*I*[a] | Hydrophobicity[b] | Carbonyl point[c] |
|---|---|---|---|---|
| Bovine albumin | 66 000 | 4.7 | 2729 | 77 |
| Egg lysozyme | 14 000 | 11 | 25 | 19 |
| Human hemoglobin | 64 500 | 6.9–7.4 | – | – |

[a] Refs. 2, 6 and 25.
[b] Ref. 26 (measured by fluorescence probe method using *cis*-parinaric acid).
[c] Refer to the number of carbonyl surface contacts per molecule (ref. 27).

TABLE III

ADSORPTION OF PROTEIN ON COLUMN

| Column | pH | Adsorption (ng/cm$^2$)[a] | | |
|---|---|---|---|---|
| | | Albumin | Lysozyme | Hemoglobin |
| Bare | 7.2 | 0.6 | 206 | 254 |
| 5% PEG | 7.2 | <0.4 | 55.2 | 7.2 |
| 20% PEG | 7.2 | 0.4 | 3.6 | 1.9 |
| 20% PEI | 7.2 | 73.2 | 181 | 273 |
| 20% PEI[b] | 4.7 | 328 | 14.5 | 50.8 |

[a] Measured by procedure A, 0.1 mg/ml protein.
[b] Measured by procedure B, 0.1 mg/ml protein.

trostatic, since the $\zeta$ potentials are progressively lower from the bare to 20% PEG bonding capillaries. It should be emphasized that even at its p*I*, hemoglobin still has obvious electrostatic interaction with the capillary. The PEI column is negatively charged at pH 7.2, but the adsorption of albumin (also negatively charged) is much stronger than that on the bare column. Therefore, strong hydrophobic interaction or hydrogen bonding must take place on the PEI column. Interactions other than electrostatic can also explain the significantly higher amount of adsorption of lysozyme and hemoglobin on the PEI column than those on the 5% PEG column, since both columns have similar $\zeta$ potentials (see Table I). At pH 4.7, the PEI column is positive charged, the adsorption of lysozyme and hemoglobin is reduced, especially lysozyme, but it is still higher than that on the 20% PEG column, while the adsorption of albumin is greatly increased. These adsorption characteristics indicated that under the condition studied, PEI column was generally poor for protein separations.

From Table III, it is found that the 20% PEG column produced the weakest adsorption. A more critical evaluation (procedure B, 0.01 mg/ml protein) was performed, with the results being tabulated in Table IV. On the 20% PEG column and at pH 7.2, all three proteins demonstrate similar adsorption. The equal amount of adsorption of albumin and lysozyme implies that the electrostatic interaction is negligible. The obvious difference of lysozyme relative to albumin and hemoglobin is its low slope ratio, *i.e.*, its desorption slope is much shallower than its adsorption slope. A low slope ratio is known to be caused by a non-linear adsorption isotherm [22] or by a slow desorption rate [23], and will deform the peak shape and lower the column efficiency. The relationship of the slope ratio to the modification layer is currently unknown.

TABLE IV

ADSORPTION OF PROTEIN ON 20% PEG BONDING COLUMN

Measured by procedure B, 0.01 mg/ml protein.

| Protein | pH | Adsorption (ng/cm$^2$) | Slope ratio | Residual |
|---|---|---|---|---|
| Bovine albumin | 7.2 | 1.0 | 0.96 | −2% |
| Egg lysozyme | 7.2 | 1.0 | 0.60 | 0% |
| Human hemoglobin | 7.2 | 0.85 | 1.05 | 5% |
| Bovine albumin | 2.1 | 0.24 | 0.93 | 0% |
| Egg lysozyme | 2.1 | 0.22 | 0.89 | 0% |
| Human hemoglobin | 2.1 | 0.09 | 0.96 | 0% |

At pH 2.1, the adsorption of all proteins is reduced further, and the slope ratio of lysozyme is improved. From the amount of adsorption and the dimension of each molecule, the fractional surface coverage can be calculated. An adsorption of 0.24 ng/cm$^2$ of albumin (30 × 150 Å) [29] corresponds to 0.10% coverage, 0.22 ng/cm$^2$ of lysozyme (45 × 30 Å) [30], 0.14%, and 0.09 ng/cm$^2$ of hemoglobin (64 × 55 Å) [31], 0.03%.

*CZE performance evaluation*

From the adsorption measurements, the most suitable column appeared to be that producing the lowest adsorption measurements. However, factors other than simple adsorption can affect the actual efficiency of the CZE capillary. Also, it was not clear by this data what the minimum adsorption value must be in order to produce acceptable separations, and whether any such lower adsorption limit would be true for a variety of proteins. Therefore, the final test of capillary surfaces was the efficiency and detectable concentration of test molecules under operating conditions.

From Table V, it can be seen that, at pH 7.2, although the protein on the 20% PEG column is only about 1 ng/cm$^2$ (see Tables III and IV), the CZE separation of proteins is still significantly degraded. At pH 2.1, the adsorption is reduced to 0.2 ng/cm$^2$ and column efficiency improved dramatically. It is believed that the reduction of adsorption is the major factor which contributes to the efficiency improvement, although it may not be the exclusive one. Fig. 5 shows the CZE separation of the probe proteins at pH 2.1 on bare and 20% PEG capillaries, while Fig. 6 presents the CZE separation of a test mixture of proteins frequently used for reversed-phase liquid chromatography. The similar column efficiency of lysozyme on the PEI column and albumin on the bare column cannot be explained from the amount of adsorption.

The behavior of lysozyme on the 20% PEG column was unexpected. At pH 7.2, lysozyme should produce efficiencies similar to albumin since they

TABLE V

COLUMN EFFICIENCY MEASURED FROM PROBE PROTEIN

0.1 mg/ml protein. The values in the Table are theoretical plate numbers.

| Protein | Bare | | 20% PEI | 20% PEG | |
|---|---|---|---|---|---|
| | pH 7.2 | pH 2.1 | pH 4.7 | pH 7.2 | pH 2.1 |
| Bovine albumin | $3.0 \cdot 10^3$ | $1.3 \cdot 10^3$ | No peak | $0.5 \cdot 10^3$ | $10 \cdot 10^3$ |
| Egg lysozyme | No peak | $24 \cdot 10^3$ | $4.0 \cdot 10^3$ | Irreversible | $70 \cdot 10^3$ |
| Phenol(neutral) | $55 \cdot 10^3$ | – | – | – | – |

have a similar degree of adsorption and no irreversible adsorption. However, during CZE operation, lysozyme demonstrates irreversible adsorption on the PEG column at pH 7.2 and gives a signal like that of frontal chromatography. The reasons are unclear at present.

In addition to the column efficiency, adsorption also affects the detectable concentration in CZE analysis. The direct measurement of the detectable concentration seems not convenient. Instead, the intercept of the plot of concentration *vs.* signal in the linear range of detection can be the alternative parameter that is parallel to the detectable concentration. For example, on 20% PEG column, at pH 2.1, the regression equation for albumin (0.02–0.2 mg/ml) is

$$C = 0.00626 + 0.00521\,A \quad (r^2 = 0.9996) \qquad (7)$$

and for lysozyme (0.02–0.2 mg/ml)

$$C = 0.000196 + 0.00634\,A \quad (r^2 = 0.9996) \qquad (8)$$

where $C$ is the sample concentration in mg/ml and $A$ is the peak area in $10^4$ count. The intercepts imply that when the concentrations of albumin and lyso-

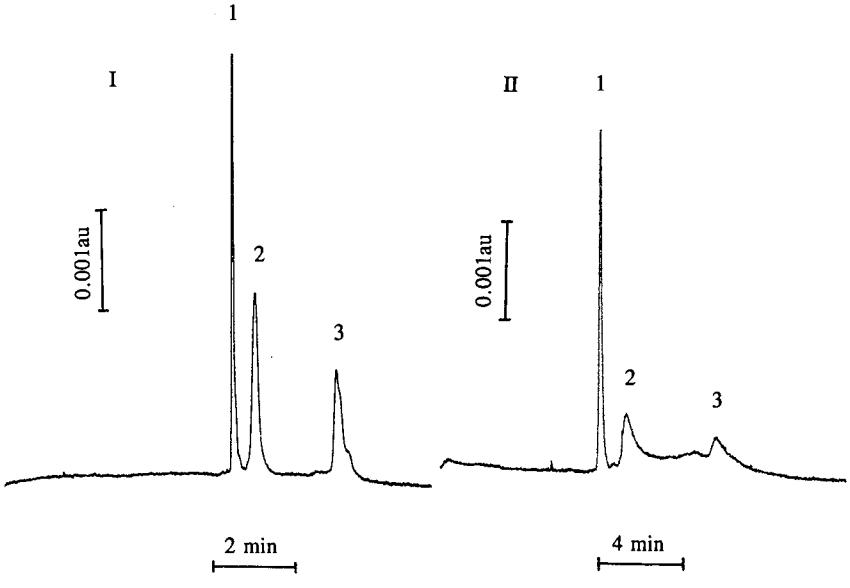


Fig. 5. Electropherograms of probe proteins. 20 m$M$ $H_3PO_4$, pH 2.1. 5 s × 5 kV injection and +12 kV running. Peaks: 1 = lysozyme; 2 = albumin; 3 = hemoglobin; 0.1 mg/ml each. (I) 20% PEG bonding capillary; (II) bare fused-silica capillary.

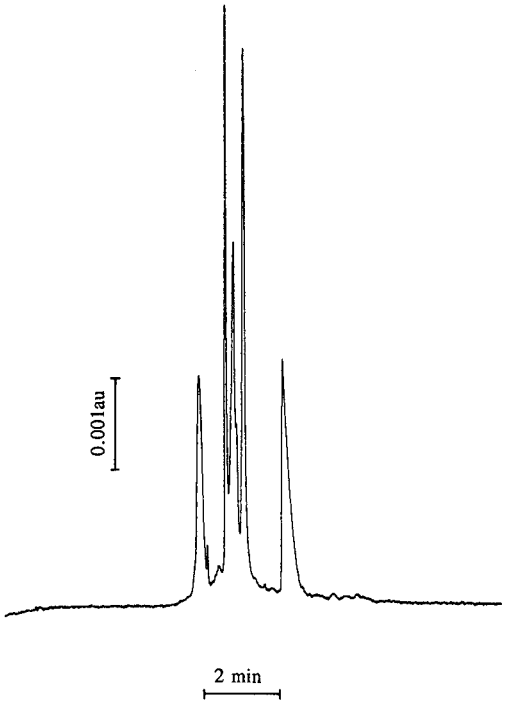


Fig. 6. Separation of protein mixture for reversed-phase high-performance liquid chromatography (insulin, cytochrome *c*, lactalbumin, carbonic anhydrase and ovalbumin). 20% PEG column, 20 m*M* $H_3PO_4$–NaOH, pH 2.5. 5 s × 5 kV injection and +15 kV running.

zyme are below 0.00626 and 0.00196 mg/ml, respectively, no peak can be detected. Although factors other than adsorption also contribute to non-zero intercepts, intercepts may be used to roughly estimate the degree of adsorption measured under the same conditions.

## CONCLUSIONS

A three-step procedure is proposed to evaluate capillaries used for protein separations in capillary electrophoresis. The $\zeta$ potential determined from the streaming potential characterizes potential for capillaries to participate in electrostatic interactions and the expected electroosmotic flow. A simple streaming potential measuring apparatus was designed, which is able to measure capillaries with 25–100 $\mu$m I.D. and with submillivolt precision. Frontal chromatographic measurement with selected probe proteins can indicate the amount of adsorption, the major interactions in the adsorption and some thermodynamic or kinetic properties of the adsorption. The simple frontal chromatographic device used in this research is able to measure adsorption as low as 0.1 ng/cm$^2$. During CZE operation, the adsorption is evaluated by peak efficiencies and the intercept of the plot of concentration *vs.* peak area.

Using the above procedures, both bare and bonded capillaries were evaluated. Generally, the 20% PEG column displays much weaker electrostatic and similar hydrophobic and/or hydrogen bonding interactions compared with the bare capillary, and performed quite well at pH 2.1. However, at pH 7.2, lysozyme demonstrated irreversible adsorption on the PEG column. PEI-bonded surfaces showed generally poor behaviour for proteins separation. It appears that protein adsorption as measured by frontal chromatography should be below 0.2 ng/cm$^2$ or *ca.* 0.1% of the capillary surface area in order to obtain good performance in CZE analysis.

## ACKNOWLEDGEMENT

This research is supported by the Center for Biotechnology, SUNY-Stonybrook and by Spectra-Physics Analytical Division. We also thank Dr. A. Yacynych at Rutgers University for his advice on the preparation of the electrodes.

## REFERENCES

1 J. W. Jorgenson and K. D. Lukacs, *Science (Washington, D.C.)*, 222 (1983) 266.
2 H. H. Lauer and D. McManigll, *Anal. Chem.*, 58 (1986) 166.
3 R. M. McCormick, *Anal. Chem.*, 60 (1988) 2322.
4 J. S. Green and J. W. Jorgenson, *J. Chromatogr.*, 478 (1989) 63.
5 S. A. Swedberg, *Anal. Biochem.*, 185 (1990) 51.
6 K. A. Cobb, V. Dolnik and M. Novotny, *Anal. Chem.*, 62 (1990) 2478.
7 A. S. Cohen and B. L. Karger, *J. Chromatogr.*, 397 (1987) 409.
8 S. Hjertén, *J. Chromatogr.*, 347 (1985) 191.
9 F. Kilar and S. Hjertén, *Electrophoresis*, 10 (1989) 23.
10 T. Wehr, M. Zhu, R. Rodriguez, D. Burke and K. Duncan, *Am. Biotech. Lab.*, 8, No. 11 (1990) 22.
11 K. D. Lukacs and J. W. Jorgenson, *J. High Resolut. Chromatogr. Chromatogr. Commun.*, 8 (1985) 407.
12 E. Grushka and R. M. McCormick, *J. Chromatogr.*, 471 (1989) 421.
13 X. Huang, W. F. Coleman and R. N. Zare, *J. Chromatogr.*, 480 (1989) 95.
14 M. Zhu, R. Rodriguez, D. Hansen and T. Wehr, *J. Chromatogr.*, 516 (1990) 123.

15 J. K. Towns and F. E. Regnier, *Anal. Chem.*, 63 (1991) 1126.
16 R. A. van Wagenen, J. D. Andrade and J. B. Hibbs, Jr., *J. Electrochem. Soc.*, 123 (1976) 1438.
17 J. C. Reijenga, G. V. A. Aben, Th. P. E. M. Verheggen and F. M. Everaerts, *J. Chromatogr.*, 260 (1983) 241.
18 A. A. A. M. van de Goor, B. J. Wanders and F. M. Everaerts, *J. Chromatogr.*, 470 (1989) 95.
19 R. N. Adams, *Electrochemistry at Solid Electrodes*, Marcel Dekker, New York, 1969, p. 291.
20 P. E. Eberly, Jr., *J. Phys. Chem.*, 65 (1961) 1261.
21 S. C. Sharma and T. Fort. Jr., *J. Colloid Interface Sci.*, 43 (1971) 36.
22 L. R. Snyder, *Principles of Adsorption Chromatography*, Marcel Dekker, New York, 1968, Ch. 3.
23 J. C. Giddings, *Anal. Chem.*, 35 (1963) 1999.
24 Y. Tashiro, K. Kataoka and Y. Sakurai, *J. Colloid Interface Sci.*, 140 (1990) 66.
25 P. G. Righetti and T. Caravaggio, *J. Chromatogr.*, 127 (1976) 1.
26 A. Kato, T. Matsuta, N. Matsudomi and K. Kobayashi, *J. Agric. Food Chem.*, 32 (1984) 284.
27 B. W. Morrissey and R. R. Stromberg, *J. Colloid Interface Sci.*, 46 (1974) 152.
28 T. A. Horbett and J. L. Brash, in J. L. Brash and T. A. Horbett (Editors), *Proteins at Interfaces*, American Chemical Society, Washington, DC, 1987, p. 1.
29 A. White, P. Handler, E. L. Smith, R. L. Hill and I. R. Lehman, *Principles of Biochemistry*, McGraw-Hill, New York, 6th ed., 1978, p. 909.
30 K. Hamaguchi, in M. Funatsu, K. Hiromi, K. Imahori, T. Murachi and K. Narita (Editors), *Proteins*, Wiley, New York, 1972, Vol. 1, p. 116.
31 R. E. Dickerson and I. Geis, *The Structure and Action of Proteins*, Harper & Row, New York, 1969, p. 57.

*Journal of Chromatography*, 594 (1992) 335–340
Elsevier Science Publishers B.V., Amsterdam

CHROM. 23 811

# Separation of plant growth regulators by capillary electrophoresis

S. K. Yeo, H. K. Lee and S. F. Y. Li*

*Department of Chemistry, National University of Singapore, Kent Ridge 0511 (Singapore)*

(First received July 30th, 1991; revised manuscript received October 18th, 1991)

ABSTRACT

Capillary electrophoresis (CE) was used for the separation of nine plant growth regulators. Cyclodextrins and cholic acid were used as modifiers in the electrophoretic buffer to enhance selectivity. Satisfactory separation was obtained using a phosphate–borate buffer containing α-, β- and γ-cyclodextrin. The effects of pH and applied voltage on the migration behaviour in this system were studied.

## INTRODUCTION

Plant growth regulators have been intensively studied by techniques such as high-performance liquid chromatography (HPLC) [1], gas chromatography [2] and bioassay [3]. However, their separation and migration behaviour in capillary electrophoresis (CE) have not been investigated. CE has recently developed into a powerful analytical technique which offers highly efficient separation. Instead of employing columns packed with stationary phase materials as is typically done in HPLC, blank fused-silica tubing can be used as the separation column. Enhancement of selectivity can be obtained by the addition of modifiers to the elctrophoretic medium [4,5]. The pseudo-stationary phase formed in this way can be easily changed by simply flushing the column with a new electrophoretic medium. Various types of modifiers have been proposed for CE separations [4–6]. In this investigation, the use of cyclodextrins and cholic acid as modifiers in the capillary electrophoretic separation of plant growth regulators was investigated. In addition, the effects of pH and applied voltage on the separation efficiency of the nine plant growth regulators were studied.

## EXPERIMENTAL

The experiments were carried out on a laboratory-built CE system. A 30-kV laboratory-built power supply was used. A fused-silica capillary tube 50 cm effective length × 50 μm I.D. (Polymicro Technologies, Phoenix, AZ, USA) was used as the separation column. The peaks were detected using an on-column UV–VIS photodiode-array detector (Model SPDM6A, Shimadzu, Kyoto, Japan). The detector cell was modified according to the procedure described by Kobayashi *et al.* [7].

The nine plant growth regulators used were purchased from Sigma (St. Louis, MO, USA). Their structures and abbreviations are shown in Fig. 1. Other chemicals were obtained from Fluka (Buchs, Switzerland). The buffer solutions were prepared from sodium dihydrogenphosphate dihydrate and anhydrous sodium tetraborate. Hydrostatic injection was used. The samples were injected at a height 6 cm above the level of the reservoir and the injection time was 8 s.

## RESULTS AND DISCUSSION

Fig. 2 shows an electropherogram obtained when no modifiers were added. The migration times in-

0021-9673/92/$05.00 

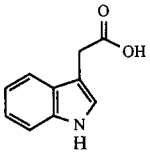

*Indole-3-acetic acid ( IAA)*

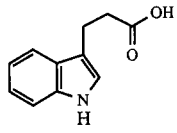

*Indole-3-propionic acid (IPA)*

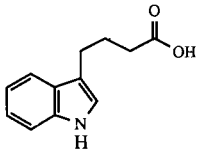

*Indole-3-butyric acid (IBA)*

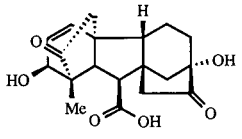

*Gibberellic Acid (GA)*

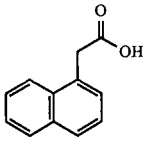

*Alpha-naphthaleneacetic acid (ANAA)*

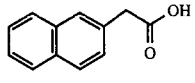

*Beta-naphthaleneacetic acid (BNAA)*

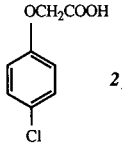

*p-chlorophenoxyacetic acid (PCPAA)*

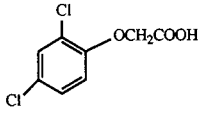

*2,4-dichlorophenoxyacetic acid (DCPAA)*

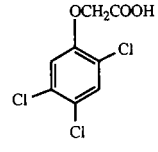

*2,4,5-trichlorophenoxyacetic acid (TCPAA)*

Fig. 1. Structures and abbreviations of plant growth regulators.

creased in the order GA < IBA < TCPAA < DCPAA, IPA < IAA, BNAA < ANAA < PCPAA.

In CE, separation is based on the differences in electrophoretic mobilities of the solutes in the presence of an electric field which is dependent on the size and charge of the solutes. In this investigation, the electroosmotic flow is towards the cathode, which is the low potential end. The direction of electrophoretic flow would depend on the charge of the solutes. For the positively charged solutes, both the electrophoretic and electroosmotic flows are in the same direction. However, for the negatively charged solutes, the electrophoretic and electroosmotic flows are in the opposite directions. Amongst the compounds investigated GA has the shortest migration time, mainly because it is the most hydrophilic among the nine plant growth regulators and its negative charge is least concentrated. Comparing the three indole acids, IBA is the first to migrate

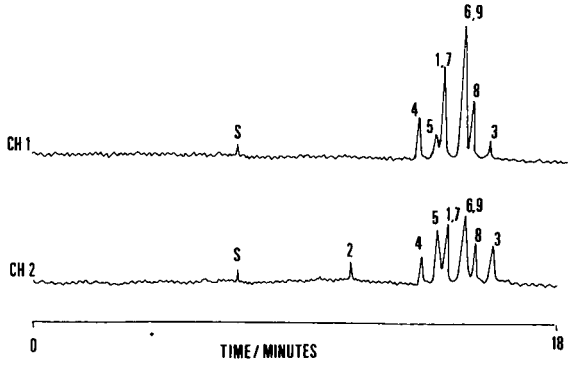


Fig. 2. Electropherogram of the nine plant growth regulators obtained with free solution capillary electrophoresis. S = methanol; 1 = DCPAA; 2 = GA; 3 = PCPAA; 4 = IBA; 5 = TCPAA; 6 = BNAA; 7 = IPA; 8 = ANAA; 9 = IAA. Electrophoretic conditions: 0.05 *M* phosphate–0.1 *M* borate buffer (pH 8.09); voltage, 15 kV; current, 36 μA; detection wavelength range, channel 1 220–230 nm, channel 2 196–210 nm; amount injected, 2 nl.

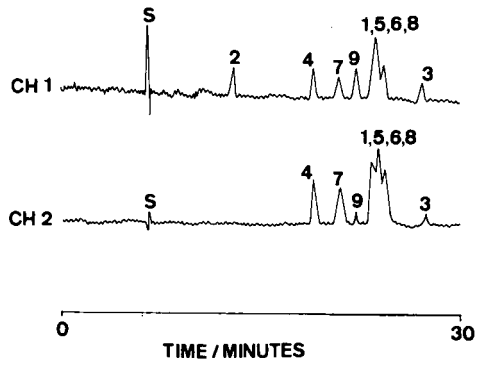


Fig. 3. Electropherogram obtained using cholic acid as modifier. S = methanol; 1 = DCPAA; 2 = GA; 3 = PCPAA; 4 = IBA; 5 = TCPAA; 6 = BNAA; 7 = IPA; 8 = ANAA; 9 = IAA. Electrophoretic conditions: 0.05 *M* phosphate–0.1 *M* borate buffer (pH 7.54)–20 m*M* cholic acid; voltage, 21 kV; current, 55 μA; detection wavelength range, channel 1 196–210 nm, channel 2 220–230 nm; amount injected, 2 nl.

out, followed by IPA and finally IAA. This could be explained by an increase in the chain length of the side-chain from acetic acid to butyric acid. An increase in chain length would lead to a decrease in the negative induction ($-I$) effect. Hence the negative charge on IAA is the most stable whereas that on IBA is the least stable. Among the three chlorophenoxyacetic acids, TCPAA has the shortest migration time followed by DCPAA and then PCPAA. This trend can be explained by the increase in the number of chloro substituents from PCPAA to TCPAA. As the number of chloro groups increased, the negative charge on the anion would be less concentrated. As TCPAA has the largest number of chloro groups, it would be expected to be the first to migrate out among the three. As BNAA is found to have a shorter migration time than ANAA, this would imply that it is either less negatively charged than ANAA or it is larger. By constructing the Stuart–Briegleb model, it is found that BNAA is indeed slightly larger than ANAA, hence it would be expected to have smaller electrophoretic mobility, resulting in a shorter migration time.

Bile salts have previously been used as modifiers in the CE separation of corticosteroids [6]. With cholic acid, compounds that are more hydrophobic would be expected to interact more with cholic acid micelles, thus leading to an increase in migration time for the more hydrophobic compounds. Hence cholic acid was investigated as a pseudo-stationary phase for the separation of plant growth regulators. The electropherogram for the plant growth regulators using cholic acid is shown in Fig. 3. In the presence of cholic acid micelles, it was observed that the less hydrophobic compounds such as the indole acids and GA migrated out faster than the more hydrophobic compounds such as the naphthaleneacetic and phenoxyacetic acids. However, DCPAA, TCPAA, BNAA and ANAA were not well resolved.

The presence of modifiers such as cyclodextrins resulted in a change in migration order and separation efficiency. This is due to the fact that the relative stabilities of cyclodextrin inclusion compounds are governed by various factors such as hydrogen bonding, Van der Waals interaction, solvation power and the ability of the molecule to fill the cavity [8,9].

Typical electropherograms obtained using cyclodextrins as modifiers are shown in Fig. 4. In the presence of α-cylodextrin as modifier (see Fig. 4a), the migration times increased in the order DCPAA < GA, PCPAA < IBA < TCPAA, IPA < BNAA, ANAA < IAA. By using the Stuart–Briegleb atomic model, one can deduce that

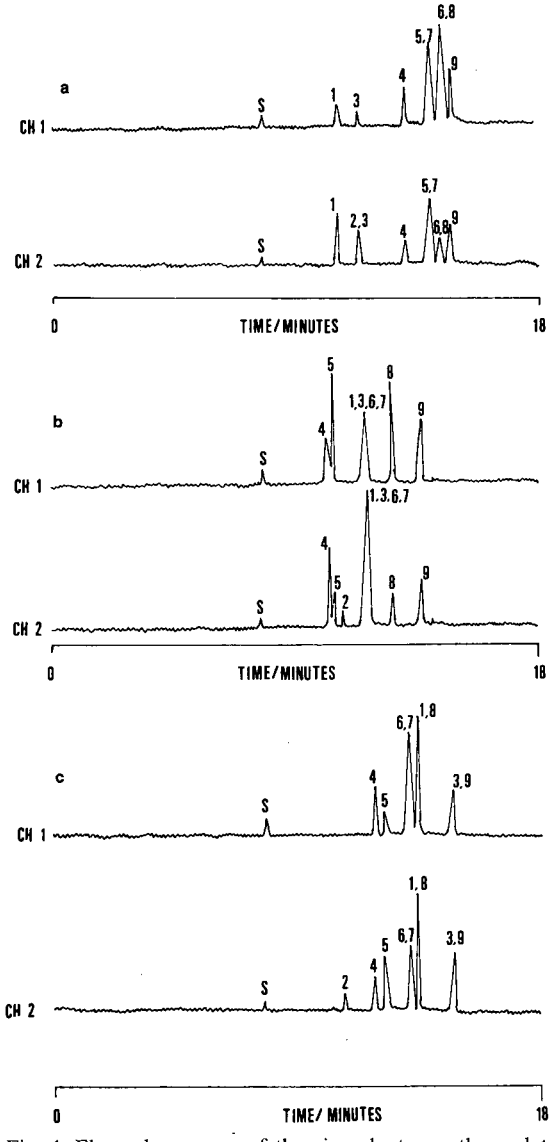


Fig. 4. Elecropherograms of the nine plant growth regulators obtained under the following electrophoretic conditions: (a) 0.05 *M* phosphate–0.1 *M* borate buffer (pH 8.09)–10 m*M* α-cyclodextrin; (b) 0.05 *M* phosphate–0.1 *M* borate buffer (pH 8.09)–10 m*M* β-cyclodextrin; (c) 0.05 *M* phosphate–0.1 *M* borate buffer (pH 8.09)–10 m*M* γ-cyclodextrin. S = methanol; 1 = DCPAA; 2 = GA; 3 = PCPAA; 4 = IBA; 5 = TCPAA; 6 = BNAA; 7 = IPA; 8 = ANAA; 9 = IAA. Voltage, 15 kV; current, 36 μA; wavelength range, channel 1 220–230– nm, channel 2 196–210 nm; amount injected, 2 nl.

DCPAA, PCPAA, TCPAA, GA, IBA and IPA cannot fit into the cavity of α-cyclodextrin completely. Solutes that can enter the cavity of α-cyclodextrin are found to have relatively longer migration times than those which are unable to enter the cavity. This observation leads one to conclude that, despite the fact that an increase in size would normally result in a decrease in electrophoretic mobility, thus resulting in a decrease in migration time [10], the bulky cyclodextrin structure results in it having a smaller overall mobility compared with the unsolubilized solutes which are much smaller. When only β-cyclodextrin was used, the migration order was (see Fig. 4b) IBA < TCPAA < GA < DCPAA, PCPAA, IPA, BNAA < ANAA < IAA. When γ-cyclodextrin was utilized, the migration order again altered (see Fig. 4c), to GA < IBA < TCPAA < BNAA, IPA < DCPAA, ANAA < PCPAA < IAA.

As the use of the three different cyclodextrins gives rise to different migration orders, a decision was made to incorporate all three cyclodextrins in order to obtain optimum conditions for the separation. The optimum conditions were obtained by the use of the overlapping resolution mapping procedure (ORM), which is a commonly used systematic optimization technique for HPLC [11–15]. Modification of the ORM procedure for use in the optimization of CE separations has been described [15]. The electropherogram for the optimum separation is shown in Fig. 5. After the optimum conditions had been obtained, the effects of applied

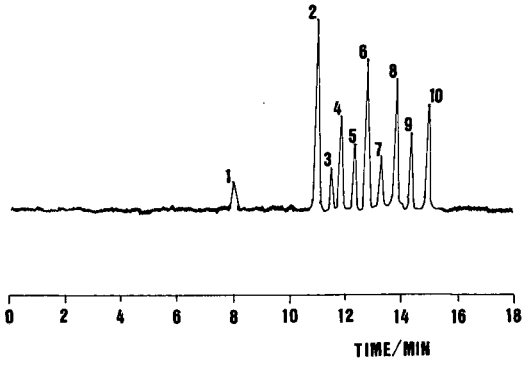


Fig. 5. Electropherogram of the nine plant growth regulators obtained under optimum conditions. S = methanol; 1 = DCPAA; 2 = GA; 3 = PCPAA; 4 = IBA; 5 = TCPAA; 6 = BNAA; 7 = IPA, 8 = ANAA; 9 = IAA. Electrophoretic conditions: 0.05 *M* phosphate–0.1 *M* borate buffer (pH 7.54)–7.5 m*M* α-cyclodextrin–1.5 m*M* β-cyclodextrin–1.0 m*M* γ-cyclodextrin; voltage, 15 kV; current, 35 μA; detection wavelength range, 196–210 nm; amount injected, 2 nl.

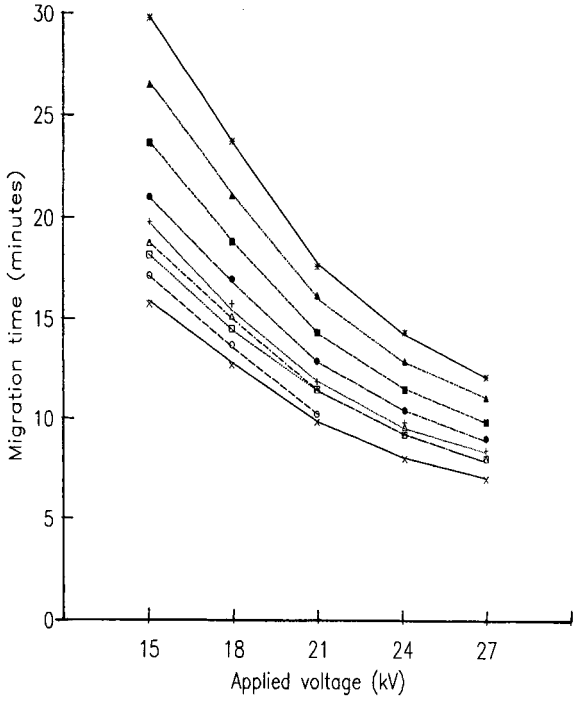


Fig. 6 Plot of migration time (min) against voltage (kV). × = DCPAA; ○ = GA; □ = PCPAA; △ = IBA; + = TCPAA; ● = BNAA; ■ = IPA; ▲ = ANAA; * = IAA.

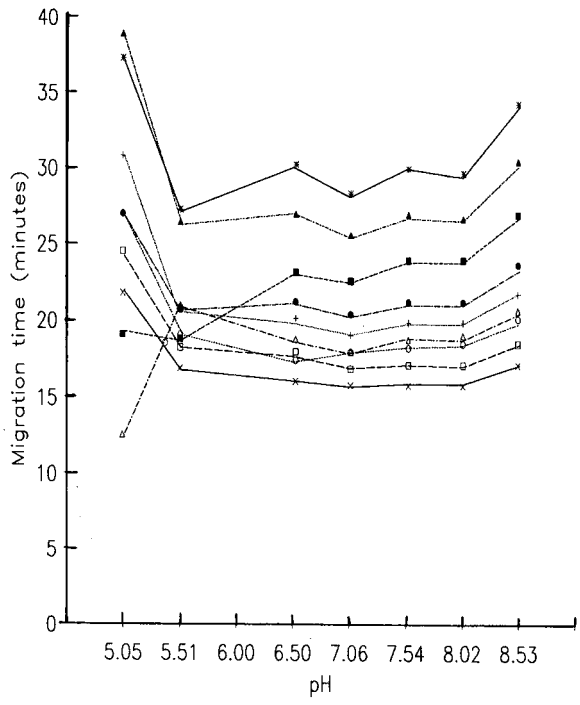


Fig. 7. Plot of migration time (min) against pH. Symbols as in Fig. 6.

voltage and pH on the separation efficiency were investigated.

Fig. 6 shows that as the applied voltage increased, the migration time decreased. This is to be expected, as the electroosmotic flow increased with increasing voltage. However, gibberellic acid was not detected at all at voltages higher than 24 kV. A possible explanation could be that it decomposes at high voltage owing to larger amounts of Joule heating.

Fig. 7 shows in general that the migration times tend to increase with increase in pH from pH 7.06 to 8.53. However, there is a general decrease in migration time from pH 5.05 to 7.06. This could be explained by an increase in electroosmotic flow when there is an increase in pH. The increase in migration time at higher pH (>7.50) could be explained by the dissociation of the acid group in the plant growth regulators resulting in the production of anions, thus increasing the migration time. At pH 4.47 (results not shown), the migration times for all the samples were found to be more than 2 h, because at low pH, the ionization of the surface silanol groups is suppressed and the electroosmotic flow approaches zero [16]. For IBA, an increase in migration time from pH 5.05 to 5.51 was observed. This could be due to fact the $pK_a$ of IBA is more than 5.05, hence it dissociates above pH 5.05, resulting in an increase in migration time.

A point to note is that the migration times obtained when the effects of pH and applied voltage were studied were longer than those obtained in the earlier part of the experiment. This is probably due to the fact the latter were investigated at a much later stage of the experiment and the increase in migration times could be due either to adsorption of a compound on the capillary wall or to the depletion of hydroxyl groups on the wall. In this instance, it is probably due to the depletion of the hydroxyl groups which resulted in the wall being less negatively charged. Consequently, a decrease in the electroosmotic flow and hence an increase in

migration times are observed. It is unlikely that the plant growth regulators are adsorbed on the wall as they would be negatively charged under the pH conditions used, which means that they would be repelled from the wall instead. Nevertheless, it was found that the migration order remained the same, so the discrepancy was not investigated further.

The use of a photodiode-array detector enables one to detect the solutes at more than one wavelength. For example, the ratio of peak heights observed at two different wavelengths was used to confirm the identity of the peaks. With reference to Figs. 2–4, it can be observed that GA was only detected in the wavelength range 196–210 nm. Further, the two naphthaleneacetic acids were found to absorb more strongly at 220–230 nm whereas the chlorophenoxyacetic acids absorb more strongly at 196–210 nm. The indole acids absorb almost identically in both wavelength ranges. Thus, by comparing the ratios of the peaks at different wavelengths and the migration times in an electropherogram, the identity of the peaks could be determined quickly and accurately.

In conclusion, CE separation of plant growth regulators can be achieved by using an electrophoretic medium containing cyclodextrins as modifier. The migration order changes with the type of cyclodextrins used and the size of their cavities. Optimum separation could be achieved when an electrophoretic medium containing $\alpha$-, $\beta$- and $\gamma$-cyclodextrin was used. The migration behaviour of the compounds in such an electrophoretic medium at different voltages and pH was studied. The general trends in the migration times could be related to the expected changes in electroosmotic flow.

ACKNOWLEDGEMENTS

The authors express their gratitude to the National University of Singapore for financial assistance and to Dr. S. C. Ng for helpful discussions.

REFERENCES

1 G. Sandberg, A. Crozier, A. Ernstsen, B. Sundberg, in H. F. Linskins and G. F. Jackson (Editors), *Modern Methods in Plant Analysis*, Vol. 5, 1987, pp. 52–71.
2 F. Hensen, A. Ernstsen and G. Sandberg, *Plant Growth Regul.*, 4 (1986) 55.
3 E. W. Weiler, J. Eberle, R. Mertens, T. Atzorn, M. Feyerabend, P. S. Jourdan, A. Arnscheidt and U. Weizorek, in T. L. Wang (Editor), *Immunology in Plant Sciences (Society for Experimental Biology Seminar Series*, No. 29), Cambridge University Press, Cambridge, 1986, pp. 27–58.
4 S. A. Sweedberg, *J. Chromatogr.*, 503 (1990) 449.
5 S. Terabe and T. Isemura, *Anal. Chem.*, 62 (1990) 650.
6 H. Nishi, T. Fukuyama, M. Matsuo and S. Terabe, *J. Chromatogr.*, 498 (1990) 313.
7 S. Kobayashi, T. Ueda and M. Kikumoto, *J. Chromatogr.*, 480 (1989) 179.
8 J. Snopek, I. Jelínek and E. Smolková-Keulemansová, *J. Chromatogr.*, 452 (1988) 571.
9 S. Fanali, *J. Chromatogr.*, 474 (1989) 441.
10 S. Terabe, H. Ozaki, K. Otsuka and T. Ando, *J. Chromatogr.*, 332 (1985) 211.
11 L. R. Snyder, *J. Chromatogr. Sci.*, 16 (1983) 223.
12 J. L. Glajch, J. J. Kirkland and L. R. Snyder, *J. Chromatogr.*, 238 (1982) 269.
13 C. P. Ong, H. K. Lee and S. F. Y. Li, *J. Chromatogr.*, 464 (1989) 405.
14 M. R. Khan, C. P. Ong, S. F. Y. Li and H. K. Lee, *J. Chromatogr.*, 513 (1990) 360.
15 S. K. Yeo, C. P. Ong and S. F. Y. Li, *Anal. Chem.*, 63 (1991) 2222.
16 W. J. Lambert and D. L. Middleton, *Anal Chem.*, 62 (1990) 1585.

*Journal of Chromatography*, 594 (1992) 341–349
Elsevier Science Publishers B.V., Amsterdam

CHROM. 23 870

# Finite difference modelling of continuous-flow electrophoresis

Terese M. Grateful and Edwin N. Lightfoot, Jr.*

*Department of Chemical Engineering, University of Wisconsin-Madison, 1415 Johnson Drive, Madison, WI 53706 (USA)*

(First received July 23rd, 1991; revised manuscript received November 12th, 1991)

ABSTRACT

A numerical scheme is used to describe the operation of isothermal continuous-flow electrophoresis. The model used accounts for the effects of diffusion, electroosmosis, and nonuniformities in convection, without the limitations on experimental parameter ranges imposed by previous solutions. Results from the numerical scheme are verified by comparison with these limiting case solutions. The flexibility of the numerical scheme provides a basic framework for the description of continuous-flow electrophoresis.

## INTRODUCTION

Along with the growth of biotechnology comes an ever increasing need for separation methods for analytical, preparative and production scale separations. Although electrophoresis has widespread application as an analytical separative tool, its potential as a production scale separation method has not been realized. Limitations imposed by complex convective heat and mass transfer processes and the lack of reliable descriptions for these processes have hindered development in even the most promising equipment in current use.

Continuous-flow electrophoresis (CFE) [1] is an attractive method for the scale-up of electrophoresis, but even it has yet to be described in enough detail and in a manner encompassing a sufficiently broad range of operating conditions to serve as a basis for process design. This deficiency exists, not because of a lack of effort in this area, but instead because previous work has primarily focused on limiting ranges of operating conditions. Although the solutions from these prior efforts do provide useful insight into the operation of CFE under limiting conditions, as indicated in the review in the next section, there is a need for a more general approach.

It now appears necessary to use a numerical description for the CFE process which not only agrees with the limiting case solutions, but also provides a solution where these asymptotic solutions are inadequate. We begin this process here, using a modified form of the method of Biscans *et al.* [2] to explore the analyses for isothermal operation. Thermal effects, as well as concentration effects, are of secondary importance in many applications, and we defer consideration of these to a later effort.

## THEORY

For this development, we will focus on the CFE apparatus represented schematically in Fig. 1. The apparatus consists of a rectangular flow chamber with chamber dimensions such that $L \gg w \gg 2d$. Carrier electrolyte flows in the axial ($x$-) direction, and an electric field is imposed across the width of the chamber, perpendicular to the electrolyte flow. The faces of the chamber at $y = \pm d$ are usually cooled. The sample is introduced into the chamber at the upstream end, and the trajectory of each sample component is determined by the vector sum of the species-dependent motion (electrophoresis) and the nonselective fluid motion (axial buffer flow and electroosmotic flow). Spatial variations exist in

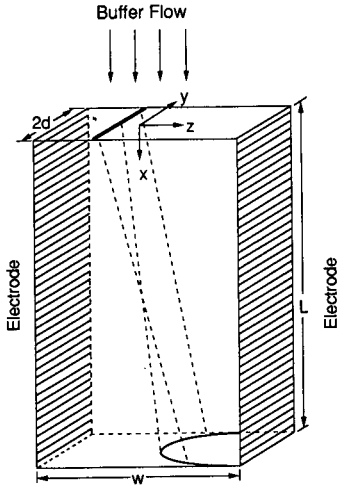


Fig. 1. Continuous-flow electrophoresis apparatus. Narrow lines indicate solute trajectories for the limiting case of zero solute diffusivity.

both components of the nonselective fluid motion, and it is this position-dependent velocity which contributes greatly to the dispersion in this system and also complicates its description.

We limit our discussion at this time to the case of isothermal operation. We also limit this discussion to the case where the concentrations of the species to be separated are sufficiently low that electrokinetic effects [3] and electrohydrodynamic spreading [4] are of secondary importance.

Assuming constant properties, we can use the following form of the continuity equation:

$$v_x\frac{\partial c_i}{\partial x} + v_{z,i}\frac{\partial c_i}{\partial z} = D_{\text{im}}\left(\frac{\partial^2 c_i}{\partial x^2} + \frac{\partial^2 c_i}{\partial y^2} + \frac{\partial^2 c_i}{\partial z^2}\right) \tag{1}$$

where $D_{\text{im}}$ is the effective binary diffusivity of component $i$ in the buffer medium, $v_x$ is the $x$-component of the buffer velocity and $v_{z,i}$ is the sum of the electrophoretic velocity of species $i$ ($v_{\text{ef},i}$) and the $z$-component of the buffer flow caused by electroosmosis ($v_z$). The terms $v_x$ and $v_{z,i}$ can be expressed as

$$v_x = v_0[1 - (y/d)^2] \tag{2}$$

and

$$v_{z,i} = v_{\text{ef},i} + v_z = v_{\text{ef},i} + v_{\text{eo}}\left\{1 - \frac{3}{2}[1 - (y/d)^2]\right\} \tag{3}$$

where $v_0$ is the maximum axial velocity and $v_{\text{eo}}$ is the electroosmotic velocity. Positive valves of $v_{\text{ef},i}$ and $v_{\text{eo}}$ indicate movement in the positive $z$-direction.

The boundary conditions for eqn. 1 are

(a) $c_i = 0$ $\quad z = \pm\infty$

(b) $\partial c_i/\partial y = 0$ $\quad y = 0, \pm d$

(c) $c_i = c_{i,0}\delta(z)$ $\quad x = 0$

(d) $c_i \to 0$ $\quad x \to \infty$

where $c_{i,0}$ is the mass input per unit area and $\delta(z)$ is a unit impulse function defined by $\delta(z) = 0$, $z \neq 0$ and $\int_{-\infty}^{\infty} \delta(z)\mathrm{d}z = 1$.

We can rewrite eqns. 1–3 in terms of dimensionless parameters as

$$v_x^*\frac{\partial c_i^*}{\partial x^*} + v_{z,i}^*\frac{\partial c_i^*}{\partial z^*} = Pe_0^{-1}\left(\frac{\partial^2 c_i^*}{\partial x^{*2}} + \frac{\partial^2 c_i^*}{\partial y^{*2}} + \frac{\partial^2 c_i^*}{\partial z^{*2}}\right) \tag{4}$$

$$v_x^* = [1 - (y^*)^2] \tag{5}$$

$$v_{z,i}^* = \frac{v_{\text{ef},i}}{v_0} + \frac{v_{\text{eo}}}{v_0}\left\{1 - \frac{3}{2}[1 - (y^*)^2]\right\} \tag{6}$$

where: $x^* = x/d$; $y^* = y/d$; $z^* = z/d$; $c_i^* = c_i d/c_{i,0}$ and $Pe_0 = v_0 d/D_{\text{im}}$. The boundary conditions become:

(a) $c_i^* = 0$ $\quad z^* = \pm\infty$

(b) $\partial c_i^*/\partial y^* = 0$ $\quad y^* = 0, \pm 1$

(c) $c_i^* = \delta(z^*)$ $\quad x^* = 0$

(d) $c_i^* \to 0$ $\quad x^* \to \infty$.

Two quantities of potential interest can be defined: the average concentration, $c_{i,\text{avg}}^*$, where

$$c_{i,\text{avg}}^* = \frac{\int_{-1}^{1} c_i^*(L/d, y^*, z^*)\mathrm{d}y^*}{\int_{-\infty}^{\infty}\int_{-1}^{1} c_i^*(L/d, y^*, z^*)\mathrm{d}y^*\mathrm{d}z^*} \tag{7}$$

and the bulk, or flow-averaged, concentration, $c_{i,\text{b}}^*$, where

$$c_{i,\text{b}}^* = \frac{\int_{-1}^{1} c_i^*(L/d, y^*, z^*)v_x^*\mathrm{d}y^*}{\int_{-\infty}^{\infty}\int_{-1}^{1} c_i^*(L/d, y^*, z^*)v_x^*\mathrm{d}y^*\mathrm{d}z^*} \tag{8}$$

From these expressions for $c_{i,\text{avg}}^*$ or $c_{i,\text{b}}^*$ and eqns.

4–6, we can see that the interactions of the experimental parameters can be summarized in terms of the following dimensionless groups: $L/d$; $Pe_0$; $v_{ef,i}/v_0$; $v_{eo}/v_0$.

Analytic solutions to eqns. 4–6 can be obtained using various simplifying assumptions, but these solutions are only valid for specific limiting cases. We review these solutions below.

*Previous work*

*Strickler and Sacks [5].* Strickler and Sacks examined the limiting case where the effects of diffusion can be neglected, and the solute profiles are strictly a result of the hydrodynamics. The angle of the deflection of a solute molecule in the chamber is determined by the ratio $v_{z,i}/v_x$, where

$$\frac{v_{z,i}}{v_x} = \frac{v_{ef,i} + v_{eo}\left\{1 - \frac{3}{2}[1 - (y/d)^2]\right\}}{v_0[1 - (y/d)^2]} = \left(\frac{v_{ef,i}}{v_0}\right)\left[\frac{1 + k_i}{1 - (y/d)^2} - \frac{3}{2}k_i\right] \quad (9)$$

and $k_i = v_{eo}/v_{ef,i}$. The result of the $y$-dependence shown in eqn. 9 is called the "crescent effect", for the crescent-shaped solute profile seen in CFE experiments. We can see from eqn. 9 that, in order to minimize the dispersion for a desired product, the electroosmotic velocity $v_{eo}$ should be equal and opposite to the electrophoretic velocity $v_{ef,i}$ of the desired product. Satisfying this condition eliminates the $y$-dependence of the migration angle for that solute and consequently eliminates the crescent-shaped profile.

*Ivory [6].* Ivory incorporated the effects of diffusion in both the $x$- and $z$-directions, but neglected diffusion in the $y$-direction. This assumption was justified as a reasonable assumption as long as the mean diffusional displacement in the $y$-direction ($\lambda_y$) is much smaller than the half-thickness ($d$). This criterion was written as

$$\frac{\lambda_y}{d} \approx \frac{(2D_{im}t)^{1/2}}{d} \approx \left[\frac{L/d}{Pe(y)}\right]^{1/2} \ll 1 \quad (10)$$

where $Pe(y) = Pe_0 v_x^*(y^*)$ and $t \approx L/v_x$ is the solute residence time.

The solution to eqn. 4 when the diffusion in the $y$-direction is neglected is

$$c_i^* = \left(\frac{\gamma x^*}{\sqrt{2\pi}}\right)\frac{K_1[\gamma(x^{*2} + z^{*2})^{1/2}]}{(x^{*2} + z^{*2})^{1/2}} \cdot \exp\left[\frac{Pe_0}{2}(x^* v_x^* + z^* v_{z,i}^*)\right] \quad (11)$$

where

$$\gamma^2 = Pe_0^2(v_x^{*2} + v_{z,i}^{*2})/4$$

$K_1(\cdot)$ is the modified Bessel function of the second kind of order one. Eqn. 11 can be numerically integrated to get $c_{i,avg}^*$ or $c_{i,b}^*$.

*Reis et al. [7].* Reis *et al.* did consider diffusion in the $y$-direction, but they used the approximation based on the Gill and Sankarasubramanian [8] extension of Taylor's method [9] for describing convective dispersion. This solution is valid for large values of $(L/d)/Pe_0$, such that the system residence time is sufficiently long that an asymptotic state is approached in which diffusion in the $y$-direction exactly balances the disturbance caused by the nonuniform axial velocity.

The solution, which is valid only for the special case when electroosmotic flows are not present ($v_{eo} = 0$), is

$$c_{i,b}^* = \frac{1}{6\pi}\int_0^\infty \frac{\exp\left[-\left(\frac{\zeta^2}{4\tau} + \frac{L_1^2}{4\xi}\right)\right]}{\sqrt{\xi\tau}}\,d\tau \quad (12)$$

where

$$\zeta = (z - v_{ef,i}t)/d$$

$$\tau = tD_{im}/d^2$$

$$L_1 = \frac{(L - \langle v_x \rangle t)}{dPe_0}$$

$$\langle v_x \rangle = \frac{1}{2d}\int_{-d}^{d} v_x\,dy$$

$$\xi = \int_0^\tau k_2(\theta)\,d\theta$$

$$k_2 = \left(\frac{1}{Pe_0}\right)^2 + \frac{8}{945} - \frac{8}{\pi^6}\sum_{n=1}^{\infty}\frac{\exp[-(n\pi)^2\theta]}{n^6}$$

In order to get the expression in eqn. 12, the

assumption was made that the ratio $\alpha \approx 1$, where $\alpha$ was defined as

$$\alpha = \frac{<c_i v_x>}{<c_i> <v_x>} \tag{13}$$

where $<\cdot> = \int_{-1}^{1} \cdot \, dy^*$. This ratio allows the conversion between the average concentration and the bulk concentration.

*Biscans et al. [2].* Biscans *et al.* proposed neglecting only axial diffusion as truly unimportant relative to axial convection. Eqn. 4 can then be written as

$$v_x^* \frac{\partial c_i^*}{\partial x^*} + v_{z,i}^* \frac{\partial c_i^*}{\partial z^*} = Pe_0^{-1}\left(\frac{\partial^2 c_i^*}{\partial y^{*2}} + \frac{\partial^2 c_i^*}{\partial z^{*2}}\right) \tag{14}$$

Finite difference methods were used to solve the equation on a plane of constant $x^*$ for grid points in $y^*$ and $z^*$ using an iterative procedure. The $x^*$-coordinate was then incremented, and the solution was determined on that $y^*$–$z^*$ plane. The boundary conditions used were

(a) $c_i^* = 0 \qquad z^* = z_0^*, z_f^*$

(b) $c_i^* = 0 \qquad y^* = \pm 1$

The boundary condition at $x^* = 0$ was not explicitly expressed in the article but was described as a squared input occupying 20–30% of the cell. Boundary condition (b) limits the validity of the solution to the case where the sample is introduced to only a small portion of the cell (in the $y^*$-direction) and the sample residence time is sufficiently short. This criterion can be expressed as

$$\left(\frac{\Delta_y}{d}\right)^2 \gg 3\left(\frac{L/d}{Pe_0}\right) \tag{15}$$

where $\Delta_y$ is the shortest distance between the sample input and the walls at $y^* = \pm 1$.

*Present work*

The solutions listed above are all limited in applicability to specific parameter ranges. The solution described by Ivory [6] is only applicable when $(L/d)/Pe_0$ is small, while that of Reis *et al.* [7] is valid for large $(L/d)/Pe_0$. The method used by Biscans *et al.* [2] is limited to both reasonably small $(L/d)/Pe_0$ and small input sample dimensions as given in eqn. 15.

Our goal is a solution capable of covering the entire parameter space of practical interest. We use for this purpose an approach similar to that of Biscans *et al.* [2], neglecting only axial diffusion as truly unimportant relative to axial convection. Our scheme differs from that of Biscans primarily in two ways. We have used a more general boundary condition in the $y^*$-direction, so our scheme is not restricted by the limitation expressed in eqn. 15. Also, we do not use an interative numerical solution, but rather a modified version of an alternating direction implicit scheme, proposed by Peaceman and Rachford [10], to find the numerical solution to eqn. 14.

For this approach, we can rewrite eqn. 14 in the form [11]

$$\frac{\partial c_i^*}{\partial x^*} = A_1 c_i^* + A_2 c_i^* \tag{16}$$

where $A_1$ and $A_2$ are linear operators, defined as

$$A_1 c_i^* = (Pe_0 v_x^*)^{-1} \frac{\partial^2 c_i^*}{\partial z^{*2}} - \frac{v_{z,i}^*}{v_x^*} \frac{\partial c_i^*}{\partial z^*} \tag{17}$$

$$A_2 c_i^* = (Pe_0 v_x^*)^{-1} \frac{\partial^2 c_i^*}{\partial y^{*2}} \tag{18}$$

The following two-step scheme is then used to get an approximation to eqn. 16:

$$(1 - \frac{\Delta x^*}{2} A_{1h}) \tilde{C}^{j+1/2}(m,n) = (1 + \frac{\Delta x^*}{2} A_{2h}) C^j(m,n) \tag{19}$$

$$(1 - \frac{\Delta x^*}{2} A_{2h}) C^{j+1}(m,n) = (1 + \frac{\Delta x^*}{2} A_{1h}) \tilde{C}^{j+1/2}(m,n) \tag{20}$$

where $C^j(m,n)$ and $C^{j+1}(m,n)$ are approximations of $c_i^*(x_j^*, y_m^*, z_n^*)$ and $c_i^*(x_{j+1}^*, y_m^*, z_n^*)$, respectively, and $\tilde{C}^{j+1/2}(m,n)$ is an intermediate variable. The terms $A_{1h}$ and $A_{2h}$ are the second-order finite difference approximations for $A_1$ and $A_2$, respectively, given by

$$A_{1h}C^j(m,n) = (Pe_0 v_x^*)^{-1}\left[\frac{C^j(m,n+1)-2C^j(m,n)+C^j(m,n-1)}{(\Delta z^*)^2}\right] - \frac{v_{z,i}^*}{v_x^*}\left[\frac{C^j(m,n+1)-C^j(m,n-1)}{2\Delta z^*}\right] \quad (21)$$

$$A_{2h}C^j(m,n) = (Pe_0 v_x^*)^{-1}\left(\frac{C^j(m+1,n)-2C^j(m,n)+C^j(m-1,n)}{(\Delta y^*)^2}\right) \quad (22)$$

The following finite difference boundary conditions are used:

(a) $C^j(m,0) = C^j(m,N) = 0$

(b) $-3C^j(0,n) + 4C^j(1,n) - C^j(2,n) = 0$

(c) $-3C^j(M,n) + 4C^j(M-1,n) - C^j(M-2,n) = 0$

with the "initial" condition

(d) $C^j(m,n) = 1, \quad x^* = 0, -1 \leqslant y^* \leqslant 1, z^* = 0$

which approximates the delta function mass type input used in the solutions of Ivory and Reis. The $y^*$ range for the finite difference scheme is given by $y_0^* \leqslant y_m^* \leqslant y_M^*$ where $y_0^* = -1$ and $y_M^* = 1$. The range for $z^*$ is $z_0^* \leqslant z_n^* \leqslant z_N^*$ where the boundaries at $z_0^*$ and $z_N^*$ are set such that these boundaries do not significantly impact the solution. This choice allows us to use the "infinite boundary" condition (a). Boundary conditions (b) and (c) are second-order, one-sided approximations for boundary conditions (b) in eqn. 4.

The requirement for the solution of this numerical scheme to show the correct convective-dispersive character is a limit on the step size in $z^*$ [11]:

$$\Delta z^* \leqslant \frac{2}{Pe_0}\left(\frac{v_0}{v_{z,i}}\right) \quad (23)$$

This condition does, however, place a lower limit on the time it takes to determine the solution by imposing a rather large minimum size for the matrix of concentrations.

## RESULTS

As shown earlier, the experimental parameters necessary to determine either $c_{i,\text{avg}}^*$ or $c_{i,b}^*$ can be summarized in terms of the following dimensionless groups: $L/d$; $Pe_0$; $v_{\text{ef},i}/v_0$; $v_{\text{eo}}/v_0$. Table I contains a summary of several recently reported experiments using the CFE apparatus. We have used the data provided in these references to obtain approximate useful ranges for the important dimensionless groups, and these ranges are reported in Table II. It is in terms of these four dimensionless parameters that we base our discussion.

For the numerical scheme to be generally applicable, it is necessary that the numerical solution approach the asymptotic solutions developed by Ivory [6] and by Reis *et al.* [7] under the limiting conditions of low and high values of $(L/d)/Pe_0$, respectively, as well as show realistic behavior between these two limits.

In an effort to verify this behavior, a series of computer simulations was performed. Figs. 2–5 compare the bulk concentrations as a function of chamber position calculated using the solutions of Ivory, Reis and the finite difference scheme presented in the previous section. The experimental parameters used in the simulations were: $Pe_0 = 2 \cdot 10^4$; $v_{\text{ef},i}/v_0 = 2.5 \cdot 10^{-3}$; $v_{\text{eo}}/v_0 = 0$. For these simulations only the dimensionless length of the chamber $(L/d)$ was varied, with $L/d = 2 \cdot 10^2$, $5 \cdot 10^3$, $1 \cdot 10^4$ and $2 \cdot 10^4$. For these values of $L/d$, the value of $(L/d)/Pe_0$ ranges from 0.01–1.0.

In Fig. 2, $(L/d)/Pe_0 = 0.01$, and we can see that the finite difference solution matches the solution of Ivory almost exactly. At this low value of $(L/d)/Pe_0$, the concentration profile seen is primarily a function of hydrodynamics, giving a purely "convective peak" which agrees with the development of Ivory.

In Fig. 3, $(L/d)/Pe_0 = 0.25$, and the convective solution no longer suffices. The hint of a double peak is now apparent, with the dispersive type solution predicted by Reis appearing as a shoulder on the convective peak. In Fig. 4, with $(L/d)/Pe_0 = 0.5$, the situation is reversed, with the convective peak now a shoulder on the dispersive peak. In Fig. 5, $(L/d)/Pe_0 = 1.0$, and the peak closely approximates the dispersive solution of Reis; the convective peak is no longer present. The difference between the concentrations predicted by the finite difference solution and the solution of Reis is due primarily to the error introduced into the Reis *et al.* solution by the assumption stated in eqn. 13 (*i.e.* $\alpha \approx 1.0$).

TABLE I

EXPERIMENTAL DATA

| Apparatus | Dimensions (cm) | | | Solutes | Residence time (min) | Ref. |
|---|---|---|---|---|---|---|
| | $L$ | $w$ | $2d$ | | | |
| ACE 710[a] | 20 | NA[b] | 0.08 | Erythrocytes | NA | [12] |
| | 18 | 4 | 0.03 | Cells | 0.5 | [13] |
| CFE system[c] | 120 | 6 | 0.15 | Cytochrome *c*, myoglobin, β-lactoglobulin, ovalbumin | 4 | [14] |
| | 120 | 8.2 | 0.18 | Granules containing growth hormone | 10.4 | [15] |
| VaP 21[d] | 25 | 10 | 0.05 | Liposomes | 1.5 | [16] |
| | | | 0.07 | Chromosomes | 2.1 | [17] |
| VaP 22[d] | 50 | 10 | 0.05 | Alcohol dehydrogenase in yeast extract | 5–20 | [18] |
| | | | | Alcohol dehydrogenase in yeast extract | 2.5–10 | [19] |
| | | | | Lysosyme in *E. coli* extract | 7.8–14.7 | [20] |
| | | | | Hemoglobin | 11.4 | [21] |
| | | | | α-amylase from *E. coli* extract | 5 | [22] |
| | | | | Myoglobin, catalase, thyroglobulin | 5 | [23] |
| | | | | Formaldehyde dehydrogenase, formate dehydrogenase, methanol oxidase | 5 | [24] |
| | | | | Endosomes, lysosomes | 3.3 | [25] |
| VaP 220[d] | 100 | 16 | 0.05 | Formaldehyde dehydrogenase, formate dehydrogenase, methanol oxidase | 3.3 | [24] |
| Lab models | 100 | 15 | 0.05 | Alcohol dehydrogenase in yeast extract | 5 | [18] |
| | 30 | 4 | 0.3 | Hemoglobin, cytochrome *c*, bovine serum albumin | 4 | [26] |

[a] Hirschmann (Munich, FRG).
[b] Not available.
[c] McDonnell Douglas (St. Louis, MO, USA).
[d] Bender & Hobein (Munich, FRG).

TABLE II

EXPERIMENTAL PARAMETER RANGES

| Parameter | Approximate range |
|---|---|
| $L/d$ | 200–4000 |
| $Pe_0$[a] | $10^3$–$10^5$ |
| $\left\|\frac{v_{ef}}{v_0}\right\|$[b], $\left\|\frac{v_{eo}}{v_0}\right\|$[c] | $10^{-3}$–$10^{-1}$ |

[a] Using estimates of solution properties.
[b] Estimated from concentration profiles given in references.
[c] Generally the same order of magnitude as $(v_{ef}/v_0)$.

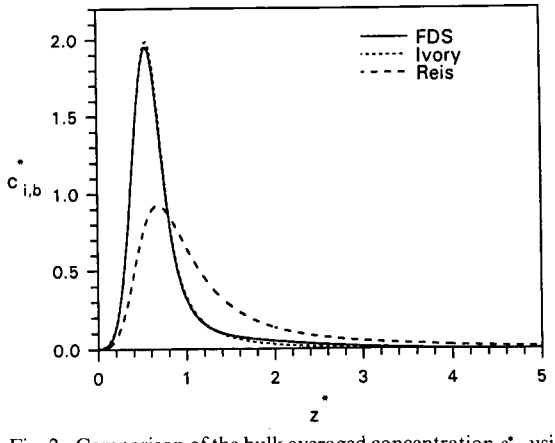


Fig. 2. Comparison of the bulk averaged concentration $c^*_{i,b}$ using the solution of Ivory, Reis *et al.* and the finite difference solution of the present work (FDS). $L/d = 2.0 \cdot 10^2$, $Pe_0 = 2 \cdot 10^4$, $v_{ef}/v_0 = 2.5 \cdot 10^{-3}$, $v_{eo}/v_0 = 0.0$.

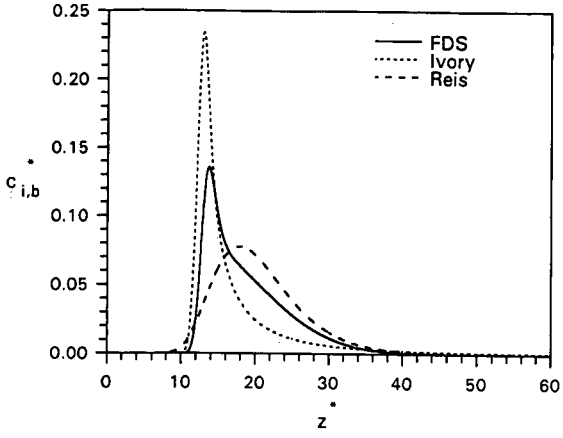


Fig. 3. Comparison of the bulk averaged concentration $c^*_{i,b}$ using the solution of Ivory, Reis *et al.* and the finite difference solution of the present work (FDS). $L/d = 5 \cdot 10^3$, $Pe_0 = 2 \cdot 10^4$, $v_{ef}/v_0 = 2.5 \cdot 10^{-3}$, $v_{eo}/v_0 = 0.0$.

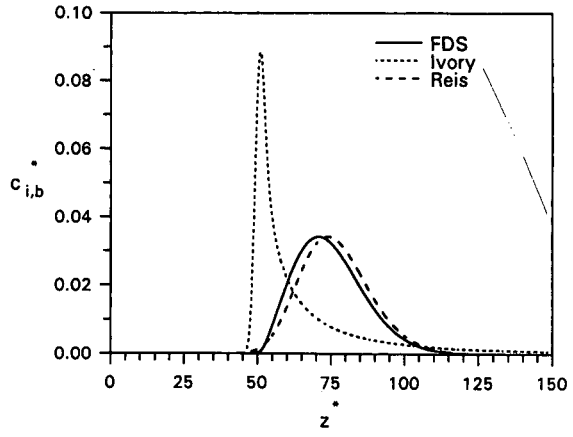


Fig. 4. Comparison of the bulk averaged concentration $c^*_{i,b}$ using the solution of Ivory, Reis *et al.* and the finite difference solution of the present work (FDS). $L/d = 1 \cdot 10^4$, $Pe_0 = 2 \cdot 10^4$, $v_{ef}/v_0 = 2.5 \cdot 10^{-3}$, $v_{eo}/v_0 = 0.0$.

Fig. 6 shows the progression of the concentration profile, calculated using the finite difference solution, from the convective result to the dispersive result. The experimental parameters are the same as in Figs. 2–5, with $L/d$ ranging from $2 \cdot 10^3$–$2 \cdot 10^4$. At low values of $(L/d)/Pe_0$, we see the steep, long-tailed peak of the convective solution. At large values of $(L/d)/Pe_0$, the effect of diffusion in the $y$-direction becomes important because the solute residence time is sufficiently long that the solute molecules are able to sample the entire $y$-range, leading to a Gaussian shaped peak. At the intermediate values of $(L/d)/Pe_0$, it appears that both peaks are present. The "double peak" seem is similar to that sometimes seen in chromatography [27] and in other mathematically similar systems [28].

It is important to note that the preceding profiles were calculated using the condition of no electroosmosis ($v_{eo} = 0$). However, under normal experimental conditions, electroosmosis does occur, and it is thus important to be able to include its effects in

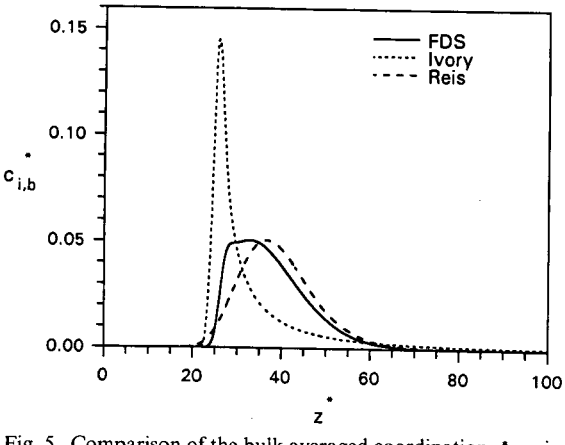


Fig. 5. Comparison of the bulk averaged coordination $c^*_{i,b}$ using the solution of Ivory, Reis *et al.* and the finite difference solution of the present work (FDS). $L/d = 2 \cdot 10^4$, $Pe_0 = 2 \cdot 10^4$, $v_{ef}/v_0 = 2.5 \cdot 10^{-3}$, $v_{eo}/v_0 = 0.0$.

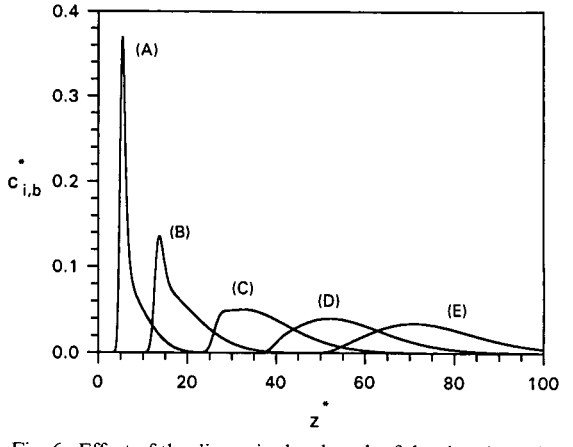


Fig. 6. Effect of the dimensionless length of the chamber $L/d$ on the bulk averaged concentration $c^*_{i,b}$ using the finite difference solution of the present work. $Pe_0 = 2 \cdot 10^4$, $v_{ef}/v_0 = 2.5 \cdot 10^{-3}$, $v_{eo}/v_0 = 0.0$. Curves are for $L/d = 2 \cdot 10^3$ (A), $5 \cdot 10^3$ (B), $1 \cdot 10^4$ (C), $1.5 \cdot 10^4$ (D), $2 \cdot 10^4$ (E).

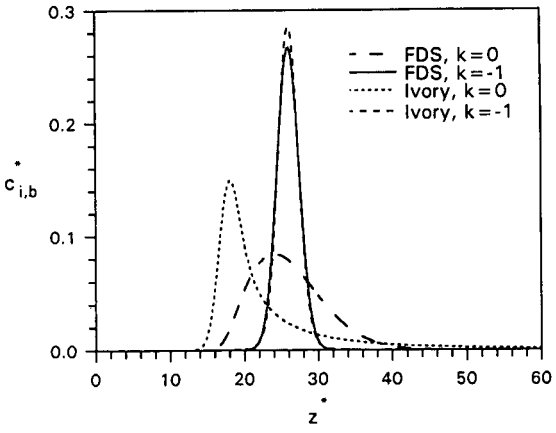


Fig. 7. Comparison of the effect of electroosmotic flow on the bulk averaged concentration $c^*_{i,b}$ using the solution of Ivory and the finite difference solution of the present work (FDS) for $v_{eo}/v_0 = 0.0$ and $v_{eo}/v_0 = -8.67 \cdot 10^{-3}$. $L/d = 2 \cdot 10^3$, $Pe_0 = 2.63 \cdot 10^3$, $v_{ef}/v_0 = 8.67 \cdot 10^{-3}$.

any description of the system. As was noted, the solution proposed by Reis *et al.* does not include the effect of electroosmosis. In Fig. 7 we show the results of a comparison between the solution of Ivory and the finite difference scheme for the conditions: $Pe_0 = 2.63 \cdot 10^3$, $v_{ef,i}/v_0 = 8.67 \cdot 10^{-3}$ and $L/d = 2 \cdot 10^3$. We compare the solutions obtained for both $v_{eo}/v_0 = 0$ and $v_{eo}/v_0 = -8.67 \cdot 10^{-3}$, corresponding to $k_i = v_{eo}/v_{ef,i} = 0, -1$. As was predicted by the expression derived by Strickler and Sacks, dispersion is minimized as the value of the electrophoretic velocity approaches a value equal and opposite to the electroosmotic velocity ($v_{eo} \rightarrow -v_{ef,i}$).

It is interesting to note in Fig. 7 that, while the solution provided by eqn. 11 does not give the correct concentration profile for $v_{eo}/v_{ef,i} = 0$, it is indeed valid for $v_{eo}/v_{ef,i} = -1$, independent of the value of $(L/d)/Pe_0$. Diffusion in the $y$-direction ceases to be important in the calculation of the final solute profile when the trajectory is independent of the $y$-position.

## DISCUSSION

We have verified that the results from the finite diffeence solution match those of the asymptotic solutions for the limiting cases. This fact, and the observation that the solution behaves as expected over the transition from the convection-dominated to the dispersion-dominated regime, verify that the use of the finite difference approximation does not introduce any significant error into the solution, and affirm our confidence in the applicability of the finite difference scheme to the entire range of the parameter space.

Although the solutions of Reis *et al.* and Ivory are analytical and thus much less time-consuming to evaluate, their use must be limited to conditions under which their assumptions hold. The use of the inappropiate model will give an error not only in the peak location, but in the peak shape as well.

The finite difference solution proposed by the present work can be easily modified to incorporate nonuniform, nonrectangular sample inputs and nonisothermal conditions, as well as alternate velocity profiles. Our scheme provides the basic framework for the description of the operation of CFE over currently useful conditions.

The intent of the present work is to show the utility of a numerical description for the system given; therefore, no optimization of the numerical method or computer code was performed. It is useful to note, however, that for a sample run such as that seen in the finite difference results shown in Fig. 7, the code took 9.5 cpu hours to execute on a VAXstation 3100 (Digital Equipment Corporation, Maynard, MA, USA). This simulation was composed of 1000 steps in $x$ and a matrix of $y$, $z$ values that was 40 × 1750. It is the stiffness of the differential equation (see eqn. 23) which requires a large number of matrix elements to accurately described the system.

## SYMBOLS

| | |
|---|---|
| $A_1, A_2$ | linear operators |
| $A_{1h}, A_{2h}$ | second order approximations to $A_1, A_2$ |
| $c_i$ | concentration of species $i$ |
| $<c_i>$ | concentration averaged with respect to $y$ |
| $c_i^*$ | dimensionless concentration |
| $c_{i,avg}$ | average concentration |
| $c^*_{i,b}$ | bulk, or flow-averaged, concentration |
| $c_{i,0}$ | mass input per unit area |
| $d$ | half-thickness of the chamber |
| $D_{im}$ | effective binary diffusivity of species $i$ |
| $k_i$ | $v_{eo}/v_{ef,i}$ |
| $L$ | length of the electrode region |

| | |
|---|---|
| $Pe_0$ | $v_0 d/D_{im}$ |
| $t$ | time |
| $v_0$ | maximum axial velocity in the chamber |
| $v_{ef,i}$ | electrophoretic velocity of species $i$ |
| $v_{eo}$ | electroosmotic velocity |
| $v_x$ | axial or $x$-component of the buffer velocity |
| $<v_x>$ | axial velocity averaged with respect to $y$ |
| $v_x^*$, $v_{z,i}^*$ | dimensionless velocities |
| $v_{z,i}$ | sum of $v_{ef,i}$ and $v_z$ |
| $w$ | width of the chamber |
| $x$, $y$, $z$ | rectangular coordinates |
| $x^*$, $y^*$, $z^*$ | dimensionless coordinates |
| $\Delta x^*$, $\Delta y^*$, $\Delta z^*$ | step sizes for $x^*$, $y^*$, $z^*$ |
| $\alpha$ | $<c_i v_x>/(<c_i> <v_x>)$ |
| $\delta(z)$ | unit impulse function |
| $\lambda_y$ | mean diffusional displacement in the $y$-direction |

## REFERENCES


1 K. Hannig, in J. R. Norris and D. W. Ribbons (Editors), *Methods in Microbiology 5B*, Academic Press, London, 1971, Ch. VIII, p. 513.
2 B. Biscans, P. Alinat, J. Bertrand and V. Sanchez, *Electrophoresis (Weinheim, Fed. Repub. Ger.)*, 9 (1988) 84.
3 M. Bier, O. A. Palusinski, R. A. Mosher and D. A. Saville, *Science (Washington, DC)*, 219 (1983) 1281.
4 P. H. Rhodes, R. S. Snyder and G. O. Roberts, *J. Colloid Interface Sci.*, 129 (1989) 78.
5 A. Strickler and T. Sacks, *Ann. N.Y. Acad. Sci.*, 209 (1973) 497.
6 C. F. Ivory, *J. Chromatogr.*, 195 (1980) 165.
7 J. Reis, E. N. Lightfoot and H. Lee, *AIChE J.*, 20 (1974) 362.
8 W. N. Gill and R. Sankarasubramanian, *Proc. R. Soc. London, A.*, 316 (1970) 341.
9 G. I. Taylor, *Proc. R. Soc. London, A*, 219 (1953) 186.
10 D. W. Peaceman and H. H. Rachford, Jr., *J. Soc. Ind. Appl. Math.*, 3 (1955) 28.
11 J. C. Strikwerda, *Finite Difference Schemes and Partial Differential Equations*, Wadsworth and Brooks/Cole Advanced Books and Software, Pacific Grove, California, 1989.
12 K. Hannig, M. Kowalski, G. Klöck, U. Zimmermann and V. Mang, *Electrophoresis (Weinheim, Fed. Repub. Ger.)*, 11 (1990) 600.
13 J. Bauer, *J. Chromatogr.*, 418 (1987) 359.
14 K. A. Knisley and L. S. Rodkey, *Electrophoresis (Weinheim, Fed. Repub. Ger.)*, 11 (1990) 927.
15 D. Hayes, C. Exton, T. Salada, K. Shellenberger, J. Waddle and W. C. Hymer, *Electrophoresis (Weinheim, Fed. Repub. Ger.)*, 11 (1990) 976.
16 R. Kessler and H. Manz, *Electrophoresis (Weinheim, Fed. Repub. Ger.)*, 11 (1990) 979.
17 F. F. Bier, U. Bettag, T. Rheingans, H. Adrian, J. Barths, M. Hausmann, H. Bühring, P. Rohwer, J. Dölle and C. Cremer, *Electrophoresis (Weinheim, Fed. Repub. Ger.)*, 10 (1989) 690.
18 S. Hoffstetter-Kuhn and H. Wagner, *Electrophoresis (Weinheim, Fed. Repub. Ger.)*, 11 (1990) 451.
19 S. Hoffstetter-Kuhn, R. Kuhn and H. Wagner, *Electrophoresis (Weinheim, Fed. Repub. Ger.)*, 11 (1990) 304.
20 R. Kuhn and H. Wagner, *J. Chromatogr.*, 481 (1989) 343.
21 R. A. Mosher, D. Dewey, W. Thormann, D. A. Saville and M. Bier, *Anal. Chem.*, 61 (1989) 362.
22 R. Kuhn and H. Wagner, *Electrophoresis (Weinheim, Fed. Repub. Ger.)*, 10 (1989) 165.
23 S. Nath, H. Schütte, H. Hustedt and W. Deckwer, *Electrophoresis (Weinheim, Fed. Repub. Ger.)*, 11 (1990) 612.
24 S. Nath, H. Schütte, G. Weber, H. Hustedt and W. Deckwer, *Electrophoresis (Weinheim, Fed. Repub. Ger.)*, 11 (1990) 937.
25 M. Marsh, in A. M. Tartakoff (Editor), *Methods in Cell Biology, Vol. 31, Vesicular Transport, Part A*, Academic Press, New York, 1989, Ch. 17, p. 319.
26 M. J. Clifton, N. Jouve, H. de Balmann and V. Sanchez, *Electrophoresis (Weinheim, Fed. Repub. Ger.)*, 11 (1990) 913.
27 S. G. Weber and P. W. Carr, in P. R. Brown and R. A. Hartwick (Editors), *High Performance Liquid Chromatography*, Wiley, New York, 1989, p. 1.
28 A. M. Lenhoff and E. N. Lightfoot, *Chem. Eng. Sci.*, 41 (1986) 2795.

*Journal of Chromatography*, 594 (1992) 351–359
Elsevier Science Publishers B.V., Amsterdam

CHROM. 23 834

# Continuous-flow electrophoresis: a separation criterion applied to the separation of model proteins

H. Roux-de Balmann* and V. Sanchez

*Laboratoire de Génie Chimique et Electrochimie, LGC CNRS URA 192, Université Paul Sabatier, 118 route de Narbonne, 31062 Toulouse Cedex (France)*

(First received July 16th, 1991; revised manuscript received October 8th, 1991)

ABSTRACT

The resolution of continuous-flow electrophoretic separations is determined by the relative importance of the migration of the products and of the widening of the corresponding peaks, both of which depend on the operating conditions and on the chamber geometry. This paper provides a separation criterion that gives a relationship between these two parameters that should be obeyed for the products to be recovered pure at the outlet of the chamber. From previous theoretical work this criterion is expressed as a function of all the operating conditions and of the chamber geometry. The theoretical calculations are first compared with experimental results for single protein samples. Both the theoretical and experimental results are found to be in good agreement in terms of migration and of peak width. The separation criterion is then further used for some model proteins in order to predict the conditions under which a complete separation could be achieved. Again, the experimental results for the separation of different proteins show that the conditions under which a total separation is achieved are very close to those expected from the calculations.

## INTRODUCTION

Continuous-flow electrophoresis is a process that enables any products, such as proteins or cells, to be purified. This process has undergone considerable development owing to the possibility of converting electrophoresis, which is a high-resolution separation method, from an analytical to a preparative scale. The separation is carried out in a thin-film flow of carrier buffer, into which the sample containing the species to be separated is continuously fed. Using an electric field in a direction perpendicular to that flow, the charged particles move as a combination of two main velocities, the carrier buffer flow velocity and the electrophoretic migration velocity. Particles having different electrophoretic mobilities should therefore have different trajectories inside the chamber. Using a fraction collector at the outlet of the separation chamber, one can then recover the separated fractions.

Unfortunately, the first trials dealing with the use of continuous-flow electrophoresis to purify biological products were very disappointing. The resolution was found to be very poor compared with that which was expected from extrapolating the results obtained on an analytical scale. Among other results, it was observed that increasing the operating conditions, *e.g.*, the electric field or the residence of the products inside the electrophoretic chamber, does not necessarily lead to an improved separation. Consequently, many theoretical studies have been undertaken in order to investigate the different phenomena involved in that process, which could be responsible for the observed results. Such studies have dealt either with hydrodynamic and thermal problems [1–3] of with transport phenomena [4–8].

Very few experimental results have been published recently compared with the large amount of theoretical work that has been done in the last few years. Most of them have dealt with the separation of cell suspensions [9–11] or latex particles [12,13] and only few have concerned the purification of protein samples [6,14]. Moreover, usually it is very difficult to interpret or compare the results owing to

0021-9673/92/$05.00 

a lack of information concerning the products investigated and the electrophoretic apparatus used.

In this work we were interested in searching for the optimum operating conditions for the purification of protein samples. Starting from previous work on hydrodynamic or dispersive effects involved in continuous-flow electrophoresis, we define a separation criterion that gives a relationship between all the relevant parameters to be fulfilled for a total separation to be achieved.

An experimental study was performed with two chambers and three different protein samples, the electrophoretic mobilities of which were chosen to be increasingly closer. In a first step single protein samples were investigated in order to compare the experimental results with those obtained from theoretical calculations. In a second step, separation experiments were performed and the results were compared with those predicted by using the resolution criterion.

## EXPERIMENTAL

### *Electrophoretic apparatus*

The electrophoresis apparatus used for the experimental study was designed and constructed in-house. The electrophoretic chamber is a rectangular channel between two polycarbonate plates. Two electrode compartments are located on each side of the chamber and are separated from it by ion-exchange membranes. At the outlet of the chamber, a collection port allows the flow to be divided into different fractions, collecting it every 1 mm along the chamber width. A multi-channel peristaltic pump located at the outlet of the separation chamber ensures the circulation of the carrier buffer fluid. The difference in flow-rate between the fractions does not exceed 3%. The sample containing the species to be separated is continuously fed at the top of the chamber through a needle, the diameter of which is about 1 mm, using a peristaltic pump. A power supply is used to apply a voltage between the two electrodes, thus creating an electric field in a direction perpendicular to the carrier buffer flow.

Two different chambers were used: chamber A, 600 mm long, 60 mm wide and 1.5 mm thick, and chamber B, 300 mm long, 40 mm wide and 3 mm thick.

A cooling system was used during the experimental runs to remove the heat dissipated by Joule heating in order to reduce the temperature gradients inside the chamber, which would otherwise give rise to convection and disturb the flows. To do that, the walls of the electrophoretic chamber were refrigerated by a cooling fluid, in order to keep the average temperature constant along the length of the cell. On the other hand, the electrode buffer was refrigerated in order to remove the heat dissipated in the region near the membranes, where the conductivity of the fluid was higher than that in the middle of the chamber, thus allowing the temperature gradients along the width of the chamber to be minimized. Some temperature sensors incorporated in the circuits allowed the efficiency of the thermal regulation to be controlled. For each set of operating conditions the temperatures of the cooling fluids were adjusted so as to maintain constant the temperature everywhere inside the chamber within $\pm 0.5$°C.

### *Fluids*

The buffer used as the carrier fluid and electrode buffer was a Tris–borate buffer with an electrical conductivity of 140 $\mu$S cm$^{-1}$. Different values pH in the range 6.5–8.5 were used.

The protein solutions were prepared by dissolving in the carrier buffer lyophilized products, purchased from Sigma. The proteins used were bovine haemoglobin (Hb), bovine serum albumin (BSA) and $\alpha$-lactalbumin.

### *Analytical methods*

The experimental results were obtained by measuring the protein concentrations in the different fractions collected at the collection port. For samples containing only one kind of protein, the concentration was obtained by absorbance measurements (406 nm for the haemoglobin samples and 280 nm for the other proteins). In the separation experiments, the concentrations of the different proteins were obtained by gel permeation chromatography using a TSK G3000 SW column with Tris–borate buffer (pH 6.5) as the eluent at a flow-rate of 0.5 ml min$^{-1}$.

## THEORETICAL APPROACH

Let us consider, for instance, the case of a sample containing two kinds of proteins, A and B, the elec-

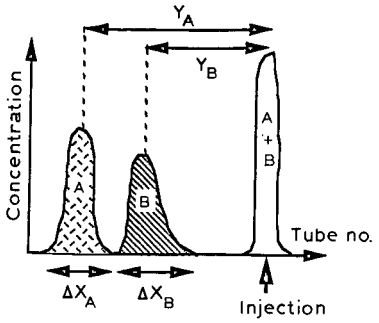


Fig. 1 Schematic representation of the separation of two proteins A and B.

trophoretic mobilities of which are $u_A$ and $u_B$, respectively. This is illustrated in Fig. 1, which shows the concentration profiles at the outlet of the chamber. After flowing through the separation chamber, the two proteins have migrated distances $Y_A$ and $Y_B$ from their positions in the injection plane. On the other hand, considering that the widths of the corresponding peaks are $\Delta X_A$ and $\Delta X_B$, respectively, one can define a "separation criterion" which gives the relationship between the values of $Y_i$ and $\Delta X_i$ to be fulfilled for the two proteins to be collected completely separated:

$$Y_A - Y_B > (\Delta X_A + \Delta X_B)/2 \qquad (1)$$

assuming that A is the more mobile species.

Some previous studies have considered the different transport phenomena involved in continuous-flow electrophoresis. From these studies one can define ranges of operating parameters in which one or the other of these phenomena becomes predominant. For this work, the operating conditions were chosen in order to minimize both free convection [2,3] and electrohydrodynamic effects [7]. This is discussed in further detail later. Under these conditions, the mass transport is then determined by a combination of the Poiseuille flow of the carrier buffer, electroosmosis and electrophoretic migration [4,8], so that one can write for the migration distance of one charged particle.

$$Y_i = E\tau[(u_i + u_{os})/(1 - z^2/d^2) - 3/2\, u_{os}] \qquad (2)$$

where $z$ represents the coordinate in the thickness of the chamber, $d$ the half-chamber thickness, $E$ the electric field, $\tau$ the average residence time inside the chamber and $u_{os}$ the electroosmotic mobility. Assuming that at the outlet of the chamber the maximum of the concentration profile corresponds to the proteins located in the centre plane of the chamber, *i.e.*, to the position $z = 0$, as it is in the injection plane, one obtains for the migration distance of the maximum of the peak the expression.

$$Y_i = E\tau(u_i - u_{os}/2) \qquad (3)$$

On the other hand, owing to the Poiseuille flow of the carrier buffer, the residence time varies along the thickness of the chamber so that the particles distributed over the section of the sample do not reach the same position. This gives rise to the so-called "crescent effect". The greatest distance will be covered by the particles located at the position $z = \pm R$, where $R$ is the radius of the sample stream. The width of the peak can therefore be written using the following expression:

$$\Delta X_i = [Y_i\,(z = \pm R) - Y_i\,(z = 0)] + 2R \qquad (4)$$

Combining eqns. 2 and 4, we have

$$\Delta X_i = \{E\tau \mid u_i + u_{os}|[1/(1 - R^2/d^2) - 1]\} + 2R \qquad (5)$$

Using eqn. 1 and combining with eqns. 3 and 5, one can rewrite the resolution criterion as

$$(u_A - u_B)E\tau > E\tau/2\{(|u_A + u_{os}| + |u_B + u_{os}|)\,[1/(1 - R^2/d^2) - 1]\} + 2R \qquad (6)$$

This relationship enables different regions to be distinguished depending on the values of $E\tau$, as illustrated in Fig. 2. The relative positions of the curves that represent the variations of the left- and right-hand sides of eqn. 6 determine whether or not a complete purification can be expected. The slope of the left-hand side of eqn. 6 depends only on the protein and on the pH of the buffer, as they both determine the value of the electrophoretic mobilities, whereas depending on the values of $R/d$ and of $|u_i + u_{os}|$ different curves can be obtained for the right-hand side of eqn. 6. For instance, in case (1), a

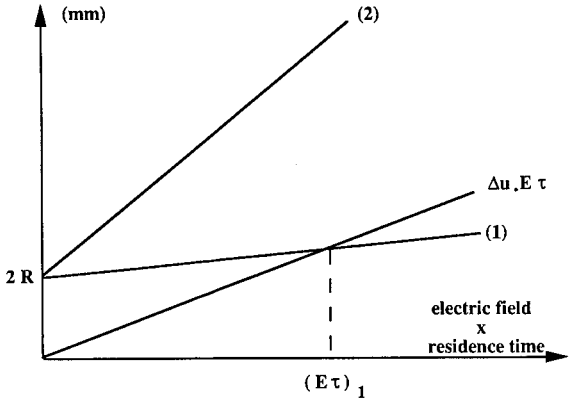


Fig. 2. Graphical interpretation of the separation criterion. (1) Right-hand side of eqn. 6 for $R/d = a1$; (2) right-hand side of eqn. 6 for $R/d = a2 > a1$.

complete separation of the two proteins should achieved for $E\tau$ values exceeding $(E\tau)_1$ whereas in case (2), which corresponds to a higher value of $R/d$, no purification is expected over the whole range of $E\tau$.

## RESULTS AND DISCUSSION

### *Electrophoresis of single protein samples*

In a first step, an experimental study was performed with single protein samples in order to determine the operating conditions to be used for further separation experiments.

Fig. 3 shows an example of results concerning the variation of the migration distance with $E\tau$. These variations are straight lines, the slope of which depends on the protein and on the pH of the carrier buffer. This linearity shows that for the operating conditions used, the influence of convective phenomena remains negligible. For a given protein, the curves obtained with the two chambers were found to be superimposed. These findings are in good agreement with eqn. 3. For each protein sample we then calculated the value of the "apparent" mobility, which is given by the slope fot the plot of the migration distance *versus* $E\tau$. The values obtained are reported in Table I for the three proteins and three pH values of the carrier buffer.

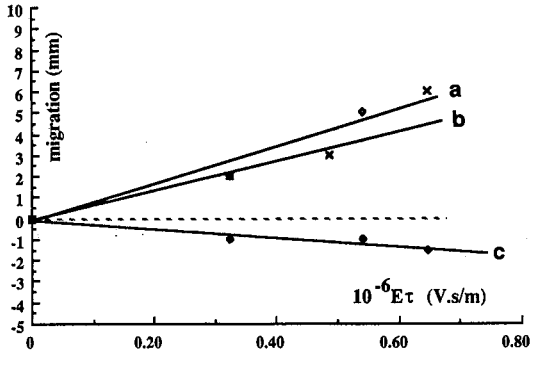


Fig. 3. Example of variation of the migration distance with $E\tau$. Operating conditions: Tris–borate buffer (pH 6.5); sample concentration, 0.3%. a = Albumin; b = α-lactalbumin; c = haemoglobin.

TABLE I

CALCULATED VALUES OF THE "APPARENT" MOBILITIES FOR VARIOUS pH VALUES OF THE TRIS–BORATE BUFFER ($\times 10^{-9}$ m$^2$ V$^{-1}$ s$^{-1}$)

| Protein | pH | | |
|---|---|---|---|
| | 6.5 | 8.0 | 8.5 |
| Haemoglobin | +2 | −9 | −9.6 |
| α-Lactalbumin | −8.6 | −13 | |
| Albumin | −9 | −16 | −19 |

To obtain the values of the electrophoretic mobilities of the proteins, one needs to know the value of the electroosmotic mobility. To obtain that value, we used a haemoglobin sample at pH 7, which is very close to its p*I* so that its electrophoretic mobility can be assumed to be zero. As a result, the slope

TABLE II

CALCULATED VALUES OF THE ELECTROPHORETIC MOBILITIES ($\times 10^{-9}$ m$^2$ V$^{-1}$ s$^{-1}$)

Electroosmotic mobility = $10.3 \cdot 10^{-9}$ m$^2$ V$^{-1}$ s$^{-1}$.

| Protein | pH | | |
|---|---|---|---|
| | 6.5 | 8.0 | 8.5 |
| Haemoglobin | +7.1 | −3.9 | −4.5 |
| α-Lactalbumin | −3.5 | −7.9 | |
| Albumin | −3.9 | −10.9 | −13.9 |

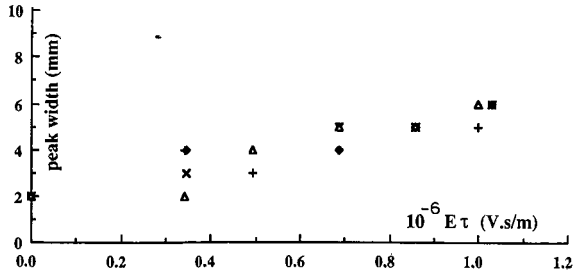


Fig. 4. Variation of the peak width with $E\tau$. Operating conditions: chamber B; Tris–borate buffer (pH 8.0); sample concentration, 0.3%; sample flow-rate = 1 ml $h^{-1}$. $E$ varied: × = BSA; ◆ = α-lactalbumine. $\tau$ varied: △ = BSA; + = α-lactalbumin.

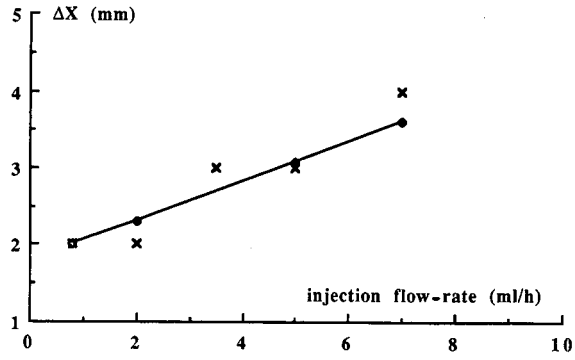


Fig. 5. Influence of sample flow-rate on the peak width: comparison between (×) experimental and (◆) calculated values. Operating conditions: chamber B; haemoglobin sample; Tris-borate buffer (pH 8.0); sample concentration, 0.3%; residence time, 120 s.

of the plot of $Y$ *versus* $E\tau$ provides the value of $u_{os}/2$ (see eqn. 3). In this way we obtained for the electroosmotic mobility a value of about $10.3 \cdot 10^{-9}$ $m^2$ $V^{-1}$ $s^{-1}$, which is very close so that which had been determined by another method in a previous study [6]. Assuming that it is constant in the pH range investigated, we then calculated for the different pH values the values of the electrophoretic mobilities of the three proteins, which are reported in Table II.

Fig. 4 shows the results concerning the peak widths that were obtained for different values of $E\tau$ with two kinds of proteins. The peak width increases as $E\tau$ increases and in the range of operating conditions investigated the points obtained by changing either the electric field or the residence time are located on a single straight line. These linear variations show that the influence of electrohydrodynamic phenomena is negligible compared with that of other transport phenomena, as the peak width should otherwise be proportional the square of the electric field [7]. This means that the assumptions that were made to write eqn. 5 are correct. From that equation another important parameter appears to be the value of $R/d$. Its influence has already been discussed in details from a theoretical point of view by many workers [4,6,8]. In a previous paper [15], we presented a visualization system that can provide a measurement of the dimensions of the sample stream inside the separation chamber. That system was used to determine the value of $R/d$ for different operating conditions.

Table III gives some values that were obtained with chamber B for different sample flow-rates. Using these values and those of the electrophoretic and elecroosmotic mobilities (see Table II), one can then calculate from eqn. 5 for a given value of $E\tau$ the variations of the peak width as a function of the injection flow-rate. Some calculated values are plotted in Fig. 5 together with the corresponding experimental values. There is good agreement between the calculated and experimental results.

Dealing with the influence of the chamber thickness, we have plotted in Fig. 6 the experimental results obtained with the two chambers for a given residence time and different electric field values. The width of the peaks is very sensitive to the thickness of the chamber, as halving the thickness makes the peaks about three times larger. Using the visualization device we obtained the values of $R/d$, which were found to be 0.9 for chamber A and 0.4 for chamber B under the operating conditions used during the experiments reported in Fig. 6. From these values we then calculated the peak width using eqn. 5 and the values were plotted in Fig. 6.

TABLE III

MEASUREMENTS OF THE VALUES OF $R/d$ FOR DIFFERENT SAMPLE FLOW-RATES

Operating conditions: chamber B; residence time, 120 s; sample, haemoglobin (0.6%).

| Injection flow-rate (ml $h^{-1}$) | 2 | 5 | 7 | 11 |
|---|---|---|---|---|
| $R/d$ | 0.4 | 0.6 | 0.65 | 0.73 |

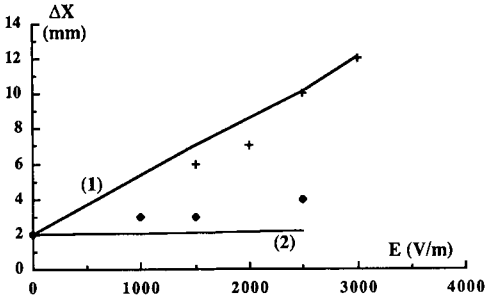


Fig. 6. Influence of chamber thickness on the variation of peak width with electric field: comparison between experimental and calculated values. Operating conditions: Tris–borate buffer (pH 8.0); BSA sample; sample concentration, 0.3%; injection flow-rate, 2 $ml^{-1}$; residence time, 220 s. Experimental: + = chamber A; ◆ = chamber B. Calculated: 1 = chamber A; 2 = chamber B.

These calculated values are very close to the experimental values.

The comparison of the widths of the peaks obtained for different proteins under given operating conditions also shows good agreement with eqn. 5, considering the influence of $|u_i + u_{os}|$. For instance, BSA and α-lactalbumin, the electrophoretic mobilities of which are very close to each other (see Table II), provide peaks having almost the same width (see Fig. 4), those obtained with Hb being wider. Finally, the influence of the pH was found to be much more sensitive with Hb, owing to a larger variation in its electrophoretic mobility.

*Separation of proteins*

The experimental results for single protein samples were found to be in good agreement with the theoretical considerations leading to eqn. 6. We therefore used that equation in order to determine the conditions for which a separation of two proteins was expected. This has already been discussed with respect to Fig. 2 in general.

Fig. 7 shows an example concerning the separation of Hb and BSA. With chamber A no total separation of the two proteins is to be expected under these operating conditions. In contrast, a total sep-

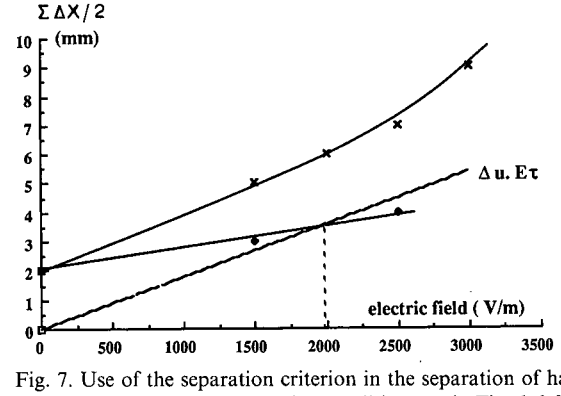


Fig. 7. Use of the separation criterion in the separation of haemoglobin and albumin. Operating conditions: as in Fig. 6; 0.3% of each protein. × = Chamber A; ◆ = chamber B.

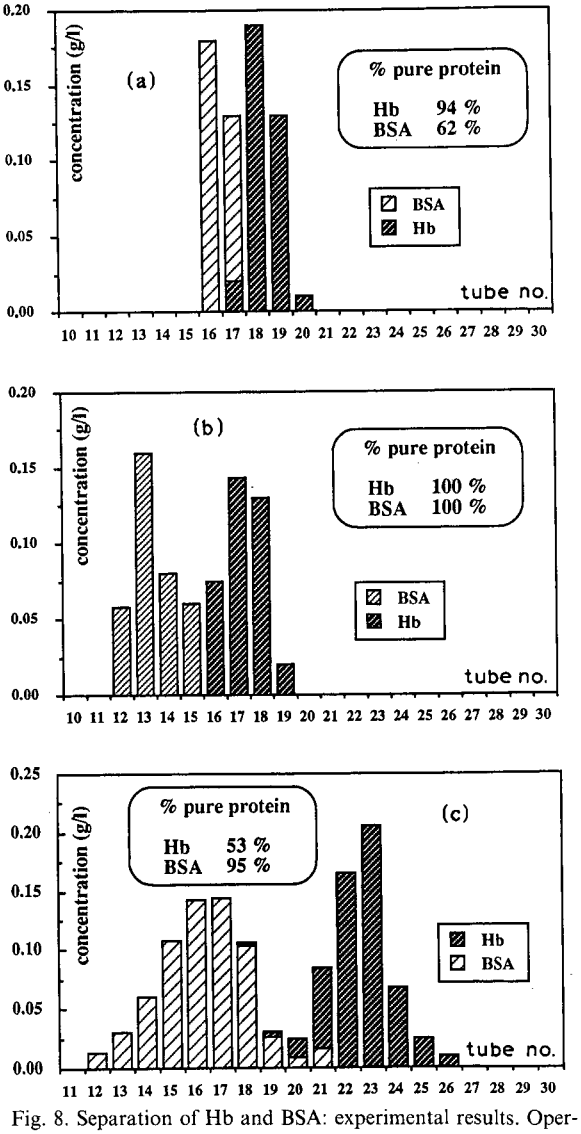


Fig. 8. Separation of Hb and BSA: experimental results. Operating conditions: as in Fig. 7. (a) Chamber B for $E$ = 1500 V $m^{-1}$; (b) chamber B for $E$ = 2500 V $m^{-1}$; (c) chamber A for $E$ = 3000 V $m^{-1}$.

aration is expected to be possible with chamber B as soon as the electric field exceeds a given value, in this instance *ca.* 2000 V $m^{-1}$. Fig. 8 shows the concentration profiles obtained under these conditions during separation experiments performed at different voltages. On the same plots we give for each protein the percentage purity, which is defined as

% of A =
= (amount of A recovered pure/total amount of A) · 100.

In this instance for a pH of 8.0 the difference in electrophoretic mobility between Hb and BSA is about $7 \cdot 10^{-9}$ $m^2$ $V^{-1}$ $s^{-1}$. Working with chamber B a total separation of the two proteins is obtained for 2500 V $m^{-1}$ whereas they are only partially separated at 1500 V $m^{-1}$. Working with chamber A only partial purification was obtained for electric fields up to 3000 V $m^{-1}$. These results are in very good agreement with those which were expected from Fig. 7.

Concerning the influence of the pH of the carrier buffer the difference in electrophoretic mobilities between Hb and BSA is about $11 \cdot 10^{-9}$ $m^2$ $V^{-1}$ $s^{-1}$ at pH 6.5 whereas it is only about $7 \cdot 10^{-9}$ $m^2$ $V^{-1}$ $s^{-1}$ at pH 8.0 (see Table III). Consequently, provided that there is no dispersive effect, the separation should be achieved more easily, *i.e.*, for lower voltages, at pH 6.5 than at pH 8.0. In Fig. 9 were plotted for the two pH values calculated variations of the left- and right-hand sides of inequality 6 *versus* the electric field strength. The value above which a separation is expected to be achieved is almost the same for the two pH values (*ca.* 2000 V $m^{-1}$). This is due to the fact that the variation in the difference in electrophoretic mobility is accompanied by a variation in the peak width, as discussed earlier. Again, the separation experiments have demonstrated that a total separation was obtained for the two pH values for an electric field above 2000 V $m^{-1}$.

As a total separation of Hb and BSA was achieved with the 3-mm thick chamber under low voltage operating conditions, we then investigated the separation of proteins with closer mobilities, such as BSA and α-lactalbumin (see Table II). The experiments were performed with chamber B at pH 8.0, where the difference in electrophoretic mobility between the two proteins is about $3 \cdot 10^{-9}$ $m^2$ $V^{-1}$ $s^{-1}$.

Fig. 10 shows the concentration profiles obtained for two values of the electrical field, the other operating parameters being kept constant. In addition, we have plotted in Fig. 11 the percentage purity *versus* the electric field strength. The percentage of

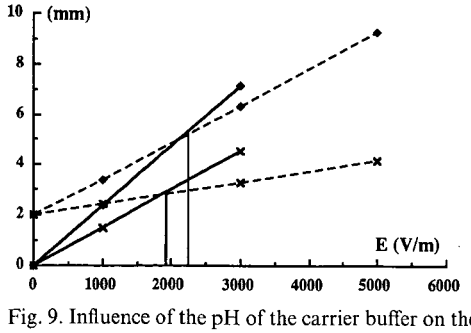


Fig. 9. Influence of the pH of the carrier buffer on the separation of Hb and BSA. Calculated variation of $\Delta Y$ (solid lines) and $\Delta X$ (dashed lines) with $E$. Operating conditions: chamber B; $R/d$ = 0.6; sample, BSA and Hb, 0.3% of each; injection flow-rate, 2 ml $h^{-1}$; residence time, 220 s. ◆ = pH 6.5; × = pH 8.0.

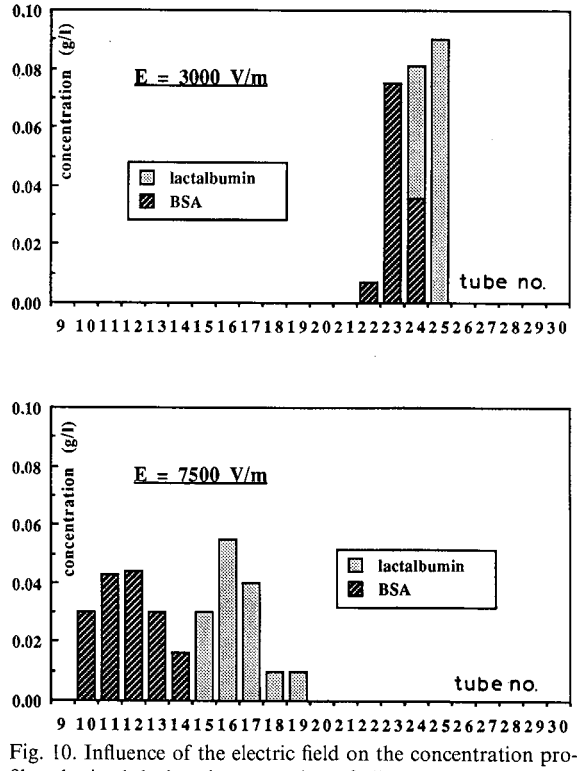


Fig. 10. Influence of the electric field on the concentration profiles obtained during the separation of albumin and α-lactalbumin. Operating conditions: chamber B; Tris–borate buffer (pH 8.0); sample concentration, 0.3% of each protein; injection flow-rate, 1 ml $h^{-1}$; residence time, 123 s.

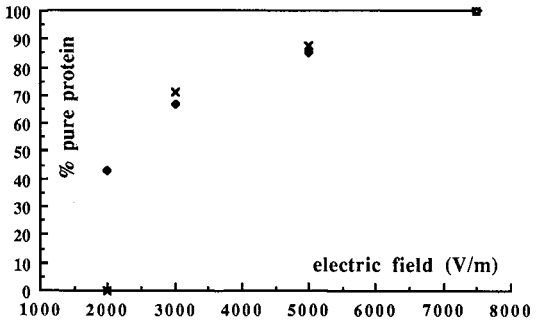


Fig. 11. Influence of electric field on the percentage of pure protein. Operating conditions: as in Fig. 10. × = BSA; ◆ = α-lactalbumin.

pure protein increases as the electric field is increased and reaches 100% at *ca.* 7000 V $m^{-1}$. This is in good agreement with the theoretical predictions. Indeed, under these conditions, for which $R/d$ was measured to be 0.3, eqn. 6 predicts that a total separation of these two proteins is reached as soon as the electric field exceeds 6500 V $m^{-1}$.

## CONCLUSION

Any electrophoretic separation is based on the difference between the electrophoretic mobilities of the compounds concerned. When performed in the continuous-flow mode, the migration is generally accompanied by a widening of the corresponding peaks. In this work we have defined a separation criterion that gives a relationship between the migration distance and the peak width that should be met for the products to be recovered pure at the outlet of the chamber.

From previous theoretical work, we have used an analytical relationship that relates both the migration distance and the peak width to the operating conditions and to the chamber geometry. In a first step an experimental study was carried out with single protein samples. It was found that in the range of operating conditions investigated both the migration and the peak width follow linear variations with $E\tau$. Using an appropriate protocol, the electroosmotic mobility was estimated, thus making it possible to obtain the values of the electrophoretic mobilities of the proteins. For each set of conditions the value of $R/d$ was measured using a previously developed visualization system. The experimental results were then compared with the calculated values and good agreement was obtained.

In a second step, the separation criterion was used in order to predict the operating conditions to be used to perform separations of proteins of known mobilites. Again, the operating ranges for which a total separation was expected were found to be very close to those given by the experimental results. Under some operating conditions a total separation of BSA and α-lactalbumin, with a difference in mobility of $3 \cdot 10^{-9}$ $m^2$ $V^{-1}$ $s^{-1}$, was obtained.

To achieve the purification of proteins of closer mobilities one has to operate either with more severe conditions, *i.e.*, higher voltages or higher residence times, or with lower values of $R/d$. When working under severer operating conditions, some other dispersive effects, *e.g.*, convection or electrohydrodynamic phenomena, can become predominant. In that event no prediction can be made directly from the results presented in this paper as the operating conditions were intentionally restricted to those making both convection and electrohydrodynamic phenomena negligible. On the other hand, whereas using lower values of $R/d$ should improve the purity of the collected products, it will also result in a decrease in the production rate, which is another important parameter to consider for this process to remain on the preparative scale.

Further work will concern the choice of the most suitable compromise between production and purity and the study of the purification of proteins from real protein mixtures.

## ACKNOWLEDGEMENTS

This work was supported by the French CNES in the frame of the GDR No. 939 CNES/CNRS "Bioseparations en Microgravité". Mr Casademont is thanked for engineering assistance.

## REFERENCES

1 P. H. Rhodes and R. S. Snyder, in R. C. Allen and P. Arnaud (Editors), *Electrophoresis '81*, Walter de Gruyter, Berlin, 1981, pp. 899–917.
2 N. Jouve and M. J. Clifton, *Int. J. Heat Mass Transfer*, 34 (1991) 1461–1471.
3 S. Ostrach, *J. Chromatogr.*, 140 (1977) 187–195.
4 A. Strickler and T. Sachs, *Ann. N.Y. Acad. Sci.*, 209 (1973) 497–514.

5 B. Biscans, P. Alinat, J. Bertrand and V. Sanchez, *Electrophoresis*, 9 (1988) 84–89.
6 M. J. Clifton, N. Jouve, H. de Balmann and V. Sanchez, *Electrophoresis*, 11 (1990) 913–919.
7 H. Roux de Balmann, C. Burgaud and V. Sanchez, *Sep. Sci. Technol.*, 26 (1991) 1481–1494.
8 J. A. Giannovario, R. N. Griffin and E. L. Gray, *J. Chromatogr.*, 153 (1978) 329–352.
9 J. A. Giannovario and R. N. Griffin, paper presented at the *10th AIAA Space Simultation Conference, New York, 1978.*
10 L. D. Plank, W. C. Hymer, M. Elaine-Kunze, G. M. Marks, J. W. Lanham and P. Todd, *J. Biochem. Biophys. Methods*, 8 (1983) 275–289.
11 R. Kuhn and H. Wagner, *J. Chromatogr.*, 481 (1989) 343–351.
12 T. Y. Miller, G. O. Wiliams and R. S. Snyder, *Electrophoresis*, 6 (1985) 377–381.
13 R. S. Snyder, P. H. Rhodes, T. Y. Miller, F. J. Micale, R. V. Mann and G. V. F. Seaman, *Sep. Sci. Technol.*, 21 (1986) 157–185.
14 K. A. Knisley and L. S. Rodkey, *Electrophoresis*, 11 (1990) 927–931.
15 H. de Balmann and V. Sanchez, *Sep. Sci. Technol.*, 26 (1990) 1365–1370.

*Journal of Chromatography*, 594 (1992) 361–369
Elsevier Science Publishers B.V., Amsterdam

CHROM. 23 862

# Continuous separation and purification of proteins by recycling isotachophoresis

Jitka Caslavska and Wolfgang Thormann*

*Department of Clinical Pharmacology, University of Berne, Murtenstrasse 35, CH-3010 Berne (Switzerland)*

(Received August 27th, 1991)

ABSTRACT

The continuous separation and purification of proteins by recycling isotachophoresis (RITP) is described. By operating the RITP fractionation process under counterflow conditions with immobilized sample zones, a configuration is available which allows the continuous feed of crude sample and withdrawal of the purified product. The concept is demonstrated by anionic RITP of bovine serum albumin (BSA) and by cationic RITP purification of ovalbumin (OVA) and lysozyme (LYSO) from a commercial OVA product containing LYSO and conalbumin as major proteinaceous impurities. For the OVA and LYSO purifications, continuous RITP provided a higher sample throughput and comparable product purity compared with batch RITP. In the BSA and LYSO separations the compounds to be purified established their isotachophoretic zones at the front of the sample stack, which represents the simplest example of continuous RITP operation. Continuous purification of OVA as a compound located at the rear of the isotachophoretic zone structure is more complex. With prolonged processing time the removal of proteinaceous impurities which accumulate in the front part of the cell, *i.e.* near the counterflow inlet, is required. Components which do not form their isotachophoretic zone at or near the edges of the zone structures can only be partially purified by continuous RITP. For such compounds a semi-continuous mode of operation in which sample infusion and the withdrawal of purified product are alternated is proposed.

## INTRODUCTION

Recycling isotachophoresis (RITP) is a relatively new free fluid approach for preparative isotachophoresis (ITP) [1–6]. In this method the fluid flows rapidly through a narrow channel and the effluent from each channel is reinjected into the electrophoresis chamber through the corresponding input port. The residence time in the separation cell is of the order of one second per single pass, which does not allow complete separation. Thus recycling is essential to attain a steady state. Immobilization of the advancing zone structure is obtained via a controlled counterflow. RITP has been shown to be an attractive purification method for egg white proteins [6].

In its simplest implementation, RITP is used as a large-scale batch process with a specified amount of sample solution being injected near one end of the separation cell, at the location of the initial interface between the leader and terminator [1–6]. This paper reports a continuous mode of operation in which the sample is continuously infused, the individual components come to rest at their appropriate position in an ITP stack held stationary by counterflow and a particular product of interest is steadily withdrawn from the appropriate channel.

## MATERIALS AND METHODS

### *Chemicals*

All chemicals used were of research grade purity. γ-amino-*n*-butyric acid (GABA), 2-amino-2-methyl-1,3-propanediol (ammediol) and β-alanine were from Sigma (St. Louis, MO, USA). Bovine serum albumin (BSA) was purchased from Fluka (Buchs, Switzerland). Ovalbumin (OVA) from chicken egg (5× crystallized, lot No. 11840/D8) and tetrapropylammonium bromide (TPAB) were from Serva (Heidelberg, Germany). Potassium acetate, formic

0021-9673/92/$05.00 

acid and acetic acid were from Merck (Darmstadt, Germany).

*RITP*

The RITP instrument used in this work is the same as described previously [5,6]. Briefly, it consists of a recycling free flow focusing apparatus (Model RF3; Protein Technologies, Tucson, AZ, USA, distributed by Rainin Instrument, Woburn, MA, USA) with modifications for RITP. Throughout this work, a separation cell of 20 cm length and 4 cm width with a fluid layer thickness of 0.75 mm and providing 30 fractions was used. The total processing volume was about 130 ml. The outlet temperature was about 15°C (cooling bath 7.5°C) with a recycling pump rate of 30% and a constant current of 50 mA. For operation in the ITP mode, the electrolyte chambers were separated from the separation channel by dialysis membranes which, for better stability, were backed up by two layers of chromatographic paper (3MM CHR; Whatman, Maidstone, UK). Electrode buffer reservoirs of 2 l (RF3 standard is 60 ml) were used and filled with buffers of ten-fold higher concentration than that used within the separation cell.

The boundary of a sample protein zone was detected by a 2138 Uvicord S instrument (Pharmacia LKB, Uppsala, Sweden) with a 277 nm filter. Its location was dependent on the purification sample (see Fig. 1). The counterflow inlet and outlet were placed in channels 30 and 1, respectively. The counterflow was generated using a low pulse peristaltic pump (Minipuls 3, Gilson Medical Electronics, Middleton, WI, USA) together with a laboratory-made pulse damper and a bubble trap. It was regulated manually with registration of the output signal from the boundary detector on a strip-chart recorder. Sample feed and bleed were executed with two independent, low-pulse peristaltic pumps (Vario Perpex, H. J. Guldener, Zürich, Switzerland).

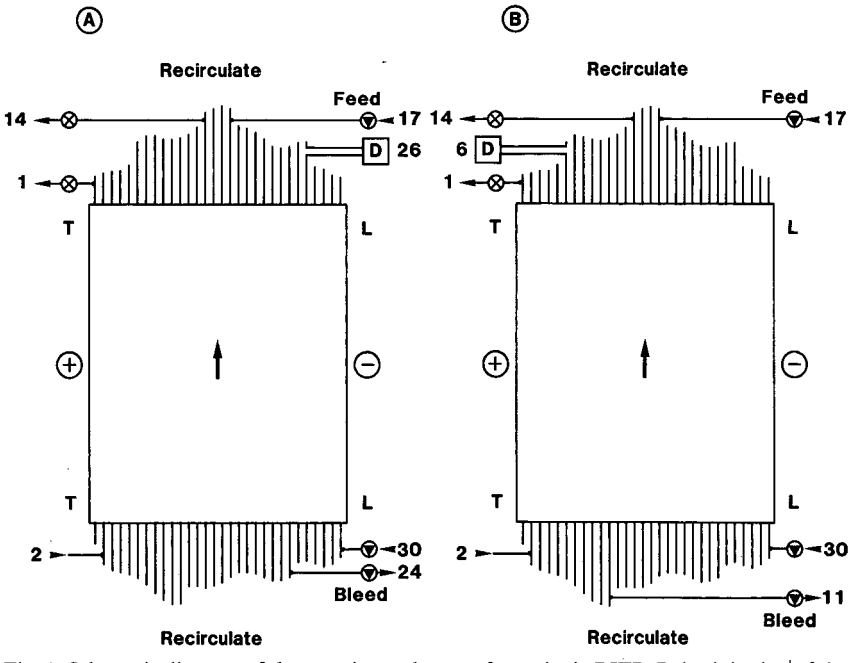


Fig. 1. Schematic diagram of the experimental set-up for cationic RITP. Bolus injection of the sample occurs through inlet 2 and the extra fluid is drained through an outlet in channel 14 (outlet 1 is closed). Counterflow is introduced into channel 30 and drained through outlet 1 (outlet 14 is closed). (A) Continuous purification of a compound at the ITP front with immobilization at channel 26, the location of the boundary detector, D. Sample feed and purified product withdrawal (bleed) are at channels 17 and 24, respectively. (B) Continuous purification of a compound which establishes its ITP zone at the end of the stack. The boundary detector is located in channel 6. Sample feed and purified product withdrawal (bleed) are at channels 17 and 11, respectively. For anionic RITP the polarity must be reversed. L and T refer to leader and terminator, respectively.

These pumps were equipped with 1/10 and 1/20 gears, respectively.

All experiments began with the separation cell filled with the leading electrolyte. The RF3 multichannel peristaltic pump was set to a pumping rate of 30% and the recycling of the electrolytes was started. The sample, dissolved in 10 ml of the leading electrolyte and filtered through a 0.45-$\mu$m membrane syringe filter (Nalgene; Nalge, Rochester, NY, USA), was slowly and carefully injected into the electrolyte stream through channel 2. After sample injection, power was applied at a constant current of 50 mA. When the absorbance in the monitoring loop changed, the counterflow was activated to maintain a constant absorbance. The ITP zone structure was thereby immobilized. Typically, the counterflow pumping rate did not exceed 2.0 ml/min. After the establishment of these steady-state conditions, the sample was continuously infused and the purified product withdrawn according to the configurations shown in Fig. 1. At the end of a run, the remaining processing fluid was collected as described for the batch process [5,6].

*Analysis of collected fractions*

For pH measurements a Model 720 pH meter and a Model 8103 SC ROSS pH electrode (both from Orion Research, Cambridge, MA, USA) were used. The conductivity was measured with a Model 101 conductivity meter (Orion Research) equipped with a Model PW 9510/65 cell (Philips, Eindhoven, Netherlands). The absorbance was measured at 280 nm in a UV–VIS Lambda 15 spectrophotometer (Perkin-Elmer, Überlingen, Germany). The fractions containing high protein concentrations had to be diluted ten times. For presentation of the data the absorbance values were multiplied by ten. Fractions containing conalbumin (CAL) showed a high turbidity and had to be filtered before analysis.

The feed and bleed solutions, in addition to selected fractions at the end of a run, were analysed by capillary ITP using a Tachophor 2127 analyser (LKB, Bromma, Sweden). This instrument was equipped with a 28 cm PTFE capillary of 0.5 mm I.D., as well as a conductivity and UV detector (filter 277 nm) at the column end. The measurements were performed at a constant current of 150 $\mu$A. The data were recorded on a two-channel stripchart recorder or with a data acquisition system consisting of a PC Integration Pack (Version 2.50, Kontron Instruments, Zürich, Switzerland) together with a Mandax AT 286 computer system, or both. This integration pack features two channels for data acquisition, automatic range switching and a dynamic sampling rate allowing a data sampling rate of up to 100 Hz for quickly changing signals. The digitized and computer-stored UV signals of the proteins were integrated (peak area determination), thus providing quantitative data for pure protein zones separated by non-absorbing spacers.

## RESULTS AND DISCUSSION

*Continuous anionic RITP of BSA*

Anionic RITP was performed as reported previously [5] with a leader composed of 10 m*M* formic acid which was adjusted to pH 9 with ammediol. The anodic electrode compartment contained a tenfold higher concentration of the same buffer. A 100 m*M* solution of $\beta$-alanine (terminator), adjusted with ammediol to pH 9.5, was used in the cathodic compartment. The RITP set-up used, but with reversed polarity, is shown in Fig. 1A and the sequence of experimental stages is summarized in Table I.

RITP was first performed with 750 mg of BSA, which was dissolved in 10 ml of 0.01 *M* leader and introduced through port 2 into the cell before the application of power. After a run time of 50 min with a constant applied current of 50 mA, the protein front reached the detection loop (channel 26) and counterflow was activated. Immobilization of the BSA zone was achieved and maintained for 25 min at a power application of about 40 W (stage II).

Continuous infusion (feed) of the sample into channel 17 (Fig. 1A), a channel containing adjusted terminating electrolyte (Fig. 2), and the withdrawal of BSA from channel 24 were then started (stage III of Table I). Using computer simulation, the composition of the terminating buffer was calculated to be 7.48 m*M* $\beta$-alanine and 33.8 m*M* ammediol (pH 9.77; conductivity 16.6 mS/cm) [7]. To minimize buffer perturbations at the location of sample infusion, the feed solution was composed of this adjusted buffer. The concentration of BSA in the buffer was 8.33 mg/ml and the pH and conductivity were 9.95 and 17.2 mS/cm, respectively. The infusion rate was 1.2 ml/min. BSA was withdrawn at a

TABLE I

EXPERIMENTAL STAGES FOR CONTINUOUS ANIONIC RITP OF 1.5 g BSA

The time represents the time interval of a stage, the charge is the total charge spent during a stage, the voltage is given as the initial and end voltage of a stage, the counterflow values represent average flow-rates and the yield is the total amount of BSA recovered during a stage.

| Stage | Time (min) | Charge (C) | Voltage (V) | Counter-flow (ml/min) | Sample feed | | Bleed rate (ml/min) | Yield of BSA (mg) |
|---|---|---|---|---|---|---|---|---|
| | | | | | Bolus (ml) | Continuous (ml/min) | | |
| I | 50 | 150 | 177–815 | Off | 10 | Off | Off | – |
| II | 25 | 75 | 815–780 | 1.5 | – | Off | Off | – |
| III | 85 | 255 | 780–670 | 1.8 | – | 1.2[a] | 0.37 | 711 |
| IV | 10 | 30 | 670–680 | 1.8 | – | Off | Off | – |
| V | 23 | 69 | 680–747 | 1.8 | – | Off | 0.30 | 161 |
| VI | 11 | 33 | 747–769 | 1.8 | – | Off | 0.77 | 198 |
| VII | Collection of all 30 RITP fractions after 204 min | | | | | | | 124[b] |

[a] Continuous feed was terminated after 70 min.
[b] From fractions 23 to 26.

rate of 0.37 ml/min. The BSA content in the bleed solution was 22.96 mg/ml, a value which is lower than that obtained previously after batch operation [5]. Under these conditions the throughput of BSA was calculated to be 510 mg/h and the amount recovered per unit charge spent was 2.79 mg. During this stage (and all subsequent stages with the bleed solution), the counterflow rate was increased to maintain the immobilized front.

After the termination of the continuous sample feed the system was stabilized for 10 min (stage IV) before further withdrawal of BSA (stages V and VI). The final processing fluid was fractionated as described for batch processes (stage VII). Fig. 2 shows the final absorbance, pH and conductivity distributions which were determined on the collected fractions. The protein content at this time was insufficient for the establishment of a plateau zone. The peak concentration (channel 24) was 14.9 mg/ml. The total recovery of BSA (stages I to VII) was 79% and the total charge spent was 612 C.

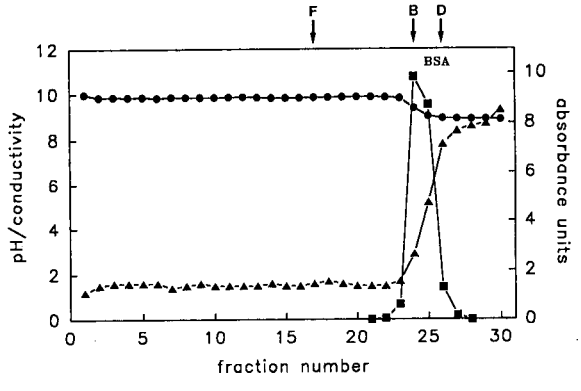


Fig. 2. RITP data after processing of 1.5 g of the BSA product with a total bleed of 1.07 g of BSA. Absorbance (280 nm, ■), pH (●) and conductivity (mS/cm, ▲) were measured on the collected fractions. D, B and F mark the positions of the boundary detector, bleed of purified product and sample feed, respectively.

*Purification of LYSO and OVA by continuous cationic RITP*

For all cationic RITP experiments a leader composed of 0.01 *M* potassium acetate and acetic acid ($pH_L$ = 4.75) was used. The cathodic electrode compartment contained a ten-fold higher concentration of the same electrolyte, whereas 0.1 *M* acetic acid (terminator) was in the anodic electrode compartment. A commercial OVA product containing LYSO and CAL as impurities was used as the sample. Previous investigations by analytical ITP and RITP showed that GABA can be used successfully as a spacer between OVA and its two major proteinaceous impurities and tetrapropylammonium (TPA) to separate CAL and LYSO [6].

For the purification of LYSO, the best RITP results were obtained with TPA added to the anodic

TABLE II

EXPERIMENTAL STAGES FOR PURIFICATION OF LYSO FROM 2.1 g OF A COMMERCIAL OVA PRODUCT BY CONTINUOUS CATIONIC RITP

The time represents the time interval of a stage, the charge is the total charge spent during a stage, the voltage is given as the initial and end voltage of a stage, the counterflow values represent average flow-rates and the yield is the total amount of LYSO recovered during a stage.

| Stage | Time (min) | Voltage (V) | Charge (C) | Counter-flow (ml/min) | Sample feed | | Bleed rate (ml/min) | Yield of LYSO (mg) |
|---|---|---|---|---|---|---|---|---|
| | | | | | Bolus (ml) | Continuous (ml/min) | | |
| I | 53 | 144–342 | 159 | Off | 10 | Off | Off | – |
| II | 45 | 342–382 | 135 | 1.8 | – | Off | Off | – |
| III | 79 | 382–350 | 237 | 1.8 | – | 1.4 | Off | – |
| IV | 15 | 350–354 | 45 | 1.8 | – | 1.4 | 0.47 | 9.1 |
| V | 14 | 354–343 | 42 | 1.8 | – | 1.4 | Off | – |
| VI | 15 | 343–366 | 45 | 1.8 | – | 1.4[a] | 0.27 | 4.9 |
| VII | 35 | 366–381 | 105 | 1.8 | – | Off | Off | – |
| VIII | 40 | 381–384 | 120 | 1.8 | – | Off | 0.23 | 13.8 |
| IX | 15 | 384–386 | 45 | 1.8 | – | Off | Off | – |
| X | Collection of all 30 RITP fractions after 311 min | | | | | | | 15.3[b] |

[a] Terminates 3 min earlier.
[b] Fractions 22 to 25.

electrode solution [6]. This configuration allowed the isolation and purification of LYSO alone. During this experiment, OVA and CAL were first pushed by electromigration towards the membrane near the sample inlet and then swept out during the counterflow operation. For continuous operation this same configuration with 50 m*M* TPAB in the anolyte was used. First 715 mg of the OVA product were processed for 53 min (stage I of Table II) and counterflow was activated for 45 min to stabilize the system at a power level of about 20 W (stage II). Then continuous sample infusion and the withdrawal of purified LYSO could be begun in the same way as described for continuous anionic RITP of BSA (Fig. 1A). Computer simulation was used to obtain an estimated composition of the adjusted terminator of 4.34 m*M* TPA and 5.1 m*M* acetic acid (pH 4.37). A feed solution of 1.4 g OVA product dissolved in 200 ml of this buffer was prepared. The infusion rate was 1.4 ml/min. First LYSO was withdrawn at a rate of 0.47 ml/min with a concentration of 1.31 mg/ml (stage IV). The throughput and amount recovered per unit charge spent were 37 mg/h and 0.20 mg, respectively. The bleed solution was then stopped for 14 min (stage V) and continued at a rate of 0.27 ml/min (stage VI; the LYSO concentration and throughput were 1.19 mg/ml and 20 mg/h, respectively). After this no feed nor bleed occurred for 35 min (stage VII) before another withdrawal of LYSO at 0.23 ml/min (stage VIII; LYSO concentration and throughput were 1.52 mg/ml and 21 mg/h, respectively). Collection of the fluid in all recycling channels occurred after 311 min of operation and 933 C of charge spent. The analytical data obtained for the 30 fractions are shown in Fig. 3. It was interesting to find that the counterflow rate could be kept constant throughout this run.

The total amount of LYSO in fractions 22 to 25 was 15.3 mg. The total LYSO yield was 43.1 mg, which represents 2.1% of the applied amount of protein. For this run, the analytical data obtained by capillary ITP are shown in Fig. 4. Panel B shows data obtained after the injection of the commercial OVA product which was spiked with GABA and TPAB. The analysis of the bleed solution and fraction 22 (with the addition of the same two spacers) are shown in panels C and D, respectively. These data show that pure LYSO was collected.

In the two runs described here, the protein of interest established its ITP zone at the beginning of

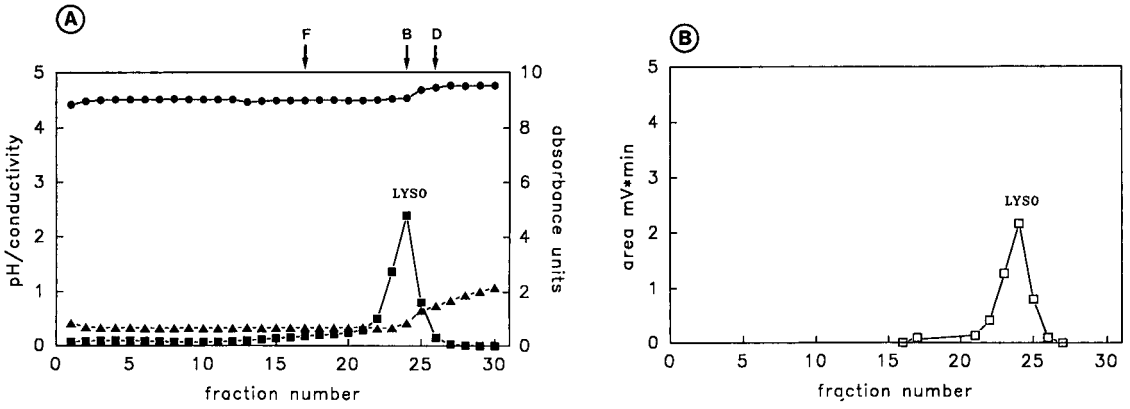


Fig. 3. RITP data after processing 2.1 g of the OVA product and bleeding off 27.8 mg of pure LYSO. Panel A shows absorbance, (280 nm, ■), pH (●) and conductivity (mS/cm, ▲) distributions measured on the collected fractions. Fractions containing CAL were filtered before analysis. Panel B shows the processed data of analytical capillary ITP runs on the Tachophor. Volumes of 1 μl of undiluted fractions and 1 μl of a spacer mixture of GABA and TPA were injected and analysed. Peak areas of the UV signals (277 nm) were determined with the PC integration pack. The peak concentration of LYSO (fraction 24, bleed channel) was 1.91 mg/ml. D, B and F mark the positions of boundary detector, bleed of purified product and sample feed, respectively.

the ITP sample stack. The third example presented in this paper consists of the continuous purification of OVA from the commercial OVA product. As this protein is the rear component in the cationic ITP stack in the potassium acetate–acetic acid system [5,6], the plumbing of the RITP set-up had to be changed (Fig. 1B). The UV monitor was inserted into recycling loop 6, which allowed the control of the rear edge of the OVA zone (Fig. 5). The sample was fed continuously into channel 17 (spacer zone) and purified OVA was withdrawn from channel 11. GABA was used as a spacer between OVA and

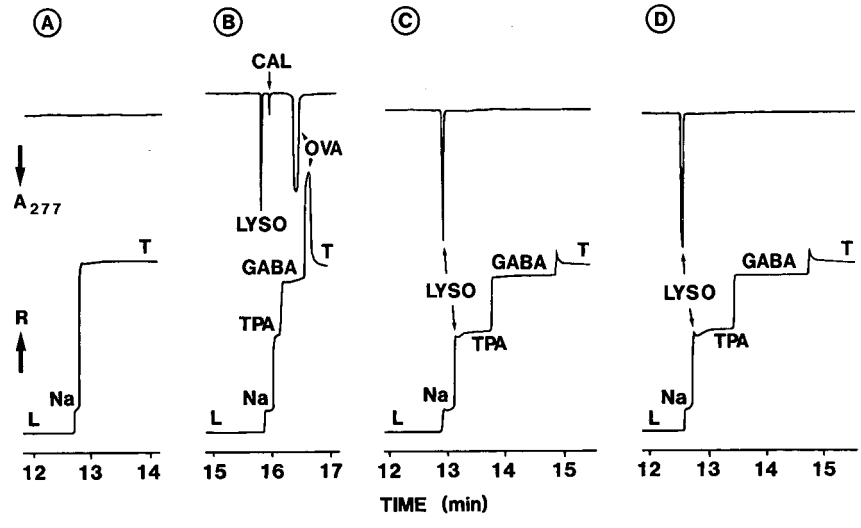


Fig. 4. Capillary ITP data for the purification of LYSO (Fig. 3, Table II) using the Tachophor analyser. Panel A shows the blank run, panel B the analysis of commercial OVA (feed), panel C the analysis of the bleed solution and panel D the analysis of fraction 24 after final fraction collection. Volumes of 1 μl of feed, bleed and the undiluted fraction and 1 μl of a spacer mixture of GABA and TPAB were injected and analysed. The lower and upper plots represent the conductivity (expressed as the increase in resistance $R$) and UV absorbance at 277 nm, respectively. L = Leader; T = terminator; Na = sodium as an impurity from electrolyte system.

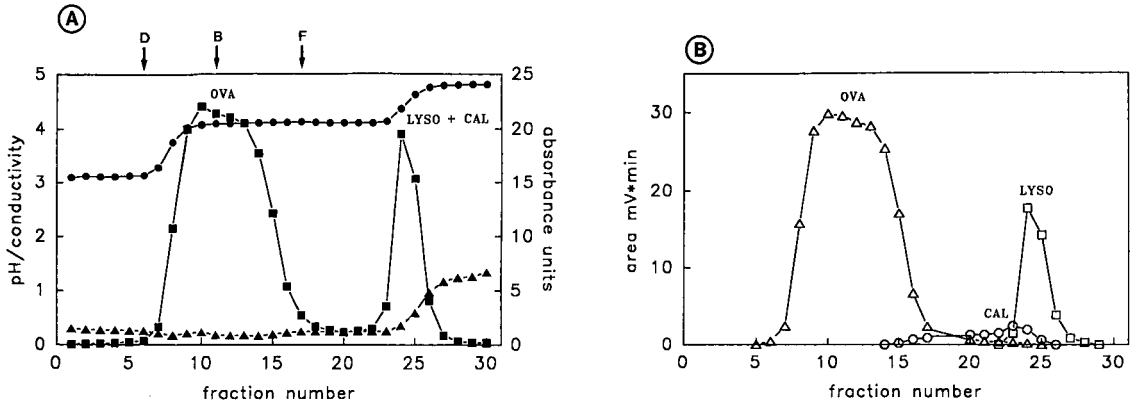


Fig. 5. RITP data after processing 2.1 g OVA and bleeding 659 mg of purified OVA. GABA was used as a spacer between OVA and the proteinaceous impurities. The OVA plateau concentration after final fraction collection was 35 mg/ml. For explanation of the data panels, refer to Fig. 3.

CAL/LYSO and the anolyte did not contain any additives. Initially, 706 mg of OVA and 32.7 mg of GABA were dissolved in 10 ml of 0.01 *M* leader and introduced through inlet 2. Cationic RITP was performed for 54 min (stage I of Table III) before 64 min of counterflow operation at a power level of about 24 W (stage II). Thereafter, the infusion of more sample occurred for 40 min at a rate of 0.6 ml/min (stage III). The feed solution was composed of 1.417 g of OVA product dissolved in 200 ml of 2.5 m*M* potassium acetate, which was adjusted to pH 4.08 (conductivity 28 mS/cm) with acetic acid. It is important to note that the feed solution did not contain any GABA, but had a similar conductivity to the established GABA spacer zone. OVA withdrawal was started at a rate of 0.12 ml/min (stage IV). The OVA concentration in the bleed solution was 22.2 mg/ml, a value which is again lower than the steady-state plateau concentration obtained with batch operation. Under these conditions a

TABLE III

EXPERIMENTAL STAGES FOR PURIFICATION OF 2.1 g OVA FROM A COMMERCIAL OVA PRODUCT BY CONTINUOUS CATIONIC RITP

The time represents the time interval of a stage, the charge is the total charge spent during a stage, the voltage is given as the initial and end voltage of a stage, the counterflow values represent average flow-rates and the yield is the total amount of OVA recovered during a stage.

| Stage | Time (min) | Voltage (V) | Charge (C) | Counter-flow (ml/min) | Sample feed | | Bleed rate (ml/min) | Yield of OVA (mg) |
|---|---|---|---|---|---|---|---|---|
| | | | | | Bolus (ml) | Continuous (ml/min) | | |
| I | 54 | 128–395 | 162 | Off | 10 | Off | Off | – |
| II | 64 | 395–471 | 192 | 1.8 | – | Off | Off | – |
| III | 40 | 471–593 | 120 | 1.0 | – | 0.6 | Off | – |
| IV | 132 | 593–638 | 396 | 1.3 | – | 0.6[a] | 0.12 | 344 |
| V | 44 | 640–585 | 132 | 1.0 | – | 2.0[b] | 0.36 | 315 |
| VI | 43 | 585–512 | 129 | 1.5 | – | Off | Off | – |
| VII | Collection of all 30 RITP fractions after 377 min | | | | | | | 800[c] |

[a] Feed rate was changed to 2.0 ml/min after 111 min.
[b] Terminates 7 min earlier.
[c] Fractions 9 to 14.

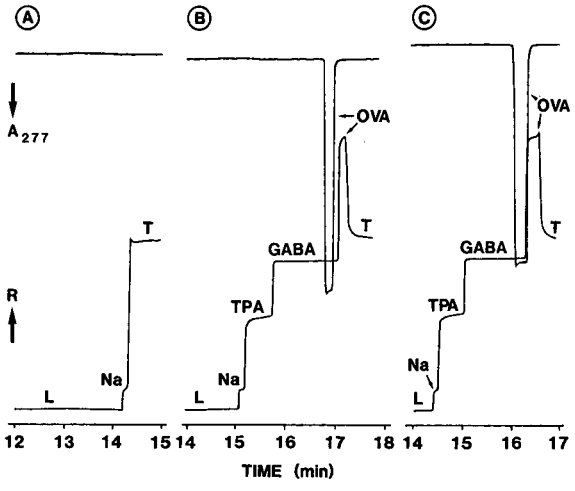


Fig. 6. Capillary ITP data of the OVA purification process (Fig. 5, Table III). Panel A shows the blank run, panel B the analysis of the bleed solution and panel C the analysis of fraction 11 after final fraction collection. Other conditions are as in Fig. 4.

yield of 156 mg/h and a recovery of 0.87 mg pure OVA per unit charge spent were obtained. A feed rate of 0.6 ml/min resulted in a protein infusion of about 250 mg/h. After 111 min of continuous operation the infusion rate was increased to 2.0 ml/min. The withdrawal rate was therefore increased to 0.36 ml/min (stage V). At this stage, the OVA concentration in the bleed solution was 19.7 mg/ml, which is equivalent to a yield of about 430 mg OVA per hour and a recovery of 2.39 mg OVA per unit charge spent. For the immobilization of the rear end of the OVA zone, the counterflow rate was readjusted for each stage.

Before the final fraction collection the system was run in the batch mode (stage VI). Collection of all recycling channels occurred after 377 min of operation and 1131 C of charge spent. A total amount of 1.46 g of pure OVA was recovered. This represents about 70% of the supplied amount of protein, a value which compares favourably with the OVA content of about 84% claimed by the supplier. Analytical data obtained for the 30 fractions are shown in Fig. 5 and the capillary ITP data are shown in Fig. 6. These analyses show that pure OVA was obtained and that, within the experimental time frame, the accumulation of CAL and LYSO did not disturb this process. An overload of these compounds is expected with longer run times, a situation which would require the continuous (or batch) removal of these proteins, *e.g.* from recycling loop 25. With a selected amount of TPAB in the original sample, and with the same instrumental set-up, it is anticipated that purified OVA and LYSO could be recovered simultaneously and continuously.

## CONCLUSIONS

RITP is a free fluid electrophoretic approach for the fractionation of proteins which features a continuous and batch mode of operation. The former mode, for which the first experimental data are reported here, is more attractive than the latter, particularly for the incorporation of RITP as a downstream processing unit operation, *i.e.* as a purification method in an industrial multistep purification protocol. As is shown with the example of BSA, the processing rate in continuous RITP is comparable with that obtained in continuous flow ITP [4]. In the examples of BSA and LYSO, the compounds to be purified established their ITP zones at the front of the sample stack. This represents the simplest example of continuous RITP in which the feed is infused into the adjusted electrolyte behind the target zone. Most sample impurities are thereby quickly removed and swept out of the cell by counterflow. Continuous purification of a compound located at the rear of the isotachophoretic zone structure, as for the OVA example, requires a more complex plumbing with sample infusion in front of the target zone in addition to occasional or continuous removal of proteinaceous impurities which accumulate within the separation cell. For compounds which form their ITP zone at neither edge of the stack, the experimental configuration has to be adapted for each sample separately and continuous purification will always be incomplete because of the migration of some contaminants through the sample zone. In this instance a semi-continuous mode of operation in which sample infusion and the withdrawal of the purified product are alternated is proposed. Such a procedure also requires an occasional removal of accumulated proteinaceous impurities, but allows a more complete purification of the centre compounds. Splitting the protein matrix by feed and bleed recycling zone electrophoresis [8] followed by purification by continuous RITP as an

edge compound would be another, but two-stage, approach worth considering.

The investigated purification of LYSO (about 40 mg/h) and OVA (about 500 mg/h) from a commercial OVA sample show the capability of using RITP to continuously isolate a minor component (here approximately 3% of the protein content) and purify a major sample constituent, respectively. Without the optimization of the various running parameters, the purities of the products were determined to be equal and the achieved throughputs were higher than those obtained in batch mode operation [6]. Scaling-up of the procedure to even higher throughputs and full automation of the continuous process are currently being studied.

## ACKNOWLEDGEMENTS

The generous loan of the Tachophor 2127 by LKB, Bromma, Sweden is gratefully acknowledged. The authors thank Kontron, Zürich, Switzerland for the loan of a PC integration pack. This work was supported by the Swiss National Science Foundation.

## REFERENCES

1 J. E. Sloan, W. Thormann, M. Bier, G. E. Twitty and R. Mosher, in M. J. Dunn (Editor), *Electrophoresis '86*, VCH, Weinheim, 1986, p. 696.
2 J. E. Sloan, W. Thormann, G. E. Twitty and M. Bier, *J. Chromatogr.*, 457 (1988) 137.
3 M. Bier, G. E. Twitty and J. E. Sloan, *J. Chromatogr.*, 470 (1989) 369.
4 W. Thormann, M. A. Firestone, J. E. Sloan, T. D. Long and R. A. Mosher, *Electrophoresis*, 11 (1990) 298.
5 J. Caslavska, P. Gebauer, A. Odermatt and W. Thormann, *J. Chromatogr.*, 545 (1991) 315.
6 J. Caslavska, P. Gebauer and W. Thormann, *J. Chromatogr.*, 585 (1991) 145.
7 W. Thormann and R. A. Mosher, *Electrophoresis*, 11 (1990) 292.
8 M. Bier, N. B. Egen, G. E. Twitty, R. A. Mosher and W. Thormann, in C. J. King and J. D. Navratil (Editors), *Chemical Separations, Vol. 1: Principles*, Litarvan Literature, Denver, 1986, p. 133.

*Journal of Chromatography*, 594 (1992) 371–378
Elsevier Science Publishers B.V., Amsterdam

CHROM. 23 839

# Study of isotachophoretic separation behaviour of metal cations by means of particle-induced X-ray emission

# III. Analysis of a crude rare earth chloride from monazite

Jian-ying Hu, Takeshi Hirokawa*, Fumitaka Nishiyama and Yoshiyuki Kiso

*Applied Physics and Chemistry, Faculty of Engineering, Hiroshima University, Kagamiyama 1, Higashi-Hiroshima, 724 (Japan)*

Kazuaki Ito and Eiji Shoto

*Environmental Science, Faculty of Engineering, Hiroshima University, Kagamiyama 1, Higashi-Hiroshima, 724 (Japan)*

(First received August 28th, 1991; revised manuscript received October 31st, 1991)

ABSTRACT

A crude rare earth chloride produced from monazite was analysed by coupled isotachophoresis–particle-induced X-ray emission (ITP–PIXE). The sample was separated and fractionated by the use of a micro-preparative isotachophoretic analyser and the dropwise fractions containing nanomole amounts of rare earth elements were analysed off-line by PIXE. By means of ITP–PIXE, the minor elements (Sm, Eu, Gd, Tb, Dy, Ho, Er, Tm, Yb, Lu and Y) co-existing with the other major lanthanoids (La, Ce, Pr and Nd) were determined accurately, because the "matrix effect" in X-ray analysis was reduced by isotachophoretic removal of the major elements. The maximum abundance found was for Ce at 47.4% with respect to total rare earths and the minimum abundance was 0.001% for Lu. The separation efficiency of the crude rare earth chloride was *ca.* 500 nmol/C. The method for the fractionation of minor elements and PIXE analysis is discussed in detail. The analytical results obtained by ITP–PIXE were confirmed by means of inductively coupled plasma atomic emission spectrometry.

## INTRODUCTION

The accurate determination of minor components co-existing with major components is often difficult when the method used depends on a preliminary separation. In isotachophoresis (ITP), when the amount of electricity is not sufficient for separation, mixed zones remain, causing the errors in determination. We have pointed out that the errors would be serious for the determination of a minor component co-existing with a major component, as the mixed zones formed in such a sample system tend to be overlooked because of the similarity between the signal of the mixed zone and that of the major component zone [1]. Therefore, the study of separation efficiency is important to avoid overloading of the sample.

The separation efficiency of a pair of separands depends not only on the mobility difference between them [2,3] but also on the amount of co-existing ionic components [1,4]. Further, the mobility difference between the separands and the co-existing components also affects the separation efficiency. Therefore, the necessary amount of electricity for complete separation varies in relation to these factors even if the sample amount of interest is kept constant. Such an effect was called the composition effect on the separation efficiency [4].

A crude rare earth chloride, which is a primary product of rare earth elements after extracting

0021-9673/92/$05.00 

thorium from monazite [5], is a typical sample containing rare earth elements with various abundances. According to the analytical results evaluated by the manufacturer using atomic absorption spectrometry, etc., the major elements were La, Ce, Pr and Nd (total abundance *ca.* 95% of the total rare earth elements) and the minor elements were Sm, Eu, Gd, Tb, Dy, Ho, Er, Tm, Yb and Y (total abundance *ca* 5%). The ratio of Ce with the maximum abundance to Yb with the minimum abundance was over $10^4$. In order to determine the minor elements, it is difficult to obtain a highly separation efficiency of the crude rare earth chloride when ITP analysis is carried out in the usual manner. In our previous paper [6], we reported a study of the separation efficiency of a binary mixture of lanthanoids and clarified that the simulated separation efficiency agreed well with that observed and that the necessary amount of electricity for the separation of minor components can be estimated from the total amount of the whole sample using coupled isotachophoresis–particle-induced X-ray emission (ITP–PIXE), where isotachophoretically separated zones were fractionated and analysed off-line by means of PIXE.

In this work, first the separation efficiency of a model crude rare earth chloride was measured, then the minor rare elements contained in a real crude rare earth chloride sample were determined by means of ITP–PIXE. Inductively coupled plasma atomic emission spectrometry (ICP-AES) was also applied in order to confirm the ITP–PIXE results.

## EXPERIMENTAL

### *Chemicals*

A crude rare earth chloride from monazite was obtained from Santoku Kinzoku (Tokyo, Japan). Lanthanoid chlorides ($LnCl_3 \cdot 6H_2O$), α-hydroxyisobutyric acid (HIB) and carnitine hydrochloride were obtained from Katayama Kagaku (Osaka, Japan). Two cationic dyes, toluidene blue (TB) and astrazon pink (AP), and hydroxypropylcellulose (HPC) were obtained from Tokyo Kasei (Tokyo, Japan). The lanthanoid chlorides and HPC were of Extra Pure grade and HIB and carnitine hydrochloride were of Guaranteed Reagent grade. The viscosity of a 2% HPC aqueous solution was 1000–4000 cP at 20°C according to the specification.

### *Samples*

Crude rare earth solutions of 8.808, 0.8808 and 0.5872 g/l were prepared by dissolving the sample in high-purity water processed with an ion exchanger (Puric-R; Japan Organo, Tokyo, Japan). The specific resistance of the water used was $18.3 \cdot 10^6$ ohm cm.

A model mixture of the crude rare earth chloride from monazite was prepared by using the chlorides of rare earths according to the analytical results supplied by Santoku Kinzoku. Stock sample solutions were prepared by dissolution in high-purity water. The concentrations of the stock solutions of La, Ce, Nd, Y and the other rare earth elements were 27.90, 53.59, 50.00, 10.89 and 5.00 m*M*, respectively. Although the presence of Lu was not specified by Santoku Kinzoku, the same amount of Lu as the trace element Yb was added. The total concentration of the model mixture was 25 m*M*. Small amounts of TB and AP were added to the above samples to monitor the migration process and to determine the timing of fractionation.

Rare earth standard solutions (1000 ppm) for atomic absorption spectrometry (Tokyo Kasei) were used as analytical standards for PIXE and ICP-AES analysis.

### *Electrolyte system*

The electrolyte system used is summarized in Table I. The leading electrolyte was 20 m*M* ammonia, which contained 10 m*M* HIB as the complex-forming reagent for the efficient separation of rare earth elements [7,8]. The utility of complex-forming reagents in ITP separations of inorganic ions including lanthanoids has been thoroughly reviewed by Bocek and Foret [9]. The pH was adjusted to 4.8 by adding acetic acid. pH measurements were carried using a Horiba (Tokyo, Japan) Model F7ss expanded pH meter. The terminating electrolyte was 10 m*M* carnitine hydrochloride. In order to make a clear interface between the leading and terminating electrolytes (no valves were used at the electrolyte interface), sucrose (20 wt.%) was added to the terminating electrolyte at the sample preseparation stage. The addition of sucrose was also effective in suppressing the convection of the terminating electrolyte. HPC (1.75%) was added to the leading electrolyte used for sample preseparation stage in order to suppress heat convection and 0.2%

TABLE I

ELECTROLYTE SYSTEM USED IN ISOTACHOPHORETIC SEPARATION

HIB = α-hydroxyisobutyric acid; CARH = carnitine hydrochloride; HPC = hydroxypropylcellulose.

| Component | Stage I[a] | Stage II[b] |
|---|---|---|
| Leading electrolyte | 20 m*M* $NH_3$ | 20 m*M* $NH_3$ |
| Complex-forming reagent | 10 m*M* HIB | 10 m*M* HIB |
| pH buffer | Acetic acid | Acetic acid |
| pH of leading electrolyte | 4.8 | 4.8 |
| Terminating electrolyte | 10 m*M* CARH | 10 m*M* CARH |
| Additive to leading electrolyte | 1.75% HPC | 0.2% HPC |
| Additive to terminating electrolyte | 20% sucrose | 0.2% HPC |

[a] Preseparation stage.
[b] Separation stage as shown in Fig. 1.

HPC in the separation and fractionation stages in order to suppress electroendosmosis.

*Preparative isotachophoretic analyser*

The preparative analyser and the method of fractionation used were reported in a previous paper [10]. A simplified diagram of the apparatus is shown in Fig. 1. The pre-separation tube was made of acrylic resin (I.D. 5 mm) and it was tapered off to 3 mm I.D. The preseparation tube was connected to the separation tube at the branch B1. The principle of fractionation was of the Arlinger type [11], except for the dropwise fractionation (*ca.* 5 μl). It was carried by applying a counter-flow of the leading electrolyte using a syringe pump. The separated zones were detected by potential gradient detection (PGD) and the fractions were analysed off-line by PIXE.

The load of leading electrolyte in the preseparation tube was made either 1.7 or 3.4 ml by extending the PTFE tube (55 cm × 2 mm I.D.) connecting the preseparation tube with the separation stage. This enabled *ca.* 10°C to be applied at the preseparation stage. In order to obtain the amount of electricity in the electrophoretic process, the migration current was integrated using a microcomputer with an analog–digital conversion interface (sampling rate 2.070 s per datum).

*PIXE analysis*

For the PIXE spectra measurements [12], a Van de Graaff accelerator was used (Model AN-2500, Nisshin High Voltage, Tokyo, Japan). The energy of the $H^+$ beam was 2 MeV and the beam current was in the range 35–50 nA. A typical single run for an ITP fraction took 190–260 s. The detector used was a highly pure Ge detector (Ortec Model GLP-10180) and the multi-channel analyser used was a Laboratory Equipment (Tokyo, Japan) Model AMS-1000.

The Nuclepore filter used as the target backing

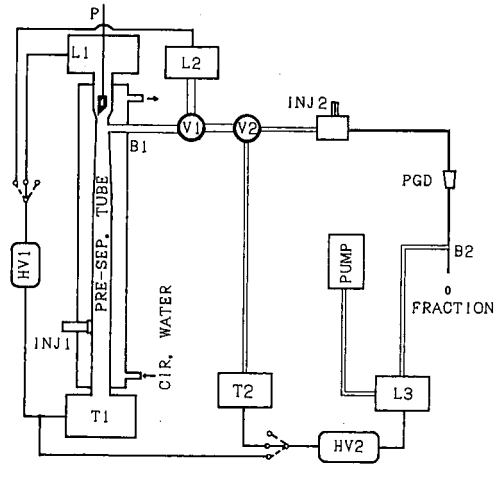


Fig. 1. Schematic diagram of the preparative isotachophoretic analyser. L1, L2, L3 = leading electrolyte compartment; T1, T2 = terminating electrolyte compartment; V1, V2 = valves to change the current path; INJ1, INJ2 = injection ports; P = PTFE plug to cut off L1 compartment; PRE-SEP. TUBE = preseparation tube; B1 = branch of preseparation tube; B2 = sample fractionating branch with a narrow-bore nozzle; PGD = potential gradient detector; HV1, HV2 = high voltage power supplies.

was of thickness 5 μm and pore size 0.1 μm and was mounted on an aluminium frame. The impurities were mainly Cr and Fe, and the abundance of Fe was one tenth of that of Cr. The fraction was dropped on the Nuclepore filter directly from the nozzle of the preparative isotachophoretic analyser (B2 in Fig. 1). The diameter of the sample spot was *ca.* 3 mm. After drying in a desiccator, it was used as the PIXE target. The amount of the rare earth element was determined by comparing its X-ray counts with those of the standard targets.

Our data reduction software PIXS was used with an option of spectrum deconvolution utilizing an X-ray relative intensity database [13]. It was useful for the X-ray spectral analysis from multi-elements containing in a target. Calculation was carried on an NEC (Tokyo, Japan) PC-9801RA microcomputer (CPU = 80 386, co-processor = 80 387, clock = 20 MHz).

The PIXE spectrum of the crude rare-earth chloride from monazite was measured and analysed in a similar manner. A 5-μl sample solution (0.5872 g/l, 2.936 μg) was spotted on the Nuclepore filter.

*ICP-AES analysis*

A Nippon Jarrel-Ash (Tokyo, Japan) Model ICAP-575 Mark II ICP-AE spectrometer equipped with a Fassel-type high salt concentration torch was operated with an input power of 1.4 kW at 27.12 MHz. The nebulizer argon flow-rate was 0.47 l/min at 1.5 kg/cm$^2$ and the sample aspiration rate was 2.4 ml/min. The emission from the plasma was observed at 15 mm above the load coil and detected with a Model R-500-01 (above 300-nm range) and a Model R-427-08 (below 300 nm) photomultiplier manufactured by Hamamatsu Photonics (Hamamatsu, Japan). An NEC PC-9801 UX21 microcomputer was used for data acquisition and processing. Quantitative analysis was carried out by comparing the strength of one or two emission lines of an element with that of a standard sample. The wavelengths of the lines used for the determination of each rare-earth element are shown in Table II.

TABLE II

WAVELENGTHS USED FOR THE DETERMINATION OF RARE EARTH ELEMENTS BY ICP-AES

| *Z* | Element | Wavelength (nm) |
|---|---|---|
| 57 | La | (i) 379.478 × 1 |
| | | (ii) 408.672 × 1 |
| 58 | Ce | (i) 399.924 × 1 |
| | | (ii) 413.38 × 1 |
| 59 | Pr | (i) 422.535 × 1 |
| 60 | Nd | (i) 406.109 × 1 |
| | | (ii) 430.358 × 1 |
| 62 | Sm | 443.388 × 1 |
| 63 | Eu | 272.778 × 3 |
| 64 | Gd | (i) 310.05 × 2 |
| | | (ii) 336.223 × 2 |
| 65 | Tb | 350.917 × 2 |
| 66 | Dy | 353.602 × 2 |
| 67 | Ho | 345.6 × 1 |
| 68 | Er | 337.271 × 2 |
| 69 | Tm | 346.22 × 2 |
| 70 | Yb | 211.667 × 3 |
| 71 | L | (i) 261.542 × 2 |
| | | (ii) 219.554 × 3 |
| 39 | Y | (i) 324.228 × 1 |
| | | (ii) 377.433 × 1 |

## RESULTS AND DISCUSSION

*Separation efficiency of the model mixture of the crude rare earth chloride*

In order to evaluate the separation efficiency of the crude rare earth chloride, first a model mixture of the crude rare earth chloride was separated and fractionated (sample volume = 200 μl, total concentration = 25 m*M*, 5000 nmol, *ca.* 700 μg). The sample constituents are shown in Table III. The zones of the major components (La, Ce, Pr and Nd) were removed at the preseparation stage. The integrated amount of electricity at the preseparation stage was 5.2 C (30 min). A further 0.92 C was added during 90 min at the separation stage.

Table III also summarizes the zone lengths of the minor components detected by the use of PGD and the recovery evaluated by means of PIXE. A mixed zone of Y and Dy was not completely resolved, although the effective mobility of Y was slightly larger than that of Dy. The time-based zone lengths of Sm, Eu, Gd and Tb were 186, 15, 141 and 13.5 s (coulomb-based zone lengths: 28, 2.25, 21.45 and 2.10 mC, respectively). The individual zone lengths of Ho, Er, Tm, Yb and Lu could not be observed owing to their low abundances (less than 0.9 nmol). Eighteen fractions were obtained in 525 s (29.2 s per

TABLE III

RECOVERY OF MINOR RARE EARTH ELEMENTS IN THE MODEL MIXTURE OF CRUDE RARE EARTH CHLORIDE BY ITP–PIXE

For experimental conditions, see text.

| Rare earth | Injected amount | | 5.2 C[a] | | 10.0 C[a] | |
|---|---|---|---|---|---|---|
| | μg | nmol | Recovery (%) | ZL (mC)[b] | Recovery (%) | ZL (mC)[b] |
| La | 163.6 | 1168 | –[c] | – | – | – |
| Ce | 331.9 | 2369 | – | – | – | – |
| Pr | 39.19 | 278.1 | – | – | – | – |
| Nd | 133.3 | 924.2 | – | – | – | – |
| Sm | 18.57 | 123.4 | 63 | 28.0 | 100 | 45.45 |
| Eu | 1.196 | 7.9 | 78 | 2.25 | 97 | 1.8 |
| Gd | 10.85 | 68.9 | 79 | 21.45 | 100 | 25.2 |
| Tb | 0.791 | 5.0 | 83 | 2.10 | 96 | 2.25 |
| Y | 3.753 | 42.2 | 101 | 15.3 | 102 | 15.75 |
| Dy | 0.770 | 4.7 | 97 | | 101 | |
| Ho | 0.141 | 0.9 | 96 | 0.45 | 94 | 0.45 |
| Er | 0.139 | 0.8 | 98 | | 97 | |
| Tm | 0.063 | 0.4 | 97 | | 98 | |
| Yb | 0.039 | 0.2 | 107 | | 107 | |
| Lu | 0.039 | 0.2 | 107 | | 97 | |
| Total[d] | 704.3 | 5000 | – | – | – | – |

[a] Amount of electricity integrated at preseparation stage.
[b] Zone length (mC) of separated zones (current: 150 μA).
[c] –, Removed at preseparation stage or not detectable.
[d] Total amount of rare earth elements.

fraction) and were analysed by PIXE. In the last fraction Ho, Er, Tm, Yb and Lu were detected.

As shown in Table III, the recovery of Sm, Eu, Gd and Tb was incomplete, suggesting that the amount of electricity applied (5.2 C) at the preseparation stage was not enough for the complete separation of Sm, Eu, Gd and Tb from the major light lanthanoids (La, Ce, Pr and Nd).

Almost all of the major lanthanoids were removed at the preseparation stage and apparently part of the Sm, Eu, Gd and Tb was not recovered because the mixed zone was not completely resolved owing to an insufficient amount of electricity. As we have already confirmed a 100% recovery of the equimolar lanthanoids under the electrolyte conditions used [9,14], when the recovery is imperfect it can be correlated with the amount of electricity applied as follows:

$$\text{Recovery}\,(\%) = \frac{\text{separable amount (nmol)}}{\text{injected amount (nmol)}} \cdot 100$$

= (applied amount of electricity per unit sample amount/necessary amount of electricity per unit sample amount) · 100

In order to obtain a 100% recovery, the necessary amount of electricity ($Q$) for the separation of a 5000-nmol sample was estimated from the minimum recovery of Sm (63%) in Table III:

$$Q = 5.2/0.63 = 8.3\text{C}$$

Consequently, the separation efficiency of the crude rare earth chloride was estimated as 602 nmol/C (= 5000/8.3).

The integrated amount of electricity was then increased to *ca.* 10 C by using the preseparation tube with a larger load of leading electrolyte. The 5000-nmol sample was fractionated and 23 fractions were obtained in 648 s (28.2 s per fraction). As summarized in Table III, the recovery of Sm–Lu was 100%, as expected, suggesting that 10 C were sufficient for

the separation of Sm–Lu from the major light lanthanoids. The zone length of Tb was almost unchanged (15 s) but that of Eu became shorter (12 s). From the PIXE analysis of the fractions, this was confirmed to be the result of the incomplete separation of the mixed zone between Eu and Gd.

From the above experimental results with the model mixture, it became evident that the separation efficiency of the crude rare earth chloride was at least 500 nmol/C (=5000/10) for the separation of the medium to heavy rare earth elements Sm–Lu from major light lanthanoids.

*ITP–PIXE analysis of real sample*

Before determining minor elements, the major elements were determined in order to obtain the abundance of total rare earth elements in the actual sample. A 6.5-$\mu$l sample (8.808 g/l, 57.3 $\mu$g) was separated and whole zones were fractionated. The preseparation stage was not used as the sample amount was small. The integrated amount of electricity was 0.603 C. The coupled tubes used were 16 cm × 1 mm I.D. × 2 mm O.D. and 32 cm × 0.5 mm I.D. × 1 mm O.D., respectively. Fig. 2 shows the observed isotachopherogram for the 57.3-$\mu$g sample, where La, Ce, Pr, Nd, Sm, Gd and Y were detected. Twenty-three fractions were obtained in 420 s (19.1 s per fraction) and were analysed by PIXE. Fig. 3 shows the analytical results. In addition to the elements detected by means of ITP, the minor elements Eu, Tb and Dy were also detected.

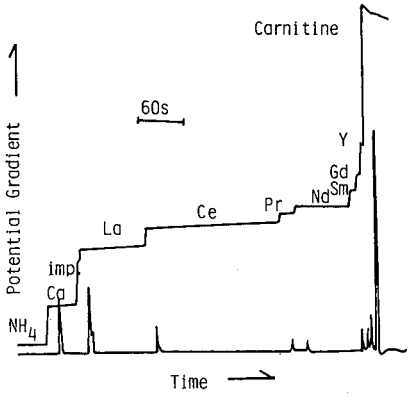


Fig. 2. Observed isotachopherogram of the crude rare earth chloride. The injected sample amount was 57.3 $\mu$g. For electrolyte conditions, see the Table I. Migration current = 150 $\mu$A. Separation stage was used (see Fig. 1). The integrated amount of electricity was 0.603 C.

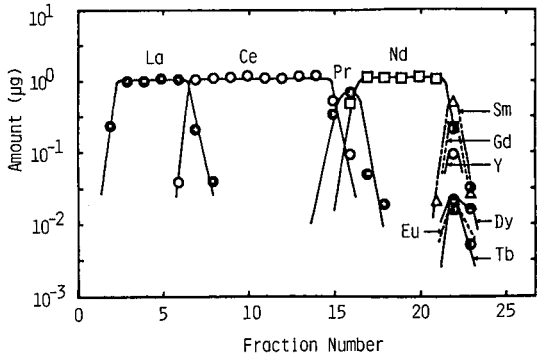


Fig. 3. Analytical results for the 23 fractions by means of PIXE. The corresponding isotachopherogram is shown in Fig. 2. For the operating conditions, see Table I.

The abundances evaluated from PIXE analysis are listed in Table IV.

In order to detect the other trace rare-earth elements, Ho, Er, Tm, Yb and Lu, the sample amount was increased to 1761.6 $\mu$g (sample solution = 200 $\mu$l, total amount of rare earth elements = 638 $\mu$g, *ca.* 4500 nmol). The amount of electricity applied during the separation was *ca.* 10 C. After removing the major elements La, Ce, Pr and part of the Nd zone, the zones containing the other minor elements were fractionated. Fig. 4 shows the observed isotachopherogram. Twenty fractions were obtained in 582 s (29.1 s per fraction). Fig. 5 shows the constituents of the fractions and the amounts evaluated by PIXE. As shown in Fig. 5, even the ultra-trace element Lu was determined. The abundances are summarized in Table IV. As discussed in the previous section, an integrated amount of electricity of 10 C was sufficient to separate Sm–Lu from major light lanthanoids (total ≈ 4500 nmol), although six elements from Dy to Lu were found in the last fraction (No. 20) only.

In order to separate these elements, a 1000-$\mu$l sample solution (total ≈ 8808 $\mu$g, 22 500 nmol) was injected at the preseparation stage. After removing the La, Ce, Pr, Nd, Sm, Eu, Gd, Tb and part of the Dy zones, the remaining zones were fractionated. The abundances of Ho, Er, Tm, Yb and Lu are given in Table IV; these elements were found in the last four fractions.

*PIXE analysis of real sample*

The limitation of the PIXE analysis itself was

TABLE IV

ABUNDANCE (%) OF THE CRUDE RARE EARTH CHLORIDES EVALUATED BY ITP–PIXE AND COMPARISON WITH OTHER METHODS

| Rare earth | ITP–PIXE | | | PIXE: 2.936 μg[a] | ICP-AES |
|---|---|---|---|---|---|
| | 57.3 μg[a] | 1762 μg[a] | 8808 μg[a] | | |
| TRE[b] | 36.20 ± 0.34[c] | 36.20 ± 0.34 | – | 37.4 ± 1.36 | – |
| La/TRE | 23.08 ± 0.11 | – | – | 22.8 ± 0.43 | 23.1 ± 0.4 |
| Ce/TRE | 47.43 ± 0.28 | – | – | 47.0 ± 0.71 | 47.8 ± 0.4 |
| Pr/TRE | 5.54 ± 0.06 | – | – | 5.40 ± 0.21 | 5.68 ± 0.13 |
| Nd/TRE | 19.57 ± 0.15 | – | – | 18.5 ± 0.43 | 19.7 ± 0.3 |
| Sm/TRE | 2.78 ± 0.04 | 2.61 ± 0.01 | – | 2.74 ± 0.16 | 2.74 ± 0.16 |
| Eu/TRE | 0.07 ± $5 \cdot 10^{-3}$ | 0.026 ± $1 \cdot 10^{-3}$ | – | 0.64 ± 0.08 | 0.022 ± $1 \cdot 10^{-3}$ |
| Gd/TRE | 1.19 ± 0.024 | 1.12 ± $7 \cdot 10^{-3}$ | – | 1.46 ± 0.13 | 1.07 ± 0.01 |
| Tb/TRE | 0.10 ± $5 \cdot 10^{-3}$ | 0.082 ± $1 \cdot 10^{-3}$ | – | 0.41 ± 0.07 | 0.15 ± $3 \cdot 10^{-3}$ |
| Dy/TRE | 0.18 ± 0.01 | 0.20 ± $7 \cdot 10^{-3}$ | – | 0.27 ± 0.06 | 0.23 ± $5 \cdot 10^{-3}$ |
| Ho/TRE | – | 0.019 ± $7 \cdot 10^{-4}$ | 0.016 ± $3 \cdot 10^{-4}$ | – | 0.029 ± $1 \cdot 10^{-3}$ |
| Er/TRE | – | 0.022 ± $2 \cdot 10^{-4}$ | 0.019 ± $6 \cdot 10^{-5}$ | – | 0.025 ± $5 \cdot 10^{-4}$ |
| Tm/TRE | – | 0.002 ± $3 \cdot 10^{-4}$ | 0.002 ± $6 \cdot 10^{-5}$ | – | 0.015 ± $2 \cdot 10^{-3}$ |
| Yb/TRE | – | 0.006 ± $5 \cdot 10^{-4}$ | 0.004 ± $2 \cdot 10^{-4}$ | – | 0.006 ± $3 \cdot 10^{-4}$ |
| Lu/TRE | – | 0.001 ± $2 \cdot 10^{-4}$ | 0.001 ± $6 \cdot 10^{-5}$ | – | 0.001 ± $5 \cdot 10^{-4}$ |
| Y/TRE | 0.45 ± 0.08 | 0.507 ± 0.02 | – | – | 0.438 ± 0.021 |

[a] Analysed sample amount.
[b] Total amount of rare earth elements.
[c] PIXE standard deviation estimated from counts.

demonstrated with the present sample. A PIXE spectrum was obtained for 2.936 μg of crude rare earth chloride (5 μl, 0.5872 g/l). By analysing the spectra using the computer program PIXS [13], La, Ce, Pr, Nd, Sm, Eu, Gd, Tb, Dy and Y were determined. The other minor rare-earth elements could not be detected owing to the limitation of deconvolution technique. The quantitative results are given in Table IV. The evaluated abundances of La, Ce, Pr, Nd, Sm and Gd agreed well with the

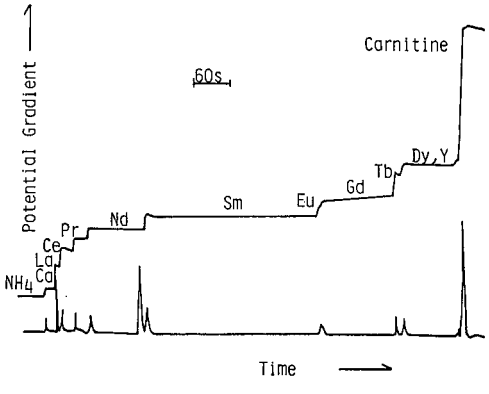


Fig. 4. Observed isotachopherogram of the crude rare earth chloride (1762 μg). The total amount of rare earth elements was 638 μg. Preseparation stage was used. For the operating conditions, see Table I.

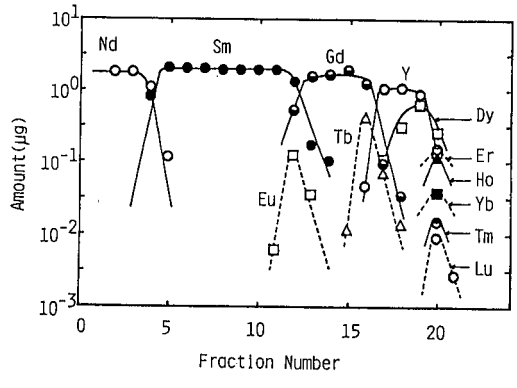


Fig. 5. Analytical results for the 21 fractions by means of PIXE. The corresponding isotachopherogram is shown in Fig. 4. The integrated amount of electricity was *ca.* 10 C.

values obtained by ITP–PIXE, except for Eu, Tb and Dy. Apparently from the results, it was necessary to remove the major elements by ITP in order to determine subsequently these elements, the abundances of which were lower than 1%.

*Analytical results by ICP-AES and comparison between ITP–PIXE and ICP-AES methods*

Table IV also summarizes the abundances of the lanthanoids evaluated by ICP-AES. The total concentration of sample solution was 8.808 g/l for the determination of ultra-trace Lu, 3.523 g/l for Yb, 0.8808 g/l for Eu, Gd, Tb, Dy, Ho, Er, Tm and Y, 0.1762 g/l for Sm, 0.04404 g/l for La, Pr and Nd, and 0.01762 g/l for Ce. Good agreement was obtained between the values obtained by ITP–PIXE and ICP-AES, except for Tb, Ho and Tm. The latter slight disagreement might be due to the overlap of the analysed spectral lines with weak lines of the major elements. Boumans *et al.* [15,16,17] have described the mutual interference among rare earth elements in ICP-AES analysis.

Fig. 6 shows the distributions of rare earth elements contained in the crude rare earth chloride from monazite which were determined by ITP–PIXE and ICP-AES. The abundances were normalized to the Ce abundance being 100%. It is well known that the natural abundance of the earth elements in their ores such as monazite should contain the whole range of rare earth elements except for the radioactive element Pm, even though some elements are present in extreme trace amounts. Also, the abundance of the elements with even atomic number should be greater than those of the neighbouring elements with odd atomic number [5]. The present results confirmed the higher accuracy of ITP–PIXE than ICP-AES, suggesting that a preseparation technique would also be necessary to obtain a higher accuracy in ICP-AES analysis.

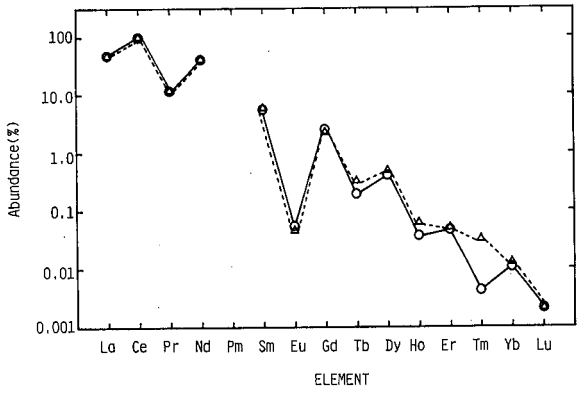


Fig. 6. Distribution of rare earth elements contained in the crude rare earth chloride from monazite. The Ce abundance was normalized as 100%. Solid line, results obtained by ITP–PIXE; dashed line, results obtained by ICP-AES.

This work confirms the analytical utility of the ITP–PIXE method. The method combines the high separability of ITP and the high sensitivity, multi-element capacity and small sample size of PIXE [12]. More complex mixtures can be analysed by ITP–PIXE. Another application to a model solution of nuclear fuel cycle waste will be published in due course.

REFERENCES

1 T. Hirokawa, A. Omori, Y. Yokota, J. Hu and Y. Kiso, *J. Chromatogr.*, 585 (1991) 297.
2 F. M. Everaerts, J. L. Beckers and Th. P. E. M. Verheggen, *Isotachophoresis —Theory, Instrumentation and Applications*, Elsevier, Amsterdam, 1976.
3 P. Bocek, M. Deml, P. Gebauer and V. Dolnik, *Analytical Isotachophoresis*, VCH, Weinheim, 1988.
4 T. Hirokawa, Y. Yokota and Y. Kiso, *J. Chromatogr.*, 545 (1991) 267.
5 N. E. Topp, *Chemistry of the Rare-Earth Elements*, Elsevier, Amsterdam, 1965.
6 J. Hu, T. Hirokawa, F. Nishiyama and Y. Kiso, *J. Chromatogr.*, 589 (1991) 339.
7 I. Nukatsuka, M. Taga and H. Yoshida, *J. Chromatogr.*, 205 (1981) 95.
8 T. Hirokawa, N. Aoki and Y. Kiso, *J. Chromatogr.*, 312 (1984) 11.
9 P. Bocek and F. Foret, *J. Chromatogr.*, 313 (1984) 189.
10 T. Hirokawa, J. Hu, K. Umeda, G. Kimra, H. Ikeda, F. Nishiyama and Y. Kiso, *J. Chromatogr.*, 513 (1990) 297.
11 L. Arlinger, *J. Chromatogr.*, 91 (1974) 829.
12 S. A. E. Johansson and J. L. Campbell, *PIXE, a Novel Technique for Elemental Analysis*, Wiley, Chichester, 1988.
13 T. Hirokawa, F. Nishiyama and Y. Kiso, *Nucl. Instrum. Methods*, B31 (1988) 525.
14 T. Hirokawa, J. Hu, S. Eguchi, F. Nishiyama and Y. Kiso, *J. Chromatogr.*, 538 (1991) 413.
15 P. W. J. M. Boumans, H.-Z. Zhuang, J. J. A. M. Vrakking, J. A. Tielrooy and F. J. M. J. Maessen, *Spectrochim. Acta, Part. B*, 43 (1988) 173.
16 P. W. J. M. Bomans, H.-Z. Zhuang, J. J. A. M. Vrakking, J. A. Tielrooy and F. J. M. J. Maessen, *Spectrochim. Acta, Part B*, 43 (1988) 1365.
17 P. W. J. M. Boumans, H.-Z. Zhuang, J. J. A. M. Vrakking, J. A. Tielrooy and F. J. M. J. Maessen, *Spectrochim. Acta, Part B*, 44 (1989) 31.

*Journal of Chromatography*, 594 (1992) 379–385
Elsevier Science Publishers B.V., Amsterdam

CHROM. 23 854

# Quantitative separation of $Cr^{3+}$ from $Mo^{6+}$, $W^{6+}$, $Hg_2^{2+}$, $Cu^{2+}$ and $Pb^{2+}$

# Chromatographic behaviour of 51 cations on papers impregnated with Sn(IV)-based inorganic ion exchangers in complex-forming acid systems

Surendra Dutt Sharma* and Smiti Misra

*Analytical Research Laboratory, Department of Chemistry, Hindu College, B-3, Jigar Colony, Moradabad-244001 (India)*

(First received July 19th, 1991; revised manuscript received November 6th, 1991)

ABSTRACT

The chromatographic behaviour of 51 metal ions was studied on tin(IV) arsenate-, tin(IV) phosphate-, tin(IV) tungstate-, tin(IV) molybdate- and tin(IV) selenite-impregnated papers in 0.5 *M* oxalic, citric and tartaric acid media. The composition and ion-exchange capacity of these papers were determined. The concentration of the anion in the exchanger deposited was found to vary directly with the $pK_a$ of the corresponding anionic acids. The selectivity of the papers for different cations is discussed. The mechanism of migration is explained in terms of ion exchange, precipitation and adsorption. A published view on the prediction of elution sequence from $R_F$ values was also checked. A number of binary and ternary separations were achieved. $Cr^{3+}$ was quantitatively separated from binary mixtures and from synthetic mixtures containing common interfering metals.

## INTRODUCTION

Chromatography of metal ions on papers impregnated with tin(IV)-based inorganic ion exchangers offers interesting separation possibilities [1–10]. These papers are highly selective and give rapid separations with simple aqueous systems. Recently, ion-exchange chromatographic separations of some anions on hydrated tin(IV) oxide-impregnated papers were also reported [11]. However, the methods of preparation of these papers by different workers during the last two decades have not always been the same and the chemical composition of the material loaded on the strips was not determined. It is important that the various ion-exchange papers should be prepared again under similar experimental conditions, their compositions determined and their selectivities for metal ions studied.

Another limitation in the earlier studies was the selection of solvents. In most instances, the non-complexing substance was used as a developer. To enhance the separation potential of these papers, it is therefore desirable to combine complexation with ion exchange. In this paper we show that the combination of these processes leads to excellent separation possibilities.

The exchangers based on tin(IV) were used to impregnate the papers owing to their high chemical stability and good ion-exchange capacity [12–16]. As these exchangers show high selectivity at low pH and decompose at high pH, weak acids were chosen as solvents so as to prevent the hydrolysis of the exchange materials. The complexing acids chosen

0021-9673/92/$05.00 

were oxalic, citric and tartaric acid. As as result, some analytically important separations were achieved, *e.g.*, $Cr^{3+}$ was quantitatively separated from $Mo^{6+}$, $W^{6+}$ and other metal ions.

## EXPERIMENTAL

### *Apparatus*

Chromatography was performed on 15 × 3.5 cm Whatman No.1 paper strips in 20 × 5 cm glass jars. A Bausch and Lomb Spectronic-20 instrument was used for colorimetry.

### *Reagents*

Tin(IV) chloride pentahydrate was used. All other chemicals and solvents used were of analytical-reagent grade from BDH.

### *Preparation of ion-exchange papers*

Papers impregnated with tin(IV)-based inorganic ion exchangers were prepared in the same manner as the tin(IV) arsenate-impregnated papers reported previously [6].

### *Test solutions and detectors*

The test solutions were generally 0.1 *M* in the metal nitrate or chloride and were prepared as described previously [5]. Conventional spot test reagents were used for detection purposes.

### *Procedure*

*Chromatography.* Chromatography was performed as described previously [5].

*Composition of paper.* Impregnated paper strips for each exchanger were separately dissolved in $HClO_4$–$HNO_3$–$H_2SO_4$ (3:1:4) and the solution was evaporated to dryness. The residue was dissolved in 4 *M* hydrochloric acid and the solution was diluted to 50 ml in each instance. The tin and the anion present were determined by methods reported previously [12–16].

*Quantitative work.* A $5 \cdot 10^4$ μg/ml stock solution of chromium chloride was prepared, then diluted 200-fold. A 20-μl volume of the solution containing 5 μg of $Cr^{3+}$ was then applied on to tin(IV) phosphate papers with the help of a lambda pipette. The other cations to be separated were also applied in the amounts shown in Table V. The strips were dried in air and saturated for 10 min with the developer and were then developed in 0.5 *M* oxalic acid until the solvent had ascended 11 cm. A pilot paper for each separation was run simultaneously in order to locate the exact position of the $Cr^{3+}$ spot with the help of a colour agent. The area on the working strip was cut into small pieces and chromium was eluted with 0.25 *M* $H_2SO_4$ at room temperature. The volume of solution was reduced by heating on a hot-plate. The paper pulp was oxidized with $HNO_3$–$HClO_4$–$H_2SO_4$ (1:3:2). The solution was then evaporated to 10 ml, cooled and 0.5 ml of 0.1 *M* $KMnO_4$ was added to oxidize [17] $Cr^{3+}$ to $Cr^{6+}$. Five drops of 5% sodium azide solution were added to decolorize the brownish tint. The solution was transfered to a 25-ml volumetric flask and 1 ml of diphenyl carbazide solution was added followed by 2 ml of $NaH_2PO_4$ solution. The blank was run in a similar way by following the entire procedure for an unspotted paper strip. The absorbance of this colour was measured at 540 nm and the amount of $Cr^{3+}$ was obtained from a calibration graph [18].

TABLE I

COMPOSITION AND ION-EXCHANGE CAPACITY OF TIN(IV)-BASED ION-EXCHANGE PAPERS

| Paper impregnated with | Concentration of reagents (*M*) | | Anion:Sn ratio | Ion-exchange capacity of impregnated papers (mequiv./g) |
|---|---|---|---|---|
| | Tin(IV) chloride pentahydrate | Sodium salt of anion | | |
| Tin(IV) arsenate | 0.10 | 0.25 | 2.15:1 | 0.38 |
| Tin(IV) molybdate | 0.10 | 0.25 | 2.75:1 | 0.40 |
| Tin(IV) phosphate | 0.10 | 0.10 | 1.44:1 | 0.34 |
| Tin(IV) tungstate | 0.10 | 0.20 | 4.8:1 | 0.30 |
| Tin(IV) selenite | 0.10 | 0.20 | 2.2:1 | 0.32 |

TABLE II

$R_F$ VALUES OF CATIONS ON TIN(IV)-BASED ION-EXCHANGE PAPERS IN COMPLEX-FORMING ACID SYSTEMS

| Cation | Tin(IV) arsenate | | | Tin(IV) phosphate | | | Tin(IV) molybdate | | | Tin(IV) tungstate | | | Tin(IV) selenite | | | Whatman No.1 | | |
|---|---|---|---|---|---|---|---|---|---|---|---|---|---|---|---|---|---|---|
| | $S_1$ | $S_2$ | $S_3$ | $S_1$ | $S_2$ | $S_3$ | $S_1$ | $S_2$ | $S_3$ | $S_1$ | $S_2$ | $S_3$ | $S_1$ | $S_2$ | $S_3$ | $S_1$ | $S_2$ | $S_3$ |
| $Ag^+$ | 0.00 | 0.00 | 0.00 | 0.00 | 0.00 | 0.00 | 0.00 | 0.00 | 0.00 | 0.00 | 0.00 | 0.00 | 0.00 | 0.00 | 0.00 | 0.00 | 0.00 | 0.00 |
| $Pb^{2+}$ | 0.00 | 0.05 | 0.11 | 0.03 | 0.14 | 0.14 | 0.81 | 0.02 | 0.30 | 0.04 | 0.04 | 0.11 | 0.05 | 0.02 | 0.30 | 0.06 | 0.90 | 0.95 |
| $Hg_2^{2+}$ | 0.68 | 0.66 | 0.76 | 0.03 | 0.71 | 0.78 | 0.80 | 0.84 | 0.87 | 0.06 | 0.00 | 0.00 | 0.15 | 0.90 | 0.80 | 0.00 | 0.72 | 0.00 |
| $Hg^{2+}$ | 0.95 | 0.65 | 0.80 | 0.85 | 0.75 | 0.76 | 0.87 | 0.76 | 0.81 | 0.82 | 0.82 | 0.86 | 0.72 | 0.74 | 0.75 | 0.00 | 0.00 | 0.00 |
| $Bi^{3+}$ | 0.50 | 0.30 | 0.07 | 0.11 | 0.75 | 0.12 | 0.90 | 0.37 | 0.17 | 0.77 | 0.07 | 0.94 | 0.25 | 0.34 | 0.32 | 0.07 | 0.95 | 0.95 |
| $Sb^{3+}$ | N.D.[a] | 0.78 | N.D. | N.D. | N.D. | 0.00 | 0.04 | 0.92 | 0.93 | N.D. | N.D. | N.D. | N.D. | N.D. | N.D. | N.D. | 0.00 | 0.00 |
| $Pd^{2+}$ | 0.91 | 0.75 | 0.82 | 0.86 | 0.93 | 0.90 | 0.84 | 0.87 | 0.92 | 0.82 | 0.86 | 0.87 | 0.87 | 0.85 | 0.90 | 0.90 | 0.90 | 0.95 |
| $Pd^{4+}$ | 0.77 | 0.81 | 0.80 | 0.10 | 0.41 | 0.80 | 0.83 | 0.87 | 0.94 | 0.86 | 0.95 | 0.81 | 0.82 | 0.85 | 0.85 | 0.84 | 0.04 | 0.00 |
| $Tl^+$ | 0.54 | 0.72 | 0.52 | 0.69 | 0.42 | 0.37 | 0.73 | 0.54 | 0.56 | 0.04 | 0.17 | 0.06 | 0.74 | 0.74 | 0.72 | 0.91 | 0.82 | 0.90 |
| $Cd^{2+}$ | 0.94 | 0.86 | 0.57 | 0.89 | 0.74 | 0.61 | 0.87 | 0.90 | 0.84 | 0.94 | 0.91 | 0.96 | 0.85 | 0.85 | 0.90 | 0.96 | 0.95 | 0.97 |
| $Fe^{2+}$ | 0.77 | 0.94 | 0.44 | 0.81 | 0.65 | 0.85 | 0.83 | 0.93 | 0.86 | 0.68 | 0.82 | 0.72 | 0.98 | 0.85 | 0.77 | 0.00 | 0.94 | 0.96 |
| $Fe^{3+}$ | 0.75 | 0.06 | 0.13 | 0.85 | T[b] | T | 0.83 | 0.92 | 0.77 | 0.70 | 0.12 | 0.10 | 0.98 | 0.74 | 0.61 | 1.00 | 0.92 | 0.98 |
| $UO_2^{2+}$ | 0.84 | 0.29 | 0.15 | 0.82 | T | T | 0.92 | 0.90 | 0.81 | 0.73 | 0.46 | 0.24 | 0.95 | 0.45 | 0.32 | 1.00 | 0.95 | 0.98 |
| $VO^{2+}$ | 0.80 | 0.89 | 0.84 | 0.86 | 0.79 | 0.82 | 0.90 | 0.83 | 0.90 | 0.91 | 0.82 | 0.89 | 0.95 | 0.92 | 0.93 | 1.00 | 0.95 | 0.98 |
| $Ir^{3+}$ | 0.91 | 0.96 | 0.98 | 0.93 | 0.98 | 0.84 | 0.75 | 0.93 | 0.95 | 0.69 | 0.95 | 0.86 | 0.95 | 0.95 | 0.92 | 1.00 | 0.98 | 0.98 |
| $Zn^{2+}$ | 0.86 | 0.81 | 0.69 | 0.95 | 0.80 | 0.88 | 0.80 | 0.90 | 0.86 | 0.70 | 0.95 | 0.87 | 0.97 | 0.95 | 0.93 | 1.00 | 0.98 | 0.98 |
| $Mn^{2+}$ | 0.72 | 0.78 | 0.98 | 0.95 | 0.82 | 0.83 | 0.85 | 0.88 | 0.75 | 0.91 | 0.92 | 0.93 | 0.95 | 0.95 | 0.92 | 1.00 | 0.98 | 0.98 |
| $Cr^{3+}$ | 0.90 | 0.94 | 0.66 | 0.90 | 0.83 | 0.87 | 0.77 | 0.91 | 0.85 | 0.80 | 0.97 | 0.89 | 0.97 | 0.90 | 0.92 | 1.00 | 0.98 | 0.98 |
| $La^{3+}$ | 0.91 | 0.96 | 0.94 | 0.93 | 0.78 | T | 0.84 | 0.84 | 0.92 | 0.93 | 0.80 | 0.20 | 0.94 | 0.85 | 0.81 | 0.97 | 0.95 | 0.97 |
| $Y^{3+}$ | 0.86 | 0.71 | 0.95 | 0.88 | 0.04 | 0.07 | 0.75 | 0.95 | 0.68 | 0.95 | 0.50 | 0.19 | 0.97 | 0.95 | 0.92 | 0.97 | 0.95 | 0.95 |
| $Pr^{3+}$ | 0.95 | 0.88 | 0.70 | 0.10 | 0.32 | 0.34 | 0.82 | 0.85 | 0.89 | 0.98 | 0.57 | 0.21 | 0.10 | 0.64 | 0.87 | 0.00 | 0.96 | 0.97 |
| $Nb^{5+}$ | 0.88 | 0.98 | 0.87 | 0.89 | 0.86 | 0.84 | 0.80 | 0.92 | 0.83 | 0.95 | 0.81 | 0.91 | 0.92 | 0.85 | 0.85 | 0.97 | 0.95 | 0.95 |
| $Ce^{3+}$ | 0.95 | 0.50 | 0.92 | 0.06 | 0.20 | 0.25 | 0.86 | 0.93 | 0.80 | 0.91 | 0.25 | 0.09 | 0.95 | 0.92 | 0.94 | 0.00 | 0.95 | 0.95 |
| $Ce^{4+}$ | 0.84 | 0.45 | 0.93 | 0.96 | 0.15 | 0.17 | 0.81 | 0.63 | 0.85 | 0.95 | 0.28 | 0.24 | 0.00 | N.D. | N.D. | 0.00 | 0.95 | 0.95 |
| $Zr^{4+}$ | 0.92 | 0.96 | 0.79 | T | T | 0.00 | 0.54 | 0.90 | 0.82 | 0.97 | 0.75 | 0.10 | 0.45 | N.D. | N.D. | 0.00 | 0.94 | 0.95 |
| $Rh^{3+}$ | 0.95 | N.D. | 0.93 | 0.77 | N.D. | 0.43 | 0.86 | 0.92 | 0.92 | 0.87 | 0.88 | 0.83 | 0.90 | 0.87 | 0.97 | 0.97 | 0.95 | 0.97 |
| $Ta^{5+}$ | 0.92 | 0.83 | 0.87 | 0.92 | 0.95 | 0.96 | 0.75 | 0.94 | 0.86 | 0.95 | 0.83 | 0.86 | 0.98 | 0.92 | 0.92 | 0.97 | 0.95 | 0.95 |
| $Cu^{2+}$ | 0.95 | 0.69 | 0.77 | 0.02 | 0.55 | 0.73 | 0.76 | 0.87 | 0.95 | 0.02 | 0.70 | 0.87 | 0.70 | 0.85 | 0.83 | 0.05 | 0.95 | 0.98 |
| $Gd^{3+}$ | N.D. | N.D. | N.D. | N.D. | 0.15 | 0.15 | 0.30 | 0.83 | 0.77 | 0.00 | 0.39 | 0.12 | 0.10 | 0.85 | 0.79 | 0.97 | 0.96 | 0.95 |
| $In^{3+}$ | 0.92 | 0.94 | 0.95 | 0.87 | 0.07 | 0.09 | 0.86 | 0.92 | 0.92 | 0.87 | 0.80 | 0.86 | 0.75 | 0.85 | 0.85 | 0.97 | 0.95 | 0.95 |
| $Ru^{3+}$ | 0.88 | 0.87 | 0.87 | 0.90 | 0.80 | 0.72 | 0.89 | 0.76 | 0.88 | 0.79 | 0.91 | 0.81 | 0.95 | 0.95 | 0.95 | 0.97 | 0.95 | 0.97 |
| $Th^{4+}$ | 0.94 | 0.80 | 0.84 | 0.17 | T | 0.20 | 0.11 | 0.74 | 0.58 | 0.10 | 0.27 | 0.18 | 0.60 | 0.75 | 0.77 | 0.20 | 0.95 | 0.95 |
| $Ti^{4+}$ | 0.33 | 0.93 | 0.27 | N.D. | 0.75 | 0.12 | N.D. | 0.92 | 0.91 | 0.88 | 0.51 | 0.97 | N.D. | 0.20 | 0.20 | T | 0.02 | 0.97 |
| $Au^{3+}$ | 0.60 | 0.31 | 0.63 | 0.51 | 0.70 | 0.61 | 0.61 | 0.55 | 0.61 | 0.54 | 0.66 | 0.70 | 0.30 | 0.45 | 0.70 | 0.20 | 0.00 | 0.50 |
| $Pt^{4+}$ | 0.98 | 0.82 | 0.95 | 0.87 | 0.98 | 0.92 | 0.00 | 0.75 | 0.82 | 0.73 | 0.91 | 0.84 | N.D. | N.D. | 0.88 | 0.93 | 0.98 | 0.95 |
| $W^{6+}$ | 0.98 | 0.98 | 0.98 | 0.00 | 0.98 | 0.98 | N.D. | 0.87 | 0.88 | N.D. | N.D. | N.D. | N.D. | N.D. | N.D. | N.D. | 0.98 | 0.95 |
| $Mo^{6+}$ | 0.92 | 0.98 | 0.95 | 0.00 | 0.00 | 0.00 | N.D. | N.D. | N.D. | 0.73 | 0.81 | 0.90 | N.D. | N.D. | N.D. | 0.05 | 0.98 | 0.95 |
| $Se^{4+}$ | 0.85 | 0.78 | 0.80 | 0.93 | 0.79 | 0.67 | N.D. | 0.32 | 0.37 | 0.61 | 0.13 | 0.52 | N.D. | N.D. | N.D. | 0.93 | 0.98 | 0.95 |
| $Te^{4+}$ | 0.95 | 0.33 | 0.81 | 0.15 | 0.07 | 0.12 | 0.40 | 0.08 | 0.06 | 0.05 | 0.00 | 0.05 | N.D. | N.D. | N.D. | 0.95 | 9.90 | 9.92 |
| $Mg^{2+}$ | 0.75 | 0.80 | 0.79 | 0.85 | 0.87 | 0.63 | 0.65 | 0.83 | 0.90 | 0.67 | 0.78 | 0.64 | 0.77 | 0.85 | 0.80 | 0.80 | 0.93 | 0.93 |
| $Be^{2+}$ | 0.90 | 0.64 | 0.23 | 0.61 | 0.10 | 0.10 | 0.90 | 0.86 | 0.90 | 0.89 | 0.98 | 0.91 | 0.98 | 0.94 | 0.93 | 1.00 | 0.96 | 0.97 |
| $Al^{3+}$ | 0.97 | 0.22 | 0.10 | 0.55 | 0.16 | 0.16 | 0.91 | 0.88 | 0.79 | 0.95 | 0.98 | 0.94 | 0.94 | 0.95 | 0.85 | 1.00 | 0.95 | 0.96 |
| $Ga^{3+}$ | 0.94 | 0.82 | 0.77 | 0.19 | 0.82 | 0.32 | 0.92 | 0.92 | 0.93 | 0.92 | 0.98 | 0.70 | 0.98 | 0.95 | 0.85 | 1.00 | 0.95 | 0.97 |
| $K^+$ | 0.92 | 0.72 | 0.80 | 0.92 | 0.83 | 0.85 | 0.79 | 0.83 | 0.92 | 0.75 | 0.86 | 0.72 | 0.95 | 0.95 | 0.84 | 0.95 | 0.98 | 0.98 |
| $Rb^+$ | 0.95 | 0.93 | 0.51 | 0.81 | 0.80 | 0.86 | 0.66 | 0.90 | 0.81 | 0.71 | 0.75 | 0.75 | 0.93 | 0.95 | 0.82 | 0.95 | 0.98 | 0.98 |
| $Cs^+$ | 0.95 | 0.92 | 0.73 | 0.87 | 0.74 | 0.78 | 0.69 | 0.90 | 0.92 | 0.42 | 0.50 | 0.40 | 0.95 | 0.95 | 0.84 | 0.95 | 0.98 | 0.98 |
| $Ba^{2+}$ | 0.44 | 0.43 | 0.86 | T | 0.72 | 0.61 | 0.44 | N.D. | N.D. | 0.44 | 0.65 | 0.26 | 0.83 | 0.94 | 0.83 | 1.00 | 0.96 | 0.95 |
| $Sr^{2+}$ | 0.95 | 0.92 | 0.93 | 0.08 | 0.82 | 0.87 | N.D. | N.D. | N.D. | 0.89 | 0.91 | 0.98 | 0.93 | 0.90 | 0.90 | 1.00 | 0.95 | 0.95 |
| $Ni^{2+}$ | 0.98 | 0.94 | 0.84 | 0.77 | 0.98 | 0.95 | 0.91 | 0.97 | N.D. | 0.83 | 0.82 | 0.66 | 0.78 | 0.75 | 0.72 | 1.00 | 0.95 | 0.95 |
| $Co^{2+}$ | 0.98 | 0.92 | 0.73 | 0.92 | 0.95 | 0.82 | 0.83 | 0.82 | 0.89 | 0.79 | 0.85 | 0.87 | 0.95 | 0.92 | 0.89 | 1.00 | 0.95 | 0.97 |
| $Ca^{2+}$ | 0.92 | 0.95 | 0.89 | 0.92 | 0.92 | 0.90 | 0.84 | 0.91 | 0.90 | 0.88 | 0.90 | 0.80 | N.D. | N.D. | N.D. | 1.00 | 0.95 | 0.95 |

[a] N.D. = Not detected.
[b] T = Tailing.

TABLE III

PRECIPITATION OF CATIONS IN MIXTURES OF SOLVENT AND IMPREGNATING MATERIAL

| Solvent | Cations + solvent | | Cations + sodium arsenate + solvent | | Cations + sodium molybdate + solvent | | Cations + sodium phosphate + solvent | | Cations + sodium tungstate + solvent | | Cations + sodium selenite + solvent | |
|---|---|---|---|---|---|---|---|---|---|---|---|---|
| | P[a] | NP[b] | P | NP | P | NP | P | NP | P | NP | P | NP |
| 0.5 *M* citric acid | None | $Hg^{2+}$,$Ti^{4+}$, $Pd^{4+}$,$Ag^{+}$, $Sb^{3+}$ | $Ag^{+}$,$Pb^{2+}$ | None | $Pb^{2+}$ | $Ag^{+}$, | NIL | $Ag^{+}$,$Mo^{6+}$ | $Pb^{2+}$ | $Ag^{+}$, $Hg_2^{2+}$ $Te^{4+}$ | $Ag^{+}$ | None |
| 0.5 *M* tartaric acid | None | $Ag^{+}$,$Sb^{3+}$ $Hg_2^{2+}$,$Hg^{2+}$ | $Ag^{+}$ | None | None | $Ag^{+}$,$Te^{4+}$ | $Zr^{4+}$ | $Ag^{+}$,$Mo^{6+}$ | None | $Ag^{+}$ $Hg_2^{2+}$ | $Ag^{+}$ | None |
| 0.5 *M* oxalic acid | $Cu^{2+}$,$Hg_2^{2+}$, $Hg^{2+}$,$Pb^{2+}$, $Ce^{3+}$,$Pr^{3}$, $Ce^{4+}$,$Th^{4+}$ | $Ag^{+}$,$Fe^{2+}$, $Zr^{4+}$ | $Ag^{+}$,$Pb^{2+}$ | None | None | $Ag^{+}$,$Sb^{3+}$, $Pt^{4+}$ | $Ag^{+}$,$Pb^{2+}$, $Zr^{4+}$,$W^{6+}$ | $Mo^{6+}$ | $Pb^{2+}$, $Cu^{2+}$,$Tl^{+}$ | $Ag^{+}$ | $Ag^{+}$,$Ce^{4+}$ | None |

[a] P = Cations that precipitate.
[b] NP = Cations that do not precipitate.

## RESULTS AND DISCUSSION

The anion:Sn ratios of the exchangers deposited on paper and the ion-exchange capacity of the treated papers are given in Table I. Chromatography was performed on tin (IV) arsenate-, tin (IV) molybdate-, tin (IV) phosphate-, tin (IV) tungstate- and tin (IV) selenite-impregnated papers in the following solvents: $S_1$, 0.5 *M* oxalic acid; $S_2$, 0.5 *M* citric acid; and $S_3$, 0.5 *M* tartaric acid. The same solvents were used for Whatman No.1 papers for comparison.

In many instances it was found possible to separate one cation from numerous metal ions. The $R_F$ values are summarized in Table II. Some useful separations were also achieved on plain papers.

Table I summarizes the composition studies on impregnated papers. A plot of anion:Sn ratio *versus* $pK_a$ of anionic acids for all the impregnated papers reveals that the concentration of the anion in the exchanger deposited varies directly with the $pK_a$ of the corresponding anionic acids (Fig. 1).

In order to study the effect of impregnation, the value of $R_i$ ($= R_F$ on Whatman No.1 papers $- R_F$ on impregnated papers) for all cations were calculated. For the cations having $R_i > 0.4$, the following conclusions can be drawn.

(1) Tin(IV) arsenate-impregnated papers in 0.5 *M* tartaric acid media are selective for $Rb^+$, $Cd^{2+}$, $Pb^{2+}$, $Bi^{3+}$, $UO_2^{2+}$, $Fe^{2+}$, $Fe^{3+}$, $Be^{2+}$ and $Al^{3+}$ owing to the higher adsorption on these papers.

(2) With tin(IV) phosphate-impregnated papers, $Be^{2+}$, $Y^{3+}$, $Rh^{3+}$ and $Ti^{4+}$ in 0.5 *M* tartaric acid, $Ba^{2+}$, $Sr^{2+}$, $Ce^{3+}$, $Pr^{3+}$ and $Ga^{3+}$ in 0.5 *M* oxalic acid and $In^{3+}$, $Zr^{4+}$ and $Th^{4+}$ in 0.5 *M* citric acid media are selectively adsorbed.

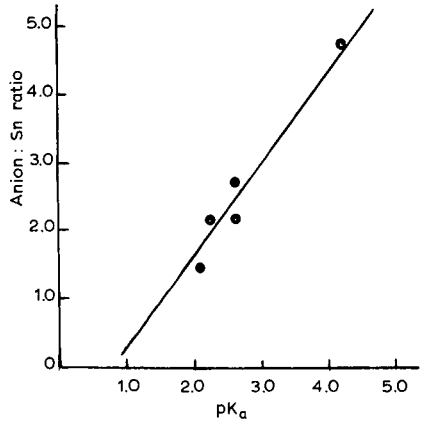


Fig. 1. Plot of anion:Sn ratio *versus* $pK_a$ for anionic acids.

(3) On tin(IV) tungstate-impregnated papers, $Cs^+$, $Pb^{2+}$, $Tl^+$, $La^{3+}$ and $Zr^{4+}$ in 0.5 *M* tartaric acid, $Se^{4+}$ and $Te^{4+}$ in 0.5 *M* citric acid and $Gd^{3+}$ in 0.5 *M* oxalic acid media show a high degree of adsorption.

(4) In 0.5 *M* oxalic acid media, tin(IV) selenite-impregnated papers are highly selective for $Pr^{3+}$ whereas tin(IV) molybdate-impregnated papers selectively adsorb $Pt^{4+}$.

The zero $R_F$ for a number of cations on impregnated papers may be due to precipitation, ion exchange and strong adsorption owing to the high charge. On mixing solutions of the cations with oxalic acid, it was found that with $Cu^{2+}$, $Hg_2^{2+}$ $Hg^{2+}$, $Pb^{2+}$, $Pr^{3+}$, $Ce^{3+}$, $Ce^{4+}$ and $Th^{4+}$ a precipitate was obtained. In such instances, the zero $R_F$ on plain papers is therefore due to the precipitation mechanism. On mixing with citric and tartaric acid, no ion was precipitated. The zero $R_F$ on plain papers in these solvents may be due to interaction with the paper matrix, as in the case of $Ag^+$ and $Sb^{3+}$. For $Zr^{4+}$, $Ti^{4+}$ and $Pd^{4+}$, the zero $R_F$ may be due to the strong adsorption owing to the high charge. In order to simulate conditions on impregnated papers, the sodium salt of the anion was added to the cation solution followed by the solvent. A number of ions precipitated under these conditions (see Table III). In these instances also the precipitation mechanism holds good.

The chromatographic behaviour of metal ions on ion-exchange columns and on impregnated papers using the same exchangers is interesting. The $R_F$ values of metal ions are related to their distribution coefficients on tin(IV)-based exchangers. For higher distribution coefficients, we observe lower $R_F$ values. This behaviour is expected because when the $K_d$ is higher, the ion is more strongly held by the ion exchanger and is less easily allowed to move further, giving a lower $R_F$ value. This trend was confirmed by determining the $R_F$ values of some common metal ions on all the impregnated papers in demineralized water. The $K_d$ values for these ions are given for comparison in Table IV, which shows that for most of the cations studied, the sequence of $K_d$ values is the same as that predicted from $R_F$ values. If

TABLE IV

COMPARISON OF $K_d$ VALUES AND $R_F$ VALUES OF SOME IONS ON TIN(IV)-BASED EXCHANGERS

Demineralized water as medium.

| Exchanger | $K_d$ [12–16,19] | $R_F$ |
|---|---|---|
| Tin(IV) arsenate | $Sr^{2+} > Ca^{2+} > Ba^{2+} > Mg^{2+}$<br>$Zn^{2+} > Cd^{2+}$<br>$In^{3+} > Y^{3+} > Al^{3+} > La^{3+} > Ga^{3+}$<br>$Ni^{2+} > Fe^{3+} > Co^{2+} > Pb^{2+} > Cu^{2+} > Mn^{2+}$<br>$Th^{4+} > Zr^{4+}$ | $Mg^{2+} > Ba^{2+} = Sr^{2+} > Ca^{2+}$<br>$Hg^{2+} > Cd^{2+} > Zn^{2+}$<br>$La^{3+} > Y^{3+} > In^{3+} > Al^{3+} > Ga^{3+}$<br>$Cu^{2+} > Co^{2+} > Ni^{2+} > Pb^{2+} Fe^{3+} > Mn^{2+}$<br>$Th^{4+} > Zr^{4+}$ |
| Tin(IV) molybdate | $Ba^{2+} > Sr^{2+} > Ca^{2+} > Mg^{2+}$<br>$Pb^{2+} > Cu^{2+} > Zn^{2+} > Cd^{2+} > Ni^{2+} > Co^{2+}$<br>$Y^{3+} > Al^{3+}$ | $Mg^{2+} > Ca^{2+} > Sr^{2+} > Ba^{2+}$<br>$Co^{2+} > Ni^{2+} > Cd^{2+} > Cu^{2+} > Zn^{2+} > Pb^{2+}$<br>$Al^{3+} > Y^{3+}$ |
| Tin(IV) tungstate | $Ba^{2+} > Sr^{2+} > Mg^{2+}$<br>$Pb^{2+} > Cd^{2+} > Zn^{2+}$<br>$Co^{2+} > Ni^{2+} > Cu^{2+}$ | $Mg^{2+} > Sr^{2+} > Ba^{2+}$<br>$Zn^{2+} > Cd^{2+} > Pb^{2+}$<br>$Cu^{2+} > Ni^{2+} > Co^{2+}$ |
| Tin(IV) phosphate | $Cu^{2+} > Ca^{2+} > Sr^{2+} > Zn^{2+} > Co^{2+}$ | $Cu^{2+} > Co^{2+} > Zn^{2+} > Sr^{2+} > Ca^{2+}$ |
| Tin(IV) selenite | $Ba^{2+} > Sr^{2+} > Ca^{2+} > Mg^{2+}$<br>$Cd^{2+} > Hg^{2+} > Zn^{2+}$<br>$La^{3+} > Y^{3+} > In^{3+} > Ga^{3+} > Al^{3+}$<br>$Cu^{2+} > Ni^{2+} > Pb^{2+} > Co^{2+} > Fe^{3+}$<br>$Zr^{4+} > Th^{4+}$ | $Mg^{2+} > Ca^{2+} > Ba^{2+} > Sr^{2+}$<br>$Zn^{2+} > Cd^{2+} > Hg^{2+}$<br>$Al^{3+} > In^{3+} > Ga^{3+} > Y^{3+} > La^{3+}$<br>$Co^{2+} > Cu^{2+} > Ni^{2+} > Fe^{3+} > Pb^{2+}$<br>$Th^{4+} > Zr^{4+}$ |

it is considered that the elution sequence can be predicted from $K_d$ values, it follows that the $R_F$ values are not reliable for such prediction for the following reasons: in paper chromatography the solvent ascent is too fast to achieve equilibrium; some of the ions definitely interact in a different manner with the paper than with the ion exchanger; and the material obtained by precipitation from solution and that deposited on paper have different compositions. As the $K_d$ values depend on the composition of the material, they are found to be different.

Owing to above facts, the Alberti and Torracca's view [20] that the elution sequence can be predicted from $R_F$ values is not very convincing. At best the $R_F$ values are a rough guide especially when they differ from one another considerably.

On the basis of $R_F$ values, a large number of binary and ternary separations are possible. Some of the important ones actually achieved are as follows:

(a) $Cr^{3+}$–$Mo^{6+}$ or $W^{6+}$, $Ag^{+}$, $Hg_2^{2+}$, $Pb^{2+}$, $Cu^{2+}$, $Ba^{2+}$ or $Sr^{2+}$ [on tin(IV) phosphate paper in 0.5 *M* oxalic acid];

(b) $Ba^{2+}$–$Sr^{2+}$ or $Ca^{2+}$, $Be^{2+}$, $Al^{3+}$, $Hg^{2+}$, $Bi^{3+}$, $Pd^{2+}$, $Pd^{4+}$, $Cd^{2+}$, $Fe^{2+}$, $Mn^{2+}$, $Cr^{3+}$ or $Cu^{2+}$ [on tin(IV) tungstate paper in 0.5 *M* tartaric acid];

(c) $Zr^{4+}$–$Th^{4+}$ or $Gd^{3+}$ or $Te^{4+}$ [on tin(IV) tungstate paper in 0.5 *M* oxalic acid];

(d) $In^{3+}$–$Al^{3+}$ or $Fe^{3+}$, $UO_2^{2+}$, $Ti^{4+}$ or $Be^{2+}$ [on tin(IV) arsenate paper in 0.5 *M* tartaric acid];

(e) $Pb^{2+}$–$UO_2^{2+}$ or $Pd^{4+}$, $Pt^{4+}$, $Tl^{+}$, $Cd^{2+}$, $Fe^{3+}$, $VO^{2+}$, $Zn^{2+}$, $Mn^{2+}$, $Cr^{3+}$ or $Mg^{2+}$ [on Whatman No.1 paper in 0.5 *M* oxalic acid];

(f) $Pb^{2+}$–$Hg^{2+}$–$Bi^{3+}$ and $Ag^{+}$–$Au^{3+}$–$Pt^{4+}$ [on tin(IV) arsenate paper in 0.5 *M* oxalic acid].

The main advantage of this work lies in the fact that $Cr^{3+}$ was quantitatively separated from binary mixtures containing larger amounts of other metal ions such as $Mo^{6+}$, $W^{6+}$, $Ag^{+}$, $Pb^{2+}$, $Cu^{2+}$, $Hg_2^{2+}$, $Ba^{2+}$ and $Sr^{2+}$ (Table V). In order to explore the possible application of the method in a wider field, two synthetic mixtures were prepared by taking $Cr^{3+}$ together with all these metal ions. $Cr^{3+}$ was successfully separated from these mixtures as indicated in Table V. The complex-forming acids were found to be very useful solvents for metal ion separations. Even on Whatman No.1 paper, such important separations such as $Cr^{3+}$–$Mo^{6+}$ (in 0.5 *M* oxalic acid), $Hg_2^{2+}$–$Hg^{2+}$ (in 0.5 *M* citric acid) and $Ti^{4+}$–$Zr^{4+}$ or $La^{3+}$ (in 0.5 *M* citric acid) were achieved.

TABLE V

QUANTITATIVE SEPARATION OF $Cr^{3+}$ IN BINARY AND SYNTHETIC MIXTURES

| Sample No. | Amount of $Cr^{3+}$ loaded ($\mu$g) | Amount of other metal ion loaded ($\mu$g) | Amount of $Cr^{3+}$ found ($\mu$g) | Error (%) |
|---|---|---|---|---|
| 1 | 5.00 | $Ag^{+}$ (340) | 5.00 | 0.00 |
| 2 | 5.00 | $Sr^{2+}$ (423) | 5.40 | −8.00 |
| 3 | 5.00 | $Pb^{2+}$ (662) | 5.00 | 0.00 |
| 4 | 5.00 | $Ba^{2+}$ (522) | 5.30 | −6.00 |
| 5 | 5.00 | $Hg_2^{2+}$ (560) | 5.35 | −7.00 |
| 6 | 5.00 | $Cu^{2+}$ (500) | 5.40 | −8.00 |
| 7 | 5.00 | $Mo^{6+}$ (412) | 5.00 | 0.00 |
| 8 | 5.00 | $W^{6+}$ (660) | 5.00 | 0.00 |
| 9 | 5.00 | Mixture | 5.60 | −12.00 |
| 10 | 5.00 | Mixture | 5.50 | −10.00 |

ACKNOWLEDGEMENT

The authors are grateful to the University Grants Commission, New Delhi (India), for financial assistance.

REFERENCES

1 M. Qureshi and S. Z. Qureshi, *J. Chromatogr.*, 22 (1966) 198.
2 M. Qureshi, K. N. Mathur and A. H. Israili, *Talanta*, 16 (1969) 503.
3 M. Qureshi, I. Akhtar and K. N. Mathur, *Anal. Chem.*, 39 (1967) 1766.
4 M. Qureshi and K. N. Mathur, *Anal. Chim. Acta*, 41 (1963) 560.
5 M. Qureshi and S. D. Sharma, *Anal. Chem.*, 45 (1973) 1283.
6 M. Qureshi and S. D. Sharma, *Talanta*, 22 (1975) 129.
7 M. Qureshi and S. D. Sharma, *Chromatographia*, 11 (1978) 153.
8 M. Qureshi, K. G. Varshney, M. P. Gupta and S. P. Gupta, *Chromatographia*, 10 (1977) 29.
9 M. Qureshi and J. P. Rawat, *Sep. Sci.*, 7 (1972) 297.
10 M. Qureshi, K. G. Varshney and R. P. S. Rajpoot, *Anal. Chem.*, 47 (1975) 1520.
11 S. K. Dabral, K. P. S. Muktawat and J. P. Rawat, *Indian J. Chem.*, Sect. A, 27 (1988) 745.
12 M. Qureshi, R. Kumar and H. S. Rathore, *J. Chem. Soc. A*, 2 (1970) 272.
13 M. Qureshi and J. P. Rawat, *J. Inorg. Nucl. Chem.*, 30 (1968) 305.
14 Y. Inoue, *J. Inorg. Nucl. Chem.*, 26 (1964) 2241.
15 M. Qureshi and K. G. Varshney, *J. Inorg. Nucl. Chem.*, 30 (1968) 3081.
16 M. Qureshi and S. A. Nabi, *Talanta*, 19 (1972) 1033.
17 B. E. Saltzman, *Anal. Chem.*, 24 (1952) 1016.
18 E. B. Sandell, *Colorimetric Determination of Traces of Metals*, Interscience, New York, 3rd ed., 1959, p. 397.
19 Y. Inoue, *Bull. Chem. Soc. Jpn.*, 36 (1963) 1316.
20 G. Alberti and E. Torracca, *J. Inorg. Nucl. Chem.*, 30 (1968) 3075.

*Journal of Chromatography*, 594 (1992) 386–391
Elsevier Science Publishers B.V., Amsterdam

CHROM. 23 914

# Short Communication

# Primary and secondary amine derivatization with luminarins 1 and 2: separation by liquid chromatography with peroxyoxalate chemiluminescence detection

Michel Tod*

*Department of Pharmacotoxicology, Avicenne Hospital, 125 Route de Stalingrad, 93000 Bobigny (France)*

Jean-Yves Legendre

*Pharmacy, Bichat Hospital, 48 rue H. Huchard, 75018 Paris (France)*

Joseph Chalom

*Eurobio, ZA Courtaboeuf, 7 avenue de Scandinavie, 919533 Les Ulis (France)*

Homan Kouwatli, Maria Poulou, Robert Farinotti and Georges Mahuzier

*Laboratoire de Chimie Analytique II, School of Pharmaceutical Sciences, rue J. B. Clément, 92290 Châtenay-Malabry (France)*

(First received September 17th, 1991; revised manuscript received November 21st, 1991)

ABSTRACT

Luminarins 1 and 2 are labelling reagents with a quinolizinocoumarin structure and an N-hydroxysuccinimide ester reactive function. They react with primary and secondary amines under relatively mild conditions (50–80°C, 20–180 min) without a catalyst and yield fluorescent and chemiluminescent derivatives. Luminarin 1 was more reactive than luminarin 2, but required an anhydrous medium to perform the derivatization. Small alkylamines were derivatized and separated by reversed-phase liquid chromatography. The fluorescence detection limit was 100 fmol injected. The limit of detection with peroxyoxalate postcolumn chemiexcitation was in the low femtomole range. Both methods were used to measure histamine with luminarin 2. Linearity of derivatization was obtained for amounts of histamine ranging from 0.5 to 5 nmol. The possibility of chemiluminescence detection in highly aqueous mobile phases (76%) was demonstrated. The results compared favourably with those of *o*-phthalaldehyde–mercaptoethanol derivatization of histamine.

## INTRODUCTION

Precolumn derivatization and chemiluminescence detection by high-performance liquid chromatography (HPLC) have been developed for the determination of trace amounts of analytes. When the analyte contains an amine functional group, several chemiluminescence derivatization reagents, such as dansyl chloride [1], fluorescamine [2], 4-chloro-7-nitrobenzo-1,2,5-oxadiazole [3], *o*-phthal-

0021-9673/92/$05.00 

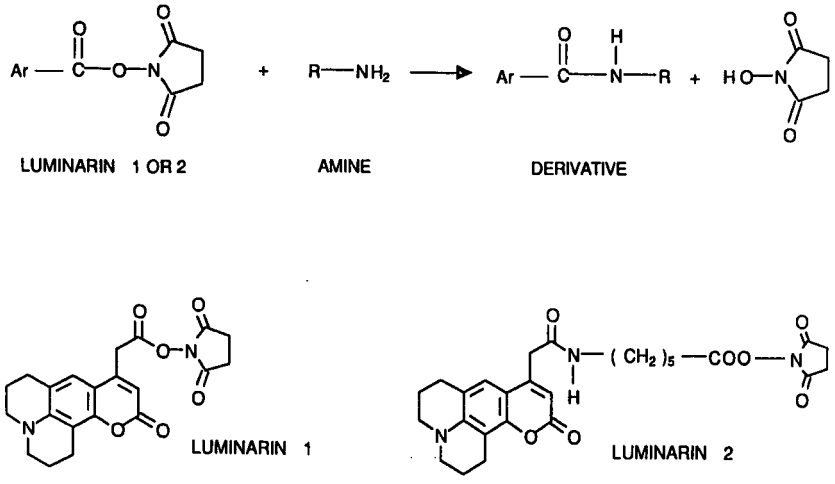


Fig. 1. Derivatization of amines by luminarins 1 and 2.

aldehyde [3], naphthalene- and anthracene-2,3-dialdehyde [4] and N-(4-aminobutyl)-N-ethylisoluminol [5] can be used.

Aminocoumarin derivatives are excellent chemiluminogenic reagents for many compounds, such as fatty acids [6] and fluoropyrimidines [7]. In previous papers we described the development of the luminarins, which are labelling reagents derived from quinolizinocoumarin [8–10]. This nucleus offers the advantage of a high chemiluminescence yield in various solvents, which results in low limits of detection (LOD) in normal- or reversed-phase chromatography. In this study, the ability of luminarins 1 and 2 (Fig. 1) to derivatize primary and secondary amines was investigated. Both reagents have an N-hydroxysuccinimide ester reactive function, which was chosen for its reactivity with [11,12] and its selectivity towards amines [13]. Alkylamines were studied as model compounds and an application to histamine was developed.

## EXPERIMENTAL

### *Reagents*

Pentylamine, nonylamine, dipropylamine, dibutylamine, bis-(2,4,6-trichlorophenyl)oxalate (TCPO) and bis-(2,4-dinitrophenyl)oxalate (DNPO) were purchased from Fluka (Buchs, Switzerland), histamine from Calbiochem (Meudon, France), luminarins 1 and 2 from Eurobio (Les Ulis, France), *o*-phthalaldehyde (OPT) and dimethylaminopyridine (DMAP) from Sigma (L'Isle d'Abeau, France) and hydrogen peroxide (30% aqueous solution) from Janssen (Beerse, Belgium). Imidazole, molecular sieves (0.3 nm) and solvents (UV or fluorescence grade) were purchased from Merck (Darmstadt, Germany). Stock solutions of luminarins 1 and 2 (0.01 *M*) were prepared in tetrahydrofuran (THF) previously dried with molecular sieves, then diluted as required and kept at −20°C.

### *Instrumentation*

For fluorescence measurements, a Chromatem 380 pump (Touzart et Matignon, Vitry, France), a Rheodyne Model 7125 injector with a 20-μl sample loop, a Shimadzu RF 530 fluorescence detector and a Shimadzu CR3A integrator (Touzart et Matignon) were used.

For chemiluminescence measurements, a Shimadzu CTO-6A column oven (Touzart et Matignon) set at 30°C and a Kratos URS051 postcolumn reactor including two pumps (Applied Biosystems, Rungis, France) were added, and the fluorescence detector was a Kratos FS970 (Applied Biosystems). With mobile phases containing a high proportion of acetonitrile (*e.g.*, 70%), the reagents and the eluate were mixed by flowing through a 60-μl PTFE capillary tube containing glass beads (Supelco, France) connected to a 120-μl delay coil placed in the col-

umn oven. With mobile phases containing a low proportion of acetonitrile (*e.g.*, 26%), TCPO and hydrogen peroxide were mixed using a 292-$\mu$l capillary tube placed in the oven, and a 60-$\mu$l capillary tube was used for mixing these reagents with the eluate before entering the detector.

*Chromatographic conditions*

For fluorescence measurements of alkylamine derivatives, an Ultrasphere ODS-2 (5 $\mu$m) column (250 × 2 mm I.D.) (Beckman, Les Ulis, France) was used and the mobile phase was acetonitrile–10 m*M* imidazole nitrate buffer (pH 7.0) (70:30, v/v) pumped at 0.3 ml/min. The excitation and emission wavelengths were 390 and 490 nm, respectively. For chemiluminescence detection, a 4.6 mm I.D. but otherwise identical column was used and the flow-rate was 1 ml/min. A 0.2 *M* hydrogen peroxide solution in THF and a 10 m*M* TCPO solution in methyl acetate were pumped at 0.25 ml/min each. The column oven was kept at 30°C and a 470-nm long-pass filter was used.

For fluorescence measurements of histamine derivatives, a Nucleosil $C_{18}$ (5 $\mu$m) column (150 × 4.6 mm I.D.) (SFCC, Neuilly-Plaisance, France) was used with a mobile phase consisting of acetonitrile-5 m*M* ammonium acetate (26:74, v/v) pumped at 2 ml/min. The excitation and emission wavelengths were 390 and 490 nm, respectively, for histamine–luminarin derivatives and 350 and 440 nm respectively, for histamine–OPT derivatives.

For chemiexcitation of the histamine–luminarin 2 derivative, a 0.4 *M* hydrogen peroxide solution in THF and a 1.1 m*M* TCPO solution in methyl acetate were pumped at 0.3 ml/min each, while the eluate flow-rate was 1.5 ml/min and the oven was set at 40°C.

*Derivatization procedure*

Alkylamines were derivatized by luminarin 1 by mixing 0.1 ml of an amine solution containing 0.2–20 nmol in THF (primary amines) or dimethyl sulphoxide (DMSO) (secondary amines) with 0.1 ml of a 1 m*M* luminarin 1 solution in THF. The solutions were heated on a water-bath for 20 min at 50°C (primary amines) or 180 min at 70°C (secondary amines). Care must be taken to avoid trace amounts of moisture. Solvents were dried using 0.4-nm molecular sieves. Alkylamines were labelled with luminarin 2 by mixing 0.1 ml of an amine solution containing 0.2–20 nmol in DMSO with 0.1 ml of a 2 m*M* luminarin 2 solution in THF. The solutions were kept at 70°C for 60 min (primary amines) or at 80°C for 180 min (secondary amines). After the reaction, the samples were diluted 1:50 (v/v) in mobile phase, in order to inject derivative amounts between 0.4 and 40 pmol.

Histamine was derivatized by luminarin 2 by mixing 0.5–5 nmol of histamine with 50 nmol of luminarin 2 in 0.5 ml of acetone and 0.1 ml of a 0.1 *M* solution of DMAP in acetone. The solution was evaporated to dryness and left for 90 min in the dark. Acetone (0.2 ml) was added just before injection.

OPT–mercapthoethanol derivatization of histamine was performed as described by Gupta and Lew [14].

## RESULTS AND DISCUSSION

*HPLC analysis*

Pentylamine, dipropylamine, dibutylamine and nonylamine were derivatized and separated according to the procedure described above, as shown in Fig. 2. Resolution between the peaks of homologous derivatives was most often complete. For example, the resolution between dipropyl- and dibutylamine–luminarin 1 derivatives was 3.5.

Other amines, such as octylamine, benzylamine and phenylethylamine, were also successfully labelled with luminarin 1 (data not shown). Luminarin 2 derivatives were less retained than luminarin 1 derivatives. The structures of pentylamine–luminarin 1 and dipropylamine–luminarin 1 derivatives were confirmed by mass spectrometry [15].

*Derivatization conditions*

The mechanism of the derivatization reaction is well known [16]. A basic dipolar solvent should *a priori* be appropriate to drive this reaction, and THF was chosen. Previously [11,12], chloroform was used as the solvent and the reaction was catalysed with triethylamine. In this study, three catalysts were tested with THF as the solvent: pyridine, triethylamine and dimethylaminopyridine. Pyridine (10 $\mu$l) inhibited the reaction; triethylamine (10 $\mu$l) accelerated the reaction but resulted in the formation of by-products; DMAP (100 $\mu$l of a 0.1 *M* solu-

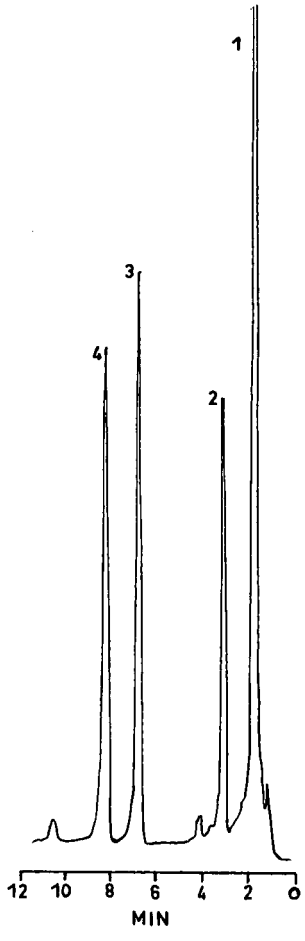


Fig. 2. Separation of luminarin 1 and 2 derivatives with fluorescence detection, 0.05 μA full-scale. Peaks: 1 = luminarin 1 (L1); 2 = pentylamine–L1; 3 = dibutylamine-L1; 4 = nonylamine–L2. 5 pmol of each derivative were injected on to the column.

tion) had no effect when THF was the solvent but increased the kinetics when histamine was derivatized by luminarin 2 in acetone or in the dry state. Accordingly, when a basic solvent such as THF is used, base catalysis has no effect. Otherwise, DMAP catalysis should be used.

Finally, alcohols as the solvent must be avoided, because they react with luminarins 1 and 2 to form the corresponding esters. This was verified with methanol, ethanol and isopropanol.

*Derivatization kinetics*

Kinetics of the pentylamine and dibutylamine reactions with luminarin 1 were determined at 50 and 70°C, respectively. The yield was measured by comparison with a standard obtained in a twofold molar excess of amine over luminarin 1. The reaction was complete (yield 95%) in 20 min for primary amines, or reached a plateau (yield 80%) in 180 min for secondary amines. As expected, the reaction was much slower with secondary amines, probably because of steric hindrance. The yield could not be improved by increasing the reaction temperature because of the degradation kinetics of luminarin 1 (see below).

Kinetics of the nonylamine and dibutylamine reactions with luminarin 2 were determined at 70 and 80°C, respectively, and the yield was measured as for luminarin 1. The plateau was reached in 60 min for primary amines (yield 88%) and 180 min for secondary amines (yield 75%). Hence the kinetics of the reaction were slower for luminarin 2 than luminarin 1.

*Hydrolysis kinetics*

The sensitivity of luminarins 1 and 2 to hydrolysis was examined, in order to determine if the reaction had to be carried out in an anhydrous medium. Hydrolysis was carried out in the reaction medium with 0.5% (v/v) water, at 50°C for luminarin 1 and 70°C for luminarin 2. Hydrolysis *vs.* time was almost linear and reached 50% in 180 min for luminarin 1 and 10% in 210 min for luminarin 2. A blank without water showed only a slight decrease. Thus, luminarin 2 is less reactive than luminarin 1 but also more resistant to hydrolysis.

*Detection and derivatization limits*

Limits of detection (signal-to-noise ratio = 3) of the pentylamine–luminarin 1 derivative with fluorescence or chemiluminescence detection was described previously [9] and were very similar for all other luminarin 1 and 2 derivatives: 100 fmol *vs.* 6 fmol injected for fluorescence *vs.* chemiluminescence detection, respectively. Hence, it should be possible to measure amounts of amines as small as 1 pmol (with fluorescence detection) if the derivatization has occurred. In fact, the derivatization limits were much higher, ranging from 200 pmol (primary amines with luminarin 1) to 500 pmol (secondary amines with luminarin 2). When the amount of amine was smaller, derivatization was poorly repro-

ducible and no linearity was observed. Hence, the limiting factor in the sensitivity of the method was not detection but derivatization. In this respect, fluorescence detection is valid for most applications, and chemiluminescence detection would be useful only when a greater selectivity of detection is required, or when the amounts of derivatives injected have to be reduced, *e.g.*, with small-bore columns.

*Application to histamine*

A classical method for histamine measurements is condensation with OPT [17], but this reaction suffers from several problems, *e.g.*, high chemical lability towards auto-oxidation and poor quantum yield of fluorescence of the isoindole derivatives (*ca.* 0.1) [18]. Condensation with OPT–mercaptoethanol [14] gives better results and was therefore compared with luminarin 2 labelling.

The kinetics of the histamine–luminarin 2 reaction in acetone were determined at 20, 60 and 80°C with a ten-fold molar excess of luminarin 2. The higher the temperature, the faster was the initial rate of the reaction, but the lower was the maximum yield; the latter then decreased. The kinetics of the reaction at 20°C in the dry state and with DMAP as the catalyst reached a plateau after 90 min with no subsequent decrease, and this procedure was used for further work. The reaction yield as a function of excess of luminarin 2 was studied in the range 1–1000. A plateau was reached for a molar ratio of 10. A higher excess of luminarin 2 resulted in the appearance of many by-products on the chromato-

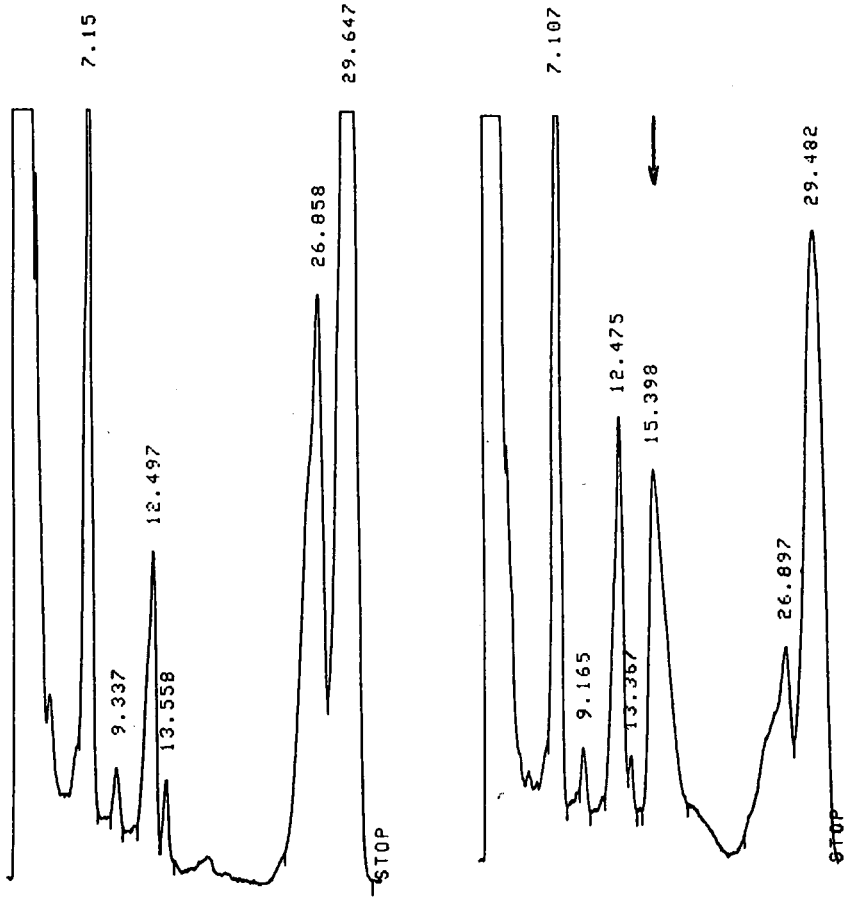


Fig. 3. Separation of the histamine–luminarin derivative with fluorescence detection, 0.5 μA full-scale. Left, blank; right, 0.5 nmol of derivatized histamine (50 pmol injected on to the column). Numbers at peaks indicate retention times in min.

gram. Under the conditions described (Fig. 3), the retention time of the histamine–luminarin 2 derivative was 15 min and that of luminarin 2 was 29 min. Peaks appearing at 7 and 12 min were impurities contained in the luminarin 2 powder. With fluorescence detection, the calibration graphs were linear for histamine amounts derivatized in each tube in the range 0.5–5 nmol ($r = 0.998$, $p < 0.01$), corresponding to 50–500 pmol of histamine derivative injected. Amounts up to 0.1 nmol of histamine could be derivatized, but the reproducibility and linearity were poor. The intra-run relative standard deviation was 8% for the 1-nmol histamine standard ($n = 5$). Once dissolved in acetone, the histamine–luminarin 2 derivative was stable for at least 4 h. Stability in the dry state was not investigated, but should be even longer. With chemiluminescence detection, the LOD was only two times lower than with fluorescence, 50 *vs.* 100 fmol (signal-to-noise ratio = 3), and was similar to that reported previously for luminarin 4 derivatives [10]. Hence luminarins, which are all derived from the quinolizinocoumarin nucleus, offer a wide range of chromatographic conditions for detection with peroxyoxalate chemiexcitation: polar mobile phases containing up to 75% of water or moderately polar mobile phases containing hexane–chloroform mixtures [9] can be used.

Derivatization of histamine by OPT (0.75 g/l) and mercaptoethanol (0.025%, v/v) in methanol was carried out for 30 min at 20°C. Under the conditions described, the retention time of the histamine–OPT derivative was 8.4 min. A linear calibration was obtained in the range 1–10 nmol of histamine, and the derivative was stable for at least 4 h in methanol. Hence both methods are similar, luminarin 2 being more sensitive but more time consuming than OPT.

## REFERENCES


1 K. Kobayashi and K. Imai, *Anal. Chem.*, 52 (1980) 424.
2 S. I. Kobayashi, J. Sekino, K. Honda and K. Imai, *Anal. Biochem.*, 112 (1981) 99.
3 G. Mellbin and B. E. F. Smith, *J. Chromatogr.*, 312 (1984) 203.
4 P. J. M. Kwakman, H. Koelewijn, I. Kool, U. A. T. Brinkman and G. J. de Jong, *J. Chromatogr.*, 511 (1990) 155.
5 K. Nakashima, K. Suetsugu, S. Akiyama and M. Yoshida, *J. Chromatogr.*, 530 (1990) 154.
6 M. L. Grayeski and J. K. de Vasto, *Anal. Chem.*, 59 (1987) 1203.
7 S. Yoshida, K. Urakami, M. Kito, S. Takeshima and S. Hirose, *Anal. Chim. Acta*, 239 (1990) 181.
8 M. Tod, R. Farinotti, G. Mahuzier and I. Gaury, *Anal. Chim. Acta*, 217 (1989) 11.
9 M. Tod, M. Prevot, M. Poulou, R. Farinotti, J. Chalom and G. Mahuzier, *Anal. Chim. Acta*, 223 (1989) 309.
10 M. Tod, M. Prevot, J. Chalom, R. Farinotti and G. Mahuzier, *J. Chromatogr.*, 542 (1991) 295.
11 H. Falter, K. Jayasimhulu and R. A. Day, *Anal. Biochem.*, 67 (1975) 359.
12 S. S. Chen, A. Y. Kou and H. Y. Chen, *J. Chromatogr.*, 276 (1983) 37.
13 D. Amir and E. Haas, *Int. J. Pept. Protein Res.*, 27 (1986) 7.
14 R. N. Gupta and M. Lew, *J. Chromatogr.*, 344 (1985) 221.
15 M. Tod, *Ph.D. Thesis*, Université Paris Sud, Faculté de Pharmacie, Paris XI, 1990, No. 138.
16 J. Mathieu and R. Panico, *Mécanismes Réactionnels en Chimie Organique*, Hermann, Paris, 2nd ed., 1980.
17 P. D. Siegel, D. M. Lewus, M. Petersen and S. A. Olenchak, *Analyst (London)*, 115 (1990) 1029.
18 L. A. Sternson, J. F. Stobaugh, J. Reid and P. de Montigny, *J. Pharm. Biomed. Anal.*, 6 (1988) 657.

*Journal of Chromatography*, 594 (1992) 392–394
Elsevier Science Publishers B.V., Amsterdam

CHROM. 23 883

# Short Communication

# Fast protein monitoring in fermentation broth using non-porous micropellicular reversed-phase columns

E. Watson* and F. Yao

*Amgen Inc., Amgen Center, Thousand Oaks, CA 91320 (USA)*

(First received May 24th, 1991; revised manuscript received November 18th, 1991)

ABSTRACT

The use of a short non-porous polymeric reversed-phase column is described for the rapid monitoring of the formation of recombinant human granulocyte colony stimulating factor in fermentation broths. The described procedure is capable of completing the assay in less than 10 min. Validation of the method showed acceptable recovery, accuracy, precision and specificity.

## INTRODUCTION

In recent years the use of high-performance liquid chromatography (HPLC) has had a major impact on the separation and isolation of proteins. As a result of the development of highly efficient columns and instrumentation, HPLC is now the preeminent analytical technique used for rapid separation and precision measurement of proteins. Of the various separation modes available, reversed-phase with covalently bonded non-polar functional groups, has been the most prominent system used. The widespread use of these bonded stationary phases arises from the simplicity, the high column resolution attainable, and the relative ease with which selectivity can be manipulated through the use of pH and organic solvents. Silica-based wide-pore, 300 Å or greater, bonded phases currently dominate the high-performance chromatographic field as stationary phase materials. Instability at high pH, $>8.0$, has long been considered a problem. In addition, low diffusivity and restricted mass transfer result in long analysis times for proteins. Recently, a number of micropellicular supports, both silica based and polymeric, have been introduced commercially. These supports have been shown to allow much faster mass transfer due to absence of intraparticle diffusional resistances, and as a result, very fast (less than 10 min) separations of peptides and proteins are possible [1–4]. Moreover, polymeric supports have been shown capable of being operated at elevated temperatures of up to 80°C and at pH 11 without any stability deleterious results [5,6].

The majority of reports published have been concerned with either peptide separations obtained from enzymatic digestion or with separation of mixtures of standard proteins. The present paper describes the use of a non-porous polymeric micropellicular column for monitoring the rate of production of recombinant human granulocyte colony stimulating factor (r-met-HuG-CSF) produced in *E. coli* cells. Analyses were carried out at room temperature with an HPLC system that has been designed to accommodate regular 25 cm × 4.6 mm

0021-9673/92/$05.00 

I.D. stainless-steel columns. Total analyses times selected were 5-min gradient with a 3-min re-equilibration time between injections.

## EXPERIMENTAL

### *Chemicals and reagents*

Recombinant r-met-HuG-CSF (approximate molecular mass 18 000) was produced at Amgen (Thousand Oaks, CA, USA). HPLC-grade acetonitrile was obtained from Fisher Scientific (Fairlawn, NJ, USA). Mercaptoethanol was obtained from Sigma (St. Louis, MO, USA). Sodium dodecyl sulfate (SDS) was obtained from Bio-Rad (Richmond, CA, USA) and sequenal-grade trifluoroacetic acid (TFA) was obtained from Pierce (Rockford, IL, USA).

### *Apparatus and chromatographic parameters*

All chromatographic analyses were carried out using a Model 8800 pump (Spectra-Physics, San Jose, CA, USA), a SPD-6A variable-wavelength detector (Shimadzu, Cole Scientific, Calabasas, CA, USA) and a Chrom Jet Integrator (Spectra-Physics). A Model 7125 injector (Rheodyne, Cotati, CA, USA) with a 10- or 5-$\mu$l loop was used to introduce the sample.

Dead volume was reduced by using 10-$\mu$l injection loops, replacing any 0.020 in. tubing with 0.010 in., inserting a low-volume gradient solvent mixing tube between pump heads and injection loop and removing dynamic/static solvent mixers. These modifications resulted in a total dead volume of 0.52 ml.

The mobile phase consist of (A) 0.1% TFA in water and (B) 0.1% TFA in acetonitrile–water (95:5). The gradients were generated from 40 to 85% B with a flow-rate of 1 ml/min. The analytical column used is commercially available from Toso Haas (Philadelphia, PA, USA). It has dimensions of 3.5 × 4.6 mm with a polymeric-based support, TSK-gel-Octadecyl-NPR (Octadecyl-NPR) covalently bonded to 2.5-$\mu$m beads.

### *Isolation of r-met HuG-CSF from fermentation media*

A 10-ml aliquot of fermentation broth was centrifuged at 10 000 rpm for 15 min. The pellet was resuspended in water and a 100-$\mu$l aliquot was removed for preparation. The sample was reduced using 2% SDS and mercaptoethanol. After heating the resulting mixture in boiling water for 10 min, the sample was passed through a 0.22-$\mu$m cellulose acetate filter and diluted prior to analysis.

## RESULTS AND DISCUSSION

Production time for r-met-HuG-CSFcompletion is relatively short, being in the order of 6–10 h. The utility of the micropellicular column for fast r-met-HuG-CSF analysis in fermentation broth extract is shown in Fig. 1. Fig. 1A shows the chromatogram obtained from fermentation media at time 0, and Fig. 1B shows the corresponding chromatogram obtained at 6 h. These chromatograms were obtained using a 5-min gradient with a 3-min solvent re-equilibration, the total assay time being 8 min. From Fig. 1A, it is seen that there are no peaks co-chromatographing with r-met-HuG-CSF or eluting nearby that could interfere with the determination of r-met-HuG-CSF using the described chromatographic conditions.

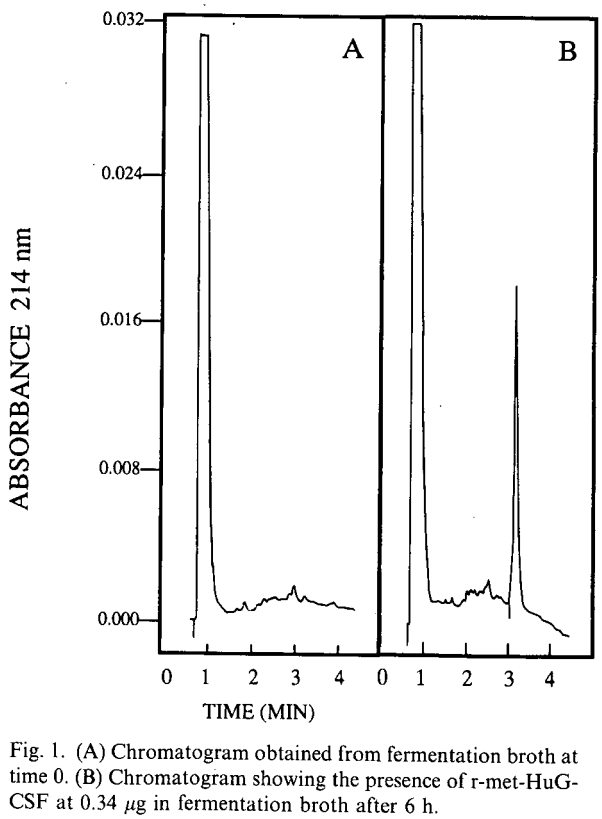


Fig. 1. (A) Chromatogram obtained from fermentation broth at time 0. (B) Chromatogram showing the presence of r-met-HuG-CSF at 0.34 $\mu$g in fermentation broth after 6 h.

The linearity of the assay was established by injecting various amounts of r-met-HuG-CSF in the range 0.1–1.0 μg and plotting area *versus* amount injected. Linearity was evident from 0.1–0.5 μg with correlation coefficients of 0.998 being obtained. From 0.5–1.0 μg, the curve showed some non-linearity but could still provide quantitative data. These results indicate that the loading capacity of the column is low and that it cannot be used for any preparative chromatography. Since the intent here is to provide fast protein determination of r-met-HuG-CSF in fermentation media, there is no absolute requirement of work within the linear range, and provided a suitable response curve is determined, a non-linear curve can be used to obtain reliable, reproducible results. Reproducibility of retention times (3.69 min ± 2.3%, $n = 7$) and peak areas (±3.0%) was determined by the repeated injection of 0.34 μg r-met-HuG-CSF.

Trifluoroacetic acid is used almost always in reversed-phase gradient elution schemes. Several other acids have been used including phosphoric and perchloric acids. The overall effect on chromatographic performance of trifluoroacetic, perchloric and phosphoric acids was compared. Phosphoric acid being the most hydrophilic caused r-met-HuG-CSF to elute the earliest while perchloric acid caused the slowest elution. Trifluoroacetic acid resulted in the sharpest peak shapes and was used in all subsequent studies for this reason.

Ghosting or hysteresis is a problem quite common to silica-based reversed-phase supports and its effect is most evident in the re-emergence of peaks from previous runs during a subsequent blank run. Frequently a blank run is required before a protein can be analyzed. Since r-met-HuG-CSF is a hydrophobic protein, the extent of ghosting was evaluated. The carry-over peak was determined to be *ca.* 0.2% and this level tended to increase as the column deteriorated. In one column that had been used quite extensively, a ghosting value of 2% was found. When this occurs, the column is cleaned with sodium hydroxide and if ghosting persists, the column is discarded.

Several publications describing the use of non-porous columns have stressed the absolute need for specialized HPLC equipment and the use of column heating ovens [7,8]. In the present study, non-porous columns were evaluated using a commercially available HPLC system that had been designed for use with conventional column dimensions, *i.e.*, 25 × 0.46 cm. The only changes made involved minimizing dead volumes.

The proposed method for the rapid determination of r-met-HuG-CSF produced in fermentation broth possesses the important characteristics of precision and specificity. In practical terms, the method has proven useful in monitoring r-met-HuG-CSF levels both in fermentation media and in the various steps involved in purification.

REFERENCES

1 K. Kalghatgi and Cs. Horváth, *J. Chromatogr.*, 398 (1987) 335.
2 K. Kalghatgi and Cs. Horváth, *J. Chromatogr.*, 443 (1988) 343.
3 Y. Kato, S. Nakatori, Y. Kitamura, Y. Yamasaki and T. Hashimoto, *J. Chromatogr.*, 502 (1990) 416.
4 K. K. Unger, G. Jilge, J. N. Kinkel and M. T. W. Hearn, *J. Chromatogr.*, 339 (1986) 61.
5 F. D. Antia and Cs. Horváth, *J. Chromatogr.*, 435 (1988) 1.
6 Y.-F. Maa and Cs. Horváth, *J. Chromatogr.*, 445 (1988) 71.
7 K. Nugent and K. Olson, *Biochromatography*, 5 (1990) 101.
8 G. P. Rozing and H. Goetz, *J. Chromatogr.*, 476 (1989) 3.

*Journal of Chromatography*, 594 (1992) 395–399
Elsevier Science Publishers B.V., Amsterdam

CHROM. 23 957

# Short Communication

# Gas chromatography of chloride and bromide as phenylboronic acid/mercuric nitrate derivatives with microwave induced plasma atomic emission detection

A. Sarafraz-Yazdi☆, M. Y. Khuhawar☆☆ and P. C. Uden*

*Department of Chemistry, Lederle Graduate Research Tower A, University of Massachusetts, Amherst, MA 01003 (USA)*

(First received October 8th, 1991; revised manuscript received December 10th, 1991)

ABSTRACT

Capillary column gas chromatography (GC) with flame ionization detection (FID) or microwave induced plasma atomic emission detection (MIP-AED) were examined for the determination of chloride, using phenylboronic acid as derivatizing reagent. Phenylboronic acid and mercuric nitrate were used in a 1:1 molar ratio to produce phenylmercuric chloride (PMC).

The limit of detection for chloride as PMC using FID was $3.3 \cdot 10^{-10}$ g and using AED, measuring the mercury response at 185 nm, it was $6.25 \cdot 10^{-11}$ g. Under the conditions used, chloride and bromide (as PMC and PMB) failed to separate adequately, but they could be determined by GC–AED using the wavelengths 478 nm and 479 nm for bromide and chloride, respectively. The specific detection limits for bromide and chloride obtained from bromine and chlorine responses were $2.9 \cdot 10^{-9}$ g and $1.8 \cdot 10^{-9}$ g per injection.

## INTRODUCTION

Packed column gas chromatographic (GC) determination of chloride following reaction with phenylmercuric nitrate (PMN) and trifluoromethylmercuric nitrate (TMN) was reported on glass columns with diethylene glycol adipate stationary flame ionization detection (FID) and electron-capture detection (ECD) [1–3].

Microwave induced plasmas (MIPs) have been employed as element-selective atomic emission detectors for GC since 1965 [4] and their analytical utility has been extensively reviewed [5–8]. They may monitor a single element or, with appropriate multi-channel spectrometers, a number of elements simultaneously. GC–atomic emission detection (AED) has been used for example for the determination of organomercuric compounds at low levels [9–14].

Phenylboronic acid (PBA) and various substituted phenylboronic acids have been used, in the presence of mercuric nitrate, as derivatizing reagents for GC determination of halides, but those studies involved packed columns and FID or ECD [3]. The present study examines capillary column GC for the determination of chloride using PBA in the presence of mercuric nitrate, and also the separation of derivatized chloride, bromide and iodide with simultaneous atomic emission detection for chlorine and bromine.

☆ Present address: Department of Chemistry, University of Meshhad, Meshhad, Iran.
☆☆ Present address: Department of Chemistry, University of Sind, Jamshoro, Sind, Pakistan.

0021-9673/92/$05.00 

## EXPERIMENTAL

A Model 3700 gas chromatograph with FID (Varian, Walnut Creek, CA, USA) and a Model 5890 II gas chromatograph [Hewlett-Packard (HP), Avondale, PA, USA] with an HP 7673A automatic injector and split/splitless capillary injection port, operated in split mode, were used. The latter instrument was coupled with an HP 5921A atomic emission detector, controlled by an HP 330 computer with HP 35920A GC–AED software. Helium was used as carrier and make-up gas, and hydrogen and oxygen were employed as reagent gases. An HP 5890A gas chromatograph equipped with an HP 5970 mass-selective detector was also used.

A DB 5 methyl-phenyl silicone fused-silica column (30 m × 0.25 mm I.D., with film thickness of 0.25 μm) and a DB-Wax polyethylene column (6 m × 0.25 mm I.D. with 0.31 μm film thickness) were used (J and W Scientific, Rancho Cordova, CA, USA).

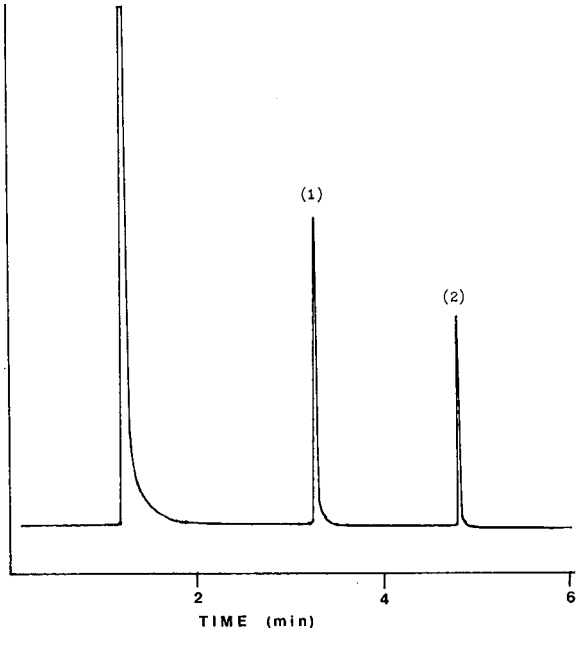


Fig. 1. Chromatographic separation of (1) phenylmercuric chloride and (2) diphenylmercury on a DB-5 (30 m × 0.25 mm, I.D.) fused-silica open tubular column, with temperature programming (150–200°C, at 10°C/min), injection port and detector temperatures 220°C, carrier gas (helium) flow-rate 1.2 ml/min and inlet split ratio 1:20.

*Preparation of phenylmercuric compounds*

PBA (0.01 *M*, 10 ml), mercuric nitrate (0.01 *M*, 10 ml), nitric acid (1 *M*, 2–3 ml) and an appropriate amount of chloride ($2 \cdot 10^{-3}$ *M*) were mixed in a separating funnel to bring the pH of the solution to 1–2. The white precipitate of PMC that was formed was extracted into chloroform, the organic layer separated and evaporated on a water bath. The residue was purified by sublimation at 0.1 Torr. The same procedure was used for the preparation of phenylmercuric bromide (PMB) and phenylmercuric iodide (PMI), using bromide and iodide reactants.

Diphenylmercury (DPM) was prepared by mixing 0.01 *M* PBA (20 ml), 0.01 *M* mercuric nitrate (10 ml) and a suitable amount of pH 10 buffer solution to keep the pH of the solution at that value, to give quantitative precipitation of DPM. The remaining procedure was as for PMC.

Standard 1000 ppm solutions of PMC and PMB were prepared from the pure compounds in benzene or methyl isobutyl ketone (MIBK). Further solutions were prepared by serial dilution in the same solvent.

## RESULTS AND DISCUSSION

*Capillary GC–FID*

The elution and possible separation of PMC from PMB and PMI was examined on DB-5 and DB-Wax columns with FID. PMC was readily eluted on DB 5 at a column temperature of 190°C, injection port and detector temperatures of 220°C, and a helium carrier gas flow-rate of 1.2 ml/min, giving fairly symmetrical peaks, but no separation between PMC, PMB and PMI. However, DPM was well separated from PMC, as shown in Fig. 1. When the DB-Wax column was evaluated, some separation between PMC, PMB and PMI was obtained (Fig. 2), but on-column adsorption of PMC and its subsequent displacement by PMB was observed (some PMC was observed to be eluted upon injection of pure PMB). Also under similar conditions, no separation between PMC and DPM was obtained. Some adsorption of PMC was also observed on the DB-5 column, but after four repeated injections, reproducible response was obtained and this column was thus chosen for further study. The identity of the prepared PMC and DPM was also

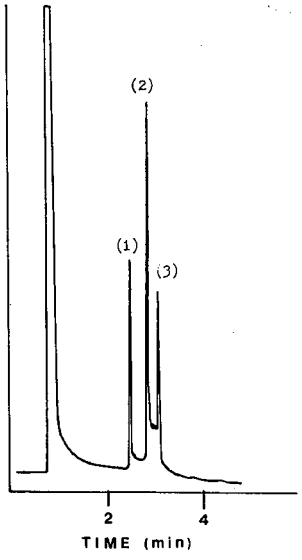


Fig. 2. Chromatographic separation of (1) phenylmercuric chloride, (2) phenylmercuric bromide and (3) phenylmercuric iodide on a DB-Wax (6 m × 0.25 mm) column with column, injection and detector temperatures 190°C, 220°C and 220°C, respectively, helium flow-rate 1.2 ml/min and inlet split ratio 1:20.

checked by GC–MS using the DB-5 column. Molecular ions for both PMC and DPM were obtained, corresponding to *m/z* 314 and 356, respectively (for $^{202}$Hg).

Quantitative response for PMC on the DB-5 column was checked by injecting different amounts of PMC in triplicate and measuring average peak areas; linear calibration was obtained up to 100 mg/ml chloride ($R^2$ = 0.998). The detection limit measured at twice the signal-to-noise ratio was $3.3 \cdot 10^{-10}$ g, a value about an order of magnitude lower than that reported on a packed column using an FID detector [1,2].

*GC–AED*

In order to obtain better sensitivity for the determination of chloride, GC–AED was performed using the same DB-5 column and monitoring the mercury response at 185 nm. A low flow-rate of make-up gas (*ca.* 30 ml/min of helium) and hydrogen and oxygen plasma reagent gases as recommended by the manufacturer for mercury were used, but an asymmetrical peak with extensive tailing was observed (Fig. 3A). Other plasma discharge tubes, silica and alumina (sapphire), were tried with little improvement. However, some improvement in peak shape was obtained upon using a high flow-rate of helium make-up gas (*ca.* 150 ml/min) (Fig. 3B). The column temperature was 190°C, and the injection port and transfer line were at 200°C. With these conditions a linear calibration curve was obtained up to 100 mg/ml chloride ($R^2$ = 0.996). An approximate limit of detection was observed at $6.25 \cdot 10^{-11}$ g chloride showing MIP-AED to be *ca.* 5 times more sensitive than FID.

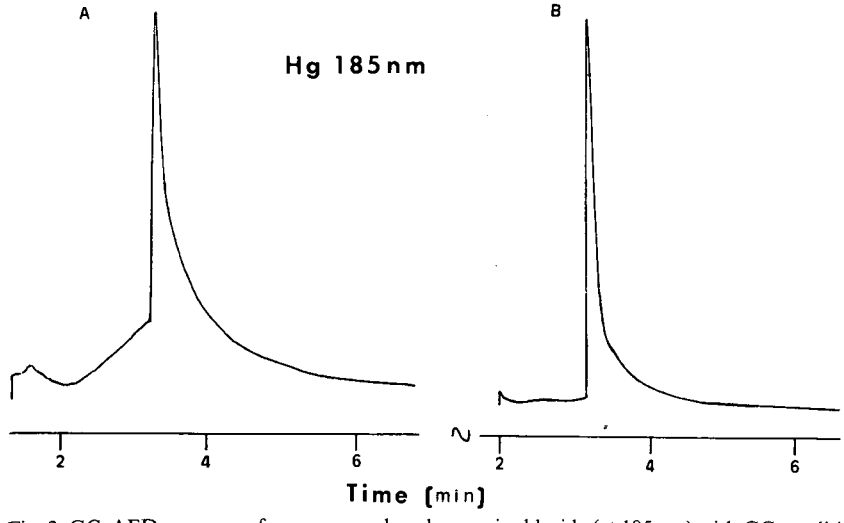


Fig. 3. GC–AED response of mercury as phenylmercuric chloride (at 185 nm) with GC conditions as Fig. 1, but using (A) $O_2$, $H_2$, low make-up flow and (B) $O_2$, $H_2$, high make-up flow.

Under the foregoing conditions, chloride and bromide co-eluted, thus only their total content should be determined by monitoring mercury emission. In order to determine chloride and bromide in a mixture, individual GC–AED monitoring of chlorine and bromine is necessary. To examine the quantitation of this response, AED responses were measured at 479 nm and 478 nm for chlorine and bromine, respectively, for an injected mixture of PMC and PMB. An optimal response for these elements was obtained by use of a high flow-rate of helium make-up gas, and oxygen as reagent gas (Fig. 4). It was noted that chlorine and bromine responses indicate similar tailing to that observed for mercury emission. However, examination of chlorobenzene under similar GC–AED flow conditions, or under those using a low flow-rate of plasma helium make-up gas, showed no appreciable peak tailing. The fact that very much less tailing was noted for PMC etc. with FID, using the same column, and also that minimal tailing occurs with many other GC peaks using the same GC–AED configuration [15], suggests that peak tailing is a function of elemental behavior in the MIP discharge tube, and that the chlorine and bromine responses are affected by the presence of the mercury in the eluent peak.

The selectivities of chlorine and bromine against carbon were measured using *n*-dodecane as a source of carbon and were found to be about $20 \cdot 10^3$ and $11 \cdot 10^3$, respectively. Despite the proximity of the emission lines used for chlorine (479 nm) and bromine (478 nm) determination, there is a reasonable selectivity of *ca.* 350 between them; the photodiode array enables the maximum emission for the two elements to be collected on diodes separated 3–4 units from each other. The detection limits for chloride and bromide as PMC and PMB were 1.8 ng (100 pg/s), and 2.98 ng (200 pg/s) respectively, as compared to the limits of *ca.* 62.5 pg (1.5 pg/s) for the undifferentiated halides obtained by measuring the mercury response. It seems probable that if some sacrifice in elemental sensitivity is acceptable for chlorine and bromine, other pairs of emission wavelengths could be chosen to afford greater selectivity between these elements.

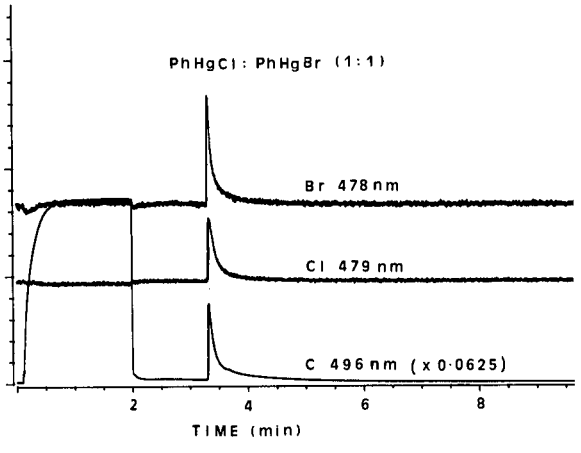


Fig. 4. Simultaneous GC–AED responses of Br, Cl and C as phenylmercuric chloride and phenylmercuric bromide at the chromatographic conditions of Fig. 1, but using $O_2$ and high make-up gas flow.

## CONCLUSIONS

The study indicates that a sensitive GC procedure for the determination of halides using FID and AED may be feasible. The method using FID is about ten times more sensitive than with a packed column; detection limits can be further improved approximately five-fold with AED. Also, in the absence of complete GC separation of the halides as PMC and PMB, chloride and bromide may be measured simultaneously using different AED wavelengths for Cl and Br detection.

## ACKNOWLEDGEMENTS

The University of Mashhad, Iran, and the Ministry of Culture and Higher Education, Islamic Republic of Iran, are acknowledged for the grant of sabbatical leave to one of us (A. S.-Y). M. Y. K. acknowledges the receipt of a Fulbright Research award. We thank the Hewlett-Packard Company, Bruce Quimby and James Sullivan for their continued interest in this project. The research was supported in part by grants from Merck Sharp and Dohme Research Laboratories and from Rhone Poulenc Rorer.

## REFERENCES

1 R. Belcher, J. R. Majer, J. A. Rodriguez-Vazquez, W. I. Stephen and P. C. Uden, *Anal. Chim. Acta*, 57 (1971) 73.

2 R. Belcher, J. A. Rodriguez-Vazquez, W. I. Stephen and P. C. Uden, *Chromatographia*, 9 (1976) 201.
3 A. Sarafraz-Yazdi, *Ph.D. dissertation*, Birmingham University, Birmingham, 1981.
4 A. J. McCormack, S. C. Tong and W. D. Cooke, *Anal. Chem.*, 37 (1965) 1470.
5 L. Ebdon, S. Hill and R. W. Ward, *Analyst*, 111 (1986) 113.
6 T. H. Risby and Y. Talmi, *CRC Crit. Rev. Anal. Chem.*, 14(3) (1983) 231.
7 P. C. Uden, *Trends Anal. Chem.*, 6(9) (1987) 238.
8 P. C. Uden, in R. M. Harrison and S. Rapsomanikis (Editors), *Environmental Analysis using Chromatography Interfaced with Atomic Spectroscopy*, Ellis Horwood, Chichester, 1989, pp. 96–125.
9 J. P. Matousek, B. J. Orr and M. Selby, *Prog. Anal. Spectrosc.*, 7 (1984) 275.
10 G. Decadt, W. Bayens, D. Bradley and L. Goeyens, *Anal. Chem.*, 57 (1985) 2788.
11 K. B. Olsen, D. S. Sklarew and J. C. Evans, *Spectrochim. Acta*, 40B (1985) 357.
12 G. M. Greenway and N. W. Barnett, *J. Anal. At. Spectrom.*, 4 (1989) 783.
13 P. Lansens and W. Bayens, *Anal. Chim. Acta*, 228 (1990) 93.
14 P. Lansens, C. Meuleman and W. Bayens, *Anal. Chim. Acta*, 229 (1990) 281.
15 B. D. Quimby and J. J. Sullivan, *Anal. Chem.*, 62 (1990) 1027.

*Journal of Chromatography*, 594 (1992) 400–402
Elsevier Science Publishers B.V., Amsterdam

CHROM. 23 844

# Short Communication

# Fast and sensitive staining technique for catalase in polyacrylamide gel

Heidi Pichorner*, Sonja Loew, Soudabeh A. A. Korori, Georg Jessner and Robert Ebermann

*Institut für Chemie, Universität für Bodenkultur, Gregor Mendelstrasse 33, A-1180 Vienna (Austria)*

(First received January 23rd, 1991; revised manuscript received November 5th, 1991)

ABSTRACT

The described staining technique for catalase activity on polyacrylamide gel leads to sharp colourless bands on a uniform brown background. It is based on the oxidation of *a*-dianisidine with hydrogen peroxide by the catalytic action of haemin. Catalase activity can be detected down to 0.25 U. The whole staining procedure needs about 30 min and parallel detection of peroxidase activity is possible.

## INTRODUCTION

Several staining techniques have been developed for visualization of the catalytic activity of catalase on gel electropherograms. A sensitive method restricted to starch gels depends upon the oxidation of iodide to iodine by hydrogen peroxide and the subsequent reaction of iodine with starch. Zones of catalase activity can be detected as colourless bands on a blue background [1–4].

Another stain uses the fact that after exposure to hydrogen peroxide the area containing the trapped gas oxygen can be stained with potassium permanganate, while the rest of the gel surface is covered with manganese dioxide. The contrast can be made more pronounced by rinsing the gels with acetic acid to remove manganese dioxide [5].

A method of distinguishing between catalase and haemoglobin is described in ref. 6 using *o*-dianisidine and "Teepol", but the mechanism of the reaction is not clear.

Catalase catalyses in a fast reaction the dismutation of hydrogen peroxide to yield water and oxygen as colourless reaction products. In contrast the peroxidase-catalysed reduction of hydrogen peroxide to water needs an external source of electrons. In the case of phenols such as *o*-dianisidine as electron donors, coloured oxidation products are formed. This different mode of hydrogen peroxide decomposition of catalase and peroxidase can be used for the simultaneous histochemical detection of catalase and peroxidase activities. Gregory and Fridovich [7] describe a method for the detection of catalase activity in polyacrylamide gels depending on the peroxidation of diphenols with hydrogen peroxide to coloured products under the catalytic influence of horseradish peroxidase (HRP). This method is still applied [8]. In the present paper we describe a more sensitive and time-saving modification of this technique using *o*-dianisidine, hydrogen peroxide and haemin as a catalytic agent.

0021-9673/92/$05.00 

## EXPERIMENTAL

### *Chemicals*

*o*-Dianisidine (3,3′-dimethoxybenzidine), bovine haemin and bovine liver catalase (C 40) were purchased from Sigma (Munich, Germany). All other chemicals were of analytical grade (Merck, Darmstadt, Germany).

### *Preparation of wood and seed extracts*

Twigs (diameter about 1 cm) were cut into splinters using a slow-turning lathe in order to prevent excess heating. Seed was milled by hand with a pestle at 4°C. Aliquots of 1 g of the splinters and the seed powder were extracted overnight at 4°C in 3 ml of buffer according to ref. 9. After removing the splinters by filtration the solution obtained was used for electrophoretic analysis without further concentration.

### *Polyacrylamide gel electrophoresis (PAGE)*

Gel electrophoresis was performed in a vertical slab gel apparatus as described earlier [10]. A separation gel containing 15.0% acrylamide, pH 8.6, cross-linked 1:75 with N,N′-bismethyleneacrylamide was used. A 50-$\mu$l sample of the wood extract and variable amounts of pure catalase solutions were used. The electrophoresis buffer system consisted of Tris–glycine, pH 8.9. The separation time was 3 h with a constant voltage of 300 V and a starting current of 120 mA. After electrophoresis the gels were washed in distilled water for 30 min.

### *Detection of catalase*

After electrophoretic separation the gel was soaked in a phosphate-buffered solution (0.06 *M*, pH 7.5) containing 0.1 m*M* *o*-dianisidine and 0.05 m*M* haemin, dissolved in a minimal volume of 0.01 *M* sodium hydroxide, for 20 min (solution A). After this the gel was rinsed with distilled water and incubated in a phosphate-buffered solution (0.06 *M*, pH 7.5) containing 0.02 m*M* *o*-dianisidine and 0.1 *M* hydrogen peroxide for 2 min (solution B). The gel was again rinsed with distilled water immediately after the zones of catalase activity appeared as transparent bands on the brown background.

## RESULTS AND DISCUSSION

The haemin-catalysed oxidation of *o*-dianisidine by hydrogen peroxide in polyacrylamide gel results in a uniform brown staining of the gel within a few minutes. At those positions where the decomposition of hydrogen peroxide is performed by catalase, sharp colourless bands appear rapidly after insertion of the gel into incubation solution B. As peroxidase is more effective in oxidizing *o*-dianisidine at the expense of hydrogen peroxide than haemin, zones of peroxidatic activity appear as dark-brown strains. After a few minutes maximum contrast between the colourless zones of catalase activity, the dark-brown zones of peroxidase activity and the amber background is obtained. Fig. 1 shows the simultaneous catalase and peroxidase staining of wood and seed extracts of *larix decidua* harvested at different altitudes. At the certain time of harvest the wood samples show peroxidase and seed catalase isoenzymes only. This result will be explored in further work.

The sensitivity of the method was determined by using serial dilutions of bovine liver catalase. Using gels with 0.75 mm thickness catalase activity can be detected down to concentrations of 0.25 U. With increasing thickness of the gel the sensitivity of the method decreases drastically even with increased incubation time for haemin and *o*-dianisidine. In gels

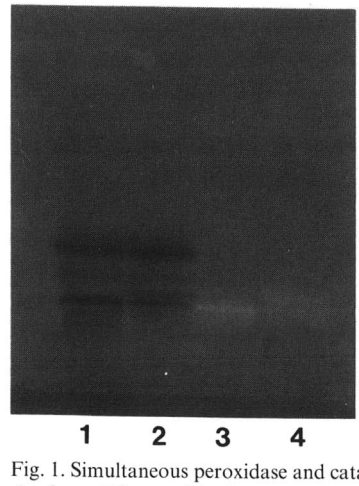


Fig. 1. Simultaneous peroxidase and catalase stain of *Larix decidua* from different altitudes. 1 = Wood of *L. decidua* from 600 m; 2 = wood of *L. decidua* from 1300 m; 3 = seed of *L. decidua* from 600 m; 4 = seed of *L. decidua* from 1300 m.

more than 4 mm thick the gel is destroyed at the positions of catalase activity by oxygen evolution.

The advantage of this technique using haemin instead of HRP is the fact that it needs less time. When gels containing concentrations of acrylamide up to 15% are used it takes several hours until HRP soaks homogeneously into the gel matrix. In contrast to HRP, with a relative molecular mass of about 40 000 daltons, haemin offers the possibility of completing the stain within 30 min because of its considerably lower molecular weight (616 daltons).

It is known that haemin displays peroxidatic function in alkaline aqueous solutions (pH $>9$) owing to the faster decay of the haematin–hydrogen peroxide complex compared with the decay of the haem–peroxide complex. In acrylamide gels the catalytic property of haemin is very well marked, even at neutral pH, possibly owing to the more hydrophobic character of the gel. Thus haemin is able to act as a perfect substitute for HRP in staining methods for catalase.

REFERENCES

1 K. Robinson, *J. Appl. Bacteriol.*, 29 (1966) 179.
2 O. Gabriel, *Methods Enzymol.*, 22 (1971) 578.
3 C. R. Shaw and R. Prasad, *Biochem. Genetics*, 4 (1970) 297.
4 A. J. Hale and J. H. Renwick, *Biochem. J.*, 80 (1961) 49.
5 O. A. Thorup, W. B. Strole and B. S. Leavell, *J. Lab. Clin. Med.*, 58 (1961) 122.
6 G. R. Tudhope, *Nature (London)*, 205 (1965) 404.
7 E. M. Gregory and I. Fridovich, *Anal. Biochem.*, 58 (1974) 57.
8 I. Goldberg and A. Hochman, *Biochim. Biophys. Acta*, 991 (1989) 330.
9 R. Ebermann and K. Stich, *Phytochemistry*, 21 (1982) 2401.
10 R. Ebermann and H. Bodenseher, *Experientia*, 24 (1968) 523.

*Journal of Chromatography*, 594 (1992) 403
Elsevier Science Publishers B.V., Amsterdam

CHROM. 23 890

# Book Review

*Advances in steroid analysis '90 (Proceedings of the 4th symposium on the analysis of steroids)* edited by S. Görög (guest editor E. Heftmann), Akadémiai Kiadó, Budapest, 1991, XIII + 493 pp., price US$58.00, ISBN 936-05-6034-8.

This volume contains the printed proceedings of the *4th Symposium on the Analysis of Steroids*, held in April 1990 in Pécs, Hungary. The first, second and third symposia of this series took place in Eger (1981), Szeged (1984) and Sopron (1987), respectively, and the proceedings were published by the same publishers, Akadémiai Kiadó (Budapest), with Elsevier (Amsterdam). These symposia present a unique forum for the discussion of current developments in steroid analysis.

The 62 papers in this book, contributed by leading experts from sixteen countries, represent the majority of lectures and posters, including the plenary and keynote lectures. Following the style in the proceedings of the previous symposia, the papers are classified according to methodology. A very wide range of analytical methods for a variety of analytes are covered. The contents consist of five main sections, on receptor binding studies, immunoassays, chromatography, spectroscopy and clinical studies.

Almost all important fields of contemporary steroid analysis are represented in a well organized fashion, such as clinical and biomedical analysis (determination of endogenous and synthetic steroid hormones, their metabolites and cardiotonic steroids, assays for the diagnosis of endocrine disorders and cancer), analyses for steroids in drugs, foods, ointments and microbial degradation products from plant sterols, officinal and industrial analysis. Among various chromatographic techniques, high-performance liquid chromatography (HPLC) appears to be the most versatile for the reliable and sensitive determination of common and less-common steroids. The utilization of mobile phase additives (*e.g.*, β-cyclodextrin), pre-column fluorescence labelling (*e.g.*, diazomethylpyrene) and post-column reactors containing immobilized enzymes (*e.g.*, hydroxysteroid dehydrogenases) is pertinently demonstrated.

Recent progress in steroid analyses for biological materials is fairly reflected in the frequent use of combined techniques, such as gas chromatography (GC)–mass spectrometry (MS), HPLC–MS and HPLC–immunoassay. GC–negative-ion chemical ionization MS combined with appropriate derivatization is particularly promising for the sensitive determination of steroids. In addition, HPLC–MS with soft ionization modes (*e.g.*, thermospray and electrospray) seems to be a powerful tool for the direct determination of steroid sulphates and glucuronides in biomedical research and clinical diagnosis.

This volume is invaluable for understanding the current trends in steroid analysis by modern instrumental techniques, and will be useful for steroid chemists, biochemists and analysts in both academic and industrial fields.

*Sendai (Japan)* Toshio Nambara

# Author Index


Abraham, M. H. and Whiting, G. S.
Hydrogen bonding. XXI. Solvation parameters for alkylaromatic hydrocarbons from gas–liquid chromatographic data 594(1992)229
André, G., see Chauret, N. 594(1992)179
Anigbogu, V. C., Muñoz de la Peña, A., Ndou, T. T. and Warner, I. M.
Retention behavior of β-cyclodextrin complexes of anthracene and pyrene using reversed-phase liquid chromatography. The effects of *tert.*-butanol and cyclopentanol 594(1992)37
Annette, D., see Graham, W. D. 594(1992)187
Araki, T., see Kimata, K. 594(1992)87
Archambault, J., see Chauret, N. 594(1992)179
Aronson, A. L., see Tyczkowska, K. L. 594(1992)195
Auriola, S. O. K., Lepistö, A.-M., Naaranlahti, T. and Lapinjoki, S. P.
Determination of taxol by high-performance liquid chromatography–thermospray mass spectrometry 594(1992)153
Baarslag, P. C., see De Bokx, P. K. 594(1992)9
Barrett, D., see Buck, C. F. 594(1992)225
Berger, R., see Tröltzsch, C. 594(1992)111
Berger, T. A. and Deye, J. F.
Correlation between column surface area and retention of polar solutes in packed-column supercritical fluid chromatography 594(1992)291
Betto, P., Gabriele, R. and Galeffi, C.
Determination of the norlignan glucosides of Hypoxidaceae by high-performance liquid chromatography 594(1992)131
Biggs, W. R., see Jinno, K. 594(1992)105
Bogoni, P., see Zonta, F. 594(1992)137
Bohm, B. A., see Koupai-Abyazani, M. R. 594(1992)117
Bradshaw, J. S., see Johnson, D. F. 594(1992)283
Buck, C. F., Mayewski, P. A., Spencer, M. J., Whitlow, S., Twickler, M. S. and Barrett, D.
Determination of major ions in snow and ice cores by ion chromatography 594(1992)225
Burford, M. D., see Langenfeld, J. J. 594(1992)297
Caruel, H., Phemius, P., Rigal, L. and Gaset, A.
Chromatographic separation of polyols by ligand exchange. Effects of the ion-exchange resin cross-linking and size 594(1992)125
Caslavska, J. and Thormann, W.
Continuous separation and purification of proteins by recycling isotachophoresis 594(1992)361
Chalom, J., see Tod, M. 594(1992)386
Chauret, N., Côté, J., Archambault, J. and André, G.
High-performance gel permeation chromatographic analysis of immunoglobulin M produced by hybridoma cell culture 594(1992)179
Cheng, J., see Wu, C. 594(1992)243
Chloupek, R. C., Hancock, W. S. and Snyder, L. R.
Computer simulation as a tool for the rapid optimization of the high-performance liquid chromatographic separation of a tryptic digest of human growth hormone 594(1992)65
Cisowski, W., see Makuch, B. 594(1992)145
Coenegracht, P. M. J., see Wieling, J. 594(1992)45
Côté, J., see Chauret, N. 594(1992)179
De Bokx, P. K., Baarslag, P. C. and Urbach, H. P.
Modelling of displacement chromatography using non-ideal isotherms 594(1992)9
De Castro, A., see Montaño, A. 594(1992)259
Delgado, C., Sancho, P., Mendieta, J. and Luque, J.
Ligand–receptor interactions in affinity cell partitioning. Studies with transferrin covalently linked to monomethoxypoly(ethylene glycol) and rat reticulocytes 594(1992)97
De Ligny, C. L., see Gelsema, W. J. 594(1992)217
Demina, N., see Polanuer, B. 594(1992)173
Deye, J. F., see Berger, T. A. 594(1992)291
DiNunzio, J. E. and Gadde, R. R.
Development of stability indicating assay methods for the determination of hydroxamic acids in topical formulations 594(1992)209
Donnelly, J. R. and Sovocool, G. W.
Gas chromatographic elution patterns of chlorinated dioxins *versus* column polarity 594(1992)269
Doornbos, D. A., see Wieling, J. 594(1992)45
Ebermann, R., see Pichorner, H. 594(1992)400
Eguchi, M., see Johnson, D. F. 594(1992)283
Farinotti, R., see Tod, M. 594(1992)386
Feldman, B. J., Mogadeddi, H. and Osterloh, J. D.
Determination of $Pb^{2+}$ in water by isotope dilution gas chromatography–mass spectrometry of tetraethyllead formed by reaction with sodium tetraethylborate 594(1992)275
Fetzer, J. C., see Jinno, K. 594(1992)105
Foley, J. P., see Jeansonne, M. S. 594(1992)1
Gabriele, R., see Betto, P. 594(1992)131
Gadde, R. R., see DiNunzio, J. E. 594(1992)209
Galeffi, C., see Betto, P. 594(1992)131
Gao, W., see Wu, C. 594(1992)243
Gaset, A., see Caruel, H. 594(1992)125
Gazda, K., see Makuch, B. 594(1992)145
Gelsema, W. J., De Ligny, C. L., Huigen, Y. M. and Schuring, J.
Determination of the mean ionic charge of the components of three $^{99m}Tc$ bone scanning agents by gel chromatography with two eluents of different electrolyte composition 594(1992)217
Gong, S., see Wu, C. 594(1992)243
Graham, W. D. and Annette, D.
Determination of ascorbic and dehydroascorbic acid in potatoes (*Solanum tuberosum*) and strawberries using ion-exclusion chromatography 594(1992)187

Grateful, T. M. and Lightfoot, Jr., E. N.
Finite difference modelling of continuous-flow electrophoresis 594(1992)341
Grunau, J. A. and Swiader, J. M.
Chromatography of 99 amino acids and other ninhydrin-reactive compounds in the Pickering lithium gradient system 594(1992)165
Hancock, W. S., see Chloupek, R. C. 594(1992)65
Hartwick, R. A., see Wang, T. 594(1992)325
Hawthorne, S. B., see Langenfeld, J. J. 594(1992)297
Hirokawa, T., see Hu, J. 594(1992)371
Hodges, R. S., see Zhu, B.-Y. 594(1992)75
Hu, J., Hirokawa, T., Nishiyama, F., Kiso, Y., Ito, K. and Shoto, E.
Study of isotachophoretic separation behaviour of metal cations by means of particle-induced X-ray emission. III. Analysis of a crude rare earth chloride from monazite 594(1992)371
Huigen, Y. M., see Gelsema, W. J. 594(1992)217
Ito, K., see Hu, J. 594(1992)371
Itoh, K., see Jinno, K. 594(1992)105
Jeansonne, M. S. and Foley, J. P.
Improved equations for the calculation of chromatographic figures of merit for ideal and skewed chromatographic peaks 594(1992)1
Jenke, D. R.
Determination of solute–polymer interaction constants via chromatography with polymer capillaries 594(1992)29
Jessner, G., see Pichorner, H. 594(1992)400
Jinno, K., Yamamoto, K., Ueda, T., Nagashima, H., Itoh, K., Fetzer, J. C. and Biggs, W. R.
Liquid chromatographic separation of all-carbon molecules $C_{60}$ and $C_{70}$ with multi-legged phenyl group bonded silica phases 594(1992)105
Johnson, D. F., Bradshaw, J. S., Eguchi, M., Rossiter, B. E., Lee, M. L., Petersson, P. and Markides, K. E.
Synthesis of (1*R-trans*)-N,N′-1,2-cyclohexylenebisbenzamideoligodimethylsiloxane copolymers for use as chiral stationary phases for capillary supercritical fluid chromatography 594(1992)283
Jonkman, J. H. G., see Wieling, J. 594(1992)45
Kakemoto, M.
Simultaneous determination of sorbic acid, dehydroacetic acid and benzoic acid by gas chromatography–mass spectrometry 594(1992)253
Khuhawar, M. Y., see Sarafraz-Yazdi, A. 594(1992)395
Kimata, K., Tanaka, N. and Araki, T.
Suppression of the effect of metal impurities in alkylsilylated silica packing materials 594(1992)87
Kiso, Y., see Hu, J. 594(1992)371
Korori, S. A. A., see Pichorner, H. 594(1992)400
Kostenko, V. G., see Nemirovskii, V. D. 594(1992)23
Koupai-Abyazani, M. R., McCallum, J. and Bohm, B. A.
Identification of the constituent flavanoid units in sainfoin proanthocyanidins by reversed-phase high-performance liquid chromatography 594(1992)117
Kouwatli, H., see Tod, M. 594(1992)386
Langenfeld, J. J., Burford, M. D., Hawthorne, S. B. and Miller, D. J.
Effects of collection solvent parameters and extraction cell geometry on supercritical fluid extraction efficiencies 594(1992)297
Lapinjoki, S. P., see Auriola, S. O. K. 594(1992)153
Lee, H.-B. and Peart, T. E.
Supercritical carbon dioxide extraction of resin and fatty acids from sediments at pulp mill sites 594(1992)309
Lee, H. K., see Yeo, S. K. 594(1992)335
Lee, M. L., see Johnson, D. F. 594(1992)283
Legendre, J.-Y., see Tod, M. 594(1992)386
Lepistö, A.-M., see Auriola, S. O. K. 594(1992)153
Li, S. F. Y., see Yeo, S. K. 594(1992)335
Lightfoot, Jr., E. N., see Grateful, T. M. 594(1992)341
Little, R. J., see Tsuji, K. 594(1992)317
Loew, S., see Pichorner, H. 594(1992)400
Lu, X., see Wu, C. 594(1992)243
Luque, J., see Delgado, C. 594(1992)97
Mahuzier, G., see Tod, M. 594(1992)386
Makuch, B., Gazda, K. and Cisowski, W.
Isolation of aristolochic acids $HA_sI$ and $HA_sII$ by preparative liquid chromatography 594(1992)145
Mant, C. T., see Zhu, B.-Y. 594(1992)75
Markides, K. E., see Johnson, D. F. 594(1992)283
Maruyama, M. and Nagayoshi, T.
Reversed-phase liquid chromatographic behaviour of alkylamines with amperometric detection and its application to trace analysis 594(1992)159
Masotti, P., see Zonta, F. 594(1992)137
Mayewski, P. A., see Buck, C. F. 594(1992)225
McCallum, J., see Koupai-Abyazani, M. R. 594(1992)117
Mendieta, J., see Delgado, C. 594(1992)97
Mensink, C. K., see Wieling, J. 594(1992)45
Michalik, M., see Tröltzsch, C. 594(1992)111
Miller, D. J., see Langenfeld, J. J. 594(1992)297
Misra, S., see Sharma, S. D. 594(1992)379
Mogadeddi, H., see Feldman, B. J. 594(1992)275
Monakhova, N. I., see Nemirovskii, V. D. 594(1992)23
Montaño, A., De Castro, A., Rejano, L. and Sánchez, A.-H.
Analysis of zapatera olives by gas and high-performance liquid chromatography 594(1992)259
Muñoz de la Peña, A., see Anigbogu, V. C. 594(1992)37
Naaranlahti, T., see Auriola, S. O. K. 594(1992)153
Nagashima, H., see Jinno, K. 594(1992)105
Nagayoshi, T., see Maruyama, M. 594(1992)159
Nambara, T.
Advances in steroid analysis (edited by S. Görög) (Book Review) 594(1992)403
Ndou, T.T., see Anigbogu, V.C. 594(1992)37
Nemirovskii, V. D., Monakhova, N. I. and Kostenko, V. G.
High-performance liquid chromatographic study of the correlation between the physico-chemical parameters of furan and benzene aldehydes and the rate of their metabolism by yeast 594(1992)23
Nishiyama, F., see Hu, J. 594(1992)371
Olsen, B. A., Stafford, J. D. and Reed, D. E.
Determination of dirithromycin purity and related substances by high-performance liquid chromatography 594(1992)203

Osterloh, J. D., see Feldman, B. J. 594(1992)275
Peart, T. E., see Lee, H.-B. 594(1992)309
Petersson, P., see Johnson, D. F. 594(1992)283
Phemius, P., see Caruel, H. 594(1992)125
Pichorner, H., Loew, S., Korori, S. A. A., Jessner, G. and Ebermann, R.
Fast and sensitive staining technique for catalase in polyacrylamide gel 594(1992)400
Polanuer, B., Sholin, A., Demina, N. and Rumiantseva, N.
Determination of glutamine, glutamic acid and pyroglutamic acids using high-performance liquid chromatography on dynamically modified silica 594(1992)173
Poulou, M., see Tod, M. 594(1992)386
Reed, D. E., see Olsen, B. A. 594(1992)203
Rejano, L., see Montaño, A. 594(1992)259
Rigal, L., see Caruel, H. 594(1992)125
Rossiter, B. E., see Johnson, D. F. 594(1992)283
Roux-de Balmann, H. and Sanchez, V.
Continuous-flow electrophoresis: a separation criterion applied to the separation of model proteins 594(1992)351
Rumiantseva, N., see Polanuer, B. 594(1992)173
Sánchez, A.-H., see Montaño, A. 594(1992)259
Sanchez, V., see Roux-de Balmann, H. 594(1992)351
Sancho, P., see Delgado, C. 594(1992)97
Sarafraz-Yazdi, A., Khuhawar, M. Y. and Uden, P. C.
Gas chromatography of chloride and bromide as phenylboronic acid/mercuric nitrate derivatives with microwave induced plasma atomic emission detection 594(1992)395
Schuring, J., see Gelsema, W. J. 594(1992)217
Sharma, S. D. and Misra, S.
Quantitative separation of $Cr^{3+}$ from $Mo^{6+}$, $W^{6+}$, $Hg_2^{2+}$, $Cu^{2+}$ and $Pb^{2+}$. Chromatographic behaviour of 51 cations on papers impregnated with Sn(IV)-based inorganic ion exchangers in complex-forming acid systems 594(1992)379
Sholin, A., see Polanuer, B. 594(1992)173
Shoto, E., see Hu, J. 594(1992)371
Snyder, L. R., see Chloupek, R. C. 594(1992)65
Sovocool, G. W., see Donnelly, J. R. 594(1992)269
Spencer, M. J., see Buck, C. F. 594(1992)225
Stafford, J. D., see Olsen, B. A. 594(1992)203
Stancher, B., see Zonta, F. 594(1992)137
Swiader, J. M., see Grunau, J. A. 594(1992)165
Tanaka, N., see Kimata, K. 594(1992)87
Thormann, W., see Caslavska, J. 594(1992)361
Tod, M., Legendre, J.-Y., Chalom, J., Kouwatli, H., Poulou, M., Farinotti, R. and Mahuzier, G.
Primary and secondary amine derivatization with luminarins 1 and 2: separation by liquid chromatography with peroxyoxalate chemiluminescence detection 594(1992)386
Tröltzsch, C., Berger, R. and Michalik, M.
Liquid chromatographic isolation and structural elucidation of methoxymethylene dimethyl dodecatrienes catalytically synthesized from methanol and three moles of isoprene 594(1992)111
Tsuji, K. and Little, R. J.
Charge-reversed, polymer-coated capillary column for the analysis of a recombinant chimeric glycoprotein 594(1992)317
Twickler, M. S., see Buck, C. F. 594(1992)225
Tyczkowska, K. L., Voyksner, R. D. and Aronson, A. L.
Solvent degradation of cloxacillin *in vitro*. Tentative identification of degradation products using thermospray liquid chromatography–mass spectrometry 594(1992)195
Uden, P. C., see Sarafraz-Yazdi, A. 594(1992)395
Ueda, T., see Jinno, K. 594(1992)105
Urbach, H. P., see De Bokx, P. K. 594(1992)9
Voyksner, R. D., see Tyczkowska, K. L. 594(1992)195
Wang, T. and Hartwick, R. A.
Capillary modification and evaluation using streaming potential and frontal chromatography for protein analysis in capillary electrophoresis 594(1992)325
Warner, I. M., see Anigbogu, V. C. 594(1992)37
Watson, E. and Yao, F.
Fast protein monitoring in fermentation broth using non-porous micropellicular reversed-phase columns 594(1992)392
Whiting, G. S., see Abraham, M. H. 594(1992)229
Whitlow, S., see Buck, C. F. 594(1992)225
Wieling, J., Coenegracht, P. M. J., Mensink, C. K., Jonkman, J. H. G. and Doornbos, D. A.
Selection of robust combinations of extraction liquid composition and internal standard. Monte Carlo simulation of improvement of assay methods with liquid–liquid extraction prior to high-performance liquid chromatography 594(1992)45
Wu, C., Cheng, J., Gao, W., Zeng, Z., Lu, X. and Gong, S.
Preparation and capillary column gas chromatographic characterization of aza-crown ether polysiloxane stationary phases 594(1992)243
Yamamoto, K., see Jinno, K. 594(1992)105
Yao, F., see Watson, E. 594(1992)392
Yeo, S. K., Lee, H. K. and Li, S. F. Y.
Separation of plant growth regulators by capillary electrophoresis 594(1992)335
Zeng, Z., see Wu, C. 594(1992)243
Zhu, B.-Y., Mant, C. T. and Hodges, R. S.
Mixed-mode hydrophilic and ionic interaction chromatography rivals reversed-phase liquid chromatography for the separation of peptides 594(1992)75
Zonta, F., Stancher, B., Bogoni, P. and Masotti, P.
High-performance liquid chromatography of okadaic acid and free fatty acids in mussels 594(1992)137

*Journal of Chromatography*, 594 (1992) 407
Elsevier Science Publishers B.V., Amsterdam

# Erratum

*J. Chromatogr.*, 587 (1991) 247–254

Fig. 6 was reproduced with the legend to Fig. 4, and Fig. 4 and the legend to Fig. 6 do not appear at all. Below are the correct figures, with their respective captions.

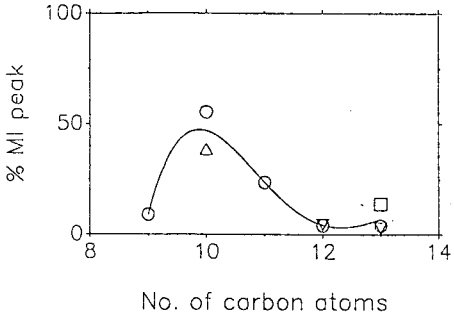


Fig. 4. Relationship between intensity of molecular ion peak and total number of carbon atoms present in the derivative. ○ = α-keto acid; △ = α-keto dicarboxylic acid; ▽ = γ-keto acid; □ = δ-keto acid.

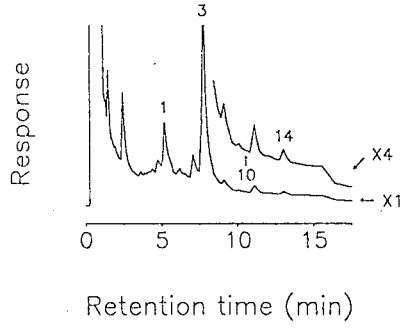


Fig. 6. Gas chromatogram of methyl esters of DNPH derivatives of keto acids extracted from *Cnidoscolus urens* and obtained on an OV-17 column. Peak assignments as in Table I.

# Journal of Chromatography

## Request for Manuscripts

M. Mills and E.M. Thurman will edit a special, thematic issue of the *Journal of Chromatography* entitled "**Principles and Applications of Solid Phase Extraction**". Both reviews and research articles will be included.

Topics such as the following will be covered:

- Surface Chemistry of Bonded Phases
- Analyte and Solvent Interaction with the Solid Phase
- Mechanisms of Isolation on Solid Phase Resins
- Automation of Solid Phase Extraction
- Innovative New Bonded Phases
- Innovative Applications of Solid Phase Extraction to Clinical and Environmental Chemistry

The deadline for receipt of submissions is **April 13th, 1992.** Five copies of the manuscript should be submitted to M. Mills, US Geological Survey, 4821 Quail Crest Place, Lawrence, Kansas 66049, USA. Tel.: (913) 842-9909; Fax: (913) 832-3500. All manuscripts will be reviewed and acceptance will be based on the usual criteria and suitability for the thematic issue, for publishing in the *Journal of Chromatography*. Potential authors of reviews should contact M. Mills prior to any submission.

Vol. 594, Nos. 1 + 2

Journal of Chromatography

# NEWS SECTION

## ANNOUNCEMENTS

### CHROMATOGRAPHY AND ECOLOGY, TALLINN, ESTONIA, SEPTEMBER 4–6, 1992

This symposium, which is dedicated to the centenary of Teodor Lippmaa, one of the first to start chromatographical investigation of plant pigments, will focus on current developments in methods of chromatography, concentrating on the applications of chromatography in ecological research.

The language of the conference will be English.

The participation fee will be approximately US$ 150. A considerably reduced fee for participants from East European and developing countries is available. The fee will cover transport costs within Estonia, Abstracts and lunches. Considering the changing currency situation in Estonia, more detailed information will be given in the Second Circular.

For further details contact: Elle Roosaluste, Department of Botany and Ecology, Lai 40, Tartu, Estonia. Tel.: (+7-1434) 35151; Fax: (+7-1434) 33472; E-Mail: KALEVI@ZBI.TARTU. EW.SU.

### ANABIOTEC '92, NOORDWIJKERHOUT, NETHERLANDS, SEPTEMBER 21–23, 1992

The 4th Anabiotec symposium will cover the rapidly developing interdisciplinary field at the interface of biotechnology and analytical methodology, enable analytical chemists and biotechnologists to exchange information in order to develop a better understanding of analysis in biotechnology, and aim towards integrating fundamental and applied research in this overlapping field of interest.

The scientific programme will consist of invited plenary lectures, submitted and invited paper presentations (both oral and poster), informal discussion sessions and scientific round tables in combination with a well balanced exhibition.

Topics to be presented will include:

*Instrumental analysis and new developments*:

- Chromatography; HPLC, GC preparative and displacement chromatography, sample preparation
- Spectroscopy; NMR, IR, MS
- Separation techniques, such as capillary zone electrophoresis (CZE), field flow fractionation (FFF)
- Flow Injection Analysis (FIA)
- Hyphenated techniques
- Kinetic methods
- New developments

*Bio-detection, biorecognition and surface (bio)chemistry:*

- Biosensors; fundalmentals and applications
- Monoclonal antibodies and DNA/RNA probes
- Glycobiology

*Application areas:*

- Fermentation/production monitoring and process control
- Regulatory aspects and environmental control
- Protein engineering
- Animal/plant cell biotechnology
- Regulatory aspects of rDNA products

An Exhibition of products and instrumentation within the scope of the symposium will be presented. As a large number of requests for exhibition space is expected (and space is limited), anyone who is interested in exhibiting is urged to make an early booking. For more information concerning the exhibition please contact the organizing bureau at the address mentioned below.

The registration fee will be approximately Dfl. 1300 (including 18.5% VAT). Transfer from Schiphol to the Leeuwenhorst will be taken care of. A discount will be available for PhD students provided they enclose a letter from the head of their department and a copy of their student identity card with their registration form. This special fee will amount to approximately Dfl. 650.00, including 18.5% VAT, two night accommodation and meals.

All those who wish to present a paper at the Anabiotec meeting should send an abstract to the organizing bureau.

For further details contact: ANABIOTEC '92, p/a CAOS, WG Plein 475, 1054 SH Amsterdam, Netherlands. Tel.: (+31-20) 616-5151; Fax: (+31-20) 689-0981.

## INTERNATIONAL ION CHROMATOGRAPHY SYMPOSIUM 1992, LINZ AUSTRIA, SEPTEMBER 21–24, 1992

This symposium will feature plenary lectures by invited speakers and contributed podium and poster presentations. The meeting features program and scientific committees of internationally recognized ion chromatography experts. This three-day meeting provides a unique opportunity for scientists from a variety of disciplines to exchange ideas and results on current ion chromatography methods and procedures.

The session topics are:

- fundamental principles and general aspects of IC
- sample handling and pretreatment
- general novel applications
- environmental applications
- industrial applications
- applications in the nuclear and power generation industry
- capillary electrophoresis for inorganic ions

Plenary lectures will be presented by: J.F.K. Huber (University of Vienna), P.R. Danesi (International Atomic Energy Agency), Petr Bocek (Czechoslovak Academy of Sciences), and M.D.H. Amey (Winfrith Technology Centre).

The program committee invites you to submit an abstract for a presentation at the symposium. Abstracts will be considered for inclusion in the program as either oral or poster presentations. An abstract book will be distributed during registration. To participated in the scientific sessions, submit an abstract of 300 words or less by March 15, 1992 to the address given below.

For further details contact: Günther Bonn, Johannes-Kepler-University, Analytical Chemistry Department, Altenbergerstrasse 69, A-4040 Linz, Austria. Tel.: (+43-732) 2468-723; Fax: (+43-732) 2468-679.

## 1st EUROPEAN SYMPOSIUM ON FPLC OF BIOMOLECULES, STRASBOURG, FRANCE, OCTOBER 19–20, 1992

The scientific programme of this symposium will consist of oral presentations, poster sessions and discussions. Submitted abstracts on the use of FPLC will be evaluated by a scientific committee and considered for oral or poster presentations on various topics, including: preparative chromatography; scaling-up; clinical applications; automation; chromatography techniques, analytical applications; troubleshooting/maintenance; industrial applications; and, multidimensional chromatography.

Abstracts describing original research using FPLC for the isolation of biomolecules, such as carbohydrates, enzymes, DNA/RNA, glycoproteins,

growth factors, membrane proteins, monoclonal antibodies, nucleotides, peptides, phosphoproteins, receptors, and recombinant proteins, are welcome. The deadline for submission of Abstracts is June 15, 1992.

Advance registration fee will be FF 2200, which will cover all scientific and social events. Qualified students will be eligible for a reduced rate of FF 1400. After September 20, 1992 the registration fee will be FF 2500 and FF 1600 for full-paying participants and students, respectively.

For further details contact: Symposium Secretariat, B.O. Conference Service, P.O. Box 100 78, S-750 10 Uppsala, Sweden. Tel. and Fax: (+46-18) 30-4074.

### BUDAPEST CHROMATOGRAPHY CONFERENCE, BUDAPEST, HUNGARY, DECEMBER 14–16, 1992

The scientific program of the conference will include both oral and poster sessions. Main topics of the conference are: theoretical aspects of chromatography; HPLC; HPTLC; electrophoretic techniques, instrumentation, calculation methods, optimization, computer application; stationary phases; chromatography of biologically active synthetic and natural products; preparative and industrial scale separations; and free communications.

An exhibition of chromatographic equipment, stationary phases, solvents and literature will be held adjacent to the Budapest Chromatography Conference.

The official language of the conference is English.

For further details contact: Organizing Bureau, Agnes v. Rubányi, Intercongress, Dózsa György u. 84/a, H-1068 Budapest, Hungary. Tel.: (+36-1) 122-2203; Fax: (+36-1) 142-4118; Telex: 223955 ici pv.

### 4TH WORKSHOP ON CHEMISTRY AND FATE OF MODERN PESTICIDES AND RELATED POLLUTANTS, PRAGUE, CZECHOSLOVAKIA, SEPTEMBER 8–10, 1993

All are invited to attend this 4th workshop dealing with modern pesticides. Due to significant environmental problems in Eastern Europe, this topic has been extended to include withdrawn pesticides: organo-Cl, PCBs. Environmental chemists, food chemists, analytical chemists, toxicologists and biologists will discuss in an interdisciplinary way relevant scientific problems. Emphasis will be placed on: residue monitoring programs, chemical and biological screening methods, quality control, toxicology and legislation.

The proceedings will be published in the *International Journal of Environmental Analytical Chemistry.*

The official language of the workshop will be English.

For further details, contact (for Eastern European countries): Dr. J. Hajslová, Department of Food Chemistry and Analysis, Institute of Chemical Technology, Suchbátarova 5, 166 28 Prague 6-Dejvice, Czechoslovakia. Fax: (+42-2) 311-4769. For all other countries, contact: IAEAC, M. Frei-Häusler, P.O. Box 46, CH-4123 Allschwil 2, Switzerland. Fax: (+41-61) 482-0805.

## COURSES

### 1992 TRAINING PROGRAM OF THE RESEARCH INSTITUTE FOR CHROMATOGRAPHY, KORTRIJK, BELGIUM

The following *Courses with Hands-on* will be held this year:

Capillary Gas Chromatography: Theory and Practice; February 5–7 and September 23–25, 1992.

Sample Preparation Methods for Capillary Gas Chromatography; March 25–27 and November 18–20, 1992.

Capillary GC–Mass Spectrometry: Interpretation of Spectra – Quantitation; April 28–30 and December 2–4, 1992.

Capillary Zone Electrophoresis and Micellar Electrokinetic Chromatography; June 17–19, 1992.

Modern Liquid Chromatography: Theory and Practice; October 14–16, 1992.

Chromatography in Environmental Analysis: Practical Validation of Official Methods; December 16–18, 1992.

The following *Seminars with Demonstrations* will be offered:

Identification in Capillary Gas Chromatography: Retention Indices, CGC–MS, CGC–FTIR, CGC–AED; May 7, 1992.

Supercritical Fluid Extraction: Possibilities and Limitations; May 15, 1992.

High Temperature Capillary GC: Possibilities and Limitations; June 12, 1992.

Microbore and Micropacked LC: 'Quo Vadis?'; October 23, 1992

Chromatographic Techniques for the Characterization of Polymers; November 6, 1992.

Chromatographic Techniques for the Analysis of Oils and Fats; November 27, 1992.

To ensure optimum communication and instrument occupation, the number of participants to each of the courses is limited to a maximum of 20. All courses listed above will be in English.

The cost of courses is BF 40 000 or DM 2000; Seminars are BF 8000 or DM 400.

For further information contact: Research Institute for Chromatography, R.I.C. bvba, Kennedypark 20, B-8500 Kortrijk, Belgium. Tel.: (+32-56)

## AWARDS

### REGINALD BENNET RECEIVES AOAC INTERNATIONAL 1991 WILEY AWARD

Reginald W. Bennett, head of the research group on serological methods and deputy chief at the U.S. Food and Drug Administration (FDA) Food Microbiology Methods Development Branch in Washington, DC, is the Recipient of the 1991 AOAC International Harvey W. Wiley award.

In a career spanning 35 years, the last 25 with FDA, Bennett's efforts have been specifically directed toward detecting microbial contamination of foods and uncovering the epidemiological causes. Among his many contributions is his work on the use of microslide gel-diffusion for detecting and semiquantifying contamination with staphylococcal enterotoxin, extraction methods for microbial toxins, methodology for purifying *Bacillus* toxins, schematization of *Listeria* serotyping, and methodology for serological renaturing (with urea) of heat-treated *S. aureus* enterotoxin. Especially noteworthy are his codevelopment of a highly specific miniaturized serological radial system for the detection and serotype identification of *S. aureus* enterotoxin; methods and simplified medium for the production of staphylococcal enterotoxin in the laboratory; and a gel filtration and cation exchange chromatography method which is the most sensitive tool developed employing column chromatography for the separation and detection of staphylococcal enterotoxin in foods.

This US$ 2500 award is given annually to honor Harvey W. Wiley, the "father" of the 1906 Pure Food and Drug Act and a founder of AOAC. The Award recognized the scientist's role in protecting the consumer and environmental quality. Nominations are accepted on an on-going basis.

For more information, contact AOAC International, Tel.: (+1-703) 522-3032; Fax: (+1-703) 522-5468.

## ANALYTICA CHIMICA ACTA CELEBRATES HER 250th VOLUME

### ANALYTICAL ADVANCES FOR THE 90's

This special volume contains papers presented at a symposium entitled "Analytical Advances for the 90's", Ootmarsum, Netherlands, May 23–26, 1991, in celebration of the publication of the 250th volume of *Analytica Chimica Acta*.

Leading analytical chemists from around the world presented lectures in four thematic sessions covering: emerging techniques in chromatography, atomic spectroscopy, molecular spectroscopy and electroanalytical chemistry/sensors.

This resulting special issue of *Analytica Chimica Acta* presents the reader with analytical method development and application areas in a broad perspective.

For further details contact: H. Kort, Elsevier Science Publishers, P.O. Box 330, 1000 AH Amsterdam, Netherlands. Tel.: (+31-20) 5862-873; Fax: (+31-20) 5862-845.

## CALENDAR OF FORTHCOMING EVENTS

**March 9–13, 1992**
**New Orleans, LA, USA**
43rd Pittsburgh Conference and Exposition on Analytical Chemistry and Applied Spectroscopy

Contact: Mrs. Alma Johnson, Program Secretary, The Pittsburgh Conference, 300 Penn Center Boulevard, Suite 332, Pittsburgh, PA 15235-5503, USA.

**April 6–8, 1992**
**Atlanta, GA, USA**
ANATECH '92, 3rd International Symposium on Analytical Techniques for Industrial Process Control

Contact: ANATECH '92, Infosciences Inc., 3000 Dundee Road, Suite 313, Northbrook, IL 60062, USA. Tel.: (708) 291-9161; Fax: (708) 291-0097.

**April 6–8, 1992**
**Nancy, France**
PREP-92, 9th International Symposium on Preparative and Industrial Chromatography

Contact: PREP-92 Secretary, E.N.S.I.C.-L.P.C.I., 1 rue Grandville, B.P. 451, F-54001 Nancy Cedex, France. Tel.: (+33) 83300276; Fax: (+33) 83350811.

□ **April 6–8, 1992**
**York, UK**
International Chiral Chromatography Course: Principles and Practice of Chiral Separation

Contact: Dr. B.J. Clark, Bradford Analytical Associated Ltd., P.O. Box 17, Leeds LS20 8TW, West Yorkshire, UK. Tel.: (+44-274) 384707; (+44-274) 725044.

□ **May 3–6, 1992**
**Warmbaths, S. Africa**
Chromatography: Mass Spectrometry '92

Contact: Joan Moncrieff, Department of Pharmacology, University of Pretoria, P.O. Box 2034, Pretoria 0001, S. Africa. Tel.: (+27-12) 319-2139.

**May 5–8, 1992**
**Liège, Belgium**
4th International Symposium on Drug Analysis

Contact: Dr. J. Crommen, Drug Analysis '92-Liège, University of Liège, Institute of Pharmacy, rue Fusch 5, B-4000 Liège, Belgium. Tel.: (+32-41) 237002; Fax: (+32-41) 221855.

**May 5–8, 1992**
**Munich, Germany**
13th International Conference on Biochemical Analysis

Contact: U. Arnold, Nymphenburger Strasse 70, D-8000 Munich 2, Germany. Tel.: (+49-89) 1234500; Fax: (+49-89) 183258.

□ **May 7–8, 1992**
**Warmbaths, S. Africa**
Combined Chromatography–Mass Spectrometry Techniques in Biochemical Analysis

Contact: Joan Moncrieff, Department of Pharmacology, University of Pretoria, P.O. Box 2034, Pretoria 0001, S. Africa. Tel.: (+27-12) 319-2139.

**May 12–14, 1992**
**La Grand Motte, France**
4th European Meeting of Groupe Français de Bio-Chromatographie

Contact: Groupe Français de Bio-Chromatographie, Unité d'Immuno Allergie, Institut Pasteur, 28 rue du Docteur Roux, 75724 Paris Cedex 15, France. Tel.: (+33-1) 45688000, ext. 7143; Fax: (+33-1) 43069835; Telex: 250609 F.

**May 17–22, 1992**
**Kyoto, Japan**
4th International Conference on Fundamentals of Adsorption

Contact: Prof. M. Suzuki, Conference Chairman, Institute of Industrial Science, University of Tokyo, 7-22-1 Roppongi, Minato-ku, Tokyo 106, Japan.

**May 25–29, 1992**
**Baltimore, MD, USA**
14th International Symposium on Capillary Chromatography

Contact: Dr. Leonard Schronk, Foundation for the ISCC, P.O. Box 663, Kennett Square, PA 19348, USA. Tel. and Fax: (+1-215) 692-4320.

**June 1–4, 1992**
**Inuyama, Aichi, Japan**
ISPAC, 5th International Symposium on Polymer Analysis and Characterization

Contact: Dr. Sadao Mori, Department of Industrial Chemistry, Faculty of Engineering, Mie University, Tsu, Mie 514, Japan. Tel: (+81-592) 32-1211, ext. 3843; Fax: (+81-592) 31-2252. Dr. Howard Barth, Dupont Com-

pany, Experimental Station, P.O. Box 80228, Wilmington, DE 19880-0228, USA. Tel: (+1-302) 695-4354; Fax: (+1-302) 695-1351.

**□ June 1–5, 1992**
**Florence, Italy**
25th International Symposium on Automotive Technology and Automation

Contact: Dr. John I. Soliman. ISATA, 42 Lloyd Park Avenue, Croydon CR0 5SB, UK. Tel.: (+44-81) 681-3069; Fax: (+44-81) 686-1490.

**June 9–12, 1992**
**Dortmund, Germany**
22nd Roland W. Frei Memorial Symposium on Environmental Analytical Chemistry and Workshop on Detection in Environmental Analysis

Contact: Symposium Office IAEAC, M. Frei-Hausler, P.O. Box 46, CH-4123 Allschwil 2, Switzerland. Tel.: (+41-61) 632789; Fax: (+41-61) 4820805.

**June 14–19, 1992**
**Baltimore, MD, USA**
HPLC '92, 16th International Conference on Column Liquid Chromatography

Contact: HPLC '92, Ms. Shirley E. Schlessinger, 400 E. Randolph Drive, Suite 1015, Chicago, IL 60601, USA. Tel.: (312) 527-2011.

**July 8–10, 1992**
**Amsterdam, Netherlands**
Amsterdam Summercourse on Capillary Electrophoresis

Contact: Dr. W.Th. Kok or Dr. J.C. Kraak, Laboratory for Analytical Chemistry, University of Amsterdam, Nieuwe Achtergracht 166, 1018 WV Amsterdam, Netherlands. Tel.: (+31-20) 525-6539/46/15; Fax: (+31-20) 525-5698.

**July 14–17, 1992**
**Montreal, Canada**
CAC-92, 5th International Conference on Chemometrics in Analytical Chemistry

Contact: Int. Conf. on Chemometrics in Analytical Chemistry, c/o Department of Chemistry, Clarkson University, Potsdam, NY 13699-5810, USA. Tel: (+1-315) 268-3861 (Dr. Hopke); (+1-315) 268-2394 (Dr. Lavine); Fax: (+1-315) 268-6670.

**□ July 27–31, 1992**
**New Hampton, NH, USA**
42nd Annual Gordon Research Conference on Statistics in Chemistry and Chemical Engineering

Contact: Dr. A.M. Cruickshank, Gordon Research Center, University of Rhode Island, Kingston, RI 02881, USA. Tel.: (+1-401) 783-4011; E-Mail: bcp101@uriacc.bitnet.

**Aug. 23–26, 1992**
**York, UK**
Capillary Electrophoresis Training Course

Contact: Dr. Terry Threlfall, Industrial Liaison Executive, Department of Chemistry, University of York, Heslington, York YO1 5DD, UK. Tel.: (+44-904) 432576/432511; Fax: (+44-904) 432516.

**Aug. 24–27, 1992**
**Jena, Germany**
COMPANA '92, 5th Conference on Computer Applications in Analytical Chemistry

Contact: COMPANA '92, Friedrich Schiller University Jena, Institute of Inorganic and Analytical Chemistry, Steiger 3, Haus 3, O-6900 Jena, Germany. Tel.: (+37-82) 25467 or (+37-82) 25029.

**Aug. 26–28, 1992**
**York, UK**
International Symposium on Capillary Electrophoresis

Contact: Dr. Terry Threlfall, Industrial Liaison Executive, Department of Chemistry, University of York, Heslington, York YO1 5DD, UK. Tel.: (+44-904) 432576/432511; Fax: (+44-904) 432516.

**Aug. 31–Sept. 3, 1992**
**Cincinnati, OH, USA**
106th Annual International Meeting and Exposition of the AOAC

Contact: Margaret Ridgell, AOAC, 2200 Wilson Boulevard, Suite 400, Arlington, VA 22201-3301, USA. Tel.: (703) 522-3032; Fax: (703) 522-5468.

**□ September 4–6, 1992**
**Tallin, Estonia**
Chromatography and Ecology

Contact: Elle Roosaluste, Department of Botany and Ecology, Lai 40, Tartu, Estonia. Tel.: (+7-1434) 35151; Fax: (+7-1434) 33472; E-Mail: KALEVI@ZBI.TARTU. EW.SU.

**Sept. 13–18, 1992**
**Aix-en-Provence, France**
19th International Symposium on Chromatography

Contact: G.A.M.S., 88 Boulevard Malesherbes, 75008 Paris,

France. Tel.: (1) 45639304; Fax: (1) 49530434

**Sept. 20–25, 1992**
**Philadelphia, PA, USA**
19th Annual Meeting of the Federation of Analytical Chemistry and Spectroscopy Societies
Contact: FACSS, P.O. Box 278, Manhattan, KS 66502, USA. Tel.: (+1-301) 846-4797.

□ **September 21–23, 1992**
**Noordwijkerhout, Netherlands**
Anabiotec '92
Contact: ANABIOTEC '92, p/a CAOS, WG Plein 475, 1054 SH Amsterdam, Netherlands. Tel.: (+31-20) 616-5151; Fax: (+31-20) 689-0981.

**Sept. 21–24, 1992**
**Linz, Austria**
International Ion Chromatography Symposium
Contact: Century International, P.O. Box 493, Medfield, MA 02052, USA. Tel.: (+1-508) 359-8777; Fax: (+1-508) 359-8778.

**Oct. 3–4, 1992**
**Salt Lake City, UT, USA**
FFF Workshop V
Contact: Julie Westwood, FFF Research Center, Department of Chemistry, University of Utah, Salt Lake City, UT 84112, USA. Tel.: (+1-801) 581-5419; Fax: (+1-801) 581-4353.

**Oct. 5–7, 1992**
**Park City, UT, USA**
3rd International Symposium on Field-Flow Fractionation (FFF)
Contact: Julie Westwood, FFF Research Center, Department of Chemistry, University of Utah, Salt Lake City, UT 84112, USA. Tel.: (+1-801) 581-5419; Fax: (+1-801) 581-4353.

**Oct. 5–8, 1992**
**Tübingen, Germany**
3rd International Symposium on Chiral Discrimination
Contact: Gesellschaft Deutscher Chemiker, Abteilung Tagungen, P.O. Box 90 04 40, D-6000 Frankfurt 90, Germany. Fax: (+49-69) 791-7475

**Oct. 6–9, 1992**
**Rome, Italy**
ITP '92, 8th International Symposium on Capillary Electrophoresis and Isotachophoresis
Contact: Dr. Salvatore Fanali, Istituto di Cromatografia del C.N.R., P.O. Box 10, 00016 Monterotondo Scalo (Rome), Italy. Tel: (+39-6) 9005328/9005836; Fax: (+39-6) 9005849; Telex: 624809 CNR ML 1.

□ **October 19–20, 1992**
**Strasbourg, France**
1st European Symposium on FPLC of Biomolecules
Contact: Symposium Secretariat, B.O. Conference Service, P.O. Box 100 78, S-750 10 Uppsala, Sweden. Tel. and Fax: (+46-18) 30-4074.

**Oct. 20–21, 1992**
**Frederick, MD, USA**
3rd Annual Frederick Conference on Capillary Electrophoresis
Contact: Margaret L. Fanning, Conference Coordinator, PRI, NCI-FCRDC, P.O. Box B, Frederick, MD 21702-1201, USA. Tel.: (+1-301) 846-1089; Fax: (+1-301) 846-5866.

**Nov. 4–6, 1992**
**Montreux, Switzerland**
9th Montreux Symposium on Liquid Chromatography–Mass Spectrometry (LC–MS, SFC–MS, CZE–MS, MS–MS)
Contact: Marianne Frei, IAEAC Secretariat, P.O. Box 46, CH-4123 Allschwil, Switzerland. Tel.: (+41-61) 632789; Fax: (+41-61) 4820805.

**Nov. 29–Dec. 2, 1992**
**Syndey, Australia**
12th International Symposium on HPLC of Proteins, Peptides and Polynucleotides
Contact: 12 ISPPP Sectretariat, GPO Box 128, Sydney NSW 2001, Australia. Tel.: (+61-2) 262-2277; Fax: (+61-2) 262-2323.

□ **December 14–16, 1992**
**Budapest, Hungary**
Budapest Chromatography Conference
Contact: Organizing Bureau, Agnes v. Rubányi, Intercongress, Dózsa György u. 84/a, H-1068 Budapest, Hungary. Tel.: (+36-1) 122-2203; Fax: (+36-1) 142-4118; Telex: 223955 ici pv

**April 4–7, 1993**
**Wrexham, UK**
Ion-Ex '93
Contact: Ion-Ex '93, Conference Secretariat, Faculty of Science, The North East Wales Institute, Connah's Quay, Deeside, Clwyd, CH5 4BR, UK. Tel.: (+44-244) 831-531 ext. 245 or 276; Fax: (+44-244) 814-305.

**May 9–14, 1993**
**Hamburg, Germany**
17th International Symposium on Column Liquid Chromatography

Contact: Gesellschaft Deutscher Chemiker, Abteilung Tagungen, P.O. Box 900440, Varrentrappstrasse 40-42, W-6000 Frankfurt am Main 90, Germany. Tel: (+49-69) 7917-360; Fax: (+49-69) 7917-475.

**Sept. 5–11, 1993**
**Edinburgh, UK**
EUROANALYSIS VIII, 8th European Conference on Analytical Chemistry

Contact: Miss P.E. Hutchinson, Analytical Division, The Royal Society of Chemistry, Burlington House, Piccadilly, London W1V 0BN, UK. Tel.: (071) 4378656; Fax: (071) 734-1227; Telex: 268001.

□ **September 8–10, 1993**
**Prague, Czechoslovakia**
4th Workshop on Chemistry and Fate of Modern Pesticides and Related Pollutants

Contact (for Eastern European countries): Dra. J. Hajslova, Department of Food Chemistry and Analysis, Institute of Chemical Technology, Suchbátarova 5, 166 28 Prague 6-Dejvice, Czechoslovakia. Fax: (+42-2) 311-4769. For all other countries, contact: IAEAC, M. Frei-Häusler, P.O. Box 46, CH-4123 Allschwil 2, Switzerland. Fax:(+41-61) 482-0805.

**June 20–24, 1994**
**Bournemouth, UK**
20th International Symposium on Chromatography

Contact: Executive Secretary, The Chromatographic Society, Nottingham Polytechnic, Burton Street, Nottingham, NG1 4BU, UK. Tel.: (0602) 500596; Fax: (0602) 500614.

□ Indicates new or amended entry

Announcements are included free of charge. Information on planned events should be sent well in advance (6 months) to: Journal of Chromatography, News Section, P.O. Box 330, 1000 AH Amsterdam, Netherlands, or by Fax: (+31 20) 5862304.

## PUBLICATION SCHEDULE FOR 1992

| MONTH | O 1991 | N 1991 | D 1991 | J | F | M | |
|---|---|---|---|---|---|---|---|
| Journal of Chromatography | 585/1 | 585/2<br>586/1<br>586/2<br>587/1 | 587/2<br>588/1+2 | 589/1+2<br>590/1<br>590/2 | 591/1+2<br>592/1+2<br>593/1+2 | 594/1+2<br>595/1 | The publication schedule for further issues will be published later |
| Cumulative Indexes, Vols. 551–600 | | | | | | | |
| Bibliography Section | | | | | | 610/1 | |
| Biomedical Applications | | | | 573/1<br>573/2 | 574/1<br>574/2 | 575/1<br>575/2 | |

## INFORMATION FOR AUTHORS

(Detailed *Instructions to Authors* were published in Vol. 558, pp. 469–472. A free reprint can be obtained by application to the publisher, Elsevier Science Publishers B.V., P.O. Box 330, 1000 AH Amsterdam, The Netherlands.)

**Types of Contributions.** The following types of papers are published in the *Journal of Chromatography* and the section on *Biomedical Applications*: Regular research papers (Full-length papers), Review articles and Short Communications. Short Communications are usually descriptions of short investigations, or they can report minor technical improvements of previously published procedures; they reflect the same quality of research as Full-length papers, but should preferably not exceed five printed pages. For Review articles, see inside front cover under Submission of Papers.

**Submission.** Every paper must be accompanied by a letter from the senior author, stating that he/she is submitting the paper for publication in the *Journal of Chromatography*.

**Manuscripts.** Manuscripts should be typed in double spacing on consecutively numbered pages of uniform size. The manuscript should be preceded by a sheet of manuscript paper carrying the title of the paper and the name and full postal address of the person to whom the proofs are to be sent. As a rule, papers should be divided into sections, headed by a caption (*e.g.*, Abstract, Introduction, Experimental, Results, Discussion, etc.). All illustrations, photographs, tables, etc., should be on separate sheets.

**Introduction.** Every paper must have a concise introduction mentioning what has been done before on the topic described, and stating clearly what is new in the paper now submitted.

**Abstract.** All articles should have an abstract of 50–100 words which clearly and briefly indicates what is new, different and significant.

**Illustrations.** The figures should be submitted in a form suitable for reproduction, drawn in Indian ink on drawing or tracing paper. Each illustration should have a legend, all the *legends* being typed (with double spacing) together on a *separate sheet*. If structures are given in the text, the original drawings should be supplied. Coloured illustrations are reproduced at the author's expense, the cost being determined by the number of pages and by the number of colours needed. The written permission of the author and publisher must be obtained for the use of any figure already published. Its source must be indicated in the legend.

**References.** References should be numbered in the order in which they are cited in the text, and listed in numerical sequence on a separate sheet at the end of the article. Please check a recent issue for the layout of the reference list. Abbreviations for the titles of journals should follow the system used by *Chemical Abstracts*. Articles not yet published should be given as "in press" (journal should be specified), "submitted for publication" (journal should be specified), "in preparation" or "personal communication".

**Dispatch. Before sending the manuscript to the Editor please check that the envelope contains four copies of the paper complete with references, legends and figures. One of the sets of figures must be the originals suitable for direct reproduction. Please also ensure that permission to publish has been obtained from your institute.**

**Proofs.** One set of proofs will be sent to the author to be carefully checked for printer's errors. Corrections must be restricted to instances in which the proof is at variance with the manuscript. "Extra corrections" will be inserted at the author's expense.

**Reprints.** Fifty reprints of Full-length papers and Short Communications will be supplied free of charge. Additional reprints can be ordered by the authors. An order form containing price quotations will be sent to the authors together with the proofs of their article.

# For Superior Chiral Separation From Analytical To Preparative.

The finest from DAICEL·····

Why look beyond DAICEL? We have developed the finest CHIRALCEL, CHIRALPAK and CROWNPAK with up to 17 types of HPLC columns, all providing superior resolution of racemic compounds.

## NEW CHIRALPAK AS

● CHIRALPAK AS

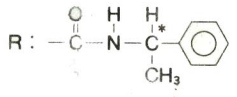

for β-Lactam antibiotics

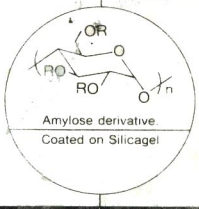


## NEW CHIRALPAK AD

● CHIRALPAK AD

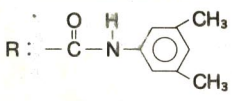

### 1-Acetoxy-2-azetidine

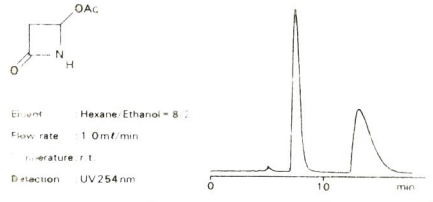


### Oxyphencyclimine

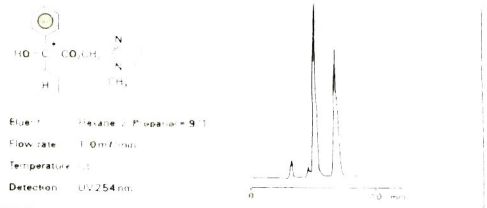


### Ofloxacine methyl ester

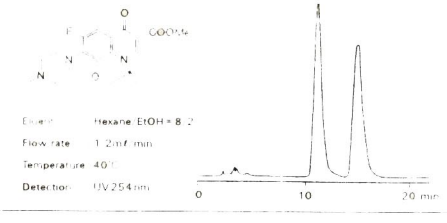


### Verapamil

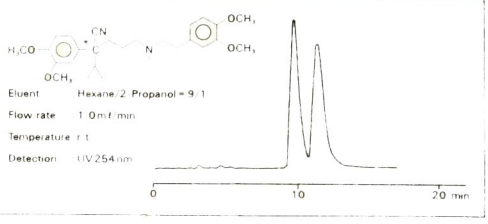


Analytical column 0.46cm × 25cm (10 μm)

CHIRALCEL OA
OB
OC
OD
OJ
OF
OG
OK

CHIRALPAK AS
AD

Normal Phase

Semi-preparative column 2cm × 25cm (10 μm)

**You can have Pure enantiomer quickly!!**

## Separation Service

- A pure enantiomer separation in the amount of 100g 10kg is now available.
- Please contact us for additional information regarding the manner of use and application of our chiral columns and how to procure our separation service.


**DAICEL CHEMICAL INDUSTRIES, LTD.**

chiral chemicals division.

8-1 Kasumigaseki 3-chome, Chiyoda-ku, Tokyo 100, Japan Phone: 03 (507) 3151 FAX: 03 (507) 3193

**DAICEL (U.S.A.), INC.**
Fort Lee Executive Park
Two Executive Drive, Fort Lee
New Jersey 07024
Phone: (201) 461-4466
FAX: (201) 461-2776

**DAICEL (U.S.A.), INC.**
23456 Hawthorne Blvd.
Bldg. 5, Suit 130
Torrance, CA 90505
Phone: (213) 791-2030
FAX: (213) 791-2031

**DAICEL (EUROPA) GmbH**
Oststr. 22
4000 Düsseldorf 1, F.R. Germany
Phone: (211) 369848
Telex: (41) 8588042 DICEL D
FAX: (211) 364429

**DAICEL CHEMICAL (ASIA) PTE. LTD.**
65 Chulia Street #40-07
OCBC Centre, Singapore 0104
Phone: 5332511
FAX: 5326454